GEOLOGIC GUIDEBOOK FOR WASHINGTON AND ADJACENT AREAS

EDITORIAL COMMITTEE

NANCY L. JOSEPH, Chairwoman
Keith L. Stoffel
James G. Evans
Thor H. Kiilsgaard
Michael A. Korosec
Robert L. Logan
Fred K. Miller
William M. Phillips
Robert E. Powell
Henry W. Schasse
J. Eric Schuster
Stephanie Z. Waggoner
Timothy J. Walsh
James W. Whipple

Prepared for the
85th Annual Meeting of the Cordilleran Section
Geological Society of America
May 8-11, 1989
Spokane, Washington

WASHINGTON DIVISION OF GEOLOGY AND EARTH RESOURCES

INFORMATION CIRCULAR 86

1989

WASHINGTON STATE DEPARTMENT OF
Natural Resources

Brian Boyle - Commissioner of Public Lands
Art Stearns - Supervisor

Division of Geology and Earth Resources
Raymond Lasmanis, State Geologist

We gratefully acknowledge generous contributions from the following companies toward publication of this guidebook:

Asamera Minerals (U.S.) Inc.
Canadian Hunter Exploration Ltd.
Cominco American Resources, Inc.
Hecla Mining Company
Meridian Oil Inc.
Shell Western E & P Inc.
Weyerhaeuser Company

This report is for sale by:

Publications
Washington Department of Natural Resources
Division of Geology and Earth Resources
Mail Stop PY-12
Olympia, WA 98504

Price	$8.35	
Tax	.65	(WA residents only)
Total	$9.00	

Mail orders must be prepaid; please add $1.00 to each order for postage and handling.
Make checks payable to the Department of Natural Resources.

Printed on acid-free paper.

Printed in the United States of America.

Foreword

The Pacific Northwest has a varied and spectacular geologic landscape. The area's geology is similar to that of other parts of the Cordillera--complex structures in rocks of diverse origins that range from miogeoclines to exotic terranes, metamorphic core complexes, and thick piles of Tertiary sedimentary and volcanic rocks. Unique to the area are the late Proterozoic Belt Supergroup and Deer Trail Group, the Miocene Columbia River Basalt Group, and the Pleistocene deposits that resulted from outburst floods of glacial Lake Missoula. The excursions in this volume sample some of the area's geologic variety.

This guidebook is published by the Washington Division of Geology and Earth Resources (DGER) for the field trips offered in conjunction with the 92nd annual meeting of the Cordilleran Section of the Geological Society of America. The meeting was held in Spokane, Washington, May 8 to 11, 1989, jointly with the Rocky Mountain Section. A companion volume titled "Guidebook to the geology of northwestern and western Idaho and surrounding areas" was published by the Idaho Geological Survey as their Bulletin 28; it covers the excursions organized by members of the Rocky Mountain Section.

The first rule governing guidebooks is that they must be available for their field trips. Consequently, this volume was prepared under a tight schedule. The texts were written during the last few months of 1988. Each contribution has had two peer reviews and additional technical and editorial review by the volume's editors and DGER geologists. Virtually all illustrations were made by the authors. The publications staff at DGER designed and prepared the volume. Because of the deadlines imposed by the meeting date, this volume has not had the normal editorial scrutiny by DGER.

This volume presents much new and previously unpublished information. The selection of papers is a significant contribution to understanding the challenging geologic problems of the region. The editors gratefully acknowledge the efforts of all those who labored to prepare this guidebook.

NLJ
January 25, 1989

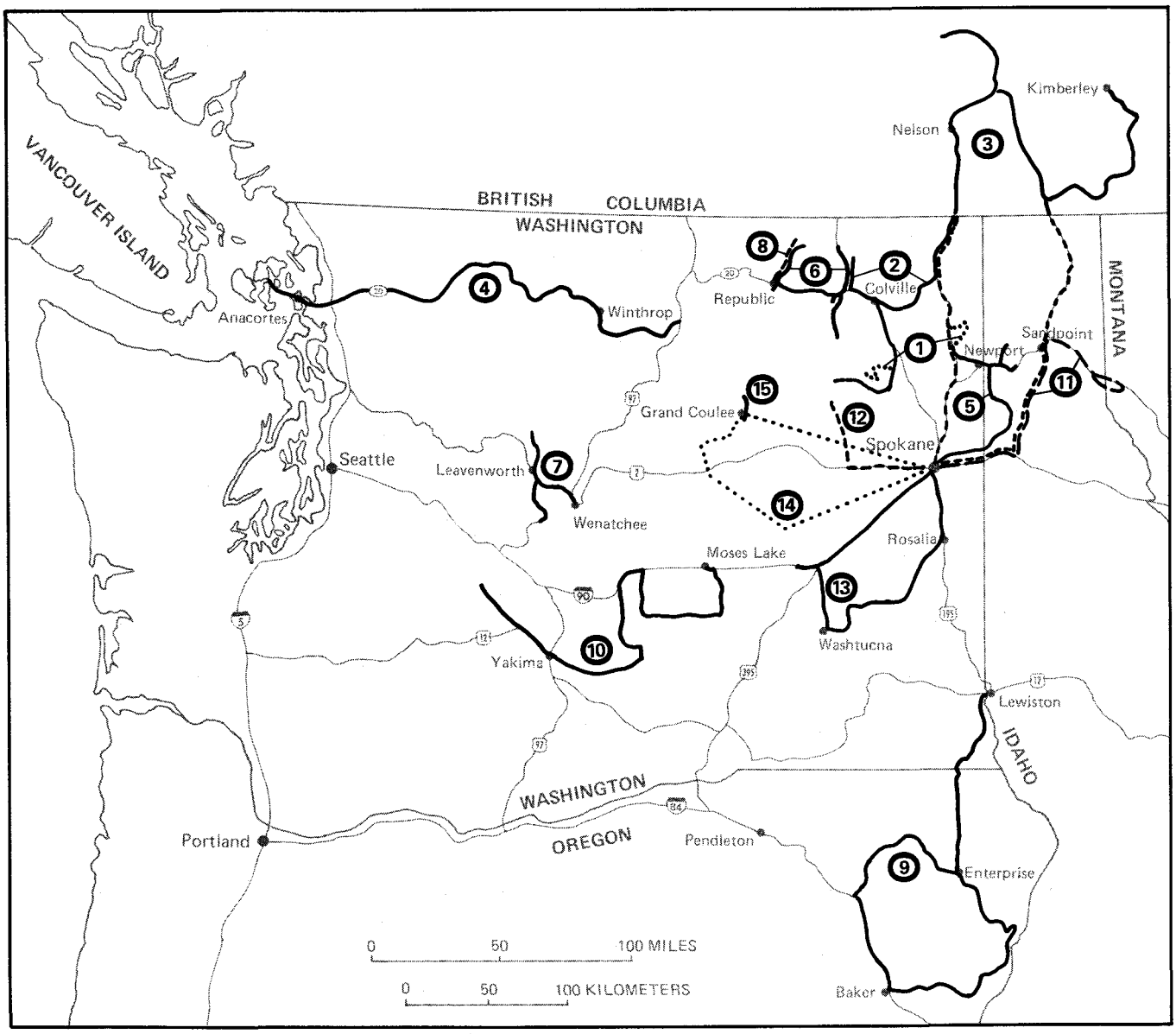

Fieldtrip routes for papers in this volume keyed to author list below.

(1) Miller and Whipple
(2) Dutro and Gilmour
(3) Lambert, Höy, and Andrew
(4) McGroder; McGroder and Miller; Haugerud; Brandon
(5) Rhodes and others
(6) Holder and others; Fox and Wilson
(7) Evans and Johnson
(8) Tschauder
(9) Hooper and Reidel
(10) Reidel and Campbell
(11) Breckenridge
(12) Kiver and others
(13) McDonald and Busacca
(14) Stradling and Kiver
(15) Behrens and Hansen

Fieldtrip Topics and Related Papers

The Deer Trail Group: Is it part of the Belt Supergroup?
Fred K. Miller and James W. Whipple 1

Paleozoic and Lower Triassic biostratigraphy of northeastern Washington
J. Thomas Dutro, Jr., and Ernest H. Gilmour 23

Tectonics and mineralization in southeastern British Columbia
Tectonics of the Kootenay Arc
Richard St J. Lambert 45
The Purcell Supergroup and the Sullivan massive sulfide deposit
Trygve Höy 55
Structure, stratigraphy , and mineral deposits of the Rossland Group, Nelson area
Trygve Höy and Kathryn Andrew 63

Elements of the Cascades 'collisional' orogen: A transect from the Methow Basin to the San Juan Islands
Introduction to a transect from the Methow Basin to the San Juan Islands, Washington
Michael F. McGroder 91
Geology of the eastern North Cascades
Michael F. McGroder and Robert B. Miller 97
Geology of the metamorphic core of the North Cascades
Ralph A. Haugerud 119
Geology of the San Juan-Cascade nappes, northwestern Cascade Range and San Juan Islands
Mark T. Brandon 137

Geology of the southern Priest River Complex and the Newport fault
Brady P. Rhodes, Tekla A. Harms, and Donald W. Hyndman 163

Volcanism, plutonism, and sedimentation, central Okanogan Highlands
Plutonism, volcanism, and sedimentation associated with core complex and graben development in the central Okanogan Highlands, Washington
R. Wade Holder, David R. Gaylord and Grace A. M. Holder 189
Kettle gneiss dome: A metamorphic core complex in north-central Washington
Kenneth F. Fox, Jr., and James R. Wilson 201

Paleogene strike-slip basins of central Washington
James E. Evans and Samuel Y. Johnson 213

Gold deposits in northern Ferry County
Richard J. Tschauder 239

Dikes and vents feeding the Columbia River basalts
Peter R. Hooper and Stephen P. Reidel 255

Structure of the Yakima Fold Belt, central Washington
Stephen P. Reidel and Newell P. Campbell 275

Fieldtrip Topics and Related Papers — Continued

The Channeled Scabland: Lake Missoula floods and sediments and loess stratigraphy

Lake Missoula floods and the Channeled Scabland
Eugene P. Kiver 307

Evidence for ice dams and floods in the Purcell Trench: Trip A
Roy M. Breckenridge 309

Glacial and multiple flood history of the northern borderlands: Trip B
Eugene P. Kiver and Dale F. Stradling 321

Record of pre-late Wisconsin floods and of late Wisconsin flood features in the Cheney-Palouse scabland: Trip C
Eric MacDonald, and Alan J. Busacca 337

The northern Columbia Plateau from the air
Dale F. Stradling and Eugene P. Kiver 347

Grand Coulee Dam
Greg W. Behrens and Phillip J. Hansen 355

The Deer Trail Group: Is It Part of the Belt Supergroup?

Fred K. Miller and James W. Whipple

The Deer Trail Group: Is It Part of the Belt Supergroup?

F. K. Miller *and* J. W. Whipple
U.S. Geological Survey
W. 920 Riverside
Spokane, WA 99201

INTRODUCTION

The Middle Proterozoic Deer Trail Group comprises an estimated thickness of 2,200 m of argillite, siltite, quartzite, and dolomite. It is exposed exclusively in the Huckleberry and Iron Mountains in northeastern Washington, in an area commonly referred to as the magnesite belt (Fig. 1). The Deer Trail Group is composed of sedimentary sequences similar to those of the Middle Proterozoic Belt Supergroup; moreover, specific lithofacies that characterize Belt Supergroup stratigraphic units appear to have counterparts in the Deer Trail Group. Despite the similarity between the two stratigraphic sequences, lithostratigraphic correlation of the two is not straightforward, even though rocks of the Belt Supergroup occur only 12 km east of the main exposure area of the Deer Trail Group. In this paper we present fairly detailed descriptions of the Deer Trail Group that provide a basis for unit-by-unit correlations with the middle and upper parts of the Belt Supergroup.

Prior attempts at correlating the Deer Trail Group with the Belt Supergroup have ranged from noting the similarities between the two sequences (Campbell and Loofbourow, 1962), to provisional unit-by-unit stratigraphic correlations (Miller and Clark, 1975; McMechan, 1981). Correlation of the two sequences is complicated chiefly by three factors:

(1) The two are separated by the Jumpoff Joe fault, a reverse or thrust fault across which the amount of lateral shortening is unknown, but could be tens of kilometers (Fig. 1).

(2) Parts of the stratigraphic sequences comprising the westernmost Belt exposures at Chewelah and Newport, Washington, with which the Deer Trail must be correlated, exhibit pronounced lithofacies changes over relatively short distances.

(3) Rocks of the Deer Trail Group are extremely deformed and show pronounced dynamothermal metamorphism; further, much of the sequence is poorly exposed.

New geologic mapping in the Huckleberry Mountains as well as reconnaissance stratigraphic and sedimentologic analysis of the Deer Trail and the two nearest Belt sections, at Chewelah and Newport, have benefited from, and built on previous work on the Deer Trail done by Weaver (1920), Bennett (1941), Campbell and Loofbourow (1962), Becraft and Weis (1963), Campbell and Raup (1964), and Evans (1987), and on that done in the Belt and Purcell Supergroups by Harrison and Jobin (1963) and McMechan (1981). We are able to make the stratigraphic correlations suggested here largely because of the quality of this previous work.

The correlations herein are based almost entirely on lithostratigraphy and represent current interpretations of ongoing work. Several units in each section correlate well on this basis, but others do not and require lithofacies changes ranging from minor to extreme. Ongoing work is not to the point, however, that we feel reliable facies models can be constructed. Although we feel fairly confident of those correlations, because the work is not complete, they should be considered a working hypothesis. The correlations, shown later in this guide in Figure 4, are similar to the stratigraphic correlation suggested by McMechan (1981) and differ in part from those suggested by Miller and Clark (1975).

It is not possible to measure either complete or composite sections of any formation in the Deer Trail Group due to a combination of (1) incomplete exposure, (2) faulting and folding, and (3) inability to accurately match thick zones of repetitious lithology containing no marker units. The internal stratigraphy and thicknesses presented here are estimates based upon the best composite section(s) for each unit, but the degree of confidence varies greatly among them.

Almost all argillite or argillitic rock in the Deer Trail Group is noticeably phyllitic. To avoid unnecessary verbiage to express degree of phyllitic development, these

From: Joseph, N. L., and others, editors, 1989, Geologic guidebook for Washington and adjacent areas: Washington Division of Geology and Earth Resources Information Circular 86.

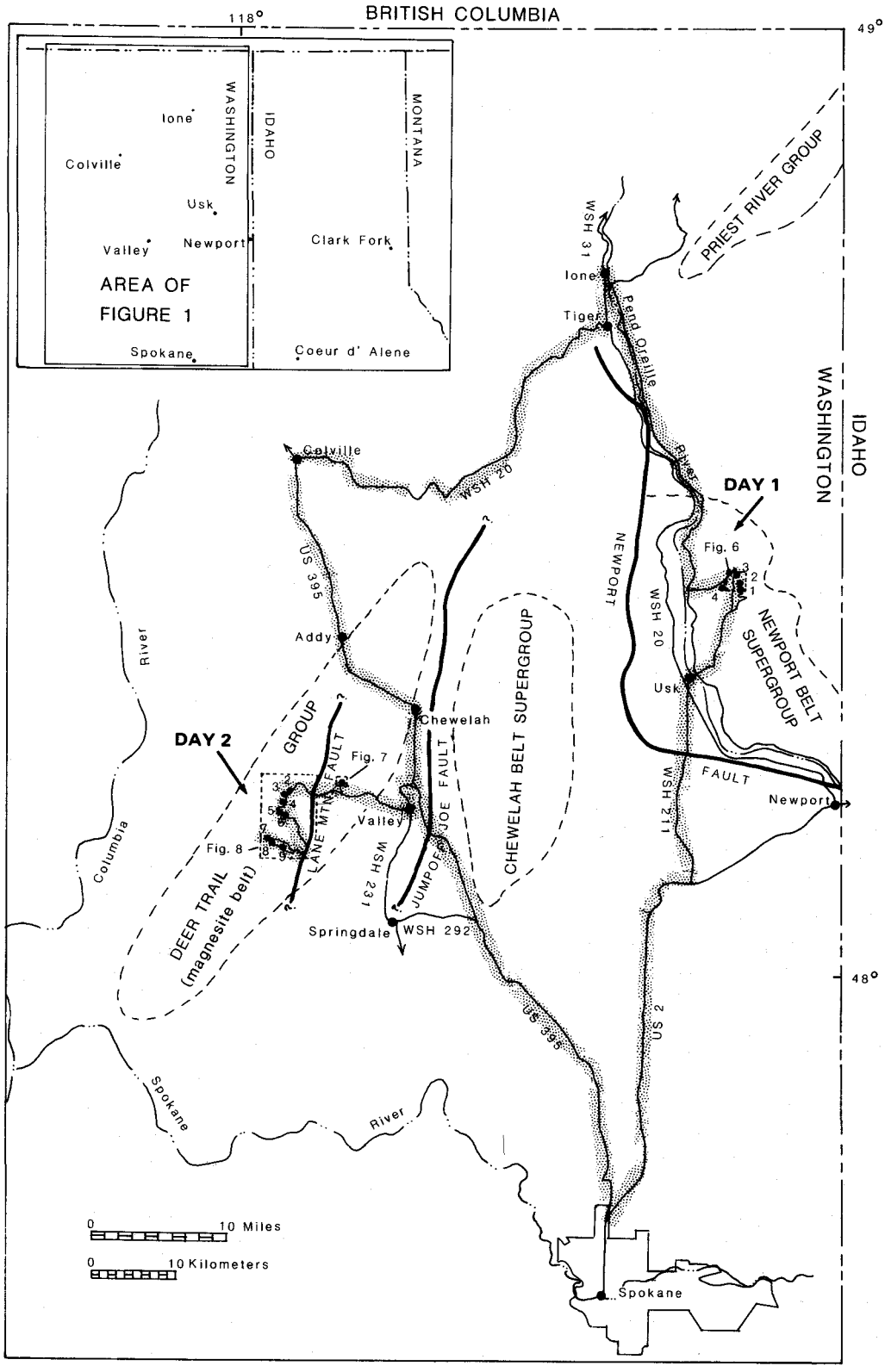

Figure 1. Index map and route of the field trip. Areas enclosed by dashed lines show approximate limits of the four Middle Proterozoic stratigraphic sequences in northeastern Washington. The sections of the Belt Supergroup at Chewelah and the Deer Trail Group are shown only 6 km apart because in several places small outliers of separate formations extend the overall unit boundaries. The main contiguous parts of the Deer Trail Group and Belt section at Chewelah, however, are about 12 km apart. Small closed circles north of Usk and west of Lane Mountain fault show approximate locations of stops. WSH, Washington State Highway, given as State Route (SR) in text.

rocks are described as argillite or argillaceous, even though almost all are phyllitic to some degree.

STRATIGRAPHY

The entire Deer Trail Group appears to be correlative with the combined Wallace Formation and the Striped Peak Formation of the Belt Supergroup as defined by Harrison and Jobin (1963) at Clark Fork, Idaho (Fig. 1). Abbreviated descriptions of the Deer Trail Group and the pertinent formations of the Belt Supergroup follow. Descriptions of some Deer Trail units are presented in greater detail than those for corresponding Belt units only because the Deer Trail stratigraphy is less familiar to most geologists. Readers are referred to cited references for further detail regarding either section.

The Newport section of the Belt Supergroup, rather than that at Chewelah (Fig. 1), was chosen for detailed comparison with the Deer Trail Group on this field trip chiefly because more of the Belt section that is correlative with the Deer Trail Group is preserved at Newport than at Chewelah. Moreover, our current mapping and stratigraphic studies indicate that the Wallace and Striped Peak sections at Chewelah must be re-evaluated and probably revised. Changes in lithofacies between Newport and Chewelah have been identified for parts of the section. Compared to changes in lithofacies between Newport and the next closest Belt section at Clark Fork, Idaho, those identified between Newport and Chewelah are relatively small. Where pertinent to Deer Trail correlations, changes in lithofacies between Newport and Chewelah are noted.

Another thick sequence of Proterozoic rocks, the Priest River Group, which is made up of the same basic lithologic types as are in the Deer Trail Group, is present about 60 km northeast of Chewelah (Fig. 1). The Priest River and Deer Trail sections are almost exactly on strike with each other, but they are separated by granitic rocks. Reconnaissance geologic mapping of the Priest River Group (Glover, 1978; Miller, 1983) and preliminary results of stratigraphic studies indicate it has the same general succession of lithic types as is found in the Deer Trail Group. Extremely complex folding and multi-stage faulting, which occur in both sections, have not yet been worked out in enough detail in the Priest River Group to permit its precise unit-by-unit correlation with the Deer Trail.

Deer Trail Group

The Deer Trail Group, from oldest to youngest, consists of: the Togo Formation, Edna Dolomite, McHale Slate, Stensgar Dolomite, and Buffalo Hump Formation. The base of the Togo is not exposed, and the Buffalo Hump is overlain unconformably by the Proterozoic Windermere Group. This unconformity cuts down-section at the northeast and southwest ends of the magnesite belt such that the maximum thickness of the Deer Trail Group is near the middle.

Greenstone dikes and sills related to a volcanic unit in the Windermere Group are common throughout the magnesite belt and intrude all formations of the Deer Trail Group. Greenstone sills(?) similar in appearance to all other greenstone in the region are present at or near the tops of both the Edna and Stensgar Dolomites almost everywhere these contacts have been seen. Because of the persistent occurrence at these two stratigraphic levels, the greenstones may actually represent extrusive rocks of Deer Trail age, although no extrusive features have been observed.

Togo Formation

Campbell and Loofbourow (1962) named the Togo Formation, but they did not designate a type section, probably because there was then, and still is, no known complete section of the formation. Because the base is not exposed and the formation is complexly faulted and folded, the original maximum thickness can only be estimated as greater than 650 m by piecing together parts from the least deformed areas. The Togo Formation is chiefly medium- and dark-gray argillite and has a few sharply defined intervals in which either quartzite or dolomite beds are concentrated. Individual beds and intervals of green argillite and green and gray siltite occur in parts of the unit, but these are distinctly subordinate in amount to the dark-gray argillite.

Bedding in the dark-gray argillite ranges from wavy, non-parallel to even parallel. Bedding thickness ranges from sub-millimeter laminae to about 10 cm; beds thicker than about 2 cm generally show even parallel bedding. Most non-parallel beds have a low to moderate angle of convergence, but in some, the angle is high, caused chiefly by soft-sediment deformation, which is common throughout the argillite. Lamination is defined by white or light-gray siltite that commonly weathers orange, probably reflecting some carbonate content.

By far the most distinctive lithologic type in the Togo is an interval of medium- to fine-grained vitreous quartzite in the uppermost part of the formation; that quartzite averages about 150 m thick and thickens to the southwest. The basal part of the quartzite is a bed-by-bed gradation from pure argillite to pure quartzite over an interval of about 5 to 10 m. The quartzite is quartz cemented and contains almost no other minerals, except in the transition zone where argillaceous material forms part of the matrix for quartz grains. As many as three other thin, possibly discontinuous quartzite intervals are scattered throughout the upper half of the formation. In the northeast part of the magnesite belt, the quartzite beds of the thick main interval are separated by sequences of dark-gray argillite that range in thickness from less than 1 mm to 2 m. Argillite becomes progressively less abun-

dant southwestward, and where the main interval is thickest at the southwest end of the magnesite belt, it contains relatively little interbedded argillite (Campbell and Loofbourow, 1962). Bedding and lamination in the uppermost quartzite interval range from even parallel to wavy non-parallel. Some of the even parallel beds are cross-bedded, and many of the wavy non-parallel beds show abundant soft-sediment deformation and compaction features (Fig. 2). Syneresis cracks and fluid escape structures are abundant.

The uppermost vitreous quartzite interval overlies about 200 m of interbedded, tan, carbonate-cemented quartzite, pale-green argillite, and tan-weathering dolomite. Bedding in this zone ranges in thickness from about 1 to 10 cm and is chiefly wavy non-parallel. Pyrite is present locally, especially in beds of dolomite. Because of its weathering characteristics, this dolomite interval crops out at only a few places in the entire magnesite belt; generally its presence is recognized by a thick, bright red-orange soil cover.

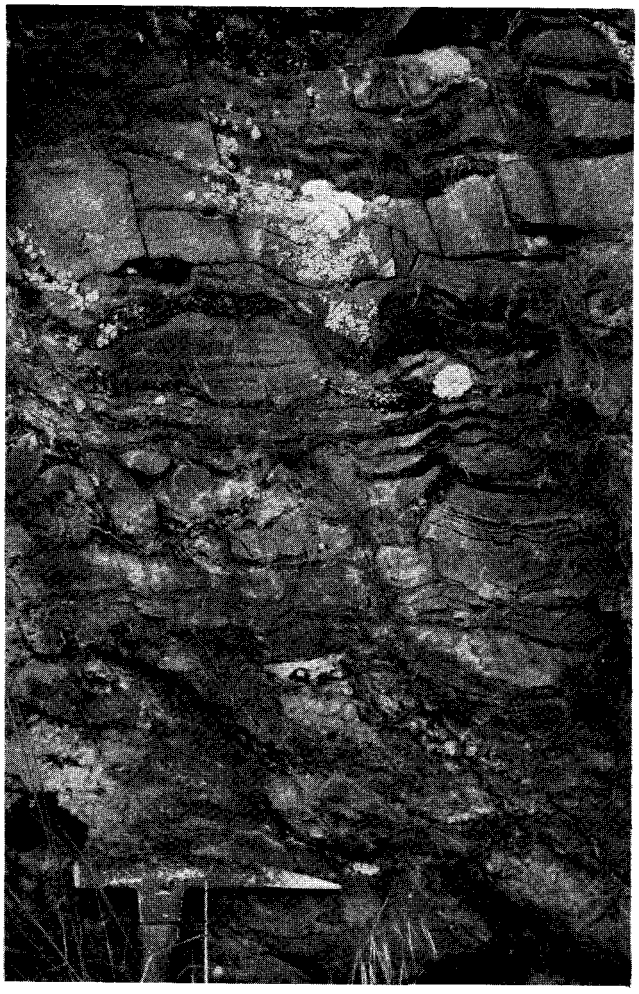

Figure 2. Vitreous quartzite of the Togo Formation. Light-colored wavy-bedded quartzite and siltite and irregularly interbedded dark-gray argillite. Load features, dewatering features, and syneresis cracks are abundant. Style of bedding and soft-sediment deformation are very similar to that in the carbonate member of the Wallace Formation at Newport. This locality is just north of the Middle Fork of Deer Creek.

Edna Dolomite

The Edna Dolomite, also named by Campbell and Loofbourow (1962), is a predominantly dolomitic unit approximately 410 m thick and contains a large proportion of argillite and quartzite. The lower half of the Edna Dolomite is very similar to the carbonate-bearing interval of the upper part of the Togo Formation that is found directly beneath the uppermost vitreous quartzite beds. The lower part of the Edna consists of mostly light-gray or pale-green argillite and siltite and interbedded pale-tan, carbonate-bearing quartzite and siltite. A few beds of impure tan dolomite also occur in this part of the section, especially near the base. Bedding and outcrop characteristics are the same as in its counterpart in the Togo Formation.

The upper half of the formation is largely thin- to thick-bedded, tan-weathering, gray and white dolomite, but thin interbeds of argillite are common. Chert-bearing dolomite is present but not abundant. Stromatolitic beds are common locally and may have been more numerous before many of the primary features in the unit were destroyed by shearing. Bedding is even parallel to wavy non-parallel, and bed thickness averages between 5 and 15 cm. Argillitic strata in this part of the Edna are commonly sheared, and at many places all sedimentary structures are destroyed.

Two prominent intervals of white and gray, thick- to thin-bedded vitreous quartzite are present in the uppermost and middle parts of the formation. Both quartzite intervals extend the entire strike length of the magnesite belt, but they are not continuously exposed. Their absence in some areas may be due to non-deposition but more likely is due to removal by small faults parallel to the strike or to lack of exposure.

McHale Slate

Campbell and Loofbourow (1962) designated all the "dark gray argillite and slate" lying stratigraphically between the Edna Dolomite and Stensgar Dolomite as the McHale Slate. Throughout its extent, the McHale is phyllitic and folded to some degree. Thickness is estimated to be about 370 m.

The McHale is almost entirely argillite, but some subdivisions based on color and bedding characteristics are recognizable. The lower 100 to 120 m of the formation is medium- to dark-gray argillite with tan, pale-gray, and white laminae. Bedding thickness ranges from laminations on a sub-millimeter scale to fining-upward couplets as much as 30 mm thick. Even parallel lamina-

tion, which is extensively disrupted by soft-sediment deformation, is most common in this part of the formation. Wavy parallel and wavy non-parallel beds are also abundant; some have prominent erosional bases.

The gray argillite interval in the lower part of the McHale grades upward into pale greenish-gray and lavender-gray argillite, which characterizes the rest of the formation. The green- and lavender-gray units alternate in intervals from 1/2 to about 30 m in thickness. The pigmentation may reflect primary differences in mineralogy or oxidation state, or both; contacts between different colored zones are sharp, and there is no gradation or color change oblique to bedding. Bedding and lamination, although well developed in almost all of the McHale, is indistinct in the upper two-thirds of the unit because beds and laminations do not contrast with one another, especially on freshly broken surfaces.

The character of the McHale Slate changes along the strike length of the magnesite belt. In the southwestern part of the belt, bedding and laminations in the upper part of the McHale Slate are almost entirely even parallel, and soft-sediment deformation is rare. The amount of soft-sediment deformation and wavy non-parallel bedding increases northeastward. In most of the magnesite belt, the upper 20 to 30 m of the McHale appears to be transitional with the dolomite of the overlying Stensgar Dolomite, but in the northeastern part of the magnesite belt, the McHale is overlain by a basal maroon argillite of the Stensgar Dolomite.

Stensgar Dolomite

The name Stensgar Dolomite was first introduced by Weaver (1920) for "a persistent dolomitic limestone" in his Deer Trail Argillite, but Bennett (1941) elevated the Deer Trail to group status and established the Stensgar as a formation. The Stensgar Dolomite is 200 to 250 m thick and may thin from east to west. Most of the Stensgar is white, tan, pink, or maroon, fairly pure dolomite. Maroon argillite beds not more than a few meters thick are restricted to a few sharply defined intervals in the upper and middle parts of the formation, and in the northeastern part of the magnesite belt, maroon argillite also occurs at or near the base. In the Jim McGraff quarry section (Figs. 1 and 7, Stop 1, Day 2), an interval of maroon argillite as much as 10 m thick is at the base of the formation. This basal argillite interval contains at least one quartzite bed. Clastic strata at the base of the Stensgar have not been observed in the southern half of the Huckleberry Mountains, perhaps due to faulting.

In the Jim McGraff quarry area, about 5 to 8 m of 10- to 100-cm-thick white to pale-tan dolomite beds that contain a few indistinct internal laminae rest with apparent conformity on the basal maroon argillite, siltite, and quartzite. Because the base is poorly exposed, the presence of dolomite below these clastic beds is uncertain. Above the dolomite beds are about 50 m of two alternating lithologic sequences: (1) white, gray, and pink, thin-bedded to thinly laminated dolomite, thin maroon argillite laminae, and thin, even-parallel interbeds of chert, and (2) massive-appearing pink, tan, or white dolomite that weathers tan. This 50-m interval is overlain by an equally thick, distinctive interval of interbedded, gray-weathering, medium- to thin-bedded dolomite and chert that is a useful marker unit in the magnesite belt; it is the only Proterozoic carbonate rock that consistently weathers gray.

Through most of the magnesite belt, the upper 100 to 150 m of the Stensgar is thin- to thick-bedded, tan-weathering, white, gray, pink, and maroon dolomite. Sparse algal structures and oolites are present just above the gray-weathering marker unit and may occur at other places in the formation. Approximately 2 to 3 m of maroon argillite about 50 to 75 m below the inferred top of the Stensgar contain abundant casts of an evaporite mineral, probably salt (Fig. 3); these salt(?) casts are obscured by shearing at many places. Nodular chert is present in sharply defined beds about 30 cm thick at several places in the formation but appears to be most

Figure 3. Salt (?) casts in an argillite interval in the upper part of the Stensgar Dolomite, north of Jim McGraff quarry.

abundant between the salt(?) cast-bearing argillite and the inferred top of the Stensgar. The contact with the overlying Buffalo Hump is either sheared or clearly faulted everywhere we have seen it.

Buffalo Hump Formation

The Buffalo Hump Formation, as defined by Campbell and Loofbourow (1962), consists of all of the Deer Trail Group above the Stensgar Dolomite and below the Proterozoic Windermere Group. The Buffalo Hump is chiefly argillite and quartzite, but both of these rock types vary greatly in appearance and possibly relative abundance. Campbell and Loofbourow (1962), Campbell and Raup (1964), and Evans (1987) noted the extreme lithologic variability of the formation from one end of the magnesite belt to the other. Campbell and Loofbourow (1962), for example, indicated that quartzite beds appear to make up most of the formation at each end of the magnesite belt, whereas thick intervals of argillite predominate in the central part. Our work suggests that this variability may be at least partly apparent and is the result of faulting, folding, and poor exposure.

The only contact between the Buffalo Hump Formation and the underlying Stensgar Dolomite that is not clearly a fault is exposed at the Double Eagle quarries near the center of the magnesite belt. Here, however, the presumed basal argillite of the Buffalo Hump is intensely sheared and lies on mineralized (magnesite) dolomite of the Stensgar. The pale, greenish-gray, phyllitic argillite at the base is about 10 m thick and faintly even-parallel laminated and contains a single 1-m-thick vitreous quartzite bed. The basal argillite is overlain by about 10 m of interbedded even-parallel, micro-laminated dark-gray argillite and even-parallel, thin-bedded siltitic argillite.

Through much of the magnesite belt, overlying the micro-laminated argillite and thin-bedded siltitic argillite is a sequence composed of (1) medium- to thick-bedded, white, gray, and pink vitreous quartzite; (2) pale, greenish-gray and lavender-gray argillite that has poorly defined lamination; and (3) green, hematite-red, and gray even-parallel and cross-bedded quartzite and siltite that is locally feldspathic. These intervals alternate in no identified order, forming a sequence which appears to be about 300 m thick. The sequence grades upward into about 220 m of argillite similar to that in the argillite intervals at the base, except that in some of it, laminations are relatively well defined. In this upper argillite unit is an interval of vitreous quartzite, about 30 to 50 m thick, interbedded with thin-bedded siltite with bedding plane partings of argillite. Much of the vitreous quartzite is very coarse grained, in places pebble-bearing, and locally has an argillaceous matrix-supported conglomerate at its base.

The maximum thickness of the Buffalo Hump, about 520 m as calculated from map width, is preserved in the central part of the magnesite belt. The unit is separated from the overlying Windermere Group by an erosional unconformity; an unknown amount of material was removed during the period of erosion.

Belt Supergroup

A section of the Belt Supergroup that is representative of the western Belt basin is exposed northwest of the town of Newport, Washington, for a distance of about 40 km (Fig. 1). All formations of the Belt, from the lower part of the Prichard Formation to the fourth member of the Striped Peak Formation, are represented, but only those stratigraphic units above and including the Wallace Formation are described here (Fig 4). The Belt section, however, is highly faulted, and for most of these formations, composite sections must be constructed.

Wallace Formation

When the Newport area was mapped by Miller (1974), the Wallace Formation was shown as undivided. Recent, as yet unpublished, mapping by Miller provisionally revises and re-assigns the strata of the Wallace in the Newport area to (in ascending order): (1) a carbonate member, (2) an argillite and siltite unit, (3) the Shepard Formation (Willis, 1902), and (4) a laminated argillite and siltite unit. Although the names of units (1) and (4) are similar to the names used by Harrison and Jobin (1963) for informal members of the Wallace Formation at Clark Fork and Shepard is a formal formation name, all are considered tentative for the Newport section at this time.

Carbonate member

In the Newport area, we are defining the carbonate member of the Wallace as consisting of those strata which are equivalent to approximately the upper 90 percent of the stratigraphic unit that was informally termed the lower calcareous member of the Wallace Formation by Harrison and Jobin (1963) in the Clark Fork area (Fig. 4). Although no unfaulted section of the carbonate member is known in the Newport area, we have pieced together a fairly well constrained 750-m-thick composite section whose thickness is similar to that shown at Clark Fork by Harrison and Jobin (1963) for corresponding strata. The carbonate member at Newport is carbonate-bearing quartzite and siltite and has abundant thin interbeds of dark-gray argillite. Numerous thick beds of relatively pure dolomite that contain irregularly shaped fillings of sparry calcite (molartooth structures) are scattered throughout the unit. Bedding is mostly wavy nonparallel. Soft-sediment deformation, load and fluid-escape structures, and syneresis cracks are abundant.

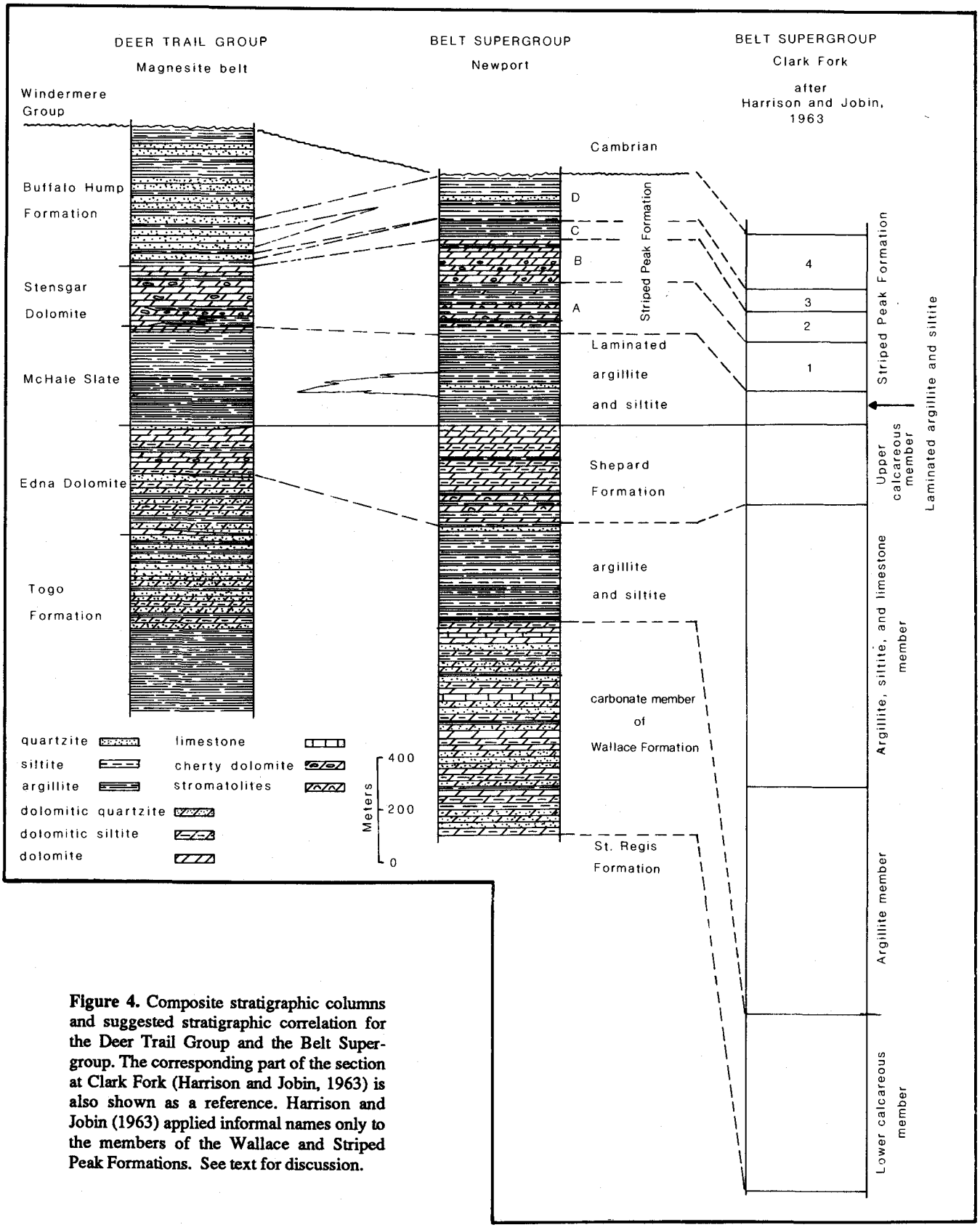

Figure 4. Composite stratigraphic columns and suggested stratigraphic correlation for the Deer Trail Group and the Belt Supergroup. The corresponding part of the section at Clark Fork (Harrison and Jobin, 1963) is also shown as a reference. Harrison and Jobin (1963) applied informal names only to the members of the Wallace and Striped Peak Formations. See text for discussion.

Argillite and siltite unit

About 380 m of interbedded argillite and siltite overlie the carbonate member of the Wallace Formation and occupy the stratigraphic position of the argillite member and argillite, siltite, and limestone member of the Wallace Formation as mapped by Harrison and Jobin (1963) in the Clark Fork section (Fig. 4). Approximately the lower one-third of the argillite and siltite unit is mostly dark-gray, wavy, non-parallel to near-parallel laminated argillite and siltite commonly arranged as fining-upward couplets and interbedded wavy non-parallel to even-parallel bedded siltite from a few centimeters to 1/2 m thick. A few, thin, fine-grained quartzite beds occur near the base and, more rarely, at irregular intervals throughout the lower half of the unit. Fining-upward couplets, ripple marks, and fluid-escape structures are common; syneresis cracks are abundant locally.

The upper two-thirds of the unit is made up of alternating 1- to 20-m-thick intervals of dark-gray, even parallel laminated argillite and gray-green siltite. The argillite intervals consist of interbedded micro-laminated argillite, and 2- to 3-cm-thick sequences of 1- to 2-mm-thick graded couplets. Fluid-escape, syneresis, and soft-sediment deformation structures are abundant in the argillite. Beds in the siltite intervals are mostly 1 to 5 cm thick, wavy non-parallel bedded siltite that contain wispy-appearing quartzite lenses and beds that are generally less than 2 cm thick. Some of the green siltite contains small amounts of carbonate minerals. In the uppermost part of this argillite and siltite unit are several 10- to 20-cm-thick, even-parallel quartzite beds.

Shepard Formation

About 360 m of dolomite, dolomitic siltite, and siltite overlying the argillite and siltite unit is here provisionally re-assigned to the Shepard Formation; the lower contact of the unit is placed at the base of the lowest dolomite bed. This unit is the approximate lithostratigraphic equivalent of Harrison and Jobin's (1963) upper calcareous member of the Wallace Formation at Clark Fork (Fig 4). The lower 50 to 75 m is white, tan, and pale-gray, tan-weathering dolomite in single- and multiple-bed zones, interbedded with medium to dark chlorite-green siltite. Siltite beds range from 3 to 30 cm thick, are faintly cross-laminated, and locally contain thin, tan quartzite beds or lenses. The siltite is micaceous, especially in the upper part of the formation, and has a few ripple-marked beds. The chlorite-green color, unusual for any Belt lithology in the Newport area, is suggestive of rocks with a volcaniclastic component and may reflect a southwestward extension of the volcanism represented by the Nicol Creek Formation of McMechan and others (1980) in southern British Columbia.

Dolomite beds are thinly laminated and commonly weather to 10- to 70-cm-thick blocks. About six or eight dolomite intervals separated by green siltite occur in this upper part of the formation and range from 10 cm to 8 m in thickness. Stromatolites and oolites are present, particularly in the uppermost dolomite intervals. On the ridge south of Browns Lake, many of the dolomite beds are pink or maroon.

The upper part of the formation is almost entirely pale-green, white, gray, or tan, tan-weathering dolomite similar to the dolomite beds below. This part of the Shepard also contains wavy parallel and non-parallel laminated beds of pale-green dolomitic siltite that weather much like the dolomite.

Laminated argillite and siltite unit

About 350 m of argillite and siltite, which are here termed the laminated argillite and siltite unit, overlie the Shepard Formation; this unit is essentially equivalent to the laminated argillite and siltite member of the upper part of the Wallace Formation as mapped by Harrison and Jobin (1963) (Fig. 4). Approximately the lower 120 m consists mostly of dark-gray, even-parallel laminated argillite. A few argillite beds are about 1 cm thick and unlaminated. Very slightly discordant erosional bases to some sets of laminae locally give a low-amplitude, long-wavelength wavy appearance to the bedding. Sub-millimeter, white siltite laminae accentuate the bedding and the wavy appearance. Fluid-escape structures and localized soft-sediment deformation are common.

The argillite grades upward over a short interval into even-parallel, thin- to medium-bedded, gray and greenish-gray siltite and interlaminated dark-gray argillite. The siltite zone is about 75 m thick and has a few 3- to 50-cm-thick white and gray fine-grained quartzite interbeds. The upper 100 m of the unit is similar to the lower part, except that there are more parallel planar 1-cm-thick non-laminated beds and the upper 50 m has tan, wavy near-parallel siltite in beds and lenses 1 to 5 mm thick that are interbedded with dark-gray argillite. Soft-sediment deformation, fluid-escape structures, and syneresis cracks are abundant in these beds.

Striped Peak Formation

Miller (1974) designated his informal members of the Striped Peak Formation at Newport, in ascending order, as members A, B, C, and D to indicate that differences between these members and the informal members of the Striped Peak (as in Harrison and Jobin, 1963) at Clark Fork (referred to herein, in ascending order, as members 1, 2, 3, and 4) were poorly understood. Subsequent work indicates that, although this part of the Newport section in general corresponds well with its Clark Fork counterpart, lithofacies differences between the individual members at these two localities are significant enough to warrant continued use of letter designations for the Newport rocks to emphasize these differences.

Member A

The laminated argillite and siltite unit that underlies the Striped Peak Formation passes upward in a short interval into pale-green, tan-weathering, siltite and argillite of member A, much of which is carbonate-bearing. Dolomite beds from 5 cm to about a meter thick are locally stromatolitic. A few dark-gray, laminated argillite intervals as much as 1 m thick are interbedded in the lower 50 m of this member, which has a total thickness of about 180 m. Gray-green, coarse, carbonate-bearing siltite and minor fine-grained quartzite make up most of the middle and upper parts of the member; dolomite beds are thicker and more numerous in the upper 50 m. Detrital muscovite is common, and hematitic stain covers most bedding plane and fracture surfaces throughout the member.

Bedding in the siltite parts of member A averages from about 1/2 to 5 cm in thickness and is mostly wavy parallel and non-parallel; some is even parallel. Graded couplets are common, and cross-lamination is present locally. Fluid-escape structures, mud cracks, mud-chip breccia, ripple marks, and salt casts are found in most parts of member A. Although similar in most other respects, member A of the Striped Peak at Newport contains more carbonate beds and does not have the abundant quartzite found in this part of member 1 of the Clark Fork section.

Member B

Member B of the Striped Peak Formation is about 160 m thick and is almost entirely gray, tan, or white dolomite. Most of the dolomite weathers tan or chocolate-brown, but unlike other Middle Proterozoic carbonate rocks, some of the dolomite weathers light gray. Stromatolites are present at several places in the member. Bedding thickness ranges from thin laminae to more than a meter. Much of this member, particularly the uppermost and lowermost parts, has hematite-red stained surfaces similar to those in member A. Gray or white chert occurs locally as nodular and irregular masses ranging from a few centimeters to 1/2 m in longest dimension. In the lower part of member B is a bed several meters thick of massive breccia-like dolomite and chert that appears to be sedimentary and not tectonic in origin.

The upper 20 m of this member consists of several thin beds of slightly phyllitic, gray argillite marking a transition into member C. The upper contact of member B is placed on top of the uppermost dolomite bed.

Member C

Member C is medium- to dark-gray, thin to microlaminated argillite. Lamination is uniformly even parallel; erosional features are rare and subtle. This member is only 70 m thick and is homogeneous throughout. Laminae of light-gray argillite or very fine grained siltite enhance the lamination. The combination of thin, even-parallel lamination and a weak bedding-plane cleavage results in flaggy, commonly paper-thin-weathering fragments. A few thin, light greenish-gray siltite beds are interbedded near the top of the member and mark a very narrow transition zone into overlying member D.

Member D

Hematitic siltite, argillite, and lesser amounts of quartzite make up nearly all of member D. This member at Newport is about 170 m thick, and it is overlain unconformably by the Cambrian Addy Quartzite. The base of the member is placed at the top of the uppermost laminated gray argillite bed of the transition zone with member C. At the base of member D is about 10 m of light gray-green quartzite, quartzitic siltite, and minor argillite. Within 2 m, this green rock passes upward into the red hues characteristic of the member.

Bedding is generally even parallel, and bed thickness ranges from less than a centimeter to just more than a meter. Cross-bedding, cross-lamination, and mud-chip breccias are common, and detrital muscovite is ubiquitous. Much of the quartzite and quartzitic siltite parts of this member is feldspathic and has a porous appearance.

STRATIGRAPHIC CORRELATIONS

The correlations suggested here between the Belt Supergroup at Newport and the Deer Trail Group in the magnesite belt are based strictly on lithostratigraphic similarities of vertical succession between the two sequences. We do not feel that the currently on-going work has reached a point that accurate facies models can be constructed, although we can identify parts of the section where facies changes between the two areas should occur.

Similarities and differences between the sections of the Deer Trail Group and Belt Supergroup at Newport exist in both the succession of major lithologic packages and the detailed lithofacies that characterize the units of each sequence. The lithostratigraphic similarities between several units in the two sections are great enough that we feel the general stratigraphic equivalence of the two sections is fairly certain. Although some of the units in one sequence that are somewhat unlike their counterparts in the other sequence leave a few specific formational correlations open to alternate interpretations, many of the dissimilarities could be related to facies changes or structural juxtaposition or both.

Figure 4 illustrates the stratigraphic correlation we feel best explains the relation between the two sequences. The succession in the rock sequence of the Belt Supergroup at Newport that is lithostratigraphically most similar to its counterpart in the Deer Trail Group is that comprising the Shepard Formation, the laminated argillite and siltite unit, and members A and B of the Striped Peak Formation. These units have very close lithologic

correlatives in the upper part of the Edna Dolomite, the McHale Slate, and the Stensgar Dolomite, respectively. In addition, member C of the Striped Peak may have a much thinned lithostratigraphic correlative in the laminated argillite beds in the lowermost part of the Buffalo Hump Formation. Green and red feldspathic quartzite and siltite beds similar to those of member D of the Striped Peak Formation are sparsely scattered throughout the lower 200 m of the Buffalo Hump Formation. However, with a few exceptions, above and below these units lithologic correspondence between the two sequences is much poorer.

Although the gross lithologic assemblages—in addition to many of the smaller scale features—are very similar for the above mentioned parts of these two sequences, there are four major differences:

(1) The upper part of the Edna Dolomite, which is considered to be the correlative of the Shepard Formation, is nearly 50 percent thinner than the Shepard at Newport. Because of the very close lithologic resemblance of the two units, however, we feel that the lesser thickness of the Edna does not detract from its correlation with the Shepard, and in fact it may eventually provide information on basin configuration and sediment dispersal to account for the different thicknesses.

(2) Approximately 75 m of fairly coarse grained strata in the middle part of the laminated argillite and siltite unit at Newport is not found in the McHale Slate, nor is the lavender and green pigmentation of the upper part of the McHale present in the Newport laminated unit. These coarser grained clastic rocks at Newport are presumed to pinch out between that locality and the magnesite belt; the difference in pigmentation may reflect slight, but important differences in sediment mineralogy or early diagenesis, or both.

(3) The Stensgar Dolomite correlates better with member B of the Striped Peak Formation than with (the combined) members A and B. Although correlation with members A and B necessitates a considerable lateral change in lithofacies, the argillitic lower part of the Stensgar in the eastern and northern parts of the magnesite belt may be the westernmost reflection of the siltitic parts of member A at Newport.

(4) The green and red, feldspathic, detrital muscovite-bearing quartzite, siltite, and argillite, which make up member D at Newport and characterize the Bonner Formation to the east, are not present as a single recognizable unit in the magnesite belt, but they occur as beds and intervals from less than a meter to more than 10 m thick interbedded with other lithologies in the lower 300 m of the Buffalo Hump Formation. We suggest that sediment represented by the coarse-grained vitreous quartzite and green and gray argillite that is interbedded with these Bonner-like lithologies in the lower part of the Buffalo Hump came from another source, which may have been to the southwest or west. Because of the other Buffalo Hump rock types interbedded with these rocks in the Deer Trail section, member D is correlated with the lower part of the Buffalo Hump only to the degree that the two units occupy the same stratigraphic position above relatively distinctive correlative units in each section.

The carbonate-bearing upper part of the Togo Formation and roughly the lower half of the Edna Dolomite are a heterogeneous mixture of lithologic types, but each taken as a whole is almost identical lithologically to the other. Together, they appear to represent a period of impure carbonate sedimentation punctuated by deposition of the vitreous quartzite beds of the Togo. This succession, except for the lack of carbonate in the vitreous quartzite, is very similar to the upper part of Harrison and Jobin's (1963) lower calcareous member of the Wallace Formation at Clark Fork with respect to overall lithology and sedimentary structures. The two differ in that the carbonate-bearing Deer Trail strata contain pale-green argillite and fewer syneresis cracks and fluid-escape structures than does the lower calcareous member of the Wallace at Clark Fork. The vitreous quartzite of the Togo, on the other hand, contains dark-gray phyllitic argillite and abundant syneresis cracks and has the bedding characteristics of the lower carbonate member of the Wallace (Fig. 2), but contains no carbonate minerals whatsoever.

If the vitreous quartzite interval of the Togo is lithologically equivalent to part of the Wallace, it represents a unique carbonate-starved facies, or else the carbonate minerals were removed during or after diagenesis. Moreover, if the succession from the middle part of the Edna to the base of the carbonate-bearing Togo correlates with the lower part of the Wallace Formation, then the unnamed argillite and siltite unit at Newport has no Deer Trail correlative, nor does the nearly pure argillite of the lower part of the Togo Formation have a correlative in the Belt section at Newport.

The thick argillite interval that makes up the lower part of the Togo Formation has no counterpart in either the Wallace Formation at Newport or the units directly beneath it and must represent a pronounced lithofacies change in this part of the section between Newport and the magnesite belt. The argillite of the Togo may represent a distal equivalent of the lowermost part of the Wallace Formation. As with the overlying vitreous quartzite, the argillite would represent a relatively carbonate-starved environment compared to the carbonate-rich Wallace at Newport.

An alternate correlation between one part of the two successions is shown in Figure 5, in which the entire laminated argillite and siltite unit of the Belt section is matched with the dark-gray argillite of the lower part of the McHale Slate. This correlation also requires that the coarser grained clastic strata of the laminated argillite and siltite unit pinch out westward. The lavender-gray and greenish-gray argillite of the upper part of the McHale, which contains a minor amount of carbonate-bearing argillite, and the red argillite at the base of the Stensgar Dolomite are correlated with member A of the Striped Peak Formation. This part of the alternate correlation would require a lateral change in lithofacies—specifically, reduction of grain size and loss of carbonate westward. The remaining part of the Stensgar is then correlated with member B of the Striped Peak. On the basis of lithofacies, the interpretation shown in Figure 4 is currently favored, but detailed sedimentologic analysis and comparison with the section of the Belt Supergroup at Chewelah may alter this or both correlations.

Because work done to date is not sufficient to construct facies models, it consequently is not sufficient to evaluate quantitatively how much of the differences in lithofacies between the Deer Trail section and the Belt section at Newport is due to differences in sedimentological environment at the time of deposition, and how much is due to later faulting. Numerous reverse faults with apparent offsets ranging from several hundred to several thousand meters each have been mapped in the magnesite belt. In addition, even greater offsets probably occurred along the Jumpoff Joe and Lane Mountain faults (Fig. 1) and a large unnamed reverse fault west of Lane Mountain (not shown on Fig. 1). Counterbalancing this horizontal shortening is horizontal extension beneath the Newport fault (Harms, 1983), proposed extensional movement on the Jumpoff Joe fault (Gager, 1982), and normal faulting and proto-rifting related to deposition of the Windermere Group (Devlin and Bond, 1988). The net relative translation of the two areas of deposition from the combination of all these movements is not known. However, the greater difference between the Deer Trail Group and the Belt section at Newport than that between the Belt section at Newport and surrounding Belt sections of comparable present-day separation suggests that net translation is more likely compressional than extensional. The magnitude of the differences between the Deer Trail Group and the Belt units at Newport suggests that the net compression may be large.

SPECULATIONS

The overall relation of the Deer Trail Group to the Belt Supergroup at Newport suggests that bottom slope, current strength, relative position with respect to sediment source and transport direction, in addition to the relative water depth in each area, differed during deposition of much of these Proterozoic sequences and changed frequently. Differences in the two sequences caused by the influence of these factors are particularly apparent in the carbonate-bearing and quartzitic parts of each.

Abundant bedded and nodular chert in the Stensgar Dolomite may be the source for the irregular chert clasts in member B of the Striped Peak Formation at Newport and suggests a transport direction for at least some of the material from west to east at this time. The persistence of this transport direction into Buffalo Hump time may be reflected in the intertonguing of Bonner-type sediment and radically different sediment types represented by the vitreous quartzite and massive argillite such that the latter types may have originated from a southwest or west source. The coarse-grained quartzite in the Buffalo Hump Formation suggests that this postulated southwest or west source terrane was much closer to the Deer Trail depocenter.

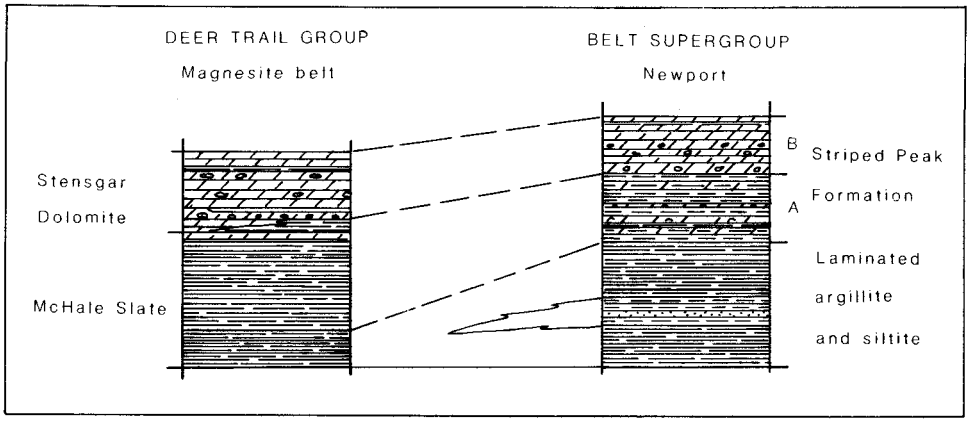

Figure 5. Alternate stratigraphic correlation for the middle parts of the Deer Trail Group and Belt Supergroup. See text for discussion.

ACKNOWLEDGMENTS

We thank D. M. Miller and R. E. Powell for thorough review of this paper.

REFERENCES CITED

Becraft, G. E.; Weis, P. L., 1963, Geology and mineral deposits of the Turtle Lake quadrangle, Washington: U.S. Geological Survey Bulletin 1131, 73 p., 6 pl., scale 1:62,500.

Bennett, W. A. G., 1941, Preliminary report on the magnesite deposits of Stevens County, Washington: Washington Division of Geology Report of Investigations 5, 25 p., 2 pl., scale 1:62,500.

Campbell, A. B.; Raup, O. B., 1964, Preliminary geologic map of the Hunters quadrangle, Stevens and Ferry Counties, Washington: U.S. Geological Survey Mineral Investigations Field Studies Map MF-276, 1 sheet, scale 1:48,000.

Campbell, Ian; Loofbourow, J. S., 1962, Geology of the magnesite belt of Stevens County, Washington: U.S. Geological Survey Bulletin 1142-F, p. F1-F53, 1 pl., scale 1:36,000.

Devlin, W. J.; Bond, G. C., 1988, The initiation of the early Paleozoic miogeocline–Evidence from the uppermost Proterozoic-Lower Cambrian Hamill Group of southeastern British Columbia: Canadian Journal of Earth Sciences, v. 25, no. 1, p. 1-19.

Evans, J. G., 1987, Geology of the Stensgar Mountain quadrangle, Stevens County, Washington: U.S. Geological Survey Bulletin 1679, 23 p., 1 pl., scale 1:24,000.

Gager, B. R., 1982, Stratigraphy, sedimentology, and tectonic implications of the Tiger Formation, Pend Oreille and Stevens Counties, Washington: University of Washington Master of Science thesis, 176 p., 21 pl.

Glover, J. K., 1978, Geology of the Summit Creek map area, southern Kootenay arc, British Columbia: Queen's University Doctor of Philosophy thesis, Kingston, Ontario, 135 p.

Harms, T. A., 1983, The Newport fault–Low angle normal faulting and Eocene extension, northeast Washington and northwest Idaho: Queen's University Master of Science thesis, Kingston, Ontario, 157 p., 14 pl.

Harrison, J. E.; Jobin, D. A., 1963, Geology of the Clark Fork quadrangle, Idaho-Montana: U.S. Geological Survey Bulletin 1141-K, 38 p., 2 pl.

McMechan, M. E., 1981, The Middle Proterozoic Purcell Supergroup in the southwestern Rocky and southeastern Purcell Mountains, British Columbia, and the initiation of the Cordilleran miogeocline, southern Canada and adjacent United States: Bulletin of Canadian Petroleum Geology, v. 29, no. 4, p. 583-621.

McMechan, M. E.; Höy, Trygve; Price, R. A., 1980, Van Creek and Nicol Creek Formations (new); A revision of the stratigraphic nomenclature of the middle Proterozoic Purcell Supergroup, southeastern British Columbia: Bulletin of Canadian Petroleum Geology, v. 28, no. 4, p. 542-558.

Miller, F. K., 1974, Preliminary geologic map of the Newport number 1 quadrangle, Pend Oreille County, Washington, and Bonner County, Idaho: Washington Division of Geology and Earth Resources Geologic Map GM-7, 7 p., 1 pl., scale 1:62,500.

Miller, F. K., 1983, Preliminary geologic map of the Gypsy Peak area, Pend Oreille County, Washington, and Bonner and Boundary counties, Idaho: U.S. Geological Survey Open-File Report 83-601, 15 p., 1 pl., scale 1:48,000.

Miller, F. K.; Clark, L. D., 1975, Geology of the Chewelah-Loon Lake area, Stevens and Spokane counties, Washington: U.S. Geological Survey Professional Paper 806, 74 p., 2 pl., scale 1:62,500.

Weaver, C. E., 1920, The mineral resources of Stevens County: Washington Geological Survey Bulletin 20, 350 p., 20 pl., scale 1:125,000.

Willis, Bailey, 1902, Stratigraphy and structure, Lewis and Livingston Ranges: Geological Society of America Bulletin, v. 13, p. 305-352.

Road Log

Day 1: Newport Area

The first day will be spent examining the middle and upper parts of the Belt Supergroup north of Newport, Washington, to provide a reference for comparison with the Deer Trail Group examined on Day 2. Representative parts of the section above the St. Regis Formation (Fig. 4) will be seen.

Cumulative mileage for the road log is given on the left; mileage between points is given in parentheses. *Set odometers at 0.0.*

0.0 (0.0) Intersection of U.S. Highway 395 and U.S. 2, north Spokane. Bear right and proceed north on U.S. 2 toward Newport. For the first 25 mi or so, the route passes through glacial and alluvial deposits, through which a few outcrops of the Columbia River Basalt Group and unnamed Cretaceous granitoid plutons protrude.

25.0 (25.0) Small septum of hornfelsed Prichard Formation between the 50-Ma Silver Point Quartz Monzonite (monzogranite) and the 100-Ma Fan Lake Granodiorite. Prominent roadcuts for the next several miles are all in the Silver Point Quartz Monzonite.

27.8 (2.8) Intersection with Washington State Route (SR) 211. Turn left toward Metaline Falls. The rock in the outcrop is Silver Point Quartz Monzonite.

36.8 (9.0) Near the beginning of the high roadcuts is the contact between the Silver Point Quartz Monzonite and Precambrian(?) gneiss and migmatite.

39.1 (2.3) The highway passes over the concealed trace of the Newport fault and is on the upper plate of this detachment until the latter part of the drive to Colville.

42.7 (3.6) Intersection with SR 20; continue straight across toward the town of Usk.

43.4 (0.7) Usk. Cross the Pend Oreille River and continue straight on the paved road.

45.0 (1.6) Intersection with a dirt road; bear left to continue on paved road (Kings Lake Road).

46.1 (1.1) Pavement ends; continue on the main road.

50.1 (4.0) Intersection with Forest Service Road (FSR) 5030; continue straight. Stay on the main road.

51.5 (1.4) Intersection with South Skookum Lake Road; bear left.

51.8 (0.3) Secondary dirt road on the left; turn left. Stay on this road.

54.3 (2.5) **STOP 1. Middle part of the argillite and siltite unit, which lies above the carbonate member of the Wallace Formation.**

Features to be noted here are thin-bedded argillite and siltite, some as fining-upward couplets; wavy non-parallel to wavy parallel bedding, syneresis cracks, fluid-escape structures, and interference and current ripple marks. Rocks are slightly hornfelsed by a Cretaceous two-mica pluton 800 m to the east.

After this stop, continue north on the road.

54.8 (0.5) **STOP 2. Argillite and siltite unit.**

Split in the road; park here. This stop entails an approximately 1.3-km hike over topography that in places is extremely steep (Fig. 6). Please use caution especially if the ground is wet.

Representative parts of the argillite and siltite unit, the Shepard Formation, and the laminated argillite and siltite unit are exposed. The contact of the carbonate member of the Wallace Formation with the argillite and siltite unit is concealed, but it is probably very near the position of the road.

Walk out the WNW-trending ridge, staying along the overgrown logging road. Float and grass-root exposures of Wallace-like rocks in the transition zone are seen at the beginning of the hike. The lower 250 m of the argillite and siltite unit are poorly exposed and slightly hornfelsed by the two-mica pluton. At the break in slope, continue down the nose of the ridge, staying on the southern side. The alternating intervals of dark-gray, laminated argillite and pale-green, carbonate-bearing siltite that characterize the upper two-thirds of the argillite and siltite unit are well exposed here.

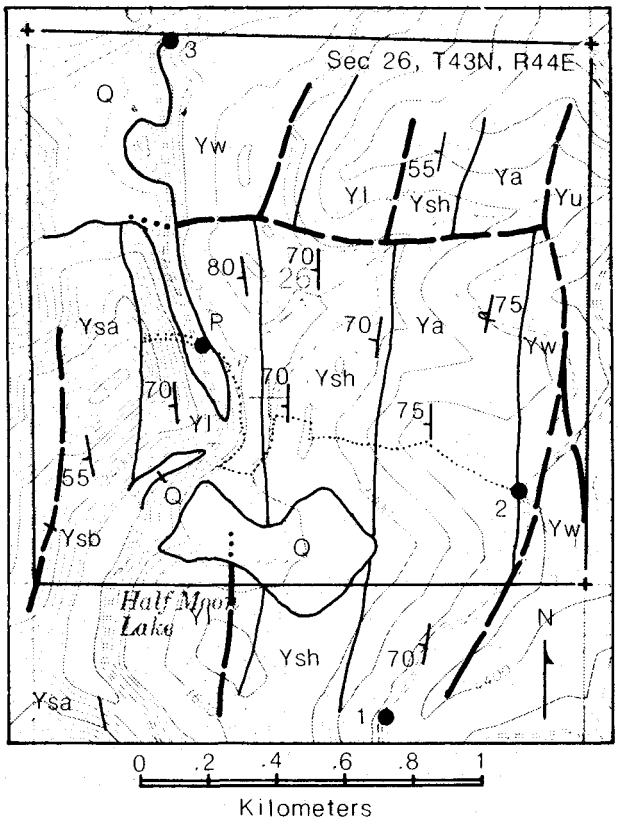

Figure 6. Geologic sketch map showing route of hike beginning at Stop 2. Route is shown by fine dotted line and ends at pick-up point (P). Route of optional hike to see middle part of laminated argillite and siltite unit is shown west of the pick-up point. Yu, Belt Supergroup undivided; Yw, carbonate member of Wallace Formation; Ya, argillite and siltite unit; Ysh, Shepard Formation; Yl, laminated argillite and siltite; Ysa, member A of Striped Peak Formation; Ysb, member B of Striped Peak Formation; Q, surficial deposits. Contacts shown by medium-weight lines, faults by dashed heavy lines. Sites to be examined shown by numbered closed circles. Square with crosses at three corners is the outline of sec. 26, T. 43 N., R. 44 E. See Figure 1 for map location. Base from USGS Browns Lake 7.5′ quadrangle. Contour interval 40 ft.

About half-way down the slope is the first impure dolomite bed of the Shepard Formation; the dolomite is interbedded with dark chlorite-green siltite. This latter rock type could have a volcaniclastic component.

Continue down the slope to the swale. The transition into the almost totally dolomitic upper part of the Shepard is covered. Climb to the top of the low ridge west of the swale. The dolomite part of the Shepard is well exposed on the upper half of this ridge.

Walk north along the ridge about 100 m and then westward to another overgrown logging road. Walk south on the logging road through the transition to the overlying laminated argillite and siltite unit. At the sharp left turn in the road (about 175 m south of where the road is first encountered), turn right and go down the nose of a short ridge through good exposures of laminated dark-gray argillite of the laminated argillite and siltite unit.

Descend to another logging road, turn right, and continue to the vehicle pick-up point at the intersection with FSR 5030. Float and outcrop of Shepard dolomite are in roadcuts on the lower part of the logging road.

Optional hike. Walk north on FSR 5030 about 100 m and climb the hill on the left. Talus covers approximately the lower 25 m of vertical elevation, but above that are good exposures of siltite and lesser amounts of quartzite that characterize the coarser grained middle part of the laminated argillite and siltite unit.

For those not going on the hike from the top of the hill at Stop 2, retrace the vehicle route 4.5 mi back to intersection of King Lake Road and FSR 5030. Locations of roadcut stops that expose representative lithologies of the section traversed by the hike are given below.

59.3 (4.5) Intersection of King Lake Road and FSR 5030; turn right onto FSR 5030. Continue north.

60.4 (1.1) Dolomite of the lower middle part of the Shepard Formation in the roadcut on the right. Continue north.

61.2 (0.8) Good exposures of the upper part of the laminated argillite and siltite unit in the roadcut on the right. Continue north.

61.6 (0.4) Intersection of an old logging road on the right. Pick-up point for the hiking party and starting point for the optional hike mentioned at end of Stop 2 above. Continue north on FSR 5030 after pick-up.

62.2 (0.6) **STOP 3. Wallace Formation.**

The road is narrow, and the stop is just past a curve. Pull over as far as possible to the left at the widest spot. Be alert for traffic while looking at rocks. Tan-weathering carbonate-bearing siltite interbedded with dark-gray argillite; wavy

uneven bedding. The rock here is typical of the Wallace Formation in the Newport area.

Continue north on FSR 5030.

62.7 (0.5) Intersection with FSR 1921 (Browns Creek Road). Turn left.

62.9 (0.2) Secondary dirt road on the right; bear left and stay on the main road.

64.9 (2.0) Secondary dirt road. Turn left, cross the creek, and continue on the road.

65.2 (0.3) **STOP 4. Striped Peak Formation.**

Park to the side of the road where space is available; this is an infrequently used road. We will walk up this road about 0.6 km.

Roadcuts begin in the lower middle part of member A of the Striped Peak Formation. (See description of the unit in the stratigraphy section.) Salt casts, ripple marks, mud cracks, mud-chip breccia, and stromatolite beds are abundant here. Member B begins at the base of the first series of thick dolomite beds. Note the abundant chert in member B, some in large irregular-shaped masses. In the lower part is a bed several meters thick of marine breccia-like dolomite. Part way through member B, several tens of meters of the roadcut have no rock exposure; this interval may conceal a fault that repeats part of the member. Member C begins at the top of the highest thick dolomite bed. The upper part of member C is covered but is uniformly similar to the lower part except for an approximately 3- to 4-m-thick siltitic transition zone into member D.

Continue southwest beyond road; climb a small brushy slope and stay on the south side of the ridge. Continue along the ridge to see member D. There is probably a small fault at or near the contact with the Cambrian Addy Quartzite.

Retrace steps to the vehicles, and retrace the route to FSR 1921.

65.5 (0.3) Intersection with FSR 1921. Turn left; continue down the canyon to the intersection with the paved road.

68.6 (3.1) Intersection with Pend Oreille River Road. Turn right (north).

69.2 (0.6) Outcrops of the Eocene and younger Tiger Formation on the right.

77.2 (8.0) View of Ruby Mountain to the left. Uppermost bold outcrops are the Cambrian Addy Quartzite that overlie hornfelsed Striped Peak(?) Formation and older Belt rocks.

79.5 (2.3) Roadcuts in the Cretaceous granodiorite of Yocum Lake; pluton underlies at least 100 km^2 to the east.

89.2 (9.7) Roadcuts on the right are in extrusive basaltic greenstone of the Late Proterozoic Leola Volcanics (Windermere Group).

95.3 (6.2) Intersection of Sullivan Lake Road. Turn left and cross the bridge over the Pend Oreille River; continue straight.

95.8 (0.5) Intersection of SR 31. Turn left (south).

98.8 (3.0) Intersection of SR 20 at the village of Tiger. Turn right and continue on the highway into Colville. Drive carefully on tight switchbacks above Tiger.

134.0 (35.2) Colville. Intersection of U.S. 395. Turn left (south).

134.7 (0.8) Benny's Panorama Motel on the left.

Day 2: Colville to Spokane

On the second day, the trip will continue south from Colville through Paleozoic carbonate rocks, Cretaceous monzogranite, Cambrian quartzite, and greenstone of the Windermere Group to the magnesite belt where representative parts of the Deer Trail Group will be seen.

Reset odometer.

0.0 Benny's Panorama Motel parking lot. Turn left (south) on U.S. 395

10.7 (10.7) Cambrian Addy Quartzite underlies the mountains to the left and right. The quartzite unconformably overlies the volcanic member of the Huckleberry Formation (a unit in the Windermere Group that is correlative with the Leola Volcanics to the northeast). In the next 8 mi, reverse faults continuous with those in the northern part of the magnesite belt repeat the greenstone-quartzite unconformity five times.

12.7 (2.0) Town of Addy to the right; continue south.

15.4 (2.7) Blue Creek. Volcanic member of the Huckleberry Formation; pillow basalt and flow breccia are exposed in the roadcut on the left.

20.0 (4.6) Cliffs on the mountain ahead are dip slopes of Addy Quartzite. Cliff-forming quartzite lies on more subdued slopes to the east formed by the thickened-westward equivalent of the laminated argillite and siltite unit that overlies the Shepard Formation at Newport.

21.1 (1.1) Town of Chewelah; continue south.

26.0 (4.9) Intersection of SR 231. Turn right and continue to the town of Valley.

27.8 (1.8) Addy Quartzite to the left. Dips are to the east (overturned) here but roll over to upright 70° west dip at the south end of this hill.

29.3 (1.5) Town of Valley. Intersection with Waitts Lake Road; turn right. Stay on main paved road.

34.3 (5.0) Intersection of a secondary dirt road on right; turn right. Stay on the main road to the top of the hill.

This road and the next stop are on private property, and permission to visit must be obtained.

35.4 (1.1) **STOP 1. Jim McGraff quarry in the Stensgar Dolomite.**

Park to one side. Follow the orange flagging 0.53 km N39°E to the northeast flank of a small, rather treeless knob on this larger hill (Fig. 7).

Although the base of the Stensgar is not exposed here, the lowermost exposures are probably near the base. (The lowest beds assigned to the Stensgar are exposed 0.30 km S53°E from the peak of the small knob, in an open area just above an overgrown logging road.) The medium- to thin-bedded chert-bearing lower part of the Stensgar is well exposed here, as is the gray-weathering dolomite.

Walk up the hill in a generally S45°W direction through areas of maximum exposure. Between here and the highest peak, most Stensgar rock types can be seen, including pink and maroon dolomite, thick-bedded dolomite, rare oolites, and stromatolites. On the southeast flank of the highest peak are exposures of maroon argillite containing salt(?) casts. Nodular chert beds can be seen in the bluff west of the quarries.

Return to the vehicles. Retrace the route to paved Waitts Lake Road.

36.5 (1.1) Intersection of Jim McGraff quarry road with Waitts Lake Road. Turn right.

39.2 (2.7) Intersection with Red Marble Road; pavement ends. Continue straight ahead and stay on the main road.

41.0 (1.8) Intersection with Keystone quarry road. Turn left.

41.4 (0.4) Keystone magnesite quarry. (See Fig. 8 for the location of the remaining stops for Day 2.)

Fork in the road. Bear left, continuing along the base of the steep dolomite slope. Strata here are the lower and lower middle parts of the Stensgar. Massive greenish-black rock is intrusive greenstone of the Windermere Group; the greenish-gray phyllite may be an argillite layer in the Stensgar. Continue on main road.

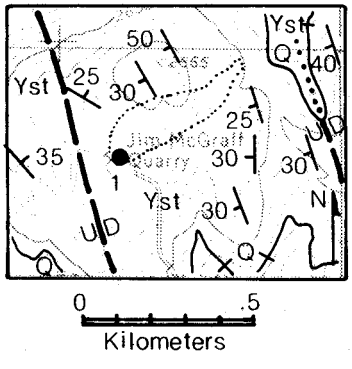

Figure 7. Geologic sketch map showing route of hike beginning and ending at Stop 1 of Day 2. Route is shown by fine dotted line. Yst, Stensgar Dolomite; Q, surficial deposits. Contacts shown by medium-weight lines, faults by dashed heavy lines. The area between the two faults could contain small concealed faults. See Figure 1 for map location. Base from USGS Waitts Lake 7.5′ quadrangle. Contour interval 40 ft.

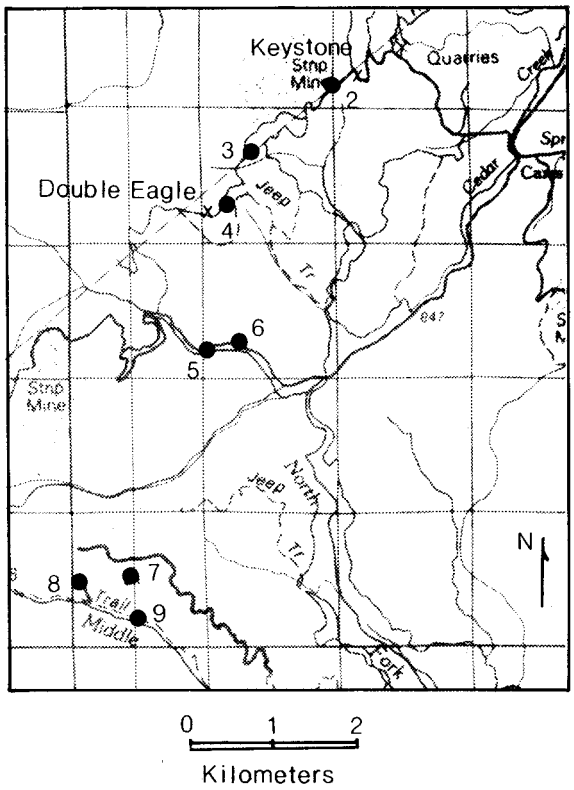

Figure 8. Sketch map showing location of Stops 2 through 9 (numbered closed circles) of Day 2 of the field trip. Double Eagle and Keystone magnesite quarries shown by x. Geology in this area is too complex to show at the scale of the map. See Figure 1 for map location. Base from USGS Chewelah 1:100,000 quadrangle (planimetric).

41.9 (0.5) Intersection with an overgrown, but passable dirt road on the right at a switchback of the main road. Turn to the right and park.

STOP 2. Buffalo Hump Formation and Striped Peak Formation.

Hike about 100 m farther up the dirt road to where rock is exposed in roadcuts.

Green and reddish quartzite and siltite beds (similar to rocks in member D of the Striped Peak Formation) in the lower part of the Buffalo Hump Formation, interbedded vitreous quartzite and indistinctly laminated and massive argillite. Farther up the road, underlying these rocks, is about 10 m of even-parallel, finely laminated to micro-laminated gray argillite. These beds may be lithologically equivalent to member C of the Striped Peak Formation at Newport. Continue eastward up the road, through a stretch with no outcrop which probably conceals a fault, to exposures of the upper part of the Stensgar.

Return to the vehicles and the main Keystone dirt road. Continue up the main Keystone dirt road.

42.1 (0.2) Approximate location of an east-dipping fault separating the Buffalo Hump Formation on the east from the McHale Slate on the west.

42.5 (0.4) **STOP 3. Pale lavender-gray and greenish-gray phyllitic argillite typical of middle and upper parts of the McHale Slate.**

The degree of folding and cleavage development is also typical of the formation throughout the magnesite belt.

Continue along the main road.

43.3 (0.8) **STOP 4. Argillite of the Buffalo Hump Formation.**

Pale greenish-gray, indistinctly laminated to massive argillite. This rock is in fault contact with the Stensgar. Walk down the road to the left for a further look at the part of section seen at the last stop.

Continue along the main road.

45.0 (1.7) Intersection with Red Marble Road. Turn left.

45.4 (0.4) **STOP 5. Upper part of the Edna Dolomite.**

Much greater heterogeneity and impurity distinguish the Edna from the Stensgar. Even in the more carbonate-rich upper part of the Edna, quartzite and argillite beds are common. Thick and thin beds are wavy non-parallel to even parallel. Oolites, stromatolites, and chert are present but not common.

Continue along the main road.

45.7 (0.3) **STOP 6. Lower part of the McHale Slate.**

The dark-gray, well-laminated lower 100 to 120 m of the McHale contrast sharply with the rest of the formation. Here and in the outcrops for the next 100 to 200 m down the road, three types of argillite that characterize the lower part of the McHale are well exposed. These are: (1) even-parallel, laminated and micro-laminated dark-gray argillite; (2) greenish-gray to khaki-colored argillite with indistinct or no lamination; (3) wavy non-parallel to even-parallel, thin-bedded and laminated dark-gray argillite that is extensively disrupted by soft-sediment deforma-

tion. Graded beds are common in the first and last rock types. No quartzite or siltite interval lithologically equivalent to that in the laminated argillite and siltite unit at Newport has been found in the McHale.

46.5 (0.8) Intersection with a dirt road. Turn right and stay on the main road.

49.9 (3.4) Intersection with Deer Creek Road. Turn right.

50.1 (0.2) Intersection with a dirt road (Middle Fork of Deer Creek Road) on the right. Turn right; stay on the main road.

50.7 (0.6) Split in the road; bear left. All rock along this road for about the next 4 mi is phyllitic and altered (bleached) lower and middle parts of the Togo Formation. This lithology, structural state, and degree of alteration and exposure are typical of much of the Togo in the magnesite belt.

52.6 (1.9) Dirt road on the right. Turn right; stay on the main road.

54.7 (2.1) Overgrown but drivable dirt road splits off to the left; bear left.

55.4 (0.7) **STOP 7. Togo Formation.**

End of the road; debark. Vehicles back-track approximately 0.1 mi and park.

Hike about 0.3 km, staying at approximately the same elevation in the clear area around the south side of this hill. Begin the traverse down the bulldozer cut to the left, bearing about S60°W, and then from the end of the dozer cut across an open area, bearing about N70°W. Continue through the vitreous quartzite interval, which ends where thick vegetation begins.

This stop's route first passes through a representative outcrop of the carbonate-bearing quartzite, siltite, and argillite beneath the vitreous quartzite interval of the Togo Formation, and then through the vitreous quartzite interval. In this part of the magnesite belt, this quartzite has numerous beds of dark-gray argillite between the thick and thin quartzite beds. Note the similarity of bedding style and sedimentary features to those in the lower part of the Wallace Formation.

Retrace the route and return to the vehicles. Then retrace the route 2.8 mi to the intersection with Middle Fork of Deer Creek Road.

58.2 (2.8) Intersection with Middle Fork of Deer Creek Road; turn right. Stay on the main road.

59.0 (0.8) Road splits; bear right.

60.2 (1.2) **STOP 8. Togo Formation.**

Overgrown logging road; park and walk up the road to the right about 0.1 km.

Rocks in the roadcut are representative of those in the carbonate-bearing zones above and below the vitreous quartzite of the Togo Formation. Although very similar to the carbonate member of the Wallace Formation at Newport, argillite in these beds is consistently pale green rather than dark gray. The green may be an alteration color developed when most of the carbonate minerals were removed from this rock.

Return to the vehicles. Turn around and proceed back down Middle Fork of Deer Creek Road.

60.8 (0.6) **STOP 9. Argillite of the Togo Formation.**

Rocks here are typical of the dark-gray, laminated argillite beneath the Togo carbonate-bearing rocks. Note graded bedding, erosional bases of some beds, and soft-sediment deformation. The degree of cleavage development is fairly typical for Togo argillite. Alteration seen at the southeast end of the roadcut increases eastward toward a large reverse fault (which repeats nearly the entire Togo Formation) and the Lane Mountain thrust fault (which repeats the entire Deer Trail Group).

This is the last stop; return to the vehicles and continue down the main road.

64.6 (3.8) Intersection with main Deer Creek Road.

65.3 (0.7) Split in the road; bear right.

67.9 (2.6) Split in the road; bear left.

71.4 (3.5) Split in the road; bear right.

72.0 (0.6) Split in the road; bear left.

73.3 (1.3) Intersection with SR 231. Turn right.

74.8 (1.5) Springdale. Stay on the main road, which makes a right-angle turn to the right at the east end of town.

75.0 (0.2) Intersection with SR 292. Turn left.

80.7 (5.7) Intersection with U.S. 395. Turn right and stay on the highway to return to Spokane.

Paleozoic and Lower Triassic Biostratigraphy of Northeastern Washington

J. Thomas Dutro, Jr., and Ernest H. Gilmour

Paleozoic and Lower Triassic Biostratigraphy of Northeastern Washington

J. Thomas Dutro, Jr.
U.S. Geological Survey
Washington, DC 20560
and
Ernest H. Gilmour
Eastern Washington University
Cheney, WA 99004

INTRODUCTION

The purpose of this field trip is to examine some of the fossiliferous outcrops that provide biostratigraphic documentation of the Paleozoic sequence in this critical part of the North American Cordillera. The area that is now northeastern Washington was located at or near the outer edge of the North American platform during most of the Paleozoic. For the most part, the successive faunas are related to those of the North American realm. During the Cambrian, carbonate platform deposits extended farther west than at any subsequent time. Onlap from west to east (in terms of present-day geography) is recorded by the Lower and Middle Cambrian deposits. Ordovician to Middle Silurian graptolitic shales reflect deeper, outer slope deposition. A time gap from Late Silurian to Middle Devonian is succeeded by upper Middle and Upper Devonian deposition, probably near the platform edge, including carbonate buildups of Frasnian age. Possibly, Mississippian carbonates were also deposited in an outer platform setting.

Now juxtaposed against this platform/slope sequence by faulting, a different Devonian and Carboniferous sequence lies to the west. Upper Devonian through Permian graywackes, argillites, and conglomerates dominate this western sequence, which was deposited on the continental slope and in distal basins. Shallow-water carbonates accumulated during the middle Permian in a few places, but the dominant signature of this western package is clastic rocks and associated mafic volcanic rocks.

Northeast Washington falls within three tectonic provinces that extend southward from British Columbia. Most of the region of this field trip (Fig. 1) is in the southwest extension of the Kootenay arc. To the east, the Kootenay arc, which comprises dominantly Paleozoic rocks, abuts the Purcell anticlinorium. Metamorphic rocks in the Kettle dome, presumably a southern extension of the Shuswap Complex, occur west of the Columbia River. A thick wedge of Upper Paleozoic and Mesozoic dominantly graywacke and argillite strata lies east of the metamorphic rocks and is in thrust contact with the miogeoclinal rocks of the Kootenay arc.

A generalized stratigraphic section is given in Figure 2. The field trip includes stops at representative exposures of each of these units.

BIOSTRATIGRAPHY

Cambrian

The oldest Paleozoic fossils in the area have been found in the lower part of the Addy Quartzite (Gypsy Quartzite)(Stop 15) where a low-diversity fauna includes: the trilobite *Nevadella addyensis* (Okulitch), the brachiopods *Micrometra*, *Kutorgina*, and *Rustella*, and hyolithids (Okulitch, 1951). The trilobite, a characteristic middle Early Cambrian genus, indicates assignment to the *Nevadella* Zone.

Archaeocyathid-bearing limestone in the immediate vicinity of Colville has been known for many years (Okulitch and Greggs, 1958; Greggs, 1959). Although these localities were originally ascribed to the "Old Dominion Limestone" (Weaver, 1920), they are now known to represent the Reeves Limestone Member of the Maitlen Phyllite (Stops 13 and 14). The Maitlen conformably overlies the Addy, and the archaeocyathid beds are also considered to be of *Nevadella*-Zone age. Greggs (1959) described a large assemblage of archaeocyathids

From: Joseph, N. L., and others, editors, 1989, Geologic guidebook for Washington and adjacent areas: Washington Division of Geology and Earth Resources Information Circular 86.

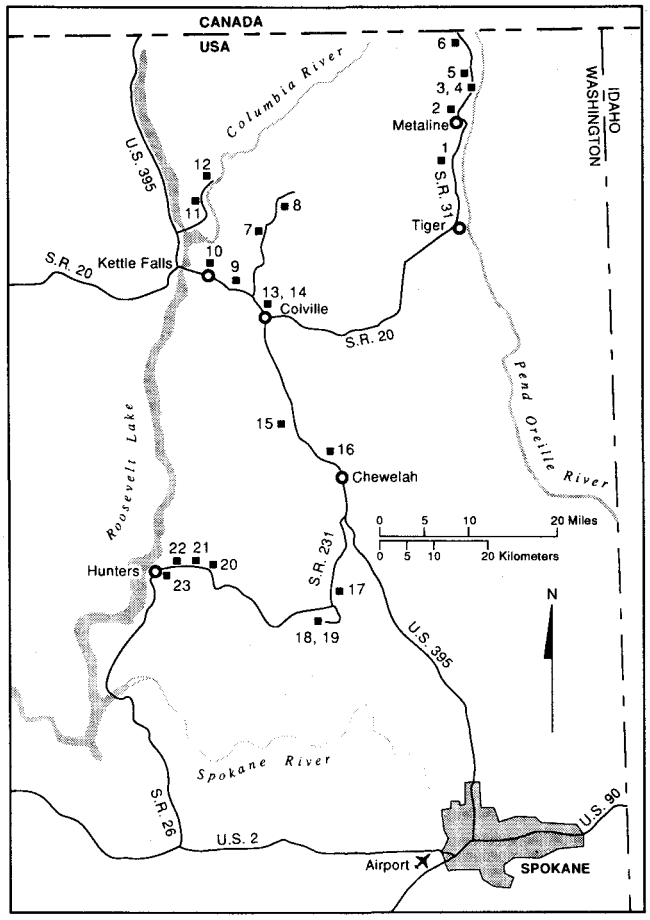

Figure 1. Index map of northeastern Washington. Numbers show approximate locations of fieldtrip stops.

from the Colville and the Salmo, British Columbia, areas. The fauna contains *Ajacicyathus nevadensis* (Okulitch), *A. rimouski* Okulitch, *Ethmophyllum americanum* Okulitch, *E. whitneyi* Meek, *Archaeocyathus atlanticus* Billings, *A. borealis* Okulitch, *Archaeopharetra typica* Bedford and Bedford, *Protopharetra dunbari* Okulitch, *Pycnoidocyathus columbianus* (Okulitch), *P. amourensis* (Okulitch), *Dendrocyathus* sp., *Archaeosycon* sp., *Claruscyathus solidus* Vologdin, *Syringocnema colvillensis* Greggs, and *Syringocyathus* sp.

The Metaline Limestone, a complex of platform carbonate facies, conformably overlies the Maitlen Phyllite. Trilobites were collected many years ago from the lower member of the Metaline in the Metaline quadrangle (Park and Cannon, 1943), and a more diversified assemblage was collected by R. G. Yates from the Leadpoint quadrangle (Yates, 1964) in the mid-1950s. A. R. Palmer (USGS, written commun., 1955, 1956) identified the following trilobite species, among others, from Yates' collections: *Alokistocare* cf. *A. sinuatum* Rasetti, *Bathyuriscus adaeus* Walcott, *Elrathia permulta* (Walcott), *Elrathina* cf. *E. cordillerae* (Rominger), *Kootenia burgessensis* Resser, *K.* cf. *K. spenceri* Resser, *Olenoides serratus* (Rominger), *Oryctocephalus burgessensis* Resser, *Pagetia* cf. *P. bootes* (Walcott), *Zacanthoides divergens* Rasetti, and *Z, romingeri* Resser. Also present were acrotretid brachiopods, the brachiopod *Nisusia* sp., and primitive mollusks. From another level in the lower part of the formation, Palmer identified the trilobites *Alokistocare paranotatum* Rasetti, *Elrathina cordillerae* (Rominger), *Ogygopsis klotzi* (Rominger), *Oryctocephalus reynoldsi* Reed, *Peronaspis columbiensis* Rasetti, *P. montis* (Matthew), and *Zacanthoides divergens* Rasetti, among others. Palmer assigned these assemblages to the *Bathyuriscus-Elrathina* Zone of the middle Cambrian. Palmer also identified some acrotretid brachiopods that may be Late Cambrian in age from beds near the top of the Metaline Limestone. The precise stratigraphic significance of this poorly fossiliferous upper Metaline remains to be determined. Together with the Early Ordovician conodonts from the Clugston Creek area (John Repetski, USGS, written commun., 1988), they cast doubt on the regional significance of the Late Cambrian-Early Ordovician hiatus.

Ordovician

The Metaline Limestone is overlain by the Ordovician Ledbetter Slate, a graptolite-bearing black slate and phyllite that contains some dark limestone and thin-bedded siltstone. Relations between the Ledbetter and the underlying Metaline are equivocal. Most geologists (Mills, 1977) have reported a disconformity, although nearly all the observable contacts are faulted (Stop 2). The evidence was examined in detail by Mills (1977), who concluded that the Ledbetter most likely lies unconformably on the Metaline.

The Ledbetter graptolites have been restudied recently by Claire Carter (1988a, b), who reports an age range of assemblages from as old as the *Oncograptus* Zone (late Arenigian) to as young as Llandoverian (Early Silurian) (Fig. 3). Most of the outcrops in the type area of the Ledbetter, west of Ledbetter Lake, produce graptolites of the *Dicranograptus clingani* Zone (Caradocian) (Stops 3 and 4). The oldest fauna recovered from the Ledbetter has not yielded graptolites but is a low-diversity assemblage of trilobites, the phyllocarid *Caryocaris*, and sponge spicules. The trilobites include *Hystricurus* aff. *H. genalatus* Ross and *Bienvillia* sp., according to M. E. Taylor (USGS, written commun., *in* Schuster, 1976), who stated that they indicate an Early Ordovician age (Tremadocian or Arenigian).

Conodonts from the upper member of the Metaline as mapped by Schuster (1976) in the Clugston Creek area (Stop 8) are identified as Early or early Middle Ordovician by John Repetski (USGS, written commun., 1988). This suggests a facies relation between the upper Metaline and the Ledbetter.

TRIASSIC	Unnamed Lower Triassic graywacke - argillite	Graywacke and argillite; Early Triassic ammonoids; at least 500m thick.
PERMIAN		
	Unnamed Permian argillite and limestone	Argillite and graywacke; Early Permian fossils; limestone at Kettle Falls contains Middle Permian fossils; at least 1000m thick.
CARBONIFEROUS	?	
	? Unnamed carbonate beds	Cherty carbonate; 200m+ thick; Mississippian conodonts and corals.
DEVONIAN	Unnamed limestone on Limestone Hill	Massive limestone; 400m thick; Frasnian corals and conodonts; Givetian conglomerate at base.
	?	
SILURIAN	? Unnamed clastic rocks	Siltstone and shale; about 600m thick; Silurian graptolites and conodonts.
ORDOVICIAN	Ledbetter Slate	Slate and argillite;700-800m thick; Middle Ordovician - Early Silurian graptolites. Early Ordovician fossils in Clugston Creek area.
	? Metaline Limestone	Carbonate sequence; Middle Cambrian trilobites in lower part; Early Ordovician conodonts in upper member; 1000-1800m thick.
CAMBRIAN	Maitlen Phyllite	Phyllite and siltstone; Reeves. Ls. Mbr. in lower 60m; archaeocyathids; as thick as 1600m.
	Addy Quartzite	Thick-bedded quartzite; Early Cambrian fossils; 1700-2700m; unconformable on Precambrian.

Figure 2. Stratigraphic column of Paleozoic and Lower Triassic strata examined on the field trip. Lower Devonian beds near Valley and Famennian strata at Greenwood cemetery are not shown.

Another anomalous situation occurs in the Pend Oreille mine where graptolites of the *Paraglossograptus tentaculus* Zone are found in lenses of slate below the top of the Metaline (Carter, 1988b). This also could be interpreted as an indication of a depositional transition or of facies intertonguing, as there is fossil evidence for continuity into the Middle Ordovician. However, regional relations indicate a considerable time gap and disconformity between the Metaline and the Ledbetter in some places (Dings and Whitebread, 1965).

Silurian

Although originally included in the Ledbetter Slate, fine-grained clastic rocks that yield Silurian fossils were locally mapped separately from the Ledbetter by Greenman and others (1977). These rocks crop out to the west of the type Ledbetter area, mostly in a 3-mi-long, north-trending belt from Beaver Mountain to Horsefly Hill (Fig. 4). Graptolites identified by W. B. N. Berry indicate an age range from late Llandoverian through Ludlovian (late Early through early Late Silurian). Conodonts identified by Brian Chatterton give a similar age range. These unnamed strata are differentiated from the Ledbetter by the increase in their siltstone content in the lower part and by sandstone and chert-pebble conglomerate in the upper part. In all probability, the lower part is gradational with the Ledbetter, and the report of Llandoverian graptolites from both formations would seem to confirm this relation. Conglomerates of Middle Devonian age overlie these Silurian beds in the vicinity of Limestone Hill, but the contact is not exposed.

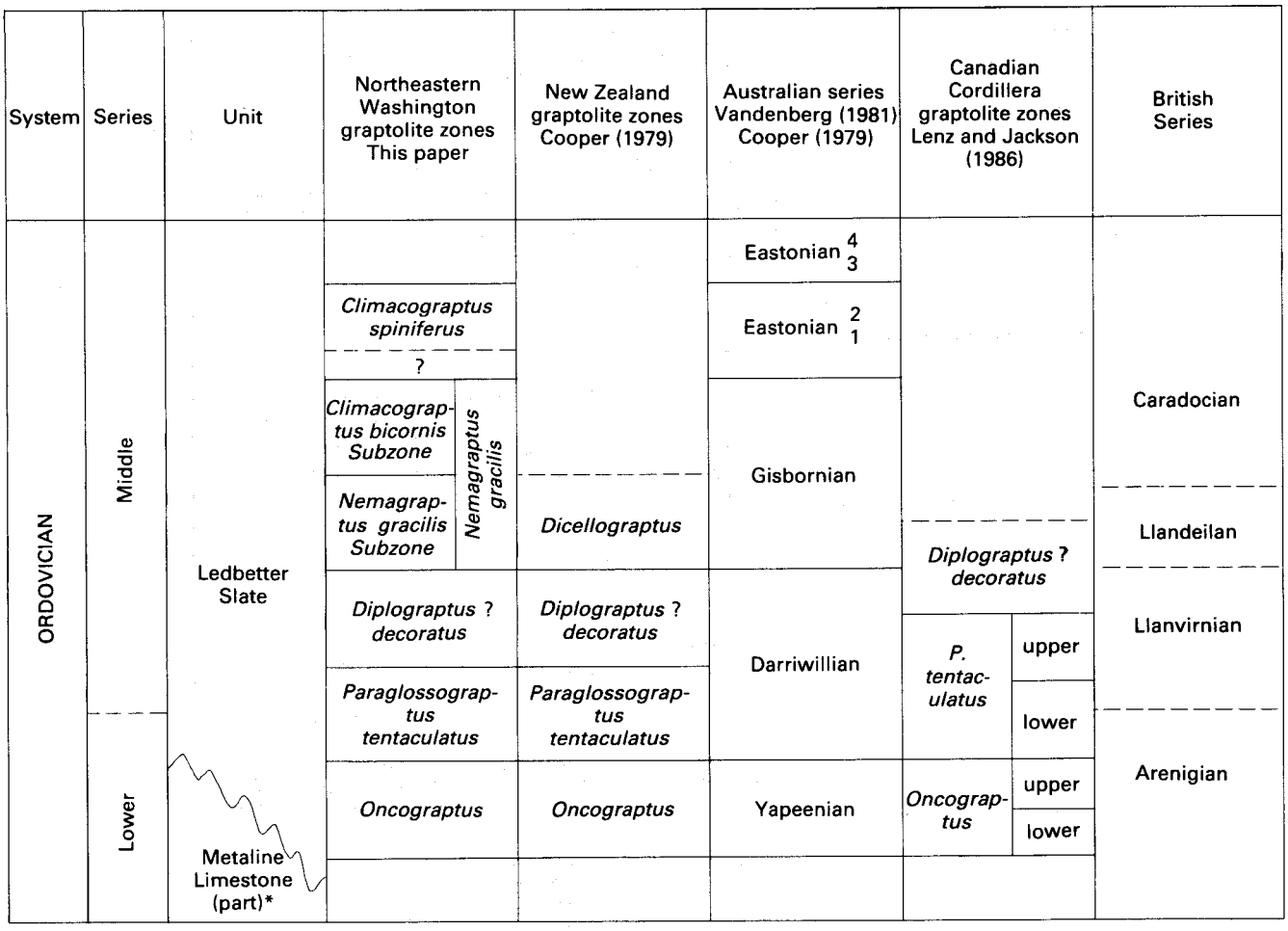

* Overall unit age is at least Middle Cambrian to Middle Ordovician.

Figure 3. Graptolite zones in the Ledbetter Slate and their correlations (from Carter, 1988b).

Devonian

Devonian rocks that will be examined on this field trip occur in two widely separated parts of this region. At Limestone Hill (Stop 5), limestone-pebble conglomerate and succeeding platform carbonates apparently overlie the Silurian clastic strata to the south. The conglomerate is probably mid-Givetian (late Middle Devonian) in age, on the basis of conodonts collected from the matrix and identified by Chatterton (Greenman and others, 1977). Clasts in the conglomerate contain early Devonian (Lohkovian and Emsian) and early Middle Devonian (Eifelian) conodonts. The massive limestones in the cliffs on the higher part of the hill have yielded several collections of Frasnian conodonts, ranging from the very earliest part of the stage to the *gigas* Zone near the top. Corals from this limestone were described by Sorauf (1972), although he ascribed a Middle Devonian age to them.

A second area of Devonian outcrop is in the Hunters quadrangle, about 4 mi east of the town of Hunters (Stop 20). Limestone crops out on the north side of a county road, just across from the Greenwood Cemetery. These beds have yielded late Late Devonian (Famennian) fossils. Brachiopods, identified by Dutro, include *Thiemella*? sp., *Schizophoria* cf. *S. australis* Kindle, *Uchtospirifer*? cf. *U. kindlei* (Stainbrook), and *Tylothyris*? cf. *T. raymondi* (Haynes).

Conodonts from this same locality were identified by Anita Harris (USGS, written commun., 1976, 1978), who assigned an age range that covers the upper two-thirds of the Famennian. The brachiopods suggest a mid-Famennian age, like that of the Trident Member of the Three Forks Formation in western Montana and the upper Palliser Formation of Alberta and British Columbia.

Conodonts of early Famennian age were identified by Anita Harris (written commun., 1988) from an outcrop east of Valley and about a mile east of U.S. Highway 395, in sec. 18, T. 31 N., R. 41 E. This is apparently the same area from which C. W. Merriam (USGS, written commun., 1965) identified Late Devonian brachiopods. From samples taken about a mile southwest of this last locality, Merriam also identified Early Devonian (Lohkovian)

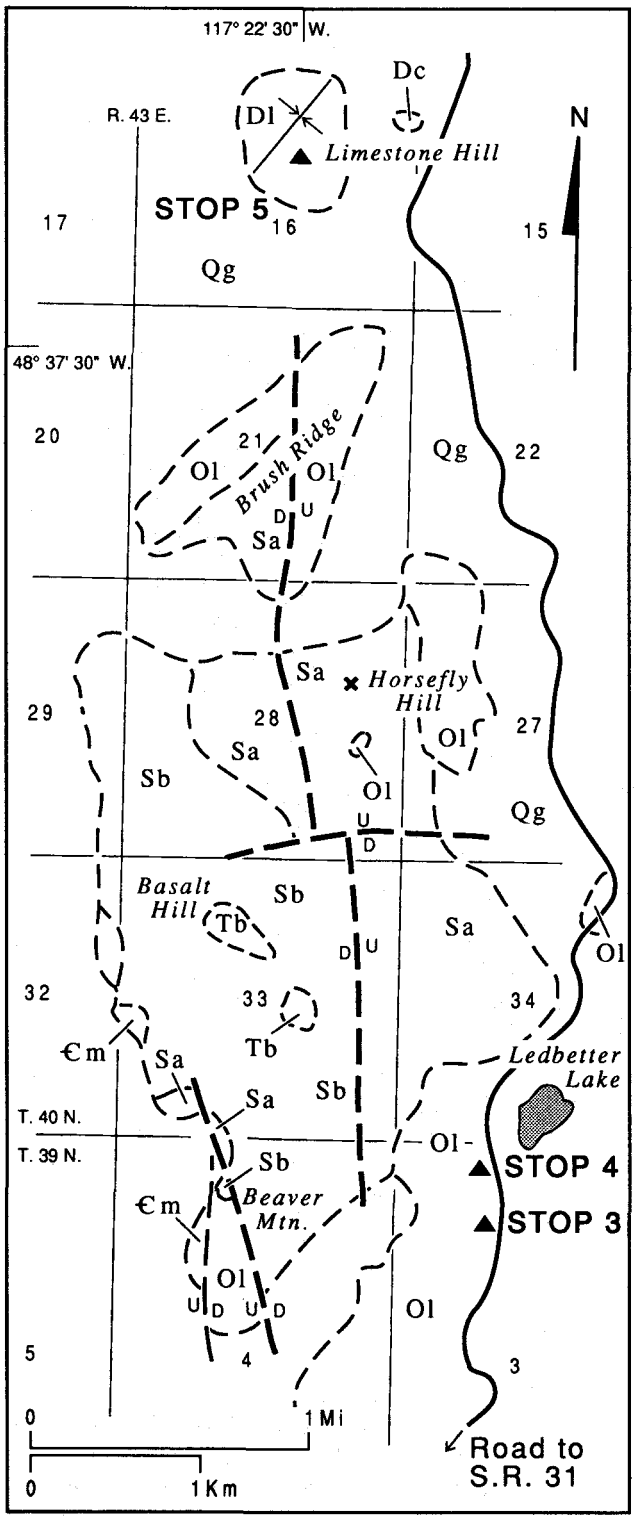

Figure 4. Geology of the Limestone Hill-Beaver Mountain area (modified from Greenman and others, 1977). Qg, glacial deposits; Tb, Tertiary basalt; Sb, unnamed upper Silurian; Sa, unnamed lower Silurian unit; Ol, Ledbetter Slate, €m, Metaline Limestone; long dashed lines, normal faults; short dashed lines, outcrop boundaries or formation boundaries.

brachiopods and corals, including *Syringaxon* sp., *Pleurodictyum* sp., ?*Trematospira* sp., *Levenea* cf. *L. carinata* (Hall), and *Leptocoelia* sp. This is of great interest because it suggests a carbonate source in the region for the clasts in the Middle Devonian conglomerate of the Limestone Hill area.

Carboniferous

The presence of rocks of early Carboniferous age can be demonstrated only in the vicinity of Springdale. Megafossils and conodonts (Bruce Wardlaw, USGS, written commun., 1985) from the most prominent outcrops on Limekiln Hill about a mile north of Springdale (Stop 17) indicate early and middle Mississippian ages, probably no younger than early Meramecian. Conodonts of a similar age range have been collected from scattered outcrops about 3 1/2 mi southwest of Springdale (Stops 18 and 19), although one conodont sample suggested the presence of rocks as young as early Morrowan (earliest Pennsylvanian) (Anita Harris, USGS, written commun., 1987). Both megafossils (brachiopods and corals) and conodonts from the Limekiln Hill area are similar to fossils from the Lodgepole Limestone of western Montana.

East of Kettle Falls, an entirely different sequence of strata of presumed Carboniferous age is faulted eastward against the early Paleozoic rocks. This is a thick, predominantly clastic, wedge of graywacke, conglomerate and sandstone and finer grained rocks. No fossils have been found in this sequence, but it is assumed to be Carboniferous on the basis of its stratigraphic position (Mills, 1985). Late Devonian conodonts have been reported by Laskowski (1982) from barite-bearing black shales associated with these coarser rocks near the Uribe mine in the NE1/4 sec. 5, T. 37 N., R. 39 E., but the stratigraphic significance of these shales has yet to be documented.

Permian

In the Kettle Falls area (Fig. 5), the Permian sequence consists of great thicknesses of argillite, siltstone, and graywacke that include limestone biohermal banks (Stop 10). Both the clastic rocks and the biohermal banks are fossiliferous and contain middle Permian assemblages. The massive, poorly bedded, biohermal banks contain fusulinids, echinodermal debris, bryozoans, brachiopods, and corals (Senter and others, 1973). Fusulinids described by Mills and Davis (1962) include *Parafusulina antimonioensis* Dunbar, *Pseudofusulinella stevensi* Mills and Davis, and *Schwagerina missionensis* Mills and Davis. Brachiopods and mollusks from the clastic strata include *Chonetes* sp., *Yakovlevia* sp. (originally listed as *Muirwoodia*), *Anidanthus minor* Cooper, *Rhynchopora* cf. *R. taylori* Girty, *Eopleurophorus*? *tropidophorus* (Meek), *Pleurotomaria euglyphea* Girty, *Euphemites urei* (Fleming), and *Plagioglypta* sp. The brachiopods were identified by G. A. Cooper (Smithsonian Institution, written commun., 1958), and the mol-

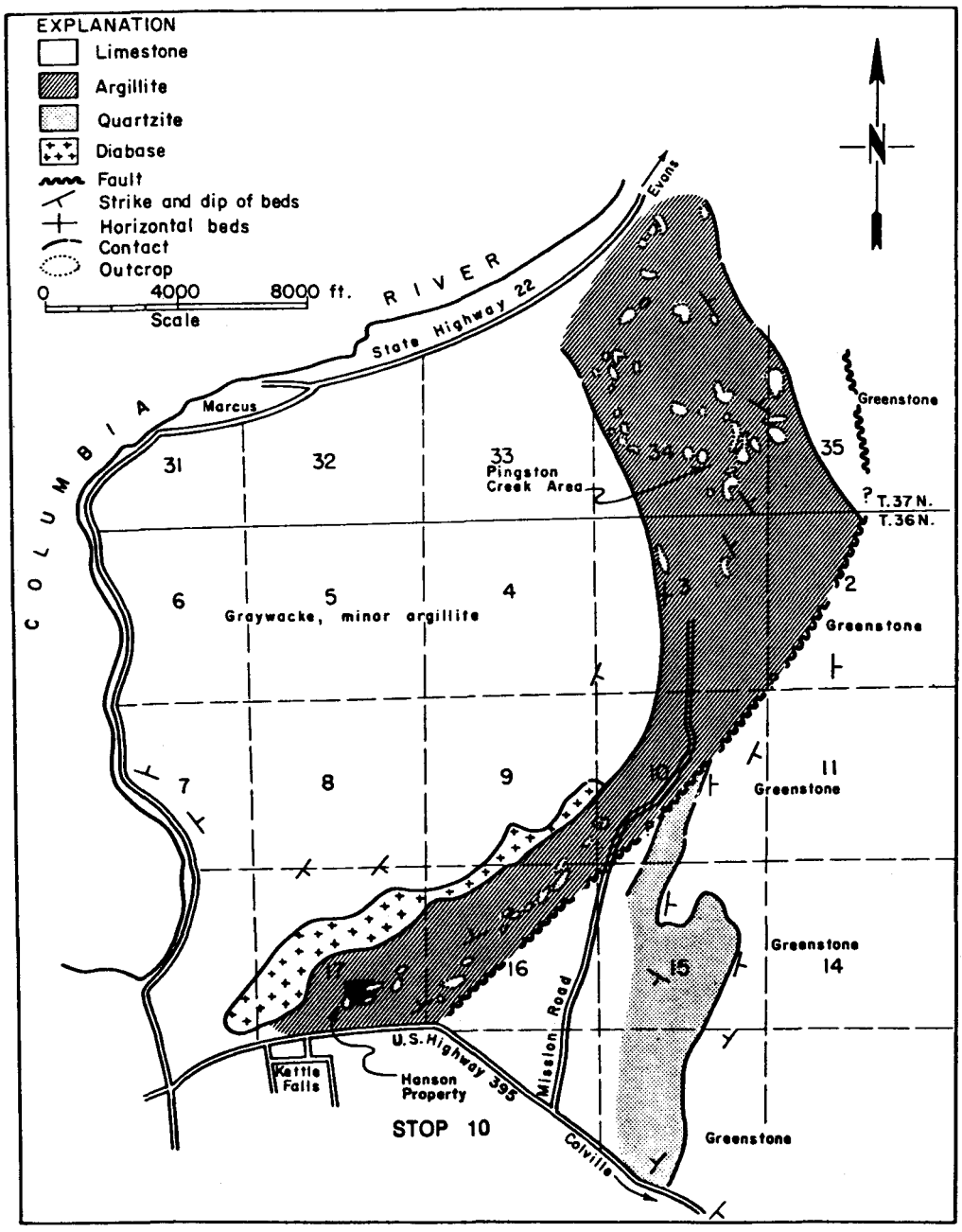

Figure 5. Sketch map of Kettle Falls area (modified from Mills, 1962).

lusks were studied by J. S. Dixon (unpub. Bachelor of Arts thesis, State College of Washington, 1958). All the fossils point to an age range of late Leonardian through Wordian (middle Permian).

Permian fusulinids were also collected by the authors from a limestone lens in the Permian argillite sequence west of the Columbia River, about a mile north of Snag Cove campground (Stop 12). These fossils were studied by R. C. Douglass (USGS, written commun., 1987), who reported that they are most like *Pseudofusulinella montis* (Thompson and Wheeler) of late Wolfcampian age. It is likely that much of the Lower and lower Upper Permian is represented in the clastic sequence in the northwestern part of the region of this field trip.

Triassic

To the west of the Permian clastic belt, a coarser clastic sequence contains Early Triassic fossils. These strata differ from those of the Permian in that they contain more siltstone and graywacke and also include massive greenstone bodies. Although there is no evidence of depositional interruption between the Permian and the Triassic, there are no Late Permian fossils to demonstrate continuity. The limestone pods in the Triassic tend to be more micritic and thin bedded than the Permian limestone bodies. Early Triassic ammonoids were described from the area west of the Columbia River, above the Permian argillite and about 1.5 mi WNW of the Snag Cove

campground (Kuenzi, 1965). We will examine an outcrop of this possible Triassic limestone about one-half mile south of the campground (Stop 11).

BIOGEOGRAPHIC AND TECTONIC SPECULATIONS

During the Paleozoic, northeastern Washington lay at the western edge of the North American platform. Some of the depositional settings were miogeoclinal, as during the Middle Cambrian and Devonian-Mississippian; at other times they were eugeoclinal, and sediments were deposited as proximal slope beds or distal basinal shales and argillites (during the Ordovician and Permian, particularly). The faunas associated with the miogeoclinal beds show close relations with correlative faunas to the east in Montana and Alberta. However, the fossils of the eugeoclinal strata are more cosmopolitan and indicate extra-North American affinities. The Ordovician and Silurian graptolite assemblages, for example, can be best correlated with those of New Zealand. This is not surprising, as it is also true of related graptolite faunas in west-central Idaho, British Columbia, Yukon, and Alaska. This is also the case for the Permian faunas, especially the fusulinids, which are not closely related to the Idaho, Nevada, and Utah miogeoclinal assemblages. Closer correlations are with the Permian of the eastern Klamath Mountains, central Oregon, and non-Tethyan parts of the Cache Creek Group of central British Columbia.

The belt of undated clastic rocks, presumably mostly Upper Devonian and Carboniferous, that lies to the east of the Permian rocks of the Kettle Falls area, is in fault contact both with the Permian and with the lower Paleozoic strata to the east. The authors have traced the latter bounding fault northward from the Hunters-Fruitland area to the vicinity of Marble on the Columbia River (Fig. 6). This fault, first recognized as a through-going feature by Snook and others (1981), appears to be offset to the east in the lower Colville River valley by a Tertiary high-angle fault.

The Permian and Triassic belts are, in turn, juxtaposed by eastward-directed thrusting against the earlier Paleozoic sequences, particularly the undated clastic belt east of Kettle Falls (Stop 9). The total amount of shortening on all these faults is speculative, but we estimate that it must have been at least a few hundred miles. The lithologies and great thickness of the Permian (at least 4,000 ft, according to Mills and Davis, 1962) suggests that these were distal deposits in a basin between the platform edge and a volcanic archipelago that may have been the origin of some of the late Paleozoic terranes that now are preserved as tectonic fragments in western North America. The Permian biohermal banks could have been deposited as fringing banks near some of those islands.

The Lower Triassic sequence suggests a similar basinal depositional setting, but there is no evidence that the Triassic limestones were shallow-water deposits.

ACKNOWLEDGMENTS

We are grateful to many people for their help and encouragement during our studies in northeastern Washington. Bob Yates introduced Dutro to the mysteries of early Paleozoic rocks in the Deep Creek area during the mid-1950s. John Bush discussed the Cambrian of the region with us and gave freely of his and his students' unpublished information. Eric Schuster introduced us to the geology of the Clugston Creek area and spent several days in the field with us, providing orientation to the general regional geology. A. R. Palmer identified many Cambrian fossils, re-evaluated some of the older collections from the Addy and the Metaline, and was a delightful field partner during the 1950s.

Anita Harris identified many of the conodont collections referred to in this guide and evaluated published conodont data, revising the ages and correlations in several instances. Claire Carter eagerly accepted the challenge of recollecting, restudying, and describing the Ordovician-Silurian graptolites from the Ledbetter and associated rocks. John Repetski and Bruce Wardlaw identified Cambrian-Ordovician and Carboniferous-Triassic conodonts, respectively. Ray Douglass identified Permian fusulinids and discussed their regional significance with us. Mike Taylor identified the early Ordovician trilobites from near the base of the Ledbetter.

John Pojeta, Jr., U.S. Geological Survey, and R. E. Grant, Smithsonian Institution, technical reviewers of this manuscript, provided helpful suggestions, as did Eric Schuster of the Washington Division of Geology and Earth Resources. The comments of all three are greatly appreciated.

Last, but not least, our work has been greatly facilitated by Nancy Joseph, Stephanie Zurenko Waggoner, and Keith Stoffel of the Spokane office of the Washington Division of Geology and Earth Resources.

To all these people, we express our deep appreciation.

SELECTED REFERENCES

Bush, J. H.; Fischer, H. J., 1981, Stratigraphic and depositional summary for Middle and Upper Cambrian strata in northeastern Washington, northern Idaho and northwestern Montana. *In* Taylor, M. E., editor, Short Papers for the 2nd International Symposium on the Cambrian System, 1981: U.S. Geological Survey Open-File Report 81-743, p. 42-45.

Campbell, A. B.; Raup, O. B., 1964, Preliminary geologic map of the Hunters quadrangle, Stevens and Ferry counties, Washington: U.S. Geological Survey Mineral Investigations Field Studies Map MF-276, 1 sheet, scale 1:48,000.

Carter, Claire, 1988a, Ordovician-Silurian graptolites from the Ledbetter Slate, northeastern Washington: U.S. Geological Survey Bulletin 1860, p. B1-B29.

Carter, Claire, 1988b, Middle Ordovician graptolites from near the contact between the Ledbetter Slate and the Metaline Limestone in the Pend Oreille Mine, northeastern Washington: U.S. Geological Survey Bulletin 1860, p. A1-A23.

Cooper, R. A., 1979, Ordovician geology and graptolite faunas of the Aorangi Mine area, northwest Nelson, New Zealand: New Zealand Geological Survey Paleontological Bulletin 47, 127 p.

Dings, M. G.; Whitebread, D. H., 1965, Geology and ore deposits of the Metaline zinc-lead district, Pend Oreille County, Washington: U. S. Geological Survey Professional Paper 489, 109 p.

Greenman, Celia; Chatterton, B. D. E.; Boucot, A. J.; Berry, W. B. N., 1977, Coarse Silurian(?) and Devonian detrital rocks in northeastern Washington–Evidence of Silurian (?) and Devonian tectonic activity. *In* Stewart, J. H.; Stevens C. H.; Fritsche, A. E., editors, Paleozoic paleogeography of the western United States: Pacific Section, Society Economic Paleontologists and Mineralogists, Pacific Coast Paleogeography Symposium 1, p. 467-479.

Greggs, R. G., 1959, Archaeocyatha from the Colville and Salmo areas of Washington and British Columbia: Journal of Paleontology, v. 33, no. 1, p. 63-75.

Kuenzi, W. D., 1965, Early Triassic (Scythian) ammonoids from northeastern Washington: Journal of Paleontology, v. 39, no. 3, p. 365-378.

Laskowski, E. R., 1982, Geology of the black shale belt of the Bruce Creek area, Stevens County, Washington: Washington State University Master of Science thesis, 113 p.

Lenz, A. C.; Jackson, D. E., 1986, Arenig and Llanvirn graptolite biostratigraphy, Canadian Cordillera. *In* Hughes, C. P.; Rickards, R. B.; Chapman, A. J., editors, 1986, Palaeoecology and biostratigraphy of graptolites: Geological Society (London) Special Publications 20, p. 27-45.

Miller, F. K., 1969, Preliminary geologic map of the Loon Lake quadrangle, Stevens and Spokane Counties, Washington: Washington Division of Mines and Geology Geologic Map GM-6, 7 p., 1 pl., scale 1:62,500.

Mills, J. W., 1962, High-calcium limestones of eastern Washington: Washington Division of Mines and Geology Bulletin 48, 268 p.

Mills, J. W., 1977, Zinc and lead ore deposits in carbonate rocks, Stevens and Ferry Counties, Washington: Washington Division of Geology and Earth Resources Bulletin 78, 171 p.

Mills, J. W., 1985, Geologic maps of the Marcus and Kettle Falls quadrangles, Stevens and Ferry Counties, Washington: Washington Division of Geology and Earth Resources Geologic Map GM-32, 18 p., 2 sheets, scale 1:24,000.

Mills, J. W.; Davis, J. R., 1962, Permian fossils of the Kettle Falls area, Stevens County, Washington: Cushman Foundation for Foraminiferal Research Contributions, v. 13, pt. 2, no. 241, p. 41-51.

Okulitch, V. J., 1951, A Lower Cambrian fossil locality near Addy, Washington: Journal of Paleontology, v. 25, no. 3, p. 405-407.

Okulitch, V. J.; Greggs, R. G., 1958, Archaeocyathid localities in Washington, British Columbia, and the Yukon Territory: Journal of Paleontology, v. 32, no. 3, p. 617-623.

Park, C. F., Jr.; Cannon, R. S., Jr., 1943, Geology and ore deposits of the Metaline quadrangle, Washington: U.S. Geological Survey Professional Paper 202, 81 p.

Schuster, J. E., 1976, Geology of the Clugston Creek area, Stevens County, Washington: Washington Division of Geology and Earth Resources Open File Report 76-8, 26 p.

Senter, L. E.; Kennedy, D. B.; Gilmour, E. H., 1973, Permian carbonate microfacies of northeastern Washington [abstract]: Northwest Scientific Association, 46th Anual Meeting, Abstracts of the Proceedings, p. 33.

Snook, J. R.; Lucas, H. E.; Abrams, M. J., 1981, A cross section of a Nevada-style thrust in northeast Washington: Washington Division of Geology and Earth Resources Report of Investigations 25, 9 p.

Sorauf, J. E., 1972, Middle Devonian coral faunas (Rugosa) from Washington and Oregon: Journal of Paleontology, v. 46, no. 3, p. 426-439.

VandenBerg, A. H. M., 1981, Victorian stages and graptolite zones. *In* Webby, B. D., editor, The Ordovician System in Australia, New Zealand, and Antarctica; Correlation chart and explanatory notes: International Union of Geological Sciences Publishing Co., p. 2-7.

Weaver, C. E., 1920, The mineral resources of Stevens County: Washington Geological Survey Bulletin 20, 350 p.

Yates, R. G., 1964, Geologic map and sections of the Deep Creek area, Stevens and Pend Oreille counties, Washington: U.S. Geological Survey Miscellaneous Geologic Investigations Map I-412, 1 sheet, scale 1:31,680.

Yates, R. G., 1971, Geologic map of the Northport quadrangle, Washington: U.S. Geological Survey Miscellaneous Geologic Investigations Map I-603, 1 sheet, scale 1:31,680.

Yates, R. G.; Robertson, J. F., 1958, Preliminary geologic map of the Leadpoint quadrangle, Stevens County, Washington: U. S. Geological Survey Mineral Investigations Field Studies Map MF-137, 1 sheet, scale 1:24,000.

Road Log

All mileages are calculated from the corner of Main and Hawthorne Streets, Colville, Washington. Cumulative mileage is given on the left; interval distances are in parentheses. The route is shown in Figure 6.

Day 1: Colville Loop Traverse

0.0 *Set odometer.* Drive north on Main Street (U.S. Highway 395).

0.8 (0.8) Intersection of U.S. 395 and Washington State Route (SR) 20; turn right on SR 20; drive east toward Tiger.

16.0 (15.2) Crystal Falls (scenic stop).

37.5 (21.5) Tiger. Intersection of SR 20 and SR 31. Turn left (north) on SR 31.

38.5 (1.0) Railroad crossing.

41.6 (3.1) Ione town center.

42.5 (0.9) Railroad crossing.

44.35 (1.85) Metaline Limestone in a roadcut on the left (west) and view of Metaline across the valley to the north.

44.6 (0.25) Turn right to Box Canyon Scenic View; optional stop.

44.7 (0.1) Scenic view of Box Canyon Dam and cliffs of Metaline Limestone to the east; higher ridges beyond are Gypsy (Addy) Quartzite and Precambrian rocks.

44.8 (0.1) Return to SR 31 and turn right (north).

45.3 (0.5) Eocene Tiger Formation gravels in two roadcuts on the left (west).

45.7 to 45.8 (0.4) Gravels of the Tiger Formation are exposed in the large roadcut on the left (west); gravels dip about 40 degrees south.

46.1 (0.3) Ledbetter Slate in the roadcut on the left (west). It is isoclinally folded and faulted; fold axes strike north (parallel to highway).

47.9 (1.8) **STOP 1. Ledbetter Slate.**

Park on the right.

Ledbetter Slate is exposed in the large roadcut on the left (west); it is isoclinally folded and faulted and displays vertical axial planes. This is a typical Ledbetter outcrop in which tectonism obscures original textures and fossils.

49.2 to 49.4 (1.3) Pleistocene sand and silt in outcrops on the left (west) side of the highway.

49.7 to 50.0 (0.5) Metaline Limestone in roadcuts on the left (west).

50.6 (0.6) Metaline town center; rest stop at the town park.

51.2 (0.6) Intersection of SR 31 and the road to Gardner Cave (Crawford State Park); turn sharp left.

52.1 (0.9) **STOP 2. Metaline Limestone.**

Park on the right.

Metaline Limestone crops out at the south end of the roadcut on the left (west); it is nearly flat lying and is overlain by Ledbetter Slate dipping north about 20 degrees. The contact is probably a fault. This is typical of the Metaline and its relations with the Ledbetter. We will contrast the two units here.

54.9 (2.8) Metaline Limestone in a small roadcut on the left (west); Ledbetter Slate in roadcuts on the left for the next 2 mi.

57.1 (2.2) **STOP 3. Ledbetter Slate type area.**

The roadcut on left (west) and the next three roadcuts are, in essence, the type area for the Ledbetter. Graptolites of the *Dicranograptus clingani* Zone are present in all these outcrops. The roadcut is opposite the south end of Ledbetter Lake, downhill to the northeast.

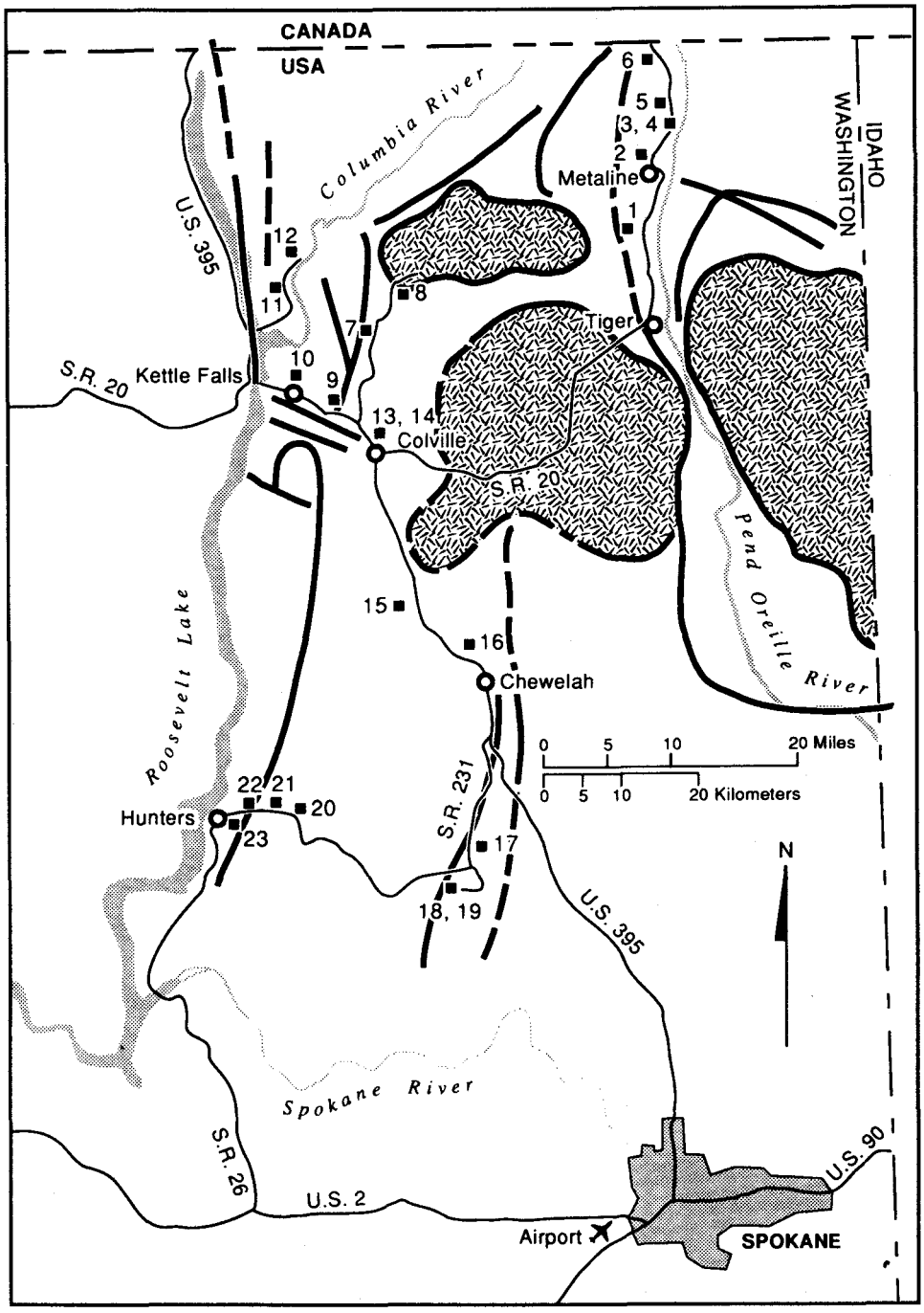

Figure 6. Simplified tectonic map of northeastern Washington; major faults approximately located. Plutons east of Colville (patterned areas) are of Late Cretaceous age. Numbers show approximate locations of field trip stops.

57.3 (0.2) **STOP 4. Graptolite-bearing Ledbetter Slate.**

Ledbetter Slate in the roadcut on the left; *D. clingani* Zone graptolites can be found here in abundance.

57.4 (0.1) U.S. Forest Service Road (FSR) 304 intersection on the left.

57.5 (0.1) Ledbetter Slate in the large roadcut on the left (west); beds dip about 40 degrees west. Good bedding features are shown, but graptolite collecting is poor.

59.0 (1.5) Metaline Limestone in the low roadcuts on the right, opposite a small lake.

59.7 (0.7) Metaline Limestone in a roadcut and low cliff on the right (east). This exposure is near the top of the Metaline, which has much brecciated black chert here.

60.8 (1.1) **STOP 5. Limestone Hill Devonian carbonate section.**

Intersection with FSR 346. Turn left on forest road and drive about 0.2 mi to the end of the pavement; park.

Cross a small creek and walk on an old road about 0.3 mi to a meadow; then climb north on the south flank of Limestone Hill to Upper Devonian limestone exposures; examine coral-bearing Frasnian reefoid bodies.

Return to the vehicles and return to the main road.

61.1 (0.3) Turn left (north) on the main road.

61.9 (0.8) Intersection with the road to Boundary Dam. Continue north on the road to Crawford State Park.

63.9 (2.0) **STOP 6. Crawford State Park;** cave in Metaline Limestone. This is our lunch stop. There may be time for a tour of Gardner Cave.

Return to SR 31.

76.3 (12.4) Turn right (south) on SR 31 and retrace the route to SR 20. Then drive west to Colville.

126.9 (50.6) Intersection of SR 20 and U.S. 395 in Colville; turn right (north) and follow U.S. 395 toward Kettle Falls.

129.0 (2.1) Intersection with Williams Lake Road; turn right (north).

134.9 (5.9) Intersection with Clugston Creek Road; turn right (east).

135.1 (0.2) Stay left (north) on the paved road.

138.8 (3.7) Ledbetter Slate in the roadcut on the left (west); Metaline Limestone in the hills to the right (east).

139.2 (0.4) Intersection; stay left on the paved road.

140.2 (1.0) **STOP 7. Tectonized Ledbetter Slate.**

Ledbetter Slate in the roadcut on the left (west). The slate is highly contorted; this roadcut is east of a major fault zone.

Continue north on the paved road.

142.1 (1.9) **STOP 8. Faulted contact between Ledbetter Slate and Metaline Limestone.**

The contact is in the main roadcut and quarry on the right side of the road (east), and Ledbetter Slate crops out at the south end of the roadcut. Abundant graptolites in the Ledbetter; Early or early Middle Ordovician conodonts have been collected from the top of and 100 ft below the top of the Metaline Limestone here.

Turn around and return to U.S. 395.

149.5 (7.4) Intersection of Williams Lake Road and U.S. 395; turn right (west).

151.9 (2.4) **STOP 9. Carboniferous (?) graywacke and conglomerate.**

Note quarry on the north side of the highway; turn onto the quarry road on the right and park.

Devonian?/Carboniferous? chert-pebble conglomerate and graywacke on Rattlesnake Mountain. These clastic rocks are thrust eastward against the Metaline/Ledbetter of the Clugston Creek belt; the fault trends northward. Contrast these lithologies with the Lower Paleozoic sequence seen as Stops 1 through 8.

Continue west on U.S. 395.

156.1 (4.2) Main intersection in Kettle Falls (Exxon station on the north side of the highway); turn right (north) toward the quarry cut on hillside.

156.3 (0.2) Pavement ends. Continue on primitive road uphill to the right.

156.4 (0.1) Quarry on the left is in Permian argillite and greenstone. Pleistocene sand and gravel are present at the top of the cut.

156.7 (0.3) **STOP 10. Permian biohermal banks.**

Park and examine the richly fossiliferous limestone outcrops about 150 ft south of the gravel road. Corals, bryozoans, brachiopods, and fusulinids are abundant in this biohermal bank.

Turn around and return to U.S. 395.

157.3 (0.6) Intersection with U.S. 395; turn right (west).

160.7 (3.4) Columbia River bridge.

161.0 (0.3) SR 20 and U.S. 395 divide; stay right on U.S. 395.

164.3 (3.3) Intersection; stay right (north) and cross Kamloops bridge and island; Kamloops campground on the left.

164.8 (0.5) Railroad crossing.

165.0 (0.2) Intersection; stay right, on the paved road; drive across terrace gravels.

170.9 (5.9) **STOP 11. Triassic (?) limestone outcrop.**

Park on the left side of the road.

The limestone crops out on the left, just south of Snag Cove campground. No fossils have yet been found here. The lithology is like that of Triassic limestones to the west that have yielded Lower Triassic ammonoids.

171.2 (0.3) Snag Cove campground.

172.5 (1.3) **STOP 12. Permian limestone.**

The outcrop is on the left (west).

Graywacke and argillite surround the limestone bodies; mafic rock float is also present. The Permian fusulinids identified by R. C. Douglass came from the limestone directly above this roadcut at 2,000 ft elevation.

Turn around and return to Colville.

175.7 (3.2) Permian clastic rocks in the roadcut on the right (west).

180.7 (5.0) Intersection with U.S. 395; turn left.

184.0 (3.3) Intersection: SR 20 joins U.S. 395 from the west. Turn left (east) and cross the Columbia River.

187.7 (3.7) Center of Kettle Falls. Drive east to Colville.

196.6 (8.9) Turn right (south) at the blinker on Main Street in Colville.

197.5 (0.9) Panorama Motel.

End of Day 1 trip.

Day 2 : Colville to Hunters Traverse.

0.0 *Reset odometer*. Drive north on Main Street through Colville.

0.7 (0.7) Intersection with SR 20. Continue straight ahead.

0.9 (0.2) Turn right (east) on 6th Street.

1.0 (0.1) **STOP 13. Lower Cambrian Reeves Limestone.**

Archaeocyathid-bearing limestone (Reeves Limestone) crops out on the northwest corner of 6th and Oak Streets (Fig. 7). Leave hammers in the vehicles—no collecting here.

Drive north on Oak Street.

1.05 (0.05) Turn left on 7th Street.

1.15 (0.1) Turn right on Main Street; drive north.

1.4 (0.25) Turn left on 11th Street and immediately right on Wynne Street.

1.6 (0.2) Pavement ends; continue uphill on the gravel road.

1.9 (0.3) Maitlen Phyllite in the bank on the right (east).

2.3 (0.4) **STOP 14. Archaeocyathid collecting locality (Reeves Limestone).**

Park on the right.

Archaeocyathid-bearing limestone crops out on the hillslope to the left (west) about 100 ft from the road. Look for thin limestone beds just beyond the brow of the hill.

Turn around; return to Colville on Main Street.

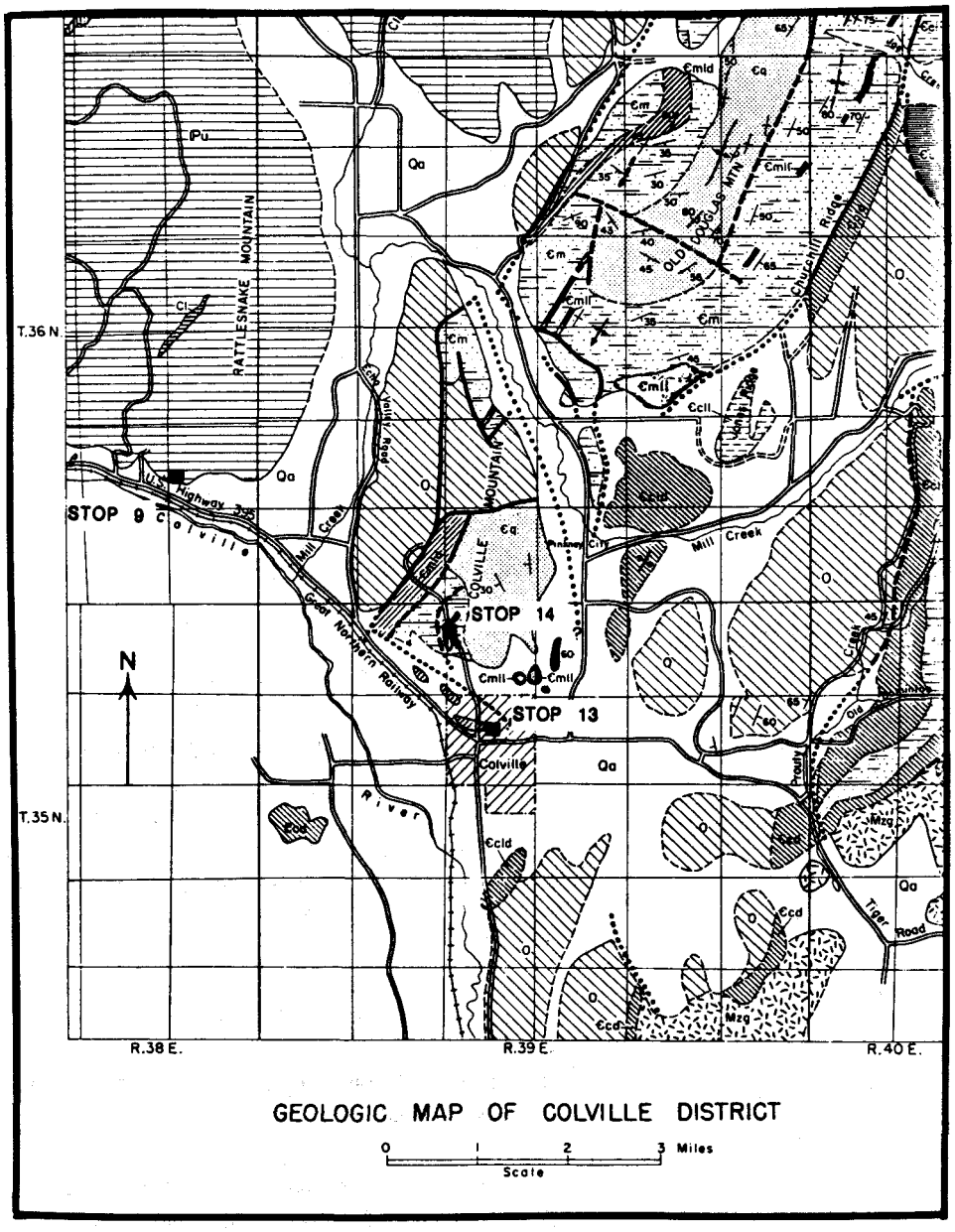

Figure 7. Geologic map of the Colville area (modified from Mills, 1962). Qa, glacial deposits and alluvium; Mzg, Mesozoic granite; Pu, undifferentiated Upper Paleozoic rocks; Cl, Carboniferous limestone; O, Ledbetter Slate; Ꞓc, Cambrian upper carbonate unit–mostly Metaline Limestone (Ꞓclu, upper limestone; Ꞓcla, limestone and argillite; Ꞓcll, lower limestone; Ꞓcld, limestone and dolomite); Ꞓm, middle unit–mostly Maitlen Phyllite (Ꞓmlu, upper limestone; Ꞓmld, limestone and dolomite; Ꞓmll, lower limestone with archeocyathids–Reeves Limestone Member); Ꞓq, Addy Quartzite.

3.6 (1.3) Turn right on 6th Street to Wynne Street and left on Wynne to U.S. 395. Continue south on Main Street.

4.6 (1.0) Corner of Main and Hawthorne Streets. Continue south on U.S. 395.

17.6 (13.0) Addy. Turn right (west) into town.

17.7 (0.1) Turn left.

17.9 (0.2) Stop sign. Turn right and cross the railroad.

18.0 (0.1) Cross the bridge over the creek. Drive south (left) around the end of the ridge.

18.4 (0.4) **STOP 15. Addy Quartzite type locality.**

Addy Quartzite crops out on the ridge to the right, north of the road beyond the Allied Chemical fence. Examine this outcrop for Early Cambrian fossils (*Nevadella* and brachiopods). *Use care*, as we are examining this outcrop with company permission. NOTE: For persons making the trip by themselves, permission must be obtained from the company before entering the area beyond the fence.

Turn around and return to Addy and U.S. 395.

18.9 (0.5) Turn right at the gas station in Addy.

19.2 (0.3) Intersection with U.S. 395; turn right (south).

24.4 (5.2) **STOP 16. Addy Quartzite sedimentary features.**

Cliffs on the left (east) are cut in the Addy. Examine the lithology, bedding, cross-bedding, and glacial surfaces by climbing the cliffs for about 200 ft.

Continue south on U.S. 395.

25.5 (1.1) Rest stop at Chewelah town park.

27.7 (2.2) Traffic light in the center of Chewelah. Continue south on U.S. 395.

32.5 (4.8) Intersection of U.S. 395 and SR 231. Turn right (west) toward Valley.

34.0 (1.5) Cliffs of Addy Quartzite on the left (east).

35.1 (1.1) Valley town limit.

36.0 (0.9) Lane Mountain silica plant on the right (west).

36.7 (0.7) Junction with SR 232; continue straight on SR 231.

36.9 (0.2) Railroad crossing.

44.2 (7.3) Intersection with the road to Hunters; continue straight ahead to Springdale.

44.9 (0.7) Springdale; turn left (north) on First Street.

45.05 (0.15) Turn left on Morton Avenue.

45.1 (0.05 Turn right on Second Street.

45.4 (0.3) Gravel road begins; continue north.

45.7 (0.3 **STOP 17. Mississippian limestone section.**

Turn right at this point and park on the dirt road.

This is the Limekiln Hill section of Mississippian limestone; type section of an unnamed formation. Climb the hill through the section (northeasterly) to examine the carbonate rock types and to collect corals, brachiopods, and conodont samples.

Turn around and return to Springdale.

46.5 (0.8) Intersection with SR 231; turn left (east) and then right (south) at the next block; lunch stop.

46.55 (0.05) Railroad crossing.

47.1 (0.55) Turn right (east) on the paved road.

47.8 (0.7) Springdale Cemetery on the right (west); pavement ends.

49.75 (1.95) Bridge across Swamp Creek.

49.85 (0.1) **STOP 18. Mississippian conodont locality.**

Park on the left on an old quarry road.

Mississippian limestone is exposed in the roadcut on the right and in the quarry on the left. Compare these rock types with those seen at Stop 17.

Continue straight on the gravel road.

50.0 (0.15) Intersection with a gravel road; continue straight ahead.

50.5 (0.5) **STOP 19. Mississippian carbonate rocks.**

Roadcuts of Mississippian carbonates along the dirt road to the right (north) and in the low ridge to the west. These rocks have yielded conodonts.

Turn around and return to Springdale.

54.3 (3.8) Junction with SR 231; turn left (north).

54.9 (0.6) Springdale. Continue straight (west) on SR 231.

55.6 (0.7) Intersection. Turn left (south) on the road to Hunters.

73.6 (18.0) Intersection with Harvey Creek road. Metaline Limestone crops out on the northwest corner of the intersection. Continue straight ahead on the Hunters road.

74.9 (1.3) **STOP 20. Upper Devonian carbonates; Greenwood Cemetery.**

Park on the left.

Unnamed Upper Devonian limestone in the roadcut on the right (north) side of the road and in the low ridge to the north. Brachiopods and conodonts can be collected here.

75.2 (0.3) **STOP 21. Limestone turbidite and slate sequence.**

Walk through the roadcut on the right (north) side of the road.

The rocks here contain Early Ordovician conodonts; this sequence may be a facies of the Ledbetter Slate. Ordovician graptolites were collected along strike across the valley to the south.

75.7 (0.5) **STOP 22. Covada Group argillite.**

Outcrops of this unit are on both sides of the road in roadcuts. Siliceous argillite (mapped as Pzch unit, part of Covada Group, by Campbell and Raup, 1964) is blocky, cleaved, and lineated. A major fault is mapped between this outcrop and the one to the east (Stop 21). Contrast the metamorphic grade of these rock with that seen at Stops 20 and 21.

77.4 (1.7) **STOP 23. Faulted Covada Group.**

Large roadcuts on both sides of the road expose graywacke, quartzite, and black slate; these have steep dips (70 degrees to vertical), mostly westerly. The fault demonstrates movement from west to east on a major fault system; isoclinal folds are overturned to the east. This unit has also been mapped as part of the Covada Group (Campbell and Raup, 1964).

This is the last stop of the trip. Continue west.

78.9 (1.5) Stop sign at the intersection with SR 25, just east of Hunters. Turn left on SR 25 and return to Spokane via the road to the airport.

124.9 (46.0) Intersection, at Davenport, with U.S. 2. Turn left (east).

154.9 (30.0) Spokane Airport.

160.9 (6.0) Spokane Convention Center.

Tectonics and Mineralization in Southeastern British Columbia

Richard St J. Lambert, Trygve Höy, and Kathryn Andrew

Tectonics and Mineralization in Southeastern British Columbia

Tectonics of the Kootenay Arc

The Purcell Supergroup and the Sullivan Mine

The Rossland Group

Road log:

- Day 1 – Sullivan Mine and journey from Kimberley to Nelson via the Kootenay Lake ferry
- Day 2 – Nelson, Kaslo, New Denver, and Slocan
- Day 3 – Salmo, Trail, to the Canadian/U.S. border
- Appendix – Spokane to Cranbrook and from the Canadian border south to Spokane.

The following introductory descriptions and road log cover the majority of the major rock units in the southern Kootenay Arc and the Purcell Anticlinorium on the Canadian side of the international border. The geologic features to be seen on the excursion are described in the three introductory papers. Responsibility for the road logs is divided as follows:

Day 1 (Part 1A): Sullivan mine and route to Creston, T. Höy;

Day 1, the remainder (Part 1B) and

Day 2 (Part 2): R. St J. Lambert;

Day 3 (Part 3A): Rossland Group, T. Höy and K. Andrew; and

Day 3, the remainder (Part 3B): R. St J. Lambert.

The Appendix is a road log prepared by Lambert. Part 1 covers the portion of the excursion from Spokane to Cranbrook. Part 2 covers the portion of the excursion from the U.S./ Canada border back to Spokane. For those using this road log on a self-guided tour, a number of possible stops are indicated by an asterisk at the beginning of the appropriate text in both parts.

Suggested citations for an introductory article and a part of the road log.

Lambert, R. St J., 1989, Tectonics and mineralization in southeastern British Columbia–Tectonics of the Kootenay Arc. *In* Joseph, N. L., and others, editors, Geologic guidebook for Washington and adjacent areas: Washington Division of Geology and Earth Resources Information Circular 86, p. 45-54.

Höy, Trygve; Andrew, Kathryn, 1989, Tectonics and mineralization in southeastern British Columbia–Road log; Part 3A, Nelson to Salmo. *In* Joseph, N. L., and others, editors, Geologic guidebook for Washington and adjacent areas: Washington Division of Geology and Earth Resources Information Circular 86, p. 79-80.

Tectonics and Mineralization in Southeastern British Columbia: Tectonics of the Kootenay Arc

Richard St John Lambert
Department of Geology
University of Alberta
Edmonton, AB
T5G 2E6 Canada

INTRODUCTION

The Kootenay Arc is a region dominated by Paleozoic rocks and extends in a gentle curve from Clearwater in the north, near 120°W, 52°N, to the Columbia River at 118°W, 48° to 49°N in the south (Fig. 1). It separates the Purcell anticlinorium in the east, with which it shares the Upper Proterozoic Windermere Group, from the Mesozoic island arcs of Quesnellia to the west. However, the western boundary is complicated by high-grade metamorphism and repeated faulting, the extent and nature of which are only partly understood. The term Kootenay Arc predates plate tectonic and terrane tectonic theory, and it has not been found to be practicable to interpret the Arc in such terms. It is quite probable that more than one terrane occurs within it, and it is certain that the boundaries of the Arc do not coincide with those of its constituent terranes. Thus the Arc is a structure which has been superimposed on several distinct terranes. Because individual terranes are in the process of definition as a result of detailed studies, there are many unanswered questions about the nature of large-scale processes in the area. It is, nevertheless, one of the best-described areas of the Canadian Cordillera, being richly mineralized and highly accessible. This excursion is designed to permit examination of both the mineralization and the tectonic problems; a superb array of exposures and of geological phenomena is presented during its three days.

There are few overviews of the Kootenay Arc, and none is current with regard to terrane theory, or incorporates Lithoprobe or COCORP seismic reflection data, or fully integrates the new knowledge of the role of Tertiary extension. Thus we precede the road log with a brief review of available information, some of which is unpublished. The reader is referred specifically to the following sources for additional information:

- Fyles (1967) for a detailed study of the Ainsworth-Kaslo mining district and a 1:12,000-scale map;
- Höy and others (1981) for detailed accounts of the Sullivan deposit and mineralization in the more northerly areas;
- Read and Brown (1981) for a map and description of part of southeastern British Columbia, including the northern part of the Kootenay Arc;
- Monger and others (1982) for the definition of the term Quesnellia and the introduction of terrane nomenclature into the geology of the Canadian Cordillera;
- Archibald and others (1983, 1984) for information on regional metamorphism, uplift and cooling;
- Struik (1986) for the definition of the Selkirk and Cariboo terranes, which, together with Quesnellia, encompass most of the units of the Kootenay Arc;
- Carr and others (1987) and Parrish and others (1988) for the latest interpretation of the western boundary of the Kootenay Arc in the area of this excursion; and
- Cook and others (1988) for relevant Lithoprobe data.

GEOLOGIC DESCRIPTION

Stratigraphy

Stratigraphic studies in the area have long been hindered by lack of fossils, geographic separation of probable correlative units, and lack of communication across the international border.

Nevertheless, a fairly complete picture has emerged. It is acknowledged, though, that the picture presented here may change as a result of new mapping. The present

From: Joseph, N. L., and others, editors, 1989, Geologic guidebook for Washington and adjacent areas: Washington Division of Geology and Earth Resources Information Circular 86.

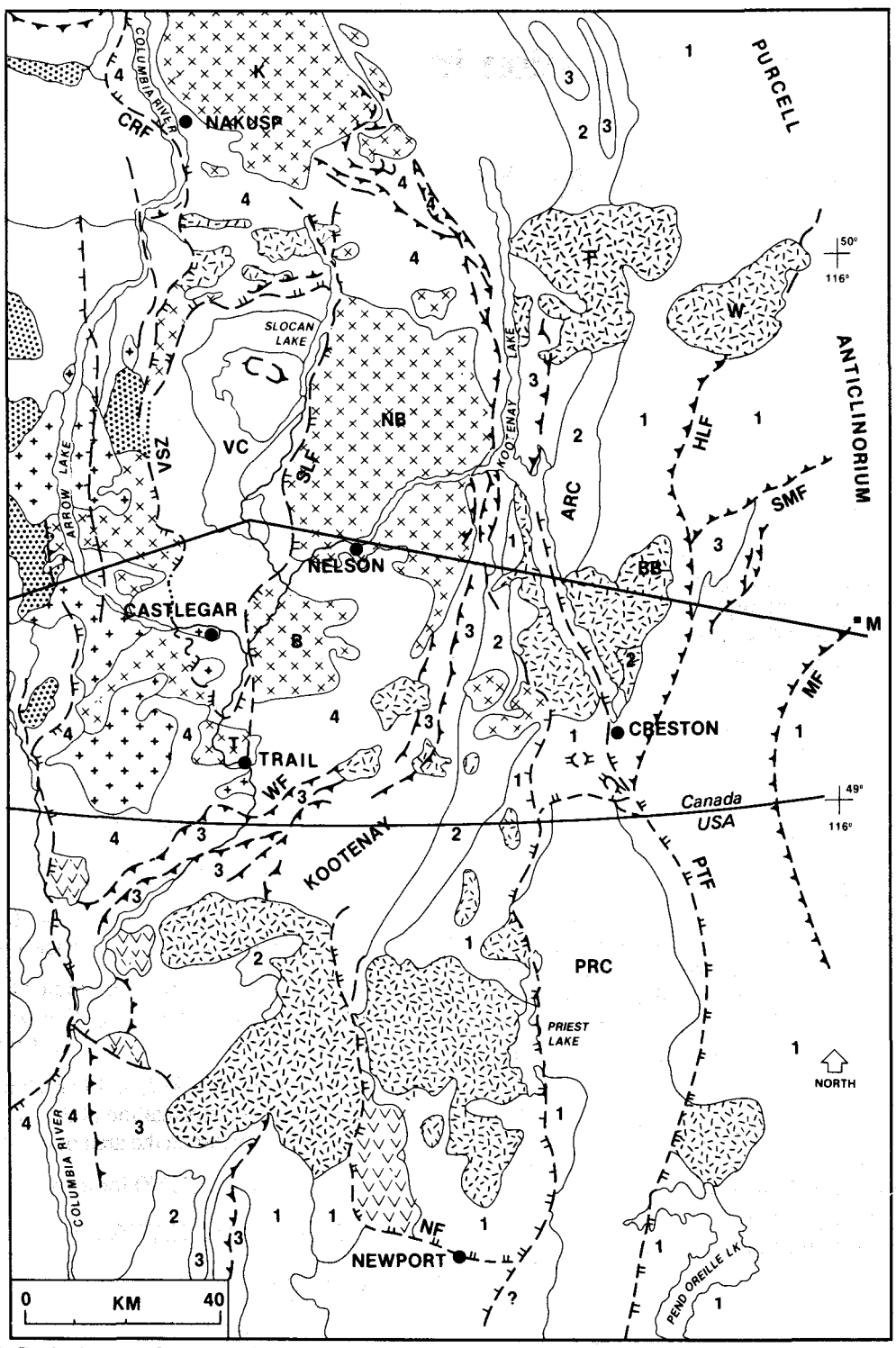

Figure 1. Geologic map of the area of the excursion, based on plate 1 of Parrish and others (1988). Symbols for igneous rocks; Jurassic, x; Cretaceous, short single lines; Ladybird granite suite, dotted; Eocene plutonic rocks, +; Eocene volcanic rocks, v. Symbols for faults: thrust faults, barbs; Eocene high-angle normal faults, double teeth; Eocene moderate-angle normal faults, single teeth. The small numerals indicate sedimentary rocks: 1, Purcell Supergroup; 2, Windermere Supergroup; 3, Paleozoic rocks; 4, Mesozoic of Quesnellia and all other allochthonous rocks. B, Bonnington pluton; BB, Bayonne batholith; CRF, Columbia River fault; F, Fry Creek batholith; HLF, Hall Lake fault; K, Kuskanax batholith; M, Moyie; MF, Moyie fault; NB, Nelson batholith; NF, Newport fault; PRC, Priest River Complex; PTF, Purcell thrust fault; SLF, Slocan Lake fault; SMF, Saint Mary's fault; T, Trail pluton; VC, Valhalla Complex; VSZ, Valkyr shear zone; W, White Creek batholith; WF, Waneta fault. The solid line is the approximate line of the Lithoprobe traverses of Figure 2a.

state of knowledge is summarized on Table 1, missing from which are the Trail and Castlegar (or Kinnaird) Gneisses, the Valkyr shear zone paragneisses and the paragneisses associated with the Priest River complex, and the Selkirk Crest batholithic complex, none of which can be assigned a protolith age with any confidence.

Structure at the Surface

Although the regional structure is generally well understood, the recent Lithoprobe and COCORP studies have raised a number of doubts about the nature and continuity of the surface features. Which, if any, structures are pre-Jurassic in age is difficult to prove, while sorting the Mesozoic compressional structures from the early Tertiary extensional structures is in its infancy.

The oldest structures are probably the northeast-trending faults in the Purcell anticlinorium. These affect the sedimentary patterns of the Purcell Supergroup. There may be a set of early folds within the Purcell, predating the unconformable deposition of the Windermere Supergroup. Likewise, the Lardeau Group and, by implication, the subjacent Cambrian and Upper Proterozoic were

Table 1. Summary of stratigraphy, Kootenay Arc and Purcell Supergroup

	(a) area east of Kootenay Lake		
	Riondel	Creston	Cranbrook
Neogene			St Eugene Fm
Cretaceous		(Bayonne batholith)	(Reade Lake stock)
Cambrian (?Lower)	Lardeau Group		
	Index Fm		
	Badshot Fm		
	Mohican Fm		
	Hamill Group		Eager Fm
			Cranbrook Fm
Proterozoic (Upper)	Windermere Supergroup.....		
	Horsethief Creek Group.....		
	Toby Fm.....		
Proterozoic (Middle)		Purcell Supergroup.....	
		Mt Nelson	Roosville
		Dutch Creek	Phillips
			Gateway
			Nicol Creek
			Van Creek
		Siyeh/Kitchener	Kitchener
		Creston	Creston
		Aldridge	Aldridge
			Fort Steele
	(b) Area west of Kootenay Lake		
	Trail and Castlegar	Nelson, Kaslo and Salmo	Route 3 west of Creston
Eocene	(Coryell syenites)		
Jurassic (M)	(Trail pluton)	(Nelson batholith)	
(L)	Hall Fm.....		
	Elise Fm (Rossland Group).....		
		Archibald Fm	
		Ymir Group	
Triassic (U)		Slocan Group	
Penn-Perm?		Kaslo Group	
Mississippian	Mt Roberts Fm	Milford Group	
Ordovician			Active Fm
Cambrian (L)?			Nelway Fm
(L)			Laib Gp:
			Reno Fm
			Qtzite
			Range Fm
Proterozoic (U)			Windermere Gp

folded and metamorphosed to a significant degree in pre-Milford Group time. The main architecture of the region was developed in four later stages, assuming that the events mentioned above are now unrecognizable in their regional framework.

(1) Post-Pliensbachian (194 Ma) and pre-Nelson batholith (NB) (164 Ma) folds affecting both the Rossland Group (RG) and its associated Pliensbachian sediments and the Slocan Group to the north of the NB. These folds also extend into the Mount Roberts Formation to the west. To the east, high-grade metamorphism and contemporaneous regional isoclinal folding of the Milford and Lardeau Groups (Höy, 1977) and, by implication, some of the Precambrian strata, must also date from this time. It is also necessary to postulate that the bounding faults of Quesnellia are of this same age; that is, the Waneta, Black Bluff, and Argillite faults south of the NB; the Lakeshore, Josephine, and Gallagher faults of the Ainsworth-Kaslo district, and the West Benard fault east of the NB (though the Ainsworth-Kaslo faults were shown as Eocene by Parrish and others, 1988).

(2) Structures associated with rapid uplift, cooling and probable convergence in the southern Kootenay Lake area, west of Creston and perhaps elsewhere. Ages of these structures are from 150 to 90 Ma. That they are to be expected is seen from the K-Ar and geobarometric studies of Archibald and others (1983, 1984) for the area between Creston and Salmo and those of Miller and others (1975) for the Newport fault zone. The existence of such a period of structural development is established by the multiple folds and lineations in the Slocan and Milford Groups (structures which also affect the Jurassic granite sills in the Ainsworth-Kaslo area) and by extensive deformation around the edges of Cretaceous batholiths. However, polyphase structures in the Lardeau and older rocks are not necessarily diagnostic of Cretaceous fold events. The Cretaceous structures may precede or, more likely, be associated with the intrusion of an arc of Cretaceous granitoids extending from 51°N (the Battle Range batholith, near Revelstoke, B.C. to 48°N (the Fan Lake pluton, south of Newport). These granitoids cut structures, such as the Hall Lake and St. Mary's faults near Cranbrook that are either associated with the eastward thrusting of the Rocky Mountains, or in other instances are possible terrane accretion boundaries. Thus an alternative interpretation of any structures of Cretaceous age in the Kootenay Arc is that they are dynamically related to genesis of the Rocky Mountain thrust sheets.

(3) Development of the Kootenay Arc. The Arc has been superimposed on the above-listed structures, the strike of which is generally parallel to the Arc and therefore changes direction by ~90 degrees along its length. That a distinct set of Cretaceous granitoids parallels the Arc in its eastern, outer part cannot be a coincidence. (But note that there are also Cretaceous granites in another arc-like pattern in Quesnellia.) The simplest explanation is that the Arc is a late structure, produced by a regional indentation process. The occurrence of the NB and parts of Quesnellia in the 'indented' region supports that view. Small-scale structures associated with the proposed indentation episode await identification.

(4) Regional extension. Tertiary extensional structures, ranging in age from 58 to 50 Ma, are prominent in the western parts of the Kootenay district. They are dominated by a set of major east-dipping shear zones which border the crystalline complexes of the Valhalla dome and cause the development of new fabrics and mylonitization (Carr and others, 1987; Parrish and others, 1988). This extensional process was accompanied by widespread igneous activity, cooling and uplift to the immediate west of Kootenay Lake, where most Rb-Sr and K-Ar ages on micas are in the 60 to 50 Ma range.

Deep Crustal Structure

The information from recent Lithoprobe and COCORP studies is illustrated on Figure 2. We see that the subsurface structure is as complicated as that at the surface, but that it does not everywhere correspond to it. West-dipping structures dominate in the east, beneath the Precambrian sediments; there is then a zone of confusion near Kootenay Lake in the Lithoprobe section (west to "Kootenay Arc" on Fig. 2a). This is followed to the west by a region with strong east- and weak west-dipping reflectors and, under the west side of the Valhalla dome, more strong west-dipping surfaces. Except under the Purcell anticlinorium, there is very little positive information for the region below ~10 km depth. Thus this seismic study clearly establishes the continuity of the Tertiary extensional surfaces to a modest depth, but unfortunately it does little to improve our knowledge of the effects of the earlier convergence in the area westward from just east of Kootenay Lake.

The COCORP section (Fig. 2b) starts in the east at the Purcell Trench, where it shows the same features as the Lithoprobe line, displaced to the west in accord with the curvature of the Kootenay Arc. Farther west, this section shows a broad zone of extension, as is clear from the surface geology; it is not yet possible, though, to correlate the deeper features between the two seismic lines.

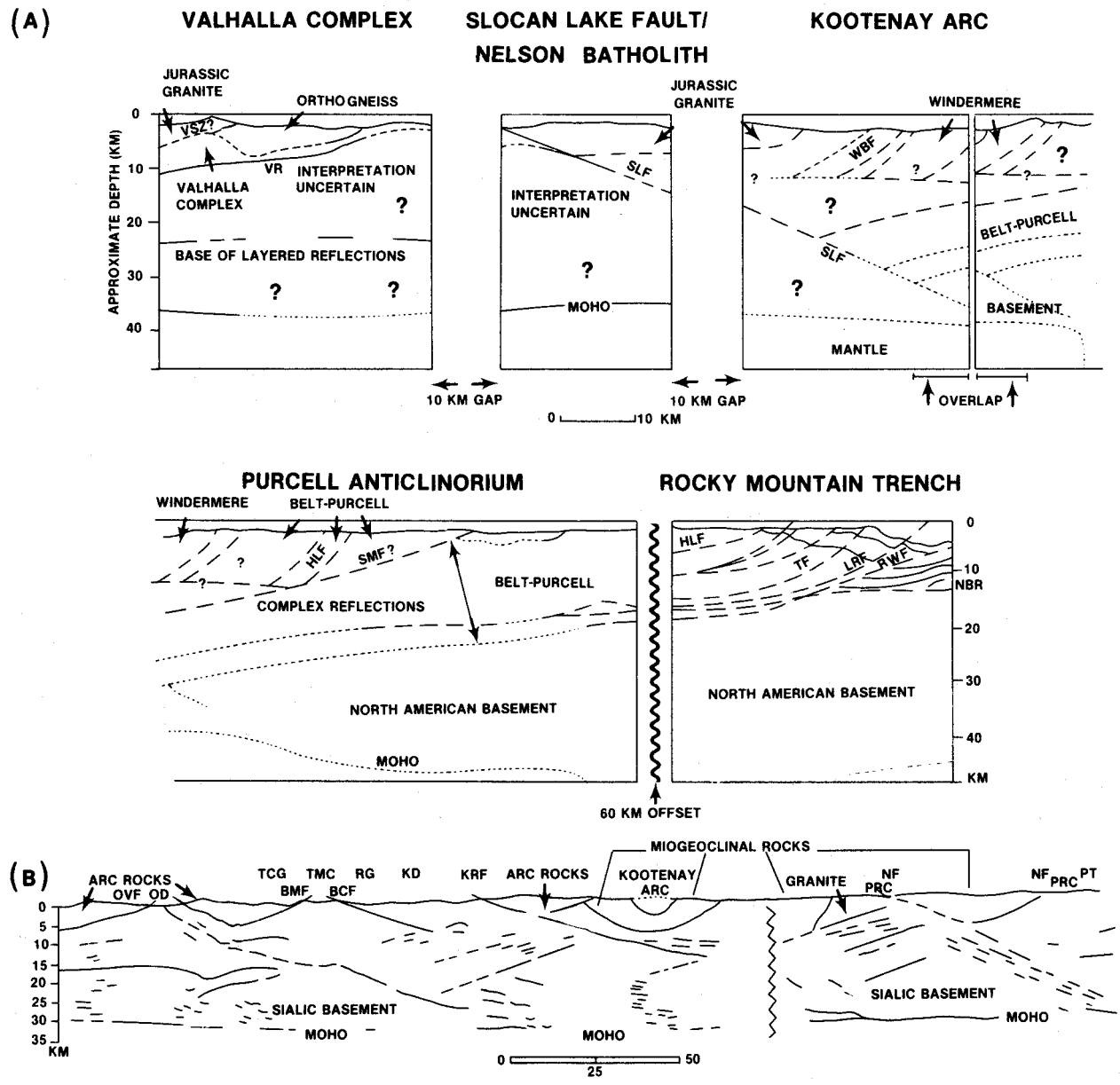

Figure 2. (a) Profile at about 49°40′N., from Lithoprobe data (Cook and others, 1988): VSZ, Valkyr shear zone; VC, Valhalla Complex; SLF, Slocan Lake fault; WBF, West Benard fault; LF, Hall Lake fault; SMF, Saint Mary's fault; TF, Torrent fault; LRF, Lussier River fault; RWF, Redwall fault. (b) Profile at about 48°N., from COCORP data (Potter and others, 1986): OVF, Okanagan Valley fault; OD, Okanagan dome; TCG, Toroda Creek graben; BMF, Bodie Mountain fault; TMC, Tenas Mary Creek fault; BCF, Bacon Creek fault; RG, Republic graben; KD, Kettle dome; KRF, Kettle River fault; PRC, Priest River Complex; NF, Newport fault; PT, Purcell thrust.

Igneous Complexes

Remarkably little has been published about the igneous rocks which lie within the area of this field trip. A few generalized field and petrographic descriptions exist, but almost no chemical or isotopic analyses of any kind have been published. Ghosh (1986) showed that all the Jurassic and Cretaceous plutons north of the border have a standard calc-alkaline chemistry and contain mafic minerals which characterize the class of I-type granites (including the Bayonne, Fry Creek, and White Creek batholiths east of Kootenay Lake). We have little information about the Tertiary granitic rocks, but the Tertiary syenites are silica-saturated, biotite-clinopyroxene bodies with an alkaline differentiation trend of the type which is controlled by pyroxene and plagioclase fractionation. The older volcanic complexes (in the Windermere, Kaslo, and Milford Groups) are an unknown quantity. The

Rossland Group (RG), south of the NB, is a suite of pyroclastic rocks and flows with the overall chemistry of calc-alkaline basaltic-andesite, andesite, and ankaramite and primitive, mantle-like O, Sr, Nd and Pb isotopic compositions (Beddoe-Stephens and Lambert, 1981; Höy and Andrew, 1988; D. K. Ghosh and R. St J. Lambert, unpub. data). Beddoe-Steven and Lambert suggested that the RG formed in a back-arc environment, whereas Ghosh concluded that the RG had never been in contact with old continental crust, unless it managed to erupt so rapidly that there could be no interaction. However, the chemical composition and mineralogy of the RG suggest that shallow fractionation has occurred, which would tend to increase, rather than decrease the likelihood of contamination. Thus these rocks point toward the existence of an oceanic rather than a continental setting for this part of eastern Quesnellia.

Regional Metamorphism, Uplift, and Cooling

From the work of Crosby (1968), Winzer (1973), Höy (1976), and Archibald and others (1983, 1984), we have a good knowledge of the nature and timing of the higher grade metamorphic and cooling events in the southern portion of the Arc in Canada. However, the lower grade peripheral regions are either only partially documented (for example, the metamorphism of the RG and of the Purcell Supergroup) or are virtually unstudied (the Slocan Group). It is clear that a Barrovian event affected the region east of the NB in the 30-m.y. interval between the eruption of the RG and the intrusion of the NB. It is possible that the facies series was of a slightly higher P/T regime than standard Barrovian, as surmised on the basis of muscovite basal spacings (Winzer, 1973). Our knowledge of metamorphism of definite Cretaceous age is confined to the areas proximal to Cretaceous plutons (Archibald and others, 1983, 1984). They reviewed and added to the existing data on regional metamorphism and provided numerous new K-Ar ages, which were used to construct a depth-time path for the area west of Creston and a regional cooling history (Figs. 3a, 3b). Sillimanite-grade metamorphism is also recorded within the Valkyr shear zone and the central part of the Valhalla dome, but it is not clear whether it predates early Eocene extension or is synchronous with it (Parrish and others, 1988).

Isotope Geology

Modern geochronological studies have been provided by Archibald and others (1983, 1984; their results are summarized in Figures 3b, 4a and 4b) and also in Parrish and others (1988).

In addition, Ghosh (1986) and D. K. Ghosh and R. St J. Lambert (unpub. data) provide a zircon age of 164 ± 1 Ma for the NB near Nelson, whereas Parrish and others (1988) mention a zircon age for an unspecified NB location of 169 ± 2 Ma. Ghosh (1986) also gives isotopic data for Sr, Nd, and Pb for samples from all the pre-Cretaceous sedimentary rocks and batholiths in the area of this guide which lie east of the Slocan Lake fault. The results for the sedimentary rocks indicate that a Proterozoic provenance is required but that younger units are increasingly oceanic in character. Modelling of the isotopic compositions of the batholiths showed that they were derived by melting of a depleted mantle, together with varying degrees of assimilation of the most probable local lower continental crust. The Sr-Nd system for some of the batholiths is illustrated in Figure 5.

Sr and Pb isotopic compositions effectively rule out any of the local upper crust as a significant contaminant. Thus, on Figure 5 only mantle and lower crust are used as end members. Most of the batholith samples lie near the center of the diagram: as a rate of assimilation/rate of crystallization (r-value) greater than 0.7 is not likely, any combination of a lower r-value and either clinopyroxene plus hornblende or plagioclase fractionation can explain the data, if the fraction of original magma remaining (F-value) is around 0.5. Ghosh (1986) concluded that 20 to 50 percent lower crustal component was required for the Nelson, Bonnington, Kuskanax, and Bayonne batholiths. In the absence of any conclusive evidence of the composition of the local lower crust, this concept of lower crustal contamination accompanying a period of fractional crystallization of pyroxene, hornblende, and plagioclase cannot be quantified more exactly.

Tectonic Theories

The task of placing the Kootenay Arc in a plate-tectonic or micro-plate setting has not been attempted explicitly. Existing theories which implicitly include the area are of three main types, according to the extent to which they incorporate paleomagnetic data and apply it to the terranes of southeast British Columbia.

The theory of Umhoefer (1987) for the paleotectonics of the western Cordillera is based on a combination of paleomagnetic data and current paleo-plate reconstructions for the eastern Pacific since the middle Late Cretaceous. It is essentially a strike-slip, latitudinal displacement theory, in which Quesnellia migrates some 2,000 km north during the Cretaceous, docking against mainland Canada to form the Rocky Mountains during the latest Cretaceous and Paleocene; eastward subduction does not play a significant role. This scheme depends heavily on the Pacific paleo-plate reconstructions; it meets with difficulty in the Jurassic batholiths which pin Quesnellia to the Eastern Assemblage of Monger and others (1982) or to Terrane III of Chamberlain and Lambert (1985) and fails to explain the origin of the Cretaceous plutons.

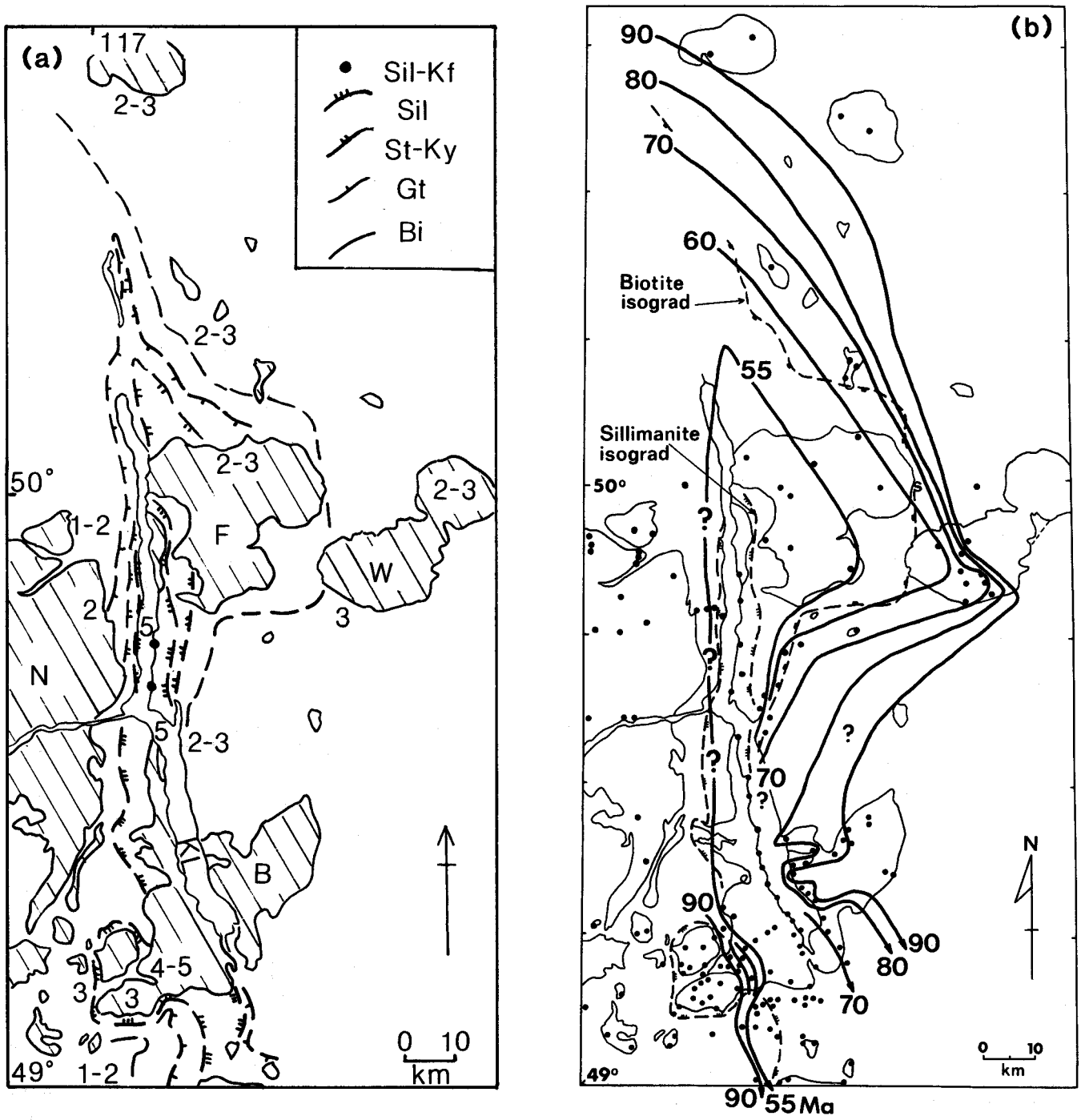

Figure 3. Kootenay Lake area: (a) Jurassic isograds, and bathograds for Cretaceous intrusions. Bathozones are indicated by numerals. B, Bayonne batholith; F, Fry Creek batholith; KL, Kootenay Lake; N, Nelson batholith; W, White Creek batholith; and (b) cooling and uplift history (based on figs. 2 and 5 in Archibald and others, 1984).

The second theory finds its most recent expression in Parrish and others (1988) and Cook and others (1988). Longitudinal displacement of the southeastern part of British Columbia plays a negligible role in this model. Evidence for northward displacement in the rest of British Columbia and Alaska is accepted, but these regions are presumed to be separated from southeast British Columbia by major strike-slip faults and(or) an area of transpression and bulk strain throughout southeastern British Columbia. The theory calls for the construction of the Rocky Mountains and the Kootenay area by a semi-continuous process of west-to-east convergence from the Middle Jurassic to the Paleocene, followed by Eocene extension. Lithoprobe data are in

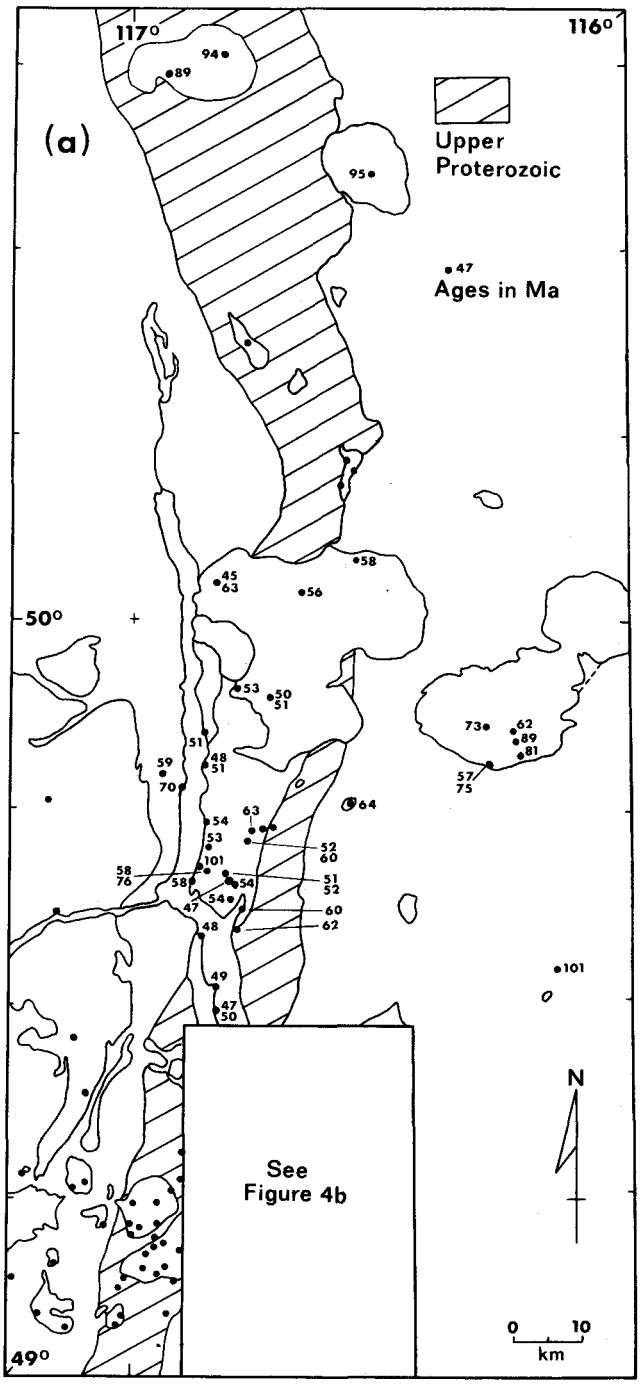

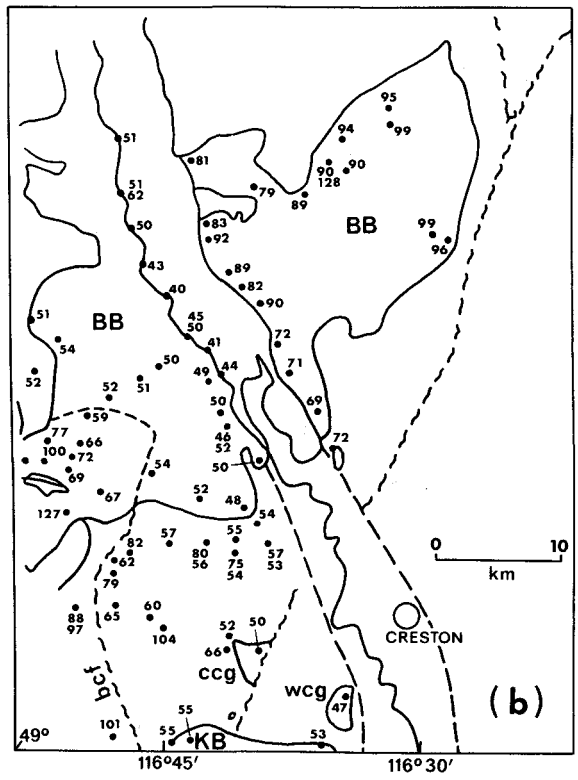

Figure 4. K-Ar ages in the Kootenay Lake area: (a) regional distribution and (b) detail for southern Kootenay Lake (based on figs. 3 and 4 in Archibald and others, 1984). In (b): BB, Bayonne batholith; bcf, Blazed Creek fault; ccg, Corn Creek gneiss; KB, Rykert batholith; wcg, West Creston gneiss.

accord with this model. Nevertheless, it faces the same difficulties as the translational model and the locations of the bounding faults and detailed features of the transpressive strain zone are not known.

The third theory possesses elements of both of the others, but it is not a compromise between them. Accepting both the paleomagnetic data and the evidence from the batholiths (both Jurassic and Cretaceous), Chamberlain and Lambert (1985) and Lambert and Chamberlain (1988) postulated that a microcontinent (Cordilleria) collided obliquely with the craton to form the Rocky Mountains in the later Cretaceous and the Paleocene. Thus the back-arc basins associated with the arcs of Quesnellia were destroyed by oblique westward subduction of the North American plate, which caused the microcontinent, on the Kula plate, to collide with continental America. The surface suture was figured to be the Purcell thrust, and the subsurface suture was shown as lying at the Purcell Trench (Kootenay Lake). That such westward subduction has occurred is manifest today in the steady westward slope of the shield surface from the prairies to the line of Kootenay Lake as revealed by Lithoprobe. The Cordilleria theory has problems with the timing and rate of northward movement. It presupposes an allochthonous origin of all sediments west of the Purcell thrust and north of the Lewis and Clark line. However, all theories accept the rifting of the continental margin during the late Precambrian and(or) the Cambrian, so the allochthonous nature of most of these units is inherent.

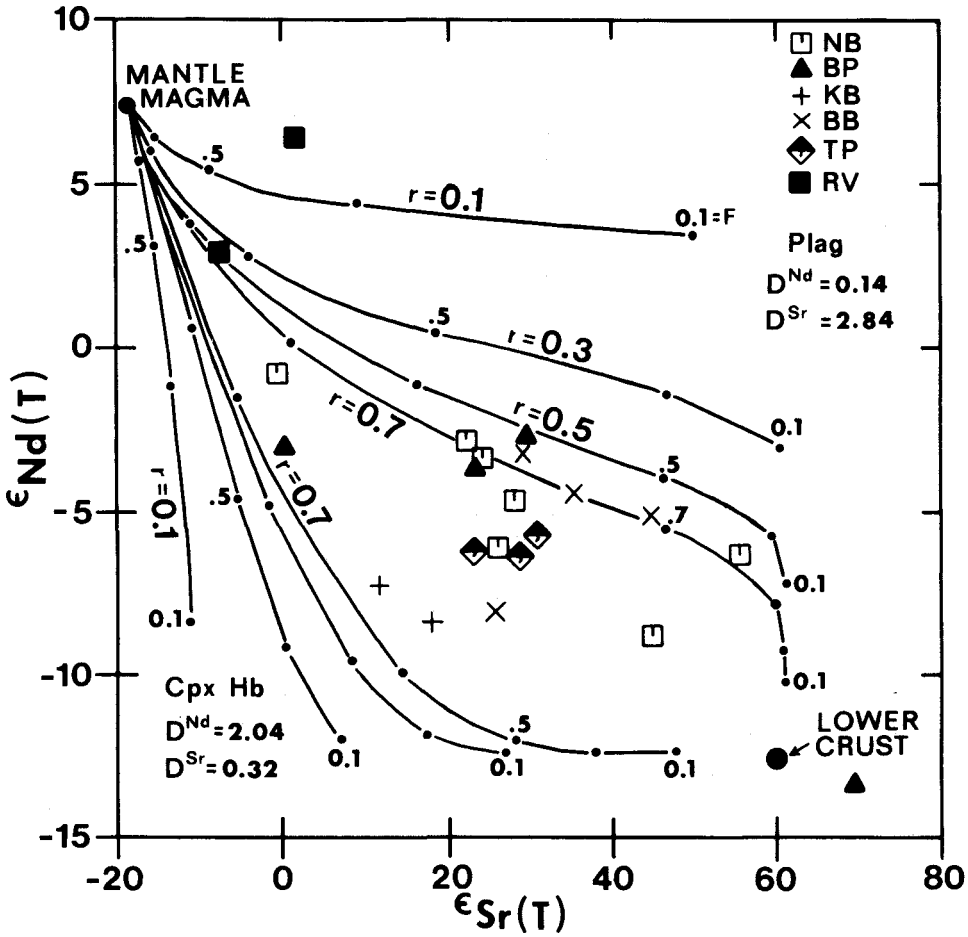

Figure 5. Sr and Nd isotopic data for batholiths, showing assimilation/fractional crystallization curves (based on data from Ghosh, 1986). NB, Nelson batholith; BP, Bonnington pluton; KB, Kuskanax batholith; BB, Bayonne batholith; TP, Trail pluton and Trail Gneiss; RG, Rossland Group.

ACKNOWLEDGMENTS

The author wishes to thank T. Höy for most useful discussions while this guide was being prepared and V. E. Chamberlain, P. Erdmer, T. Kiilsgaard, and the editors for their reviews of the text.

REFERENCES CITED

Aadland, R. K.; Bennett, E. H.; and others, compilers, 1979, Geologic map of the Sandpoint quadrangle, Idaho and Washington: Idaho Bureau of Mines and Geology Geologic Map Series, 1 sheet, scale 1:250,000.

Addie, G. G., 1970, The Reeves-MacDonald mine, Nelway, British Columbia. *In* Weissensborn, A. E., editor, Lead-zinc deposits in the Kootenay Arc, northeastern Washington and adjacent British Columbia: Washington Division of Mines and Geology Bulletin 61, p. 79-88.

Archibald, D. A.; Glover, J. K.; Price, R. A.; Farrar, E.; Carmichael, D. M., 1983, Geochronology and tectonic implications of magmatism and metamorphism, southern Kootenay Arc and neighbouring regions, southeastern British Columbia; Part I, Jurassic to Mid-Cretaceous: Canadian Journal of Earth Sciences, v. 20, no. 12, p. 1891-1913.

Archibald, D. A.; Krogh, T. E.; Armstrong, R. L.; Farrar, E., 1984, Geochronology and tectonic implications of magmatism and metamorphism, southern Kootenay Arc and neighbouring regions, southeastern British Columbia; Part II, Mid-Cretaceous to Eocene: Canadian Journal of Earth Sciences, v. 21, no. 5, p. 567-583.

Beddoe-Stephens, B.; Lambert, R. St J., 1981, Geochemical, mineralogical and isotopic data relating to the origin and tectonic setting of the Rossland volcanic rocks, southern British Columbia: Canadian Journal of Earth Sciences, v. 18, no. 5, p. 858-868.

Carr, S. D.; Parrish, R. R.; Brown, R. L., 1987, Eocene structural development of the Valhalla complex, southeastern British Columbia: Tectonics, v. 6, no. 2, p. 175-196.

Chamberlain, V. E.; Lambert, R. St J., 1985, Cordilleria, a newly defined Canadian microcontinent: Nature, v. 314, no. 6013, p. 707-713.

Cook, F. A.; Green, A. G.; Simony, P. S.; Price, R. A.; Parrish, R. R.; Milkereit, B.; Gordy, P. L.; Brown, R. L.; Coflin, K. C.; Patenaude, C., 1988, Lithoprobe seismic reflection structure of the southeastern Canadian Cordillera–Initial results: Tectonics, v. 7, no. 2, p. 157-180.

Crosby, Percy, 1968, Tectonic, plutonic and metamorphic history of the central Kootenay Arc, British Columbia, Canada: Geological Society of America Special Paper 99, 94 p., 2 pl.

Fyles, J. T., 1967, Geology of the Ainsworth-Kaslo area, British Columbia: British Columbia Department of Mines and Petroleum Resources Bulletin 53, 125 p., 6 pl.

Fyles, J. T.; Hewlett, C. G., 1959, Stratigraphy and structure of the Salmo lead-zinc area: British Columbia Department of Mines Bulletin 41, 162 p.

Ghosh, D. K., 1986, Geochemistry of the Nelson-Rossland area, southeastern British Columbia: University of Alberta Doctor of Philosophy thesis , 310 p.

Griggs, A. B., 1976, The Columbia River Basalt Group in the Spokane quadrangle, Washington, Idaho and Montana: U.S. Geological Survey Bulletin 1413, 39 p.

Höy, Trygve, 1976, Calc-silicate isograds in the Riondel area, southeastern British Columbia: Canadian Journal of Earth Sciences, v. 13, no. 8, p. 1093-1104.

Höy, Trygve, 1977, Stratigraphy and structure of the Kootenay Arc in the Riondel area, southeastern British Columbia: Canadian Journal of Earth Sciences, v. 14, no. 10, p. 2301-2315.

Höy, Trygve, 1980, Geology of the Riondel area, central Kootenay Arc, southeastern British Columbia: British Columbia Ministry of Energy, Mines and Petroleum Resources Bulletin 73, 89 p.

Höy, Trygve, 1982, Stratigraphic and structural setting of stratabound lead-zinc deposits in southeastern B.C.: Canadian Institute of Mining and Metallurgy Bulletin v. 75, p. 114-134.

Höy, Trygve; Andrew, Kathryn, (in press), The Rossland Group, Nelson map area, southeastern British Columbia: British Columbia Ministry of Energy, Mines and Petroleum Resources Paper 1989-1.

Höy, Trygve; Edmonds, F. R.; Hamilton, J. M.; Hauser, R. L.; Muraro, T. W.; Ransom, P. W., 1981, Lead-zinc and copper-zinc deposits in south-eastern British Columbia. *In* Thompson, R. I.; Cook, D. G., editors, Field guide to geology and mineral deposits: Geological Association of Canada annual meeting, Calgary, p. 41-67.

Lambert, R. St J.; Chamberlain, V. E., 1988, Cordilleria revisited, with a three dimensional model for Cretaceous tectonics in British Columbia: Journal of Geology, v. 96, no. 1, p. 47-60.

Little, H. W., 1960, Nelson map-area, west half, British Columbia (82F W1/2): Geological Survey of Canada Memoir 308, 205 p.

Monger, J. W. H.; Price, R. A.; Templeman-Kluit, D. J., 1982, Tectonic accretion and the origin of the two major metamorphic and plutonic welts in the Canadian Cordillera: Geology, v. 10, no. 2, p. 70-75.

Parrish, R. R.; Carr, S. D.; Parkinson, D. L., 1988, Eocene extensional tectonics and geochronology of the southern Omineca belt, British Columbia and Washington: Tectonics, v. 7, no. 2, p. 181-212.

Potter, C. J.; Sanford, W. E.; Yoos, T. R.; Prussen, E. I.; Keach, R. W., II; Oliver, J. E.; Kaufman, Sidney; Brown, L. D., 1986, COCORP deep seismic reflection traverse of the interior of the North American Cordillera, Washington and Idaho: Tectonics, v. 5, no. 7, p. 1007-1027.

Read, P. R.; Brown R. L., 1981, Columbia River fault zone–Southeastern margin of the Shuswap and Monashee complexes, southern British Columbia: Canadian Journal of Earth Sciences, v. 18, no. 7, p. 1127-1145.

Sangster, D. F., 1968, Some chemical features of lead-zinc deposits in carbonate rocks: Geological Survey of Canada Paper 68-39, 17 p.

Simony, P. S., 1979, Pre-Carboniferous basement near Trail, British Columbia: Canadian Journal of Earth Sciences, v. 16, no. 1, p. 1-11.

Struik, L. C., 1986, Imbricated terranes of the Cariboo gold belt with correlations and implications for tectonics in southeastern British Columbia: Canadian Journal of Earth Sciences, v. 23, no. 8. p. 1047-1061.

Umhoefer, P. J., 1987, Northward translation of "Baja British Columbia" along the late Cretaceous to Paleogene margin of western North America: Tectonics, v. 6, no. 4, p. 377-394.

Winzer, S. R., 1973, Regional metamorphism in the Central Kootenay Arc: University of Alberta Doctor of Philosophy thesis, 335 p.

[The road log for this paper can be found in Parts 1B, 2, and 3B of the road log that completes this suite of text for the excursion.]

Tectonics and Mineralization in Southeastern British Columbia: The Purcell Supergroup and the Sullivan Massive Sulfide Deposit

Trygve Höy
Ministry of Energy, Mines and Petroleum Resources
Parliament Buildings
Victoria, BC
V8V 1X4 Canada

INTRODUCTION

The fieldtrip excursion will visit the Sullivan deposit at Kimberley, a large stratiform lead-zinc-silver deposit in turbidites of the middle Proterozoic Purcell Supergroup. It will also examine rocks of the Purcell Supergroup as the trip crosses the Purcell anticlinorium into highly deformed rocks of the Kootenay Arc to the west.

The Purcell anticlinorium is a broad north-plunging structure cored by rocks of the Purcell Supergroup and flanked by late Proterozoic Windermere rocks and lower Paleozoic platformal rocks (Fig. 1). The anticlinorium is cut by a number of generally east- or northeast-trending transverse faults that have had intermittent movement on them since middle Proterozoic time (Leech, 1958; Lis and Price, 1976; Höy, 1982). The latest movement on one of these faults, the St. Mary fault, is constrained by an intrusion that cut and apparently sealed it by 94 Ma (Höy and van der Heyden, 1988).

THE PURCELL SUPERGROUP

The oldest rocks exposed in the core of the Purcell anticlinorium are quartzites, siltstones, and argillites of the Aldridge Formation, which is correlated with the Prichard Formation in the United States (Fig. 2). The lower Aldridge comprises at least 1,500 m of rusty-weathering argillite, siltstone, and quartzite (Fig. 3). The contact between the lower and middle Aldridge is gradational over a few tens to several hundred meters. Locally, an intraformational conglomerate occurs at or near the top of the lower Aldridge, at the same stratigraphic position as the Sullivan deposit.

The middle Aldridge comprises thick, grey quartz wacke beds and interlayered laminated siltstone layers, intruded by some regionally extensive metagabbro sills (Fig. 3). In general, quartz wacke beds are thinner and less abundant higher in the middle Aldridge section (Höy and Diakow, 1982). The quartz wacke beds have numerous sedimentary structures indicative of turbidity current deposition (Bishop and others, 1970). Paleocurrent data in the Moyie Lake and Kimberley areas indicate a northerly current transport direction (Fig. 4).

Interturbidite argillaceous siltstone in the central part of the middle Aldridge commonly consists of a sequence several meters thick of alternating dark and light laminations less than a millimeter to a few millimeters thick. Laminations in about a dozen of these sequences can be matched across distances of as much 300 km (Edmunds, 1977; Huebschman, 1973). They are reliable stratigraphic markers that allow correlation within the 3-km-thick middle Aldridge succession.

The upper Aldridge includes 300 to 400 m of generally rusty-weathering dark-grey argillite and lighter grey siltstone.

The overlying Creston Formation consists of light-green, brown, and pale-purple argillaceous quartzite, siltstone, and argillite that contains numerous shallow-water sedimentary structures. The Creston is overlain by shallow-water carbonate and clastic rocks of the Kitchener Formation, subtidal to supratidal clastic rocks of the Van Creek Formation, and andesitic volcanic rocks of the Nicol Creek Formation (Fig. 3). The volcanic rocks

From: Joseph, N. L., and others, editors, 1989, Geologic guidebook for Washington and adjacent areas: Washington Division of Geology and Earth Resources Information Circular 86.

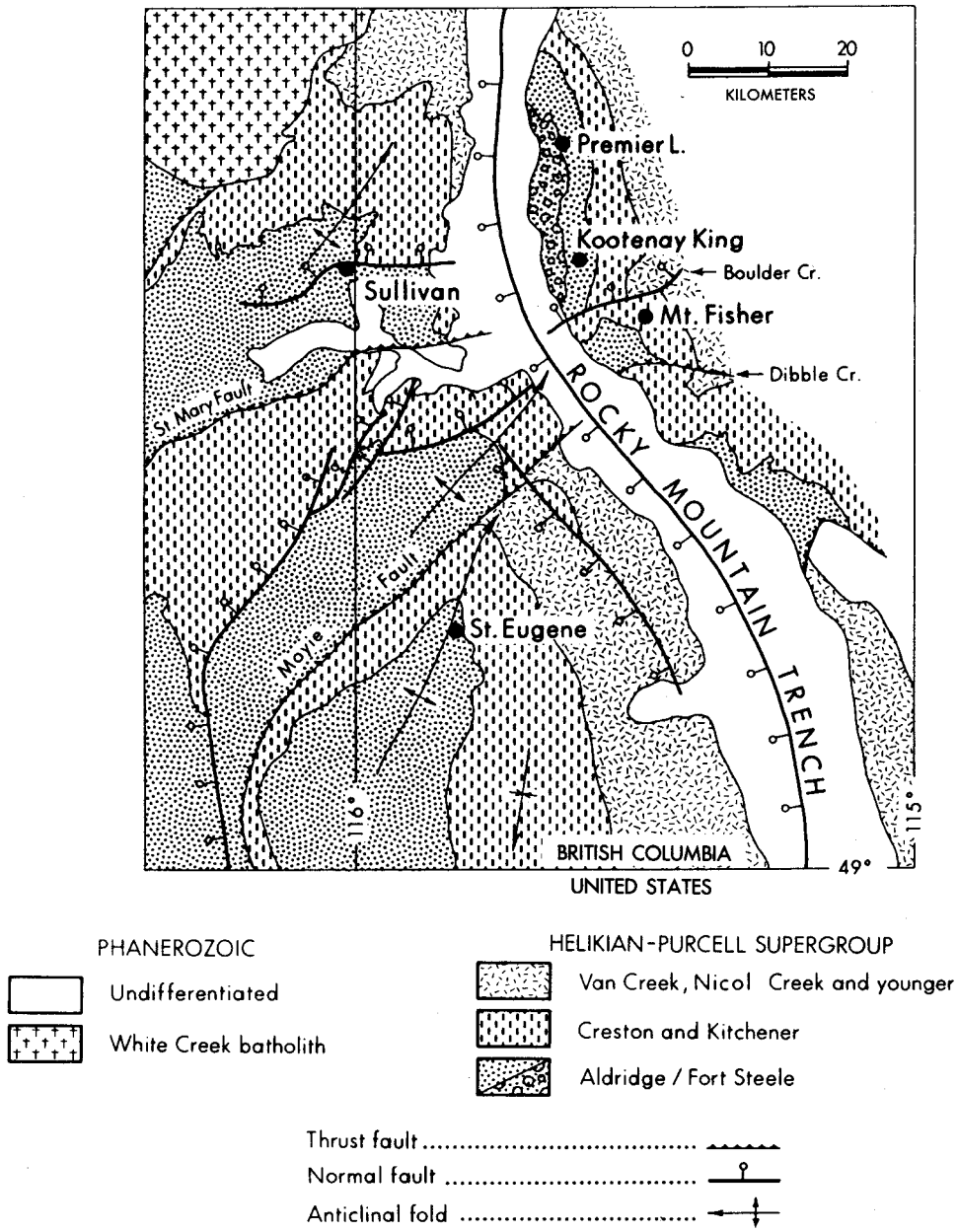

Figure 1. Geologic map of the Purcell Supergroup in Fernie west half map sheet and part of Nelson east half (compiled from Höy and Carter, 1988; Rice, 1941; Reesor, 1973; Leech, 1958).

occur only east of the Rocky Mountain Trench and along the eastern flank of the Purcell anticlinorium. Elsewhere, grey and green argillite, dolomite, and quartzite of the Dutch Creek Formation (Fig. 2) overlie the "Siyeh" Formation (Reesor, 1973) and are overlain by oolitic and stromatolitic dolomite and dolomitic limestone, argillaceous limestone, and argillite of the Mount Nelson Formation (Rice, 1941; Reesor, 1973; Carter and Höy, 1987).

Laterally extensive gabbroic sills, referred to as the Moyie intrusions, intrude the lower and the lower part of the middle Aldridge Formation. They are a few tens to several hundred meters thick, with medium- to coarse-grained equigranular central parts and finer grained margins. A thin hornfelsed zone occurs adjacent to some sill contacts. Locally, Moyie intrusions also form dikes. Although Moyie intrusions have isotopic ages indistinguishable from those of the host Aldridge rocks (approximately 1,440 Ma, Zartman and others, 1982; Höy, 1988), it has generally been accepted that they are coeval with deposition of the upper Aldridge Formation or Creston rocks (Zartman and others, 1982; Hamilton

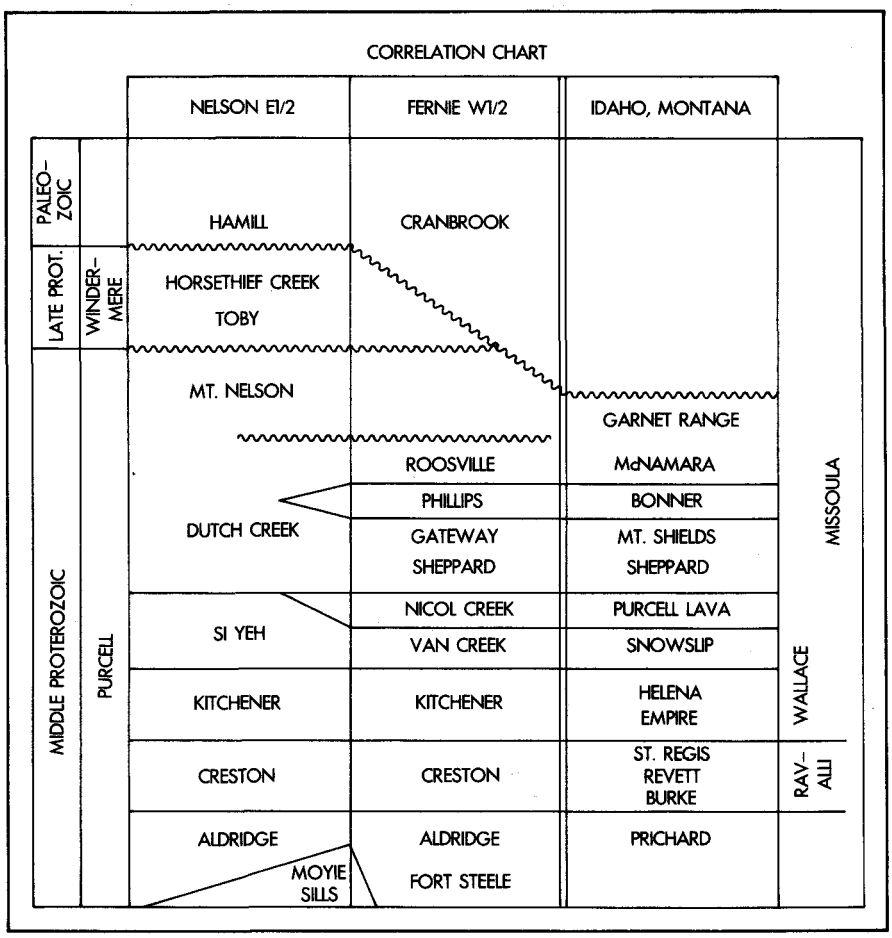

Figure 2. Correlation chart, southeastern British Columbia and northern Idaho and Montana.

and others, 1983) or perhaps with Nicol Creek lavas (McMechan, 1981). However, Höy (1984a, b) presents evidence that suggests that they were early and emplaced into water-saturated Aldridge sediments a few tens to a few hundreds of meters below the sediment surface. Hence, the Moyie sills are evidence of a regional igneous/thermal event during deposition of lower and middle Aldridge rocks, during formation of stratiform sulfide deposits. A modern example of intrusion of basaltic sills into highly porous unconsolidated turbidite sediments was described by Einsele and others (1980) from drill sites in the Guaymas Basin, Gulf of California.

Moyie intrusions are restricted to early Aldridge time, dying out in late middle Aldridge time at the same time as the volume of coarse turbidites decreased. The abundance, volume, spatial distribution, and temporal restriction of Moyie intrusions to a stratigraphic interval dominated by turbidite deposition and the geochemistry of the intrusive rocks (Höy, unpub. data) suggest that lower Aldridge and early middle Aldridge sedimentation took place during a period of continental rifting. However, it is not possible, from the chemistry of the sills, to determine if rifting produced an intracratonic basin, as suggested by Winston and others (1984) or a miogeocline partially underlain by oceanic crust.

East of the Rocky Mountain Trench, in the area of the Kootenay King deposit and Premier Lake (Fig. 1), coarse fluvial quartzite and tidal-flat deposits of the Fort Steele Formation are at the base of the exposed Purcell succession (Fig. 5) (Höy, 1979, 1982). They are overlain by deeper water siltstone and quartzite of the Aldridge Formation, dominantly shallow-water tidal-flat, floodplain, and deltaic deposits of the Creston Formation, and platformal carbonates of the Kitchener Formation. The Kootenay King deposit is a laminated, stratiform lead-zinc deposit in middle Aldridge siltstone.

The Boulder Creek fault coincides approximately with a marked transition in the character of lower Purcell rocks: from the dominantly fluvial, shallow-water, and minor turbidite deposits to the north into a thick succession of turbidites to the south that are similar to those in the Purcell Mountains west of the Rocky Mountain Trench (McMechan, 1981; Höy and Diakow, 1982).

In summary, the lower exposures of Purcell rocks in the Kootenay King mine area are dominantly fluvial and floodplain deposits, in contrast with considerably thicker, basinal turbidite facies to the south and west. This indicates that in lower Purcell time, the Kootenay King area was near the edge of a deep, structural basin that lay to the south and west. Rapid thinning and fining of sedi-

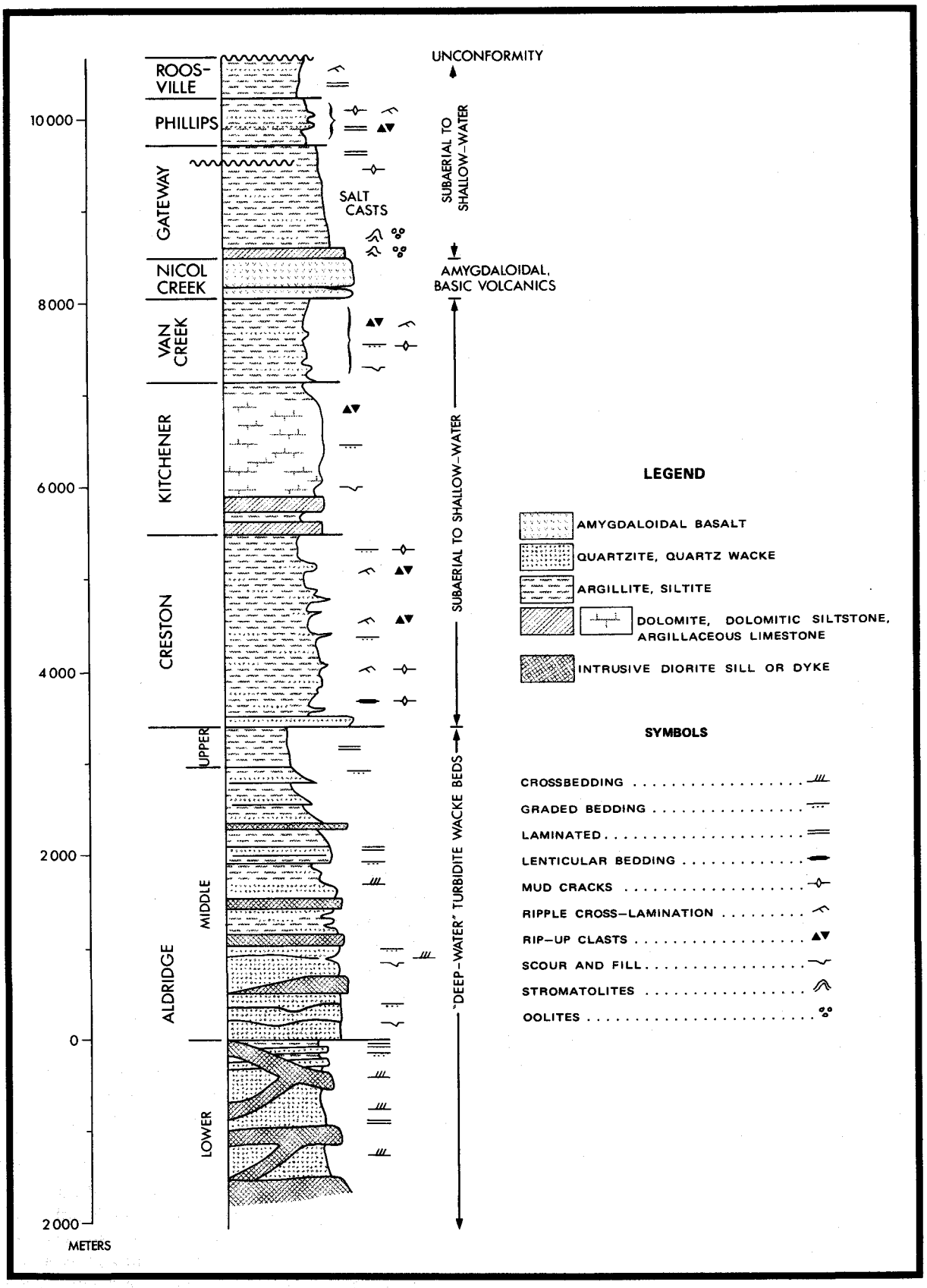

Figure 3. Composite stratigraphic column of the Purcell Supergroup in the Moyie Lake area.

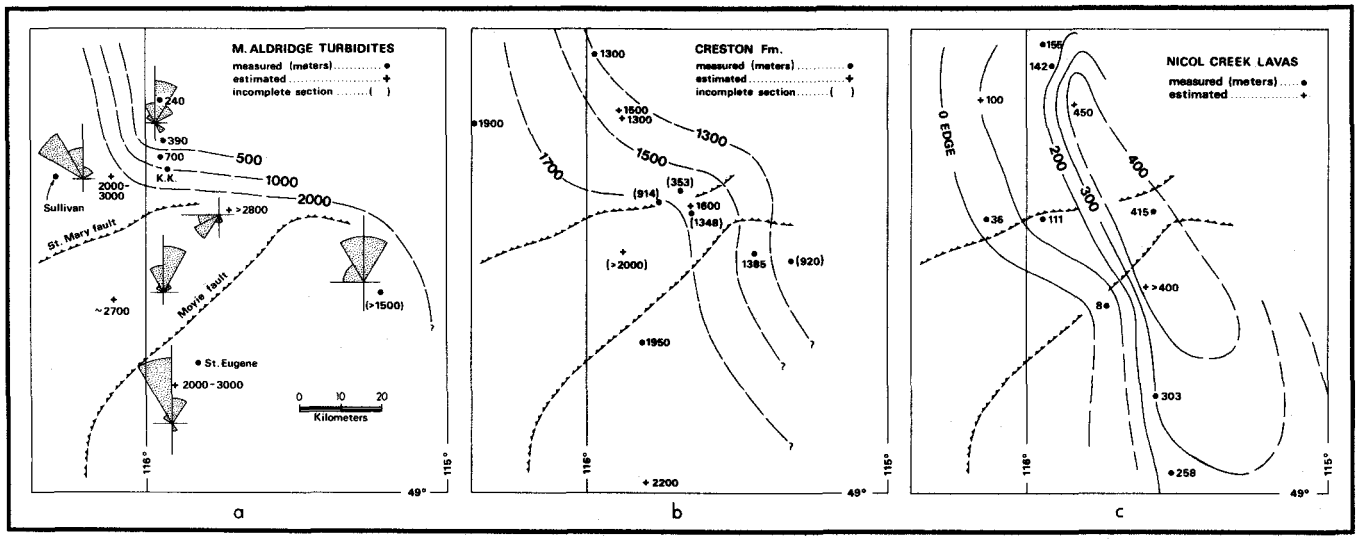

Figure 4. Isopach maps of middle Aldridge turbidites (a) and the Creston Formation (b) and isolith map of Nicol Creek lavas (c), southeastern B.C., restored for movements on Moyie, St. Mary, Dibble Creek, and Boulder Creek faults. (Data sources: Benvenuto and Price, 1979; Höy, 1979, 1984c, 1985; Höy and Diakow, 1982; McMechan, 1981 and unpub. data).

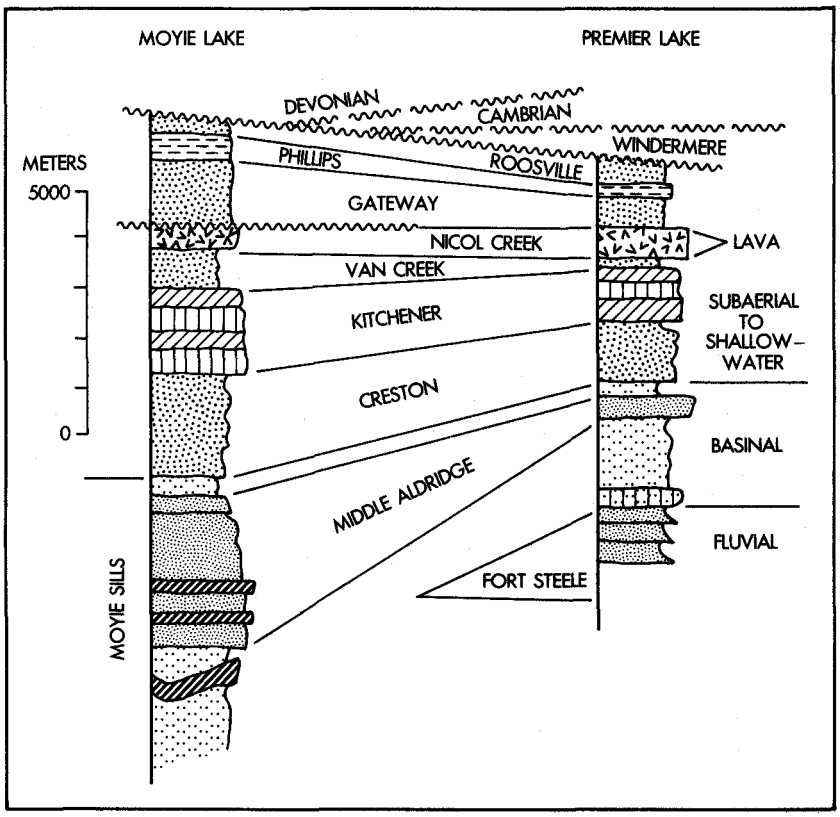

Figure 5. Composite stratigraphic sections (data from Höy, 1985).

ments in the Kootenay King area, northward-directed paleocurrents, dramatic thickening of turbidites just to the south, and coarse pebble conglomerates located near the basin/platformal transition (Höy, 1979, 1982) suggest that the basin edge developed by growth faulting.

Facies trends and palinspastically restored isopach maps (Höy, 1984b) indicate a marked westward deflection in the basin margin near the present position of the St. Mary and Boulder Creek faults (Fig. 4). The deflection coincides approximately with the northern edge of a postulated older, southwest-trending, Precambrian rift structure, recognized from geophysical data and postulated to extend in Hudsonian basement rocks beneath the cover rocks into southeastern British Columbia (Kanasewich and others, 1969). It is suggested that bowing up of the crust near the northern margin of the older, southwest-trending, tectonic zone, recorded in northward shedding of fluvial Fort Steele sediments (Höy, 1979), preceded incipient rifting (Price, 1981). Early stages in the development of the basin are marked by the thick accumulations of Aldridge turbidites and voluminous intrusions of basic sills. North- to northwest- (and locally westerly) directed paleocurrents generally paralleled the margin of the basin. Upper Purcell shallow-water rocks prograded westward over the basin margin and turbidite flysch package, but differential downwarping continued periodically within the basin. In later Purcell time, faults along the basin margin were re-activated, probably to deep crustal levels, and resulted in local surface relief that produced erosional contacts with locally coarse, fluvial conglomerates (Höy and Diakow, 1982; Carter and Höy, 1987) and in the extrusion of the Nicol Creek basalts centered near the early Purcell platform-basin hinge line.

THE SULLIVAN DEPOSIT

The Sullivan deposit is one of the largest massive sulfide base metal deposits in the world. It has been described in a number of papers, recent ones including Ethier and others (1976), Hamilton and others (1982, 1983), and guidebooks (Höy and others, 1985). Hence it is only briefly described here. The Sullivan deposit has produced in excess of 130 million tons of ore from an original reserve of 160 million tons containing 6 percent lead, 6 percent zinc, 28 percent iron, and 67 g/tonne silver (Ransom and others, 1985).

The western part of the orebody is approximately 2,000 m in diameter and 100 m thick (Fig. 6). It comprises massive pyrrhotite with scattered wispy layers of galena, overlain by layers of mixed pyrrhotite, sphalerite, galena, and pyrite that is intercalated with clastic layers. Its eastern part, separated from the more massive western part by an irregular transition zone, includes five distinct conformable layers of generally well laminated sulfides separated by clastic rocks. The sulfide layers thin to the east, away from the transition zone, and are replaced at the limits of the ore deposit by iron sulfide bands.

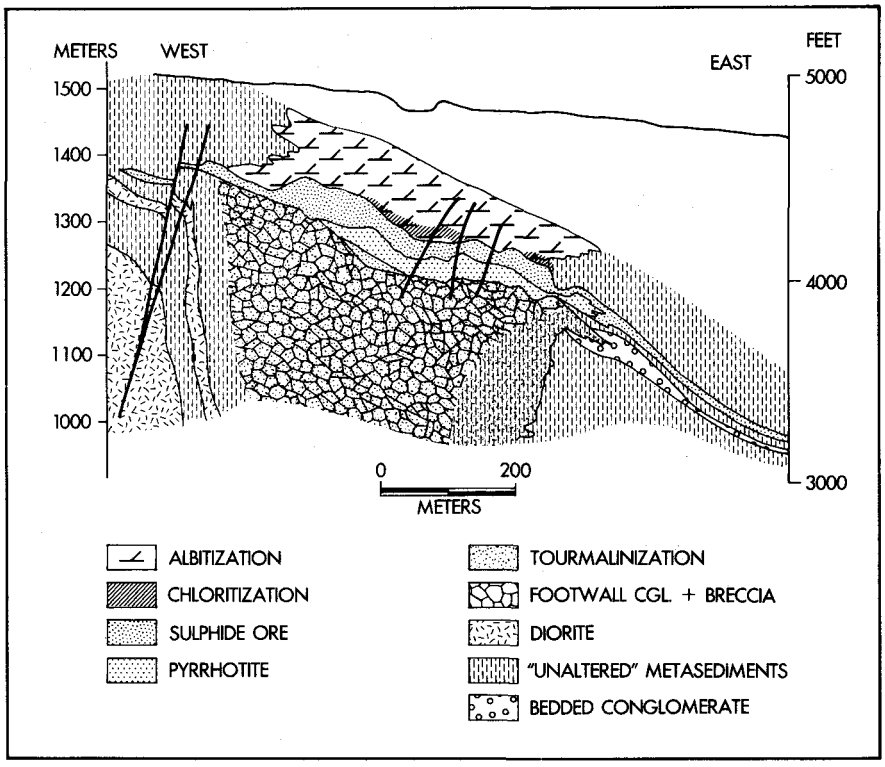

Figure 6. East-west vertical sections through the Sullivan orebody (modified from Hamilton and others, 1982, 1983; Ransom and others, 1985).

An extensive brecciated and altered zone underlies the massive western part of the orebody. (See also Shaw and Hodgson, 1980.) Linear, north-trending breccia zones, disseminated and vein sulfides, and extensive alteration to a dark, dense chert-like tourmaline-rich rock are conspicuous features of the altered footwall. Albite-chlorite-pyrite alteration is also restricted to the western part of the orebody, occurring in cross-cutting zones in the footwall tourmalinite, in the orebody itself, and as much as 100 m above the orebody in the hanging wall (Hamilton and others, 1982; Shaw and Hodgson, 1980).

The deposit is zoned: lead/zinc and silver values decrease toward the margin in the eastern part. Tin is concentrated in the western part. In general, metal distribution patterns are directly related to proximal chaotic breccia; higher absolute values and higher lead/zinc and silver/lead ratios are known in rocks that overlie the breccia zones (Ransom and others, 1985; Hamilton and others, 1982).

Sullivan is interpreted to be a hydrothermal synsedimentary deposit that formed in a small submarine basin. The western part lies directly above the conduit zone, the brecciated and altered footwall of the deposit.

ACKNOWLEDGMENTS

Observations and discussions about the genesis of the Sullivan deposit and on rocks of the Purcell Supergroup have been developed over many years by a large number of geologists. This guide draws heavily on this previous work. In particular, I thank the staff of Cominco Ltd. for the support they have shown researchers both within and outside the company. Their free exchange of ideas and publications on the geology of Sullivan have advanced considerably our understanding of this deposit and other similar massive sulfide deposits.

REFERENCES CITED

Benvenuto, G. L.; Price, R. A., 1979, Structural evolution of the Hosmer thrust sheet, southeastern British Columbia: Bulletin of Canadian Petroleum Geology, v. 27, no. 3, p. 360-394.

Bishop, D. T.; Morris, H. C.; Edmunds, F. R., 1970, Turbidites and depositional features in the lower Belt-Purcell Supergroup [abstract]: Geological Society of America Abstracts with Programs, v. 2, no. 7, p. 497.

Carter, G.; Höy, T., 1987, Geology of the Skookumchuck map area (W1/2), southeastern British Columbia: B.C. Ministry of Energy, Mines and Petroleum Resources Open File Map 1987-8, scale 1:50,000.

Edmunds, F. R., 1977, Kimberley to Creston, stratigraphy and lithology of the lower Belt Series in the Purcell Mountains, British Columbia. *In* Lead-zinc deposits of southeastern British Columbia: Geological Association of Canada Fieldtrip Guidebook 1, p. 22-32.

Einsele, G.; Gieskes, J. M.; Curray, J.; [and others], 1980, Intrusion of basaltic sills into highly porous sediments, and resulting hydrothermal activity: Nature, v. 283, no. 5746, p. 441-445.

Ethier, V. G.; Campbell, F. A.; Both, R. A.; Krouse, H. R., 1976, Geological setting of the Sullivan orebody and estimates of temperatures and pressure of metamorphism: Economic Geology, v. 71, no. 8, p. 1570-1588.

Hamilton, J. M.; Bishop, D. T.; Morris, H. C.; Owens, O. E., 1982, Geology of the Sullivan orebody, Kimberley, B.C., Canada. *In* Hutchinson, R. W.; Spence, C. D.; Franklin, J. M., editors, Precambrian sulphide deposits, H. S. Robinson Memorial Volume: Geological Association of Canada Special Paper 25, p. 597-665.

Hamilton, J. M.; Hauser, R. L.; Ransom, P. W., 1983, The Sullivan orebody. *In* Stratabound base metal deposits in southeastern British Columbia and northwestern Montana: Geological Association of Canada Fieldtrip Guidebook 13, p. 44-59.

Höy, Trygve, 1979, Geology of the Estella-Kootenay King area, Hughes Range, southeastern British Columbia: B.C. Ministry of Energy, Mines and Petroleum Resources Preliminary Map 36, scale 1:50,000.

Höy, Trygve, 1982, The Purcell Supergroup in southeastern British Columbia–Sedimentation, tectonics, and stratiform lead-zinc deposits. *In* Hutchinson, R. W.; Spence, C. W.; Franklin, J. M., editors, Precambrian sulphide deposits, H. S. Robinson Memorial Volume: Geological Association of Canada Special Paper 25, p. 127-147.

Höy, Trygve, 1984a, Structural setting, mineral deposits, and associated alteration and magmatism, Sullivan camp, southeastern British Columbia: British Columbia Ministry of Energy, Mines and Petroleum Resources Paper 1984-1, p. 24-35.

Höy, Trygve, 1984b, The Purcell Supergroup near the Rocky Mountain Trench, southeastern British Columbia. *In* Hobbs, S. W., editor, The Belt: Montana Bureau of Mines and Geology Special Publication 90, p. 36-38.

Höy, Trygve, 1984c, Geology of the Cranbrook sheet and Sullivan map-area: B.C. Ministry of Energy, Mines and Petroleum Resources Preliminary Map 54, scale 1:50,000.

Höy, Trygve, 1985, The Purcell Supergroup, Fernie west-half, southeastern British Columbia; Part A—Stratigraphy-measured sections: British Columbia Ministry of Energy, Mines and Petroleum Resources Bulletin 76, 79 p.

Höy, Trygve, 1988, Early tectonic and magmatic evolution of the middle Proterozoic Purcell basin, southeastern Canadian Cordillera (abstract): Geological Association of Canada, Pacific Section, Programme and Abstracts, p.16.

Höy, Trygve; Berg, N.; Fyles, J. T.; Delaney, G. D.; McMurdo, D.; Ransom, P. W., 1985, Stratabound base metal deposits in southeastern British Columbia. *In* Tempelman-Kluit, Dirk, editor, Field guides to geology and mineral deposits in the southern Canadian Cordillera: Geological Society of America Cordilleran Section Fieldtrip 13, 32 p.

Höy, Trygve; Carter, G., 1988, Geology of the Fernie west half map sheet (and part of the Nelson east half): B.C. Ministry of Energy, Mines and Petroleum Resources Open File Map 1988-14, scale 1:100,000.

Höy, Trygve; Diakow, L., 1982, Geology of the Moyie Lake area: British Columbia Ministry of Energy, Mines and Petroleum Resources Preliminary Map 49, scale 1:50,000.

Höy, Trygve; van der Heyden, Peter, 1988, Geochemistry, geochronology, and tectonic implications of two quartz monzonite intrusions, Purcell Mountains, southeastern British Columbia: Canadian Journal of Earth Sciences, v. 25, no. 1, p. 106-115.

Huebschman, R. P., 1973, Correlation of fine carbonaceous bands across a Precambrian stagnant basin: Journal of Sedimentary Petrology, v. 43, no. 3, p. 688-699.

Kanasewich, E. R.; Clowes, R. M.; McCloughan, C. H., 1969, A buried Precambrian rift in western Canada: Tectonophysics, v. 8, no. 4-6, p. 513-527.

Leech, G. B., 1958, Fernie map-area, west half, British Columbia, 82G W1/2: Geological Survey of Canada Paper 58-10, 40 p.

Lis, M. G.; Price, R. A., 1976, Large-scale block faulting during deposition of the Windermere Supergroup (Hadrynian) in southeastern British Columbia: Geological Survey of Canada Paper 1976-1A, p. 135-136.

McMechan, M. E., 1981, The middle Proterozoic Purcell Supergroup in the southeastern Rocky and southeastern Purcell Mountains, British Columbia and the initiation of the Cordilleran miogeocline, southern Canada and adjacent United States: Bulletin of Canadian Petroleum Geology, v. 29, no. 4, p. 583-621.

Price, R. A., 1981, The Cordilleran foreland thrust and fold belt in the southern Canadian Rocky Mountains. *In* McClay, K. R.; Price, N. J., editors, Thrust and nappe tectonics: Geological Society of London Special Publication 9, p. 427-448.

Ransom, P. W.; Delaney, G. D.; McMurdo, D., 1985, The Sullivan orebody. *In* Stratabound base metal deposits in southeastern British Columbia: Geological Society of America Cordilleran Section Fieldguide 11, 32 p.

Reesor, J. E., 1973, Geology of the Lardeau map-area, east half, British Columbia: Geological Survey of Canada Memoir 369, 129 p., 2 pl.

Rice, H. M. A., 1941, Nelson map-area, east half, British Columbia: Geological Survey of Canada Memoir 228, 86 p., 1 pl.

Shaw, D. R.; Hodgson, C. J., 1980, Wall-rock alteration at the Sullivan mine, Kimberley, British Columbia (abstract): Canadian Institute of Mining and Metallurgy Bulletin, v. 73, no. 821, p. 75.

Winston, Don; Woods, Marvin; Byer, G. B., 1984, The case for an intracratonic Belt-Purcell Basin–Tectonics, stratigraphic and stable isotopic considerations. *In* McBane, J. D.; Garrison, P. B., editors, Northwest Montana and adjacent Canada: Montana Geological Society Field Conference and Symposium, p. 103-119.

Zartman, R. E.; Peterman, Z. E.; Obradovich, J. D.; Gallego, M. D.; Bishop, D. T., 1982, Age of the Crossport C Sill near Eastport, Idaho. *In* Reid, R. R.; Williams, G. A., editors, Society of Economic Geologists' Coeur d'Alene field conference: Idaho Bureau of Mines and Geology Bulletin 24, p. 61-69.

[The road log for this paper is Part 1A of the road log that completes the suite of text.]

Tectonics and Mineralization in Southeastern British Columbia: Structure, Stratigraphy, and Mineral Deposits of the Rossland Group, Nelson Area

Trygve Höy *and* Kathryn Andrew
Ministry of Energy, Mines and Petroleum Resources
Parliament Buildings
Victoria, BC
V8V 1X4 Canada

INTRODUCTION

This part of the 3-day excursion will examine excellent road exposures of the Lower Jurassic Elise Formation, the central volcanic unit of the Rossland Group, along Highway 6 south of Nelson. The Bonnington pluton, a satellite of the Nelson batholith, will be seen en route to Castlegar. The Trail Gneiss, Trail pluton, tectonics of fault systems near Trail, and the Reeves-MacDonald mine will also be examined. (See Lambert, this volume).

THE ROSSLAND GROUP

The Rossland Group is exposed in a broad arcuate belt in southeastern British Columbia, bounded to the east, north, and west by granitic rocks of the Middle to Late Jurassic Nelson batholith and in fault contact with lower Paleozoic rocks of the Kootenay Arc on the south (Fig. 1). It is intruded by numerous small, irregular stocks, most of which are correlative with the Nelson batholith (Little, 1964), by apophyses of the Nelson batholith, and by Coryell alkalic intrusions of Eocene age.

The Rossland Group is subdivided into a lower, generally highly deformed sequence of predominantly fine-grained clastic rocks of the Ymir Group and Archibald Formation, a middle part that is a thick accumulation of mafic flows and pyroclastic and epiclastic volcanic rocks of the Elise Formation, and overlying these, generally less intensely deformed clastic rocks of the Hall Formation. The age of the Elise Formation is bracketed by Sinemurian fossils in the Archibald Formation and Toarcian fossils in the overlying Hall Formation (Frebold and Tipper, 1970; Tipper, 1984); no fossils have been found in the Ymir Group.

The Rossland Group has been a major producer of precious metals, with more than 84,000 kg of gold and 105,000 kg of silver recovered from the Rossland camp (Fyles, 1984), the second largest gold producing camp in British Columbia, and more than 16,750 kg of gold and 190,000 kg of silver recovered from the Nelson and Ymir camps. Exploration continues to be active in these camps and throughout the length of exposures of Rossland Group rocks, particularly with the recent discoveries of significant gold deposits at both the Willa property near Silverton and the Tillicum property near Nakusp, both within roof pendants of the Nelson batholith north of Nelson.

Deposit types within the Nelson area include mesothermal gold-silver-copper and silver-gold-lead-zinc veins; porphyry or stockwork molybdenum-copper; skarn tungsten, molybdenum, or copper; a gold skarn deposit; and "conformable gold" deposits. "Conformable gold", an informal name applied to a variety of gold deposits that are conformable with either the foliation or bedding, is currently receiving considerable exploration interest. These deposits are associated with synvolcanic intrusions, have extensive alteration halos, and are sheared and foliated together with their host rocks. These deposit types are concentrated in the more northern exposures of the Rossland Group southwest of Nelson (Mulligan, 1952; Little, 1982a; Andrew and Höy, 1988), east and northeast of Ymir (Cockfield, 1936; McAllister, 1951), and in the Rossland camp itself (Fyles, 1984).

From: Joseph, N. L., and others, editors, 1989, Geologic guidebook for Washington and adjacent areas: Washington Division of Geology and Earth Resources Information Circular 86.

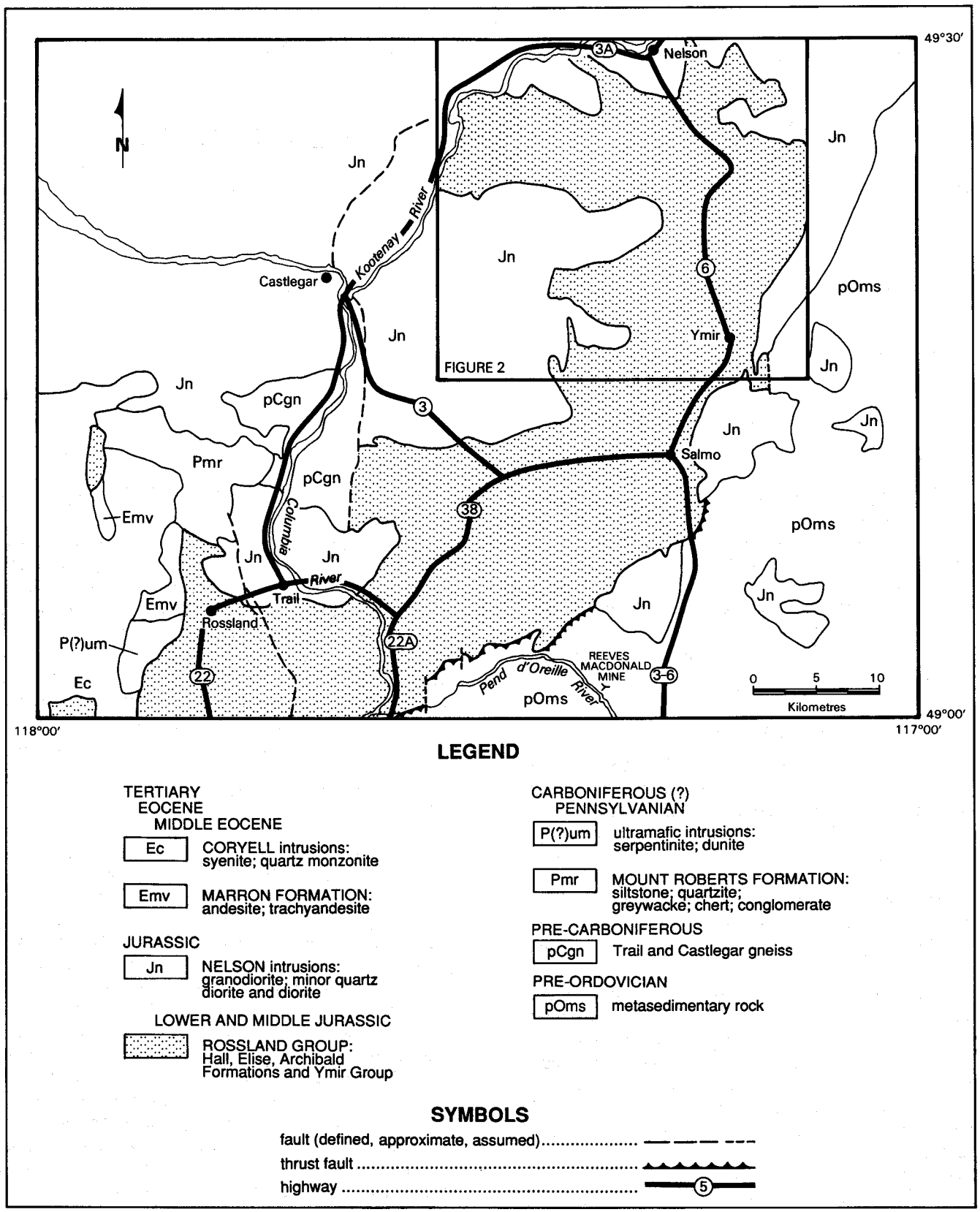

Figure 1. The distribution of the Rossland Group in southeastern British Columbia. Regional geology after Little (1960, 1964, 1982a, b), Fyles (1984), Simony (1979), Corbett and Simony (1984), and Parrish (1984).

GEOLOGY OF THE NELSON AREA

The structure of the Nelson area (Fig. 2) is dominated by north-trending tight folds and associated shears. The Hall Creek syncline, a tight south-plunging, west-dipping overturned fold, is the most prominent fold in the area. It is cored by the Hall Formation and repeats the Ymir-Archibald and Elise Formations in its limbs.

The Elise Formation south of Nelson, in the area crossed by the excursion, consists of an upper and a lower part. The lower part of the succession includes dominantly mafic flows and flow breccias as much as 1 km thick that lie with apparent conformity on the Ymir Group. Autoclastic fragments, including broken amygdaloidal pillows, characterize the lower Elise and are incorporated in flows 0.5 to 1 m thick. The upper part of the Elise Formation is a sequence of mafic to intermediate tuffs, flows, and subvolcanic intrusions, and minor epiclastic deposits. It is characterized by a number of cyclical sequences that typically comprise lapilli tuff and blocky tephra overlain by crystal tuff and fine tuff (Fig. 3). These units interfinger extensively, and, in detail, several units may be represented in a single outcrop. Conformable, locally sheared plagioclase porphyry bodies in the upper Elise, including the Silver King porphyry, are interpreted to be coeval subvolcanic intrusions.

The Elise Formation has been described in detail by Höy and Andrew (1988, in press).

The distinction between the upper and lower parts of the Elise on the west limb of the Hall Creek syncline (Fig. 2) is less evident. Here, the Elise Formation comprises 1.5 to 2 km of mafic, coarse pyroclastic breccias interlayered with minor augite porphyry flows and prominent sections of waterlaid crystal and lapilli tuff (Höy and Andrew, 1989).

Southwest of Salmo, the abundance of epiclastic rocks in the Elise Formation increases considerably (Fitzpatrick, 1985).

Rock and mineral chemical analyses of Rossland volcanic rocks (Beddoe-Stephens and Lambert, 1981; Ghosh, 1986; Höy and Andrew, 1988 and unpub. data) indicate that the Elise volcanic rocks are dominantly undersaturated basic volcanic rocks of mainly subalkaline but also alkaline affinity. Most analyses fall in the alkaline field on an alkali versus silica diagram (Fig. 4),

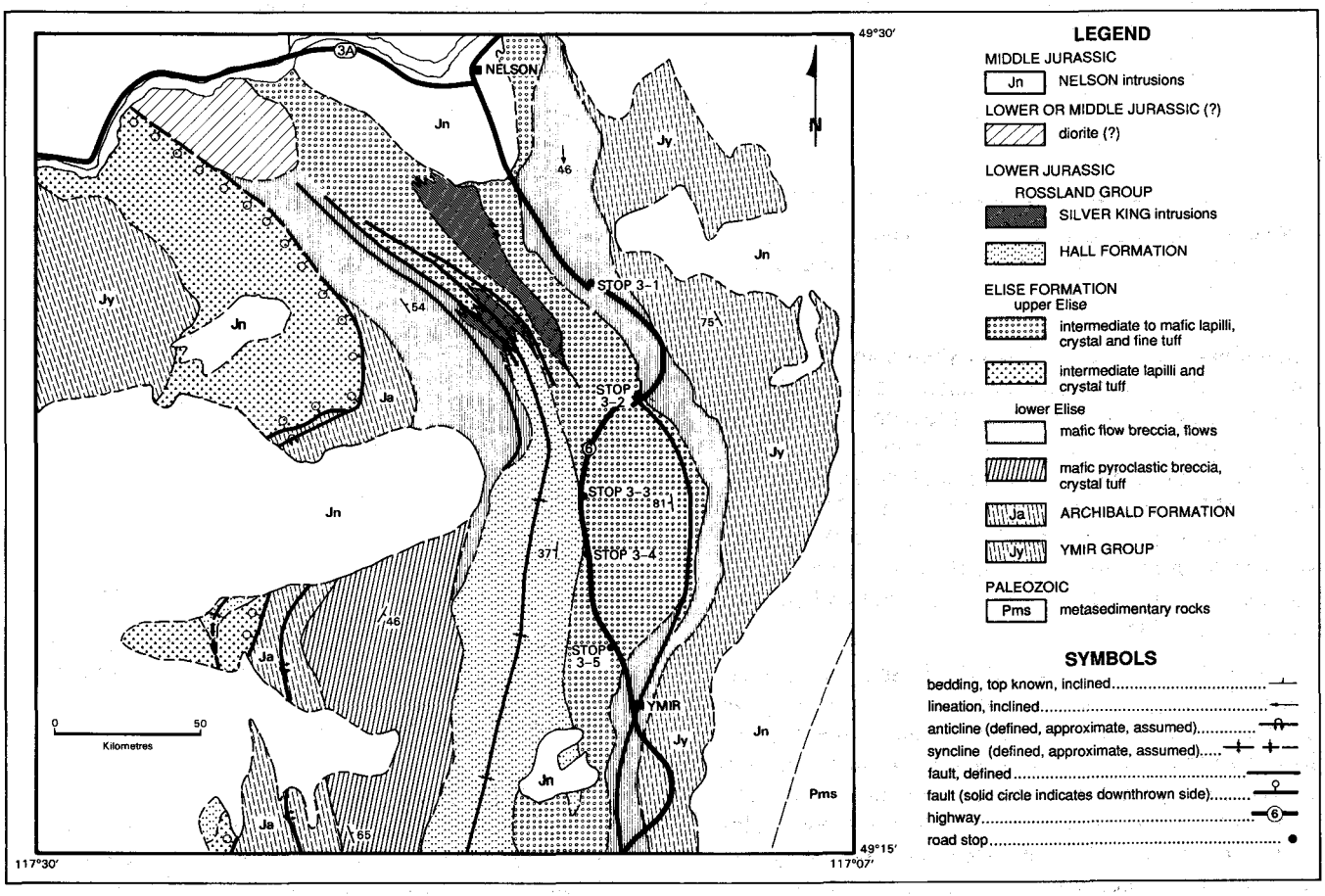

Figure 2. Geology of the Nelson map-area (from Andrew and Höy, 1988: Höy and Andrew, 1989; McAllister, 1951; Mulligan, 1952; Little, 1964, 1982a).

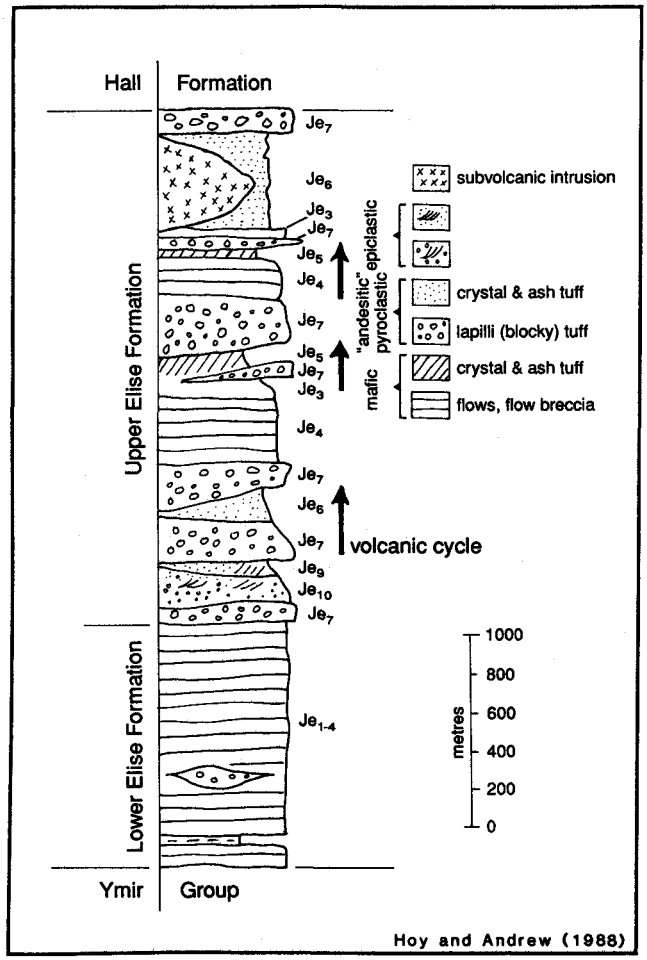

Figure 3. A composite volcanic succession of the Elise Formation along Highway 6 south of Nelson (from Höy and Andrew, 1988).

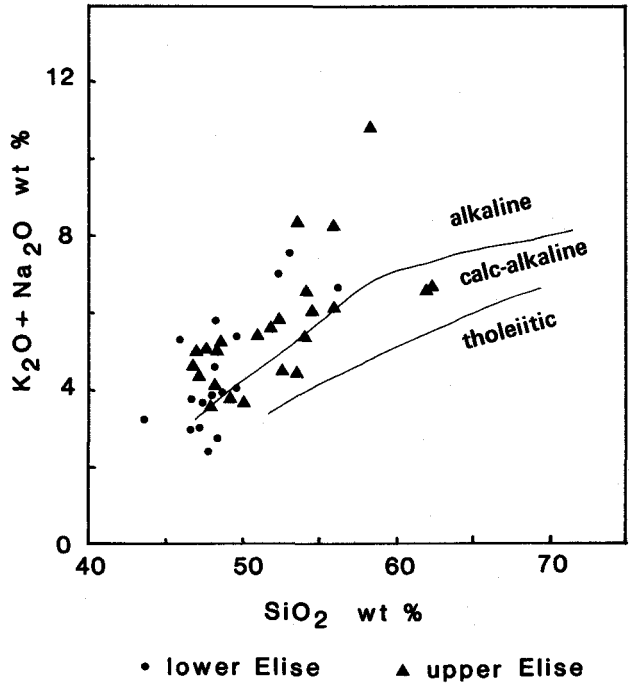

Figure 4. Alkali-silica plot of Elise Formation volcanic rocks showing the distinct alkaline trend; field boundaries from Kuno (1966).

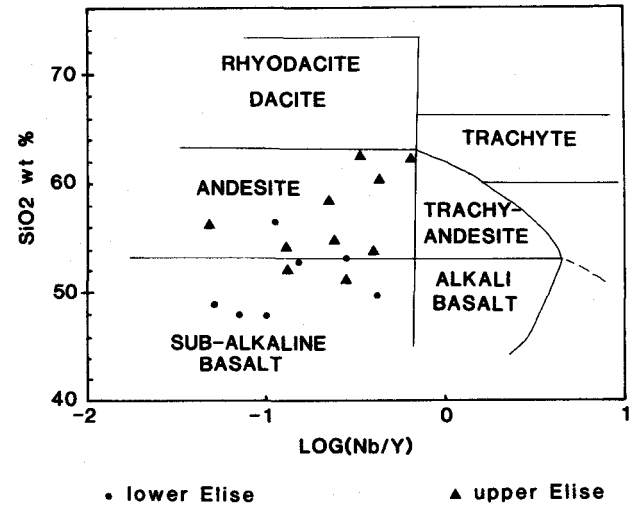

Figure 5. SiO_2-Nb/Y diagram illustrating the subalkaline nature of Elise volcanic rocks; lower Elise, dominantly basaltic; upper Elise, dominantly andesitic; field boundaries from Winchester and Floyd (1977).

due mainly to the very high potassium content. However, on plots using essentially incompatible trace elements (Fig. 5), they plot as subalkaline andesite and basalt. The contradicting whole-rock and trace-element geochemistry, low titanium content, high potassium/sodium ratios (Mackenzie and Chappell, 1972), and low titanium/vanadium ratios (Shervais, 1982) support a shoshonitic association for the Elise volcanic rocks, as has been shown by Beddoe-Stephens and Lambert (1981) and Spence (1985).

The shoshonitic nature of the Elise Formation supports the suggestion that the Rossland Group was deposited in a volcanic arc environment (Spence, 1985; Ray and Spence, 1986). Shoshonitic volcanism appears to be associated with disturbance or steepening of a subduction zone, possibly due to plate collision (Joplin, 1968; Gill, 1970). Rossland Group shoshonitic rocks may therefore record arc volcanism as a subduction zone was dying just prior to plate collision. This collision possibly involved accretion of Quesnellia in Terrane I (Monger and others, 1982) to the North American craton in Jurassic time. Continued compressional tectonics, bracketed by a late Early Jurassic age for the Rossland Group and a post-tectonic late Middle Jurassic age for the Nelson batholith, may have resulted in the intense regional deformation of Rossland Group rocks in the Nelson area.

ACKNOWLEDGMENTS

We thank M. Fournier, M. Holmes, and C. Lund for their capable, cheerful, and enthusiastic assistance during mapping in the 1987 and 1988 field seasons. Field visits and discussions with J. Fyles, V. Preto, R. Smyth, W. McMillan, G. Ray, R. St J. Lambert, P. Simony, and G. Nixon were both helpful and stimulating. Financial support for this project is provided by the Geological Survey Branch of the British Columbia Ministry of Energy, Mines and Petroleum Resources.

REFERENCES CITED

Andrew, Kathryn; Höy, Trygve, 1988, Preliminary geology and mineral occurrences in the Rossland Group between Nelson and Ymir, southeastern British Columbia: British Columbia Ministry of Energy, Mines and Petroleum Resources Open File Map 1988-1, scale 1:20,000.

Beddoe-Stephens, B.; Lambert, R. St J., 1981, Geochemical, mineralogical, and isotopic data relating to the origin and tectonic setting of the Rossland volcanic rocks, southern British Columbia: Canadian Journal of Earth Sciences, v. 18, no. 5, p. 858-868.

Cockfield, W. E., 1936, Lode gold deposits of Ymir-Nelson area, British Columbia: Geological Survey of Canada Memoir 191, 78 p., 1 plate.

Corbett, C. R.; Simony, P. S., 1984, The Champion Lake Fault in the Trail-Castlegar area of southeastern British Columbia: Geological Survey of Canada Paper 84-1A, p. 103-104.

Fitzpatrick, Mark, 1985, The geology of the Rossland Group in the Beaver Valley area, southeastern British Columbia: University of Calgary Master of Science thesis, 150 p., 2 pl.

Frebold, Hans; Tipper, H. W., 1970, Status of the Jurassic in the Canadian Cordillera of British Columbia, Alberta, and southern Yukon: Canadian Journal of Earth Sciences, v. 7, no. 1, p. 1-21.

Fyles, J. T., 1984, Geological setting of the Rossland mining camp: British Columbia Ministry of Energy, Mines and Petroleum Resources Bulletin 74, 61 p., 3 pl.

Ghosh, D. K., 1986, Geochemistry of the Nelson-Rossland area, southeastern British Columbia: University of Alberta Doctor of Philosophy thesis, 310 p.

Gill, J. B., 1970, Geochemistry of Viti Levu and its evolution as an island arc: Contributions to Mineralogy and Petrology, v. 27, p. 179-203.

Höy, Trygve; Andrew, Kathryn, 1988, Preliminary geology and geochemistry of the Elise Formation, Rossland Group, between Nelson and Ymir, southeastern British Columbia: British Columbia Ministry of Energy, Mines and Petroleum Resources Paper 1988-1, p. 19-30.

Höy, Trygve; Andrew, Kathryn, in press, The Rossland Group, Nelson map area, southeastern British Columbia: British Columbia Ministry of Energy, Mines and Petroleum Resources Paper 1989-1.

Joplin, C. A., 1968, The shoshonite association – A review: Geological Society of Australia, v. 15, p. 274-275.

Kuno, Hisashi, 1966, Lateral variation of basalt magma types across continental margins and island arcs: Bulletin of Volcanology, v. 29, p. 195-222.

Little, H. W., 1960, Nelson map-area, west-half, British Columbia: Geological Survey of Canada Memoir 308, 205 p.

Little, H. W.; McAllister, A. L.; Fyles, J. T.; Hewlett, C. G., 1964, Geology, Ymir (Nelson, east half), British Columbia: Geological Survey of Canada Map 1144A, scale 1:63,360.

Little, H. W., 1982a, Geology, Bonnington map-area, British Columbia: Geological Survey of Canada Map 1571A, 1 sheet, scale 1:50,000.

Little, H. W., 1982b, Geology of the Rossland-Trail map-area, British Columbia: Geological Survey of Canada Paper 79-26, 38 p.

Mackenzie, D. E.; Chappell, B. W., 1972, Shoshonitic and calc-alkaline lavas from the Highlands of Papua New Guinea: Contributions to Mineralogy and Petrology, v. 35, no. 1, p. 50-62.

McAllister, A. L., 1951, Ymir map-area, British Columbia: Geological Survey of Canada Paper 51-4, 58 p.

Monger, J. W. H.; Price, R. A.; Templeman-Kluit, D. J., 1982, Tectonic accretion and the origin of the two major metamorphic and plutonic welts in the Canadian Cordillera: Geology, v. 10, no. 2, p. 70-75.

Mulligan, Robert, 1952, Bonnington map-area, British Columbia: Geological Survey of Canada Paper 52-13, 37 p.

Parrish, R. R., 1984, Slocan Lake fault – A low angle fault zone bounding the Valhalla gneiss complex, Nelson map-area, southern British Columbia: Geological Survey of Canada Paper 84-1A, p. 323-330.

Ray, G. E.; Spence, Andree, 1986, The potassium-rich volcanic rocks at Tillicum Mountain–Their geochemistry, origin, and regional significance: British Columbia Ministry of Energy, Mines and Petroleum Resources Paper 1986-1, p. 45-49.

Shervais, J. W., 1982, Ti-V plots and the petrogenesis of modern and ophiolitic lavas: Earth and Planetary Science Letters, v. 59, no. 1, p. 101-118.

Simony, P. S., 1979, Pre-Carboniferous basement near Trail, British Columbia: Canadian Journal of Earth Sciences, v. 16, no. 1, p. 1-11.

Spence, Andree, 1985, Shoshonites and associated rocks of central British Columbia: British Columbia Ministry of Energy, Mines and Petroleum Resources Paper 1985-1, p. 426-442.

Tipper, H. W., 1984, The age of the Jurassic Rossland Group of southeastern British Columbia: Geological Survey of Canada Paper 84-1A, p. 631-632.

Winchester, J. A.; Floyd, P. A., 1977, Geochemical discrimination of different magma series and their differentiation products using immobile elements: Chemical Geology, v. 20, no. 4, p. 325-343.

[The road log for this paper is Part 3A of the road log that completes the suite of text for this excursion.]

Tectonics and Mineralization in Southeastern British Columbia: Road Log

Part 1A, Kimberley to Creston

[Text prepared by Trygve Höy.]

The first part of this 3-day excursion crosses the Purcell anticlinorium, from the Sullivan deposit at Kimberley to the town of Creston at the southern end of the Canadian portion of the Kootenay Arc (Fig. 1 of Höy, this volume). At the successive stops we will review the main lithologies of the Purcell Supergroup, beginning with an exposure of the lower part of the Aldridge a few kilometers south of Kimberley (Fig. 1) and moving generally up-section to a Kitchener Formation exposure at Moyie Lake (Fig. 2). Most stops are in the Moyie Lake area (Höy and Diakow, 1982), in the southern Purcell Mountains near the central part of the Purcell anticlinorium. The Moyie Lake area (Fig. 2) is cut by the northeast-trending Moyie fault that continues northeast across the Rocky Mountain Trench into the Rocky Mountains and southwest into Idaho and Montana. The fault appears to follow the locus of an older fault along which the north side was relatively down-dropped in pre-late Devonian time (Leech, 1958). North of the Moyie fault, a thick sequence of Cambrian rocks lies unconformably on upper Purcell Supergroup rocks, whereas south of the fault Devonian rocks unconformably overlie Purcell rocks. Late, right-lateral and reverse movement on the Moyie fault has resulted in a net vertical displacement of several kilometers, and at the north end of Moyie Lake, lower Aldridge rocks on the north hanging wall of the fault are juxtaposed against Kitchener Formation footwall rocks.

The structure of the area south of the fault, the "Moyie block" of Benvenuto and Price (1979), is dominated by the Moyie anticline, a northeast-plunging upright anticlinal fold. The western limb of the Moyie anticline is cut by the Moyie fault. Lower and middle Aldridge rocks are folded into moderately tight to open, north- to northeast-trending folds that are outlined by metagabbro sills. In the hanging wall immediately adjacent to the Moyie fault, folds are tight and locally overturned. The lower Aldridge is exposed in two overturned anticlinal folds just west of the north end of Moyie Lake and west of Cranbrook Mountain (Fig. 1).

Parts of the following road log are based on Höy and others (1985). See Höy (this volume for references cited.)

We will take Highway 95A from Kimberley to Cranbrook and Highway 3/95 from Cranbrook to Creston. Travel distance for this log is given in kilometers on the left, with miles in parentheses. The distance is cumulative only. *Set odometers.*

0 (0) **STOP 1. Lower Aldridge Formation.**

Mark Creek at Marysville. Lower Aldridge sedimentary rocks within a few meters of the Sullivan mine horizon are exposed in the gorge below the bridge. In general, these are thin wacke and argillite beds. The stop provides a basis for comparison with medium-bedded turbidites of the middle Aldridge Formation at Stop 2. Particularly note the bedding thickness here, which is thinner and less well defined than in the middle Aldridge.

The route continues south through essentially flat-lying, poorly exposed lower middle Aldridge Formation. Cliffs visible in places on the north side of the highway are metagabbro sills.

2.8 (1.75) The trace of the St. Mary fault, a right-lateral reverse fault with 12 km of apparent strike separation (Fig. 1). South of the fault, Cambrian rocks lying unconformably on Nicol Creek and Gateway Formations are exposed, whereas north of the fault, lower and middle Aldridge rocks are exposed (Höy, 1984c).

14.3 (8.9) St. Mary River. Outcrops of Kitchener Formation are present along the river bank.

22.4 (14.0) Junction with Highway 3/95 from Radium and Fernie.

From: Joseph, N. L., and others, editors, 1989, Geologic guidebook for Washington and adjacent areas: Washington Division of Geology and Earth Resources Information Circular 86.

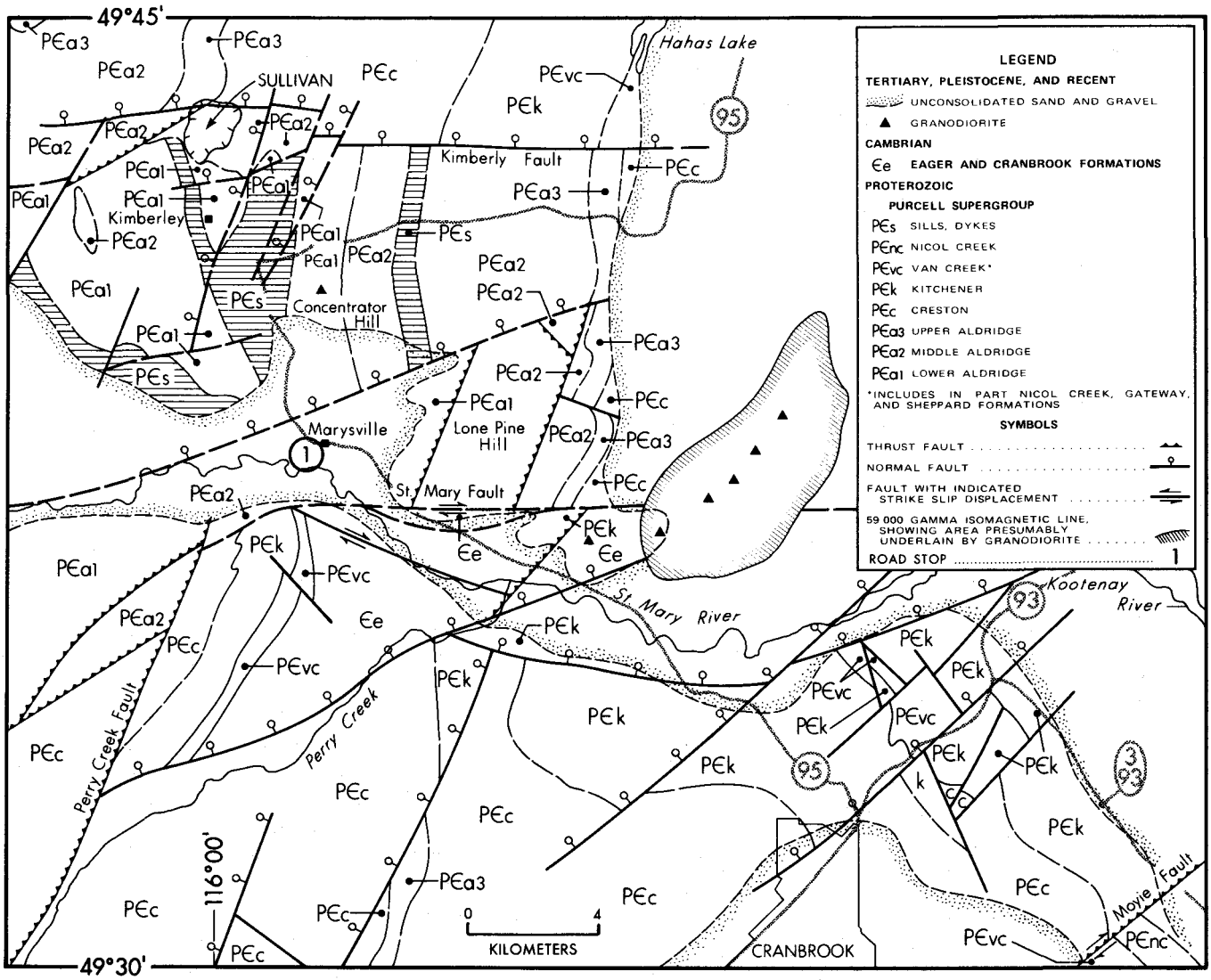

Figure 1. Geologic map of the Kimberley area, showing excursion route (after Höy, 1984c).

22.4 to 29.2 (14-18.2) City of Cranbrook.

41.8 (26.0) **STOP 2. Middle Aldridge Formation.**

A sequence of interbedded turbidites and argillites is exposed on the east side of the highway just opposite the Lumberton turnoff. It lies in the middle Aldridge, about 1,000 m above the base. The presence of AE turbidites as much as 1 m thick may be contrasted with the lower Aldridge lithology of Stop 1 and rocks seen in the Sullivan Mine.

The turbidite units here are generally graded only at the top, but a few are graded in a reverse manner in their basal part; the central part of coarser grained turbidite beds is commonly massive. Within the silt and fine sand-sized turbidites, parallel laminations, convolute laminations, ripple bedding, and flame structures can be seen. Sole markings, including grooves, flute marks, furrows and ridges, tool marks, and load casts are common. Current indicators in middle Aldridge turbidite deposits in the Moyie Lake area show a northerly transport direction. Concretionary bodies and rip-up clasts are present in some beds, and large crystal casts with the swallow tail form of selenite are in some of the more argillaceous beds.

46.8 (29.2) **STOP 3. Metagabbro** (Moyie sill).

Outcrops of a metagabbro sill are present on both sides of the highway and in a railway cut

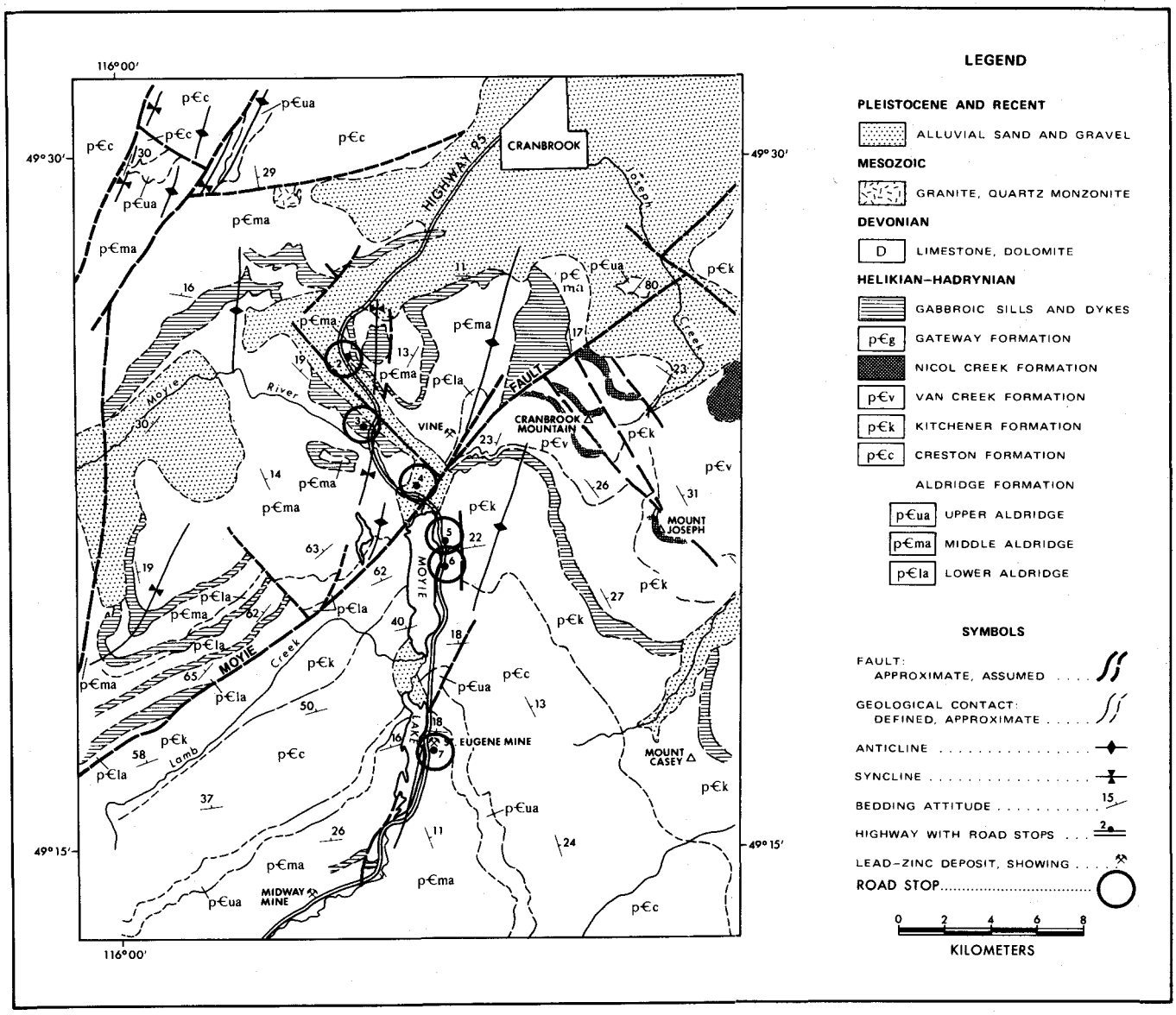

Figure 2. Geologic map of the Moyie Lake area, showing excursion route (after Höy and Diakow, 1982).

50 m to the north. Moyie sills comprise a considerable portion of the lower and middle Aldridge succession in the Purcell Mountains. They are regionally extensive and in the Moyie Lake area have been used as stratigraphic markers (Höy and Diakow, 1982). These sills have yielded a concordant U-Pb zircon age of 1,445 ± 10 Ma (Höy, 1988), an age similar to the 1,433 ± 10 Ma date of the Crossport C sill in Idaho (Zartman and others, 1982).

47.5 (29.7) **STOP 4. Middle Aldridge Formation.**

An outcrop on the north side of the highway just east of the Moyie River bridge exposes a middle Aldridge Formation "marker argillite". The marker argillite is at the base of the cliff toward the north end. It is about 3.5 m thick but includes as much as a meter of non-laminated sedimentary rock. This marker unit, and other similar units within the middle Aldridge, can be matched, lamination for lamination, over distances of several hundred kilometers.

48.8 (30.5) Trace of the Moyie fault.

Lower Aldridge rocks exposed in an anticlinal fold on the northwest or hanging-wall side of the fault are juxtaposed against Kitchener

Formation on its southeast side (Fig. 2). The Moyie fault is one of a number of northeast-trending faults that transect the Purcell anticlinorium. Repeated movements in the vicinity of these faults have had a fundamental control on stratigraphy and tectonics in southeastern British Columbia. The most recent displacement on the Moyie fault is right-lateral and reverse.

52.7 (32.9) **STOP 5. Kitchener Formation.**

Lower units of the Kitchener Formation are exposed on both sides of the highway on the east side of Moyie Lake. They are interbedded argillaceous dolomites and dolomitic argillites. Of particular interest are structures referred to as "molar tooth" that consist of small crenulated veinlets of calcite, approximately perpendicular to the bedding, which weather in negative relief. The form of these structures is quite varied, in some places being almost tubular. In addition, ripple-marked surfaces and scour-and-fill structures can be found in the more argillaceous units. Elsewhere in the Kitchener, stromatolites have been identified. The transitional contact with the underlying Creston Formation occurs about 100 m to the south.

54.5 (34.0) **STOP 6. Creston Formation.**

The Creston Formation crops out on the cliffs on the east side of the highway. The outcrops are quartzite and wacke beds in different shades of green, dull grey-green, and maroon from near the top part of the Creston Formation.

The numerous sedimentary structures include desiccation and syneresis cracks, mud-chip breccias, scour-and-fill structures, ripple marks, cross-bedding, and graded bedding generally indicative of shallow-water conditions. The characteristic bed-form is thin-bedded, commonly laminated argillite-siltite couplets.

55.9 (34.9) Exposures of the transition between the upper Aldridge Formation and the Creston Formation. The upper Aldridge is a dark, carbonaceous, thin-bedded argillite succession. The Creston in the transition zone is an alternation of basically green, rusty-weathering, thin argillites and wackes (Aldridge characteristic); relatively fresh surfaces are slightly green. Some sandstone lenses can be found, as well as silt "intrusions" and penecontemporaneous pull-apart structures.

59.3 (37.0) Town of Moyie.

60.5 (37.8) **STOP 7. St. Eugene mine.**

The entrance to the St. Eugene mine is on the east side of the highway. Adits and associated dumps can be seen up the hillside to the east. On the far shore of Moyie Lake, the Aurora mine, in an extension of the St. Eugene vein, is visible.

The St. Eugene mine lies about 2,000 m above the base of the middle Aldridge Formation. It was discovered in the late 1890s by a Kootenay Indian and acquired by the owners of the Trail smelter in 1905 to supplement diminishing supplies of concentrates. The mine exploited a ladder-vein system, striking WNW and dipping steeply south. The ore was essentially argentiferous galena and sphalerite. By 1916, when reserves were exhausted at 620 m below the headframe, production had amounted to 846,755 tons grading 12 percent lead, 1 percent zinc, and 200 g/tonne silver.

The veins produced lead, silver, and zinc that were derived mainly from argentiferous galena and sphalerite. Tetrahedrite and chalcopyrite were present in small amounts. Vein gangue minerals included quartz, biotite, chlorite, garnet, amphibole, pyrrhotite, pyrite, and magnetite with localized epidote, grunerite, and fluorite. These minerals occured in tabular ore shoots in steeply-dipping veins and within cymoid structures. Average mineable width was 2 to 3.5 m. This overall vein system can be traced for 3,500 m along strike and 1,400 m down dip.

67.3 (42.0) Midway mine. This is a small gold-quartz vein deposit. Associated metallic minerals are arsenopyrite, pyrite, galena, sphalerite, and chalcopyrite. The earliest records are from 1933, when the property was acquired by the B.C. Cariboo Goldfields Limited. Only a few ore shipments have been made.

91.3 (57.0) Town of Yahk. The lowest stratigraphic exposures of middle Aldridge rocks, in the block south of the Moyie fault, occur in the vicinity of Yahk. For the last 40 km the route along Highways 3/95 generally descends through middle Aldridge stratigraphy as it passes obliquely through the western limb of the north-plunging Moyie anticline.

The road trip continues westward along Highway 3 to Creston, a distance of approximately 40 km (25 mi). The remainder of the first day of this 3-day excursion is described in Part 1B of this road log.

Road Log: Part 1B, Creston to Nelson

[Text prepared by R. St J. Lambert]

This text accompanies the preceding Part 1A to complete the first day of the excursion. References cited in this log are listed at the end of Lambert (this volume).

After arriving in Creston, follow Highway 3 through the town centre, bearing right at the end of the main shopping street, and continue on Highway 3 to the north edge of the town. The route is now in the Purcell Trench, which is followed north for 80 km to the ferry from Kootenay Bay to Balfour (Fig. 1). From the ferry, we shall drive 36 km west to Nelson. This last part of the journey is described in Part 2 of this road log, which covers the second day of the excursion.

Note that all distances in the following log are in kilometers and participants are frequently directed to reset odometers to zero. This is to simplify mental arithmetic and to minimize error due to poorly calibrated odometers. An 8:5 conversion of kilometers to miles is usually adequate, as there are many location checks provided in the log, but more exactly, 1.6093 km = 1.0 mi.

0.0 Junction of Highways 3 and 3A at the north end of Creston. *Reset odometers.* Continue on Highway 3A along the line of the Purcell Trench.

3.2 Viewpoint. The roadcut is in the Creston Formation, which crops out ahead as far as Wyndell. From there, the Kitchener Formation is discontinuously exposed as far as 10.2 km.

11.6 First outcrop of the Bayonne batholith, followed to the north by schists of the Dutch Creek Formation, which occur in screens near the edge of the batholith.

21.2 IMASCO rock-crushing plant.

29.6 **STOP 8. Bayonne batholith.**

Good parking will be found on both sides of the road.

The Bayonne batholith, exposed here and at several more optional stops to the north, is a biotite-hornblende granodiorite which contains xenoliths of amphibolite. It is strongly crushed in most outcrops along the road, a feature which is related to faulting along the Trench, but it is also highly altered on the mountains to the east. Samples from the outcrops in the Trench have strongly disturbed isotopic systems. Elsewhere along the road section, the Bayonne consists of tonalite or quartz-monzonite, as well as other types of granodiorite. It has not yet been mapped in detail.

39.0 Glass House, which is built of embalming fluid bottles.

40.1 North contact of the Bayonne batholith. Although not exposed at the roadside or on the shore, the contact with the Dutch Creek Formation can be found some 300 m up the valley to the east.

40.2 **STOP 9. Toby Conglomerate.**

There is good parking on the west of the road.

At this locality, strongly stretched quartz clasts lie in a phyllitic matrix. The gradation into pebbly Horsethief Creek Group is well seen to the north. Note that there are 'clasts' of amphibolite in the latter: these were once dolomite clasts which reacted with the chloritic matrix during regional metamorphism (R. Adair and R. St J. Lambert, unpub. data).

49.7 The Heidelberg Inn.

65.7 Grey Creek. The route has passed through the Horsethief Creek Group all the way from the last stop to here.

67.2 Fresh outcrops of the Grey Creek stock. This is a biotite granodiorite of probable Cretaceous age, on the basis of its compositional affiliation. However, it yields only Eocene ages on separated minerals.

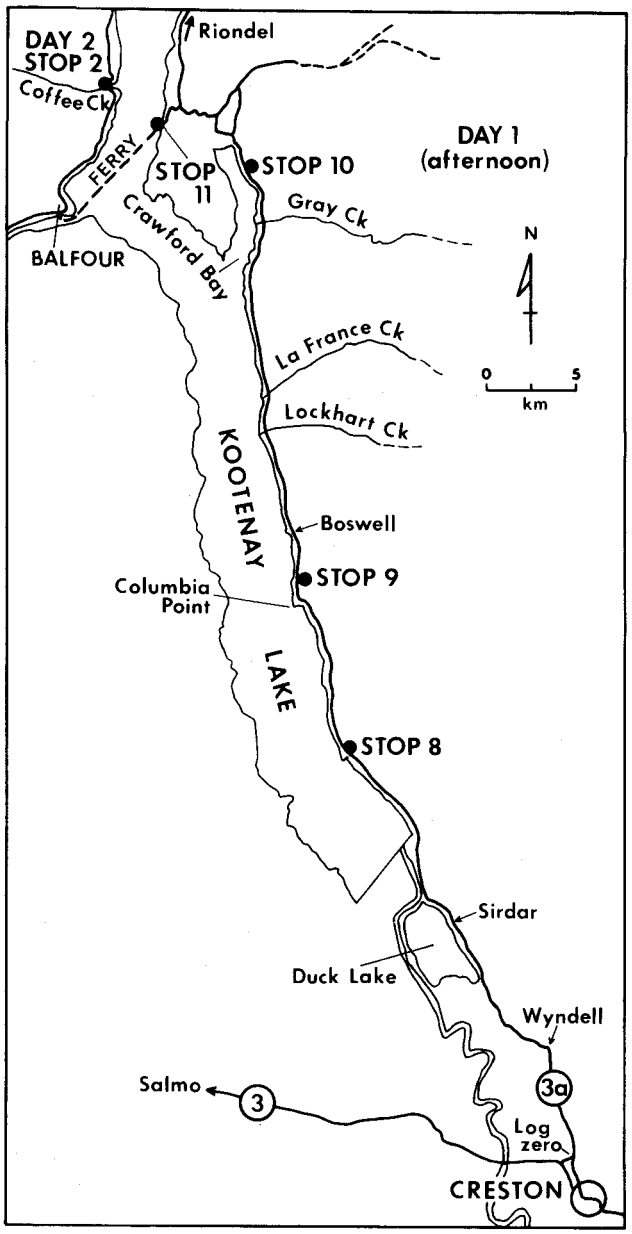

Figure 1. Route of field trip, Creston to Nelson.

70.0 **STOP 10. Badshot Formation.**

This stop may be made at any one of several suitable parking places.

Roadcuts and shoreline exposures display dolomitic marbles, which are associated with a highly varied suite of calc-schists, amphibolites and mica-schists, all of which are intruded by numerous pegmatites and microgranite dikes (Höy, 1982). This sequence must be assigned to the Mohican Formation and the Badshot Formation. The latter, however, was formerly identified as a single, major unit of marble. In the 2.0 km of road and shore exposures between the northern contact of the Grey Creek stock and the road junction at the northeast corner of Crawford Bay, there are at least seven bands of marble. Whether the marble is repeated by folding or whether there were several beds of impure dolomite has not been resolved. Some of the marbles contain diopside and tremolite, the latter occurring in crystals up to 80 cm long at the former timber landing stage on the shore. The assemblage diopside-tremolite-quartz-calcite is common in this section, closely defining the grade of metamorphism as the lower limit of the amphibolite facies.

78.5 **STOP 11. Lardeau Group.**

Park at the Kootenay Bay ferry terminal and examine the Lardeau Group in whatever time is available before the ferry arrives. The service is every 50 minutes in the summer, but only every 2 hours for the rest of the year.

From the last locality, the road has traversed Lardeau Group calc-schists, mica-schists, and amphibolites, with prominent garnetiferous pegmatites and aplites. To the north of the terminal, Kootenay Point (which is all private land) shows excellent sections in these rocks. Owners of the houses on the promontory do not normally object to small parties exploring the exact shoreline on the south side of the point, but it is recommended that visitors ask permission. Please do not remove any of the dramatic reaction zones which border the small granitic dikes! This promontory was mapped in detail by Winzer (1973).

After crossing the lake and leaving the ferry, turn west (left) at the end of the access road to the ferry terminal and proceed straight to Nelson.

[References for this log are given in the preceding article by Lambert.]

Road Log:
Part 2, Nelson to Balfour, Kaslo, and New Denver and Return to Nelson

[Text prepared by R. St J. Lambert.]

The day's route is designed to illustrate the nature of the upper part of the Paleozoic sequence along Kootenay Lake, the lower part of the Quesnellia sequence, and the structure of the Nelson batholith and its relation to the Valhalla complex to the west. The Ainsworth and Slocan mining camps are included in the route. The major tectonic features are the eastern boundary of Quesnellia and the Eocene extensional structures to the west of the Nelson batholith, including the Slocan Lake fault and the Valkyr shear zone.

The route from Nelson traverses the Nelson batholith (NB) eastward to near Balfour (Fig. 1), where it crosses on to the poorly exposed Milford Group and then the Lardeau Group. The latter group is seen in numerous roadcuts and along the shoreline between Balfour and Kaslo. A side excursion up Woodbury Creek traverses the Lardeau-Milford contact, near which are poor exposures of old Pb-Zn mines in the Ainsworth mining camp. The abandoned Bluebell mine is visible across the lake at Riondel. To the northwest of Kaslo, poor exposure in the river valley reduces inspection of the Lardeau, Milford, and Kaslo Groups to a minimum, but the black slate facies of the Slocan Group is well exposed. Nearer to New Denver, the Slocan Group is more varied and hosts the Slocan mining camp. Turbidites and graphitic limestones, together with satellites of the Nelson batholith, can be seen. From New Denver southward, the Slocan Group is traversed at first, but along Slocan Lake the valley follows the Slocan Lake fault and the Valkyr shear zone. Gneisses associated with these structures are well displayed. On the final leg of the route, east toward Nelson, dioritic and granodioritic phases of the Nelson batholith crop out over broad areas.

Note that all distances in the following log are in kilometers and participants are frequently directed to *reset odometers to zero*. This is to simplify mental arithmetic and to minimize error due to poorly calibrated odometers. An 8:5 conversion of kilometers to miles is usually adequate, as there are many location checks provided in the log, but more exactly, 1.6093 km = 1.0 mi.

0.0 North end of the bridge over the west arm of Kootenay Lake at the east exit from Nelson. Proceed northeast on Highway 3A.

2.5 **STOP 1. Nelson batholith.**

Parking on the south side of the road.

This roadcut displays medium-grained hololeucocratic garnetiferous granite with rare K-feldspar and beta-quartz phenocrysts, which are indicative of a high-pressure origin. Qualitative portable scintillometer measurements show this to be the only phase of the NB which contains appreciable uranium. This phase of the NB is known only from this locality.

16.4 **STOP 2. Nelson batholith.**

Roadcut at Crescent Beach Resort, with parking at its west end.

Porphyritic granodiorite of the NB crops out here; it contains K-feldspar phenocrysts as much as 5 cm long, abundant partially digested amphibolite xenoliths, leucocratic veins, and two mafic dikes of unknown age. D. K. Ghosh and R. St J. Lambert (unpub. data) record an age of 164 ± 1 Ma for concordant zircon from this granodiorite.

20.9 Last roadcut in the NB on the eastbound journey. All roadcuts between here and Nelson are in granodiorites of NB, except at Stop 1 (granite). The NB has not been mapped in detail: inspection of the forests and the thick scree, boulder clay, and soil cover will show why. Between here and Balfour, small roadcuts exhibit schists and amphibolites of the Lardeau (and Milford?) Group.

30.5 Balfour. Keep on the main road. From here to Kaslo all roadcuts are in the Lardeau Group, which consists of staurolite to sillimanite-grade schists. The grade rises from Balfour to Woodbury Point and then falls again to Kaslo. The Lardeau Group consists of a variety of mica-schists, calc-silicate schists, psammitic schists, and marbles. Intrusive (garnet-) amphibolite sheets are seen south of Ainsworth, and gneissic hololeucocratic biotite-granites are common in

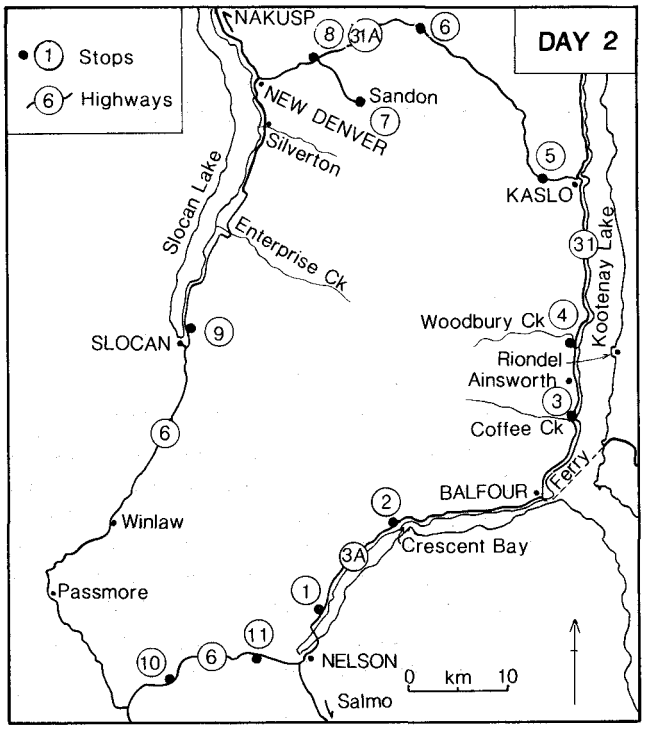

Figure 1. Route of field trip, Nelson to Balfour, Kaslo, and New Denver and return to Nelson.

all sections (Fyles, 1967). These granite-gneiss sills are subparallel to the principal foliation but are clearly intrusive. Analysis shows them to consist of a bimodal suite of tonalite and granite, both very rich in Sr and Ba, indicative of calc-alkaline affinity. No ages have been determined on them.

40.3 **STOP 3. Lardeau Group.**

Coffee Creek. Parking is available near the bridge. *Beware of traffic.*

The roadcut to the northeast presents the best continuous roadside dip section in the Lardeau Group. From west to east, we have (rough distances along the road): 140 m of biotite-schist (± carbonate), garnet-staurolite-schist and biotite-psammite; 25 m of scree at the culvert; 40 m of calc-silicate schists (with diopside-tremolite-calcite-quartz); an 80-m sill of gneissic microtonalite, which contains hololeucogranite sheets, with a shear zone at its base; 16 m of calc-silicate schists; 14 m of marble with included boudins of microgranite; and 15 m of calc-silicate schists with boudinaged micro-granite or microtonalite. Finally, all the way round the corner to the end of the outcrop, a microgranite cut by mafic dikes is exposed.

44.9 Ainsworth village center; hot springs.

49.0 **STOP 4. Lardeau and Milford Groups.**

Follow a minor road west up Woodbury Creek, leaving the main road at a narrow angle just north of Woodbury Creek bridge. The first part of the road is steep and rough and may be unsuitable for cars. It is only a few minutes' walk, though, to the parking spot at the first clearing after the road levels out in the hanging valley.

Two hundred meters farther along the road is a decline to the left, at the end of which a remnant of an exposure of the Vigilant vein is seen as a 5-cm seam of galena in a fissure striking across the track. On the road above, an old adit marks the same vein.

For the next kilometer, tourmaline-bearing two-mica, garnet schists of the Lardeau Group are discontinuously exposed. This series of outcrops is terminated by an abrupt gully, in which brecciated schists indicate that a fault occurs (the Lakeshore fault). For about 200 m the road crosses hornblende- and biotite-hornblende schists, terminating in a pure marble. This assemblage is in the Milford Group.

Another fault, known as the "Woodbury soft lead", crosses at this point. It is marked by a broad gully, which contains gossan, talc schists, graphite schists, and unidentified crush-rocks. To the west, more amphibolites are cut by meter-thick sheets of crushed garnetiferous microgranites, which are folded concentrically, in contrast to the multiply refolded basic rocks. A series of faults cuts this part of the section, which is extensively veined by carbonate. After a gap, a band of two-mica schist is truncated by a 150-m-thick 'granite' sheet, possibly an offshoot of the NB. Beyond the granite, chlorite schists are possibly part of the Kaslo Group.

Note the extraordinary contrasts in structural style and grade of metamorphism along this section: it may well contain the eastern boundary of Quesnellia. From the last outcrop, it is possible to continue west to the contact of the NB across the Kaslo and Slocan Groups, but we shall return to the main road and continue north. *Distances in the log do not include this side trip.*

70.4 Junction of Highways 3A and 31A in Kaslo. *Reset odometers here.* Follow 31A to New Denver, and after 0.5 km, turn left at the stop sign, staying on 31A. The road climbs up to another hang-

ing valley, passing across the Lardeau Group, which contains granite-gneiss sills, as it did farther south.

4.8 **STOP 5. Milford Group (?).**

Roadcut in mica schists and psammites, with parking on the south side.

These rocks may be in the Milford Group: note the sharp drop in metamorphic grade from the Lardeau Group, as at Woodbury Creek. There are at least seven bands of arenaceous-appearing rock in this section, three of which are: (1) a quartz-pebble arenite, (2) a microtonalite, and (3) a crushed porphyritic microgranite.

Mississippian conodonts have been recovered from near this roadcut.

7.0 Start of poor exposures of Kaslo Group greenschists.

9.4 Start of a long series of roadcuts in strike section in black slates and phyllites of the upper division of the Slocan Group. As throughout the Slocan Group, Sr and Nd in the slates has been partly derived from a Proterozoic continental source, but most of the Sr has probably come from sea water via calcareous organisms, the Slocan being generally calcareous.

24.7 On the north side of the road, the adit of a former Pb-Zn mine is to be seen. The mine was one of many near here which were developed in a galena-sphalerite vein system hosted by a fine-grained graphitic marble.

26.3 **STOP 6. Ruins of Retallack mine.**

This was formerly a Pb-Zn mine. As sphalerite was not recovered from this mine because of low prices for Zn and difficulty in processing, there is still plenty to be found. The host of this vein deposit is a thinly cleaved black slate. In the creek, 200 m east, boulders of mafic and ultramafic rocks from the Kaslo Group are common.

29.5 Campsite at the east end of Fish Lake, near the summit of the pass. From here the road descends toward New Denver through the Slocan Group, which is generally more arenaceous and less calcareous than it is farther east. Stratigraphy and structure are, however, poorly understood.

A magnificent series of beaver dams can be seen to the south of the road for the next several kilometers.

38.3 Turn south to Sandon. A side trip to this ghost town is well worth the journey.

44.2 **STOP 7. Sandon.**

The valley is in another black slate division of the Slocan Group. At Sandon, the Dickenson (Sylvana) mine is worked in a shear zone which contains disseminated PbS and ZnS. The processing plant and tailings pond are on the west side of the valley at Sandon. Access to the mine is from adits on the track up the mountainside to the southwest, which leads to Idaho Peak. (If individuals wish to gain access to the mine, *permission should be sought in advance* from the manager in New Denver.) The ore body is about 1 m thick and dips at about 20 degrees to the west under Silver Ridge (the area of highest Ag grades in the Slocan camp).

The ore has a lateral extent of about 1.5 x 0.6 km, but it occurs in 100-m-long lenses. Below the slates of the footwall of the shear zone is a veneer of meta-turbidites overlying a diorite, part of the NB system, but the shear zone cuts into the diorite in places. Pb isotopic studies by D. K. Ghosh and R. St J. Lambert show that the Pb in the ores in the Slocan Group is almost entirely derived from the sediments of the Slocan Group itself.

50.1 Sandon turn. Resume the route to New Denver.

51.3 **STOP 8. Satellite of the Nelson batholith.**

Park on the corner overlooking the valley to the west.

Weather permitting, there is an excellent view of the gneisses of the Valhalla Range. Outcrops of a porphyritic diorite of the NB suite are present along the roadside. Good sections of slates of the Slocan Group crop out within a few hundred meters to both east and west.

58.5 Junction of Highways 6 and 31A in New Denver. *Reset odometers to 0.0* and proceed south on Highway 6 over Slocan Group slates and meta-turbidites. At 4.7 km cross Silverton Creek.

17.2 Enterprise Creek. Beginning of exposures of gneisses associated with the Valkyr shear zone.

25.1 Start of narrow road. For 1.0 km there are excellent outcrops of the gneisses of the Valkyr shear zone, locally mylonitized in the Slocan Lake fault. A car may be parked at either end of this one-lane road and the cliffs examined by foot.

The danger from traffic is such that this section cannot be recommended for a large party.

29.9 **STOP 9. Gneisses of the Valkyr shear zone.**

The parking place is on the west.

This locality is opposite one of many new roadcuts in gneisses, and it offers good views of the Slocan valley and the regional structure. As elsewhere along this road section, the gneisses are a varied mixture of garnet-(sillimanite-) paragneiss, amphibolite, tonalite gneiss, and pegmatite and granite gneiss. Parrish and others (1988) obtained a suite of zircons from a 200-m-thick, strongly foliated mylonitic granite-gneiss of the Ladybird granite which crops out in this section. On a U-Pb diagram, these zircons lie in the midst of an array of points which define an age of 58 ± 1 Ma. It was argued that this closely approximated the age of movement on the Valkyr shear zone. Greenschist-facies mylonitization was dated by Rb-Sr on biotite as 54.5 ± 1 Ma. The paragneiss and amphibolite have not been dated precisely, but J. Schutze and R. St J. Lambert (unpub. data) obtained a 850 ± 50 Ma whole-rock isochron on the paragneisses from this section. Many of these rocks are strongly chloritized, and the meaning of this figure is not clear.

The Slocan Lake fault and its associated mylonites are subparallel to and below the Valkyr shear zone at this locality. The upper limit of the gneisses of the Valkyr shear zone appears to be by gradation into the NB; thus these gneisses might be part of the protolith of the NB, which has both mantle and lower-crustal Sr and Nd components (Ghosh, 1986).

32.1 Road junction to Slocan. Keep on the main road, which lies along the Slocan Lake fault, which separates the Ladybird granite suite from the NB and coincides with the Valkyr shear zone. Exposures are poor near the road, but the broad banding of the gneisses in the shear zone is clearly seen on the hills to the east.

78.5 Junction of Highways 6 and 3A; turn east toward Nelson.

83.9 **STOP 10. Diorites of the Nelson Batholith.**

Park on the south side of the road to examine hornblende diorite.

This unit was mapped as part of the NB by Little (1960). Ghosh (1986) showed that this diorite is continuous chemically with the granodiorites of the main part of the NB. It also appears to merge with the dioritic parts of the Bonnington pluton, but not enough detailed mapping has yet been done to establish the true relation.

91.5 Bridge over the Kootenay River.

94.6 **STOP 11. Granodiorite of the Nelson Batholith.**

Roadcuts in porphyritic NB granodiorite. This variety of the NB is probably the most typical and widespread type. It is locally rich in amphibolite xenoliths and, in this section, is cut by mafic dikes of unknown age.

98.3 Highway 3A passes under Highway 6 at the west end of Nelson. This is the end of the second day of the excursion, during which we have traveled 227 km.

Road Log: Part 3A, Nelson to Salmo

[Text prepared by Trygve Höy and Kathryn Andrew.]

On the morning of the third day of the excursion, we will drive along Highway 6 from Nelson south to Salmo. The distance traveled is given in kilometers on the left, with equivalent miles in parentheses. Safe parking is available at each stop.

The five stops along Highway 6 illustrate the variety of lithologies in volcanic rocks and comagmatic intrusive rocks of the Elise Formation, the volcanic succession in the central part of the Lower Jurassic Rossland Group. The Rossland Group and the geology of this area is described in the introductory paper by Höy and Andrew (this volume). Further details are given in Andrew and Höy (1988) and Höy and Andrew (in press).

The afternoon of the third day permits further examination of the eastern boundary of Quesnellia and, to the west, the relations of the boundary and several satellites of the Nelson batholith to crystalline complexes along a Tertiary extentional zone. In addition, the Bonnington and Trail plutons, the Salmo mining camp, and the Columbia River fault zone will be seen. [See the appendix for text covering the return trip to Spokane.]

0.0 (0.0) Junction of Highways 6 and 3A southwest of Nelson. The route begins in porphyritic phases of the Nelson batholith, and numerous exposures are visible on both sides of the highway.

7.8 (4.8) **STOP 1. Lower Elise Formation.**

Outcrops on the east side of the highway are coarse-grained augite porphyry flows and flow breccias of the lower Elise Formation. These are dark green, massive, compound flows (0.5-1 m thick) that have 20 to 40 percent augite phenocrysts commonly as much as 1 cm in diameter and only minor plagioclase phenocrysts. Typically the flows are autobrecciated; the subangular to subrounded fragments range from 2 to 10 cm in diameter. Due to the similarity of fragment and matrix composition, the autoclastic nature is in many places difficult to confirm. Generally, fragments are finer grained and more felsic and tend to have more augite phenocrysts and calcite amygdules than the matrix.

14.0 (8.7) **STOP 2. Lower and upper Elise Formation.**

On the south side of the highway is an outcrop of massive augite porphyry flows of the lower Elise. The massive flows here are, however, subordinate to those with autoclastic fragments.

On the north side of the highway is a 200-m-long outcrop of tuffaceous siltstone and conglomerate near the base of the upper Elise. The pale-green volcanic siltstone is interbedded with coarser, tuffaceous, plagioclase-rich beds that contain small lithic fragments. The siltstone is thinly bedded and finely laminated and has well-defined graded beds, basal scours, crossbeds, and channels indicative of emplacement in a high-energy, shallow-marine environment. The conglomerate is an interbedded sequence of conglomerate, grit, sandstone, and siltstone of predominantly volcanic or subvolcanic provenance. The most abundant clasts are subrounded boulders and cobbles of feldspar porphyry that are similar in texture and composition to the Silver King porphyry. Other clasts include chert, uncommon mafic volcanic, and rare felsic volcanic fragments.

18.4 (11.5) **STOP 3. Elise Formation, Hall Formation.**

A portion of the old highway is just east of the new highway and makes a good parking lot.

Pyroclastic and epiclastic volcanic rocks at the top of the upper Elise and argillite and siltstone at the base of the Hall Formation are exposed along the railroad tracks just below the old highway. North along the railroad tracks, plagioclase-augite crystal tuff and lapilli tuff outcrops of the Elise are typified by 5 to 20 percent subrounded pyroclasts ranging from 2 mm to 6 cm in diameter. Crystals in the matrix are dominantly euhedral plagioclase laths, and less than 5 percent are subhedral augite.

Approximately 150 m north along the exposure, the rocks appear to be dominantly

epiclastic volcanic conglomerates rather than pyroclastic. However, a prominent foliation (with associated flattening of all clasts) makes it difficult to more closely interpret the nature of these tuffites.

22.0 (13.7) Barrett Creek bridge.

23.4 (14.6) **STOP 4. Pillow basalt.**

Augite porphyry pillow basalt in the upper Elise is well exposed on the west side of the highway. The amygdaloidal pillows are as large as 1 m in diameter and have glassy rinds.

24.9 (15.5) **STOP 5. Plagioclase porphyry intrusion.**

Plagioclase porphyry, similar to the Silver King intrusions, crops out on both sides of the highway. The porphyry is characterized by 20 to 30 percent euhedral plagioclase phenocrysts as much as 1 cm across and less than 5 percent hornblende laths. This unit may be coeval with the Elise Formation because similar clasts of plagioclase porphyry are found in epiclastic units in the Elise. Supporting textural evidence for a subvolcanic origin for these plutons includes several percent resorbed quartz phenocrysts.

The excursion continues south to Ymir; the road log resumes with Part 3B.

Road Log:
Part 3B: Ymir to Nelway via Salmo and Trail

[Text prepared by R. St J. Lambert.]

The log in Part 3B is continuous with that in Part 3A; the route south first crosses a monzonite of the Coryell plutonic suite on the way into Salmo (Fig. 1). Turning west and northwest, the Bonnington pluton, a satellite of the NB, will be seen on the way to Castlegar. Between Castlegar and Trail, on the way south again, the Trail Gneiss and Trail pluton will be examined, and the complex geology of the Columbia valley will be visible. After passing through Trail, another outcrop of the gneisses associated with the Tertiary extension can be seen, followed by more RG on the road back to Salmo. South of Salmo, part of the old Salmo mining camp will be traversed. One of the major bounding faults of Quesnellia will be seen at Black Bluff, a magnificent section through Ordovician(?) slate and Cambrian phyllite. Before crossing the border, a side excursion will be made to the Reeves Limestone at the former Reeves-MacDonald mine area.

References cited in this part of the road log are list in the preceding article by Lambert.

Note that all distances in the following log are in kilometers and participants are frequently directed to reset odometers to zero. This is to simplify mental arithmetic and to minimize error due to poorly calibrated odometers. An 8:5 conversion of kilometers to miles is usually adequate as there are many location checks provided in the log, but more exactly, 1.6093 km = 1.0 mi.

27.0 Northern turnoff to Ymir; continue on the main road.

29.6 **STOP 6. Monzonite of the Coryell Suite.**

Beware of traffic! Park to the north of the roadcut. This suite of biotite-augite-monzonite has been dated at 51.3 ± 1.0 Ma (Rb-Sr mineral isochron; K. Berndt, Department of Geology, University of Alberta, written commun., 1983). A short distance to the east, by the railway line, a small quarry for ornamental stone was opened in a highly feldspathic phase of this stock because of its richness in iridescent feldspar.

39.9 Main street of Salmo. Continue west. To the southeast, the hills are carved from the Salmo pluton, a member of the Nelson batholith (NB) suite. Near Salmo, it intrudes the RG, but to the east it cuts the continental miogeocline or Terrane III, as do the NB and the Late Jurassic Kuskanax batholith to the north (Chamberlain and Lambert, 1985). These batholiths pin Quesnellia to Terrane III.

40.5 Junction of Highways 3 and 6; turn to the northwest toward Trail. The road crosses RG, cut by minor intrusions of the NB suite.

51.0 Junction of Highways 3 and 3B; turn northwest on Highway 3. Roadcuts in RG continue for another 4 km.

55.0 The Bonnington pluton (BP) is exposed in numerous roadcuts for the next 20 km.

60.9 **STOP 7. Bonnington pluton (BP).**

Park at any suitable point near the summit on the highway. The nearby roadcuts are all in xenolithic granodiorites.

Most exposures of BP show a high degree of epidotic and chloritic alteration, which accompanied brecciation. This alteration can also be well seen nearer Castlegar, before the descent down the hill into the Columbia River valley and the beginning of the outcrops of the envelope of RG to the northwest of BP.

76.9 Junction of Highways 3 and 3A. Turn west on Highway 3 toward Castlegar, crossing the Columbia River at 77.5 km.

78.7 Junction of Highways 3 and 22. *Reset odometers to 0.0 km* and turn south.

5.3 Kinnaird (Castlegar) Gneiss

10.9 Garnetiferous Trail Gneiss.

11.4 Genelle turn. Keep on the main road.

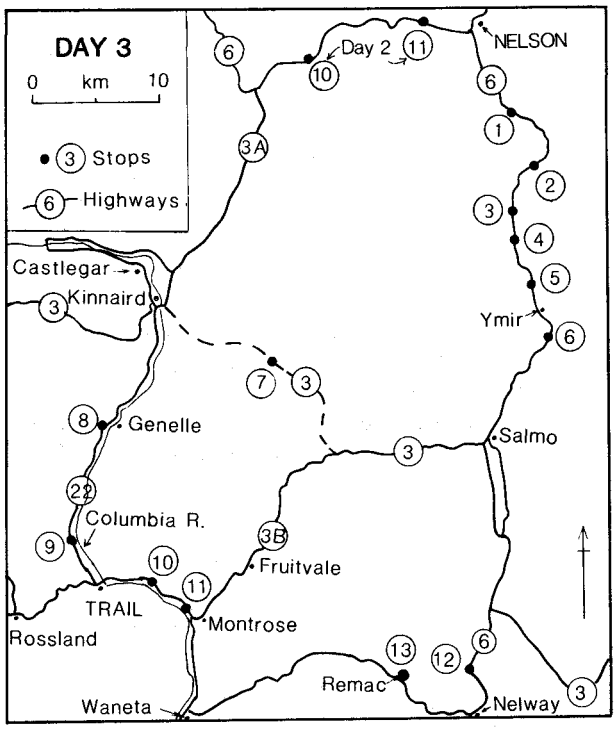

Figure 1. Route of field trip, Nelson to Salmo, Trail and Nelway.

13.3 Large roadcut in Trail Gneiss. This exposure is chiefly of paragneiss, but there is also an igneous component of dioritic to granodioritic composition.

14.0 **STOP 8. Trail Gneiss.**

Parking is available at any suitable point.

At this locality a sample of the Trail Gneiss had epsilon Nd and Sr values 160 m.y. ago which are virtually identical to those of the Trail pluton (Nd(t) = -6, Sr(t) = +30; Ghosh, 1986). These values indicate a moderate fraction of a crustal component in both complexes; they may also indicate that the Trail Gneiss is, at least, partly of the same age as the Trail pluton.

20.5 Roadcuts in the Trail pluton. This grey diorite is weakly gneissic and is intruded by biotite lamprophyre at the south end of the more northerly cut. There are good views to the east of the Trail Gneiss and the regional structure: the principal foliation in the gneisses dips gently east.

23.5 **STOP 9. Trail pluton.**

Park on the east side of the road.

The Trail pluton, a grey diorite as at the last roadcut, is cut by lamprophyre dikes in this section. At several other places in and around Trail and Rossland, these lamprophyres occur as diatremes, some of which contain xenoliths of basement gneisses.

424.3 Stoney Creek road.

26.7 Junction of Highways 3B and 22 in Trail; go east on 3B toward Salmo.

27.4 Center of the bridge over the Columbia River.

32.3 **STOP 10. Trail Gneiss (?).**

Park in the small turnoff west of the road.

Lineated Trail Gneiss is exposed in the river bank and appears to underlie the RG to the east. Both appear to be intruded by the Trail pluton just to the north. The area around this locality was described in detail by Simony (1979).

33.9 Junction of Highways 3 and 22A: the road to Waneta and the United States. Keep on the main road (Highway 3).

35.9 **STOP 11. Agglomerates in the Rossland Group.**

The parking place is on the west side of the road.

Opposite is a long section in agglomeratic andesites of the RG, cut by dikes of the NB suite. The route continues east in poorly exposed RG, at all points here in the greenschist facies, albeit at a lower grade than on the road south of Nelson. The metamorphism is regional and is pre-NB in age.

57.3 Junction of Highways 3 and 3B. Continue east toward Salmo.

67.8 Junction of Highways 3 and 6 at Salmo. Keep right, to the south, observing roadcuts in pyritiferous black slate at 70 km and RG at 72.0 and 73.4 km. The valley is bounded here to the east by small horsts of black slate, hornfelsed by Jurassic plutons, a faulted and brecciated remnant of one of which may be seen at the end of the ridge at 75.0 km.

81.9 Junction of Highways 3 and 6. Turn south on Highway 6 (Highway 3 east provides an excellent section of the Cambrian and the Windermere Group, including the Toby Conglomerate).

87.1 **STOP 12. Black Bluff fault.**

Park on the west side of the road.

The fault plane is exceptionally clearly seen on the east side of the road, where it is host to a biotite lamprophyre dike. It separates black slate on the north, mapped as Active Formation (Ordovician), from grey, multiply cleaved and folded phyllite and impure limestone of the Nelway Formation to the south. This is one of the three major faults which bound the RG (and thus Quesnellia) on its eastern edge. The others lie short distances to the west and east, together defining the "Argillite Belt", famous for its Pb-Zn deposits.

92.2 Turn west on a minor road to Waneta, which exits the main road about 100 m north of the United States border. *Reset odometers for the side trip.*

5.7 Thin beds of limestone are interbedded with black shale along the roadside. The black shales continue west in roadcuts for 0.5 km and are mapped as Active Formation (= Ledbetter Slate to the south). However, a random selection of these rocks gives a 160 ± 8 Ma Rb-Sr isochron with initial ratio = 0.7166 ± 0.0003 (Ghosh, 1986). Thus either these very low grade rocks are actually Middle or Late Jurassic or the region was subjected to hydrothermal metamorphism at that time.

6.8 **STOP 13. Reeves Limestone.**

Remac (Reeves-MacDonald) mine road junction.

The Reeves Limestone can be examined along the road to the west. The Reeves-MacDonald mine is one of a number of Pb-Zn deposits which were formerly mined in the Salmo camp, including the Emerald, Jersey, and H. B. deposits (Fyles and Hewlett, 1959; Addie, 1970). It produced, until its closure in 1977, 5.8 million tonnes of ore containing 0.98 percent lead, 3.42 percent zinc, and 3.4 g/tonne silver.

Ore deposits in the Reeves-MacDonald mine are in the south limb of the Salmo River anticline. They consist of "bands, lenses and disseminated grains of pyrite, honey-coloured sphalerite and galena, in dolomite" (Fyles and Hewlett, 1967, p. 144). The Reeves orebody, one of several orebodies in the mine, is in the limb and hinge zone of an attenuated syncline. A dolomite zone surrounds the orebody. Much of the ore is well banded and is locally highly contorted. Some ore is brecciated, with angular clasts of limestone and dolomite in a massive sulfide matrix. The origin of the Reeves-MacDonald and other southern Kootenay Arc deposits is enigmatic. Fyles and Hewlett (1959) described them as replacement deposits, controlled by phase 2 folds and by faults. Sangster (1970) and Addie (1970) both concluded that the deposits accumulated in small basins in a carbonate platform and were thus syngenetic. Höy (1982) suggests that the Kootenay Arc deposits were early, spanning the syngenetic-diagenetic interval, accommodating features cited as evidence for both syngenetic and Mississippi-type epigenetic origin.

Return to the main road, where the log restarts again at 0.0 km; *reset odometers.*

13.6 Junction with Highway 6, with Customs to the right.

13.7 Customs and Immigration; limited hours of operation.

End of road log for the third day of this excursion. See the appendix for the continuation from the border to Spokane.

Road Log:
Appendix : Log for Roads between Spokane, Washington, and Southeastern British Columbia

[Text prepared by R. St J. Lambert.]

Part I: Spokane, Washington, to Cranbrook, British Columbia

The route from Spokane to Cranbrook first follows the east-west valley of the Spokane River east to Coeur d'Alene, the same route that the great late-Pleistocene floods from glacial Lake Missoula followed in a westerly direction. Near Spokane, the valley is narrow, but at Post Falls it widens quickly to form a triangular basin, the Rathdrum Prairie. This is the first of many Tertiary basins which will be seen on this excursion. It is bounded on its east side by part of a broadly north-south linear feature which extends into Canada as the Purcell Trench and southward as far the Lewis and Clark line at the south end of Coeur d'Alene Lake and, possibly, though offset, as the set of linear faults along the western edge of the Idaho batholith.

From Coeur d'Alene, U.S. 95 will be followed north to the border. It follows a series of fault-controlled valleys as far as Junction 1 north of Bonners Ferry, where U.S. 95 is in the Purcell Trench, but the route then turns northeast to Cranbrook, out of the north-south linear system.

At Spokane, and at least as far as 35 km north of Coeur d'Alene and along the valleys of the St. Joe and St. Maries Rivers to the southeast, some 80 km distant from Coeur d'Alene, all valleys are underlain by varied combinations of the Columbia River Basalt Group (CRBG), Miocene and Pliocene sediments and Quaternary outwash gravels, the latter alone reaching a thickness of 330 m. These valleys are therefore pre-CRBG—that is, more than 15 m.y. old (Griggs, 1976). It seems that the last part of the Wanapum Formation (Wanapum Basalt of U.S. usage) of the CRBG, the Priest Rapids Member, may have poured over the edge of the plateau into the northern valley system, but the situation is not that simple, because flows of the CRBG are found at a wide range of elevations, particularly near Coeur d'Alene. Post-CRBG faulting has clearly occurred in many places. In addition, flows of early Wanapum age (Dodge Member; basalt of Dodge in U.S. usage) are found in valleys southeast of Coeur d'Alene, where there is evidence for the occurrence of a local feeder system in the form of eruptive centres and at least one sill.

The following only provides the briefest of introductions to the geology of northern Idaho and Washington; additional information can be obtained from the geologic map of the Sandpoint quadrangle (1:250,000; Aadland; Bennett; and others, 1979). Asterisks indicate possible stopping points on the journeys from Spokane to Canada and back again.

The road log is in kilometers throughout: an 8:5 conversion of kilometers to miles is usually adequate, as there are many location checks provided in the log, but more exactly, 1.6093 km = 1.0 mi.

0.0 U.S. Highway 95/Appleway junction in Coeur d'Alene, just north of Interstate Highway 90.

13.2* U.S. 95/Idaho State Highway (SH) 53 junction. Flows of the CRBG form a cliff to the east. The view south is to the line of hills south of Coeur d'Alene, at the beginning of the fault system associated with the Lewis and Clark line and the end of the Purcell Trench fault system.

21.6 CRBG on a cliff to east. The road continues NNE for another 3 km along the axis of the northern extension of Rathdrum Prairie, after which it turns north for 8 km.

35.0* This is southernmost roadcut of the Selkirk Crest batholithic complex, a group of Tertiary I-type plutons which makes up most of the mountains on the west of the Purcell Trench as far as the border. It is not to be confused with any part of the Priest River complex proper, which lies to its west.

41.0 Careywood store. The road follows a fault line for the next 17 km, along which a series of small basins have developed, perhaps pull-aparts. One is at Careywood, another at Cocolalla Lake. At

47.3 km the road traverses a transverse ridge, a horst across the valley, which bounds the Cocolalla basin.

55.1 Another transverse ridge.

69.0 Sandpoint. The southernmost outcrops of Precambrian gneisses in the west wall of the trench are northwest of Sandpoint.

72.7 U.S. 95/Idaho SH 200 junction at the outskirts of Sandpoint. The Hope fault, which trends ESE from here, is the northernmost of the series of major dextral faults which cause the feature known as the Lewis and Clark line.

84.0 On the western side of this valley, Precambrian gneisses form knolls on the ends of east-west spurs, which stand out from the main mass of the Selkirk Crest batholithic complex.

88.7 Pack River bridge. The road, railway, and river wind their way across another transverse horst.

93.0* Precambrian gneiss is present on both sides of the road. That on the east rests on a west-dipping thrust, placing it against the Belt Supergroup.

118.0* Geological site and parking place: "Glacial Lakes".

124.3 Bonners Ferry bridge.

128.6 U.S. 95/Idaho SH 2 junction. (Last gas and shops this side of the border). The road lies in the middle of another triangular basin, scattered in which are small inliers of granodiorite. The basin separates the Selkirk Crest batholithic complex from Belt Supergroup, which is intruded by a Cretaceous pluton.

148.9 U.S. 95/Idaho SH 1 junction; turn northeast to Cranbrook. The route crosses granodiorite to the top of the hill and then stays on Belt-Purcell Supergroup all the way to Cranbrook.

167.2 Customs and Immigration, Kingsgate; this facility is open 24 hours a day.

248.1 Cranbrook, junction of 4th Street and Highway 95; traffic lights.

Part 2. Canada/U.S. Border to Spokane

The return route to Spokane traverses the structurally complex valley of the Pend Oreille River on its way across the southern extension of the Kootenay Arc into the Newport fault zone. The route also crosses examples of the Cretaceous plutonic suite, which parallel the arcuate trend of the Paleozoic rocks to the west.

0.0 Canada/U.S. border. Customs and Immigration; limited operation hours.

Reset odometers at 0.0.

The route south lies in the Sandpoint quadrangle (Aadland, Bennett, and others, 1979). The road (now Washington State Route 31) crosses the border at 117°18′W and lies entirely within the Cambrian as far as the Tertiary basin south of Metaline Falls. The majority of the roadside outcrops are in shales (Maitlen Phyllite); on this route south, the Metaline Limestone starts to crop out near Metaline Falls.

16.7 Sullivan Lake road; begin descent into Metaline Falls.

20.4* Bridge over the Pend Oreille River. Metaline Formation shale and dolomite.

27.4 Roadcut in Cambrian slate and phyllite.

31.4* Tiger Formation: Tertiary sand and gravel.

32.5 Cambrian dolomite at the bend in the road.

34.3 The road enters a Tertiary-Quaternary pull-apart basin, developed on the trace of the Newport fault (NF).

43.1 Junction with State Route 20: continue south toward Newport. The low hills to the west are in the Paleocene or Eocene Phillips Lake granodiorite.

48.6 The barren hillside to the east is the southernmost exposure of the Windermere Group along this valley. Maitlen phyllite occurs at the base of the hills.

51.7 The Cretaceous Kaniksu batholith is to the east. To the west is the southern end of a range of low hills of Tertiary sands and gravels of the Tiger Formation.

56.5* Roadcut in leucogranite of the Phillips Lake pluton. The road follows a narrow valley along the Newport fault, which separates Kaniksu granitoids in the upper plate from the Phillips Lake pluton to the west. At 62.9 km (*) there is a roadcut in the Phillips Lake pluton.

63.6 David Thompson marker.

66.6 The NF swings to the west, so that we enter the upper plate of the Newport fault system. Immediately, there is a roadcut in the Kaniksu batholith, here a granodiorite. A small area of Wallace Formation of the Belt Supergroup lies south of this granodiorite and west of the road.

73.0 The route enters a large Tertiary basin, bounded on the west and south by the NF, which can be traced by mylonite on the ends of the bordering hills. The eastern edge is along a major set of faults in the Burke Formation of the Belt Supergroup. Tertiary gravel is common around the edge of the basin, indicating a Tertiary extensional regime.

93.2 Junction with SR 211; follow 211 toward Spokane.

99.9 At a cross-roads and milepost 11 is the location of the NF. A ridge of Precambrian gneisses lies to the south in the footwall of the NF.

100.9* Crushed rocks in the NF zone; 1 km farther south, outcrops of gneisses occur opposite a lake.

103.6* For about 1.5 km, outcrops of the Tertiary Silver Point quartz-monzonite can be seen.

117.6 Junction of SR 211 and U.S. 2. Turn to the west on U.S. 2, crossing over the southwest end of a small Tertiary basin.

120.0* Numerous roadcuts in the Cretaceous Fan Lake pluton.

127.0 Spokane County line; southernmost outcrop of granite.

129.0 Approximate edge of Columbia River basalt plateau.

163.0 U.S. 2 meets U.S. 395 at the northern edge of Spokane. The approximate distance from the international border to downtown Spokane is 170 km (106 mi).

Elements of the Cascades 'Collisional' Orogen: A Transect from the Methow Basin to the San Juan Islands

Michael F. McGroder, Robert B. Miller, Ralph A. Haugerud, and Mark T. Brandon

Elements of the Cascades 'Collisional' Orogen: Introduction to a Transect from the Methow Basin to the San Juan Islands, Washington

Michael F. McGroder
Department of Geological Sciences, AJ-20
University of Washington
Seattle, WA 98195

INTRODUCTION

Since the pioneering work of Peter Misch and his students from the 1950s through the 1970s, it has become widely accepted that rocks underlying the northern part of the Cascade Range (or North Cascades) in Washington experienced a major orogenic event in mid-Cretaceous time (for example, Monger and others, 1982). More recently it has become clear that the major pulse of contractional deformation, as determined from studies in fold belts both east and west of the axis of the range, took place in a fairly short time, between about 115 and 85 Ma (Brandon and others, 1988; McGroder, 1988). Although most thrusting in the Cascades had apparently ceased by early Late Cretaceous time, rocks in the mountain belt continued to deform in a complex manner as the newly assembled orogenic belt became dismembered along a series of northwest-trending strike-slip faults (for example, Monger, 1986).

Workers studying the record of the mid-Cretaceous orogenic event in different parts of the range have devised a number of orogenic models to explain the evolution of this belt (for example, Monger, 1986; Brown, 1987; Brandon and others, 1988; McGroder, 1988). However, the orogeny is expressed so differently in the various segments of the range (Fig. 1) and Tertiary modification has locally been so intense that no consensus has been reached on many important questions about orogenesis. Such first-order problems as the direction of regional thrust transport, the palinspastic position of most nappes, the mechanisms responsible for inverting and closing a long-lived sedimentary basin in the eastern Cascades, and the causal relation of thrust faulting to regional metamorphism remain controversial. One of the most significant uncertainties yet to be fully addressed is how the crustal shortening recorded in the two fold-and-thrust belts at the margins of the orogenic welt is accommodated in the deeper, internal portion of the mountain belt.

The structural evolution of the Cascades bears on a larger problem in Cordilleran tectonics—the nature of the Insular-Intermontane superterrane boundary—because the mountain belt straddles the margins of the two superterranes. These superterranes parallel the trend of the Cordillera and extend from Washington to northern British Columbia and Alaska (Fig. 1). While many workers (for example, Monger and others, 1982; Garver and others, 1988) speculate that the collision of the two superterranes precipitated the mid-Cretaceous orogeny in the Cascades, no consensus has emerged about whether that collision was driven by the subduction of a small ocean basin between the superterranes (Monger, 1986), by the impingement of a diverse group of coastwise-migrating terranes against a buttress or salient in the continental margin (Brandon and others, 1988), or whether the so-called "collisional deformation" was really nothing more than the manifestation of the collapse of a single continental-margin arc due perhaps to an increase in plate convergence velocities (van der Heyden and Woodsworth, 1988).

This introductory paper provides a geologic overview of the Cascades and briefly summarizes several competing models of orogenic development. The three succeeding papers in this guidebook (by McGroder and Miller, by Haugerud, and by Brandon) are intended first to provide the reader with a detailed account of more specific aspects of Cascade geology in the three main areas of the range, and second, to place those details in a regional context so that the various orogenic models can be most effectively evaluated.

From: Joseph, N. L., and others, editors, 1989, Geologic guidebook for Washington and adjacent areas: Washington Division of Geology and Earth Resources Information Circular 86.

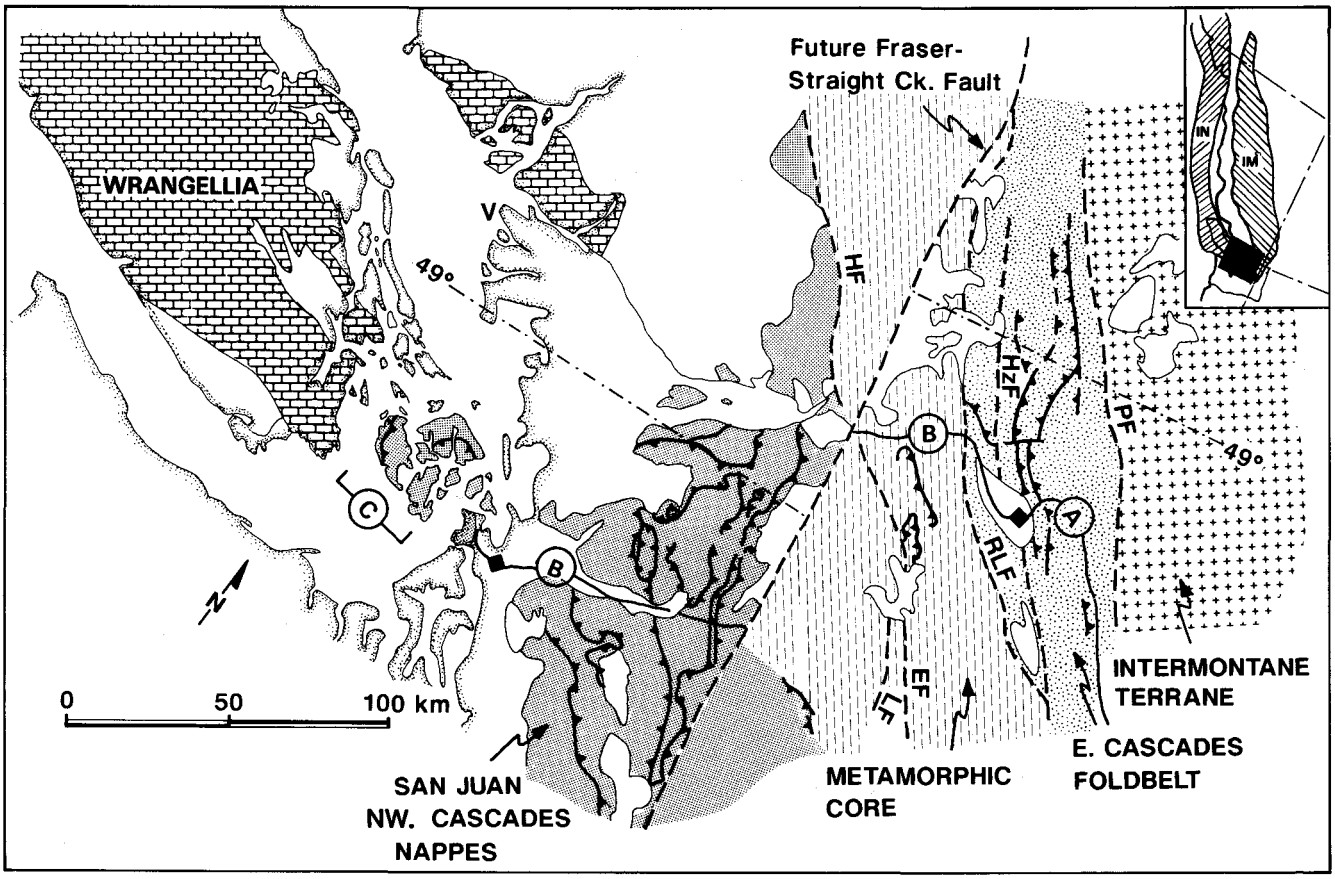

Figure 1. Simplified regional geologic map of northwestern Washington and southwestern British Columbia showing the five structural-metamorphic provinces or domains in the Cascade orogenic belt. Map has been restored to pre-Fraser-Straight Creek configuration after Monger (1985) and Vance (1985) in order to emphasize along-strike continuity of domains. Also shown is the approximate trace of Washington State Route 20, labelled by A, B, and C, which refer to areas covered by three companion field guides (A, McGroder and Miller; B, Haugerud; C, Brandon). V, Vancouver, British Columbia. Late- to post-orogenic faults: EF, Entiat fault; LF, Leavenworth fault; HF, Harrison fault; HzF, Hozameen fault; PF, Pasayten fault; RLF, Ross Lake fault. White areas denote plutons, Tertiary deposits, and alluvium. Insert shows Cascades straddling boundary between Intermontane (IM) and Insular (IN) composite terranes.

REGIONAL GEOLOGY

The Cascades orogen can be subdivided into five structural-metamorphic provinces or domains that trend roughly north-northwest (Fig. 1). The structures separating the domains are in most cases late- to post-orogenic, high-angle faults that have accommodated both dextral strike-slip and some vertical motion.

The westernmost structural element in the orogen underlies Vancouver Island and is composed of the Wrangellia terrane, which we will not visit on this trip. The Wrangellia terrane is one component of the Insular superterrane. Evidence suggests that the rocks now exposed on Vancouver Island were only mildly deformed during middle Cretaceous time (Muller, 1977).

East of there, in the northwest Cascades and San Juan Islands, a record of severe crustal contraction is preserved in a thick pile of thrust sheets (or nappes) that incorporate diverse terranes bearing radiometric signatures as old as Precambrian and fossils as young as late Albian (about 100 Ma) (Misch, 1966; Brown, 1987; Brandon and others, 1988). Many of the terranes in the San Juans and northwest Cascades probably evolved independently prior to their incorporation into the Cascades in mid-Cretaceous time, although all were probably adjacent to the continental margin by Late Jurassic time (Brandon and others, 1988).

Rocks in the most internal zone of the orogen, to the east of the area underlain by the nappes and separated from it by the Tertiary Fraser-Straight Creek fault, were undergoing regional greenschist to upper amphibolite facies metamorphism during Cretaceous and Paleogene time (Mattinson, 1972). Some parts of the metamorphic core were probably uplifted shortly after they were

buried; others (for example, Skagit Gneiss) remained deeply buried until the Eocene (Haugerud, 1985; Evans and Berti, 1986; McGroder, 1988).

Like the area adjacent to the west side of the metamorphic core, the area bounding the east side of the core is underlain by a fold-and-thrust belt, although less Cretaceous crustal shortening occurred there than in the western Cascades (McGroder, 1988). The eastern Cascades fold belt resides almost entirely within the Jurassic and Cretaceous Methow basin, although a Permian to Jurassic oceanic assemblage known as the Hozameen (Hozomeen of some authors) terrane is structurally interleaved in the fold belt as well (Misch, 1966). The Methow basin was the site of marine deposition until approximately late Albian time (Coates, 1974; McGroder, unpub. data). It ceased to be a sedimentary basin at the beginning of Late Cretaceous time due to infill of orogenic clastics, internal deformation, and regional uplift (McGroder, 1988).

The Intermontane composite terrane, which forms the eastern external zone of the orogen and the easternmost of the five structural-metamorphic domains in the Cascades orogenic belt, lies east of the Pasayten fault and will not be visited on this trip. At the latitude of the Washington Cascades, the Intermontane terrane is composed of Paleozoic and lower Mesozoic rocks of Quesnellia, which are intruded by numerous plutons of mostly Jurassic and Cretaceous age (Monger and others, 1982). Like rocks of Wrangellia in the western external block of the orogenic belt, Intermontane terrane rocks in the eastern external block were apparently only mildly deformed during the Cretaceous Cascades orogeny (McGroder, 1988).

During Late Cretaceous and Paleogene time, following the fairly short-lived episode of major crustal contraction, the crust underlying the Cascades was cut by a series of late- to post-orogenic, northwest-trending, high-angle, oblique-slip faults (Fig. 1) and probably at least one low-angle normal fault. These faults represent fundamental crustal breaks in the Cascades and have so dismembered the orogen that nowhere is it possible to walk up-structure out of the metamorphic core toward the external zones without crossing several of them. In the portions of the orogen that remained deeply buried during latest Cretaceous to Paleogene time, strain that may have accumulated as a result of transpressive motion on the oblique-slip faults transposed or obliterated fabrics formed during the early phases of orogeny. The multiple episodes of deformation that have affected rocks throughout much of the Cascades have caused two questions to take on added importance in recent years: How are given rock fabrics dated, and what do they signify about local or regional tectonic transport directions?

OROGENIC MODELS AND OUTSTANDING PROBLEMS

Mid-Cretaceous Orogeny

Models of Cretaceous orogenesis in the Cascades have historically fallen into two groups—those that treat development of the three major structural-metamorphic elements (northwest Cascades-San Juan nappes, metamorphic core, eastern Cascades fold belt) independently (Misch, 1966; Davis and others, 1978; Brown, 1987), and those that attribute metamorphism of the core and structural evolution of the Methow basin directly to the process of nappe emplacement (Brandon and Cowan, 1985; McGroder and Mohrig, 1987; McGroder, 1988).

The models of Misch (1966), Davis and others (1978), and Brown (1987) all call on a significant component of orogen-parallel strike-slip motion to assemble the major elements in the orogen. Misch (1966) and Davis and others (1978) interpreted the Ross Lake fault to have been an active dextral strike-slip fault that separated the Methow basin from the rest of the Cascades during middle Cretaceous time. However, more recent studies within the basin (McGroder, 1988; Garver and others, 1988) and along the Ross Lake fault zone (McGroder and Miller, this volume) have failed to support that hypothesis. Brown (1987) interpreted the major direction of thrust transport in the northwest Cascades to be toward the north-northwest on the basis of kinematic analysis of small-scale structures in deformed rocks in the northwestern Cascades. He hypothesized that northward translation of thrust sheets was driven in part by distributed displacement on a series of orogen-parallel dextral strike-slip faults. Neither Misch (1966), Davis and others (1978), nor Brown (1987) provided an explanation for the coeval development of the northwest Cascades contractional system and the Cascades metamorphic core.

The models of Brandon and Cowan (1985), McGroder and Mohrig (1987), and McGroder (1988) (and to a large extent, that of Misch, 1966) are based on the hypothesis that during the middle Cretaceous, the Cascade orogen was deforming predominantly upon west-vergent thrust faults. These workers argue that strike-slip activity was probably an important means of juxtaposing the diverse tectonostratigraphic elements prior to mid-Cretaceous time and was certainly important in dismembering the orogen in latest Cretaceous and Paleogene time, but it was not a significant factor in constructing the orogen during the peak of orogeny. These workers view the major constructional episode or orogeny to have occurred in an Alpine-type mountain belt with most relative motion occurring in the east-west (present coordinates) plane.

The most important problem facing those attempting to reconstruct the kinematic evolution of middle Cretaceous orogeny in the Cascades is determination of the direction, magnitude, and precise timing of nappe translation. Perhaps as significant a problem is whether upgraded rocks in the metamorphic core have an affinity with or are direct correlatives of units outside the core. Lithologically, many units in the core resemble rocks outside the core (for example, Napeequa schist and Twisp Valley Schist resemble the Hozameen terrane; see Haugerud, this volume). If these and certain other units inside and outside the core are directly correlative, then those correlations have major implications about prethrusting paleogeography and the location of sutures within the core.

Paleogene Tectonics

Unlike more classic collision belts like the Alps and the Himalaya, the Cascades orogen remained near the boundary between a continental and an oceanic plate even after the peak of contractional deformation. As a consequence, strains that accumulated as a result of oceanic-continental plate interactions during latest Cretaceous and Paleogene time, that is, *after* the peak of contractional deformation, were sufficiently intense that the orogen became thoroughly reconfigured late in its history.

Most kinematic models of development of the suite of northwest trending, high-angle faults that cut the Cascades ascribe their formation to dextral transpressive activity at the western edge of the North American plate (for example, Vance, 1982; Brown, 1987; Umhoefer, 1987). The key questions about these structures pertain to their age and the magnitude of displacement they have accommodated. If they were active as early as earliest Late Cretaceous time, then they must have played a role in mid-Cretaceous orogenic evolution (Brown, 1987).

The high-angle faults and associated structures also present important questions in their own right. For example, what is the temporal and kinematic relation of the moderate- to high-angle faults in the Cascades to the numerous low-angle normal faults that occur so extensively just to the east of the Cascades? Both sets of structures were apparently active at about the same time (McGroder and Miller, this volume). Related questions are: Did the Cascades faults parallel the paleoplate boundary? Did they localize along inherited crustal weaknesses formed during peak orogenesis? Or did they form where they did for both of the above reasons?

The key to these and the many related questions lies in detailed structural analysis of the pertinent structures coupled with continued geochronologic investigation. The three papers that follow summarize where current investigations stand and identify the most important unresolved questions in various parts of the Cascades. Many years of work lie ahead before workers can expect to reach agreement on many of the fundamental questions about Cretaceous and Paleogene tectonic history in the Pacific Northwest.

ACKNOWLEDGMENTS

I thank Susan Monsen, M. A. Korosec, J. A. Vance, and J. G. Evans for reviews of this manuscript. I gratefully acknowledge support from NSF EAR-8305937 to J. Bourgeois and EAR-8508239 to D. Cowan and J. Bourgeois. My studies in the Cascades have also been supported by a Shell Doctoral Fellowship. I also thank Steve Kiorpes for help with this manuscript.

REFERENCES

Brandon, M. T.; Cowan, D. S., 1985, The Late Cretaceous San Juan Islands-northwestern Cascades thrust system [abstract]: Geological Society of America Abstracts with Programs, v. 17, no. 6, p. 343.

Brandon, M. T.; Cowan, D. S.; Vance, J. A., 1988, The Late Cretaceous San Juan thrust system, San Juan Islands, Washington: Geological Society of America Special Paper 221, 81 p., 1 pl.

Brown, E. H., 1987, Structural geology and accretionary history of the northwest Cascades system, Washington and British Columbia: Geological Society of America Bulletin, v. 99, no. 2, p. 201-214.

Coates, J. A., 1974, Geology of the Manning Park area, British Columbia: Geological Survey of Canada Bulletin 238, 177 p., 9 pl.

Davis, G. A.; Monger, J. W. H.; Burchfiel, B. C., 1978, Mesozoic construction of the Cordilleran "collage", central British Columbia to central California: *In* Howell, D. G.; McDougall, K. A., editors, Mesozoic paleogeography of the western United States; Pacific Coast Paleogeography Symposium 2: Society of Economic Paleontologists and Mineralogists, Pacific Section, p. 1-34.

Evans, B. W.; Berti, J. W., 1986, Revised metamorphic history for the Chiwaukum Schist, north Cascades, Washington: Geology, v. 14, no. 8, p. 695-698.

Garver, J. I.; McGroder, M. F.; Umhoefer, P. J.; Bourgeois, Joanne, 1988, Pre- to syn-collisional sedimentation in the Jura-Cretaceous Methow-Tyaughton basin, northern Washington, southern British Columbia [abstract]: Geological Society of America Abstracts with Program, v. 20, no. 7, p. A274.

Haugerud, R. A., 1985, Geology of the Hozameen Group and the Ross Lake shear zone, Masilpanik area, north Cascades, southwest British Columbia: University of Washington Doctor of Philosophy thesis, 263 p.

Mattinson, J. M., 1972, Ages of zircons from the northern Cascade Mountains, Washington: Geological Society of America Bulletin, v. 83, no. 12, p. 3769-3784.

McGroder, M. F., 1988, Structural evolution of the eastern Cascades fold belt–Implications for late Mesozoic accretionary tectonics in the Pacific Northwest: University of Washington Doctor of Philosophy thesis, 140 p.

McGroder, M. F.; Mohrig, D., 1987, Piggyback to foreland transition in the Methow basin, Washington–2, A balanced cross-section of the Cascade orogen [abstract]: Geological Society of America Abstracts with Programs, v. 19, no. 7, p. 766.

Misch, Peter, 1966, Tectonic evolution of the northern Cascades of Washington–A west-Cordilleran case history. *In* Canadian Institute of Mining and Metallurgy; and others, A symposium on the tectonic history and mineral deposits of the western Cordillera in British Columbia and neighbouring parts of the United States, Vancouver, 1964: Canadian Institute of Mining and Metallurgy Special Volume 8, p. 101-148.

Monger, J. W. H., 1985, Structural evolution of the southwestern Intermontane Belt, Ashcroft and Hope map areas, British Columbia: Geological Survey of Canada Paper 85-1A, p. 349-358.

Monger, J. W. H., 1986, Geology between Harrison Lake and Fraser River, Hope map-area, southwestern British Columbia: Geological Survey of Canada Paper 86-1B, pp. 669-706.

Monger, J. W. H.; Price, R. A.; Templeman-Kluit, D. J., 1982, Tectonic accretion and the origin of the two major metamorphic belts and plutonic welts in the Canadian Cordillera: Geology, v. 10, no. 2, p. 70-75.

Muller, J. E., 1977, Evolution of the Pacific margin, Vancouver Island, and adjacent regions: Canadian Journal of Earth Sciences, v. 14, no. 9, p. 2062-2085.

Umhoefer, P. J., 1987, Northward translation of "Baja British Columbia" along the Late Cretaceous to Paleocene margin of western North America: Tectonics, v. 6, no. 4, p. 377-394.

van der Heyden, Peter; Woodsworth, G. J., 1988, Tectonic evolution of the Coast Plutonic Complex, British Columbia–Implications of new U-Pb and K-Ar dates: Geological Society of America Abstracts with Program, v. 20, no. 3, p. 239.

Vance, J. A., 1982, Paleogene magmatism and tectonics in the Washington Cascades [abstract]: Eos (American Geophysical Union Transactions), v. 63, no. 8, p. 173.

Vance, J. A., 1985, Early Tertiary faulting in the north Cascades [abstract]: Geological Society of America Abstracts with Programs, v. 17, no. 5, p. 415.

Geology of the Eastern North Cascades

Michael F. McGroder
Department of Geological Sciences, AJ-20
University of Washington
Seattle, WA 98195
and
Robert B. Miller
Department of Geology
San Jose State University
San Jose, CA 95192

CRETACEOUS GEOLOGY OF THE METHOW BASIN

Basin Morphology

The Methow basin is here defined as including those Mesozoic sedimentary and volcanic rocks lying between the Ross Lake fault on the west and the Pasayten fault on the east, excluding rocks assigned to the Bridge River-Hozameen terrane (Fig. 1). To the southeast the basin is in fault contact with a block of pre-Late Cretaceous crystalline rocks (Stop 1-1). Where basement to the sedimentary succession crops out near Hope, British Columbia, it is composed of MORB-type basalt of probable Early Triassic age (Ray, 1986).

Stratigraphy

Strata within the basin range in age from Lower Jurassic to Tertiary. On the basis of the continuity of stratigraphy from north to south, McGroder (1988) subdivided the Methow basin into northern and southern subterranes (Fig. 1). The discussion below summarizes the stratigraphy and basin evolution of the northern subterrane, where stratigraphic relations are well understood. Stratigraphic relations in the southern subterrane, where many units have been assigned to the Upper Jurassic-Lower Cretaceous Newby Group (Barksdale, 1975), are poorly known and will not be discussed here. However, we will visit a fieldtrip locality in the Newby Group (Stop 1-3).

The Mesozoic part of the section can be divided into four unconformity-bounded sequences that differ in thickness, composition, and other stratigraphic and sedimentologic details (Fig. 2): (1) Sinemurian through Bajocian clastics and minor volcanics of the Ladner Group, (2) Oxfordian through Tithonian and Hauterivian through Aptian fine-grained clastics of the Thunder Lake sequence and lower Jackass Mountain Group, (3) Albian and possibly Cenomanian strata of the Harts Pass and Virginian Ridge Formations and Winthrop Sandstone, and (4) Cenomanian(?) red beds and andesite breccias and flows of the Midnight Peak Formation (Coates, 1974; Barksdale, 1975; O'Brien, 1986). We refer to units in the lower two sequences in the discussion of basin structures, but their stratigraphic record has little bearing on middle Cretaceous tectonics in the region, so the reader is referred elsewhere for more comprehensive descriptions of those rocks (for example, Jeletzky, 1970; Coates, 1974; O'Brien, 1986). We will discuss rocks in sequences 3 and 4, which do contain a record of middle Cretaceous tectonic activity, in succeeding paragraphs.

Overlaps and Source Links with Adjacent Terranes

Overlaps and source links with terranes neighboring the Methow basin have been established with varying degrees of certainty. The timing of juxtaposition of the basin with the Intermontane terrane to the east can only be demonstrated unequivocally by Tertiary strata of the Island Mountain volcanic unit, which straddle the Pasayten fault (White, 1986). However, a good case has been made that units overlying the Mount Lytton Complex in the western Intermontane terrane, near Spences Bridge, B.C., are equivalent to Aptian-Albian strata west of the Pasayten fault (Monger, 1985). The Spences Bridge strata are largely andesitic volcanic rocks, which led Monger (1985) to interpret them as a late Early Cretaceous arc coupled with a forearc basin (Methow) to the west. Previous workers (Tennyson and Cole, 1978)

From: Joseph, N. L., and others, editors, 1989, Geologic guidebook for Washington and adjacent areas: Washington Division of Geology and Earth Resources Information Circular 86.

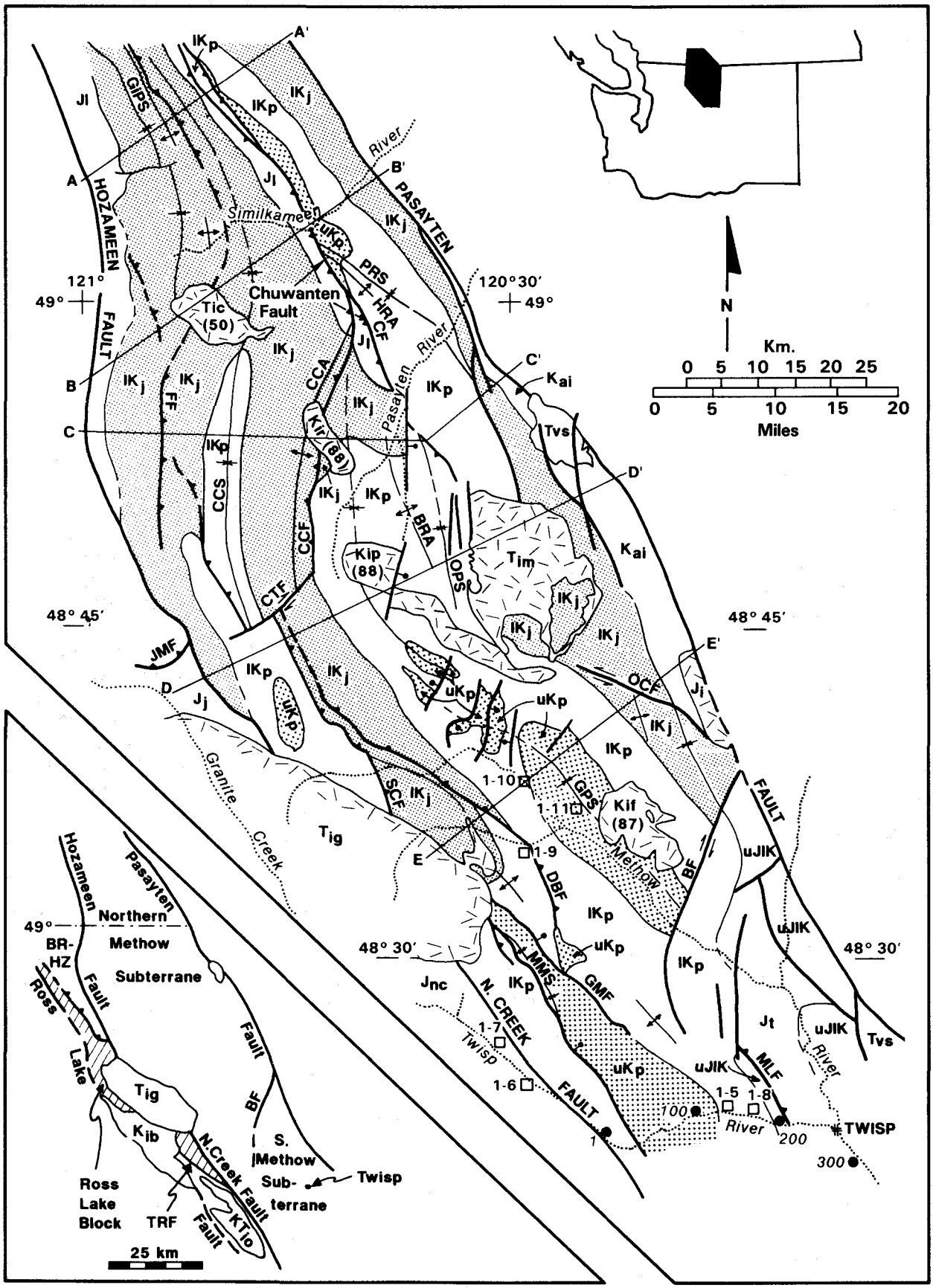

A'
A
B'
B
C
C'
D'
D
E'
E
IKp
IKj
Jl
GIPS
HOZAMEEN
FAULT
PASAYTEN
River
Similkameen
uKp
PRS
HRA
CF
Chuwanten
Fault
Tic
(50)
121°
49°
120°30'
49°
Pasayten
River
CCA
Kir
(88)
FF
CCS
CCF
CTF
BRA
OPS
Kip
(88)
Tim
Kai
Tvs
48° 45'
48° 45'
JMF
Jj
Granite
Creek
SCF
Tig
1-10
1-11
GPS
Kif
(87)
Methow
BF
DBF
1-9
uJIK
48° 30'
48° 30'
Jnc
N. CREEK
FAULT
MMS
GMF
1-7
Twisp
1-6
1
100
River
200
300
1-5
1-8
MLF
Jt
TWISP
River
N
Km.
0 5 10 15 20 25
0 5 10 15 20
Miles
Hozameen
Pasayten
Northern
Methow
Subterrane
49°
BR-
HZ
Ross
Fault
Lake
Tig
Kib
N.Creek Fault
Fault
BF
S.
Methow
Sub-
terrane
Twisp
Ross
Lake
Block
TRF
KTio
25 km

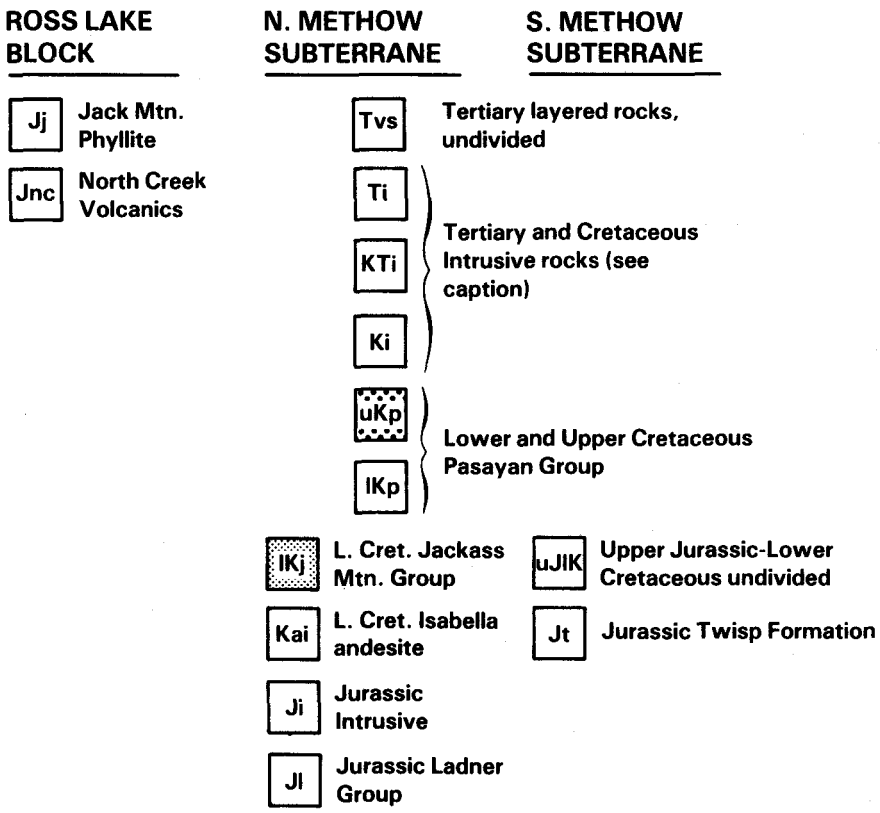

Figure 1 (Facing page). Simplified geologic map of the eastern Cascades fold belt, north of Twisp, Washington. Field trip stops are shown by boxes. Washington State Highway 20 follows the Methow River. See explanation for unit names. The Intermontane terrane underlies the area east of the Pasayten fault. Other names, not in legend: BR-HZ, Bridge River-Hozameen terrane; Kib, Black Peak batholith; Kif, Fawn Peak stock; Kip, Pasayten stock; Kir, Rock Creek stock; KTio, Oval Peak batholith; Tig, Golden Horn batholith; Tim, Monument and Lost Peak stocks. Faults: BF, Boesel fault; CTF, Canyon Creek tear fault; DBF, Driveway Butte fault; FF, Freezeout fault; GMF, Gardner Mountain fault; JMF, Jack Mountain fault; MLF, Mocassin Lake fault; OCF, Ortell Creek fault; SCF, Slate Creek fault. Folds: BRA, Buckskin Ridge anticline; CCA, Canyon Creek anticline; CCS, Castle Creek syncline; GPS, Goat Peak syncline; GiPS, Gibson Pass syncline; HRA, Holdover Ridge anticline; MMS, Midnight Mountain syncline; OPS, Osceola Peak syncline; PRS, Ptarmigan Ridge syncline. Numbers 1 - 300 along lower Twisp River refer to shot points on COCORP Washington Line 7. Cross-section C-C' is shown in Figure 3; the other cross-sections are not discussed. See Figure 2 for subdivisions of Pasayten and Jackass Mountain Groups.

had also interpreted Methow sediments as recording the unroofing of a volcanic-plutonic source terrain east of the Pasayten fault. More U-Pb zircon dating will need to be conducted before the volume and areal extent of Early Cretaceous volcanic and plutonic rocks can be quantified and the arc-forearc hypothesis verified. Todd (1987) reported that dikes of similar composition and age (early Late Cretaceous) occur east and west of the Pasayten fault, which she interpreted to mean that major motion on that structure had ceased by that time.

Pre-late Early Cretaceous links between the Methow and Intermontane terranes are difficult to verify, but it is conceivable that rocks as old as Lower to Middle Jurassic (Ladner Group, Ashcroft Formation) that now occur on opposite sides of the Pasayten fault are lateral equivalents of one another (cf. Coates, 1974; Travers, 1978). In summary, the Pasayten fault has a long and complex history, and the problem of ascertaining when terranes on opposing sides of this structure were first juxtaposed is difficult to resolve.

The oldest source link between the Bridge River-Hozameen terrane to the west and the Methow basin is the chert-pebble conglomorate in the middle Albian Virginian Ridge Formation. Chert pebbles in the Virginian Ridge contain radiolarians of Triassic or Jurassic age (Trexler and Bourgeois, 1985). Cherts that have similar ages have been reported from the Hozameen terrane by Haugerud (1985). Although Albian time could conceivably be the first time the Methow and Bridge River-Hozameen were adjacent to one another, it is impossible to rule out the possibility that they were sutured together as early as the middle Jurassic.

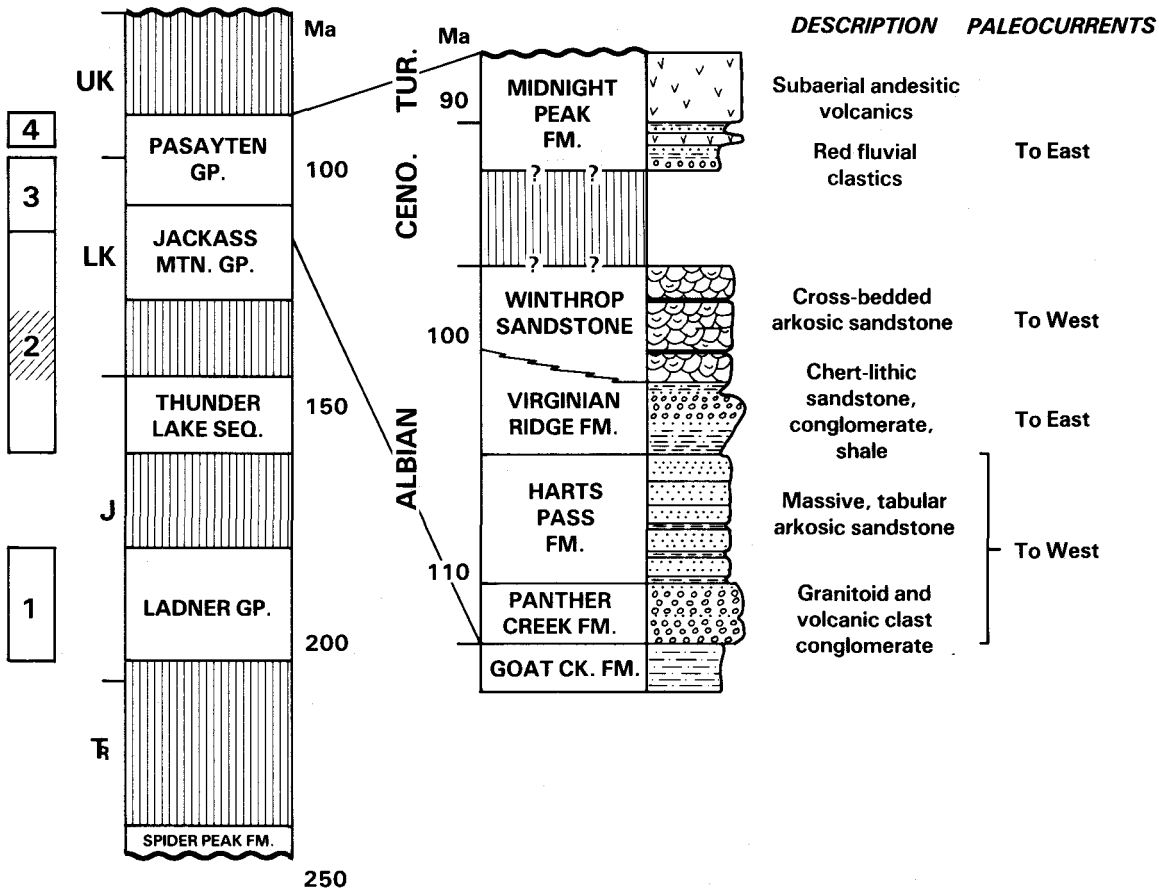

Figure 2. Stratigraphic column showing stratigraphy of the Methow basin. Numbers 1 to 4 refer to first-order depositional sequences most of which are unconformity bounded. Information on paleocurrents obtained from Cole (1973), Kleinspehn (1985), and D. Mohrig (Univ. of Washington, unpub. data).

Stratigraphic Record of mid-Cretaceous Orogeny

The Methow basin was the site of active deposition before and during the onset of crustal deformation in the Cretaceous and is therefore a logical place to address problems about the Cretaceous orogenic evolution of the Cascades. The long-lived basin, which had received sediment exclusively from the east throughout most of its Jurassic and Early Cretaceous history, began to close in middle Albian time, as indicated by the inversion of the basin and by the onset of widespread dispersal of coarse clastic sediment from an uplifted western source terrane (Cole, 1973; Coates, 1974; Tennyson and Cole, 1978; Davis and others, 1978). The west-derived chert-pebble conglomerate in the Virginian Ridge Formation came to be widely regarded as the deposit that heralded the arrival of exotic terranes to the west (for example, Cole, 1973; Tennyson and Cole, 1978; Davis and others, 1978; Trexler and Bourgeois, 1985).

Recent workers view the greatest change in depositional trends within the basin as marked by the rapid acceleration of basin-marginal uplift and basin subsidence. This is recorded in the conglomeratic Panther Creek Formation and the thick, turbiditic Harts Pass Formation, which underlie the Virginian Ridge (Garver and others, 1988). Granitoid clasts in the conglomerate record uplift of a plutonic terrane east of the basin. Sandstones and shales of the Harts Pass Formation, which is lower to middle Albian in age, exceed 3.5 km in thickness and record tectonic subsidence in the basin. The two units overlying the Harts Pass Formation, the chert-lithic Virginian Ridge Formation and the arkosic, east-derived Winthrop Sandstone, are also very thick (4-5 km cumulatively). Their thickness, provenance, and paleocurrents record: (a) continued subsidence within the basin, and (b) east-west swings of the topographically lowest point in the basin. The onset of basin subsidence may mark the beginning of thrust faulting in the region, but we are uncertain of the geometry of that thrusting.

The Midnight Peak Formation represents the fourth and uppermost unconformity-bounded sequence in the basin. While underlying units may contain the record of early thrusting in the eastern Cascades, there is little evidence in the form of widespread angular unconfor-

mities within those units that the sedimentary basin itself was deforming at that time. The Midnight Peak Formation, however, appears to reflect the encroachment of active thrust deformation into the basin (McGroder, 1988). The Midnight Peak is composed of two informal members, one known as the Ventura member and composed of red clastic rocks, deposited on east-sloping alluvial plains (Mohrig and Bourgeois, 1986) and the other composed of interbedded andesitic volcanic breccias and flows from widespread arc volcanism of probable early Late Cretaceous age. Both the red beds and volcanic rocks lie above a regional unconformity that is markedly angular in the vicinity of mapped thrusts, and the two members are themselves separated locally by an angular unconformity. These relations and the presence of clasts derived from underlying Methow strata in the Ventura member demonstrate that the basin was actively deforming during early Late Cretaceous time (McGroder, 1988).

Structure of the Methow Basin

During and after the final stages of basin filling, the Methow basin was deformed into a southeast-plunging synclinorium underlain by the east-vergent Chuwanten thrust (Fig. 1; McGroder, 1988). During mid-Cretaceous time, more than 50 km of shortening occurred on the Chuwanten and related faults in the north end of the basin (Fig. 3), while in the south, only about 20 km of contraction occurred. This displacement gradient generated enough structural plunge to allow well constrained, balanced cross-sections to be drawn to a depth of about 11 km below sea level in the basin (McGroder, 1988).

Perhaps the most curious aspect of the structure in the basin is that in the north, major folds and thrusts appear east-vergent, whereas in the south, tectonic transport was apparently westward. McGroder (1988) interpreted that relation to indicate that crustal contraction was accomplished largely by tectonic wedging, in which eastward motion of an allochthon was accomodated at near-surface levels by west-vergent thrusting (Fig. 3). In other words, the tectonic wedge burrowed eastward into the basin and unpeeled the strata, instead of riding structurally atop the basin on a single, east-vergent thrust.

The youngest thrusting within the basin can not be proven to be Cretaceous, but most thrust-related deforma-

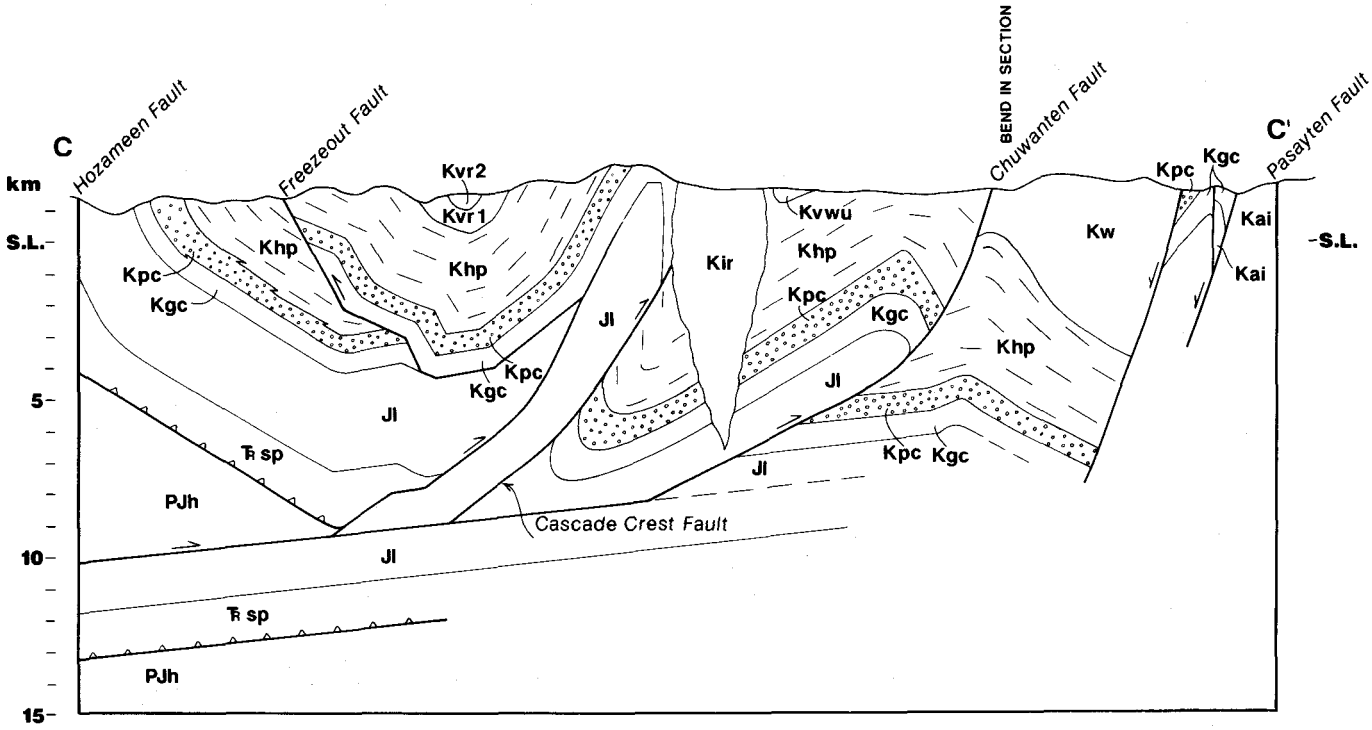

Figure 3. Geologic cross-section C-C' from location shown on Figure 1. No vertical exaggeration. Unit symbols: PJh, Hozameen Group; Trsp, Spider Peak Formation; Jl, Ladner Group; Kgc, Goat Creek Formation; Kpc, Panther Creek Formation; Khp, Harts Pass Formation; Kvr1, Kvr2, Virginian Ridge Formation; Kw, Winthrop Sandstone; Kvwu, Virginian Ridge and Winthrop formations, undivided; Kai, Isabella andesite; Kir, Rock Creek stock. Teeth on fault represent fossil suture of uncertain age between Methow and Bridge River-Hozameen terranes. Apparent distortion of unit thicknesses between Cascade Crest and Chuwanten faults due to 30 degrees plunge of structure there. The west end of the section illustrates the geometry of the tectonic wedge in the Methow basin. In the south end of the basin, along the fieldtrip route, the Chuwanten and Cascade Crest faults did not propagate to the surface, and so the structures at the surface are west-vergent thrusts that make up the lid to the tectonic wedge.

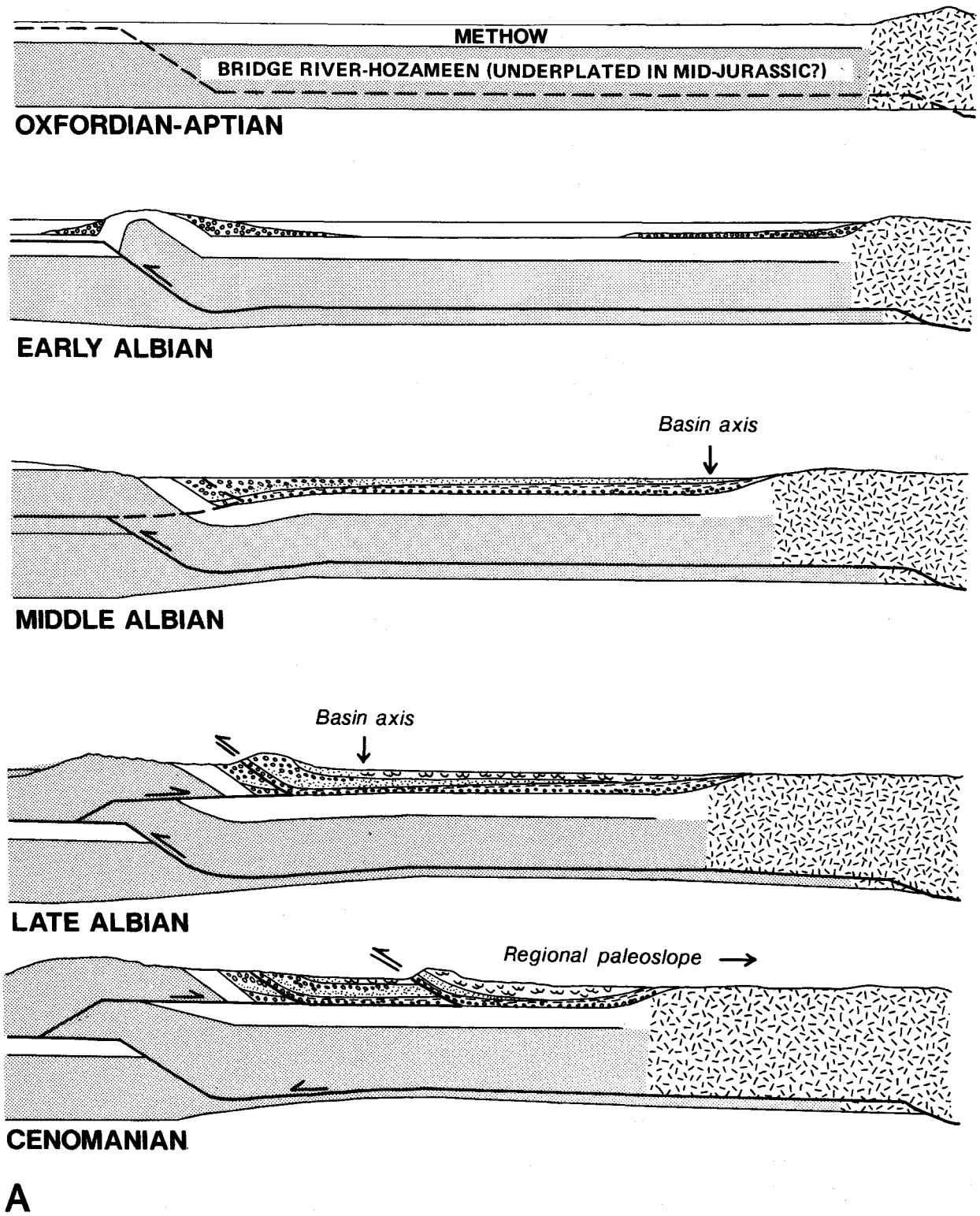

Figure 4. Two models for basin evolution in the eastern Cascades. A, Piggyback model, where basin resides in structurally high, piggyback position during early and middle Albian time; B, Foreland model, in which basin resides in structurally low, foreland position throughout Albian and Cenomanian time.

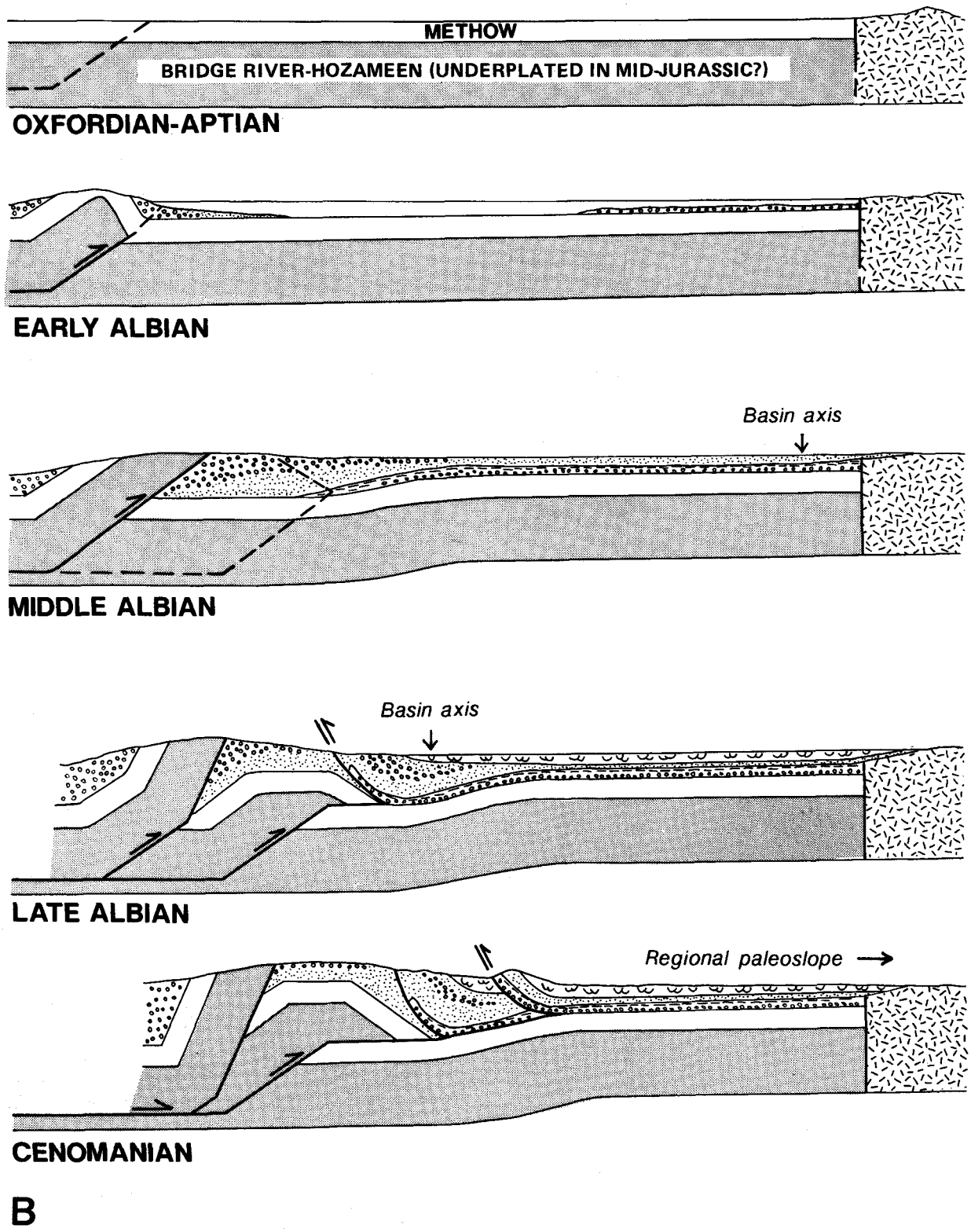

Figure 4. Two models for basin evolution in the eastern Cascades (continued).

tion is bracketed between 100 and 88 Ma. The 88 Ma (K-Ar, hornblende, recalculated from Tabor and others, 1968) Rock Creek stock cuts the map trace of the Cascade Crest fault, which is essentially a splay or imbrication of the Chuwanten thrust (Fig. 1). Also, the relations concerning the sub-Midnight Peak unconformity discussed above indicate that west-vergent thrusting in the lid to the tectonic wedge had commenced before deposition of the Midnight Peak Formation. Although the Midnight Peak is not dated directly, it is cut by the 89 Ma (K-Ar) Fawn Peak stock (Riedell, 1979). Therefore, the bulk of intrabasinal thrusting was accomplished by about 88 Ma, and we suspect that the shortening had ceased altogether in the eastern Cascades by shortly thereafter.

Basin Evolution Model

A few historical remarks about the evolution of thought on Methow basin development are in order. Since the work of Tennyson and Cole (1978), the Cretaceous strata in the basin have been interpreted as having been deposited in a forearc position. As far as we are aware, the first reference to thrusting in the Cascades as a mechanism for changing the regional slope in the basin to eastward was made by Cole (1973; see his fig. 27). Five years later, in an influential summary paper, Davis and others (1978) reinterpreted the west-derived clastics in the Methow basin as recording active right-lateral, strike-slip faulting along a proto-Ross Lake fault. The wrench basin model (for example, Trexler and Bourgeois, 1985; Kleinspehn, 1985) has persisted until very recently and probably still has some proponents today. However, the recent analyses by Mohrig and Bourgeois (1986), McGroder and Mohrig (1987), McGroder (1988), and Garver and others (1988) have demonstrated that during Albian and Cenomanian time, the basin was deforming during regional overthrusting and that there is little evidence for syndepositional strike-slip activity. Moreover, the available evidence on the timing of strike-slip activity suggests that most dextral motion on high-angle faults in this region is Tertiary in age. (See section on high-angle faults, below.)

While we favor a thrust-kinematic model for basin evolution, we realize that many aspects of the models presented below are conjectural and will undoubtedly be refined with future work in the basin. In spite of their immaturity, we have chosen to present two preliminary models of basin evolution below (Fig. 4a and 4b). Both models recognize that in early Late Cretaceous time, dominant thrust transport direction was to the east. The two models differ primarily in how they explain the Albian structural development of the basin. In one, the Methow is asserted to lie in a structurally high, "piggyback" position; in the other, the basin lies in a structurally low "foreland" position throughout its history. Current investigations in the Tyaughton basin, which lies in the southern Coast Ranges of British Columbia and likely represents the offset western edge of the Methow basin, may resolve this uncertainty (J. I. Garver, Univ. of Washington, oral commun., 1988).

Palinspastic Relations

The west side of the northern Methow basin abuts against the Hozameen fault. The east-vergent thrust faults that intersect the surface within the basin must descend section to the west and therefore must occur west of the Hozameen fault, albeit at a deeper structural level. The only recognized candidate for the deep level of one or more of the faults in the Chuwanten system is the Jack Mountain thrust fault of Misch (1966) (Fig. 1).

If the east side of the Methow basin is held fixed, the excess 50 km of crust preserved in the thrust system within the basin must be relocated to the west in order to restore the basin to a pre-thrusting configuration. The excess 50 km of crust will not fit in the approximately 7-km-wide slot between the Ross Lake and Hozameen faults, and so the question becomes: Does the remaining 43 km of unshortened section restore to a position atop or beneath the Skagit Gneiss, which lies west of the Ross Lake fault? Because no clasts of Skagit have been identified from Methow strata, and because available geochronologic data, summarized in a following section, indicate that uplift of the Skagit Gneiss occurred in Tertiary time, we believe that the Jack Mountain-Chuwanten thrust roots over the Skagit.

The obvious question posed by the above analysis is: Does the Methow restore to a palinspastic position west of the crystalline core? We believe the answer is "no" because a strong case can be made that all the nappes currently residing in the northwestern Cascades and San Juan Islands were derived from atop or *east* of the Cascades crystalline core. Brandon and Cowan (1985) and McGroder (1988) argue that stacking of those nappes and the subsequent translation of them from their homeland to where they rest today is the mechanism most likely to have induced core metamorphism. In that scenario, the east-vergent Jack Mountain-Chuwanten thrust probably acted as a backthrust system during regional overthrusting, so that the structurally highest rocks (Jack Mountain-Chuwanten allochthon-Shuksan allochthon) in the Cascades had the configuration of a crustal-scale flake or pop-up. In other words, following the culmination of thrusting, they were floored to the east by an east-vergent, crustal-scale thrust system and to the west by a west-vergent, crustal-scale thrust system. The whole flake moved from east to west over the orogenic footwall, which is now exposed in a tectonic window of sorts in the metamorphic core of the range.

POST-CRETACEOUS NNW-TRENDING HIGH-ANGLE FAULTS

Major NNW-striking high-angle faults have broken the Late Cretaceous North Cascades orogen into several large structural blocks. These structures include the Pasayten fault, Ross Lake fault zone, Entiat fault, Leavenworth fault, and Straight Creek fault (Fig. 5). Movement is generally not precisely dated, but some of the faults were active in the early and middle Eocene, and most have been postulated to record dextral strike-slip motion (for example, Misch, 1977; Tabor and others, 1984; Monger, 1986). The Straight Creek fault is the youngest of these structures and has the best documented evidence for major strike slip. Displacements probably were on the order of 80 to 110 km (Vance and Miller, 1981; Monger, 1985; Kleinspehn, 1985), although as much as 190 km of movement has been proposed (Misch, 1977).

Ross Lake Fault Zone

The Ross Lake fault zone (RLFZ) is the most complex of the NNW-striking high-angle structures and will be viewed in some detail on the field trip. The RLFZ forms the northeastern border of the dominantly Mesozoic and early Cenozoic crystalline core of the North Cascades, and in general it separates amphibolite-facies rocks from weakly metamorphosed Jurassic and Cretaceous strata of the Methow basin (Misch, 1966). Many workers consider the fault zone to be a fundamental Cretaceous structure of the North Cascades. Misch (1966) originally noted possible Cretaceous strike slip on this structure, and Davis and others (1978) postulated a minimum of 160 km of Late Jurassic-Early Cretaceous dextral slip. Hamilton (1978) suggested that the RLFZ was originally a suture across which the North Cascades were accreted, and Brandon and Cowan (1985) postulated that the "root zone" for the San Juan Islands-Northwestern Cascades thrust system may have been in the vicinity of the RLFZ. We show below, however, that well-documented deformation in the fault zone is early Tertiary in age, and that any Cretaceous deformation has been severely overprinted by Paleogene deformation, plutonism, and metamorphism. From a larger perspective, much of the displacement in the zone may have occurred during a time when the Okanogan complex and other metamorphic core complexes east of the North Cascades were undergoing a major thermal and extensional event (Fig. 5).

Misch (1966, 1977) originally defined the RLFZ as a ~15-km-wide system of steep NNW- to northwest-trending faults and associated fault zones. These include the Ross Lake fault, Gabriel Peak tectonic belt, Twisp River fault, Foggy Dew fault, and Hozameen-North Creek fault. The RLFZ is the site of numerous Late Cretaceous to Eocene plutons. The largest plutons are, from north to south, the Ruby Creek plutons, Black Peak batholith, Golden Horn batholith, Oval Peak batholith, and Cooper Mountain batholith (Fig. 6). In the following discussion, we will briefly describe each of the major structures in the RLFZ, generally proceeding from northeast to southwest, and then summarize the timing and significance of this tectonic element.

The steeply dipping Hozameen fault is the easternmost structure in the RLFZ (Figs. 5 and 6). Along its northern extent the fault separates the oceanic Permian to Jurassic Hozameen Group on the west from strata of the Methow basin on the east; to the south it appears to truncate the Jack Mountain thrust (Staatz and others, 1971; Tennyson, 1974). Farther south, volcanic and sedimentary strata of the Little Jack unit occur on the west side of the fault. The Hozameen fault is intruded by the Eocene (~50 Ma) Golden Horn batholith (McGroder, 1987). The North Creek fault represents the continuation of the Hozameen fault south of the batholith. This fault separates the pre-Late Cretaceous North Creek Volcanics, which may be lower-grade equivalents of the Little Jack unit, from the middle Cretaceous Virginian Ridge Formation of the Methow basin.

Farther south lies a critical junction between the North Creek fault, Foggy Dew fault, and Twisp River fault (Fig. 6). (See Stop 1-6.) The Foggy Dew and North Creek faults lie nearly on strike and a continuous mylonitic zone occurs on the southwest sides of the Twisp River and Foggy Dew faults. Thus, the North Creek and Twisp River faults are both splays of the Foggy Dew fault.

The Twisp River and Foggy Dew faults are major discontinuities that separate medium- to high-grade rocks on the southwest from sub-greenschist- to lower-greenschist-facies volcanic and sedimentary strata on the east. Bedding is locally well preserved in the volcanic and sedimentary rocks, and ductile deformation is generally absent.

The Foggy Dew fault is the southernmost mapped segment of the RLFZ (Fig. 6). It separates a 1-km-wide zone of amphibolite-facies mylonites derived from the crystalline core of the North Cascades from Jurassic(?) to middle Cretaceous rocks of the Methow basin. The mylonitic foliation dips moderately to steeply, and a prominent stretching lineation plunges 0 to 35 degrees southeast. Abundant kinematic indicators record oblique slip, with components of dextral strike slip and normal dip slip (Miller, 1987). Some of the mylonites are derived from the Paleocene Oval Peak pluton, whereas abundant amphibolites are at least in part derived from mafic intrusive rocks, and rare sillimanite-bearing schists are interpreted as mylonitized Twisp Valley Schist.

The Twisp River fault juxtaposes the pre-Late Cretaceous Twisp Valley Schist and Paleocene Oval Peak pluton with the North Creek Volcanics (Barksdale,

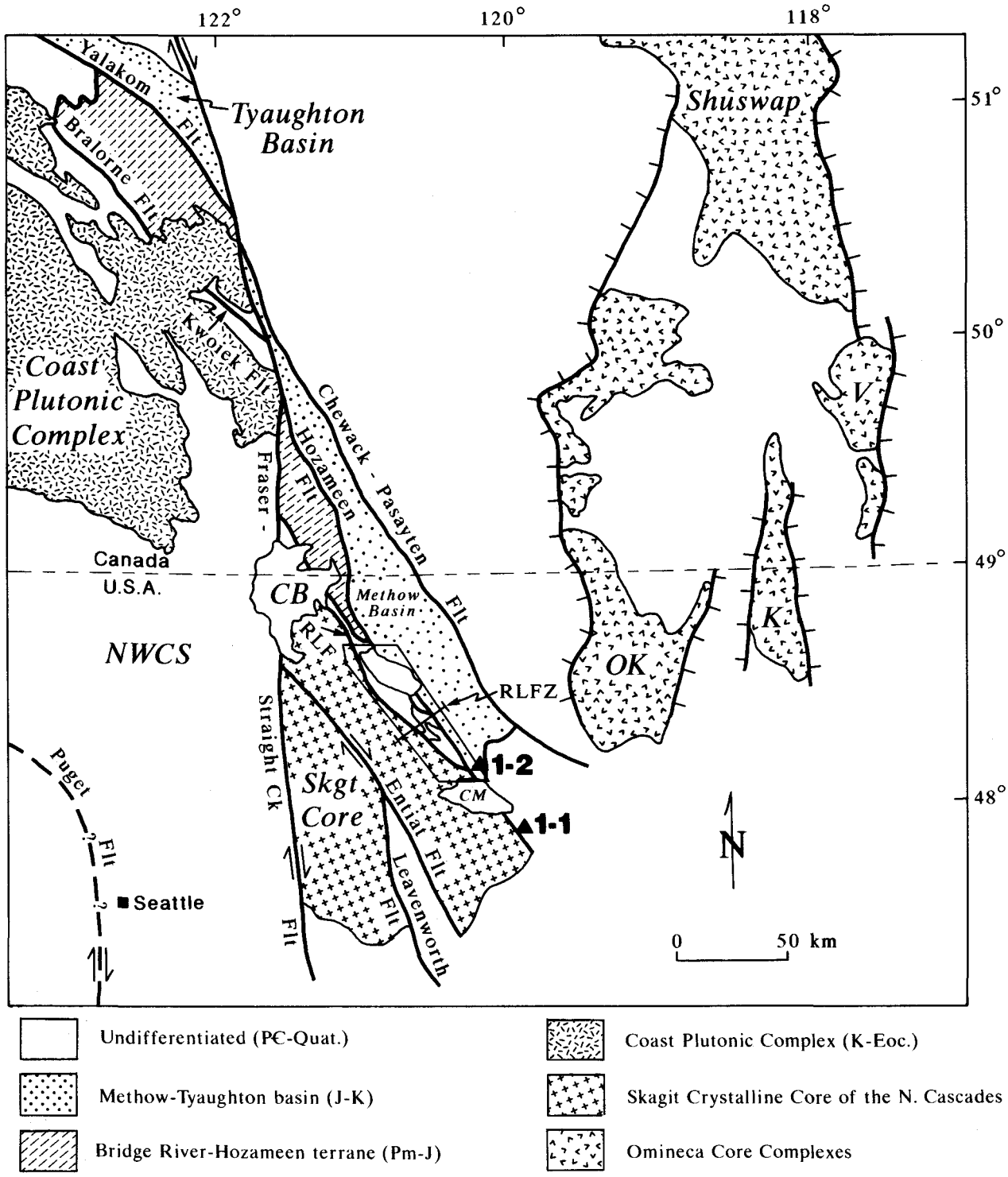

Figure 5. Simplified map showing the location of the crystalline core (Skagit core) of the North Cascades and its spatial relation to the southern Coast Plutonic Complex and the Omineca metamorphic core complexes. Major high-angle early Cenozoic and Cretaceous(?) faults are also emphasized, as are major Eocene extensional faults (ticks on upper plate) along the margins of the core complexes. Fieldtrip stops 1-1 and 1-2 and several units discussed in the text are also shown. The outlined area delineates the location of Figure 6. CB, Chilliwack batholith (Oligocene-Miocene); CM, Cooper Mountain batholith (48 Ma); K, Kettle dome; NWCS, Northwest Cascades-San Juan Islands thrust system; OK, Okanogan Complex; RLF, Ross Lake fault; RLFZ, Ross Lake fault zone; V, Valhalla Complex. Modified from Johnson (1985), Parrish and others (1988), Price and others (1985), and Roddick and others (1979).

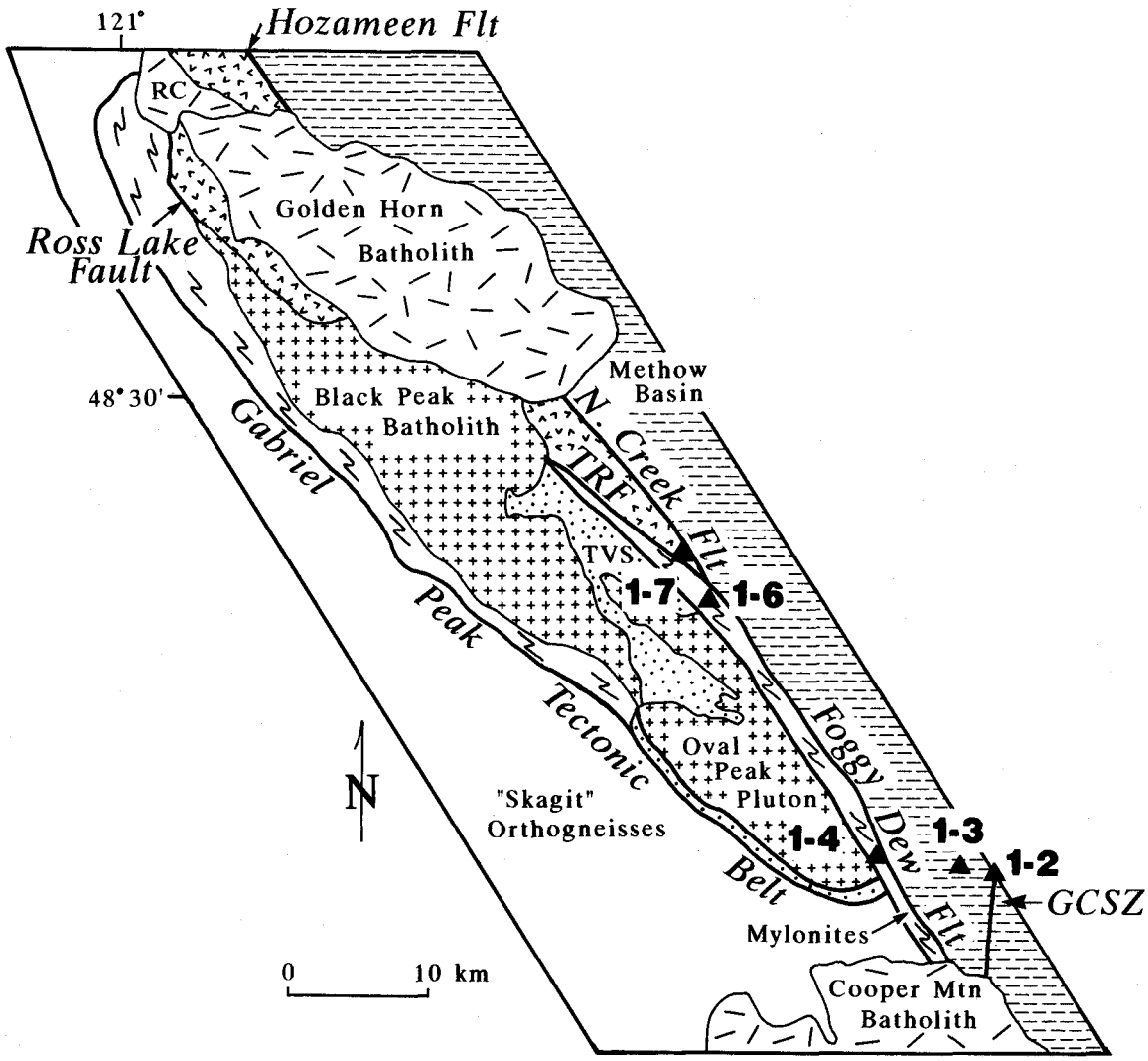

Figure 6. Simplified map of the southern segment of the Ross Lake fault zone. Fieldtrip stops within and near the fault zone are also shown. +, Late Cretaceous and Paleocene plutons; random dashes, Eocene plutons; v, North Creek Volcanics; squiggles, mylonites; GCSZ, Gold Creek shear zone; RC, Ruby Creek heterogeneous plutonic belt; TRF, Twisp River fault; TVS, Twisp Valley Schist. Modified from Misch (1966, 1977), Barksdale (1975), and Miller (1987).

1975). Steeply dipping mylonites displaying a strong subhorizontal lineation are well developed near the fault and suggest a greater component of strike-slip motion than in the Foggy Dew fault zone. The mylonite zone narrows to the north (Miller, 1987), and the Twisp River fault does not continue through the Black Peak batholith (discussed below) (Misch, 1966; Barksdale, 1975).

The Ross Lake fault occurs north of the Black Peak batholith, but it lies west of the projection of the Twisp River fault. In Washington the Ross Lake fault consists of several short vertical or steeply west-dipping segments that are separated by plutonic rocks (Misch, 1966). The fault generally places the Skagit Gneiss on the southwest against the Little Jack unit on the northeast which is upgraded to amphibolite facies near the fault. In southern British Columbia the fault is a distributed shear zone that juxtaposes the Skagit Gneiss and the Hozameen Group (Haugerud, 1985). Normal dip-slip displacement telescoped metamorphic facies in the latter rocks, and dextral strike slip is suggested by gently plunging post-46 Ma stretching lineations and scattered kinematic indicators in mylonites (Haugerud, 1985; this volume). Along Washington State Route 20, a 48 Ma phase of the Ruby Creek heterogeneous plutonic belt was possibly emplaced while the Ross Lake fault was active (Misch, 1977; Miller and others, 1988). In southern British Columbia the fault is cut by the 30 Ma main phase of the Chilliwack batholith (Richards and McTaggart, 1976).

The continuation of the Ross Lake fault south of its intersection with the Black Peak batholith is difficult to discern. It may step to the west side of the batholith to the Gabriel Peak tectonic belt, which is a moderately to

steeply northeast-dipping zone of highly strained rocks (Fig. 6) (Miller, 1987). In the northwest this tectonic belt is marked by the deformed western margin of the Cretaceous (90 Ma) Black Peak batholith (Misch, 1977) and by mylonitic orthogneisses of the Skagit Gneiss (Miller, 1987), one of which has yielded a crystallization age of 68 Ma (Hoppe, 1982). South of the Black Peak batholith, the Gabriel Peak tectonic belt is defined by the deformed southwestern margin of the Paleocene Oval Peak pluton (Miller, 1987).

The variation in orientations of small-scale structures in the Gabriel Peak tectonic belt probably records a complex kinematic history. In the northwest part of the belt stretching lineations plunge gently, and kinematic indicators suggest dextral strike-slip motion (Miller, 1988). However, in the southeastern part of the belt, the stretching lineation plunges down-dip, and dip-slip movement clearly occurred.

Timing of Deformation

Both strike-slip and dip-slip motion occurred on the various strands of the Ross Lake system, and motion was diachronous. Several workers have argued for pre-Black Peak (pre-90 Ma) displacement in the system. Misch (1966) first postulated such motion on the basis of map relations, whereas Trexler and Bourgeois (1985) contended that their sedimentological data indicate that the Ross Lake fault was active during mid-Cretaceous deposition in the Methow basin. Davis and others (1978) and Hamilton (1978) also postulated Mesozoic movement on the basis of inferred regional tectonic relations.

However, it is difficult to prove that motion occurred prior to intrusion of the Black Peak batholith. At first glance, the map pattern (Fig. 6) suggests that the Twisp River fault is intruded by the Black Peak batholith near where that pluton has been dated at 90 Ma (K-Ar hornblende) (Misch, 1963; 1966). However, the Twisp River mylonite zone probably involves rocks of the Paleocene Oval Peak pluton. These seemingly contradictory relations may be resolved if motion on the Twisp River fault is transferred westward at its northwest termination to the portion of the Gabriel Peak tectonic belt which probably experienced dextral strike-slip displacement (Miller, 1987; 1988). In this interpretation, shortening between the left-stepping en echelon pair of dextral strike-slip fault zones is accommodated by widespread ENE-striking, reverse-slip ductile shear zones in the Black Peak batholith (Fig. 6) (Miller, 1988). It seems unlikely that such a transfer mechanism accommodates large displacements. Perhaps much of the movement in this part of the RLFZ is taken up by the Foggy Dew and North Creek faults.

Complex relations at the northern end of the Black Peak batholith are also ambiguous with respect to pre-90 Ma movement. Misch's (1966, 1977) mapping suggests that the Ross Lake fault is truncated by the batholith. The fault cuts mylonitic orthogneisses of the Gabriel Peak tectonic belt (Misch, 1977), however, and at least some mylonitic granitoids in this belt have crystallization ages of 68 Ma (Hoppe, 1982) and 59 Ma (S. A. Bowring, Washington University, written commun., 1988).

The earliest documented motion in the RLFZ is latest Cretaceous and/or early Paleocene mylonitization in the Gabriel Peak tectonic belt. Hoppe (1982) presented U/Pb sphene and Rb/Sr data which he interpreted to indicate that epidote-amphibolite-facies metamorphism and mylonitization of a 68 Ma Skagit orthogneiss (see above) in the belt occurred at ~65 Ma. Age data from the southwest margin of the Oval Peak batholith, the Twisp Valley Schist, and orthogneisses of the Skagit Gneiss bracket ductile deformation in the southeastern part of the Gabriel Peak tectonic belt between ~60 and 55 Ma (Paleocene-early Eocene) (R. B. Miller and S. A. Bowring, unpublished data). Latest motion in the Gabriel Peak belt occurred along a fault which places a weakly foliated 50 Ma Skagit orthogneiss against the deformed western margin of the Black Peak batholith (Hoppe, 1982).

Mylonitization in the Foggy Dew fault zone occurred between the Paleocene and middle Eocene. The mylonite zone truncates the 61 Ma Oval Peak batholith (Miller, 1987), and some of the mylonitization probably occurred by about 55.8 ± 3.6 Ma, the K-Ar hornblende age of an amphibolite in the fault zone. However, latest motion continued into the middle Eocene because a 50 Ma tonalite shows a mylonitic fabric (R. B. Miller and S. A. Bowring, unpublished data) and the undeformed 48 Ma Cooper Mountain batholith truncates the Foggy Dew fault (Barksdale, 1975; Wade, 1988). Movement on the North Creek fault and southern part of the Hozameen fault also ended by about 50 Ma.

There is evidence for some post-50 Ma displacement in other parts of the RLFZ, particularly in southern British Columbia, where the Ross Lake fault was active after 46 Ma (Haugerud, 1985). Renewed movement also occurred in the Gabriel Peak belt, as discussed above.

Although dextral strike-slip displacement has been reasonably well documented for some of the faults (Ross Lake fault, Foggy Dew fault), there are no reliable estimates of the magnitude of slip. Normal dip-slip motion in the RLFZ is consistently down to the northeast. This is in agreement with the differing metamorphic grades and apparent structural levels across the RLFZ.

Regional Implications

These observations on the RLFZ must be considered in any broader interpretation of the tectonic evolution of the North Cascades. They demonstrate the importance of Paleogene strike-slip faulting along the northeastern margin of the crystalline core, and they further support the in-

terpretation that such faulting was widespread in the Paleogene in central and western Washington (for example, Tabor and others, 1984; Johnson, 1984; Vance, 1985). Transcurrent motion also is in good agreement with the plate motion reconstructions of Engebretson and others (1985), which postulate highly oblique convergence for this time interval.

The recent studies of the RLFZ are of relevance to the debate over whether the mid-Cretaceous North Cascade orogen (~90 Ma) was dominantly related to major east-west crustal shortening or to dextral transpressional faulting (cf. Misch, 1966, 1988; Davis and others, 1978; Brown, 1987; Brandon and others, 1988). We find no direct evidence to support Cretaceous wrench faulting in the RLFZ. Subhorizontal northwest-trending stretching lineations west of the crystalline core are inferred to be related to Cretaceous strike-slip motion by Brown (1987). However, our work clearly shows that similarly oriented fabrics in the eastern North Cascades are of Paleocene and Eocene age. Thus the possibility that such fabrics west of the Straight Creek fault are also Tertiary in age must be considered (cf. Tabor and others, in press). We also find no evidence for Cretaceous shortening in the RLFZ. Any Cretaceous deformation in this fault zone, regardless of tectonic regime, may have been essentially obliterated by the intense early Cenozoic deformation, metamorphism, and plutonism along the northeastern margin of the cystalline core.

From a broader viewpoint, the RLFZ may in part record a transition during the Paleogene between two tectonic regimes. Extension occurred to the east in the Omineca metamorphic core complexes (for example, Parrish and others, 1988; Orr and Cheney, 1987), and strike-slip faulting occurred to the west of the crystalline core (Fig. 5) (for example, Johnson, 1984). This transitional nature of the RLFZ is well shown by the oblique-slip Foggy Dew fault zone which records components of both dextral strike slip and normal slip. Mylonitization in this northeast-dipping zone occurred between 61 and 48 Ma, and in part overlaps in time with the major east-dipping ductile extensional shear zones in the Omineca belt, such as bound the Valhalla Complex (Fig. 5) (Parrish and others, 1988).

ACKNOWLEDGMENTS

This guide was improved by helpful reviews from S. Monson, J. A. Vance, M. A. Korosec, and J. G. Evans. McGroder acknowledges support from National Science Foundation Grants EAR-8305937 (to J. Bourgeois) and EAR-8508239 (to D. Cowan and J. Bourgeois). Miller's work has been supported by National Science Foundation Grant EAR-8707956, by the Washington Division of Geology and Earth Resources, and by a San Jose State University Faculty Research Grant.

REFERENCES CITED

Barksdale, J. D., 1975, Geology of the Methow Valley, Okanogan County, Washington: Washington Division of Geology and Earth Resources Bulletin 68, 72 p., 1 pl.

Brandon, M. T.; Cowan, D. S., 1985, The Late Cretaceous San Juan Islands–Northwestern Cascades thrust system [abstract]: Geological Society of America Abstracts with Programs, v. 17, no. 6, p. 343.

Brandon, M. T.; Cowan, D. S.; Vance, J. A., 1988, The Late Cretaceous San Juan thrust system, San Juan Islands, Washington: Geological Society of America Special Paper 221, 81 p.

Brown, E. H., 1987, Structural geology and accretionary history of the northwest Cascades system, Washington and British Columbia: Geological Society of America Bulletin, v. 99, no. 2, p. 201-214.

Coates, J. A., 1974, Geology of the Manning Park area, British Columbia: Geological Survey of Canada Bulletin 238, 177 p., 9 pl.

Cole, M. R., 1973, Petrology and dispersal patterns of Jurassic and Cretaceous sedimentary rocks in the Methow River area, north Cascades, Washington: University of Washington Doctor of Philosophy thesis, 110 p.

Davis, G. A.; Monger, J. W. H.; Burchfiel, B. C., 1978, Mesozoic construction of the Cordilleran "collage", central British Columbia to central California. *In* Howell, D. G.; McDougall, K. A., editors, Mesozoic paleogeography of the western United States; Pacific Coast Paleogeography Symposium 2: Society of Economic Paleontologists and Mineralogists, Pacific Section, p. 1-32.

DiLeonardo, C. G., 1987, Structural evolution of the Smith Canyon fault, northeastern Cascades, Washington: San Jose State University Master of Science thesis, 85 p, 2 pl.

Engebretson, D. C.; Cox, Allan; Gordon, R. G., 1985, Relative motions between oceanic and continental plates in the Pacific Basin: Geological Society of America Special Paper 206, 59 p.

Garver, J. I.; McGroder, M. F.; Umhoefer, P. J.; Bourgeois, Joanne, 1988, Pre- to syn-collisional sedimentation in the Jura-Cretaceous Methow-Tyaughton basin, northern Washington, southern British Columbia [abstract]: Geological Society of America Abstracts with Programs, v. 20, no. 7, p. A274.

Haugerud, R. A., 1985, Geology of the Hozameen Group and the Ross Lake shear zone, Maselpanik area, north Cascades, southwest British Columbia: University of Washington Doctor of Philosophy thesis, 263 p.

Hamilton, Warren, 1978, Mesozoic tectonics of the western United States. *In* Howell, D. G.; McDougall, K. A., editors, Mesozoic paleogeography of the western United States; Pacific Coast Paleogeography Symposium 2; Society of Economic Paleontologists and Mineralogists, Pacific Section, p. 33-70.

Hopkins, W. N., 1987, Geology of the Newby Group and adjacent units in the southern Methow trough, northeast Cascades, Washington: San Jose State University Master of Science thesis, 95 p., 1 pl.

Hoppe, W. J., 1982, Origin and age of the Gabriel Peak Orthogneiss, north Cascades, Washington: University of Kansas Master of Science thesis, 79 p., 2 pl.

Jeletzky, J. A., 1970, Lower Cretaceous and late Upper Jurassic biochronology and facies of Manning Park area, British Columbia: Geological Survey of Canada Paper 70-1, part A, p. 214-223.

Johnson, S. Y., 1982, Stratigraphy, sedimentology, and tectonic setting of the Eocene Chuckanut Formation, northwest Washington: University of Washington Doctor of Philosophy thesis, 221 p., 4 pl.

Johnson, S. Y., 1984, Evidence for a margin-truncating transcurrent fault (pre-Late Eocene) in western Washington: Geology, v. 12, no. 9, p. 538-541.

Kleinspehn, K. L., 1985, Cretaceous sedimentation and tectonics, Tyaughton-Methow basin, southwestern British Columbia: Canadian Journal of Earth Sciences, v. 22, no. 2, p. 154-174.

McGroder, M. F., 1987, Yalakom-Foggy Dew fault–A 500(+) km long Late Cretaceous-Paleogene oblique-slip fault in Washington and British Columbia [abstract]: Geological Society of America Abstracts with Programs, v. 19, no. 6, p. 430.

McGroder, M. F., 1988, Structural evolution of eastern Cascades foldbelt–Implications for late Mesozoic accretionary tectonics in the Pacific Northwest: University of Washington Doctor of Philosophy thesis, 140 p.

McGroder, M. F.; Mohrig, D., 1987, Piggyback to foreland transition in the Methow basin, Washington, 2–A balanced cross-section of the Cascade orogen [abstract]: Geological Society of America Abstracts with Programs, v. 19, no. 7, p. 766.

Miller, R. B., 1987, Geology of the Twisp River-Chelan Divide region, north Cascades, Washington: Washington Division of Geology and Earth Resources Open File Report 87-17, 12 p., 12 pl.

Miller, R. B., 1988, Possible role of ductile shear zones in linking overstepping strike-slip faults, Ross Lake fault zone, north Cascades, Washington [abstract]: Geological Society of America Abstracts with Programs, v. 20, no. 7, p. A108.

Miller R. B.; Bowring, S. A.; Hoppe, W. J., 1988, New evidence for extensive Paleogene plutonism and metamorphism in the crystalline core of the north Cascades [abstract]: Geological Society of America Abstracts with Programs, v. 20, no. 6, p. 432-433.

Misch, Peter, 1963, New samples for age determinations from the northern Cascades. *In* Kulp, J. L., and others, Investigations in isotopic geochemistry: Columbia University Lamont Geological Observatory (under contract NYO-7243 to U.S. Atomic Energy Commission), Report 8, p. 26-40, Appendix K, p. 1-4.

Misch, Peter, 1966, Tectonic evolution of the northern Cascades of Washington–A west-Cordilleran case history. *In* Canadian Institute of Mining and Metallurgy; and others {Gunning, H. C. , editor,], A symposium on the tectonic history and mineral deposits of the western Cordillera in British Columbia and neighbouring parts of the United States, Vancouver, 1964: Canadian Institute of Mining and Metallurgy Special Volume 8, p. 101-148.

Misch, Peter, 1977, Bedrock geology of the north Cascades. *In* Brown, E. H.; Ellis, R. C., editors, Geological excursions in the Pacific Northwest; Geological Society of America Annual Meeting, 1977: Western Washington University, p. 1-62.

Misch, Peter, 1977, Dextral displacements at some major strike faults in the north Cascades [abstract]: Geological Association of Canada Program with Abstracts, v. 2, p. 37.

Misch, Peter, 1988, Tectonic and metamorphic evolution of the North Cascades–An overview. *In* Ernst, W. G., ed., Rubey Volume v. 11, p. 179-195.

Mohrig, D. C.; Bourgeois, Joanne, 1986, A new source terrane for Methow basin (WA) sediments–Evidence from the Cenomanian(?) Ventura member, Midnight Peak Formation, southern Canadian Cordillera [abstract]: Geological Society of America Abstracts with Programs, v. 18, no. 2, p. 159.

Monger, J. W. H., 1985, Structural evolution of the southwestern Intermontane Belt, Ashcroft and Hope map areas, British Columbia: Geological Survey of Canada Paper 85-1A, p. 349-358.

Monger, J. W. H., 1986, Geology between Harrison Lake and Fraser River, Hope map area, southwestern British Columbia: Geological Survey of Canada Paper 86-1B, p. 699-706.

O'Brien, Jennifer, 1986, Jurassic stratigraphy of the Methow Trough, southwestern British Columbia: Geological Survey of Canada Paper 86-1B, p. 749-756.

Orr, K. E.; Cheney, E. S., 1987, Kettle and Okanogan domes, northeastern Washington and southern British Columbia. *In* Schuster, J. E., editor, Selected papers on the geology of Washington: Washington Division of Geology and Earth Resources Bulletin 77, p. 55-71.

Parrish, R. R.; Carr, S. D.; Parkinson, D. L., 1988, Eocene extensional tectonics and geochronology of the southern Omineca belt, British Columbia and Washington: Tectonics, v. 7, no. 2, p. 181-212.

Raviola, F. P., 1988, Metamorphism, plutonism and deformation in the Pateros-Alta Lake region, north-central Washington: San Jose State University Master of Science thesis, 182 p, 1 pl.

Ray, G. E., 1986, The Hozameen fault system and related Coquihalla serpentine belt of southwestern British Columbia: Canadian Journal of Earth Sciences, v. 23, no. 7, p. 1022-1041.

Richards, T. A.; McTaggart, K. C., 1976, Granitic rocks of the southern Coast Plutonic Complex and northern Cascades of British Columbia: Geological Society of America Bulletin, v. 87, no. 6, p. 935-953.

Riedell, K. B., 1979, Geology and porphyry copper mineralization of the Fawn Peak intrusive complex, Methow Valley, Washington: University of Washington Master of Science thesis, 52 p.

Staatz, M. H.; Tabor, R. W.; Weis, P. L.; Robertson, J. F.; Van Noy, R. M.; Pattee, E. C.; 1972, Geology and mineral resources of the Pasayten Wilderness area, Washington: U.S. Geological Survey Bulletin 1359, 132 p.

Tabor, R. W., Engels, J. C.; Staatz, M. H., 1968, Quartz diorite-quartz monzonite and granite plutons of the Pasayten River area, Washington–Petrology, age, and emplacement: U.S. Geological Survey Professional Paper 600-C, p. C45-C52.

Tabor, R. W.; Frizzell, V. A., Jr.; Vance, J. A.; Naeser, C. W., 1984, Ages and stratigraphy of lower and middle Tertiary sedimentary and volcanic rocks of the central Cascades, Washington–Application to the tectonic history of the Straight Creek fault: Geological Society of America Bulletin, v. 95, no. 1, p. 26-44.

Tabor, R. W.; Haugerud, R. A.; Miller, R. B., in press, Overview of the geology of the North Cascades. *In* Tabor, R. W.; Haugerud, R. A.; Miller, R. B.; Brown, E. H.; Babcock, R. H., Accreted terranes of the North Cascades, Washington: International Geological Congress Trip T307, American Geophysical Union.

Tennyson, M. E., 1974, Stratigraphy, structure and tectonic setting of Jurassic and Cretaceous sedimentary rocks in the west-central Methow-Pasayten area, northeastern Cascade Range, Washington and British Columbia: University of Washington Doctor of Philosophy thesis, 155 p., 3 pl.

Tennyson, M. E.; Cole, M. R., 1978, Tectonic significance of upper Mesozoic Methow-Pasayten sequence, northeastern Cascade Range, Washington and British Columbia. *In* Howell, D. G.; McDougall, K. A., editors, Mesozoic paleogeography of the western United States, Pacific Coast Paleogeography Symposium 2: Society of Economic Paleontologists and Mineralogists Pacific Section, p. 499-508.

Todd, V. R., 1987, Jurassic and Cretaceous plutonism in and near the Methow basin, north-central Washington–Preliminary K-Ar data [abstract]: Geological Society of America Abstracts with Program, v. 19, no. 6, p. 458.

Travers, W. B., 1978, Overturned Nicola and Ashcroft strata and their relation to the Cache Creek Group, southwestern Intermontane Belt, British Columbia: Canadian Journal of Earth Sciences, v. 15, no. 1, p. 99-116.

Trexler, J. H., Jr., 1985, Sedimentology and stratigraphy of the Cretaceous Virginian Ridge Formation, Methow basin, Washington: Canadian Journal of Earth Sciences, v. 22, no. 9, p. 1274-1285.

Trexler, J. H., Jr.; Bourgeois, Joanne, 1985, Evidence for mid-Cretaceous wrench faulting in the Methow basin, Washington–Tectonostratigraphic setting of the Virginian Ridge Formation: Tectonics, v. 4, no. 4, p. 379-394.

Vance, J. A.; Miller, R. B., 1981, The movement history of the Straight Creek fault in Washington State [abstract]: Geological Association of Canada Cordilleran Section Programme and Abstracts, p. 39-41.

Vance, J. A., 1985, Early Tertiary faulting in the north Cascades [abstract]: Geological Society of America Abstracts with Programs, v. 17, no. 6, p. 415.

Wade, W. M., 1988, Geology of the northern portion of the Cooper Mountain batholith, north-central Cascades, Washington: San Jose State University Master of Science thesis, 88 p, 1 p.

White, P. J., 1986, Geology of the Island Mountain area, Okanogan County, Washington: University of Washington Master of Science thesis, 80 p., 1 pl.

Road Log

The mileage in this log is cumulative.

Pateros To Mazama

0.0 Junction of U.S. Highway 97 and State Route (SR) 153 near Pateros. Drive east on SR 153.

0.3 **STOP 1-1. Migmatites of the Alta Lake complex.**

Parking spot is 0.2 mi ahead on the right.

The Alta Lake complex consists mainly of variably migmatized amphibolites and trondhjemitic orthogneisses, with lesser biotite schists and rare quartzites (Raviola, 1988). Migmatization resulted from metamorphic differentiation and injection, according to Raviola. Hornblende from an amphibolite in the complex yielded a conventional K-Ar age of 104 ± 5 Ma (Raviola, 1988), which may date the metamorphism or may reflect resetting and/or cooling.

The Alta Lake complex occupies a critical position between the southernmost extension of the Ross Lake fault zone and the projection of the Chewack-Pasayten fault (Fig. 5). The relation of the Alta Lake complex and other crystalline rocks between the two major faults to the crystalline core of the North Cascades to the west and to the Okanogan complex to the east is enigmatic. The K-Ar age is more compatible with geochronologic results from the Okanogan complex, as few K-Ar ages in the core of the North Cascades are greater than 90 Ma. The crystalline belt containing the Alta Lake complex is in fault contact with the Methow basin which lies along strike to the northwest (Barksdale, 1975).

1.7 Alta Lake State Park turnoff. Continue on SR 153.

3.8 Bridge over the Methow River. A large raft of schist in the pre-Late Cretaceous Methow Gneiss is exposed along the river. The Methow Gneiss is a tonalitic orthogneiss of batholithic dimensions which intruded the Alta Lake complex prior to, or contemporaneous with dynamothermal metamorphism (Raviola, 1988). The Methow generally has a gently dipping foliation, and its structural patterns show some similarities to those of a gneiss dome.

11.4 Enter the community of Methow.

11.6 Leave Methow. Between here and the turnoff from SR 153 there are isolated outcrops of Methow Gneiss.

17.6 Junction of Gold Creek Road and SR 153. Turn left on Gold Creek Road.

Reset odometer.

0.0 Junction of Gold Creek Road and SR 153.

0.1 Methow Gneiss.

0.9 Junction. Turn left (west).

2.0 Junction with the South Fork Gold Creek Road. Proceed straight ahead.

3.3 to 3.6 **STOP 1-2. Gold Creek shear zone.**

Strongly foliated greenschists and minor phyllites (east end of the outcrop) of the Gold Creek shear zone. This >1-km-wide shear zone strikes NNE, at a significant angle to the regional northwest trend of the North Cascades (Fig. 6). The gently north-plunging stretching lineation and steep foliation suggest that this is a strike-slip zone, and DiLeonardo (1987) has postulated dextral slip on the basis of sparse kinematic indicators. Kinks of the foliation are widespread. This high strain zone deforms the Late Jurassic and Early Cretaceous Newby Group of the Methow basin and is truncated by the Eocene Cooper Mountain batholith.

Continue straight ahead (northwest).

3.7 Junction. Continue straight ahead.

3.9 to 4.0 Large outcrops of the Newby Group.

6.0 **STOP 1-3. Newby Group**

Outcrops of well-bedded volcaniclastic sedimentary rocks of the Newby Group, which are the oldest exposed strata of the southern Methow basin. Hopkins (1987) described graded and cross-laminated beds in these rocks, which he interpreted as turbidites that apparently were

derived from a volcanic arc to the east. These rocks are probably the protoliths for some of the strongly foliated greenschists in the Gold Creek shear zone of Stop 1-2.

Proceed straight ahead (west).

6.1 Turnoff to Foggy Dew Campground. Pavement ends. Continue straight ahead (northwest).

7.6 Junction with Crater Creek Road. Turn left, toward the Crater Creek trail.

7.7 Cross Gold Creek.

9.7 Amphibolites in the Foggy Dew fault zone are exposed on the right and on the hill above to the north.

10.0 Mylonitic gneisses and amphibolites in the Foggy Dew fault zone are exposed in the roadcut on the right. A gneiss from this outcrop has been dated at about 50 Ma (U-Pb, zircon) by S. A. Bowring (Washington University, written commun., 1988).

10.1 Small roadcut in mylonite on the right.

10.2 **STOP 1-4. Foggy Dew fault zone.**

Eagle Lakes-Crater Creek trailhead. Park and walk up the trail about 0.3 mi.

At this stop is a long series of outcrops of mylonitic gneisses, amphibolites, and rare schists of the Foggy Dew fault zone (Fig. 6). This 1-km-wide mylonite zone is the southernmost recognized segment of the Ross Lake fault zone. The Foggy Dew fault separates the amphibolite-facies mylonites from weakly metamorphosed rocks of the Methow basin to the northeast. The mylonites record oblique slip with components of dextral strike slip and normal dip slip, down to the northeast (Miller, 1987). Ductile deformation is bracketed between 61 and 48 Ma.

Some of the mylonitic gneisses in these outcrops are derived from the Paleocene Oval Peak pluton. Intrusive contacts are locally preserved between the Oval Peak-derived gneisses and the amphibolites. The amphibolites have yielded a K-Ar hornblende age of 55.8 ± 3.6 Ma and may be derived from metadiabases and metagabbros which occur locally in the fault zone. Rare metasedimentary rocks in these outcrops include sillimanite-bearing schists that may be derived from the Twisp Valley Schist. Preliminary thermo-barometric work on one of these schists yielded a temperature of approximately 600° to 625° C and pressures of 4 to 5 kb (D. L. Whitney, University of Washington, written commun., 1988).

The northwest-striking mylonitic foliation in the fault zone dips moderately to steeply to the northeast, and the stretching lineation typically plunges about 25 to 30 degrees to the southeast. Abundant type-1 and type-2 S-C fabrics, and lesser shear bands, asymmetric porphyroclasts and foliation fish provide evidence for oblique dextral slip. Asymmetric folds of foliation are also common in the amphibolites.

Retrace the route to the junction at 0.9 mi from SR 153 and *reset odometer*.

0.0 Turn left (north) at the junction toward Twisp.

0.4 to 0.5 Large outcrops of Methow Gneiss.

1.6 Junction with SR 153. Turn left toward Twisp.

4.1 Junction with Libby Creek Road. Stay on SR 153.

4.2 to 4.5 Large outcrops mapped as the pre-Late Cretaceous Leecher Metamorphics by Barksdale (1975). These rocks apparently belong in the same structural block as the Alta Lake complex and Methow Gneiss.

5.0 Thick, flat shear zone in the Leecher Metamorphics.

5.1 Cross the Methow River.

5.2 Enter Carlton.

13.9 Junction. SR 153 ends. Proceed straight ahead (north) onto SR 20.

15.9 Cross the Methow River and enter Twisp.

Reset odometer at the north end of Twisp at the junction of SR 20 and the Twisp River Road. Travel west on the Twisp River Road.

0.0 Intersection of Twisp River Road and SR 20.

0.7 Outcrop of Newby Group volcanics. The age of these rocks is unknown, but nearby they are intruded by a 137 Ma stock (K-Ar, hornblende, V. Todd, USGS, written commun., 1986).

1.3 Intersection. Stay right. Newby volcanics in the quarry to the left.

4.0 Heterolithic Patterson Lake conglomerate of probable middle Albian age (McGroder, unpublished data). This unit used to be lumped with the Virginian Ridge Formation (Barksdale, 1975) but has more recently been separated because the clasts are almost exclusively sedimentary and volcanic rock fragments, much unlike the Virginian Ridge conglomerates, which contain predominantly chert clasts. The Patterson Lake unit lies directly above undivided rocks of the Newby Group and therefore takes the place of the thick, Lower Cretaceous, turbiditic Jackass Mountain group in the south end of the basin. It locally contains 1-m-diameter clasts and may record local high-angle faulting at the south end of the basin in late Early Cretaceous time (Trexler, 1985).

5.1 Virginian Ridge Formation outcrop on the right.

6.2 Small outcrop of Winthrop Sandstone.

6.7 Winthrop Sandstone outcrop.

7.0 **STOP 1-5. Winthrop Sandstone.**

The purposes of this stop are twofold. First, examine the degree of lithification and lack of metamorphism in the Winthrop for the purpose of contrasting the rocks with those found on the other side of the Foggy Dew and Twisp River faults at the next stop. The Winthrop at this locality appears as it does throughout much of the basin—friable to moderately indurated. In addition, it is deformed into large folds, commonly associated with fairly widely spaced thrust faults. It lacks cleavage and is not penetratively deformed in most places in the basin. The next stop will show how abruptly the structural style and metamorphic grade change as one crosses two faults in the Ross Lake system.

This stop also serves to introduce the basic stratigraphy of the Methow basin and to examine the sandstone petrology of the Winthrop Sandstone. The Winthrop lies high in the section, above the chert-lithic Virginian Ridge Formation and below the Midnight Peak Formation. It is probably Albian in age on the basis of its flora, and is composed predominantly of sandstone containing abundant quartz, feldspar, biotite, and minor muscovite. Paleocurrent and provenance studies have led virtually all workers who have studied the Winthrop to conclude that it was derived from the plutonic terrane of the Okanogan Range, east of the Pasayten fault (for example, Cole, 1973; Tennyson and Cole, 1978; Trexler, 1985). The Winthrop is similar in composition to most of the other east-derived Upper Jurassic-Lower Cretaceous clastic rocks in the section, although it contains a higher proportion of plutonic detritus and a correspondingly smaller amount of volcanic lithics than underlying strata.

The Winthrop was deposited in sand-bedded rivers in a rapidly subsiding basin and exceeds 4 km in thickness east of the Methow Valley. Basal strata of the Winthrop interfinger to the west with the uppermost strata in the Virginian Ridge Formation. For reasons that are not understood at present, those two formations lose their individual integrity in the north end of the basin and interfinger on the scale of meters over a stratigraphic thickness of more than a kilometer.

There is some uncertainty about the structural setting in which the Winthrop was deposited. We tentatively ascribe westward progradation of the Winthrop to the onset or rejuvenation of east-vergent thrusting in the western reaches of the basin. Tectonic loading associated with that thrusting would have drawn the basin axis (the topographically lowest part of the active, two-sided depositional system) westward from where it stood at the time when the Virginian Ridge clastic wedge had prograded to its easternmost limit.

Continue west on Twisp River Road.

7.1 Newby Creek Road. Continue straight ahead.

7.7 Andesitic volcanic rocks of the Midnight Peak Formation.

8.3 Little Bridge Creek Road on the right. Continue straight ahead.

11.1 Road to Black Pine Lake and Buttermilk Creek on the left. Continue straight ahead.

12.5 Volcanic rocks assigned to the Winthrop Sandstone (McGroder, unpublished data). These rocks were originally assigned to the Midnight Peak Formation (Barksdale, 1975). They apparently record intrabasinal volcanism in the Methow during Albian time.

14.7 War Creek Campground.

14.9 Go left on Forest Service Road (FSR) 4430 across the Twisp River.

15.1 Bear right.

15.3 **STOP 1-6. Twisp River fault zone.**

A series of roadcuts exposes mylonites associated with the Twisp River fault, which is concealed by alluvium in the valley of the Twisp River a short distance to the northeast. This major structure is part of the Ross Lake fault zone and separates the polydeformed Twisp Valley Schist and other rocks of the crystalline core of the North Cascades from the lower grade North Creek Volcanics. The latter consists of altered intermediate volcanic rocks and arkoses of uncertain age which may be part of the lower section of the Methow basin or part of a separate terrane (McGroder, 1988).

The Twisp River fault zone consists mainly of mylonitic gneisses, garnet-biotite schists, and porphyries. The latter may have been intruded into the fault zone and now form the lineated mylonites exposed at this locality. They contain relict plagioclase phenocrysts that can be recognized in thin section, but that are more difficult to discern by hand lens.

The subhorizontal stretching lineation and the steep foliation are most compatible with strike-slip motion in the mylonite zone. Kinematic indicators are scarce but indicate dextral slip. Furthermore, the mylonite zone is continuous with, and probably is a splay of the Foggy Dew fault zone which provides ample evidence of dextral slip. (See Stop 1-4.) Barksdale (1975), however, favored sinistral slip for the fault.

Mylonitic tonalitic gneisses occur a few tens of meters southwest of these roadcuts. The gneisses contain the assemblage quartz-plagioclase-biotite-muscovite-epidote and display plagioclase porphyroclasts and prominent quartz ribbons. The gneisses may be derived from the Oval Peak pluton, but they are separated from that intrusion by garnet-biotite schist of the Twisp Valley Schist.

Continue straight (northwest)

15.5 Road to War Creek trailhead. Continue straight ahead.

19.3 Turn right to Mystery Camp.

19.35 **STOP 1-7 (optional). North Creek Volcanics.**

Moderately deformed sedimentary rocks assigned to the North Creek Volcanics of Misch (1966) are exposed here, and the structural style and metamorphic grade can be contrasted with rocks at the preceding stops. This unit lies in the triangular fault sliver between the Twisp River fault on the west and the North Creek fault on the east. It exhibits a style and intensity of deformation that appear more ductile and intense than in the Winthrop Sandstone and less penetrative and less intense than in rocks at the preceding stop near War Creek. Note the two lineations in the outcrop, both of which trend generally northwesterly and plunge gently. The type of strain and the metamorphic gradient shown by the last three stops are characteristic of the high-angle oblique-slip fault systems on the east margin of the Cascades metamorphic core.

Head southeast toward Twisp on the Twisp River Road.

23.5 Pass War Creek campground on the way back to Twisp.

29.9 Little Bridge Creek Road on the left.

32.7 Elbow Coulee Road on the left.

33.0 **STOP 1-8. Virginian Ridge Formation.**

Chert-pebble conglomerates like the ones at this outcrop are the hallmark of the Virginian Ridge Formation and signal an abrupt and important change in the source terrain of Methow basin clastics in about middle Albian time. Paleocurrent studies, provenance analysis, and the age of radiolarians (Triassic-Jurassic) from the chert pebbles all point to the Bridge River-Hozameen terrane as the most obvious and likely source terrane. (See Trexler, 1985.)

The Virginian Ridge was probably deposited in a steep fan-delta system that prograded eastward through time. Basal pro-delta(?) turbidites are overlain by thickening and coarsening upward deltaic cycles that are typically

capped by sheets of laterally extensive pebble and cobble conglomerate like the one at this stop.

The Virginian Ridge exceeds 4 km in thickness at the west edge of the basin and thins dramatically to the east. This gives it a wedge-shaped three-dimensional geometry. These traits suggest that the unit was deposited in a structural moat adjacent to an active thrust-cored uplift.

Return to Twisp.

38.2 Highway intersection. Turn left (north) onto SR 20 toward Winthrop.

39.4 Bluffs of Paleogene Pipestone Canyon Formation at 2 to 3 o'clock. Boulder conglomerate, granitic sandstone, and finely laminated siltstone were probably deposited as alluvial fans and lake beds against an active Pasayten fault scarp. The unit was then tilted eastward during continued motion on the fault and now dips at 20 to 45 degrees.

40.3 Deformed Twisp Formation. This unit has not been dated, but it has been tentatively correlated with the Lower to Middle Jurassic Ladner Group in British Columbia on lithologic grounds (Barksdale, 1975).

45.0 Milepost 195. Twisp Formation.

46.6 Cross Methow River and enter Winthrop.

47.2 Turn left at four-way intersection, staying on SR 20. Cross Chewack (Chewuch) River and continue north out of town.

53.2 Type section of the Winthrop Sandstone.

54.0 Approximate trace of the Boesel fault, which divides the Methow into a northern basin or subterrane that contains a thick Lower Cretaceous turbidite package (Jackass Mountain or Harts Pass Group) and a southern basin or subterrane that does not contain such rocks. Midnight Peak Formation crops out on the right for next several miles.

55.6 Cross the Methow River.

56.0 Eastward-dipping flatirons of the Ventura red bed member of the Midnight Peak Formation on the left for the next mile. The red beds and underlying units form the west limb of the Goat Peak syncline, a major structure that extends northward approximately 50 km from this latitude to nearly the U.S.-Canadian border. Many drainages in the Methow Valley area are incised into the Ventura, which is composed of nonresistant mudstone, sandstone, and minor conglomerate.

60.9 Road to Mazama; Goat Peak on the right. Continue straight ahead on SR 20.

62.7 Cross Early Winters Creek.

64.6 Cross Early Winters Creek again.

65.1 Go left at the Cedar Creek trailhead road (FSR 200). Drive to the back (south) end of the gravel pit at the end of the road.

66.3 **STOP 1-9. Driveway Butte overview.**

This stop presents a representative view of the characteristic structural style of rocks in the Methow basin. Figure 7 is a line drawing made from a photograph taken from this location. It shows elements of a west-vergent imbricate system along the Driveway Butte fault. The Driveway Butte fault dips steeply east at this location and places the Harts Pass Formation atop the Virginian Ridge Formation. The footwall rocks of the fault lie in the hanging wall of the Slate Creek fault, and so they are also tilted eastward. The fault zones themselves are typically covered, but where exposed they locally contain downdip stretching lineations in deformed conglomerates. On the basis of the stratigraphic position of rocks involved in west-vergent thrusting, those faults do not appear to have accommodated tremendous displacement. However, the main east-vergent thrust in the basin, which daylights north of the field trip route, places Lower Jurassic above Upper Cretaceous and therefore accomodated substantial displacement. An explanation for these relationships will be offered at the final stop of the day.

Return to SR 20.

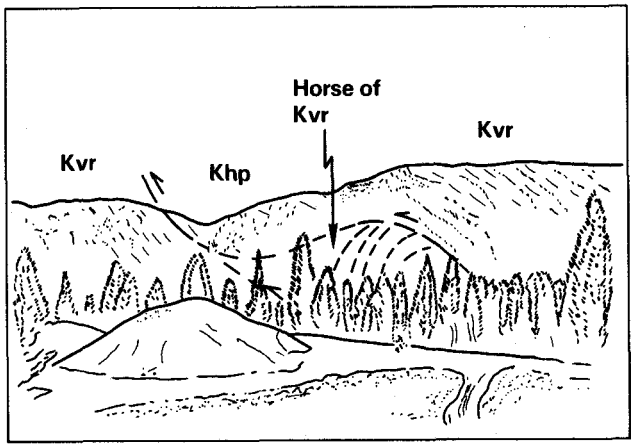

Figure 7. Sketch of Driveway Butte, showing oblique view of Driveway Butte fault as viewed from south. Kvr, middle Albian Virginian Ridge Formation; Khp, lower to middle Albian Harts Pass Formation. Fault-bounded sliver or horse of Kvr makes up knob in foreground. Apparent curved trace of fault above horse is due to the oblique view of the structure coupled with topographic effects. The fault and the beds above it are roughly planar and dip east, or to the right.

67.5 Junction with SR 20. Turn right (east).

71.6 Make a left turn toward Mazama.

71.8 Cross the Methow River.

72.0 Go left on the road toward Harts Pass and pass the Mazama Country Store. At Harts Pass and nearby Slate Peak, you can see beautiful high mountain scenery and peaks as far west as Mount Baker, as well as a thick section of the Harts Pass and Virginian Ridge formations.

74.9 Small outcrops of Ventura red beds for the next couple of miles.

77.0 **STOP 1-10. Overview of sub- and intra-Midnight Peak unconformities.**

Stop at the old barn and find a place to turn around.

An important unconformity has recently been discovered between the Winthrop Sandstone and overlying Midnight Peak Formation. The view from this spot on the Harts Pass road affords one of the better opportunities to see the angular unconformity from a distance. Figure 8 is a sketch of Last Chance Point drawn from approximately this location. It shows how the basal red beds of the Ventura member overlie a bevelled Winthrop Sandstone with about 20 degrees of

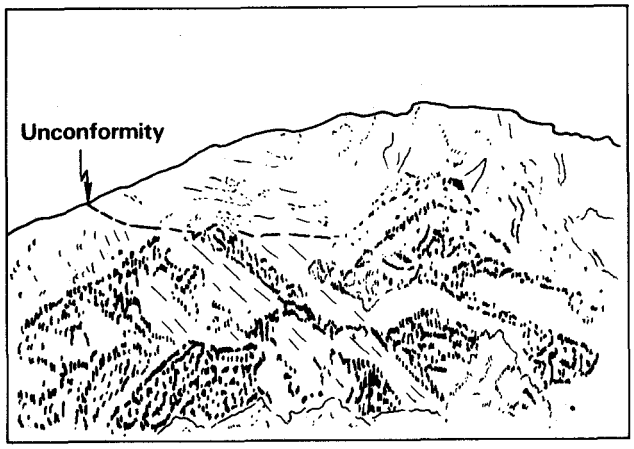

Figure 8. Sketch of Last Chance Point, viewed from the south. View shows angular unconformity separating Winthrop Sandstone below (dip 40°-45° east) from basal red beds of Midnight Peak Formation above (dip 15°-20° east).

discordance. The steeper dip of the Winthrop with respect to the Ventura and the location of a structural high defined by isopach data (Fig. 9) suggest that folding and uplift of the Winthrop in this area was coupled to and driven by motion on the Driveway Butte and(or) Slate Creek thrusts.

Above the road and to the east, in the steep hillslope beneath Goat Peak, the volcanic member of the Midnight Peak appears to cut downsection westward into the Ventura member. This intraformational unconformity lies east of the one beneath the Ventura member and probably records continued growth of the structural high above the west-vergent thrust(s) during deposition of the Midnight Peak Formation. Folding obviously outlasted deposition of this unit because the volcanic rocks themselves are folded.

Return to the intersection just south of the Mazama country store.

81.9 At the intersection, go left toward Winthrop on the old state highway. You will follow the old highway for several miles.

83.9 Turn left at Goat Peak Road.

86.6 Turn left toward the Goat Peak lookout.

91.2 **STOP 1-11.Volcanic rocks of the Midnight Peak Formation and overview of Methow basin structure.**

The Midnight Peak Formation is characterized by pyroxene-plagioclase andesite brec-

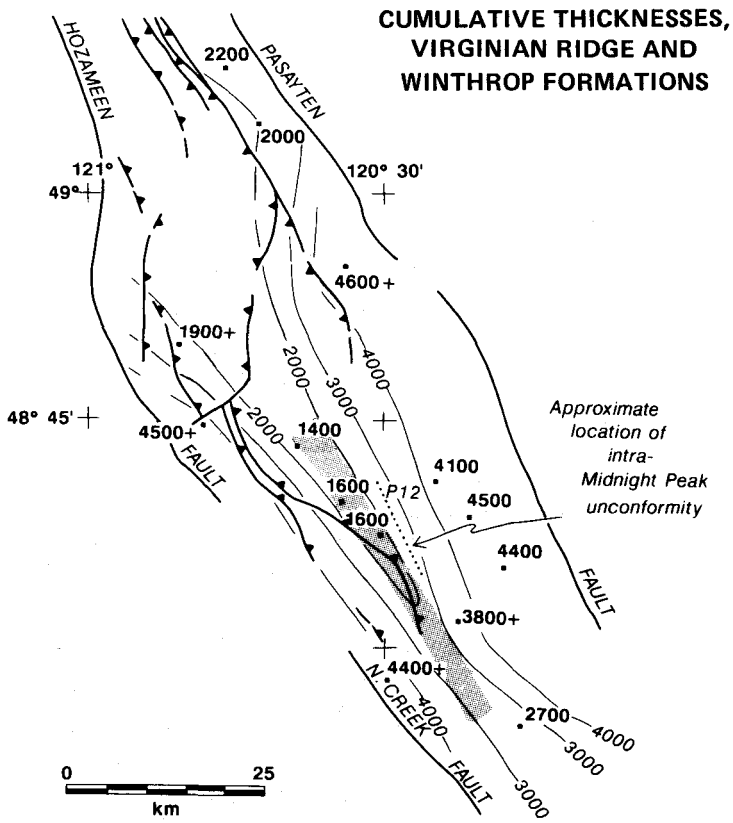

Figure 9. Isopach map showing cumulative thicknesses, in meters, of Virginian Ridge and Winthrop Formations. Shaded area represents region where the sub-Midnight Peak unconformity is demonstrably angular. Note spatial coincidence of angular unconformity, isopach low, and the two thrusts, the Driveway Butte and Slate Creek Peak faults. These relations strongly suggest that the structural high (isopach low) and angular unconformity formed in the hangingwall of the two thrusts while one or both were active. Because the two faults were kinematically linked to the Chuwanten thrust as the top and bottom of a tectonic wedge, some motion on the Chuwanten thrust is bracketed between late Albian and about 89 Ma, the upper age limit on the Midnight Peak Formation.

cias that weather to various shades of green, maroon, and red. Hornblende is quite rare in the Midnight Peak and so the unit has never been dated directly, but field relations and geochemistry suggest that the volcanic rocks are extrusive equivalents of a group of 86 to 90 Ma stocks in the basin (V. Todd, USGS, oral commun., 1985). These early Late Cretaceous rocks are part of a widespread magmatic arc that appears to intrude most Cascades terranes and, except in the deep part of the metamorphic core, crystallized during and after the last stages of regional contractional deformation. Related arc rocks are the Black Peak batholith, the Pasayten, Rock Creek, and Fawn Peak stocks, the Eldorado Orthogneiss, the Ten Peak pluton, and the Mount Stuart batholith.

This overview is near the axial trace of the Goat Peak syncline (Fig. 1). The east limb of the syncline exposes fairly deep rocks in the Methow section, yet the deep level of neither of the west-vergent thrusts that emerge to the west (Stop 1-9) occurs in that limb. Seismic reflection data collected along the Twisp River Road and balanced cross-sections constructed by downplunge projection suggest that the east-dipping faults in the hillside we are viewing emanate from the nose of a tectonic wedge floored by an east-vergent thrust (McGroder, 1988). The nose of this wedge, where the east- and west-vergent thrusts intersect, probably now underlies the axial trace of the Goat Peak syncline, approximately beneath this stop. The insertion of this wedge into the basin delaminated the Methow strata along west-vergent thrusts (for example, Driveway Butte, Slate Creek) that propagated through the section by folding rocks at high structural levels. In the the north end of the basin, the sole fault to the wedge eventually climbed all the way to the surface. Lesser displacement at the latitude of Mazama stranded the nose of the wedge in the subsurface. This displacement gradient generated the southeasterly regional plunge in the basin.

As discussed above, most of the deformation preceded and accompanied deposition of the Midnight Peak Formation, that is, occurred between about 100 and 88 Ma. Balanced cross-sections suggest that shortening exceeded 50 km at the present latitude of the U.S.-Canadian border (McGroder, 1988).

The prominent peaks in the distance are composed of granite of the Golden Horn batholith, which is described at the first stop on the companion road guide (Haugerud, this volume).

Return to Winthrop.

Geology of the Metamorphic Core of the North Cascades

Ralph A. Haugerud
U.S. Geological Survey
345 Middlefield Road
Menlo Park, CA 94025

INTRODUCTION

Eocene faults segment the Cretaceous and earliest Tertiary North Cascades orogen into several blocks (Fig. 1) among which there are significant differences in stratigraphy, thermal history, and(or) deformational history. Medium- and high-grade regionally metamorphosed rocks of the orogen are restricted to the region between the Straight Creek fault and the Ross Lake fault zone—commonly referred to as the "metamorphic core" or "Skagit core"—and a narrow area along the northeast side of the Ross Lake and North Creek faults.

This paper contains a geologic overview and road log for a one-day field trip across the Ross Lake fault zone and metamorphic core along Washington State Route (SR) 20. The road log continues into the mildly metamorphosed rocks west of the Straight Creek fault; however, for an overview of the geology of of the western North Cascades, the reader should refer to the companion paper by Brandon (this volume).

Within the metamorphic core the Entiat fault is a significant boundary. Much of the block to the northeast of the fault was ductilely deformed in the Eocene, and a large fraction of K-Ar cooling ages there are Eocene (disregarding those ages associated with younger plutons of the Cascade arc). No Eocene ductile deformation has been recognized in the block southwest of the Entiat fault, where most cooling ages are Late Cretaceous (Engels and others, 1976; Haugerud, 1987). Discussion herein of the metamorphic core is, in general, applicable only to the region northeast of the Entiat fault.

GEOLOGIC OVERVIEW

The gross structural relations among major pre-Eocene lithologic units discussed here are summarized in Figure 2. The geology and geography of the field trip are sketched in Figure 3 (Ross Lake fault zone and metamorphic core) and Figure 4 (western North Cascades).

Fieldtrip stops emphasize three themes: (1) several pre-Late Cretaceous terranes that are the fundamental building blocks of this part of the range, (2) deformation and metamorphic recrystallization of these terranes during Late Cretaceous and earliest Tertiary orogeny, and (3) Eocene reworking of the orogen and coeval magmatism of the "Challis" event. Oligocene and younger magmatic rocks of the Cascade arc are neglected, though they comprise much of this part of the range.

Pre-Late Cretaceous(?) Terranes

Rocks within the Ross Lake Fault Zone

Three units of metamorphosed sedimentary and volcanic strata which crop out between the Hozameen fault and Ross Lake fault proper, within the Ross Lake fault zone, comprise two terranes. Below the Jack Mountain thrust, phyllite and semischist with minor amounts of intercalated ribbon chert, greenish tuffaceous schist, and scattered ultramafic pods constitute the Jack Mountain Phyllite of Misch (1966b) (Stop 2-2); associated with this unit is the higher grade, largely metavolcanic, Elijah Ridge Schist of Misch (1966b). The North Creek Volcanics of Misch (1966b) may be correlative with the Elijah Ridge Schist. Tabor and others (in press [a]) lump these units together as the Little Jack terrane. These units predate the Late Cretaceous Black Peak and middle Eocene Golden Horn batholiths.

Above the Jack Mountain thrust lies the Permian to Middle Jurassic Hozameen Group of Cairnes (1944)(Hozomeen of other authors), composed of basaltic greenstone (metamorphosed pillow basalt, tuff, breccia, massive lava), chert, and argillite with minor amounts of limestone, gabbro, sandstone, and dacite(?) (McTaggart and Thompson, 1967; Tennyson and others, 1982; Haugerud, 1985; Ray, 1986).

North of 49°N, the Maselpanik schist unit of Haugerud (1985) is the along-strike metamorphic equivalent of the Elijah Ridge Schist and Jack Mountain Phyllite, although McTaggart and Thompson (1967) and

From: Joseph, N. L., and others, editors, 1989, Geologic guidebook for Washington and adjacent areas: Washington Division of Geology and Earth Resources Information Circular 86.

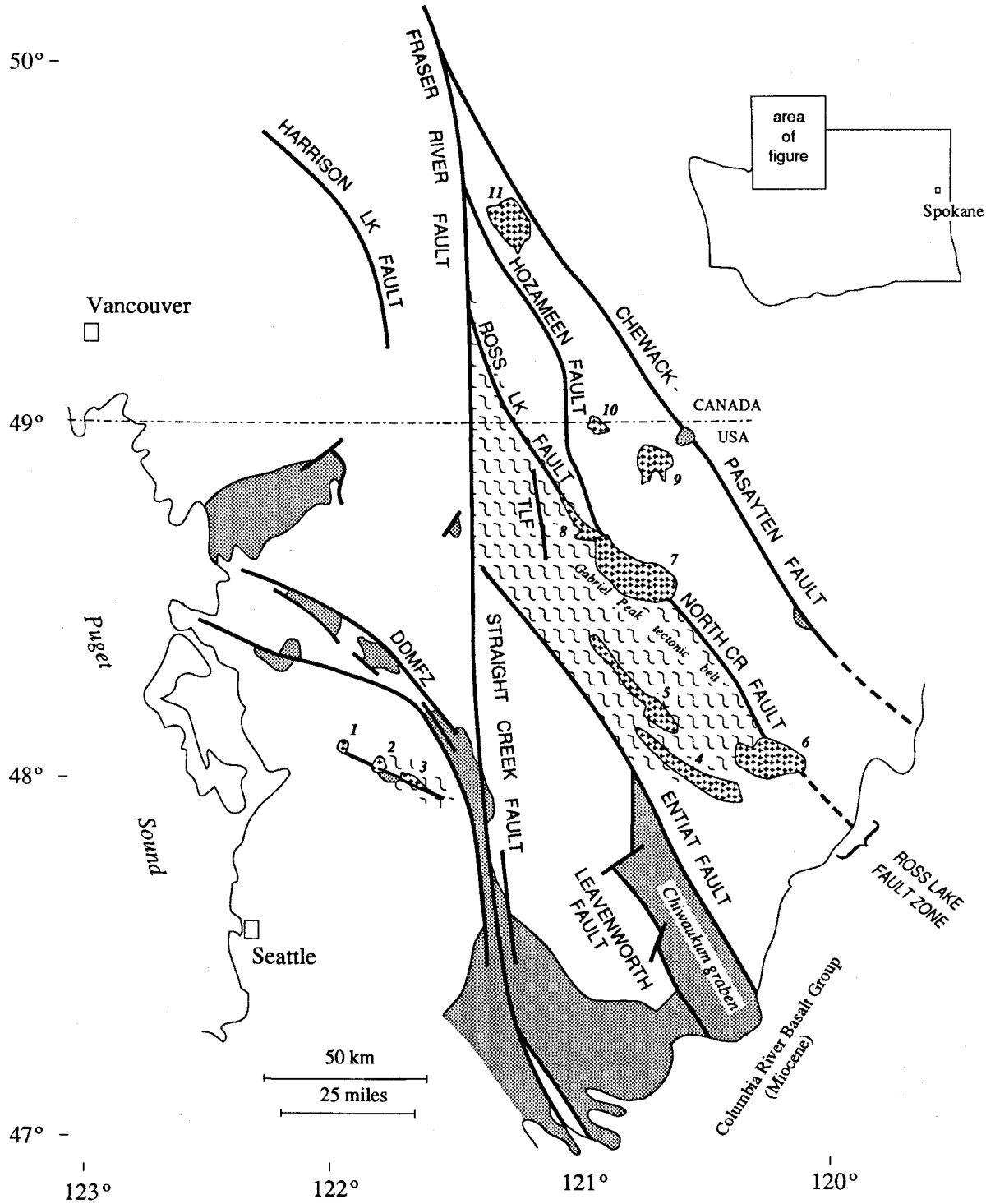

Figure 1. North Cascades area and significant Eocene features. Shaded areas, Eocene sedimentary and volcanic rocks; crosses, Eocene plutons (1, Granite Falls; 2, Mount Pilchuck; 3, Bald Mountain; 4, Duncan Hill; 5, Railroad Creek; 6, Cooper Mountain; 7, Golden Horn; 8, Ruby Creek; 9, Monument Peak/Lost Peak; 10, Castle Peak; 11, Needle Peak); wavy lines, regions of Eocene ductile deformation and(or) Eocene K-Ar regional-metamorphic cooling ages; DDMFZ, Darrington-Devils Mountain fault zone; TLF, Thunder Lake fault. Eocene ages of some features are inferred.

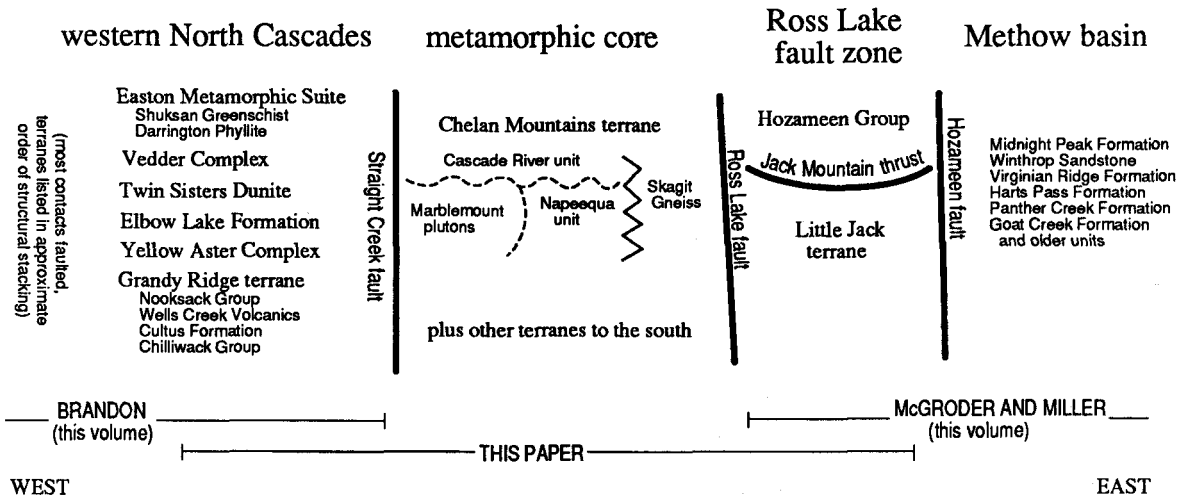

Figure 2. Gross structural relations of major pre-Eocene rock units along Washington State Route 20, showing area covered by this paper and companion papers by McGroder and Miller (this volume) and Brandon (this volume). Synorogenic plutons omitted. Nomenclature does not conform to current usage by U.S. Geological Survey.

Haugerud (1985) inferred that this unit has a Hozameen protolith.

Rocks between the Ross Lake and Straight Creek Faults

Tabor and others (in press [a]) assign schists and gneisses on the fieldtrip route between the Ross Lake and Straight Creek faults to four units. First is the Napeequa unit (Stop 2-6), which consists of metachert, amphibolite, calcareous and amphibolitic schist, rare marble, and scattered ultramafic bodies. The second unit, the Cascade River unit, consists of thick sections of granitoid-clast metaconglomerate as well as metasandstone, lesser metapelite, and some metavolcanic rock. Associated with these two units is the third, the tonalitic, 220 Ma Marblemount Meta Quartz Diorite of Misch (1966b) and related plutons. These three units are part of the Chelan Mountains terrane. (Nomenclature used here is that of Tabor and others, 1988, in press [a]). The Cascade River Schist of Misch, 1966, includes all of the Cascade River unit and parts of the Napeequa unit. Our work suggests that the Cascade River Schist should be restricted to the metaclastic schists and their interstratified metavolcanic rocks. As used here, the Chelan Mountains terrane includes the Mad River terrane of Tabor and others (1987a).

Relations among these three units are not well understood. My preferred hypothesis is that the Marblemount plutons intruded the Napeequa unit and that the Cascade River unit once overlay both depositionally. A pre-metamorphic fault between the Napeequa and Cascade River units is also plausible. Constraints are: (a) boulders of Marblemount(?) tonalite occur in metaconglomerate of the Cascade River unit; (b) the oceanic, ribbon chert- and basalt-rich Napeequa unit and the coarse-clastic-rich Cascade River unit are incompatible depositional assemblages; (c) Mattinson (1972) interpreted a discordant U-Pb zircon age from meta-keratophyre of the Napeequa unit (collected in the Holden area) to indicate crystallization at about 265 Ma, before intrusion of the 220 Ma Marblemount plutons; and (d) the Cascade River unit is in part coeval with the Marblemount unit, as metatuff in the Cascade River unit has given a 219 Ma U-Pb zircon age (John Stacey, U.S. Geological Survey, written commun., 1988).

The fourth unit of the metamorphic core at this latitude, the Skagit Gneiss of Misch (1966b), is largely orthogneiss (Stop 2-5) with subsidiary banded gneiss which contains significant paragneiss (Stop 2-4). Both are commonly migmatitic. Near Big Devil Peak, south of Newhalem, schist of the Napeequa unit grades into banded gneiss of the Skagit Gneiss; similar schist reappears at the northeast margin of the Skagit Gneiss, on the upper slopes of Ruby Mountain. For these reasons Tabor and others (in press [a]) include all Skagit paragneisses in the Chelan Mountains terrane, though it is possible that other pre-metamorphic terranes (for example, the Skymo unit, Stop 2-3) are hidden by the veil of high-grade metamorphism and migmatization in the Skagit.

Farther south, other pre-Late Cretaceous terranes lie within the metamorphic core of the North Cascades. These include the largely metapelitic Nason terrane, the meta-arkosic(?) Swakane terrane, and the (in part unmetamorphosed) ophiolitic Ingalls Complex of Miller (1985). Descriptions of these terranes and further references are in Tabor and others (1987a).

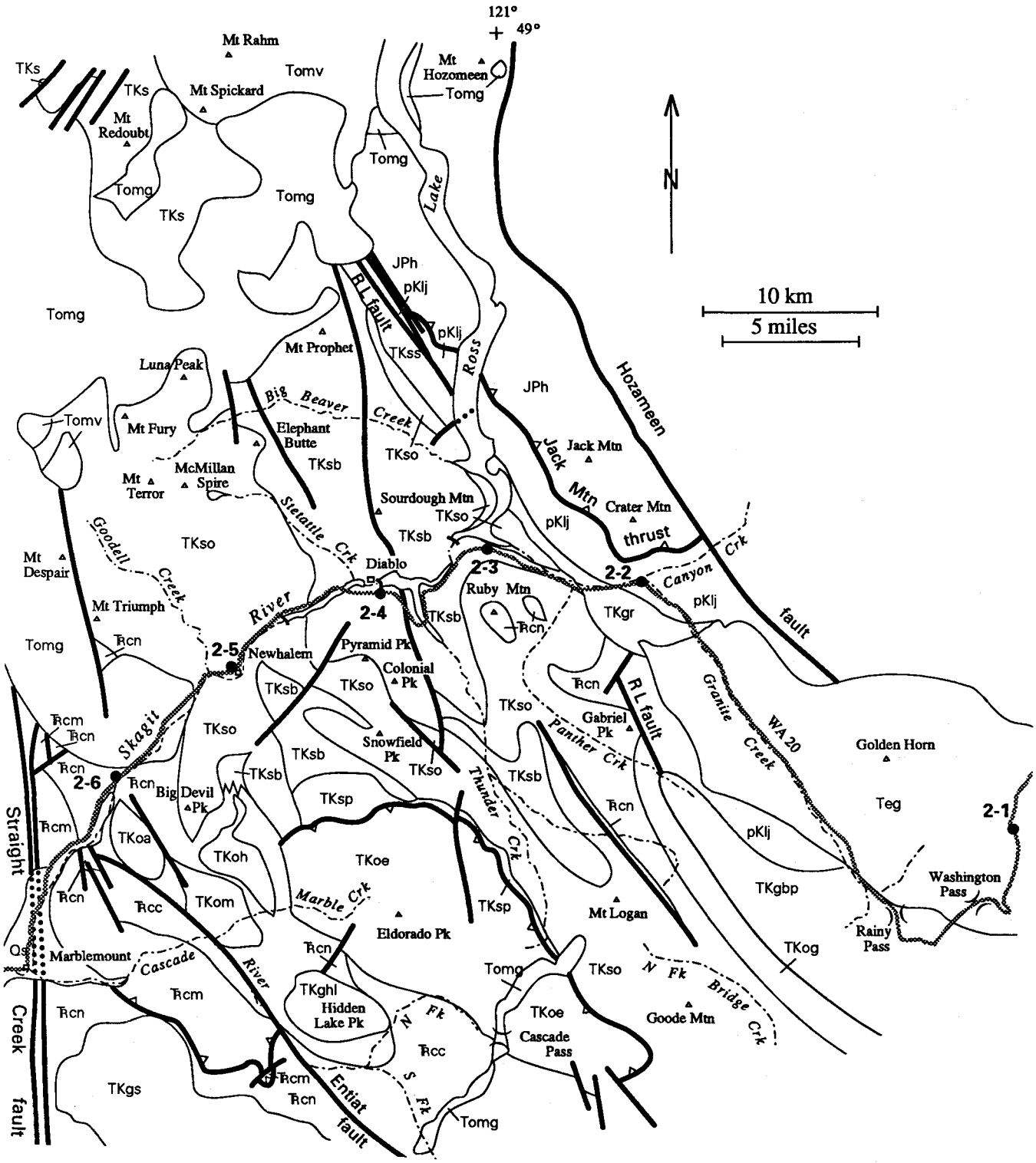

Figure 3. Geologic map of the area along the fieldtrip route between the Hozameen and Straight Creek faults. Compiled from Tabor (1961), Staatz and others (1972), Barksdale (1975), Misch (1977), Miller (1987), Tabor and others (1988), and Tabor and Haugerud (unpublished USGS field maps). Absolute ages are primary intrusive or depositional ages interpreted from U-Pb zircon dating as reported by Mattinson (1972), Hoppe (1984), Miller and others (1988), Haugerud and others (1988), and J. S. Stacey (USGS, written commun., 1987, 1988). See facing page for explanation.

EXPLANATION

Q Surficial deposits

ROCKS OF THE CASCADE ARC

Tomg Miocene and Oligocene granitoid rocks
Tomv Miocene and Oligocene volcanic rocks

ROCKS OF THE "CHALLIS" EVENT

Teg Eocene granite of the Golden Horn batholith--50 Ma

EOCENE TO LATE CRETACEOUS OROGENIC ROCKS

Skagit Gneiss of Misch (1966)--Largely migmatitic. Divided into:
TKsb Banded gneiss (metamorphic age)--derived from strata of the Chelan Mountains terrane
TKss Skymo unit--Troctolite, norite, and gabbro
TKso Orthogneiss--65 and 74 Ma, in part
TKsp Pegmatite--At northeast border of Eldorado pluton

Orthogneiss--Divided into:
TKoa Alma Creek pluton
TKom Marble Creek pluton--75 Ma
TKoh Haystack Creek pluton
TKog Gabriel Peak Orthogneiss of Misch (1966)--65 Ma
TKoe Eldorado Orthogneiss of Misch (1966)--90 Ma

Granitoid plutons--Little-deformed to undeformed. Divided into:
TKgr "Ruby Creek Heterogeneous Plutonic Belt" of Misch (1966)--48 Ma, in part
TKghl Hidden Lake pluton--75 Ma
TKgs Snowking pluton
TKgbp Black Peak batholith--90 Ma, in part

PRE-OROGENIC TERRANES

JPh Hozameen Group of Cairnes (1944) (Middle Jurassic to Permian)

pKlj Pre-Late Cretaceous rocks of the Little Jack terrane--Metamorphosed during Late Cretaceous to Eocene orogeny

Triassic (and older?) rocks of the Chelan Mountains terrane--Metamorphosed during Late Cretaceous to Eocene orogeny. Divided into:
TRcc Cascade River unit--219 Ma, in part
TRcn Napeequa unit--Pre(?)-220 Ma, in part
TRcm Marblemount Meta Quartz Diorite of Misch (1966) and correlative tonalitic plutons--220 Ma

contact fault low-angle fault
2-2 fieldtrip stop

Rocks West of the Straight Creek Fault

Rocks west of the Straight Creek fault have close affinities with rocks of the San Juan Islands and are described by Brandon (this volume).

The discerning reader will note possible parallels between rock units east and west of the Straight Creek fault: for example, might the Elbow Lake Formation, Napeequa unit, and Hozameen Group be equivalent? What of the similarities between the Cultus Formation and Cascade River unit? Such correlations should be good fodder for the beer hour.

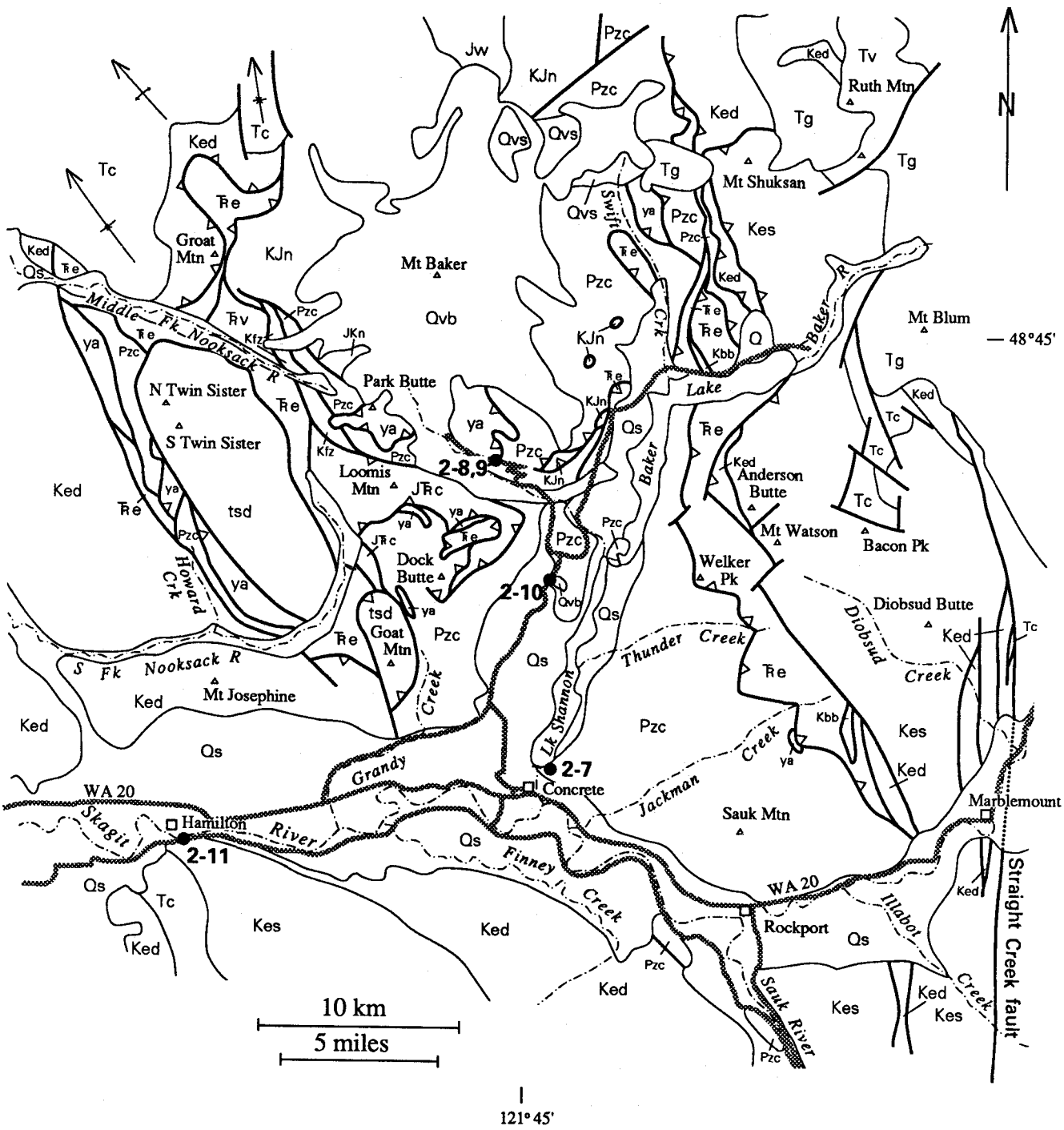

Figure 4. Geologic map of the area along fieldtrip route west of the Straight Creek fault. Simplified from Brown and others (1987). Age assignments are from cited references and C. D. Blome (USGS, written commun., 1988). See facing page for explanation.

EXPLANATION

Qs Surficial deposits

ROCKS OF THE CASCADE ARC

Qvb Quaternary volcanic rocks of Mount Baker
Qvs Volcanic rocks of Swift Creek--Pre-Mount Baker age
Tv Tertiary volcanic rocks
Tg Pliocene to Oligocene granitoid rocks

EOCENE SEDIMENTARY ROCKS

Tc Chuckanut Formation

PRE-LATE CRETACEOUS ROCKS

(in approximate order of structural stacking)

Easton Metamorphic Suite (Early Cretaceous; metamorphic age)--Divided into:
Kes Shuksan Greenschist
Ked Darrington Phyllite

TRv Vedder Complex of Armstrong and others (1983) (Triassic; metamorphic age)

Kbb Baker Lake Blueschist of Brown and others (1987) (Cretaceous(?); metamorphic age)

ya Yellow Aster Complex of Misch (1966)

tsd Twin Sisters Dunite of Misch (1966)

TRe Elbow Lake Formation of Brown and others (1987) (Triassic?, may in part be younger and older)

Grandy Ridge terrane--Divided into:
KJn Nooksack Group of Misch (1966) (Cretaceous and Jurassic)
Jw Wells Creek Volcanics of Misch (1966) (Jurassic)
JTRc Cultus Formation of Monger (1970) (Jurassic and Triassic)
Pzc Chilliwack Group of Cairnes (1944) (Paleozoic)

Kfz Cretaceous fault zone

contact fault low-angle fault

2-11 fieldtrip stop

Late Cretaceous and Earliest Tertiary Orogeny

Most rocks within the metamorphic core of the North Cascades are schist or gneiss formed during Late Cretaceous recrystallization and deformation, which locally lasted into the early Tertiary. Roughly contemporaneous with this metamorphism was the intrusion of numerous plutons.

Peak regional-metamorphic conditions along the fieldtrip route ranged from chlorite zone near the Hozameen-North Creek fault, to sillimanite zone in much of the Skagit Gneiss, back down to chlorite zone near Marblemount (Misch, 1966b, 1968, 1977, 1979). Thermobarometry suggests peak conditions of about 720°C and 9 kb in Skagit Gneiss having the highest metamorphic grade (Whitney and Evans, 1988).

Synorogenic plutons are mostly tonalitic. Mattinson (1972) demonstrated that one of the largest of these, the Eldorado Orthogneiss of Misch (1966b), is ~90 Ma, thus part of a suite of mid-Cretaceous plutons that includes the Mount Stuart, Spuzzum, Pasayten, and several other bodies in the North Cascades and adjacent Coast Mountains. More recently, Miller and others (1988), Haugerud

and others (1988), and John Stacey (U.S. Geological Survey, written commun., 1988) have obtained U-Pb zircon ages of 60 to 75 Ma from several plutons in the Ross Lake fault zone and that part of the metamorphic core northeast of the Entiat fault (Stop 2-5). The younger plutons seem to be restricted to this region.

Ductile deformation in the metamorphic core and at the southwest edge of the Ross Lake fault zone postdates Upper Triassic and Middle Jurassic protoliths and locally lasted into (or was revived in) the middle Eocene (Stop 2-4). Within the Skagit Gneiss, early Tertiary deformation has obliterated most evidence of earlier phases of deformation. Xenoliths in a 64 Ma orthogneiss in the Skagit preserve an older, pre-intrusion foliation (Haugerud, 1985; Haugerud and others, 1988). An older fabric is also preserved in well-foliated schist which is intruded by the slightly deformed ~75 Ma Hidden Lake Peak stock (Fig. 3). By analogy, all of the Skagit Gneiss was probably deformed before 75 Ma. Along the fieldtrip route, the dominant fabric in rocks of the core is a northwest-trending subhorizontal lineation associated with steeply dipping northwest-striking foliation. These orientations largely reflect the youngest, Eocene, penetrative deformation.

Metamorphic recrystallization is not well dated, but must postdate Late Triassic strata of the Chelan Mountains terrane and Middle Jurassic Hozameen strata that grade into the Maselpanik schist unit of Haugerud (1985). Pre-kinematic porphyroblasts in schists adjacent to the Hidden Lake Peak stock demonstrate pre-75 Ma recrystallization. The ~75 Ma tonalitic Marble Creek pluton (Fig. 3) contains magmatic epidote, indicating pressures ≥6 kb at that time (Zen and Hammarstrom, 1984). The 65 Ma pluton at Newhalem (Stop 2-5) has participated in migmatization. Most metamorphic recrystallization within the Skagit Gneiss predates middle Eocene dikes and sills; these dikes and sills cross-cut the main metamorphic fabric and have igneous textures modified only by mylonitic grain-size reduction.

Eocene Orogeny

The North Cascades lie at the junction of two Eocene tectonic regimes. To the east, east-west extension of the Omineca belt in the early and middle Eocene was accompanied by low-angle normal faulting; basin development; ductile deformation, unroofing, and cooling of mid-crustal rocks; and by the extensive and intense Challis magmatic event (Ewing, 1980; Parrish and others, 1988). To the west, parts of the continental margin were transported northward on a network of north- to northwest-trending steep faults at about the same time (for example, Cowan, 1982; Johnson, 1984).

Eocene deformation of the North Cascades seems to reflect the interaction of these regimes: The few K-Ar ages from the Skagit Gneiss and adjacent schists (Engels and others, 1976; Richards and McTaggart, 1976) indicate unroofing and consequent cooling in the middle Eocene, apparently during or shortly after post-46 Ma ductile extension (Stop 2-4). Challis-age magmatic rocks are present in much of the range (Stops 2-1 and 2-4), and sedimentary basins developed in the western North Cascades, in the central Cascades, and east of the metamorphic core. However, the extension direction in the Skagit Gneiss is northwest-southeast, subparallel to the continental margin, and associated faults are steep and dominated by dextral strike slip. Eocene features in the North Cascades are sketched in Figure 1.

Mylonitic fabrics, cooling at the same time as unroofing of metamorphic complexes in the Okanogan region to the east, and sharp changes in metamorphic grade at the northeast margin of the Skagit Gneiss all invite comparison with metamorphic core complexes elsewhere in the Cordillera, but the characteristic low-angle normal faults seem to be missing.

Unroofing of the Skagit Gneiss was accommodated by at least three mechanisms: (1) an unknown amount of erosion; (2) vertical thinning within the Skagit Gneiss, and presumably the once-overlying rocks, evidenced by uniaxial prolate strains in late lineated orthogneiss dikes—that is, horizontal extension with apparent shortening in all directions, including the vertical, at right angles to the extension direction; and, necessarily coupled with these mechanisms, (3) the dip-slip component of motion on the Ross Lake, Entiat, and Straight Creek faults (Haugerud, 1985). Along-strike depth changes in the Duncan Hill pluton (Fig. 1) (Hopson and others, 1970; Dellinger and Hopson, 1988) suggest up-to-the-northwest tilting at the southern margin of the Skagit Gneiss.

Seemingly contradictory evidence for timing of motion in the Ross Lake fault zone (Fig. 3) is reviewed by McGroder and Miller (this volume). Though one strand of the zone is plugged by the Black Peak batholith—dated at one locality at 90 Ma—and the 50 Ma Golden Horn batholith plugs another strand, other strands displace rocks as young as 48 Ma, and fault-associated fabrics affect 46 Ma orthogneiss north of 49°N. The contrast in metamorphic facies across the fault zone suggests significant dip-slip motion, whereas fabrics within the zone show both dextral strike slip and oblique slip (Haugerud, 1985; Tabor and others, in press [a]; McGroder and Miller, this volume).

Kriens (1988) studied the Ross Lake fault proper near SR 20 and found no evidence for significant early Tertiary dextral displacement. Perhaps much of the Eocene motion documented by Haugerud (1985) to the north and Miller (Miller and others, 1985; McGroder and Miller, this volume) to the south is localized on faults or zones of distributed shear west of the region Kriens examined.

The southern portion of the Entiat fault is a strike-slip feature that had considerable displacement, as suggested by its straightness and development of mylonites (Laravie, 1976; Whetten and Laravie, 1976). It probably was an active wrench fault during middle Eocene filling of the Chiwaukum graben (Fig. 1). However, the Entiat fault is not well defined where it meets the Straight Creek fault near Marblemount, and at this point it may have had little strike-slip displacement.

The Straight Creek fault (Fraser fault in Canada) was first recognized by Vance (1957) and interpreted as a dextral strike-slip fault by Misch (1966b). Estimates of dextral slip have ranged from 85 to 200 km; perhaps the best-founded of these is Kleinspehn's (1985) observation that undoing 110 km of dextral slip restores the Albian depositional system in the Methow–Tyaughton basin. However, no restoration of the Straight Creek fault is entirely satisfactory.

North of the Skagit River, the Straight Creek fault cuts undated (probable Eocene) fluvial sediments (Monger, 1970; Misch, 1979; Fugro Northwest, Inc., 1979) and is plugged by 35 Ma and younger plutons of the Chilliwack batholith (Richards and McTaggart, 1976). Where cross-cutting relations between northwest-southeast elongation of the Skagit Gneiss and north-south faulting on the Straight Creek system are visible north of 49°N, Straight Creek deformation is younger (Haugerud, 1985).

However, given the possible 48 to 50 Ma inception of the Straight Creek fault (Vance, 1985; but see Tabor and others, 1984, in press [b]), the cross-cutting relations may merely reflect the last increments of each process, and extension of the Skagit Gneiss and motion on the Ross Lake zone and Straight Creek fault may be contemporaneous. This implies that offset on the Straight Creek fault must change along strike, with less offset to the north. The lack of Tertiary regional metamorphism west of the Straight Creek fault indicates a substantial component of post-middle Eocene east-side-up vertical displacement.

ACKNOWLEDGMENTS

My understanding of North Cascades geology has matured in the course of three summers mapping the Mount Baker 30 x 60 minute quadrangle with Rowland Tabor; the work and ideas presented here are in large part his. These ideas will undoubtedly grow further as this mapping is completed. Conversations with E. H. Brown, the late P. Misch, D. L. Whitney, G. J. Woodsworth, and others have been helpful. The road log draws heavily from guides by Misch (1977) and Tabor and others (in press [a]). Reviews by J. G. Evans, M. A. Korosec, R. E. Powell, R. W. Tabor, and J. A. Vance have helped improve the text. Special thanks to M. F. McGroder for organizing all of this.

REFERENCES CITED

Armstrong, R. L.; Misch, Peter, 1987, Rb-Sr and K-Ar dating of mid-Mesozoic blueschist and late Paleozoic albite-epidote-amphibolite and blueschist facies metamorphism in the North Cascades, Washington and British Columbia, and fingerprinting of eugeosynclinal rock assemblages. *In* Schuster, J. E., editor, Selected papers on the geology of Washington, Washington Division of Geology and Earth Resources Bulletin 77, p. 85-105.

Armstrong, R. L.; Harakal, J. E.; Brown, E. H.; Bernardi, M. L.; Rady, P. M., 1983, Late Paleozoic high pressure metamorphic rocks in northwestern Washington and southwestern British Columbia–The Vedder Complex: Geological Society of America Bulletin, v. 94, no. 4, p. 451-458.

Babcock, R. S., 1970, Geochemistry of the main-stage migmatitic gneisses in the Skagit Gneiss Complex: University of Washington Doctor of Philosopy thesis, 147 p.

Babcock, R. S.; Armstrong, R. L.; Misch, Peter, 1985, Isotopic constraints on the age and origin of the Skagit Metamorphic Suite and related rocks [abstract]: Geological Society of America Abstracts with Programs, v. 17, no. 6, p. 339.

Barksdale, J. D., 1975, Geology of the Methow Valley, Okanogan County, Washington: Washington Division of Geology and Earth Resources Bulletin 68, 72 p., 1 pl.

Blackwell, D. L., 1983, Geology of the Park Butte-Loomis Mountain area, Washington (Eastern margin of the Twin Sisters dunite): Western Washington University Master of Science thesis, 253 p., 4 pl.

Boggs, R. C., 1980, Okanoganite, a new rare-earth borofluorosilicate from the Golden Horn batholith, Okanogan County, Washington: American Mineralogist, v. 65, no. 11-12, p. 1138-1142.

Boggs, R. C., 1984, Mineralogy and geochemistry of the Golden Horn batholith, northern Cascades, Washington: University of California, Santa Barbara, Doctor of Philosophy thesis, 187 p., 2 pl.

Brandon, M. T.; Cowan, D. S., 1985, The Late Cretaceous San Juan Islands–Northwestern Cascades thrust system [abstract]: Geological Society of America Abstracts with Programs, v. 17, no. 6, p. 343.

Brandon, M. T.; Cowan, D. S.; Vance, J. A., 1988, The late Cretaceous San Juan thrust system, San Juan Islands, Washington: Geological Society of America Special Paper 221, 81 p.

Brown, E. H., 1986, Geology of the Shuksan Suite, North Cascades, Washington. *In* Evans, B. W.; Brown, E. H., editors, Blueschists and eclogites: Geological Society of America Memoir 164, p. 143-154.

Brown, E. H., 1987, Structural geology and accretionary history of the northwest Cascades system, Washington and British Columbia: Geological Society of America Bulletin, v. 99, no. 2, p. 201-214.

Brown, E. H.; Blake, M. C., Jr, 1987, Correlation of Early Cretaceous blueschists in Washington, Oregon, and northern California: Tectonics, v. 6, no. 6, p. 795-806.

Brown, E. H.; Wilson, D. L.; Armstrong, R. L.; Harakal, J. E., 1982, Petrologic, structural, and age relations of serpentinite, amphibolite, and blueschist in the Shuksan Suite of the Iron Mountain-Gee Point area, north Cascades, Washington: Geological Society of America Bulletin, v. 93, no. 11, p. 1087-1098.

Brown, E. H.; Blackwell, D. L.; Christenson, B. W.; Frasse, F. I.; Haugerud, R. A.; Jones, J. T.; Leiggi, P. A.; Morrison, M. L.; Rady, P. M.; Reller, G. J.; Sevigny, J. H.; Silverberg, D. S.; Smith, M. T.; Sondergaard, J. N.; Ziegler, C. B., 1987, Geologic map of the northwest Cascades, Washington: Geological Society of America Map and Chart Series MC-61, 10 p., 1 pl., scale 1:100,000.

Cairnes, C. E., 1944, Hope, Yale, and New Westminster Districts, British Columbia: Geological Survey of Canada Map 737A, 1 sheet, scale 1:253,400.

Cowan, D. S., 1982, Geological evidence for post-40 m.y. B.P. large-scale northwestward displacement of part of southeastern Alaska: Geology, v. 10, no. 6, p. 309-313.

Danner, W. R., 1966, Limestone resources of western Washington: Washington Division of Mines and Geology Bulletin 52, 474 p.

Dellinger, D. A.; Hopson, C. A., 1988, Compositional zoning within the Duncan Hill pluton, North Cascades [abstract]: Geological Society of America Abstracts with Programs, v. 20, no. 3, p. 154.

Dungan, M. A.; Vance, J. A.; Blanchard, D. P., 1983, Geochemistry of the Shuksan greenschists and blueschists, North Cascades, Washington–Variably fractionated and altered metabasalts of oceanic affinity: Contributions to Mineralogy and Petrology, v. 82, no. 2-3, p. 131-146.

Engels, J. C.; Tabor, R. W.; Miller, F. K.; Obradovich, J. D., 1976, Summary of K-Ar, Rb-Sr, U-Pb, Pb-alpha, and fission-track ages of rocks from Washington State prior to 1975 (exclusive of Columbia Plateau basalts): U.S. Geological Survey Miscellaneous Field Studies Map MF-710, 2 sheets.

Ewing, T. E., 1980, Paleogene tectonic evolution of the Pacific Northwest: Journal of Geology, v. 88, no. 6, p. 619-638.

Fugro Northwest, Inc., 1979, Interim report on geologic feasibility studies for Copper Creek dam: Seattle City Light, 145 p., 2 pl.

Godinot, A., 1988, Comment on "Pipe vesicles in Hawaiian basaltic lavas–Their origin and potential as paleoslope indicators": Geology, v. 16, no. 1, p. 90.

Haugerud, R. A., 1985, Geology of the Hozameen Group and the Ross Lake shear zone, Maselpanik area, North Cascades, southwest British Columbia: University of Washington Doctor of Philosophy thesis, 263 p.

Haugerud, R. A., 1987, Argon geochronology of the Tenpeak pluton and untilting of the Wenatchee block, north Cascade Range, Washington [abstract]: Eos (American Geophysical Union Transactions), v. 68, no. 52, p. 1814.

Haugerud, R. A.; Morrison, M. L.; Brown, E. H., 1981, Structural and metamorphic history of the Shuksan Metamorphic Suite in the Mount Watson and Gee Point areas, North Cascades, Washington: Geological Society of America Bulletin, v. 92, no. 6, Part I, p. 374-383.

Haugerud, R. A.; Tabor, R. W.; Stacey, John; van der Heyden, Peter, 1988, What is in the core of the North Cascades, Washington? A new look at the structure and metamorphic history of the Skagit Gneiss of Misch (1966) [abstract]: Geological Society of America Abstracts with Programs, v. 20, no. 3, p. 168.

Hoppe, W. J., 1984, Origin and age of the Gabriel Peak Orthogneiss, North Cascades, Washington: University of Kansas Master of Science thesis, 79 p., 2 pl.

Hopson, C. A.; Cater, F. W.; Crowder, D. F., 1970, Emplacement of plutons, Cascade Mountains, Washington [abstract]: Geological Society of America Abstracts with Programs, v. 2, no. 2, p. 104.

Johnson, S. Y., 1984, Evidence for a margin-truncating transcurrent fault (pre-Late Eocene) in western Washington: Geology, v. 12, no. 9, p. 538-541.

Kleinspehn, K. L., 1985, Cretaceous sedimentation and tectonics, Tyaughton-Methow basin, southwestern British Columbia: Canadian Journal of Earth Sciences, v. 22, no. 2, p. 154-174.

Kriens, B. J., 1988, Tectonic evolution of the Ross Lake area, northwest Washington-southwest British Columbia: Harvard University Doctor of Philosophy thesis, 214 p., 7 pl.

Laravie, J. A., 1976, Geological field studies along the eastern border of the Chiwaukum graben, central Washington: University of Washington Master of Science thesis, 56 p., 1 pl.

Liszak, J. L., 1982, The Chilliwack Group of Black Mountain: Western Washington University Master of Science thesis, 104 p.

Mattinson, J. M., 1972, Ages of zircons from the northern Cascade Mountains, Washington: Geological Society of America Bulletin, v. 83, no. 12, p. 3769-3784.

McTaggart, K. C.; Thompson, R. M., 1967, Geology of part of the northern Cascades in southern British Columbia: Canadian Journal of Earth Sciences, v. 4, no. 6, p. 1199-1228.

Miller, R. B., 1985, The ophiolitic Ingalls complex, north-central Cascade Mountains, Washington: Geological Society of America Bulletin, v. 96, no. 1, p. 27-42.

Miller, R. B., 1987, Geology of the Twisp River-Chelan Divide region, North Cascades, Washington: Washington Division of Geology and Earth Resources Open-File Report 87-17, 12 p., 12 pl.

Miller, R. B.; Bowring, S. A.; Hoppe, W. J., 1988, New evidence for extensive Paleogene plutonism and metamorphism in the crystalline core of the North Cascades: Geological Society of America Abstracts with Programs, v. 20, no. 6, p. 432-433.

Miller, R. B.; Misch, Peter; Hoppe, W. J., 1985, New observations on the central and southern segments of the Ross Lake fault zone, N. Cascades, Washington [abstract]: Geological Society of America Abstracts with Programs, v. 17, no. 6, p. 370.

Misch, Peter, 1966a, Alkaline granite amidst the calc-alkaline intrusive suite of the northern Cascades, Washington [abstract]: Geological Society of America Special Paper 87, p. 216-217.

Misch, Peter, 1966b, Tectonic evolution of the northern Cascades of Washington–A west-cordilleran case history. *In* Canadian Institute of Mining and Metallurgy; and others, A symposium on the tectonic history and mineral deposits of the western Cordillera in British Columbia and neighbouring parts of the United States, Vancouver, 1964: Canadian Institute of Mining and Metallurgy Special Volume 8, p. 101-148.

Misch, Peter, 1968, Plagioclase compositions and non-anatectic origin of migmatitic gneisses in northern Cascades of Washington State: Contributions to Mineralogy and Petrology, v. 17, no. 1, p. 1-70.

Misch, Peter, 1977, Bedrock geology of the North Cascades. *In* Brown, E. H.; Ellis, R. C., editors, Geological excursions in the Pacific Northwest: Geological Society of America Annual Meeting, Seattle, 1977: Western Washington University, p. 1-62.

Misch, Peter, 1979, Geologic map of the Marblemount quadrangle, Washington: Washington Division of Geology and Earth Resources, Geologic Map GM-23, 1 sheet, scale 1:48,000.

Monger, J. W. H., 1966, The stratigraphy and structure of the type area of the Chilliwack Group, southwestern British Columbia: University of British Columbia Doctor of Philosophy thesis, 158 p.

Monger, J. W. H., 1970, Hope map-area, west half (92 H W1/2), British Columbia: Geological Survey of Canada Paper 69-47, 75 p., 3 pl.

Parrish, R. R.; Carr, S. D.; Parkinson, D. L., 1988, Eocene extensional tectonics and geochronology of the southern Omineca belt, British Columbia and Washington: Tectonics, v. 7, no. 2, p. 181-212.

Ray, G. E., 1986, The Hozameen fault system and related Coquihalla serpentine belt of southwestern British Columbia: Canadian Journal of Earth Sciences, v. 23, no. 7, p. 1022-1041.

Richards, T. A.; McTaggart, K. C., 1976, Granitic rocks of the southern Coast Plutonic Complex and northern Cascades of British Columbia: Geological Society of America Bulletin, v. 87, no. 6, p. 935-953.

Silberling, N. J.; Jones, D. L.; Blake, M. C., Jr.; Howell, D. G., 1987, Lithotectonic terrane map of the western conterminous United States: U.S. Geological Survey Miscellaneous Field Studies Map MF-1874-C, 20 p., 1 pl., scale 1:2,500,000.

Smith, M. T., 1988, Deformational geometry and tectonic significance of a portion of the Chilliwack Group, northwestern Cascades, Washington: Canadian Journal of Earth Sciences, v. 25, no. 3, p. 433-441.

Staatz, M. H.; Tabor, R. W.; Weis, P. L.; Robertson, J. F.; Van Noy, R. M.; Pattee, E. C., 1972, Geology and mineral resources of the northern part of the North Cascades National Park, Washington: U.S. Geological Survey Bulletin 1359, 132 p.

Stull, R. J., 1969, The geochemistry of the southeastern portion of the Golden Horn batholith, northern Cascades, Washington: University of Washington Doctor of Philosophy thesis, 127 p., 1 pl.

Tabor, R. W., 1961, The crystalline geology of the area south of Cascade Pass, northern Cascade Mountains, Washington: University of Washington Doctor of Philosophy thesis, 205 p.

Tabor, R. W.; Frizzell, V. A., Jr.; Vance, J. A.; Naeser, C. W., 1984, Ages and stratigraphy of lower and middle Tertiary sedimentary and volcanic rocks of the central Cascades, Washington–Application to the tectonic history of the Straight Creek fault: Geological Society of America Bulletin, v. 95, no. 1, p. 26-44.

Tabor, R. W.; Zartman, R. E.; Frizzell, V. A., Jr., 1987a, Possible tectonostratigraphic terranes in the North Cascades crystalline core, Washington. *In* Schuster, J. E., editor, Selected papers on the geology of Washington: Washington Division of Geology and Earth Resources Bulletin 77, p. 107-127.

Tabor, R. W.; Frizzell, V. A., Jr.; Whetten, J. T.; Waitt, R. B.; Swanson, D. A.; Byerly, G. R.; Booth, D. B.; Hetherington, M. J.; Zartman, R. E., 1987b, Geologic map of the Chelan 30-minute by 60-minute quadrangle, Washington: U.S. Geological Survey Miscellaneous Investigations Map I-1661, 29 p., 1 pl., scale 1:100,000.

Tabor, R. W.; Booth, D. B.; Vance, J. A.; Ort, M. H., 1988, Preliminary geologic map of the Sauk River 1° x 1/2° quadrangle, Washington: U.S. Geological Survey Open-File Report 88-692, 50 p., 1 pl., scale 1:100,000.

Tabor, R. W.; Haugerud, R. A.; Miller, R. B.; Brown, E. H.; Babcock, R. S., in press [a], Accreted terranes of the North Cascades Range, Washington: 28th International Geologic Congress, Trip T307.

Tabor, R. W.; Frizzell, V. A., Jr.; Booth, D. B.; Waitt, R. B.; Whetten, J. T.; Zartman, R. E., in press [b], Geologic map of the Skykomish 30-minute by 60-minute quadrangle, Washington: U.S. Geological Survey Miscellaneous Investigations Map I-1963, scale 1:100,000.

Tennyson, M. E.; Jones, D. L.; Murchey, Benita, 1982, Age and nature of chert and mafic rocks of the Hozameen Group, north Cascades Range [abstract]: Geological Society of America Abstracts with Programs, v. 14, no. 4, p. 239-240.

Vance, J. A., 1957, The geology of the Sauk River area in the northern Cascades of Washington: University of Washington Doctor of Philosophy thesis, 312 p.

Vance, J. A., 1985, Early Tertiary faulting in the North Cascades [abstract]: Geological Society of America Abstracts with Programs, v. 17, no. 6, p. 415.

Wallace, W. K., 1976, Bedrock geology of the Ross Lake fault zone in the Skymo Creek area, North Cascades National Park, Washington: University of Washington Master of Science thesis, 111 p., 1 pl.

Whetten, J. T.; Laravie, J. A., 1976, Preliminary geologic map of the Chiwaukum 4 NE quadrangle, Chiwaukum graben, Washington: U.S. Geological Survey Miscellaneous Field Studies Map MF-794, 1 sheet, scale 1:24,000.

Whitney, D. L.; Evans, B. W., 1988, Revised metamorphic history for the Skagit Gneiss, North Cascades–Implications for the mechanism of migmatization [abstract]: Geological Society of America Abstracts with Programs, v. 20, no. 3, p. 242-243.

Yardley, B. W. D., 1978, Genesis of the Skagit migmatites, Washington and the distinction between possible mechanisms of migmatization: Geological Society of America Bulletin, v. 89, no. 6, p. 941-951.

Zen, E-an; Hammarstrom, J. M., 1984, Magmatic epidote and its petrologic significance: Geology, v. 12, no. 9, p. 515-518.

Road Log

This log covers the second day of a three-day field trip. It includes more stops than we can comfortably make in one day. Depending on weather, snowpack, time, and the interests of the group, we will omit some of the following stops.

The road log begins on Washington State Route (SR) 20, several miles up-valley (northwest) of the communities of Winthrop and Twisp. For most of the day, mileage is referenced to the mileposts along SR 20 (milepost numbers are lower to the west), not to elapsed distance.

179.6 Turnoff to Mazama and Harts Pass.

167.7 **STOP 2-1. Rapakivi (plagioclase mantling potassium feldspar) granite of the undeformed, high-level, ~50 Ma Golden Horn batholith.**

Look carefully for miarolitic cavities at this stop. Elsewhere, granite of the Golden Horn batholith bears arfvedsonite (Boggs, 1984; earlier workers considered the sodic amphibole to be riebeckite) and aegirine. Because the batholith has intruded the Hozameen-North Creek fault, motion on this stretch of the fault must be older than 50 Ma.

The Golden Horn batholith is the best known (Misch, 1966a; Stull, 1969; Engels and others, 1976; Hoppe, 1984; Boggs, 1980, 1984) of a suite of middle Eocene granite and granodiorite plutons that extends across much of the range. The suite also includes the late lineated dikes of the Skagit Gneiss (Stop 2-4) and the Castle Peak, Monument Peak, Cooper Mountain, Duncan Hill, Railroad Creek, Bald Mountain(?), and Mount Pilchuck plutons. Most older and younger plutons in the North Cascades are tonalite.

162.4 Washington Pass (5,477 ft), where the Chelan and Methow Rivers divide; both streams flow into the Columbia River.

160.0 Roadcuts are in undeformed tonalite of the Black Peak batholith. Samples from near here have yielded ~90 Ma U-Pb zircon and K-Ar ages (Hoppe, 1984; Engels and others, 1976).

157.5 Rainy Pass (4,840 ft) on the Skagit-Chelan divide. For the next 16 mi we travel northwest along the Ross Lake fault zone, here totally obliterated by the younger Golden Horn batholith.

141.2 **STOP 2-2. Jack Mountain Phyllite at Canyon Creek trail head.**

Park on the right (north).

Roadcuts on the south side of SR 20 are in Jack Mountain Phyllite (Little Jack terrane). They display typical biotite porphyroblasts and deformed leucocratic sills, all with a gently southwest-plunging lineation. Across the valley to the north, the lower two-thirds of the hillside is also Jack Mountain Phyllite. The upper slopes are greenstone of the Hozameen Group.

139.9 Northwest of the Golden Horn batholith the Ross Lake fault zone has been invaded by numerous granitoid intrusions, some of which are foliated. These range in composition from granite to hornblende diorite. The intrusions are the "Ruby Creek Heterogeneous Plutonic Belt" of Misch (1966b). The complicated intrusive relations and large amounts of included country rock are probably the result of intrusion into an active fault zone (Misch, 1977).

At this location, Ruby Creek agmatites range from varieties with equant and angular inclusions to varieties with elongate, rounded, foliated fragments. The latter are Misch's "pollywog agmatite". Most inclusions are probably Jack Mountain Phyllite or Elijah Ridge Schist. The trondhjemite matrix of the pollywog agmatite has given a 48 Ma U-Pb zircon date (Miller and others, 1988).

138.5 Panther Creek bridge.

135.1 **STOP 2-3. Ross Lake overlook.**

Park in the large turnout on the right.

Across the road are complex migmatites of the Skagit Gneiss (Chelan Mountains terrane, see Stop 2-6). Good views to the north of (right to left) Little Jack, Jack, and Hozomeen Mountains, Ross Lake, and Mount Prophet, highest point on the left. Mount Prophet (7,650 ft) is carved from marble, paragneiss, and orthogneiss of the Skagit Gneiss. One of the few sillimanite localities in the Skagit Gneiss is on its southern

slope. Ridges to the right of Mount Prophet are underlain by the Skymo unit of Wallace (1976): troctolite and olivine norite intruded by medium- to coarse-grained gabbro. Brittle, north- and northwest-trending faults separate the Skymo unit from the Skagit Gneiss, but Skymo gabbro is intruded by pegmatite of the Skagit Gneiss (Staatz and others, 1972). Rocks of the Skymo unit extend southeast to the shore of Ross Lake.

To the northeast, but on the west side of the lake, are schists, semischists and phyllites of the Little Jack terrane, in which metamorphic grade decreases to the east. Farther to the northeast are greenstone and chert of the Hozameen Group. In the distance, beyond the head of the lake in Canada, is Silvertip Mountain. Closer to the overlook, the sharp horns to the right are Hozomeen Mountain (8,066 ft). Small stocks of the Chilliwack batholith are present on both Silvertip and Hozomeen Mountains and their contact-metamorphic effects have helped produce rugged mountains out of otherwise less competent chert, argillite, and greenstone of the Hozameen Group.

The massive peak to the right is Jack Mountain (9,066 ft). On its lower slopes, near timberline, the gently northeast-dipping Jack Mountain fault places the Hozameen Group above semischist, phyllite, talc schist, and metaporphyry of the Little Jack terrane. Little Jack Mountain (6,745 ft) is the grassy ridge below and to the right of Jack Mountain.

Although the Little Jack terrane here is in fault contact with the Hozameen Group and the Skymo unit of the Chelan Mountains terrane, it displays a steep metamorphic gradient from the high-grade rocks to the southwest to the slightly metamorphosed Hozameen Group. A similar but less faulted gradient occurs north of 49°N, though in rocks probably correlative with the Hozameen Group (McTaggart and Thompson, 1967; Haugerud, 1985).

The Hozameen Group and Little Jack terrane most likely overlay the Skagit Gneiss during Late Cretaceous to early Tertiary metamorphism, and the abruptness of the present metamorphic gradient probably reflects the dip-slip component of post-metamorphic deformation along this part of the Ross Lake fault zone. The metamorphic gradient is too steep to present a (now-tilted) depth-controlled thermal gradient. It is likewise too steep to be a stable lateral thermal gradient, and differences in peak metamorphic pressure indicate that the steep gradient does not represent a wider lateral thermal gradient condensed by strike-slip shearing. (See Haugerud, 1985, for a more complete discussion.)

The low peninsula extending from the east into Ross Lake, separating Ross Lake from Ruby Arm to the right, is underlain by homogeneous Skagit orthogneiss with nearly flat foliation. Between this orthogneiss and the Little Jack terrane on the slopes above are intrusive rocks and agmatite of the "Ruby Creek Heterogeneous Plutonic Belt" of Misch (1966b).

133.5 Horsetail Creek and John Pierce Falls. East of the bridge are spectacular roadcuts of banded migmatitic gneiss, locally with layers of metamorphosed ultramafic rock.

131.8 Diablo Lake overlook. Stop here (though not today) to admire the view southwest across Thunder Arm of Diablo Lake to Colonial Peak (7,771 ft) and neighboring summits. To the north, across Diablo Lake, peaks made of Skagit Gneiss are (left to right) Davis Peak (7,051 ft), Elephant Butte (7,380 ft) and Sourdough Mountain (6,106 ft), on which is a fire lookout that was manned by poet Gary Snyder during the mid-1950s.

The outcrop across the highway is massive biotite-hornblende quartz diorite orthogneiss, veined by extensive light-colored dikes. From this point to beyond the turnoff to Diablo, outcrops are dominantly paragneiss.

130.5 Bridge across Thunder Arm of Diablo Lake.

129.5 Thunder Lake. The valleys of Stetattle Creek and Thunder Creek are localized along strands of a group of north- and NNW-trending brittle faults. These faults must be of late Eocene or earliest Oligocene age because they cut Skagit Gneiss with its ductile middle Eocene fabric and do not offset the early Oligocene phases of the Chilliwack batholith to the north. Sourdough Creek (which drains toward us on the south face of Sourdough Mountain), Thunder Lake, and a large notch on the east ridge of Colonial Peak are located on the Thunder Lake fault, the most conspicuous of these structures.

127.4 **STOP 2-4. Skagit Gneiss at the Diablo Dam turnoff.**

Roadcuts here display migmatitic banded gneiss with both older, pegmatitic, main-phase

leucosomes and finer grained, cross-cutting late lineated dikes.

There is no consensus on the petrogenesis of Skagit migmatites. Plagioclase compositions in most leucosomes and their wall rocks do not differ substantially (Misch, 1968; Yardley, 1978), indicating that the leucosomes are not injected melts. The wide range of leucosome plagioclase compositions, lack of K-feldspar, common lack of nearby melanosomes, and estimated metamorphic temperatures of 600°C led Misch (1968) to infer that the leucosomes are not segregated partial melts. Misch (1968) and Babcock (1970) favored large-scale metasomatism at sub-solidus conditions to generate the leucosomes. Yardley (1978) agreed that the migmatites formed without melting but favored local metamorphic differentiation.

More recently, Whitney and Evans (1988) estimated peak metamorphic conditions of ~720°C and ~9 kb. Given these conditions, parts of the Skagit must have been partially molten, yet the pegmatitic texture of most leucosomes suggests that their constituent grains grew in a hydrous fluid, not a melt. Melts at 9 kb are very effective H_2O reservoirs. Magmas intruding the Skagit could have arrived with substantial dissolved H_2O, and in-situ melts would have trapped any water passing through the crustal pile. Perhaps most leucosomes in the Skagit are pegmatites formed by protracted exsolution of this H_2O during regional uplift. Slow exsolution would favor collection of fluid into scattered large bubbles (Godinot, 1988). Besides carrying substantial dissolved solids, such fluid would speed grain-size coarsening in the regions it wetted.

Late lineated dikes have a range of compositions, but most common are cream-colored granites, commonly with minor biotite, locally with garnet and(or) muscovite. The granitic composition is distinctive: along the Skagit River most older parts of the Skagit Gneiss lack potassium feldspar. The dikes commonly cross-cut foliation in the host gneiss, yet are themselves lineated parallel to the northwest-trending low-angle lineation in the gneiss. Locally the dikes are foliated. These relations indicate that the dikes were intruded after most regional metamorphism but while the gneiss complex was still hot. They were subsequently stretched northwest-southeast along with the rest of the complex. Whole-rock Rb-Sr analyses of a suite of these dikes from along SR 20 define a 45 ± 3 Ma isochron (Babcock and others, 1985). U-Pb dates from a structurally and lithologically similar pluton a few kilometers north of 49°N (Haugerud, 1985) indicate intrusion at about 46 Ma (Peter van der Heyden, University of British Columbia, written commun., 1988).

126.2 Bridge across Gorge Lake followed by the turnoff to the town of Diablo. Roadcuts on the right after crossing Gorge Lake are in banded gneiss, including garnet biotite schist, amphibolite, and thin layers of (mostly) biotite tonalite orthogneiss, all threaded with coarse-grained leucotonalite (trondhjemite). Massive orthogneiss is more abundant to the southwest, and beyond Gorge Lake it is the predominant rock of the canyon.

120.9 Enter the town of Newhalem (526 ft). Above on the west are the orthogneiss buttresses of Mount Ross (6,052 ft).

120.3 **STOP 2-5. Skagit orthogneiss at Newhalem.**

Turn left onto the parallel gravel road and park by the prominent buttress of rock.

Bluffs of gray rock immediately north of the road are "incipiently migmatized" (Misch, 1977, p. 35) gneissic hornblende-biotite tonalite orthogneiss. This outcrop has yielded U-Pb zircon dates of ~65 Ma (Haugerud and others, 1988). Similar rock a few kilometers across strike to the south yields U-Pb zircon dates of ~75 Ma (John Stacey, U.S. Geological Survey, written commun., 1987, 1988). Along with the ~64 Ma age of the more strongly migmatized Custer orthogneiss unit of Haugerud and others (1988) north of 49°N, these dates demonstrate that deformation and migmatization of the Skagit Gneiss are in part Tertiary.

As we leave Newhalem and cross Goodell Creek, look to the right (north) for a view of the southern Picket Range, eroded out of Skagit orthogneiss.

118.2 First outcrops of the Oligocene and younger Chilliwack composite batholith.

114.9 Light-colored waterlaid volcanic ash in roadcuts. This deposit must be postglacial, yet the present-day Skagit River is an unlikely agent to deposit such fine-grained material. Landslide(s) farther downstream probably dammed the Skagit and these beds were laid down in the resulting lake.

114.6 **STOP 2-6. Schist of the Napeequa unit of the Chelan Mountains terrane, with sills of late-metamorphic orthogneiss.**

Park on the river side of the road.

At the upstream end of the outcrop are intricately folded quartz-rich biotite schists—with thicker quartzite and thinner biotite-rich laminae—typical of metacherts in the Napeequa unit. The intricate fold style is common in much lower grade ribbon chert, and by analogy it is likely that these folds largely predate amphibolite-facies metamorphism.

For the next 2 mi outcrops of schist of the Napeequa unit are in the toes of large landslides. Rapids in this stretch of the Skagit River are formed by blocks of landslide debris. Rock types in the roadcuts include biotite schist, two-mica schist, quartzose schist, amphibole-bearing schist, and chlorite-rich mafic schist. Less abundant are pods and layers of talc and talc-carbonate schists, locally with forsterite, tremolite, and anthophyllite. All are metamorphosed in amphibolite facies (Misch, 1977). Vein quartz is locally extensive enough to have been mined to make glass.

110.7 Bridge over Bacon Creek.

110.4 Marblemount Meta Quartz Diorite of Misch (1966). Here the Marblemount is predominantly a muscovite-chlorite-epidote-albite-quartz gneiss. From these outcrops Mattinson (1972) obtained a 220 Ma (Late Triassic) zircon U-Pb age. The Marblemount and its equivalent Late Triassic plutons form a belt extending from the Straight Creek fault, only about 1 km to the west of here, southeast for 150 km before they are covered by the Miocene Columbia River Basalt Group.

106.1 Town of Marblemount. The broad valley junction here is eroded out along two strands of the Eocene Straight Creek fault. Lookout Mountain looming up to the east is underlain by Marblemount Meta Quartz Diorite. Forested bluffs to the west are Shuksan Greenschist of the Easton terrane.

Refer to the paper by Brandon (this volume) for an overview of lithologies and tectonics relevant to the following part of the road log.

103.0 Corkindale Creek. To the north, east of Corkindale Creek, steep wooded hillsides are underlain by Shuksan Greenschist. West of the creek are greenstones and low-grade metasedimentary rocks of the upper Paleozoic Chilliwack Group of Cairnes (1944), and high on the ridge are thick chert beds and greenstone of the Permian(?) to Jurassic(?) Elbow Lake formation of Brown and others (1987).

97.7 Junction with SR 530, the Darrington-Rockport road.

Roadcuts to the east are in basaltic greenstone and associated sedimentary rocks of the Chilliwack Group.

89.6 At the east edge of the town of Concrete, before crossing the bridge over the Baker River, turn right onto Everett Avenue, then left onto East Main Street. Just before crossing the old Baker River bridge, turn uphill (right) onto East Lake Shannon Road. Follow this road up the hill, turn left onto the road to the top of Lower Baker Dam, and then take the right fork at "Y". Stop at the gate and walk around the corner into the abandoned quarry.

STOP 2-7. Quarry in limestone of the Chilliwack Group of Cairnes (1944).

Mount Shuksan, Mount Baker, and Grandy Ridge can be seen from here on a clear day, and this stop is convenient for orienting ourselves amidst the controversy and confusion of northwest Cascades tectonics.

Age-definitive fossils have not been reported from this quarry, but on the basis of large crinoid columnals (present in some talus blocks on the east side of the quarry), Danner (1966) correlated these beds with limestone of his Lower Pennsylvanian Red Mountain sequence, which was reinterpreted by Liszak (1982) to be Late Mississippian in age.

Like much of the remainder of the Chilliwack Group, this limestone lens has been tectonically dismembered: the upper and lower contacts are faults, and the limestone cannot be traced along strike. Similar, though smaller, fault-bounded lenses of Devonian to Permian limestone are scattered throughout the Chilliwack Group. North of 49°N, Monger (1966, 1970) used such lenses to trace a coherent stratigraphy. Such stratigraphy is only locally recognizable south of the border.

The Chilliwack Group also contains arc volcanic rocks and volcaniclastic sedimentary rocks. Felsic and intermediate Permian(?) volcanic rocks of the Chilliwack Group and associated volcaniclastic strata are difficult to distinguish from similar Triassic rocks in the Cultus Formation of Monger (1970) (Blackwell, 1983). The Cultus Formation probably was deposited on the Chilliwack Group, though we have not seen the contact. Younger than most of the Cultus are dacitic tuffs and flows of the Middle Jurassic Wells Creek Volcanics of Misch (1966b) and the overlying, Upper Jurassic to Lower Cretaceous argillite and sandstone of the Nooksack Group of Misch (1966b). The base of the Wells Creek Volcanics is not exposed, but I believe the unit overlies the Cultus Formation. Tabor and others (in press [a]) lump all these units together as the Grandy Ridge terrane.

Return to East Main Street, turn right, cross the old bridge over the Baker River, and follow the road up hill to the stop sign. Turn right onto Main Street and continue west through downtown Concrete to the stop sign at Main and Superior. Turn right on Superior, go uphill, and turn left onto the Burpee Hill Road. Follow the Burpee Hill Road past outcrops of glacial outwash deposits (note collapse features) about 4 mi to:

0.0 Junction of Burpee Hill Road and Baker Lake Highway at Lake Tyee. *Reset odometer* and turn right onto Baker Lake Highway. The next part of this trip is measured by road miles, not mileposts.

1.7 The low hill in the foreground is of young, but pre-Vashon age (latest continental glaciation), olivine basalt (see Stop 2-10).

5.8 Rocky Creek bridge; at the north end of the bridge, turn left onto U.S. Forest Service Road (FSR) 12 and follow signs to Schreibers Meadow.

~8 Cross Sulphur Creek. Beyond here the road is on top of olivine basalt flows. Morphology and vegetative cover suggest that flows of at least two ages, both postglacial, erupted from the cinder cone south of Schreibers Meadow. The oldest flows extend almost to Upper Baker Dam. These flows overlie the glacial-outwash deposits that fill the lower Baker River valley.

~10 Junction of FSR 12 and FSR 13. Keep right on FSR 13, past three hairpin turns, to:

~12 **STOP 2-8. Yellow Aster Complex of Misch (1966b).**

Park near the road-metal quarry on the right side of the road.

The Yellow Aster Complex is a hodge-podge of fault-bounded igneous and metamorphic rock fragments in the northwest Cascades. Radiometric dating (Mattinson, 1972) indicates that some gneisses and granitoid rocks of the complex crystallized at ~415 Ma; these plutons intrude older clinopyroxene-bearing gneisses which Misch and Mattinson interpreted as metamorphosed 1,400 Ma plutons. Younger mafic intrusions, mostly diabase, intrude the gneisses and granitoid rocks.

This outcrop is in the >6-km-long Park Butte slab of imbricated gneiss of the Yellow Aster Complex and volcanic rock of the Chilliwack Group, which caps ridges on the south side of Mount Baker. Hornblende diorite and gneissic diorite here are typical of the younger elements of the Yellow Aster Complex. The cross-cutting mafic dikes are also typical.

Older clinopyroxene-plagioclase-quartz gneiss, calc-silicate gneiss, and marble are present at the west end of this slab; the lithologic association strongly suggests that the older gneisses are metasedimentary. Good talus exposures of these older gneisses can be reached via a short (~1 mi) walk from the end of FSR 13 to the base of Survey Point, immediately west of Schreibers Meadow.

Retrace the route 1/4 mi back down FSR 13 to:

STOP 2-9. Low-angle fault zone beneath Park Butte slate of the Yellow Aster Complex.

Park at the blocked spur road (on the left, or north, side of FSR 13) adjacent to the stream culvert 100 m west of the margin of a recent clearcut.

Below FSR 13 the stream has carved a broad, steep gully which exposes the low-angle fault zone beneath the Yellow Aster Complex. Walk through logging slash and brush along the east margin of the washout until you can descend into the gully to reach excellent exposures of the fault zone, which extends to the base of the

hillside some 200 m below. Most rock is tectonized shale, siltstone, and sandstone of the Nooksack Group. Imbricated with the Nooksack are blocks of greenstone (Chilliwack Group?) and, on the east side of the gully, a 1 m x 2 m lozenge of light-colored, poorly cemented, chert-lithic sandstone and granule conglomerate with thin coaly seams. This last lithology is common in early Tertiary sandstones in the northwest Cascades. Similarly, poorly cemented sandstone, commonly with abundant quartz grains and minor detrital muscovite, is present at several other localities in low-angle fault zones south and east of Mount Baker. Low-angle faults in the northwest Cascades have been considered mid-Cretaceous thrusts (Misch, 1966b; Brandon and Cowan, 1985; Brown, 1987; Smith, 1988), and the low-grade, lawsonite-aragonite metamorphism of the northwest Cascades has been thought a consequence of burial by these thrusts (Brandon and others, 1988). Yet some sandstones in the low-angle fault zones appear unmetamorphosed! Do these sandstones owe their unmetamorphosed appearance to leaching by ground water, or are the Tertiary tectonics of the foothills more complicated than previously realized?

Return to the junction with the Baker Lake highway.

0.0 At the junction, *reset odometer* and turn right, toward Concrete.

0.9 **STOP 2-10. Nooksack Group.**

Park on the left side of the road at this long roadcut.

One of the more frustrating aspects of mapping in the northwest Cascades is that volcaniclastic strata such as those here can reasonably be assigned to the Paleozoic (Chilliwack Group), Triassic (Cultus Formation), or Jurassic and Cretaceous (Wells Creek Volcanics and Nooksack Group). Misch (1966) considered rocks at this outcrop to be part of the Nooksack Group; Brown and others (1987) mapped them as Chilliwack Group. I think these outcrops are Nooksack because they are structurally conformable with fine-grained, chocolate-weathering, locally marly strata in which I have recently found belemnites and one ammonite, all characteristic of Nooksack strata south of Mount Baker. However, green-gray to black strata here are richer in coarse-grained volcanic detritus than most of the Nooksack south of Mount Baker.

At the north end of the roadcut, Nooksack Group rocks are overlain by Quaternary deposits of (in ascending stratigraphic order) unconsolidated gravel, basaltic agglomerate, olivine basalt with poorly formed columns, and clay-rich till. The basalt is similar to—but must be older than—the postglacial Sulphur Creek flows. Two small hills immediately to the east, possibly the dissected vent, are composed of olivine basalt, basaltic agglomerate, and bedded cinders.

Return to Concrete via the Burpee Hill Road (about 9 mi). [If Stop 2-11 is to be skipped in a rush to reach Interstate Highway 5 (I-5), do not turn left onto Burpee Hill Road at Lake Tyee, but follow the Baker Lake highway down Grandy Creek to SR 20, turn right onto SR 20, and follow SR 20 to I-5. Blocky-weathering, siliceous, volcanic siltstones in roadcuts near Grandy Lake, 1.8 mi beyond the Burpee Hill Road junction, belong to the Cultus(?) Formation.]

At the intersection of Superior and Main Streets in Concrete (stop sign), continue straight ahead (south) 0.1 mi to SR 20.

0.0 At junction with SR 20 *reset odometer* and turn right.

0.4 Turn left onto the South Skagit highway.

1.3 Bridge over the Skagit River. At the south end of the bridge, follow the South Skagit highway to the right. Darrington Phyllite of the Easton Metamorphic Suite crops out at the south abutment.

11.7 **STOP 2-11. Well-recrystallized greenschist and blueschist of the Shuksan Greenschist.**

The Easton Metamorphic Suite (Tabor and others, in press [b]), commonly referred to as the Shuksan Metamorphic Suite of Misch (1966b) and also known as the Shuksan terrane of Silberling and others (1987), includes the Darrington Phyllite and Shuksan Greenschist. Protoliths of the Darrington and Shuksan were marine shale and minor sandstone and MORB-type submarine basalt which probably underlay the shale (Haugerud and others, 1981; Dungan and others, 1983; Brown, 1986). From their

isotopic studies, Brown and others (1982), Brown (1986), and Armstrong and Misch (1987) suggest that the protolith age of the Easton Metamorphic Suite is Jurassic and metamorphism is Early Cretaceous (pre-120 Ma). Metamorphic assemblages testify to metamorphism at 7 to 9 kb and 300° to 400°C (Brown, 1986). Regionally extensive blueschists with very similar metamorphic history and lithologies occur in northern California (Brown and Blake, 1987).

While the Shuksan Greenschist is in blueschist facies, most of the unit is (obviously) greenschist, with subordinate blueschist. The stability of actinolite (greenschist) versus glaucophane or crossite (blueschist) depends on the bulk composition of the rock, especially the Fe^{2+}/Fe^{3+} ratio.

Thorough recrystallization and a well-developed metamorphic fabric distinguish rocks of the Easton Metamorphic Suite from most other rocks in the western North Cascades. You may see small knots of epidote with foliation wrapping around them. These are relics from an earlier, static metamorphism which predates synkinematic blueschist-facies metamorphism. This earlier event was probably sea-floor hydrothermal alteration (Haugerud and others, 1981).

The Easton Metamorphic Suite is bounded by post-metamorphic faults. Though most of these faults are high angle, some evidence suggests that the Easton is structurally high, above the Grandy Ridge terrane and the overlying Elbow Lake unit.

End of trip.

To reach I-5, continue west on the South Skagit highway:

25.0 The South Skagit highway passes beneath an overpass and loops left to join SR 9.

25.4 Junction with SR 9. Turn right (south) on SR 9.

26.5 First of two railroad crossings in the town of Clear Lake.

29.7 Junction of SR 9 with SR 538 (at mile 49.8 of SR 9). Turn right on SR 538.

33.5 Intersection of SR 538 (Clear Lake Road) with I-5, milepost 227.

To continue west on SR 20 to Anacortes for the Day 3 trip, take I-5 north to exit 230, exit onto SR 20 and turn west (left).

Geology of the San Juan-Cascade Nappes, Northwestern Cascade Range and San Juan Islands

Mark T. Brandon
Department of Geology and Geophysics
Yale University
P.O. Box 6666
New Haven, CT 06511

INTRODUCTION

The San Juan-Cascade nappes (Fig. 1) lie in a northwest-trending belt which is bounded by the Skagit metamorphic core (Haugerud, this volume) to the northeast and Wrangellia to the southwest. Wrangellia is a large coherent terrane that underlies much of Vancouver Island. At present, the nappe sequence has a cross-strike width of at least 150 km, extending from the westernmost thrust in the San Juan Islands (labeled Late Cretaceous suture in Fig. 1) to the Ingalls ophiolite in the Mount Stuart area (shown as Decatur terrane on Fig. 1). A common interpretation is that the San Juan-Cascade nappes represent a long-lived accretionary system that formed by successive arrival of far-traveled terranes (for example, Whetten and others, 1978). This view is certainly consistent with the varied assortment of Mesozoic and Paleozoic terranes in the nappes. More recent work (Brandon and others, 1988), however, has shown that large parts of the nappe sequence were assembled during a short-lived orogenic event, bracketed between 100 and 84 Ma. Brandon and Cowan (1985) argue that this orogenic event was associated with the collision of Wrangellia. The San Juan-Cascade nappes are considered to be a system of Late Cretaceous thrust sheets that were driven to the southwest over Wrangellia. Many parts of the nappe sequence were also affected by a synchronous high-pressure metamorphic event (characteristic assemblage: prehnite-lawsonite-aragonite) caused by rapid structural burial and subsequent uplift within an advancing thrust wedge (Brandon and others, 1988).

The discussion section of this paper provides an overview for field stops in the San Juan-Cascade nappes, which are Stops 2-7 to 2-11 in the western Cascades (Haugerud, this volume) and Stops 3-1 to 3-8 in the San Juan Islands (described below). The discussion focuses on the following three topics: (1) pre-Late Cretaceous terranes within the nappe sequence, (2) continental accretion of these terranes prior to the Late Jurassic, and (3) the tectonic setting associated with Late Cretaceous thrusting.

DISCUSSION

Pre-Late Cretaceous Terranes in the San Juan-Cascade Nappes

The San Juan-Cascade nappes are commonly identified as a composite terrane (for example, Jones and others, 1983) because of the pervasive effects of Late Cretaceous thrusting. In the extreme, each nappe or fault slice might be considered a separate terrane, and the Late Cretaceous faults viewed as fundamental terrane boundaries. A more conventional approach is to use geologic relations within each nappe to piece together the larger tectonostratigraphic units that existed prior to the Late Cretaceous. An example of this approach is the analysis of Brandon and others (1988), which employs stratigraphic relations, paleontological ages, isotopic dates, and chemical analyses to identify and characterize pre-Late Cretaceous terranes in the San Juan Islands. The results of this analysis are extended here to all parts of the San Juan-Cascade nappes (Table 1, Figs. 1 and 2). This analysis should be viewed as preliminary considering that the internal stratigraphy and age of many of the Cascade nappes are just starting to be resolved.

Seven pre-Late Cretaceous tectonostratigraphic units are identified in Table 1 (shown as major headings). Each of these contains one or more affiliated rock units (listed below the major headings). Three types of tec-

From: Joseph, N. L., and others, editors, 1989, Geologic guidebook for Washington and adjacent areas: Washington Division of Geology and Earth Resources Information Circular 86.

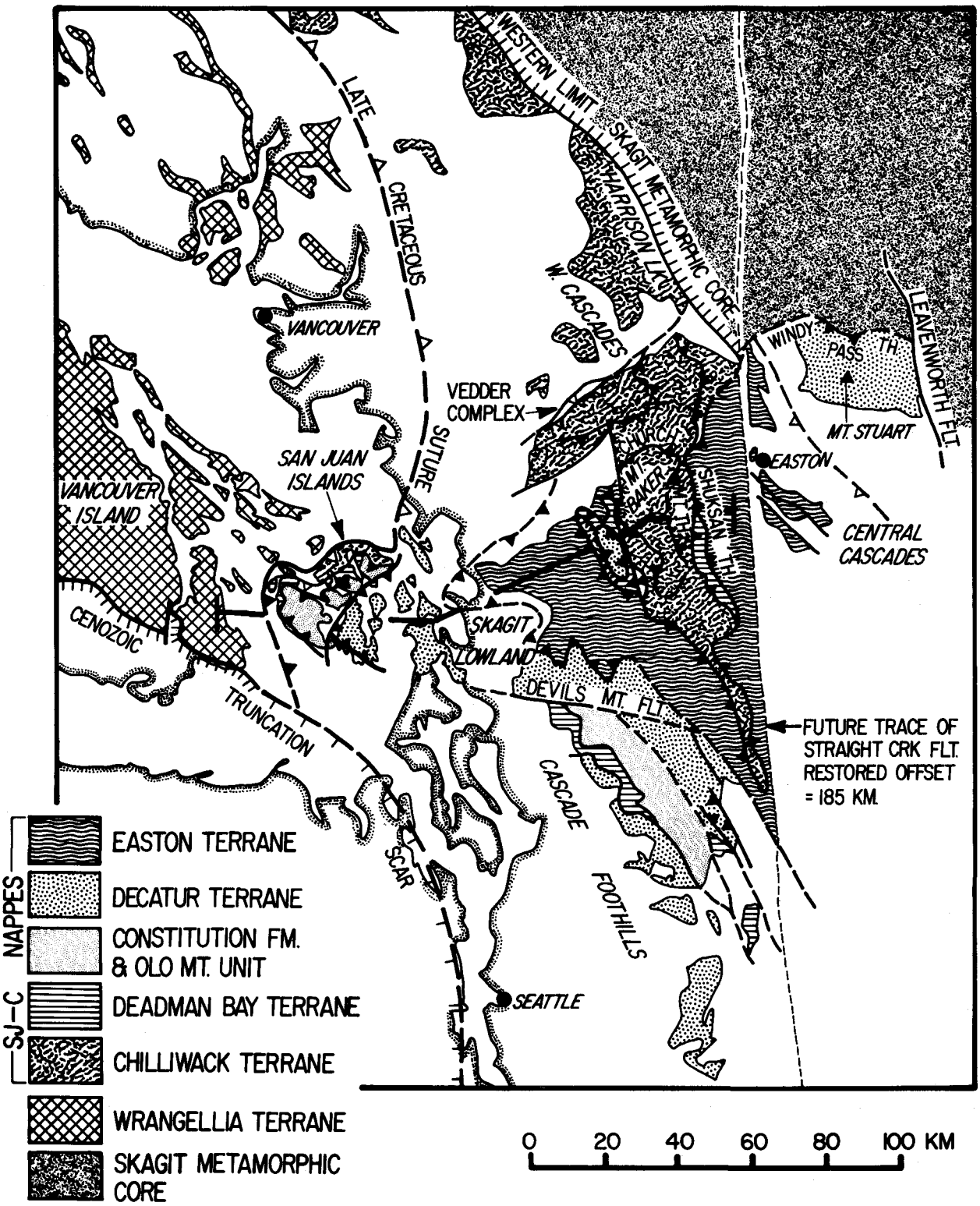

Figure 1. Generalized map of tectonostratigraphic units in the San Juan-Cascade nappes. The Straight Creek fault is restored based on the interpretation of Misch (1977b), which matches metamorphic units in the Skagit Core (Chiwaukum and Settler Schists). The Vedder terrane, Richardson basalts, and Lopez Structural Complex are too small to show here. One exception is a large outcrop of Vedder terrane at Vedder Mountain (labeled "Vedder Complex"). The east-west line across the San Juan Islands and Mount Baker locates the cross-section in Figure 4. The fault labeled "Late Cretaceous suture" marks the western limit of the San Juan-Cascade nappes. The fault labeled "Cenozoic truncation scar" marks the location of an inferred early Cenozoic fault that truncated the southwest side of the Cascade orogen (Brandon, 1985).

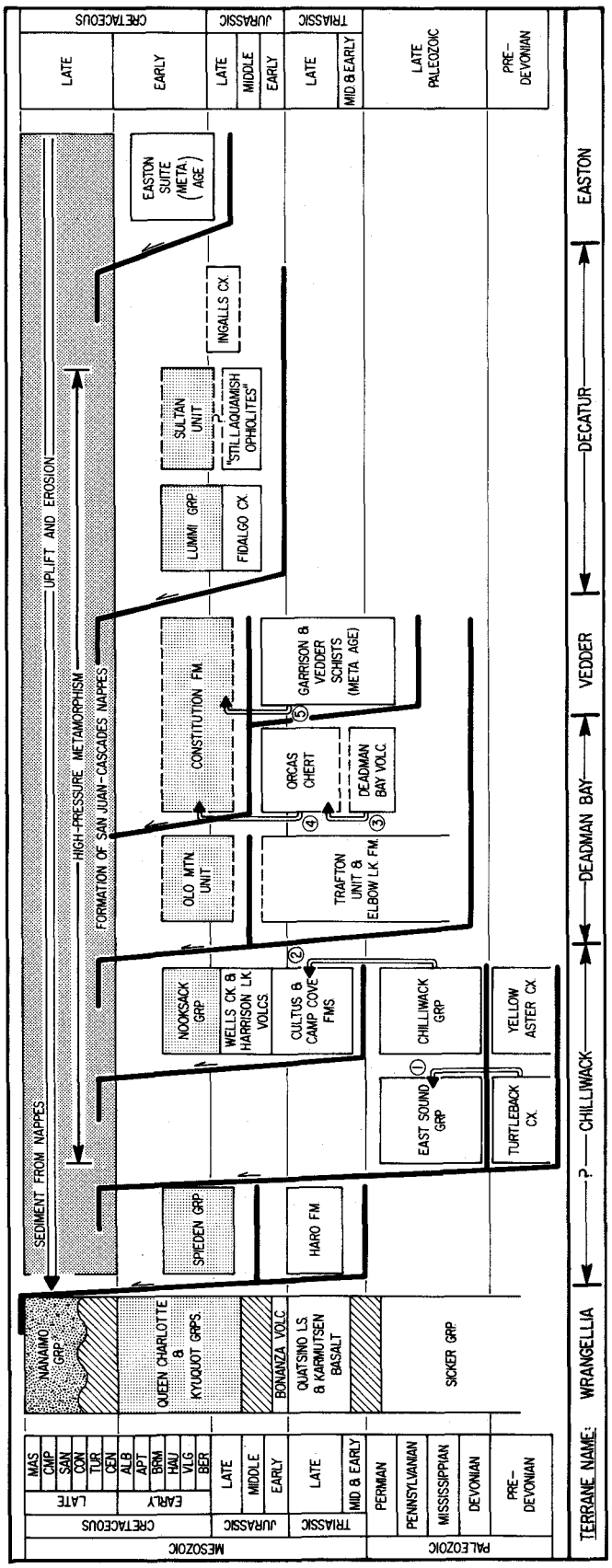

Figure 2. Pre-Late Cretaceous terranes in the San Juan-Cascade nappes (modified from Brandon and others, 1988; see Table 1 for further details). Each column represents a separate terrane with its name appearing below. The continuous portion of a column shows rock units that are connected by demonstrable stratigraphic contacts. Breaks in a column indicate that stratigraphic contacts are not preserved. Stratigraphic hiatuses are hachured, and dashed horizontal lines indicate that the age range of the unit is not known. Arrows with numbers indicate other types of geologic ties between rock units within a terrane. The numbers refer to the following comments: (1) dikes related to the East Sound Group are found in the Turtleback Complex, and a poorly preserved unconformity between the two units is locally present (Brandon and others, 1988); (2) cobbles of Chilliwack Group limestone are found in the Camp Cove Formation (Monger, 1986; Monger and Berg, 1987); (3) similarities in chert ages and basalt chemistry (Brandon and others, 1988); (4) Tethyan fusulinid-bearing limestone cobbles in the Constitution Formation (Brandon and others, 1988); and (5) Garrison schist cobbles and detritus in the Constitution Formation (Brandon and others, 1988). Stippled units are Jurassic and Cretaceous clastic linking sequences, which are inferred to postdate accretion of the pre-Late Cretaceous terranes to continental America. The timing of Late Cretaceous thrusting and regional high-pressure metamorphism is shown at the top of the diagram. Heavy lines are meant to schematically represent thrust faults within the San Juan-Cascade nappes. The lower flats of these faults underlie the units that they involve, and the upper flats marks the time of movement of the fault. The Nanaimo Group is a syn-orogenic unit that was deposited on Wrangellia and received detritus from the San Juan-Cascade nappes.

Table 1. Pre-Late Cretaceous units in the San Juan-Cascade nappes. Tectonostratigraphic headings are listed in an order that approximates their relative positions, from top to bottom, in the nappe sequence.

==========

EASTON TERRANE (METAMORPHIC)

Easton Metamorphic Suite (= Shuksan Suite of Misch, 1966) [WC & CC; 2, 12, 14]: Metamorphism is primarily Early Cretaceous (120-130 Ma). A coherent high-pressure metamorphic unit composed of basalt (ocean-floor chemistry), graphitic quartzose phyllite, minor sandstone, and rare metalliferous sediments. Locally includes minor Late Jurassic barroisite schist. Isotopic dating suggests a Jurassic depositional age for the clastic sediments.

DECATUR AND RELATED TERRANES (COHERENT)

Middle and Late Jurassic ophiolite and arc-volcanic complex; also includes overlying Jura-Cretaceous clastic strata.

Fidalgo Igneous Complex [SJ; 1]: Middle and Late Jurassic. Ultramafite, gabbro, and low-potassium basalt, andesite and dacite. In the San Juan Islands, the associated volcanic sequence contains interbedded radiolarian argillite and chert, and breccia with clasts derived from the underlying plutonic and volcanic sequence.

Miscellaneous ophiolitic units in the Cascades Foothills [CF; 9, 11]: Middle and Late Jurassic. A group of ophiolitic units which based on age and lithology are broadly correlative to the Fidalgo Complex. Includes the Twin Sisters dunite, the Haystack unit [9, 10], the Stillaguamish ophiolite [11], volcanic and plutonic rocks of the Western Melange [8], and the Deer Creek volcanics [2].

Ingalls Complex [CC; 3,4]: Late Jurassic. A complexly faulted assemblage of ultramafite, gabbro, mafic and silicic volcanics, ribbon chert, and sandstone.

Lummi Group [SJ; 1, 13]: Latest Jurassic and Early Cretaceous. Marine clastic strata overlying the Fidalgo Complex.

Clastic units associated with ophiolitic rocks of the Cascades Foothills [CF]: Late Jurassic and Early Cretaceous. Consists of poorly exposed and variably disrupted mudstone, turbidite, conglomerate and minor chert. Includes the Sultan unit [7] and units pTwa and pTwak in the Western Melange [8].

PILLOW BASALTS OF RICHARDSON (EXOTIC FAULT SLICE)

Basalts of Richardson [SJ; 1]: Middle Cretaceous (latest Albian, 100 Ma). A small fault-bounded pillow basalt unit found in the Lopez Structural Complex, a Late Cretaceous imbricate fault zone in the San Juan Islands. Another slice of this unit may be present on northern Cypress Island [13]. High-Ti basalt chemistry suggests an ocean-island affinity. The age of this unit provides a lower bound for thrusting and regional high-pressure metamorphism in the San Juan Islands.

CONSTITUTION FORMATION (FAULT-BOUNDED LINKING SEQUENCE)

Constitution Formation [SJ; 1]: Jurassic or Early Cretaceous. Stratified sequence of volcaniclastic sandstone, mudstone, ribbon chert and green tuff with slide blocks of pillowed basalt and dacite. Contains clasts and cobbles derived from the Garrison Schist and a fusulinid-bearing limestone cobble from the Deadman Bay Volcanics.

Possibly correlative units in the Cascade Foothills [CF; 9]: Late Jurassic and Early Cretaceous. Poorly exposed and variably disrupted assemblage of mudstone, sandstone, chert, basalt and green tuff. Includes the Olo Mountain unit [7, 9] and units pTws and pTwsv in the Western Melange [8].

VEDDER AND RELATED TERRANES (METAMORPHIC)

Vedder Complex [WC; 2] and Garrison Schist [SJ; 1]: Permian and Triassic metamorphic ages. Metabasaltic schist with minor metachert; grade ranges from greenschist to albite-epidote amphibolite and blueschist. In the San Juan Islands, the Garrison occurs as isolated fault slices along the Rosario thrust.

Table 1. Pre-Late Cretaceous units in the San Juan-Cascade nappes (continued).

DEADMAN BAY AND RELATED TERRANES (COHERENT)

Upper Paleozoic and Lower Mesozoic high-Ti pillow basalts, chert and limestone with Tethyan fusulinid fauna.

Deadman Bay Volcanics and Orcas Chert [SJ; 1]: Early Permian to Early Jurassic. A disrupted stratigraphic sequence composed of chert, mudstone, pillow basalt, and limestone. Basalt chemistry indicates an oceanic-island affinity. Limestones contain Tethyan fauna.

Elbow Lake Formation [WC; 2]: Poorly dated (Pennsylvanian?, Jurassic?). Ribbon chert and mudstone with minor green tuff, limestone and high-Ti basalt.

Trafton unit [CF; 7, 9]: Mississippian to Jurassic. Ribbon chert, mudstone, green tuff, basalt and limestone. Limestones contain Tethyan fusulinid fauna.

CHILLIWACK AND RELATED TERRANES (COHERENT)

Paleozoic to Middle Jurassic arc-volcanic rocks with McCloud-type fusulinid fauna; includes overlying Jura-Cretaceous clastic sequence.

Yellow Aster [WC; 2] and Turtleback [SJ; 1] Igneous Complexes: Mostly Early Paleozoic, possibly a Precambrian component as well. A plutonic complex composed of tonalite and subordinate gabbro. Relationships in the San Juan Islands suggest that these units are basement for the Chilliwack-East Sound volcanics [1].

Chilliwack [WC; 2] and East Sound [SJ; 1] Groups: Early Devonian to Early Permian. An arc-volcanic sequence with minor interbedded limestone. Limestones contain McCloud-type fauna.

Cultus [WC; 2], Camp Cove [HL; 5] and Haro [SJ; 1] Formations: Triassic and Early Jurassic. Volcaniclastic and pyroclastic sediments, radiolarian-bearing siliceous argillite, shelly interbeds and subordinate silicic volcanic rocks. The Camp Cove contains fossiliferous limestone cobbles derived from the Chilliwack [6].

Wells Creek [WC; 2] and Harrison Lake [HL; 5] Volcanics: Early and Middle Jurassic. Andesitic and dacitic volcanic flows and pyroclastic rocks.

Nooksack [WC & HL; 2, 5] and Spieden [SJ; 1] Groups: Late Jurassic and Early Cretaceous. Well bedded marine clastic strata derived primarily from an arc-volcanic source.

NOTE: Brackets enclose locations and references. Locations are: **WC** western Cascades, **SJ** San Juan Islands, **HL** west side of Harrison Lake, **CF** Cascade foothills south of Devils Mountain fault, and **CC** central Cascades (Mount Stuart area).

REFERENCES: [1] Brandon and others, 1988; [2] Brown and others, 1987; [3] Southwick, 1974; [4] Miller, 1985; [5] Arthur, 1986; [6] Monger and Berg, 1987; [7] Danner, 1957, 1966; [8] Frizzel and others, 1987; [9] Whetten and others, 1988; [10] Whetten and others, 1980; [11] Vance and others, 1980; [12] Frizzel and others, 1984; [13] Garver, 1988a; [14] Armstrong and Misch, 1987.

tonostratigraphic units have been recognized (terms in parentheses following major headings in Table 1):

(1) *coherent terrane*, which comprises a stratigraphically related sequence of units with an associated crustal basement;

(2) *metamorphic terrane*, which refers to a package of rocks that have been so thoroughly reconstituted that they are best characterized by their metamorphic history; and

(3) *linking sequence*, defined as an epiclastic unit that demonstrates, by virtue of provenance or stratigraphic overlap, the juxtaposition of two disparate terranes or the incorporation of an oceanic terrane into a continental margin setting.

Some parts of the San Juan-Cascade nappes are better characterized by their Late Cretaceous structural history than by their pre-Late Cretaceous history. They constitute a fourth type of tectonostratigraphic unit, called a *structural complex*, which is a heterogeneous and highly faulted assemblage of rock units. At present, there is only one designated structural complex in the San Juan-Cascade nappes (Lopez Structural Complex in the San Juan

Islands; Brandon and others, 1988), although some of the highly imbricated zones in the western Cascades are likely candidates. An important aspect of these structural complexes is the common occurrence of small slices of exotic rock units which are stratigraphically unrelated to units outside of the complex (for example, the Richardson pillow basalts in the Lopez Complex; see Table 1). The presence of these exotic elements suggests that these zones have accommodated large displacements.

Some of the linking relations that are used to tie various rock units to specific terranes are shown in Figure 2. Some of these assignments are tentative (for example, Haro Formation and Spieden Group in the Chilliwack terrane), but in most cases they can be well supported (references given in Table 1). Five pre-Late Cretaceous terranes are recognized: three coherent terranes, the Chilliwack, Deadman Bay, and Decatur; and two metamorphic terranes, the Easton and Vedder.

The oldest terrane is the Chilliwack (Monger and Berg, 1987), which records intermittent arc-magmatism from at least the Cambrian to Middle Jurassic. This terrane is synonymous with the Grandy Ridge terrane of Haugerud (this volume) and the Turtleback terrane of Brandon and others (1988). The Chilliwack terrane contains an early Paleozoic, and possibly Precambrian igneous basement (Turtleback and Yellow Aster Complexes) and a Lower Devonian to Middle Jurassic sequence of volcanic rocks with subordinate limestone and epiclastic sediments. Units within this terrane are examined at Stops 2-7 and 2-8 (Haugerud, this volume). The Chilliwack terrane is commonly correlated with arc-volcanic rocks in the eastern Klamath Mountains and eastern Sierra Nevada of northern California, and with the Quesnellia terrane of British Columbia (Davis and others, 1978; Saleeby, 1983). These terranes are considered to be remnants of a late Paleozoic and early Mesozoic magmatic arc that fringed the western margin of North America. Permian limestones in this belt are distinguished by the McCloud fusulinid fauna, a provincial fauna of western North America (Monger and Ross, 1971; Saleeby, 1983).

Two other terranes include Paleozoic rocks: the Deadman Bay and Vedder terranes. They overlap in age with the Chilliwack terrane but are otherwise distinct. The Deadman Bay terrane (Stop 3-7) comprises a Lower Permian to Lower Jurassic stratigraphic sequence of oceanic-island pillow basalt, limestone, and ribbon chert. In addition to obvious lithological contrasts with the Chilliwack, Permian limestones in the Deadman Bay terrane contain a Tethyan fusulinid fauna considered to be exotic to North America. The Deadman Bay is probably equivalent to parts of the Cache Creek terrane of British Columbia and the North Fork-Hayfork terrane of the Klamath Mountains (Davis and others, 1978; Saleeby, 1983).

The Vedder terrane (Stop 3-6) consists chiefly of fine-grained metabasaltic schist ranging in grade from greenschist to albite-epidote amphibolite and blueschist (Brown and others, 1987; synonymous with the Garrison terrane of Brandon and others, 1988). The largest outcrop is at Vedder Mountain in the western Cascades (labeled Vedder Complex in Fig. 1). All other occurrences are less than several hundred meters across and are too small to show in Figure 1. Isotopic dates cluster between 286 and 219 Ma (Armstrong and Misch, 1987), indicating Permian or Triassic metamorphism. Thus, metamorphism of the Vedder coincided with volcanism and chert deposition in the Chilliwack and Deadman Bay terranes. The Vedder may be related to other Permian and Triassic metamorphic units in the western Cordillera, such as the Pinchi Lake blueschist of British Columbia (Paterson and Harakal, 1974) and the Fort Jones blueschists of the Klamath Mountains (Davis and others, 1978; Irwin, 1981). A common feature of these Permian and Triassic metamorphic rocks is that they are typically associated with Deadman Bay-like units composed of upper Paleozoic and lower Mesozoic chert, basalt, and limestone. An inference is that the Vedder and Deadman terranes formed in a common tectonic setting, possibly at a late Paleozoic-early Mesozoic subduction zone (Davis and others, 1978). In the San Juan-Cascade nappes, Late Cretaceous faulting has obscured any obvious evidence of an early connection between these two terranes.

The youngest terranes in the San Juan-Cascade nappes are the Decatur and Easton terranes. The Decatur terrane (Stops 3-1 and 3-2) is floored by a Middle to Upper Jurassic ophiolite and contains a superimposed Upper Jurassic arc-volcanic complex. The ophiolitic basement of the Decatur allows this terrane to be clearly distinguished from older San Juan-Cascade terranes. The Decatur terrane is strikingly similar in age and stratigraphy to the Coast Range ophiolite of California (Hopson and others, 1981; Shervais and Kimbrough, 1985; Garver, 1988b).

The Easton terrane (Stop 2-11 in Haugerud, this volume) comprises a suite of Early Cretaceous metamorphic rocks, metamorphosed under blueschist conditions (P = 800-900 Mpa [8-9 kb], T = 300°-400° C; Brown and Blake, 1987). Its distinctive metamorphic history distinguishes the Easton from the other terranes listed above. The Easton appears to be of the same age, lithology, and degree of metamorphism as metamorphic rocks in northern California and southern Oregon (Brown and Blake, 1987). These rocks are located in the eastern part of the Franciscan Complex (South Fork Mountain and Colebrook schists) and in a thrust window in the Klamath Mountains (Condrey Mountain schist) and apparently

were formed during an early stage in the development of the Franciscan subduction complex.

Another potential tectonostratigraphic unit is the middle Cretaceous pillow basalts of Richardson. This unit appears to be restricted to two small fault slices in the San Juan Islands (approximate dimensions: 2.5 km x 250 m-500 m). The main slice (Stop 3-4) is in the Lopez Structural Complex at the town of Richardson, southern Lopez Island (labeled "R" in Fig. 3). Garver (1988a) has tentatively identified a second slice on northern Cypress Island (labeled "R?" in Fig. 3), but paleontological ages from this locality are poorly resolved. The Richardson basalts are important to San Juan geology because they are the youngest rocks affected by Late Cretaceous thrusting and high-pressure metamorphism. Foraminifera from interbedded shale at the Richardson locality have been identified as latest Albian (100 Ma) (Brandon and others, 1988).

An important question is whether to designate the Richardson basalts as a terrane. Arguing in favor is the fact that this unit is in some respects similar to the exotic limestone-basalt terranes in the Franciscan Complex (for example, Laytonville), which are interpreted as accreted fragments of seamounts. An important difference is that the middle Cretaceous Franciscan terranes contain pelagic limestone and chert, indicating an open-ocean setting (Sliter, 1984), whereas sediments in the Richardson basalts are limited to interbeds of hemipelagic shale with minor sand-sized grains of volcanic quartz. I feel that tectonostratigraphic classification is not warranted at this time. The main problem is that there are no coeval units to compare with the Richardson basalts. The tentative discovery of these basalts in the middle of the Decatur terrane ("R?" in Fig. 3) raises the possibility that they are a younger part of the Decatur terrane. If correct, the Richardson slice in the Lopez Complex ("R" in Fig. 3) could be explained as a fault slice derived from the adjacent Decatur terrane.

To the west and northwest of the San Juan-Cascade nappes lies Wrangellia (Jones and others, 1977) (Fig. 1), a coherent and regionally extensive terrane that underlies most of Vancouver Island. Wrangellia comprises a stratified sequence of Paleozoic arc-volcanic rocks, Triassic flood basalts, and Lower Jurassic arc-volcanic rocks (Muller, 1977). The oldest rocks are pre-Devonian, and probably Silurian (Brandon and others, 1986). This terrane is distinguished from adjacent terranes by its distinctive Triassic stratigraphy and also by the presence of a Boreal fusulinid fauna in Permian limestones (Monger and Ross, 1971). Wrangellia of Vancouver Island was not significantly affected by Late Cretaceous thrust faulting and shows no evidence of high-pressure metamorphism. It must have been near the nappes during the Late Cretaceous because it is overlain by synorogenic deposits of the Upper Cretaceous Nanaimo Group, which were derived, at least in part, from erosion of the San Juan-Cascade nappes (Brandon and others, 1988).

Timing of Continental Accretion

Most of the structural boundaries that separate terranes within the San Juan-Cascade nappes and also separate the nappes from Wrangellia are probably Late Cretaceous faults. There is evidence, however, that these terranes were accreted to continental America long before the Late Cretaceous. This conclusion is based on stratigraphic distinctions between terranes, which are pronounced during the Permian and Triassic and become almost insignificant during the Late Jurassic and Early Cretaceous.

This point is illustrated in Figure 2. All Upper Jurassic and Lower Cretaceous units (stippled units in Fig. 2) are composed almost entirely of marine epiclastic strata. In some places, these epiclastic units are in stratigraphic contact with older terranes (Kyuquot Group for Wrangellia; Lummi Group for Decatur terrane; Nooksack Group for Chilliwack terrane). In other places, these units are fault-bounded but can be tied to older terranes by a provenance link (for example, Constitution Formation contains clasts derived from Deadman Bay and Vedder terranes; Brandon and others, 1988).

All of these Jurassic and Cretaceous units are composed mainly of volcaniclastic sediments (p. 77 in Sutherland Brown, 1968; p. 36-39 in Muller and others, 1974; p. 25-31 in Muller and others, 1981; Brown and others, 1987; Brandon and others, 1988; Garver, 1988a), indicating that their source regions were dominated by intermediate to silicic arc-volcanic rocks. K-Ar dates of volcanic cobbles in the Spieden Group indicate that at least some of these volcanic rocks are Late Jurassic in age. The volcanic material cannot have been derived from San Juan-Cascade terranes or from Wrangellia because at that time these terranes were covered by Jurassic and Cretaceous marine strata.

The volume of sediment represented by these epiclastic units and other coeval epiclastic units to the north and south requires subaerially exposed source regions with continent-scale dimensions (Brandon and others, 1988). Thus, these epiclastic units are considered to be linking sequences that tie the San Juan-Cascade terranes and Wrangellia to a large continent-like mass, presumably the American continent, by the Late Jurassic. It is important to note that these linking sequences provide no information about the relative latitudinal position of each of the terranes along the Late Jurassic margin and do not preclude the possibility of younger coastwise translation.

Pre-Late Jurassic accretion is consistent with the accretionary history of similar terranes in the southern part of the Cordillera. In California, terranes similar to the

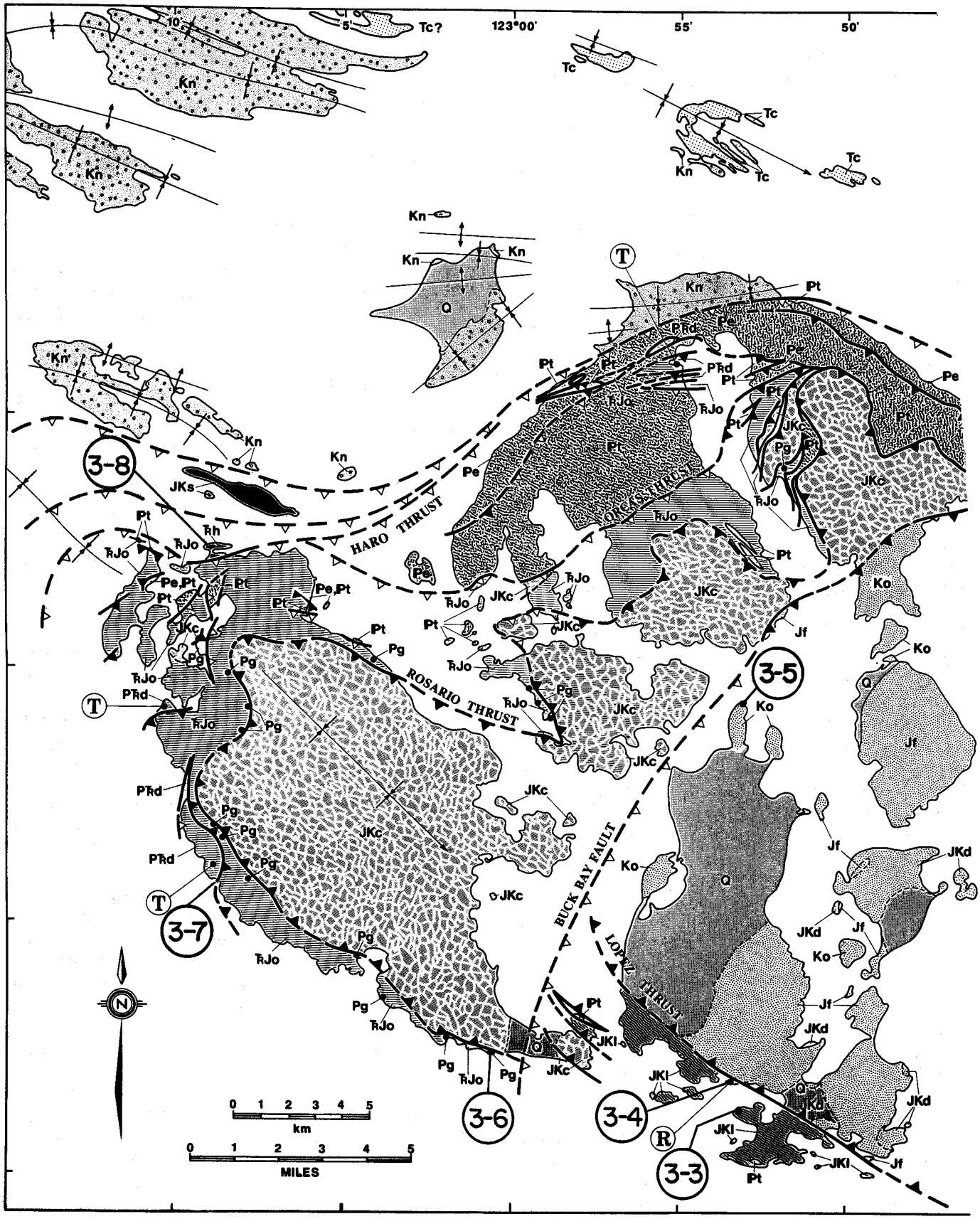

Figure 3. Geologic map of the San Juan Islands (modified from Brandon and others, 1988). Numbers refer to field stop locations.

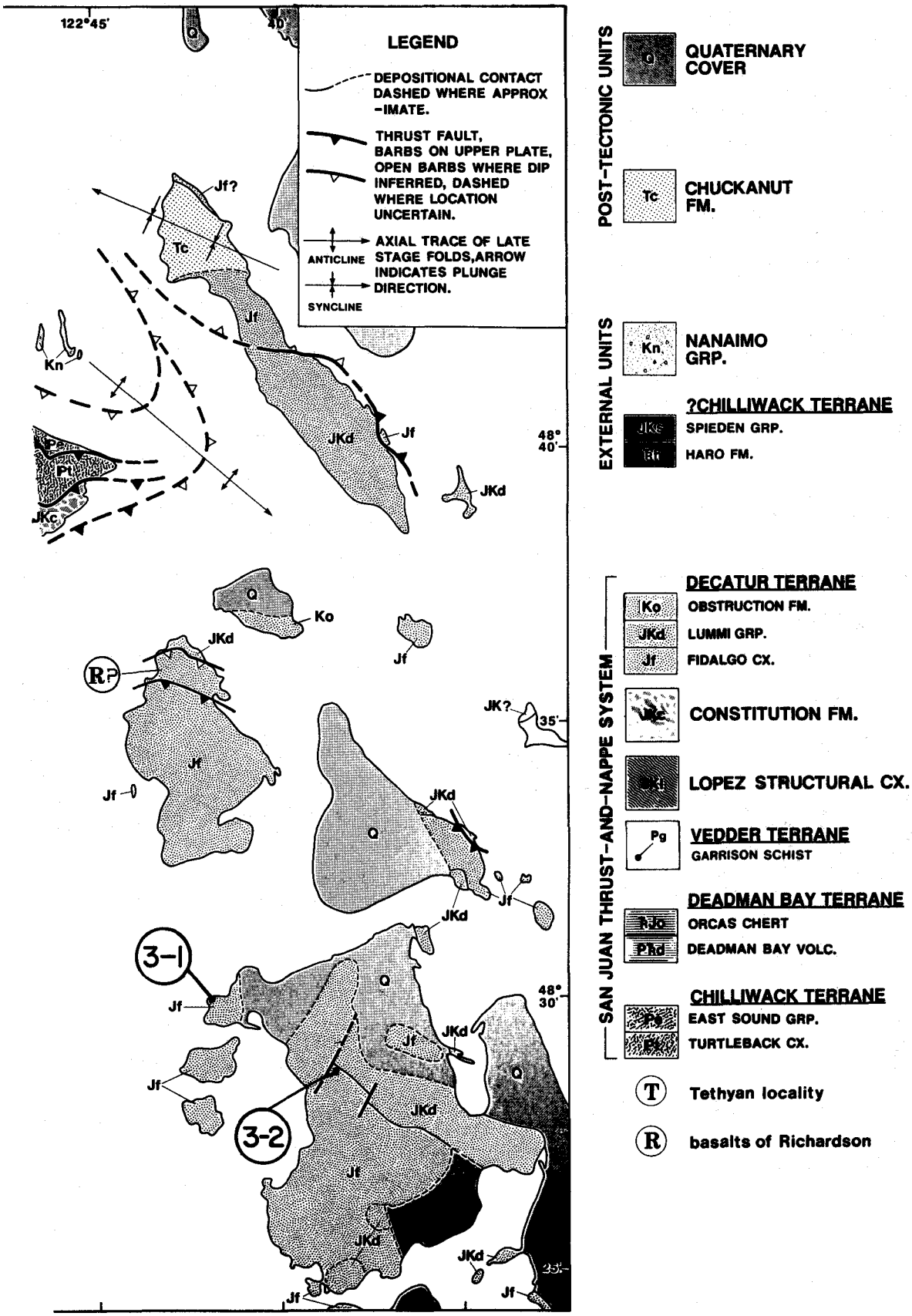

Figure 3. Geologic map of the San Juan Islands, continued.

Chilliwack, Deadman Bay, Vedder, and Decatur were accreted to continental North America by the Middle and Late Jurassic. The nature of this accretionary event remains uncertain: Did it involve the collisional arrival of an oceanic island arc (Schweickert, 1981) or non-collisional shortening of an in-situ arc system (Saleeby, 1981)? Regardless of the interpretation, this Middle to Late Jurassic event marks an important stratigraphic transition to widespread epiclastic sedimentation during the Late Jurassic and Early Cretaceous, as recorded by the Great Valley Group and Franciscan Complex. The Great Valley Group was deposited in a forearc setting with older accreted terranes forming the basement beneath the arc and forearc. The San Juan-Cascade terranes, and perhaps Wrangellia as well, may have been situated in a similar tectonic setting somewhere else along the Jurasic and Cretaceous Cordilleran margin. One readily identifiable remnant of this convergent margin setting is the Easton terrane.

Tectonic Setting of Late Cretaceous Orogeny

The formation and stacking of the San Juan-Cascade nappes is considered to be the hallmark of the Late Cretaceous Cascade orogeny (for example, Misch, 1966; Vance, 1977). The internal structure of the thrust belt is best preserved in the Mount Baker area and in the San Juan Islands (Fig. 1) where the superimposed effects of Tertiary deformation are minor. The east-west cross-section in Figure 4 provides a schematic view of the regional-scale structure of the thrust system. Though greatly simplified, this section shows that a regular stacking order is present at a regional scale. Misch (1966, 1977a) was first to recognize the broad aspects of this stacking order in the Mount Baker area. Further work in the Mount Baker area (Brown and others, 1987) and in the San Juan Islands (Vance, 1975, 1977; Whetten and others, 1978; Brandon and others, 1988) has substantiated and extended Misch's interpretation.

Misch (1966, 1977a, 1988) recognized three structural divisions in the Mount Baker area, from top to bottom: the Shuksan plate, the Church Mountain plate, and the "autochthon". The Shuksan plate forms the highest recognized nappe in the San Juan-Cascade system. It is composed solely of a fairly coherent section of Easton terrane and has a structural thickness that may approach 10 km. This plate is floored by the Shuksan thrust, which shows little imbrication with rocks of the underlying

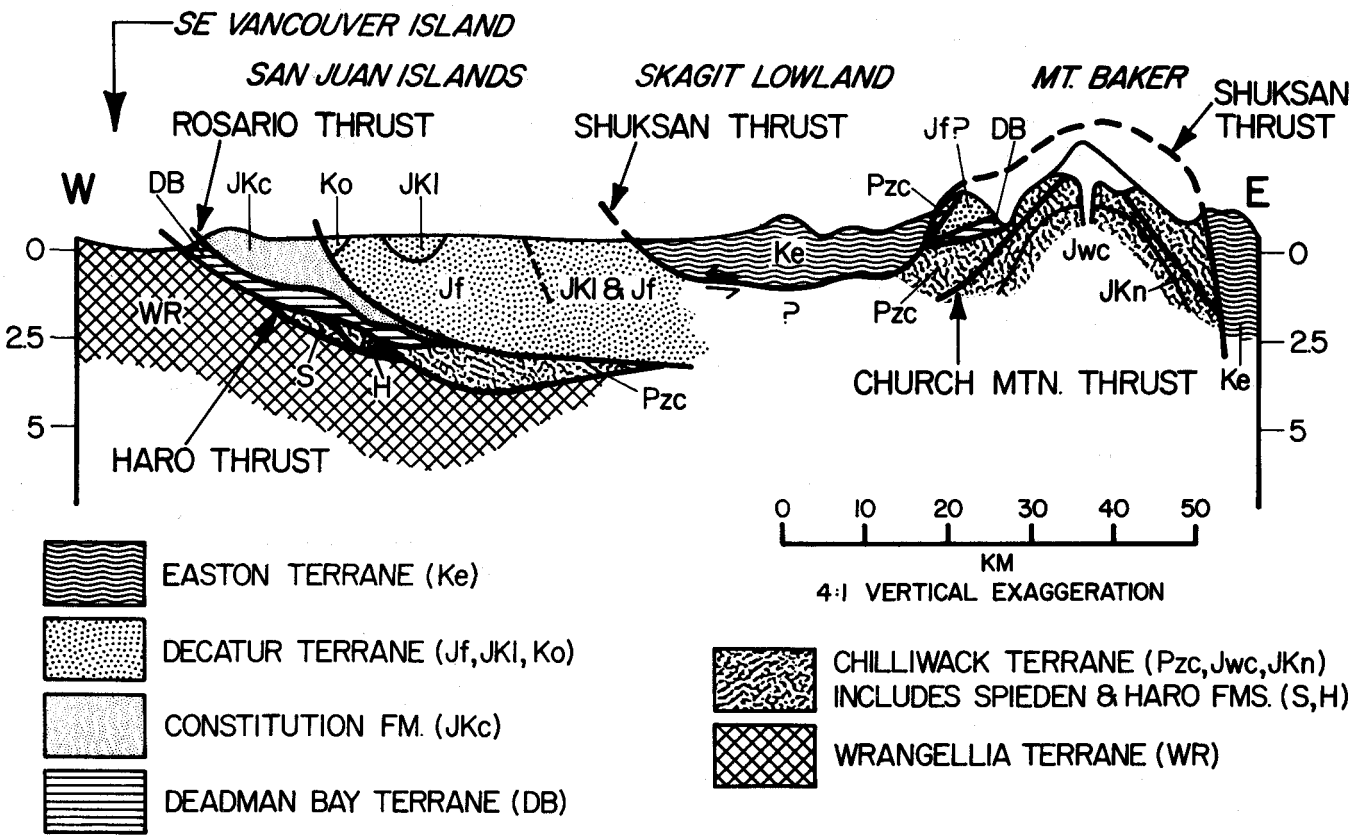

Figure 4. A schematic east-west cross section across the western Cascades and San Juan Islands (modified from Brandon and others, 1984). The location of the section is shown in Figure 1. Subsurface geology is projected in from the northwest using an average structural plunge of 12° to the southeast. Tectonostratigraphic units are defined in Table 1. The Vedder terrane, the Richardson basalts, and the Lopez Structural Complex are too small to portray here.

Church Mountain plate. The Church Mountain plate consists of a highly imbricated and heterogeneous assemblage derived mainly from the Chilliwack terrane and to a lesser degree from the Deadman Bay, Decatur, and Vedder terranes. The Church Mountain plate, which might be best represented as a structural complex, does occupy a specific structural level within the San Juan-Cascade nappes. Beneath the Church Mountain plate, which is floored by the Church Mountain thrust, lies the "autochthon" which consists of a relatively coherent section of Jurassic and Lower Cretaceous rocks of the Chilliwack terrane (Wells Creek Volcanics and Nooksack Group). Misch recognized that an unexposed thrust may underlie his "autochthon", and thus used this term merely as a label.

The extension of Misch's structural divisions west into the San Juan Islands is complicated by poor exposure in the intervening Skagit lowland (Fig. 1). The highest nappe found in the San Juans is the Decatur terrane. The Shuksan plate may have extended over the San Juan nappes (discussed below), but at present its western erosional limit is restricted to the Skagit lowland. The structural sequence in the San Juans, from top to bottom, consists of: Decatur terrane, Lopez Structural Complex, Constitution Formation, Vedder terrane, Deadman Bay terrane, and the Chilliwack terrane. (The Lopez Complex and Vedder terrane are too small to show in Fig. 4.) This sequence may represent a western extension of Misch's Church Mountain plate. Parts of the San Juan nappe sequence are highly imbricated; for example, see descriptions of the Orcas, Rosario, and Lopez faults in Brandon and others (1988). However, the San Juan sequence does not seem to be as pervasively faulted as the Church Mountain plate. Lying beneath the San Juan nappes are some small fault slices of Triassic and Jurassic and Cretaceous rocks (Haro Formation and Spieden Group, labeled "H" and "S" in Fig. 4) that may be equivalent to Misch's "autochthon". The presence of low-pressure zeolite assemblages in these rocks indicates that they were not subjected to the high-pressure metamorphic history that characterizes the rest of the San Juan-Cascade nappes.

In Figure 1, the San Juan-Cascade nappes are shown extending to the south and east of the Mount Baker area. This conclusion is based largely on the fact that almost all units in these areas can be correlated with units in the San Juan Islands and Mount Baker area. In some areas, particularly in the region south of the Devils Mountain fault (Fig. 1), Late Cretaceous structures are difficult to identify because of subsequent early Tertiary faulting and plutonism. However, these rocks do contain the same high-pressure metamorphic assemblage found in nappes of the San Juan Islands and Mount Baker area, suggesting a common tectonic history (discussed below).

A distinctive aspect of the San Juan-Cascade nappes is their metamorphic history. Much of the nappe sequence shows some evidence of a very low temperature, high-pressure metamorphism characterized by the formation of minor amounts of prehnite, lawsonite, and aragonite (McMillan, 1966; Monger, 1966; Vance, 1968; Misch, 1971; Beaty, 1974; Glassley and others, 1976; Brown and others, 1981). The details of this metamorphic event are best resolved in the San Juan Islands where Brandon and others (1988) have demonstrated that high-pressure metamorphism was caused by rapid structural burial during Late Cretaceous thrusting. Stratigraphic ages constrain this metamorphic event to the interval 100 to 84 Ma: (1) the youngest rocks involved in thrusting and metamorphism are the uppermost Albian (100 Ma) Richardson basalts; and (2) sandstone cobbles with lawsonite-prehnite assemblages are found in lowermost Campanian (84 Ma) strata of the Nanaimo Group, a synorogenic clastic sequence exposed to the north and northwest of the San Juan Islands. The Nanaimo Group also contains detritus from other parts of the San Juan-Cascade nappes, with the most obvious source being the Easton and Deadman Bay terranes. In the San Juan Islands, metamorphic conditions culminated at about 150°C and 600 Mpa (6 kb). These constraints require structural burial to depths of about 20 km and then uplift and return to the surface within a 16-m.y. interval, indicating a round trip with vertical velocities averaging about 2 km/m.y. Structural burial beneath an advancing thrust wedge to depths of 20 km implies much greater horizontal displacements, estimated to be at least 70 km or more.

Some parts of the nappe sequence were not affected by this high-pressure metamorphic event. Most notable is the Easton terrane (part of the Shuksan plate), although an isolated occurrence of metamorphic aragonite (Evans and Misch, 1976) may be related to the Late Cretaceous event. (Evans and Misch, 1976, attributed the aragonite to Early Cretaceous metamorphism of the Easton terrane.) The general absence of Late Cretaceous metamorphic assemblages in the Easton suggests that it may have formed a large part of the structural overburden required for high-pressure metamorphism of the lower part of the nappe sequence. Cobbles of Easton rocks in the Nanaimo Group demonstrate that the Easton was at the surface during Late Cretaceous thrusting. The easternmost part of the nappe sequence, the Ingalls ophiolite (shown in Fig. 1 as Decatur terrane in the Mount Stuart area), also lacks evidence of the prehnite-lawsonite-aragonite metamorphism. This part of the San Juan-Cascade nappes lies above the Skagit metamorphic core and thus would have been affected by higher thermal gradients in this more interior part of the orogen. The Skagit core does record an increase of at least 10 km in metamorphic depth during the Late Cretaceous (Evans and Berti, 1986), possibly caused by the emplacement of San Juan-Cascade nappes over the core.

At present, a controversial issue is the direction of transport and tectonic setting of the San Juan-Cascade

nappes. One group (Brandon and Cowan, 1985; McGroder, 1988) argues that the nappes were formed by the impingement of Wrangellia with the American continental margin, during which the San Juan-Cascade nappes were driven to the southwest over a footwall plate composed of Wrangellia. Another group (Brown, 1987; Smith, 1988) argues that the nappes formed in a northwest-trending transpressive shear zone. A third group (Davis and others, 1978; Vance and others, 1980; Miller, 1985) favors northward obduction of Decatur ophiolitic terranes from sites within the "Columbian embayment", a postulated oceanic embayment thought to lie in the vicinity of southwest Washington and western Oregon. This assemblage was then affected to various degrees by a younger episode of southwest-directed thrusting.

Much of this controversy centers on differing opinions about the transport direction of the San Juan-Cascade nappes. The argument for top-to-the-southwest transport is based largely on regional-scale features of the orogen, such as the northwesterly trend of the Skagit metamorphic core and the synorogenic Nanaimo basin. These features are interpreted to have formed during collision, with the metamorphic core marking the site of greatest crustal thickening and the Nanaimo basin representing a flexurally induced foredeep. They record the regional-scale configuration of the orogen and thus provide information about the overall shortening direction across the orogen.

The main argument for transpressive shear rests on the interpretation of small-scale structures in the Mount Baker area, which Brown (1987) and Smith (1988) attributed to Late Cretaceous faulting. Strain indicators show a pronounced horizontal elongation, but the trend of this elongation varies from northwest in the region south of Mount Baker to southwest in the region north of Mount Baker. Shear-sense indicators also vary considerably—only 60 percent of them are consistent with transpressive dextral shear in a northwest direction.

Another argument that Brown (1987) uses to support the transpressive shear interpretation is the fact that many of the faults in the Mount Baker area are steep, which he interprets as evidence that they formed as strike-slip faults. This conclusion is poorly founded because the present attitudes of the faults cannot be confidently related to their initial orientations. It is well known that thrust imbrication causes old thrust faults to rotate into steeper orientations. Furthermore, the steep attitudes of these faults could also be caused by younger deformation. Upper Cretaceous and Lower Tertiary strata in the Cascades and San Juan Islands commonly have moderate or steep dips, and in a few places are even overturned. Even so, it is important to point out that the top-to-the-southwest interpretation, based on regional-scale features of the orogen, appears inconsistent with most of the kinematic data of Brown (1987) and Smith (1988). As such, the controversy remains. An important aspect of the work of Brown (1987) and Smith (1988) is that it has demonstrated the need to better resolve and integrate outcrop-scale and orogen-scale kinematic evidence.

ACKNOWLEDGMENTS

I want to first acknowledge the efforts of Mike McGroder, who has been the prime mover for this field trip. This paper was significantly improved through careful reviews by J. G. Evans, S. A. Monsen, W. M. Phillips, and J. A. Vance. I thank D. Gusey and E. H. Brown for permission to reproduce text and figure from Gusey and Brown (1987) and the Geological Society of America for permission to use figures from Brandon and Cowan (1987).

REFERENCES

Armstrong, R. L.; Misch, Peter, 1987, Rb-Sr and K-Ar dating of mid-Mesozoic blueschist and Late Paleozoic albite-epidote-amphibolite and blueschist metamorphism in the North Cascades, Washington and British Columbia, and Sr-isotope fingerprinting of eugeosynclinal rock assemblages. *In* Schuster, J. E., editor, 1987, Selected papers on the geology of Washington: Washington Division of Geology and Earth Resources Bulletin 77, p. 85-105.

Arthur, A. J., 1986, Stratigraphy along the west side of Harrison Lake, southwestern British Columbia: Geological Survey of Canada Paper 86-1B, p. 715-720.

Beaty, R. J., 1974, Low grade metamorphism of Permian to Early Cretaceous volcanic and volcaniclastic rocks near Chilliwack, British Columbia: University of British Columbia Bachelor of Science thesis, 68 p.

Brandon, M. T., 1985, Mesozoic melange of the Pacific Rim complex, western Vancouver Island. *In* Tempelman-Kluit, Dirk, editor, 1985, Field guides to geology and mineral deposits in the southern Canadian Cordillera; Geological Society of America Cordilleran section meeting: Geological Survey of Canada, p. 7.1-7.28.

Brandon, M. T.; Cowan, D. S., 1985, The Late Cretaceous San Juan Islands-Northwestern Cascades Thrust System [abstract]: Geological Society of America Abstracts with Programs, v. 17, no. 6, p. 343.

Brandon, M. T.; Cowan, D. S., 1987, The Late Cretaceous San Juan thrust system, Washington–Nappes related to the arrival of Wrangellia. *In* Hill, M. L, editor, 1987, Cordilleran Section of the Geological Society of America: Geological Society of America DNAG Centennial Field Guide 1, p. 383-388.

Brandon, M. T.; Cowan, D. S.; Muller, J. E.; Vance, J. A., 1983, Pre-Tertiary geology of San Juan Islands, Washington and southeast Vancouver Island, British Columbia: Geological Association of Canada Victoria Section Field Trip 5, 65 p.

Brandon, M. T.; Johnson, S. Y.; Steward, R. J.; McClain, K. J., compilers, 1984, Geologic cross section B-B′-B″. *In* Kulm, L. D., and others, editors, 1984, Western North American continental margin and adjacent ocean floor off Oregon and Washington: Ocean Drilling Program, Regional Atlas Series 1; Marine Science International, [Woods Hole, MA], p. 19-20.

Brandon, M. T.; Orchard, M. J.; Parrish, R. R.; Sutherland Brown, A.; Yorath, C. J., 1986, Fossil ages and isotopic dates from the Paleozoic Sicker Group and associated intrusive rocks, Vancouver Island, British Columbia: Geological Survey of Canada Paper 86-1A, p. 683-696.

Brandon, M. T.; Cowan, D. S.; Vance, J. A., 1988, The Late Cretaceous San Juan thrust system, San Juan Islands, Washington: Geological Society of America Special Paper 221, 81 p., 1 plate.

Brown, E. H., 1977, The Fidalgo ophiolite. Part 1 of Cowan, D. S.; Whetten, J. T.; Brown, E. H., 1977, Geology of the southern San Juan Islands; Field trip No. 11. *In* Brown, E. H.; Ellis, R. C., editors, 1977, Geological excursions in the Pacific Northwest; Geological Society of America annual meeting: Western Washington University, p. 309-320.

Brown, E. H., 1987, Structural geology and accretionary history of the northwest Cascades system, Washington and British Columbia: Geological Society of America Bulletin, v. 99, no. 2, p. 201-241.

Brown, E. H.; Blake, M. C., Jr., 1987, Correlation of Early Cretaceous blueschists in Washington, Oregon and northern California: Tectonics, v. 6, no. 6, p. 795-806.

Brown, E. H.; Bernardi, M. L.; Christensen, B. W.; Cruver, J. R.; Haugerud, R. A.; Rady, P. M.; Sondergaard, J. N., 1981, Metamorphic facies and tectonics in part of the Cascade Range and Puget Lowland of northwestern Washington: Geological Society of America Bulletin, v. 92, no. 4, part I, p. 170-178.

Brown, E. H.; Blackwell, D. L.; Christensen, B. W.; Frasse, F. I.; Haugerud, R. A.; Jones, J. T.; Leiggi, P. A.; Morrison, M. L.; Rady, P. M.; Reller, G. J.; Sevigney, J. H.; Silverberg, D. L.; Smith, M. T.; Sondergaard, J. N.; Ziegler, C. B., 1987, Geologic map of the northwest Cascades, Washington: Geological Society of America Map and Chart Series, MC-61, 1 sheet, scale 1:100,000, with 10 p. text.

Cowan, D. S.; Whetten, J. T., 1977, Geology of Lopez and San Juan Islands. Part 2 of Cowan, D. S.; Whetten, J. T.; Brown, E. H., 1977. Geology of the southern San Juan Islands; Field trip No. 11. *In* Brown, E. H.; Ellis, R. C., editors, 1977, Geological excursions in the Pacific Northwest; Geological Society of America annual meeting: Western Washington University, p. 321-338.

Danner, W. R., 1957, A stratigraphic reconnaissance in the northwestern Cascade Mountains and San Juan Islands of Washington State: University of Washington Doctor of Philosophy thesis, 562 p., 7 pl.

Danner, W. R., 1966, Limestone resources of western Washington: Washington Division of Mines and Geology Bulletin 52, 474 p.

Davis, G. A.; Monger, J. W. H.; Burchfiel, B. C., 1978, Mesozoic construction of the Cordilleran "collage", central British Columbia to central California. *In* Howell, D. G.; McDougall, K. A., editors, 1978, Mesozoic paleogeography of the western United States: Society of Economic Paleontologists and Mineralogists, Pacific Section, Pacific Coast Paleogeography Symposium 2, p. 1-32.

Evans, B. W.; Berti, J. W., 1986, A revised metamorphic history for the Chiwaukum Schist, north Cascades, Washington: Geology, v. 14, no. 8, p. 695-698.

Evans, B. W.; Misch, Peter, 1976, A quartz-aragonite-talc schist from the lower Skagit Valley, Washington: American Minerologist, v. 61, no. 9-10, p. 1005-1008.

Frizzell, V. A., Jr.; Tabor, R. W.; Booth, D. B.; Ort, K. M.; Waitt, R. B.; Jr., 1984, Preliminary geologic map of the Snoqualmie Pass 1:100,000 quadrangle, Washington: U.S. Geological Survey Open-File Report 84-693, 42 p., 1 pl.

Frizzell, V. A., Jr.; Tabor, R. W.; Zartman, R. E.; Blome, C. D., 1987, Late Mesozoic or early Tertiary melanges in the western Cascades of Washington. *In* Schuster, J. E., editor, 1977, Selected papers on the geology of Washington: Washington Division of Geology and Earth Resources Bulletin 77, p. 129-148.

Garver, J. I., 1988a, Stratigraphy, depositional setting and tectonic significance of the clastic cover to the Fidalgo Ophiolite, San Juan Islands, Washington: Canadian Journal of Earth Sciences, v. 25, no. 3, p. 417-432.

Garver, J. I., 1988b, Fragment of the Coast Range ophiolite and the Great Valley sequence in the San Juan Islands, Washington: Geology, v. 16, no. 10, p. 948-951.

Glassley, W. E.; Whetten, J. T.; Cowan, D. S.; Vance, J. A., 1976, Significance of coexisting lawsonite, prehnite, and aragonite in the San Juan Islands, Washington: Geology, v. 4, no. 5, p. 301-302.

Gusey, D. L., 1978, The geology of southwestern Fidalgo Island: Western Washington University Master of Science thesis, 85 p., 1 pl.

Gusey, D. L.; Brown, E. H., 1987, The Fidalgo Ophiolite, Washington. *In* Hill, M. L., editor, 1987, Cordilleran Section of the Geological Society of America: Geological Society of America DNAG Centennial Field Guide 1, p. 389-392.

Hopson, C. A.; Mattinson, J. M.; Pessagno, E. A., Jr., 1981, Coast Range ophiolite, western California. *In* Ernst, W. G., editor, 1981, The geotectonic development of California: Rubey Volume I: Prentice-Hall, p. 418-510.

Igo, Hisayoshi; Koike, Toshio; Igo, Hisaharu; Sashida, Katsuo; Hisada, Kenichiro; Isozaki, Yukio, 1984, On the occurrence of conodonts and radiolarians from the San Juan Islands, Washington and Vancouver Island, British Columbia: University of Tsukuba Institute of Geoscience Annual Report 10, p. 86-91.

Irwin, W. P., 1981, Tectonic accretion of the Klamath Mountains. *In* Ernst, W. G., editor, 1981, The geotectonic development of California, Rubey Volume I: Prentice-Hall, p. 29-49.

Johnson, S. Y., 1978, Sedimentology, petrology, and structure of Mesozoic strata in the northwestern San Juan Islands, Washington: University of Washington Master of Science thesis, 106 p., 4 pl.

Jones, D. L.; Silberling, N. J.; Hillhouse, J., 1977, Wrangellia–A displaced terrane in northwestern North America: Canadian Journal of Earth Sciences, v. 14, no. 11, p. 2565-2577.

Jones, D. L.; Howell, D. G.; Coney, P. J.; Monger, J. W. H., 1983, Recognition, character and analysis of tectonostratigraphic terranes in western North America. *In* Hashimoto, M.; Uyeda, S., editors, 1983, Accretion tectonics in the circum-Pacific regions: D. Reidel Publishing Company, p. 21-35.

McGroder, M. F., 1988, Structural evolution of eastern Cascades foldbelt [abstract]: Geological Society of America Abstracts with Programs, v. 20, no. 3, p. 213.

McMillan, W. J., 1966, Geology of Vedder Mountain, near Chilliwack, British Columbia: University of British Columbia Master of Science thesis, 59 p.

Miller, R. B., 1985, The ophiolitic Ingalls Complex, north-central Cascade Mountains, Washington: Geological Society of America Bulletin, v. 96, no. 1, p. 27-42.

Misch, Peter, 1966, Tectonic evolution of the northern Cascades of Washington State–A west-Cordilleran case history. *In* Canadian Institute of Mining and Metallurgy; and others, 1966, A symposium on the tectonic history and mineral deposits of the western Cordillera in British Columbia and neighbouring parts of the United States, Vancouver, 1964: Canadian Institute of Mining and Metallurgy Special Volume 8, p. 101-148.

Misch, Peter, 1971, Metamorphic facies types in north Cascades [abstract]: Geological Association of Canada Cordilleran Section Meeting Program and Abstracts, p. 22-23.

Misch, Peter, 1977a, Bedrock geology of the north Cascades. *In* Brown, E. H.; Ellis, R. C., editors, 1977, Geological excursions in the Pacific Northwest; Geological Society of America annual meeting: Western Washington University, p. 1-62.

Misch, Peter, 1977b, Dextral displacements at some major strike faults in the north Cascades [abstract]: Geological Association of Canada [annual meeting], Programs with Abstracts, v. 2, p. 37.

Misch, Peter, 1988, Tectonic and metamorphic evolution of the North Cascades: an overview. *In* Ernst, W. G., editor, 1988, Metamorphism and crustal evolution of the western United States: Rubey Volume VII, Prentice Hall, p. 180-195.

Monger, J. W. H., 1966, The stratigraphy and structure of the type area of the Chilliwack Group, southwestern British Columbia: University of British Columbia Doctor of Philosophy thesis, 158 p.

Monger, J. W. H., 1970, Hope map-area, west half (92H W1/2) British Columbia: Geological Survey of Canada Paper 69-47, 75 p., 3 pl.

Monger, J. W. H., 1986, Geology between Harrison Lake and Fraser River, Hope map-area, southwestern British Columbia: Geological Survey of Canada Paper 86-1B, p. 699-706.

Monger, J. W. H.; Berg, H. C., 1987, Lithotectonic terranes of western Canada and southeastern Alaska: U.S. Geological Survey Miscellaneous Field Studies Map MF-1874-B, 1 sheet, scale 1:2,500,000, with 12 p. text.

Monger, J. W. H.; Ross, C. A., 1971, Distribution of fusulinaceans in the western Canadian Cordillera: Canadian Journal of Earth Sciences, v. 8, no. 2, p. 259-278.

Muller, J. E., 1977, Evolution of the Pacific Margin, Vancouver Island, and adjacent regions: Canadian Journal of Earth Sciences, v. 14, no. 9, p. 2062-2085.

Muller, J. E.; Northcote, K. E.; Carlisle, D., 1974, Geology and mineral deposits of Alert-Cape Scott map-area, Vancouver Island, British Columbia: Geological Survey of Canada Paper 74-8, 77 p., 2 pl.

Muller, J. E.; Cameron, B. E. B.; Northcote, K. E., 1981, Geology and mineral deposits of the Nootka Sound map-area (92 E), Vancouver Island, British Columbia: Geological Survey of Canada Paper 80-16, 53 p., 1 pl.

Paterson, I. A.; Harakal, J. E., 1974, Potassium-argon dating of blueschists from Pinchi Lake, central British Columbia: Canadian Journal of Earth Sciences, v. 11, no. 7, p. 1007-1011.

Raleigh, C. B., 1965, Structure and petrology of an alpine peridotite on Cypress Island, Washington, U.S.A.: Contribution to Mineralogy and Petrology [Beitrage zur Mineralogie und Petrographie], v. 11, no. 7, p. 719-741.

Saleeby, J. B., 1981, Ocean floor accretion and volcanoplutonic arc evolution of the Mesozoic Sierra Nevada. *In* Ernst, W. G., editor, 1981, The geotectonic development of California, Rubey Volume I: Prentice-Hall, p. 132-181.

Saleeby, J. B., 1983, Accretionary tectonics of the North American Cordillera: Annual Reviews of Earth and Planetary Sciences, v. 11, p. 45-73.

Schweickert, R. A., 1981, Tectonic evolution of the Sierra Nevada Range. *In* Ernst, W. G., editor, 1981, The geotectonic development of California, Rubey Volume I: Prentice-Hall, p. 87-131.

Shervais, J. W.; Kimbrough, D. L., 1985, Geochemical evidence for the tectonic setting of the Coast Range ophiolite–A composite island arc-oceanic crust terrane in western California: Geology, v. 13, no. 1, p. 35-38.

Sliter, W. V., 1984, Foraminifers from Cretaceous limestone of the Franciscan Complex, northern California. *In* Blake, M. C., Jr., editor, 1984, Franciscan geology of northern California: Society of Economic Paleontologists and Mineralogists, Pacific Section, Field Trip Guidebook 43, p. 149-162.

Smith, M. T., 1988, Deformational geometry and tectonic significance of a portion of the Chilliwack Group, northwestern Cascades, Washington: Canadian Journal of Earth Sciences, v. 25, no. 3, p. 433-441.

Southwick, D. L., 1974, Geology of the alpine-type ultramafic complex near Mount Stuart, Washington: Geological Society of America Bulletin, v. 85, no. 3, p. 391-402.

Sutherland Brown, A., 1968, Geology of the Queen Charlotte Islands, British Columbia: British Columbia Department of Mines and Petroleum Resources Bulletin 54, 226 p., 7 pl.

Vance, J. A., 1968, Metamorphic aragonite in the prehnite-pumpellyite facies, northwest Washington: American Journal of Science, v. 266, no. 4, p. 299-315.

Vance, J. A., 1975, Bedrock geology of San Juan County. *In* Russell, R. H., editor, 1975, Geology and water resources of the San Juan Islands, San Juan County, Washington: Washington Department of Ecology Water Supply Bulletin 46, p. 3-19.

Vance, J. A., 1977, The stratigraphy and structure of Orcas Island, San Juan Islands. *In* Brown, E. H.; Ellis, R. C., editors, 1977, Geological excursions in the Pacific Northwest; Geological Society of America annual meeting: Western Washington University, p. 170-203.

Vance, J. A.; Dungan, M. A.; Blanchard, D. P.; Rhodes, J. M., 1980, Tectonic setting and trace element geochemistry of Mesozoic ophiolitic rocks in western Washington: American Journal of Science, v. 280-A, part 1, p. 359-388.

Whetten, J. T.; Jones, D. L.; Cowan, D. S.; Zartman, R. E., 1978, Ages of Mesozoic terranes in the San Juan Islands, Washington. *In* Howell, D. G.; McDougall, K. A., editors, 1978, Mesozoic paleogeography of the western United States: Society of Economic Paleontologists and Mineralogists, Pacific Section, Pacific Coast Paleography Symposium 2, p. 117-132.

Whetten, J. T.; Zartman, R. E.; Blakely, R. J.; Jones, D. L., 1980, Allochthonous Jurassic ophiolite in northwest Washington: Geological Society of America Bulletin, v. 91, no. 6, part I, p. 359-368.

Whetten, J. T.; Carroll, P. I.; Gower, H. D.; Brown, E. H.; Pessl, Fred, Jr., 1988, Bedrock geologic map of the Port Townsend 30- by 60-minute quadrangle, Puget Sound region, Washington: U.S. Geological Survey Miscellaneous Investigations Series Map I-1198-G, 1 sheet, scale 1:100,000.

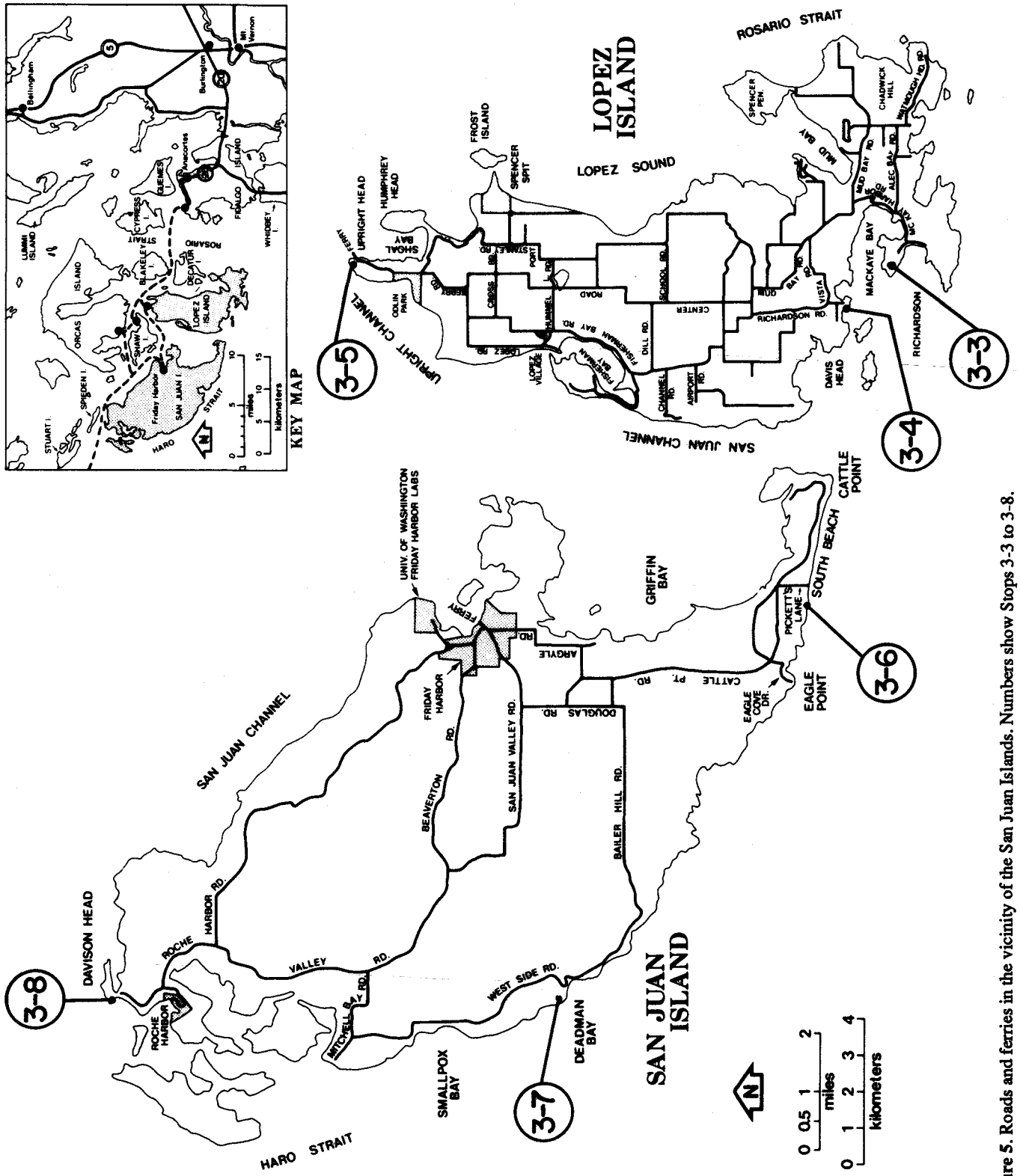

Figure 5. Roads and ferries in the vicinity of the San Juan Islands. Numbers show Stops 3-3 to 3-8.

Road Log

This log describes eight field stops (3-1 to 3-8 in Figs. 3 and 5) in the San Juan Islands. It is complemented by four field stops in the western North Cascades (2-7 to 2-11 in Haugerud, this volume). Collectively, these stops focus on the geology of the San Juan-Cascade nappes. Our goals are to: (1) examine timing constraints for thrusting and regional high-pressure metamorphism, (2) inspect outcrop-scale structures associated with some of the major thrusts, and (3) look at representative parts of the pre-Late Cretaceous tectonostratigraphic units found in the nappes. Other more comprehensive field guides to the San Juan Islands and surrounding areas are Brandon and others (1983), Brown (1977), Vance (1977), Cowan and Whetten (1977), Misch (1977), Brandon and Cowan (1987), and Gusey and Brown (1987). Several of the locality descriptions below are reproduced, with minor modifications, from the following original sources: Gusey and Brown (1987) for Stops 3-1 and 3-2 on Fidalgo Island; and Brandon and Cowan (1987) for Stops 3-4, 3-6, and 3-7.

Field Stops on Fidalgo Island

The first two stops are in the Fidalgo ophiolite (Decatur terrane), on the west side of Fidalgo Island (Figs. 3 and 6). From Interstate Highway 5, take exit 230 at Burlington and head west to Anacortes on Washington State Route (SR) 20 (inset map in Fig. 5). In Anacortes, follow the signs to the Washington State ferry terminal (Fig. 6), which will take you north on Commercial Avenue and then west (left) onto 12th Street (a spur of SR 20). Stay in the left lane at the junction to the ferry terminal and proceed straight ahead to Washington Park (Fig. 6). For the next two stops, cumulative mileage is shown in parentheses, starting at the park entrance.

Follow the loop road in the park. Stop near the leaning tree (0.4 mi).

STOP 3-1: Washington Park, Fidalgo Island—Serpentinized ultramafic rocks of the Fidalgo Igneous Complex.

The following text is reproduced with permission from Gusey and Brown (1987).

"Tidal exposures in this vicinity and to the west for several hundred meters display the ultramafic rock of the Fidalgo ophiolite. Look for chromite layers, relict pyroxenes, and original dunite-peridotite contacts in the serpentinite.

"The serpentinite exposed here is part of an ultramafic belt that is also exposed on nearby Burrows and Cypress Islands. Detailed analysis of the ultramafic rock on Cypress Island has shown the unserpentinized parts of the mass are largely harzburgite with a tectonite fabric, but possible relict igneous textures are visible (Raleigh, 1965).

"The serpentinite is thought to be the base of the Fidalgo ophiolite. Nowhere on Fidalgo Island, or elsewhere in the San Juan Islands, has a primary, unfaulted contact between the serpentinite and layered gabbro been observed. However, the close spatial relation of gabbroic and ultramafic rock and the indication from graded bedding in the gabbro suggest that the serpentinite lies down-section from the gabbro [Fig. 6]. Also, a small (30 x 50 m) lens of serpentinized peridotite occurs within the plagiogranite dike complex near the southern end of Fidalgo Island. "

To reach Stop 3-2, proceed along the loop road to the park exit (2.4 mi) and head east on Sunset Avenue. Turn right (3.0 mi) onto Anaco Beach Road which becomes Marine Drive. Turn left (5.9 mi) onto Havekost Road and then turn right (6.8 mi) into the Marine Asphalt Company quarry. This quarry is still active. Stop at the office to ask for permission to enter.

STOP 3-2: Marine Asphalt Quarry, Fidalgo Island—Basal breccia and siliceous argillite resting on plutonic rocks of the Fidalgo Igneous Complex.

The following text is reproduced with permission from Gusey and Brown (1987).

"Here, plagiogranite exposed in the south quarry wall is overlain along an irregular contact by coarse sedimentary breccia containing clasts of plagiogranite, keratophyre, and spilite. Exposed on the west quarry wall, depositionally overlying the breccia, is steeply dipping pelagic argillite.

"Elsewhere on Fidalgo Island, sedimentary breccias apparently occupying the same stratigraphic position, that is, beneath pelagic argillite, contain clasts of serpentinite, cumulate gabbro, and pegmatitic diorite, as well as plagiogranite and volcanic rocks. Clast size ranges from 1 to 30 cm. These breccias may represent talus accumulations at the base of a submarine fault.

"Generally, the pelagic argillite unit is a radiolarian-bearing, metal-enriched, carbonate-free chloritic argillite with local minor tuf-

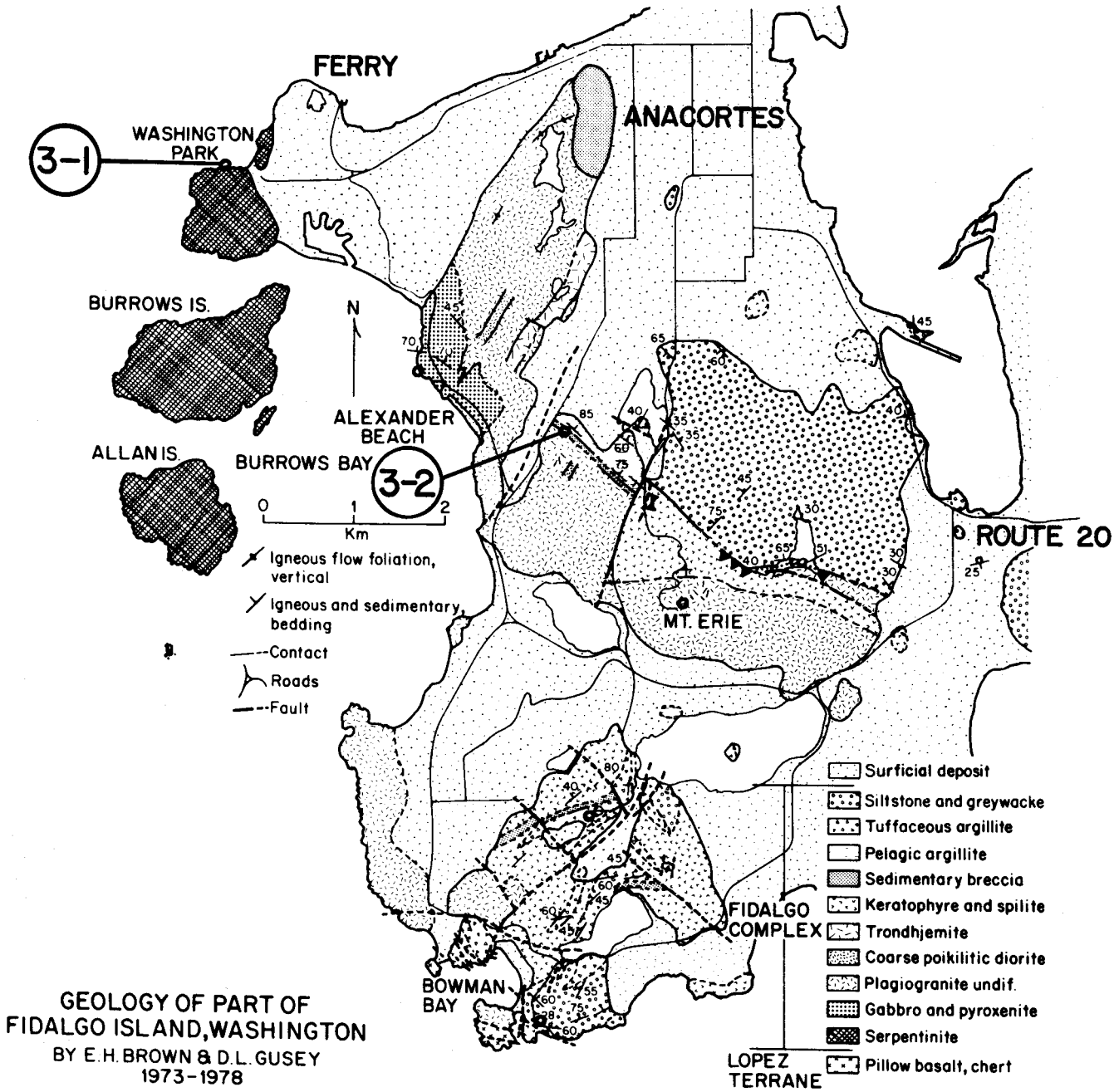

Figure 6. Geologic map of Fidalgo Island for Stops 3-1 and 3-2. Numbers refer to field stops locations. Reprinted with permission from Gusey and Brown (1987).

faceous debris. Radiolarians from an argillite bed approximately 55 m from the base of the unit have been dated as Late Kimmeridgian to Early Tithonian (Gusey, 1978). The concentration of metals (Ba, Cu, Ni, Co, and Mn) in the pelagic argillite is similar to that in present-day Pacific pelagic sediments (Brown, 1977).

"Of special interest within the pelagic argillite unit are thin (5 cm) interbeds of a chloritic sandstone. This sandstone consists of sand-sized chlorite grains in a micritic matrix. Diffractograms of the clay-size fraction indicate the presence of a well-crystallized, expandable chlorite. In thin section, mesh textures and cleavage traces are common in the chlorite. Also chlorite has been observed replacing pyroxene. Accessory minerals include chromite, quartz, plagioclase, clinopyroxene, garnet, amphibolite,

and volcanic and sedimentary rock fragments. These beds are interpreted to have been deposited by turbidity currents from a nearby ultramafic source and subsequently chloritized (Gusey, 1978)."

To return to the Anacortes ferry terminal, retrace your way to the intersection of Anaco Beach Road and Sunset Avenue. Turn right on Sunset Avenue, then left at the entrance road to the Anacortes ferry terminal. Ferries from this terminal provide frequent service for cars and passengers to Lopez, San Juan, Orcas, and Shaw Islands. Long waits are to be expected on summer weekends.

Experience indicates that a road map is preferable to cumulative mileages for finding field stops in the San Juans because roads are too closely spaced for easy differentiation. Thus, the map in Figure 5 will be used for subsequent directions.

Field Stops on Lopez Island

For Stops 3-3, 3-4, and 3-5, take the Lopez Island ferry. The ferry disembarks at Upright Head on Lopez Island.

From the ferry terminal, head south on Ferry Road. At the T-intersection, turn left and then right onto Center Road and continue south to the next T-intersection, where you turn left and right again onto Mud Bay Road. Take the second right turn onto McKay Harbor Road. Follow this road to the intersection with Aleck Bay Road, and then continue southwest on McKay Harbor Road for another 0.5 mi to an unnamed dirt road that turns off to the right (north). Drive 0.3 mi on this road to a large grassy parking area adjacent to a wharf. The headland here, called Johns Point, is private property; you *must* ask permission to enter (currently at the small house about 75 m west of the parking area). Walk around the west end of the point where you will find nearly continuous exposures of bedrock.

STOP 3-3: Johns Point, Lopez Island—Fault slices and deformation in the Lopez Structural Complex.

The Lopez Structural Complex, which is the focus of Stops 3-3 and 3-4, is exposed along the south coast of Lopez Island and on the southeast tip of San Juan Island (Figs. 3 and 7). It represents a 2.5-km-thick imbricate fault zone that separates two fairly coherent Mesozoic units: the structurally lower Constitution Formation and the overlying Decatur terrane. At map scale (Fig. 7), the Lopez Complex consists of an imbricated series of elongate, lenticular fault slices, which dip moderately northeast beneath the Decatur terrane. Many of the fault slices are similar to, and were probably derived from the Constitution Formation and Decatur terrane; others contain exotic units that cannot be related to rock units in the footwall or the hangingwall. These exotic units are early Paleozoic tonalite (Turtleback Complex in Fig. 7, derived from the Chilliwack terrane) and the middle Cretaceous Richardson basalts.

The structural base of the Lopez Complex is not exposed. The top is the Lopez thrust, which marks the uppermost limit of significant structural interleaving of disparate rock units. This particular thrust is fairly easy to follow because it generally places igneous rocks of the Decatur terrane (Fidalgo Igneous Complex) over sedimentary units of the Lopez Complex. The most prominent structure visible in most outcrops in the Lopez is a northeast-dipping flattening cleavage. In the past, this cleavage was attributed to shearing within the fault zone, but subsequent work (Brandon and others, 1988) has shown that the cleavage formed by pressure-solution flow, that it is not restricted to the Lopez Complex, and that it postdates thrust faulting and regional high-pressure metamorphism. I attribute cleavage formation to late-stage ductile shortening as thrust slices moved through the warmest part of the thrust wedge (see fig. 29 of Brandon and others, 1988).

Most of the Lopez Complex is composed of two rock units derived from the Decatur terrane: (1) well-bedded turbidite sandstone and mudstone, with minor shale-chip and chert-pebble conglomerate; and (2) Jurassic pillow basalt and minor brecciated gabbro. Rock units from the Constitution Formation include: (1) chaotic mudstone-rich sequences composed mainly of olistostromal pebbly and bouldery mudstones, with clasts of sandstone, basalt, and chert dispersed in a black mudstone matrix; and (2) sandstone sequences with interbedded chert, green tuff, and basalt. The first of the Constitution-like units has yielded Early Cretaceous (Valanginian) *Buchia*, and the second has yielded Jurassic or Cretaceous radiolarians from interbedded chert (Brandon and others, 1988).

All rock units in the Lopez Complex show some evidence of high-pressure metamorphism: sandstones contain lawsonite and aragonite; the slices of Turtleback tonalite contain rare lawsonite; basalts, including the Richardson basalts,

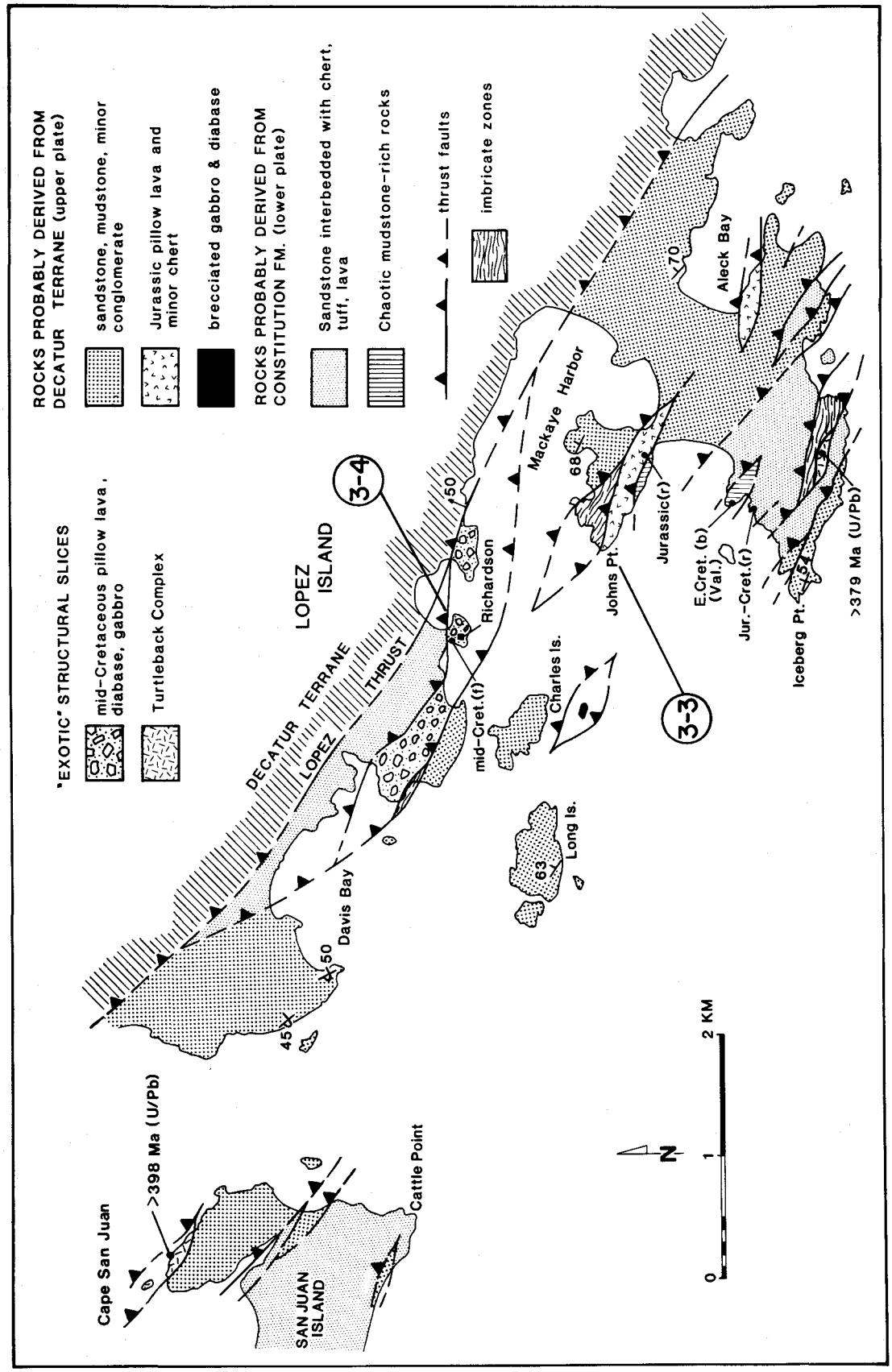

Figure 7. Geologic map for Stops 3-3 and 3-4 showing the internal structure of the Lopez Structural Complex, exposed on the southern perimeters of Lopez and San Juan Islands (Brandon and others, 1988). Numbers refer to the field stop locations. All contacts are faults. Strike and dip symbols show bedding attitude in stratified units. Fossil ages and isotopic dates are indicated by: "f" for foraminifera from mudstone at Richardson, "r" for radiolarians from chert, "b" for *Buchia pacifica* (Valanginian) from sandstone, and "U/Pb" for U/Pb zircon dates from Turtleback tonalite.

contain aragonite, pumpellyite, and chlorite; and gabbro associated with the Richardson basalts contains rare blue amphibole.

The diverse geology of Johns Point is representative of the Lopez Complex as a whole. As one moves from north to south around the peninsula, one can examine the following fault slices (Fig. 7): relatively coherent turbidites, a highly deformed fault zone, a thick slice of Jurassic pillow basalt (ocean-floor chemistry), and a polymictic pebbly mudstone with rounded clasts.

The pebbly mudstone unit highlights a persistent problem to unraveling the deformational histories of units like the Lopez Complex. There is abundant evidence, both at map scale and outcrop scale, for thrust-related imbrication and shearing; however, rock units within the complex also show evidence of syn-depositional mass-wasting. Thus, it becomes difficult to determine how much of the intermixing within the complex occurred by faulting and how much predates the development of the fault zone.

A good example of this problem is present at Johns Point. At the southern contact of the Jurassic basalt where it lies adjacent to pebbly mudstone, one can see thin mud-filled fissures in the basalt. The mud was presumably derived from the adjacent pebbly mudstone. These features certainly attest to the mobility of the mud, but past debates at this outcrop have produced two very different interpretations. The first concludes that the pebbly mudstone must have been soft and unlithified, and thus in a near-surface setting, when the basalt block was emplaced. In this case, the basalt is considered to be a submarine slide block, produced by a Late Jurassic or Early Cretaceous rock fall that travelled into a mud-rich basin. The second interpretation argues that the block/mudstone contact is a product of Late Cretaceous thrusting since much of the present structure of the Lopez Complex appears to be thrust related. The mobility of the mud is attributed to cataclastic flow of the mudstone matrix within a zone of large shear strain. This interpretation maintains that mud can remain highly mobile even at great depths.

To reach the next stop, follow McKay Harbor Road back to the T-intersection with Mud Bay Road. Turn left onto Mud Bay Road. Turn at the next left onto Vista Road, and then turn left at the T-intersection onto Richardson Road. Drive south to the hamlet of Richardson. Park at the Richardson store where the road ends in a cul-de-sac. The outcrops to be examined are on the east side of the road and on the coast extending 75 m north of the store.

STOP 3-4: Richardson, Lopez Island—An exotic slice of middle Cretaceous Richardson basalts in the Lopez Structural Complex.

The brownish-red mudstone bed in the 3-m-high roadcut opposite the store is very important because it has yielded the youngest fossils from the San Juan nappes. Foraminifera from these mudstones, first discovered by Danner (1966), have been identified as latest Albian (mid-Cretaceous, about 100 Ma). The mudstone bed forms a 1.5-m-thick interval in a sequence otherwise composed of basalt and minor gabbro. As already discussed, the Richardson basalts are unusual in that they do not appear to have been derived from the units bounding the Lopez Complex and thus may represent an exotic unit. In the Lopez Complex, these basalts are restricted to a single fault slice about 2.5 km long and 275 m thick (Fig. 7). At outcrop scale, the unit shows little evidence of fault deformation. Amygdules and veins of metamorphic aragonite and pumpellyite are present in the Richardson basalts, indicating that regional high-pressure metamorphism postdates the 100 Ma age of these basalts.

More of this volcanic unit is exposed in the steep, 5-m-high seacliff immediately north of the store. Note that the mudstone is part of a northeast-dipping stratigraphic sequence including, from bottom to top: pillow basalt, red and black mudstone, pillow breccia, and finally more pillow basalt at the north end of the outcrop. The pillows indicate that the sequence is upright.

On the basis of their trace-element composition (high TiO_2, light rare-earth element enriched; Brandon and others, 1988), these pillowed basalts probably erupted in an "oceanic-island" setting and thus may represent part of a middle Cretaceous seamount. The mudstone contains small lenses of sand-sized volcanic quartz and feldspar, indicating the proximity of an intermediate volcanic arc.

An isolated outcrop of gabbro is exposed at the northeast end of the coastal exposures at Richardson. The gabbro is chemically similar to the basalts (p. 67 *in* Brandon and others, 1988) and thus is included in the Richardson unit.

Retrace the route to the ferry terminal at Upright Head. While waiting for the ferry, we can examine the coastal outcrops in the vicinity of the loading ramp.

STOP 3-5: Upright Head, Lopez Island—Middle Cretaceous Obstruction Formation.

Upright Head exposes conglomerates that belong to the upper member of the Obstruction Formation (unit Ko in Figs. 3 and 4), a new unit recognized and studied by Garver (1988a). The Obstruction is composed of a lower sandstone member (> 400 m thick) and an upper conglomerate member (> 800 m thick). The base and top of the unit are not exposed, and age-diagnostic fossils have not been found.

The significance of this unit lies in Garver's discovery that the Obstruction Formation is younger than the Richardson basalts and that deposition of the unit probably postdates regional high-pressure metamorphism. The age of the unit is based on a suite of fission-track ages for detrital grains of zircon from a sandstone sample. The sandstone was not subjected to the zircon annealing temperature, so detrital ages provide a maximum limit for the depositional age of the sandstone. The youngest peak of the detrital age suite is 95 ± 6.8 Ma (error at 95% confidence level), indicating deposition at some time after the Albian (Garver, 1988a).

The Obstruction Formation lacks evidence of the regional high-pressure metamorphism. The observed assemblage is calcite-clay-white mica. Nearby Decatur terrane rocks contain prehnite plus rare aragonite. This metamorphic contrast does not require a difference in pressure-temperature conditions. Carbonate-clay-white mica assemblages are found elsewhere in the San Juan nappes and probably formed by excess CO_2 in the fluid phase (Brandon and others, 1988). Even so, Garver's interpretation of post-metamorphic deposition seems plausible, given the young age of the Obstruction. Further dating, especially apatite fission-track dating, would help to resolve the thermal history of the Obstruction.

If Garver's interpretation is correct, the Obstruction Formation would have been deposited on the San Juan nappes late in their thrust history, perhaps as a piggyback basin (a basin that forms on top of a moving thrust sheet). Conglomerates in the Obstruction contain clasts that may have been derived from the older nappes (chert, porphyritic dacite, metadiorite, bull quartz, and lawsonite-bearing meta-quartzite). Radiolarians from chert pebbles indicate a Lower Jurassic and possibly Middle Jurassic chert-rich source, with the Deadman Bay terrane a likely candidate (Garver, 1988a).

At Upright Head, the conglomerate clasts range up to 10 cm in diameter and are mainly chert with lesser mudstone, volcanic rock, and sandstone (Cowan and Whetten, 1977). In contrast to the Lopez Complex, the clasts are not noticeably flattened, and a cleavage is not present.

Field Stops on San Juan Island

Take the ferry to San Juan Island, which disembarks at Friday Harbor. Outcrops in the vicinity of Friday Harbor consist mainly of weathered massive sandstone of the Constitution Formation. The metamorphic assemblages in sandstones from this area include prehnite with minor lawsonite, whereas sandstones from the southern parts of Lopez and San Juan Islands include lawsonite without prehnite. This change is caused by a reaction which forms prehnite at the expense of lawsonite (Brandon and others, 1988).

To reach Stop 3-6, drive from the ferry terminal; follow the main street through the town of Friday Harbor. Leave town on San Juan Valley Road (Fig. 5). Follow the road as it turns left and becomes Douglas Road. This road makes another left and becomes Cattle Point Road. Follow Cattle Point Road into the park at the south end of the island. Turn right on Pickett's lane, which leads to a parking area at South Beach. Follow the dirt road to the right about 0.3 mi and park adjacent to the outcrops at the west end of the beach. The area of interest starts at these first outcrops (the most easterly outcrops in Fig. 8) and continues about 600 to 800 m to the west along the coast.

STOP 3-6: South Beach, San Juan Island—Exotic slices of Permian and Triassic metamorphic rock within the Rosario thrust zone.

The South Beach outcrops lie at the southwest end of the Rosario thrust zone, which extends offshore beyond this point. The thrust dips northeast here, placing massive sandstone of the Constitution Formation over a structurally complex assortment of mudstone, green volcanic rocks (locally pillowed), green tuff, and ribbon chert, which are collectively assigned to the Orcas Chert (Deadman Bay terrane; see Brandon and others, 1988). The best evidence for large thrust displacements across the fault is the presence of exotic slices of Garrison Schist (Vedder terrane) lying within the fault zone. The Garrison is a thoroughly recrystallized metamorphic rock that was metamorphosed under greenschist and amphibolite conditions during the Permian and Triassic, long before its tectonic emplacement along the Late Cretaceous Rosario thrust (Brandon and others, 1988).

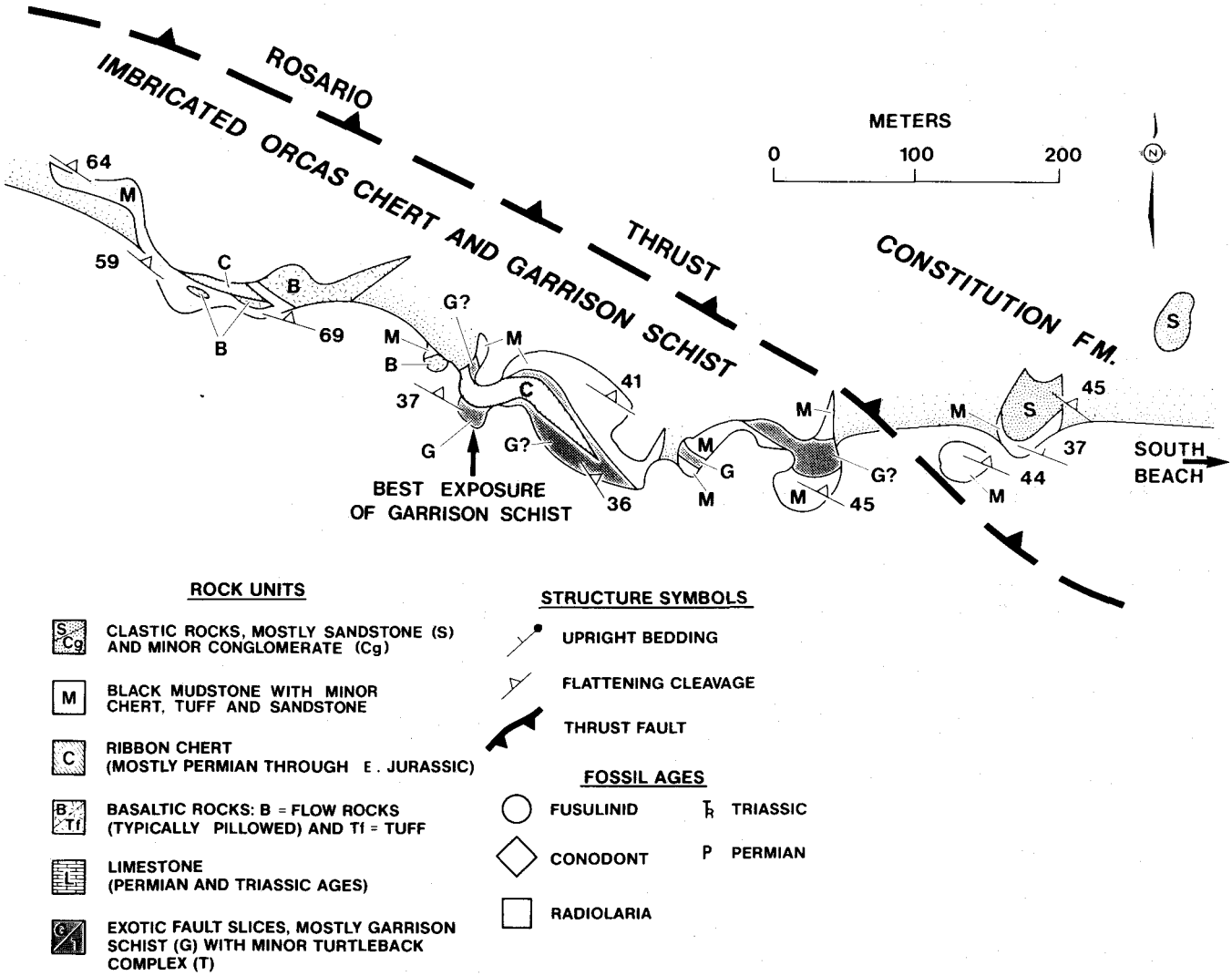

Figure 8. Outcrop map for Stop 3-6 showing the internal structure of the imbricate zone beneath the Rosario thrust at South Beach, southern San Juan Island (Brandon and others, 1988). Explanation is for both Figs. 8 and 9. Massive sandstone (S) and mudstone (M) of the Constitution Formation lie above the Rosario thrust. The area below the thrust consists of an imbricated fault zone containing ribbon chert (C) and pillow basalt (B) of the Orcas Chert, and small fault slices of Garrison Schist (G). The mudstone-rich unit (M) beneath the Rosario thrust is of uncertain affinity, and may belong to the Constitution or to the Orcas.

At the east side of the area shown in the map (Fig. 8), the first outcrops belong to the Constitution Formation (labeled "M" and "S" in Fig. 8) and consist of a northeast-dipping depositional sequence that includes a thin horizon of mudstone, green tuff, and ribbon chert, overlain by a thick massive sandstone unit. Of particular interest is the clear interbedding of clastic rocks with radiolarian-bearing ribbon chert.

Farther west along the coast is a highly imbricated sequence of Orcas Chert with exotic slices of Garrison Schist. These rocks lie beneath the Rosario thrust, which is the highest recognized thrust within this imbricated fault zone. Here, and elsewhere in the San Juan Islands, the slices of dark- to light-green Garrison Schist are localized in a 100- to 200-m-thick zone beneath the Rosario thrust. The Garrison in the South Beach area is a brecciated, fine-grained mafic schist consisting of chlorite + actinolite + epidote + plagioclase. Brecciation and cataclasis are attributed to tectonic emplacement of these fault slices. Structural relations are best exposed at the location indicated in Figure 8 where a large, tabular slice (2 x 6 x 6 m) of Garrison is surrounded by disrupted black mudstone, ribbon

chert, and minor unfoliated basalt of the Orcas Chert. Note the small imbricate fault zone developed beneath the south side of this Garrison slice. These exotic slices were emplaced into the Rosario fault zone prior to high-pressure regional metamorphism (lawsonite-prehnite-aragonite) as indicated by thin-section textures which show the cataclastic fabric of the schist cut by undeformed veins of aragonite.

Return to Cattle Point Road and drive north toward Friday Harbor. Turn west and connect with Bailer Hill Road, which becomes West Side Road where it meets the coast. Deadman Bay is a small cove located just south of where the road makes two sharp switchbacks (Fig. 9). Park on the short road off West Side Road just before the first switchback. Walk southwest to the coast.

STOP 3-7: Deadman Bay, San Juan Island—Tethyan-fusulinid limestones in the Deadman Bay Volcanics.

Deadman Bay is located at the southern end of a 4-km-long fault slice of Deadman Bay Volcanics (Table 1, Fig. 9). Gray and green ribbon chert exposed at the south side of the bay belongs to the Orcas Chert, which structurally overlies the Deadman Bay Volcanics along a northeast-dipping thrust fault. The trace of this fault follows the West Side Road to the north.

The Deadman Bay Volcanics are well exposed along the coast on the rocky headlands between the bay and the lighthouse to the north. The unit is dominated by red and green pillow basalt, breccia, and tuff with subordinate interbedded limestone. It is distrupted in many places by faults, but it generally has a persistent easterly strike and, in this area, a near-vertical dip. Geopetal structures indicate younging to the north. Limestones in the unit are massive and gray, and they contain small amounts of intercalated green tuff. Bedding, where present in the limestones, is typically contorted and appears to have been deformed by soft-sediment slumping. Carbonate material occurs interstitially in the pillowed flows and might have been sucked into the pillowed framework by rapidly convecting currents generated by the cooling submarine flows or by churning as the lavas flowed across carbonate accumulations. Some of the limestones were converted to aragonite marble during Late Cretaceous high-pressure metamorphism.

Crinoid debris and fragments of other fossils can be found in many limestone pods. A thin limestone bed, clearly interbedded in the pillow basalt sequence at Deadman Bay, has yielded late Early Permian (late? Leonardian) conodonts (conodont locality at south end of map in Fig. 9). Limestone in a nearby quarry has yielded early Late Permian (early Guadalupian) fusulinids (fusulinid localities at south end of map in Fig. 9). These fusulinids are Tethyan, which suggests that the Deadman Bay Volcanics are exotic to North America. Trace-element chemistry (high TiO_2 and light rare-earth element enrichment; Brandon and others, 1988) indicates that the volcanics were probably erupted in an "oceanic-island" setting.

To reach the last stop on this trip, continue north on West Side Road, and turn right onto Mitchell Bay Road, which ends in a T-intersection with Roche Valley Road. Turn left and follow this road to a narrow causeway about 1 mi north of the town of Roche Harbor. This causeway connects Davison Head with San Juan Island. Park on the causeway. The best exposures are on the west side of Davison Head. The description below is modified from Brandon and others (1988).

STOP 3-8: Davison Head, San Juan Island—Upper Triassic Haro Formation.

A 700-m-thick section of steeply dipping, Upper Triassic Haro Formation crops out in the area surrounding Davison Head and also extends along the coast south of the causeway for a short distance (Vance, 1975; Johnson, 1978). The unit is not found elsewhere in the San Juan Islands. The Haro consists of well-bedded siltstone, sandstone, tuff, conglomerate, and breccia, all of which contain abundant andesitic and dacitic volcanic detritus. The local presence of crystal tuff indicates volcanism was contemporaneous with deposition (Johnson, 1978). South of Davison Head, thin coquina beds contain *Halobia* indicating a Carnian or Norian age. Minor interbeds of siliceous shale at two localities have yielded radiolarians with ages similar to that of *Halobia* (Igo and others, 1984: Carnian to Norian for one locality, and Norian to Pliensbachian for the other).

The Haro Formation and the Upper Jurassic and Lower Cretaceous Spieden Group, which underlies Spieden Island to the north of Davison

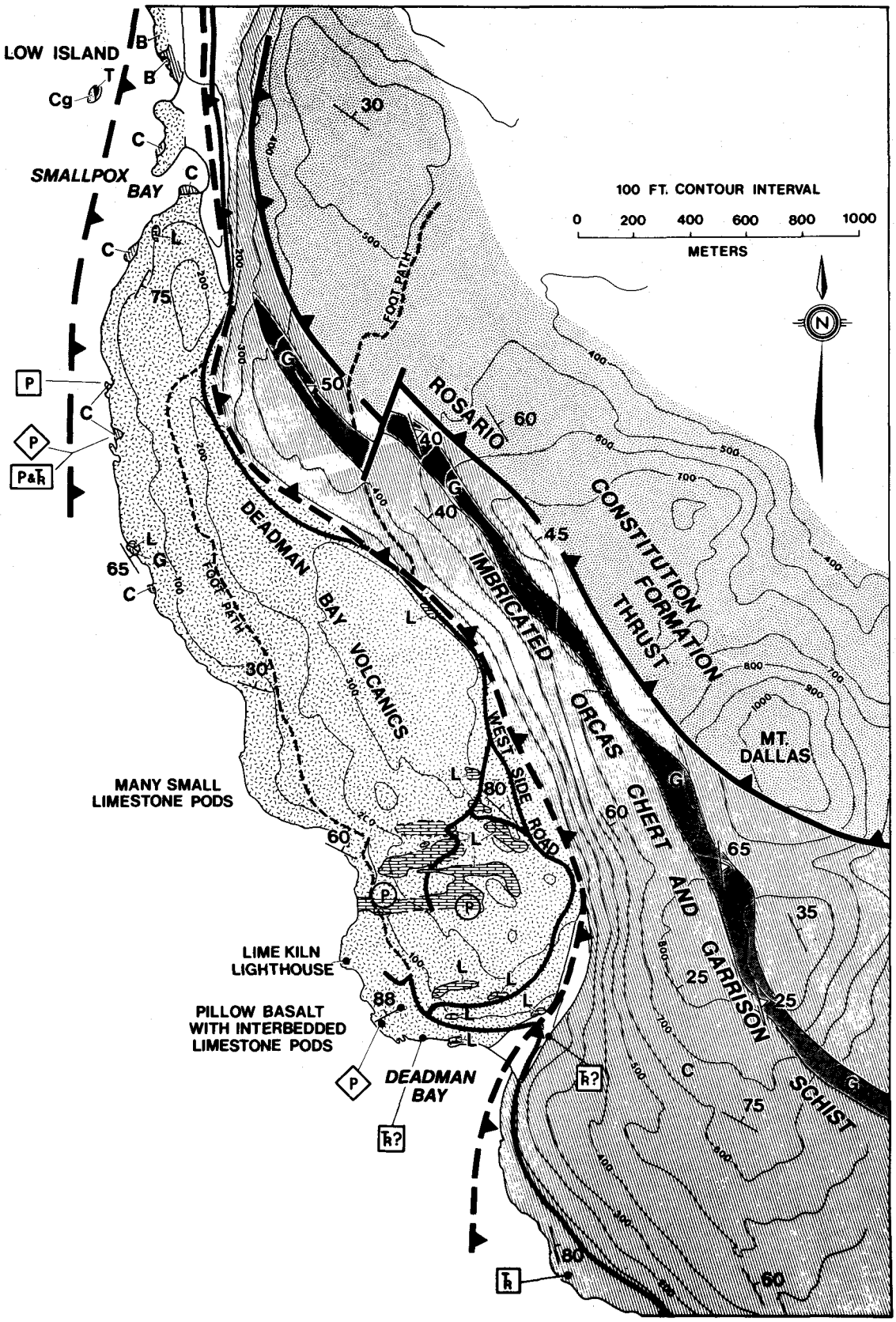

Figure 9. Geologic map for Stop 3-7 showing a large fault slice of Deadman Bay Volcanics on the west coast of San Juan Island. Map is from Brandon and others (1988); fossil localities are described there. See Figure 8 for explanation.

Head, are the only two pre-Late Cretaceous units in the San Juan Islands that have not been subjected to regional high-pressure metamorphism. Metamorphism of these two units is restricted to zeolite facies. For this reason, Brandon and others (1988) considered the Haro and Spieden to be external units within the San Juan-Cascade thrust system. Unlike many of the other thrust faults in the San Juan nappes, the Haro fault (Fig. 3), which separates the Haro Formation from nappes to the south, must postdate regional high-pressure metamorphism. Brandon and others (1988) argue that this fault is one of several post-metamorphic thrust faults bordering the northern and western perimeters of the San Juan nappes. It is suggested here that these faults represent the youngest thrusts of the San Juan-Cascade system. They are envisioned to have carried the already erosionally thinned nappes westward into the Nanaimo Basin and to have emplaced the nappes over rock units, such as the Haro and Spieden, which were never subjected to substantial structural burial. An implication of this interpretation is that the San Juan nappes have also overridden a substantial portion of the Nanaimo Basin and thus are underlain by Upper Cretaceous strata of the Nanaimo Group.

The Haro Formation appears to be unrelated to other nearby Upper Triassic units. It is clearly different from the chert-rich Deadman Bay terrane. Coeval units in the Wrangellia terrane of Vancouver Island consist of tholeiitic basalt overlain by limestone and shale (Karmutsen, Quatsino, and Parsons Bay Formations: Muller, 1977), with no evidence of intermediate or silicic volcanic rocks. One unit that may be correlative is the Upper Triassic and Jurassic Cultus Formation (Table 1, Fig. 2) of the Cascade Range, which belongs to the Chilliwack terrane. In its type area in southernmost British Columbia, the Cultus consists of volcaniclastic sandstone and siltstone (Monger, 1970) but lacks the coarse-grained pyroclastic sediments that characterize the Haro. However, the Cultus as mapped in the Mount Baker area (Brown and others, 1987) and the Harrison Lake area (Camp Cove Formation in Monger, 1970; Arthur, 1986) is dominated by volcanic flows and pyroclastic rocks with distinctive radiolarian siliceous argillites. Radiolarians and conodonts from siliceous argillites at Harrison Lake are Middle Triassic, indicating that these rocks are slightly older than the Haro. Nonetheless, the common occurrence of volcanogenic rocks and siliceous argillites suggests that the Haro may be related to the Cultus. This possibility warrants further study and comparison.

Geology of the Southern Priest River Complex and the Newport Fault

Brady P. Rhodes, Tekla A. Harms, and Donald W. Hyndman

Geology of the Southern Priest River Complex and the Newport Fault

Brady P. Rhodes
Department of Geological Sciences
California State University
Fullerton, CA 92634

Tekla A. Harms
Department of Geology
Amherst College
Amherst, MA 01002

and

Donald W. Hyndman
Department of Geology
University of Montana
Missoula, MT 59812

This paper consists of two parts. The first part describes the southern Priest River complex and was written by B. P. Rhodes and D. W. Hyndman. The second part discusses the Newport fault and was written by T. A. Harms. Together they set the stage for a field trip through northeastern Washington and northern Idaho.

SOUTHERN PRIEST RIVER COMPLEX

Introduction

A region of amphibolite-grade, predominantly pelitic and semipelitic metasedimentary rocks and associated granitic rocks defines the Priest River complex (PRC) of northern Idaho and northeastern Washington (Fig. 1). The protoliths of the metasedimentary rocks likely include both the sedimentary rocks of the Proterozoic Belt Supergroup and pre-Belt crystalline basement. The granitic rocks apparently range in age from Precambrian (Evans and Fischer, 1986) to Tertiary (Miller and Engels, 1975; M. E. Bickford, Univ. of Kansas, unpublished data); most are late Cretaceous to early Tertiary (Miller and Engels, 1985). A NNE-trending gently antiformal zone of mylonitization defines the Spokane dome (Fig. 2) (Cheney, 1980; Rhodes and Hyndman, 1984).

The PRC lies in a large region of unmetamorphosed to lower greenschist facies rocks of the Belt Supergroup and relatively shallow Mesozoic plutons. The Purcell Trench forms the sharp to gradational boundary of the complex to the east, whereas to the west the degree of metamorphism gradually increases to greenschist-grade Belt Supergroup rocks (Rhodes and Hyndman, 1984). To the south, the complex is covered by flows of the Miocene Columbia River basalt; scattered exposures of metamorphic rocks in windows through the basalt suggest this boundary may also represent gradational metamorphism. To the north, the spoon-shaped Newport fault block covers much of the northern part of the complex (Miller, 1971; Harms, 1982; Harms and Price, 1983). High-grade metamorphic rocks and granite form the footwall of the Newport fault on its eastern, western, and southern limbs.

The Spokane Dome Mylonitic Zone

In the southern part of the PRC the 4-km-thick Spokane dome mylonitic zone affected both the granitic rocks of the Mount Spokane granite and Newman Lake Gneiss, as well as paragneiss of the Hauser Lake Gneiss (Fig. 2) (Rhodes and Hyndman, 1984). The mylonitic foliation is broadly warped into a NNE-trending arch that plunges north and projects beneath nonmylonitic rocks in the northern part of the complex. The mylonitic zone probably extends well beneath the Newport fault and northeastern PRC. An east-west COCORP seismic line just north of Sandpoint shows a zone of subhorizontal reflectors beginning at a depth of about 5 km and extending to 9 km (Potter and others, 1986); this zone closely corresponds to the extrapolated position of the crest of the Spokane dome.

The southern part of the mylonitic zone is covered by alluvium in the Spokane River valley. South of the valley (Fig. 1) the zone re-emerges, dipping 20 to 30 degrees to the south. Approximately 3 to 5 km farther south the mylonitization fades structurally downward into Hauser Lake Gneiss that exhibits a steeply dipping crystal-

From: Joseph, N. L., and others, editors, 1989, Geologic guidebook for Washington and adjacent areas: Washington Division of Geology and Earth Resources Information Circular 86.

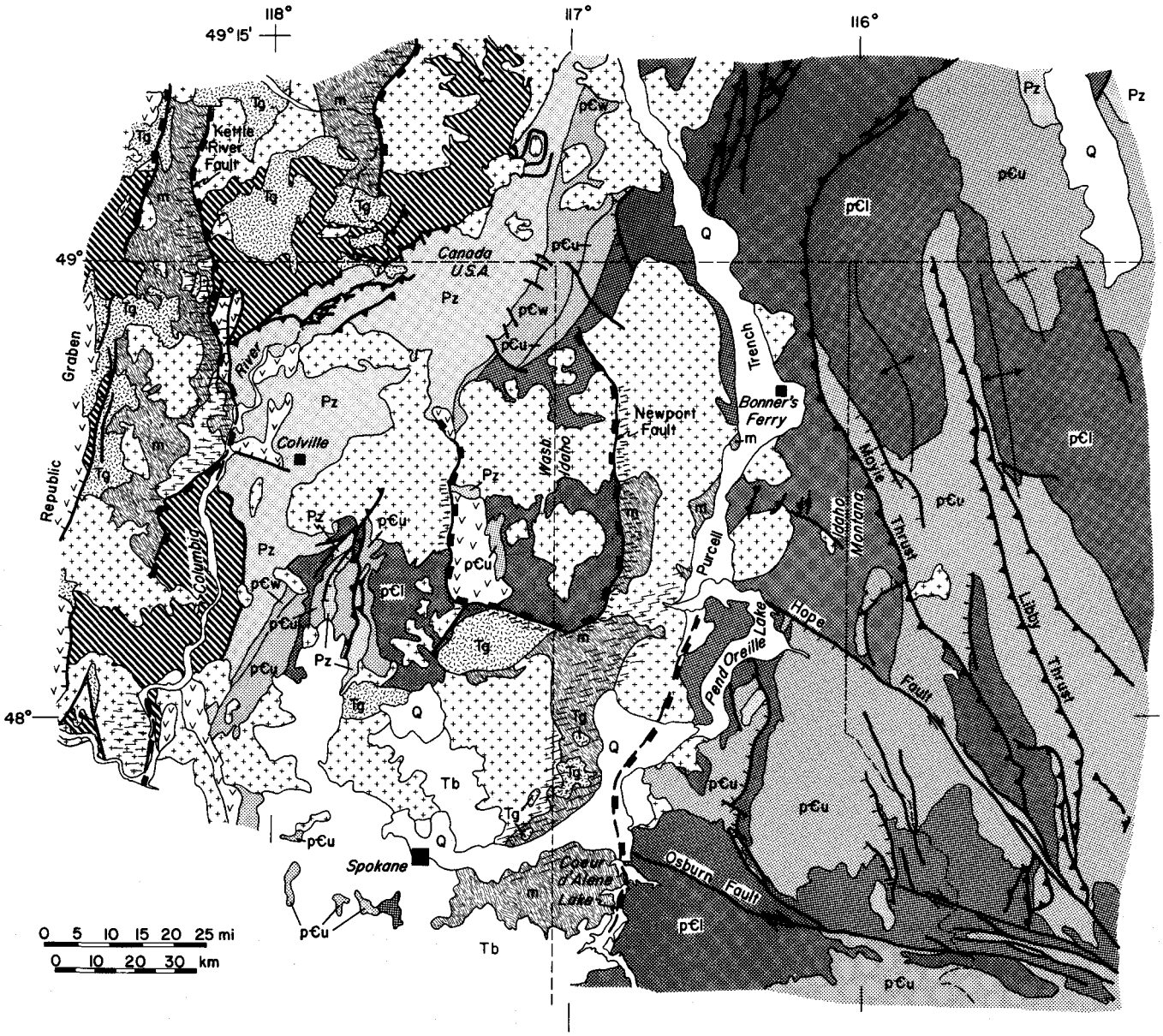

EXPLANATION

- Q — Quaternary surficial deposits
- Tb — Miocene basalt
- Eocene volcanic and sedimentary rocks
- Tg — Tertiary granitic rocks
- Cretaceous granitic rocks
- Pz — Lower Paleozoic miogeoclinal rocks
- eugeoclinal rocks of Quesnellia
- Windermere (pЄw) and upper Belt Supergroup (pЄu)
- pЄl — Lower Belt Supergroup
- m — metamorphic rocks
- mylonitic rocks
- contact
- thrust fault
- Low-angle normal fault
- High-angle normal fault
- Strike-slip fault
- High-angle fault with unknown slip
- anticline
- syncline

Figure 1. Geologic map of a part of northeastern Washington, northern Idaho, northwestern Montana, and southern British Columbia. See Rhodes and Hyndman (1988) for sources.

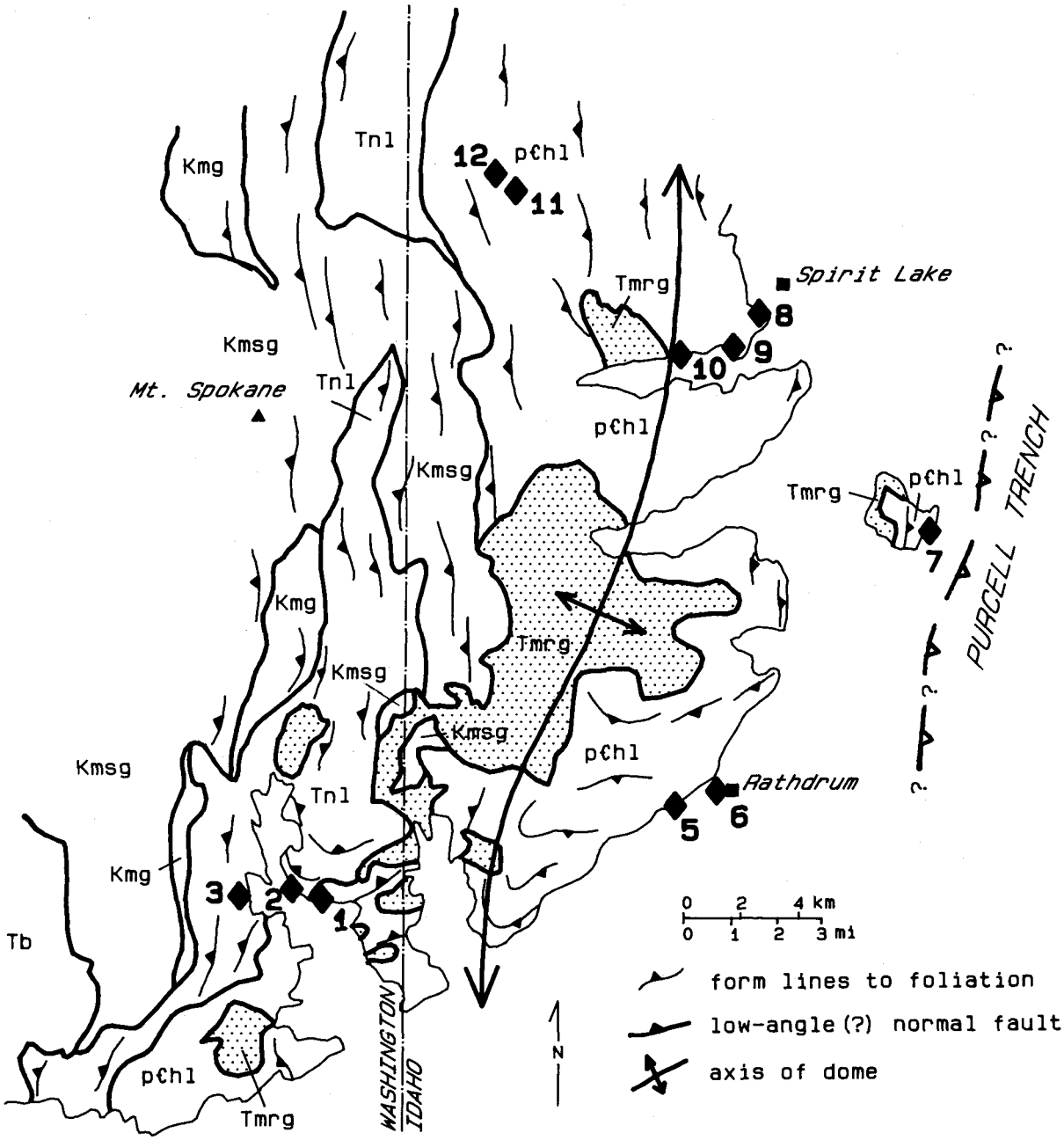

Figure 2. Geologic map of the southern part of the Priest River complex showing fieldtrip stops 1-3 and 5-12. p€hl, Hauser Lake Gneiss; Kmsg, Mount Spokane granite; Kmg, muscovite-megacryst-bearing granite; Tnl, Newman Lake Gneiss; Tmrg, Mount Rathdrum granite (shaded); Tb, Columbia River basalt. After Rhodes (1986) and Weissenborn and Weis (1976).

loblastic foliation that has no trace of mylonitization. On the western flank of the Spokane dome, the mylonitization grades structurally upward into the undeformed or weakly foliated Mount Spokane granite. Within the core of the dome, erosion has breached the mylonitic zone, exposing unmylonitized paragneiss with a steeply inclined crystalloblastic foliation that is progressively transposed upward into the gently east-dipping mylonitic foliation along a zone <100 m thick (Rhodes, 1986). The east flank of the dome dips into the Purcell Trench. The apparent thickness of the east limb is much less than 4 km; thus the east limb may be truncated by buried faults in the trench (Rhodes and Hyndman, 1984).

The mylonitic foliation contains a ubiquitous lineation, defined by slickenside-like striae or elongate mineral grains. Over most of the complex the lineation has a fairly consistent trend of approximately S70°W to N70°E with local variations of as much as 20 to 30 degrees in a single outcrop. Along the Purcell Trench the lineation gradually swings to a more nearly east-west

trend. This alone might suggest an overprinting along the Purcell Trench by a younger mylonitic event having a more nearly due-east slip line. However, this hypothesis is refuted by the gradational change in trend of the lineation and by the lack of discontinuities within the zone or direct cross-cutting relations between two distinct lineations. All the evidence suggests that the east-dipping mylonitic rocks adjacent to the Purcell Trench and the west-dipping mylonites on the west limb are part of a single zone that was regionally domed during uplift. Abundant S-C surfaces in the mylonitic rocks and other kinematic indicators are present in virtually all rock types and show clearly that movement along the zone was top-to-the-east on both the east and west limbs of the dome, suggesting that doming came after the major episode of slip on the mylonitic rocks (Rhodes and Hyndman, 1984).

The fine- to medium-grained Mount Rathdrum granite forms several small plutons that intrude the mylonitic rocks (Fig. 2). Most of the larger bodies of the Mount Rathdrum granite are undeformed or have a weak nonmylonitic foliation and(or) lineation (Weissenborn and Weis, 1976). However, many thin dikes, sills, and small masses both cut across the metamorphic foliation and exhibit an incipient mylonitic foliation and lineation that are parallel to the foliation and lineation in the surrounding rocks. Thus, we infer that the Mount Rathdrum granite is late synkinematic; the crystallization of the larger bodies outlasted mylonitization, but the smaller, faster cooling dikes and sills solidified before the last movement along the mylonitic zone. The age of the Mount Rathdrum granite is, therefore, critical to bracketing the age of mylonitization. Preliminary U-Pb geochronology suggests that the granite may be early Eocene (52 Ma) (Bickford and others, 1985); if true, then most of the mylonitization is early Eocene or older, with the last movement occurring as the granite crystallized.

Metamorphism

Two distinct metamorphic pulses can be recognized in the PRC. The earlier metamorphism occurred at pressures exceeding 5 kb, in the uppermost amphibolite facies, with sillimanite + K-feldspar being the most common assemblage and with kyanite + sillimanite locally preserved (Rhodes, 1986). Evidence of partial melting, such as numerous pegmatite pods and masses with mafic selvages, is locally apparent, and thus this metamorphism may be related to the generation and intrusion of large quantities of granite during the Mesozoic. A steeply inclined crystalloblastic foliation developed during the peak of this earlier metamorphism and lacks an accompanying penetrative lineation. Sillimanite grew parallel to this foliation but without a preferred linear orientation. This earlier foliation is preserved both beneath and above the Spokane dome mylonitic zone.

A second phase of metamorphism, which reached the middle-amphibolite facies, accompanied mylonitization and partially re-equilibrated the rocks. Reactions diagnostic of this younger event include the widespread growth of muscovite at the expense of sillimanite and K-feldspar, the exchange of Mg between garnet and biotite (leaving the garnet rims depleted in Mg), and locally developed andalusite replacing kyanite. At a few localities, all three Al_2SiO_5 polymorphs occur together within a single rock, with complex textural relations suggesting that kyanite and sillimanite are relict from the older metamorphism, and that andalusite and a subsequent second growth of sillimanite belong to the younger event. Geothermobarometry suggests that this second metamorphism, and hence mylonitization, occurred at <3.5 kb (Rhodes, 1986). Rocks outside the mylonitic zone commonly show no evidence of the younger event.

The Purcell Trench

The Purcell Trench extends from southern British Columbia to about 25 km south of Coeur d'Alene, Idaho. Over most of its length, the trench consists of a narrow (<10 km) topographic trough filled with Pleistocene glacial sediments and Holocene alluvium. High-grade metasedimentary rocks and granite predominate west of the trench, and essentially unmetamorphosed Belt rocks occur to the east. Recent reconnaissance and detailed studies (Rhodes, unpublished data) suggest that the trench probably does not contain a through-going structure along its entire length.

Within the United States the trench can be broken into three segments. The northern segment, from the Canadian border to just south of Bonners Ferry, is a linear valley that now contains the Kootenay River (Fig. 1). The west side of the valley consists of amphibolite-facies metasedimentary rocks that have a generally steeply dipping crystalloblastic foliation that locally strikes into the trench. Farther to the west, orthogneiss and granite intrude the metasedimentary rocks (Aadland and Bennett, 1979). The east side of the valley is underlain by unmetamorphosed Belt rocks intruded by undeformed granite. These granitic bodies apparently intruded at a much shallower depth than those to the west of the trench. No granite exposures are known within the trench. The linearity of the valley and the contrasting structural levels across the trench are consistent with a fault buried within the valley (Harrison and others, 1972). However, given the 8- to 10-km width of the unexposed interval, a more gradational boundary cannot be completely ruled out.

The central segment of the trench, extending from south of Bonners Ferry to just west of the southern tip of Pend Oreille Lake, is topographically indistinct. Just north of Pend Oreille Lake, outcrops of nonmylonitic metasedimentary rocks intruded by granite are nearly continuous across the extrapolated position of the trench. The metasedimentary rocks are gradually less metamorphosed to the east, grading from migmatitic gneisses into

muscovite-biotite schists, white-mica phyllites, cleaved argillite, and finally unmetamorphosed lower Belt argillites. A few miles west of Pend Oreille Lake, undeformed granite of unknown age continues across the trench in nearly continuous exposures. On the west side of the trench, small bodies of metasedimentary rock in the granite are of low grade, ranging from phyllite to slate. Here, the actual boundary of the PRC must lie west of the Purcell Trench, where it is masked by the abundant granite rocks. Although numerous small faults may exist among the scattered outcrops, no major structures can be located along this segment of the trench. Rather, the trench here may consist of a crustal-scale monocline, the Purcell Trench being located along the limb where the gradation from deep to shallow crustal levels is masked by abundant granitic rocks.

The southern segment of the trench, extending from the southern tip of Pend Oreille Lake to Coeur d'Alene Lake, consists of a much broader sediment-filled trough. Here, the western side of the trench is underlain by mylonitic rocks that dip into the trench. Widely scattered exposures of unmetamorphosed Belt rocks within the trench extend to within about 3 km of the mylonitic rocks. The mylonitic rocks are near the base of the 4-km-thick zone, and, given the gentle eastward dip, there is not sufficient space to accommodate the remaining thickness of the mylonitic zone in the trench to the west of the outcrops of Belt rocks. Thus either a fault lops off the upper part of the mylonitic zone, or the mylonitic zone thins abruptly from more than 4 km to less than 3 km.

Tectonic Setting of Mylonitization

The interpretation of the kinematics and timing of mylonitization within the PRC is the basis for inferences concerning the late Mesozoic and early Tertiary tectonic evolution of the northwestern Cordillera in the United States. For the reasons listed below, we believe that the mylonitic rocks of the Spokane dome developed during deep crustal shortening correlative with thrusting both to the east in the Northern Rocky Mountains (for example, Price, 1981) and to the west within the Kootenay Arc (for example, Miller and Clark, 1976; Ellis, 1986):

- The preliminary radiometric bracketing of the age of mylonitization suggests that most of the strain occurred prior to the emplacement of the 52-m.y.-old (?) Mount Rathdrum granite (M. E. Bickford, Univ. of Kansas, unpublished data) and that a significant portion of strain followed the late Cretaceous emplacement of the composite Mount Spokane granite; thus much of the mylonitization may have occurred during the late Cretaceous.
- The thickness of the Mount Spokane mylonitic zone is more compatible with thickening the crust during compression and stands in contrast to the much thinner Newport fault zone, which clearly developed during extensional strain.
- If the mylonitic zone developed as an east-dipping normal fault that was later domed, then the mylonites must re-surface to the west at some breakaway zone. No such zone has yet been recognized; instead, the Spokane dome mylonitic zone may link up with subhorizontal reflectors that appear on a COCORP seismic reflection traverse in eastern Washington that are also interpreted as thrust-related (Potter and others, 1986).
- No continuous zone of chloritic breccia that is characteristic of Tertiary low-angle normal-sense mylonitic zones throughout the Cordillera overlies the Spokane dome mylonitic zone. Thus this zone apparently was born, lived, and died as a mid-crustal shear zone, and its uplift to the upper levels of the crust came well after motion on the zone had ceased. Uplift of the PRC is dated by the widespread K-Ar cooling ages of 50 Ma (Miller and Engels, 1975).
- The Spokane dome mylonitic zone is cut locally by thin (<5 cm) west-dipping shears that clearly show a top-to-the-west sense of offset. We suggest that these shears developed synchronously with the Newport fault and record a distinctly younger stage of extension and uplift.

THE NEWPORT FAULT ZONE

Introduction

The Newport fault zone is a shallow-dipping, north-plunging, spoon-shaped fault across which a sedimentary suprastructure of Proterozoic Belt Supergroup, Paleozoic miogeoclinal, and Tertiary basin-fill strata are juxtaposed over a crystalline infrastructure of high-grade metamorphic and plutonic rocks, the Priest River complex. The fault zone has a distinctive U-shaped trace that results from its three-dimensional spoon shape: it dips extremely shallowly west along the eastern trace, east on the western side, and north along the southern side. The fault is continuous in the subsurface from the east to the west traces below the hanging wall. As a result, the Newport fault divides the region into two structurally and lithologically distinct terranes: (1) a hanging wall "flap" attached to the north where displacement across the fault diminishes and the fault traces terminate and (2) a footwall, which extends along the three sides of the U-shaped fault and is continuous beneath the hanging wall.

The hanging wall is composed predominantly of the Proterozoic Belt Supergroup, which has an estimated thickness of 9,100 m (Miller, 1974) and is affected by only chlorite-grade burial metamorphism. This is overlain by a thin (1,200 m) sequence of Paleozoic(?) shelf strata that is, in turn, unconformably overlain by flows of the Eocene Sanpoil Volcanics (50 Ma, according to Pear-

son and Obradovich, 1977) and by coarse clastic sediments of the alluvial-fluvial Tiger Formation. Lower Belt strata of the hanging wall are intruded by a number of granitic plutons. They are accompanied by relatively narrow contact metamorphic aureoles. These units of the hanging wall are characteristic of relatively high suprastructural levels of the crust.

In contrast, the footwall terrane of the Newport fault includes two basic components: Cretaceous peraluminous granitic batholiths intruding mostly undated medium- to high-grade schists and gneisses that may be Belt basement, metamorphosed Belt strata, or both. Along the southern trace of the Newport fault, the footwall domain includes the Silver Point Quartz Monzonite. This pluton is distinct from other footwall intrusive bodies in that it is biotite-hornblende-sphene-bearing and Eocene in age (48 Ma, according to Miller and Engels, 1975; Reynolds and others, 1981). Footwall units are characteristic of a mid-crustal level metamorphic and plutonic infrastructure. Rocks of the hanging wall have few counterparts in the footwall of the fault. Belt and Paleozoic(?) sequences homotaxial with those of the hanging wall occur beyond the footwall terrane, to the east of the Purcell Trench fault (Rehrig and Reynolds, 1981) in the area of Pend Oreille Lake (Harrison and Jobin, 1965) and in the west, near Chewelah, gradationally above metamorphosed Prichard Formation of the western footwall. Each of the hanging wall and footwall lithologies described above is in some place cut and truncated by the Newport fault zone.

Newport Fault Zone

The Newport fault is marked by a wide zone of both cataclastic and mylonitic fault rocks. There is a regular pattern of variation in fault rock texture across the fault zone. This pattern is consistent along the entire trace of the fault so that the fault zone can be divided into two parallel tabular subzones. Chlorite microbreccia forms a mappable layer 1 to 5 m thick everywhere at the top of the Newport fault zone. Detachment of the hanging wall strata occurs at the top of the microbreccia. The chlorite microbreccia is a cohesive, massive, extremely fine grained and homogeneous crush rock with no ordered fabric whatsoever. It is characterized by white feldspar clasts floating in a green siliceous and chloritic matrix. It stands in marked contrast to the underlying broad, diffuse zone of well foliated and lineated mylonites of the second subdomain of the fault zone. (Use of the term "mylonite" in this discussion is consistent with the definition of Sibson, 1977.) These mylonites are gradational downward over a distance ranging to 500 m into nonmylonitic rocks of the footwall terrane.

The overall mineral composition of Newport mylonites is remarkably uniform along the length of the fault. Quartz and potassium and plagioclase feldspars are the major constituents; biotite is a common accessory. This consistent composition can be attributed to its derivation from footwall plutonic and metamorphic protoliths that are all fundamentally quartzo-feldspathic. Various minor secondary minerals that occur locally within the mylonite zone can also be related to the composition of the protolith: for example, sphene and hornblende in mylonites developed adjacent to the Silver Point Quartz Monzonite, or sillimanite and muscovite in mylonites derived from high-grade schists.

Across the Newport fault zone, mylonites show a variety of textures and a range in development of fabric, which, due to the limited mineralogic composition of the protoliths, reflect differing amounts of strain. Seams of mylonite showing greater deformation anastamose throughout the mylonite zone, isolating lens-like masses of less deformed rock. However, on a map scale, there is a consistent progression in decreasing degree of mylonitization across the fault zone from intense ductile deformation adjacent to the chlorite microbreccia downward to normal crystalline and crystalloblastic textures of the protoliths in the footwall.

Newport fault mylonites are characteristically strongly foliated and lineated. In most Newport mylonites there occur both a penetrative flattening fabric (an "S-fabric"; Berthe and others, 1979) composed of strongly flattened or ribboned quartz grains and aligned mica basal cleavage, and a discontinuous, spaced shear fabric ("C-fabric") that sigmoidally offsets the S-fabric and along which there is a concentration of comminuted mica and feldspar. The ubiquitous mylonitic lineation is defined by preferred orientation of acicular minerals, parallelism of elongate quartz ribbons, and tails of crushed feldspar grains.

Three-point calculations based on outcrop distribution of the chloritized microbreccia show that over intervals of one to several kilometers the microbreccia forms essentially planar segments which together resolve into the single, continuous curviplanar surface of the fault. There is near-perfect parallelism between the orientation of the chlorite microbreccia subzone and the orientation of the foliation in immediately underlying mylonites. The microbreccia does not cross or cut the mylonite zone, although locally mylonite is overprinted by brecciation or other forms of brittle deformation. Mylonitic foliation conforms to the shape of the fault zone; it is west dipping on the east side, east dipping on the west side and north dipping along the southern trace. The mylonitic lineation lies within the local mylonitic foliation but otherwise has a consistent, regional WSW-ENE trend (azimuth 70°) throughout the fault zone. This orientation of the lineation is disturbingly similar, if not identical to that seen in the Spokane dome mylonites (Rhodes and Hyndman, 1984). The Newport fault zone mylonitic lineation marks the direction of maximum elongation during deformation.

Both chlorite microbreccia and mylonite subzones of the Newport fault cut the mid-Eocene Silver Point Quartz Monzonite in the footwall along the southern trace of the fault zone. Both fault rock types therefore postdate the pluton. Exposures within the body of the Silver Point Quartz Monzonite, as much as several kilometers from the Newport fault trace, commonly show a poorly developed primary igneous foliation and a lineation which is on average aligned with the mean fault zone mylonitic lineation. This suggests that the Silver Point Quartz Monzonite is late synkinematic; the regional stress accompanying displacement on the Newport fault occurred while the pluton was still sufficiently plastic to have acquired a primary fabric.

The tectonic fabric of Newport fault zone mylonites provide the basis for establishing the nature of offset along the fault (Harms, 1982; Harms and Price, 1983). The direction of shear during displacement on the fault is assumed to lie parallel to the prominent WSW-ENE mylonitic lineation. The sense of shear in that direction is determined from (1) the sense of asymmetry between the S- and C-fabrics (Ramsay and Graham, 1970; Burg and Laurent, 1978; Berthe and others, 1979; Ponce de Leon and Choukroune, 1980) and between recrystallized subgrains and large ribbon grains of quartz (Vauchez, 1980; Lister and Snoke, 1984), and (2) the shape asymmetry of porphyroclasts (Simpson and Schmid, 1983) analyzed in oriented thin sections of samples collected along the fault trace. All samples from the eastern and western north-south-trending traces of the fault show unequivocally that the hanging wall moved down with respect to the footwall, down and to the west along the eastern trace and down and to the east along the western trace. (Because the fault trace parallels the mylonitic lineation along the southern segment of the fault, the sense of displacement shown in mylonite samples from that segment is more complex. Those samples indicate predominantly penetrative attenuation with little absolute differential displacement of the hanging wall either north-south or east-west.) The microfabric of the Newport fault mylonites demonstrates that the Newport fault is a low-angle normal fault.

Polished and slickensided surfaces in the chlorite microbreccia of the Newport fault zone are consistent with extensional strain along the fault zone. These minor faults are not the surface of detachment of the hanging wall; they occur within the microbreccia subzone and commonly strike or dip opposite to the fault zone as a whole. However, slickensides show normal dip-slip displacement on these surfaces within the east and west segments of the Newport fault, and normal oblique-slip displacement along the southern trace. The offset within the microbreccia zone is thus kinematically compatible with that determined from Newport mylonites.

Sibson (1977) points out that the vertical distribution of cataclastic and mylonitic fault rocks within a fault zone is determined largely by quartz ductility, which is dependent on temperature and thus on depth. With significant dip-slip displacement, cataclasites and mylonites that form simultaneously at different depths will ultimately be juxtaposed by the displacement which created them. Mylonites will be brought up into the brittle regime and can become overprinted by brittle deformation as an inherent consequence of an episode of crustal-scale dip-slip displacement. The pattern of transition from fault rocks that formed under brittle conditions to fault rocks that formed under conditions of higher quartz ductility and greater depth thus records the sense of displacement on the fault as well as the initial vertical distribution of fault rock types. Along the entire trace of the Newport fault, chlorite microbreccia overlies mylonitic rocks that occur on the footwall side of the fault zone and are derived from footwall rocks, demonstrating that the microbreccia was dropped down into juxtaposition over the mylonites by normal fault displacement.

These consistent kinematic indicators, as well as the parallelism and contemporaneity of both the chlorite microbreccia and mylonite, support the conclusion that the Newport fault is normal in sense along all of its U-shaped trace and that it is the result of a single episode of crustal-scale extensional dip-slip faulting.

Low-Angle Normal Faulting and Extensional Tectonics

As the hanging wall of the Newport structure was displaced down inward-facing listric normal fault surfaces relative to the hanging wall, the eastern and western segments of the Newport fault footwall rocks must have moved out and upward relative to the hanging wall. The juxtaposition of deeper mid-crustal infrastructure in the footwall directly below supracrustal rocks of the hanging wall indicates significant dip-slip offset. The spoon shape and shallow dip of the Newport fault zone geometrically require that this vertical component of slip was accompanied by an equivalent horizontal component of relative displacement. The footwall now exposed east and west of the fault originally occupied a position beneath the hanging wall and was essentially pulled out from under it, resulting in tectonic denudation of the footwall infrastructure. This interpretation is consistent with the suggestion by Price (1979) that the Newport fault structure represents crustal-scale boudinage such as proposed by Davis (Davis and Coney, 1979) as a model for the distinctive structures and large exposures of infrastructure in and around metamorphic core complexes. By this hypothesis, under regional extension the crustal infrastructure necks by concentrated penetrative flow, while the interiors of adjacent crustal boudins remain relatively untectonized. The more brittle suprastructure extends concurrently by slip on discrete listric normal faults and is displaced into the neck zone along surfaces of ductile shear, which are the deeper extensions of the

listric faults. Thus, in the Newport structure, the eastern and western infrastructural culminations are two north-south-trending crustal-scale boudins produced in response to WSW-ENE-directed extension indicated by the Newport mylonitic lineation (Fig. 3). The Silver Point Quartz Monzonite was intruded into the dilatant zone in the extending neck below and south of the U-shaped fault. Displacement on the Newport fault is a consequence of compensation in the suprastructure for extensional boudinage in the infrastructure. There is a progressive northward reduction in tectonic denudation and in exposure of deeper infrastructure along the Newport fault trace; suprastructural extension along the Newport fault ends at its two northern terminations, analogous to closure at the tip of a tension gash. The hanging wall is a flap of rent upper crust that is attached at the north end but detached to the south above an extending base.

The strength of this hypothesis lies in the variety of geologic features in the Newport area for which it accounts:

(1) In three dimensions the Newport fault, as represented by the chlorite microbreccia zone, has a curved, spoon-like shape. At the present level of exposure along most of its trace, the fault dips beneath the hanging wall at 25 to 30 degrees. At least locally, however, the fault is constrained to have been more steeply dipping at higher structural levels by the present topography of the footwall rocks immediately beyond the fault. The fault flattens to near horizontal in places and can be projected at a negligible dip under the hanging wall. Together, these attitudes show that the Newport fault is a listric fault. Belt and lower Paleozoic strata in the hanging wall lie in a broad north-trending anticlinal warp. Along both the east and west traces of the fault, beds of the hanging wall dip down to intersect the fault surface at a consistent angle of 60 degrees. Displacement on a listric fault that cuts horizontal strata at the surface at the ideal theoretical angle of 60 degrees results in a progressive rotation of hanging-wall beds but a preservation of the original 60 degree angle of intersection between bedding and the fault surface. The observed concave fault surface shape and 60 degree angle of intersection between fault and hanging-wall bedding in the Newport structure are consistent with an interpretation of the Newport fault as the shallow dipping to horizontal sole of a listric normal fault. The broad anticlinal warp of Belt strata in the hanging wall results from symmetric rotation of beds along each of the east and west, parallel, inward-facing listric segments of the Newport fault.

(2) The nonmarine, coarse clastic Tiger Formation (Gager, 1984) and the underlying Sanpoil volcanic flows, both Eocene in age, are restricted to a basin in the western hanging wall of the Newport fault. They occur as a west-dipping homocline, overlying the Belt and Paleozoic strata to the east with angular unconformity. The Tiger Formation has a similar trend to, but a shallower westerly dip than the underlying Belt and Paleozoic rocks. Ideally, with listric normal faulting, older strata undergo fault-related rotation initiating development of an associated basin. Subsequently, basin-fill deposits are tilted as they accumulate, but undergo progressively less net rotation. The configuration of the Tiger Formation and Sanpoil Volcanics suggests they are just such syntectonic basin-fill deposits. The distinctive listric spoon shape of the Newport fault is thus an integral factor in the formation of hanging wall structures and deposits (Fig. 3).

(3) Units in the hanging wall of the Newport fault are part of a distinctive stratigraphic sequence comprising Proterozoic rocks of the Belt Supergroup overlain directly by a poorly dated continental margin sequence of Paleozoic rocks. It is similar to homotaxial sequences to the east beyond the eastern footwall and to the west in the Chewelah

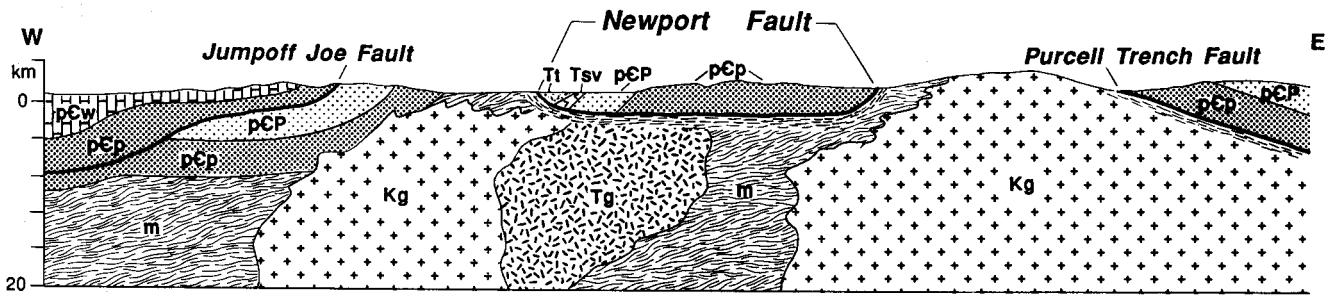

Figure 3. Generalized geologic cross-section across the Newport fault zone and related structures at approximately 48°50′ latitude. Horizontal and vertical scales equal. Short dash pattern shows zone of mylonitization; m, metamorphic rocks of uncertain age; pЄp, lower Belt Supergroup (Prichard Formation); pЄP, upper Belt Supergroup and Paleozoic strata; pЄw, Windermere-equivalent (Deer Trail Group); Kg, Cretaceous granite; Tg, Tertiary granite (Silver Point Quartz Monzonite); Tsv, Sanpoil Volcanics; Tt, Tiger Formation. After Harms (1982).

area below the Jumpoff Joe thrust fault. It is distinct from the sequence in the thrust panel above the Jumpoff Joe fault which, along with the Belt Supergroup, includes Windermere-equivalent strata and a thicker, deeper water Paleozoic facies. The hanging wall of the Newport fault cannot be the eastward extension of the Jumpoff Joe thrust sheet. The hanging wall occupies its pre-Newport-fault relative position with respect to, but has been separated from initially continuous homotaxial sequences to the east and west by the denudation and upward and outward movement of the footwall "boudins".

(4) Miller and Engels (1975) have reported a large set of mineral pair K-Ar ages from the crystalline infrastructure of the Newport footwall. "Chrontours" on these apparent ages parallel the Newport fault and cross individual plutons. They show a domain of concordant 45 to 50 Ma dates nearest to the trace of the fault and a domain of concordant 90 to 100 Ma dates both east of the Purcell Trench and 25 to 35 km west of the western fault trace (as well as in the plutons of the hanging wall). A domain of discordant ages that range from 50 to 100 Ma is gradational between the 45 to 50 Ma domain and the flanking 90 to 100 Ma domains. Harms and Price (1983) interpret this distribution (and supplementary age data presented by Archibald and others, 1983) as representing secular cooling of mid-Cretaceous batholiths in which concordant mid-Cretaceous ages record the rapid quenching of magmas intruded into cold country rocks and discordant 50 to 100 Ma ages record slow secular cooling in the deeper crustal levels of the same batholiths. Concordant ages ranging from 45 to 50 Ma, which occur closest to the Newport fault, result from abrupt quenching due to tectonic denudation of the initially deepest, hot crustal infrastructure during east-west crustal extension and low-angle normal faulting on the Newport fault zone.

Age of Newport Fault Displacement

The time of regional extension and low-angle normal faulting along the Newport fault can be closely constrained by the ages and structural relations of various units in the Newport area. The Silver Point Quartz Monzonite occurs in what was the extending neck zone of the Newport infrastructure. Both mylonite and chlorite microbreccia of the Newport fault cut the 48 Ma Silver Point Quartz Monzonite, which elsewhere bears a weak primary igneous fabric paralleling the mylonitic fabric. Therefore, the Silver Point Quartz Monzonite is considered to be late synkinematic. The 50 Ma Sanpoil Volcanics, rhyodacitic in composition (Miller, 1974), may be the extrusive equivalent of the Silver Point Quartz Monzonite. Immediately overlying Tiger Formation strata have yielded lower to middle Eocene pollen (A. P. Audretch, unpublished data, cited *in* Harms, 1982). Together, the Sanpoil Volcanics and Tiger Formation represent syntectonic, hanging-wall basin-fill deposits. Finally, concordant 45 to 50 Ma K-Ar quenching ages in plutonic rocks of the Newport fault infrastructure constrain the timing of footwall denudation. All available data indicate a 50 to 48 Ma age of displacement on the Newport fault. Movement on the fault was neither prolonged nor episodic. Both cataclastic and mylonitic fault rocks of the Newport fault zone developed in this brief period, and both must be the result of one extensional event.

ACKNOWLEDGMENTS

This research was supported in part by National Science Foundation Grant EAR83-07690 to D. W. Hyndman. B. P. Rhodes makes acknowledgment to the Donors of the Petroleum Research Fund, administered by the American Chemical Society, for partial support of his research. We thank Fred Miller, Dave Alt, John Cooper, and Stephanie Zurenko Waggoner for thorough and very helpful reviews of this paper.

REFERENCES CITED

Aadland, R. K., Bennett, E. H.; and others, compilers, 1979, Geologic map of the Sandpoint quadrangle, Idaho and Washington: Idaho Bureau of Mines and Geology Geologic Map Series, 1 sheet, scale 1:250,000.

Archibald, D. A.; Glover, J. K.; Price, R. A.; Farrar, E.; Carmichael, D. M., 1983, Geochronology and tectonic implications of magmatism and metamorphism, southern Kootenay Arc and neighbouring regions, southeastern British Columbia; Part I – Jurassic to mid-Cretaceous: Canadian Journal of Earth Sciences, v. 20, no. 12, p. 1891-1913.

Berthe, D.; Choukroune, P.; Jegouzo, P., 1979, Orthogneiss mylonite and non-coaxial deformation of granites–The example of the South Armorican Shear Zone: Journal of Structural Geology, v. 1, no. 1, p. 31-42.

Bickford, M. E.; Rhodes, B. P.; Hyndman, D. W., 1985, Age of mylonitization in the southern Priest River Complex, northern Idaho and northeastern Washington [abstract]: Geological Society of America Abstracts with Programs, v. 17, no. 6, p. 341-342.

Burg, J. P.; Laurent, P., 1978, Strain analysis of a shear zone in a granodiorite: Tectonophysics, v. 47, no. 1-2, p. 15-42.

Cheney, E. S., 1980, The Kettle dome and related structures in northeastern Washington. *In* Crittenden, M. D., Jr.; Coney, P. J., Davis, G. H., editors, Cordilleran Metamorphic Core Complexes: Geological Society of America Memoir 153, p. 463-484.

Davis, G. H.; Coney, P. J., 1979, Geologic development of the Cordilleran metamorphic core complexes: Geology, v. 7, no. 3, p. 120-124.

Ellis, M. A., 1986, Structural morphology and associated strain in the central Cordillera (British Columbia and Washington)–Evidence of oblique tectonics: Geology, v. 14, no. 8, p. 647-650.

Evans, K. V., and Fischer, L. B., 1986, U-Pb geochronology of two augen gneiss terranes, Idaho–New data and tectonic implications: Canadian Journal of Earth Sciences, v. 23, no. 12, p. 1919-1927.

Gager, B. R., 1984, The Tiger Formation–Paleocene fluvial sediments deposited adjacent to a deforming Cordilleran core complex, northeastern Washington: Sedimentary Geology, v. 38, no. 1/4, p. 393-420.

Harms, T. A., 1982, The Newport fault–Low-angle normal faulting and Eocene extension, northeast Washington and northwest Idaho: Queen's University Master of Science thesis [Kingston, Ontario], 157 p.

Harms, T. A.; Price, R. A., 1983, The Newport fault–Eocene crustal stretching, necking and listric normal faulting in NE Washington and NW Idaho [abstract]: Geological Society of America Abstracts with Programs, v. 15, no. 5, p. 309.

Harrison, J. E.; Jobin, D. A., 1965, Geologic map of the Packsaddle Mtn. quadrangle, Idaho: U.S. Geological Survey Geologic Quadrangle Map GQ-375, 1 sheet, scale 1:62,500, with 4 p. text.

Harrison, J. E.; Kleinkopf, M. D.; Obradovich, J. D., 1972, Tectonic events at the intersection between the Hope fault and the Purcell Trench, northern Idaho: U.S. Geological Survey Professional Paper 719, 24 p., 1 pl.

Lister, G. S.; Snoke, A. W., 1984, S-C mylonites: Journal of Structural Geology, v. 6, no. 6, p. 617-638.

Miller, F. K., 1971, The Newport fault and associated mylonites, northeastern Washington: U.S. Geological Survey Professional Paper 750-D, p. D77-D79.

Miller, F. K., 1974, Preliminary geologic map of the Newport Number 1 quadrangle, Pend Oreille County, Washington and Bonner County, Idaho: Washington Division of Geology and Earth Resources Geologic Map GM-7, 6 p., 1 pl., scale 1:62,500.

Miller, F. K.; Clark, L. D., 1975, Geology of the Chewelah-Loon Lake area, Stevens and Spokane Counties, Washington: U.S. Geological Survey Professional Paper 806, 76 p., 2 pl., scale 1:62,500.

Miller, F. K.; Engels, J. C., 1975, Distribution and trends of discordant ages of the plutonic rocks of northeastern Washington and northern Idaho: Geological Society of America Bulletin, v. 86, no. 4, p. 517-528.

Pearson, R. C.; Obradovich, J. D., 1977, Eocene rocks in northeast Washington–Radiometric ages and correlation: U.S. Geological Survey Bulletin 1433, 41 p., 1 pl.

Ponce de Leon, M. I.; Choukroune, P., 1980, Shear zones in the Iberian Arc: Journal of Structural Geology, v. 2, no. 1/2, p. 63-68.

Potter, C. J.; Sanford, W. E.; Yoos, T. R.; Prussen, E. I.; Keach, R. W.; Oliver, J. E.; Kaufman, Sidney.; Brown, L. D., 1986, COCORP deep seismic reflection traverse of the interior of the North American Cordillera, Washington and Idaho–Implications for orogenic evolution: Tectonics, v. 5, no. 7, p. 1007-1026.

Price, R. A., 1979, Intracontinental ductile crustal spreading linking the Fraser River and northern Rocky Mountain Trench transform fault zones, south-central British Columbia and northeast Washington [abstract]: Geological Society of America Abstracts with Programs, v. 11, no. 7, p. 499.

Price, R. A., 1981, The Cordilleran foreland thrust and fold belt in the southern Canadian Rocky Mountains. *In* MacClay, K. R.; Price, N. J., editors, Thrust and Nappe Tectonics: Geological Society of London Special Publication 9, p. 427-448.

Ramsay, J. G.; Graham, R. H., 1970, Strain variation in shear belts: Canadian Journal of Earth Sciences, v. 7, p. 786-813.

Rehrig, W. A.; Reynolds, S. J., 1981, Eocene metamorphic core complex tectonics near the Lewis and Clark Zone, western Montana and northern Idaho [abstract]: Geological Society of America Abstracts with Programs, v. 13, no. 2, p. 102.

Reynolds, S. J.; Rehrig, W. A.; Armstrong, R. L., 1981, Reconnaissance Rb-Sr geochronology and tectonic evolution of the Priest River crystalline complex of northern Idaho and northeastern Washington [abstract]: Geological Society of America Abstracts with Programs, v. 13, no. 2, p. 103.

Rhodes, B. P., 1986, Metamorphism of the Spokane dome mylonitic zone, Priest River Complex–Constraints on the tectonic evolution of northeastern Washington and northern Idaho: Journal of Geology, v. 94. no. 4, p. 539-556.

Rhodes, B. P.; Hyndman, D. H., 1984, Kinematics of mylonites in the Priest River "metamorphic core complex", northern Idaho and northeastern Washington: Canadian Journal of Earth Sciences, v. 21, no. 10, p. 1161-1170.

Rhodes, B. P.; Hyndman, D. W., 1988, Regional metamorphism, structure, and tectonics of northeastern Washington and northern Idaho. *In* Ernst, W. G., editor, Metamorphism and Crustal Evolution of the Western United States: Prentice Hall, p. 271-295.

Schroeder, M. C., 1952, Geology of the Bead Lake district, Pend Oreille County, Washington: Washington Division of Mines and Geology Bulletin 40, 57 p., 1 pl.

Sibson, R. H., 1977, Fault rocks and fault mechanisms: Geological Society of London Journal, v. 133, part 3, p. 191-213.

Simpson, Carol; Schmid, S. M., 1983, An evaluation of criteria to deduce the sense of movement in sheared rocks: Geological Society of America Bulletin, v. 94, no. 11, p. 1281-1288.

Vauchez, A., 1980, Ribbon texture and deformation mechanisms of quartz in a mylonitized granite of Great Kabylia (Algeria): Tectonophysics, v. 67, no. 1-2, p. 1-12.

Weissenborn, A. E.; Weis, P. L., 1976, Geologic map of the Mount Spokane quadrangle, Spokane County, Washington, and Kootenai and Bonner Counties, Idaho: U.S. Geological Survey Geologic Quadrangle Map GQ-1336, 1 sheet, scale 1:62,500.

Road Log

This road log describes a two-day trip that departs from Spokane and finishes along U.S. Route 2 (U.S. 2), just west of Sandpoint, Idaho. The route of the field trip is shown on Figure 4. The authors divided the responsibility for this log as follows: Stops 1 through 12, B. P. Rhodes; Stops 13 through 19, T. A. Harms; and Stops 20 and 21, D. W. Hyndman. Any inferences or interpretations in the road log are the views of the author for that stop; the other authors may or may not agree!

In the road log, cumulative mileage is given at the left, the interval mileage in parentheses.

Day 1: Southern Priest River Complex and Newport fault.

0.0 (0.0) *Set odometers.* Begin field trip at the traffic light at the end of the eastbound exit ramp off Interstate Highway 90 (I-90) exit 289. From downtown Spokane, take I-90 east to the Pines Road/Opportunity exit (exit 289). Turn left on Pines Road.

0.1 (0.1) Continue straight through two stop lights.

0.4 (0.3) The road climbs a hill, passing grayish drab outcrops of Newman Lake Gneiss.

1.1 (0.7) Pines Road dead ends into Trent Road at a traffic light. Turn right on Trent Road.

1.4 (0.3) Bridge over the Spokane River.

2.2 (0.8) Intersection with Evergreen Road. Continue straight on Trent Road.

3.0 (0.8) Sullivan Road exit. Continue straight on Trent Road.

5.0 (2.0) Road passes a large roadcut in Hauser Lake Gneiss.

Here the exposure consists of gently inclined, lineated sillimanite-biotite-feldspar-quartz gneiss and schist, pegmatite, and several layers of amphibolite, including a garnetiferous amphibolite near the west end of the cut. *Note: this road is heavily travelled, and this is not a good place to stop.*

5.1 (0.1) From the *right lane*, continue straight toward Rathdrum, Idaho, on Washington State Route (SR) 290.

5.9 (0.8) Low hills and outcrops to the north are gently west-dipping Hauser Lake Gneiss.

7.1 (1.2) Small roadcut of sphene-bearing amphibolite gneiss, which is part of the Newman Lake Gneiss.

9.4 (2.3) Turn left toward Newman Lake on Starr Road, just before Conoco gas station.

10.0 (0.6) Junction with Lincoln Road. Continue straight on Starr Road.

10.4 (0.4) Junction with Morris Road. Continue straight on Starr Road.

11.5 (1.1) Junction with West Newman Lake Road. Continue straight on Starr Road.

13.0 (1.5) **STOP 1. Hauser Lake Gneiss.**

Stop at the Y-junction (Hauser Lake Road to the right and Newman Lake Drive to the left). Park in the gravel area at the junction and walk 50 yd east to the roadcut (behind two pine trees) on the north side of Newman Lake Drive. The roadcut extends to the west up a private drive. Please do not go beyond the gate on the driveway.

The Hauser Lake Gneiss consists of spectacularly lineated, sillimanite-bearing mylonitic biotitic gneiss. Sillimanite defines the strong lineation. Close examination shows that, when viewed down the lineation, the foliation is not as strong and is locally folded, with the fold axes parallel to the lineation.

At the west end of the cut, at the base of the driveway, a dike of fine-grained, whitish Mount Rathdrum granite cuts across the foliation in the Hauser Lake Gneiss at a low angle. The granite is lineated and contains a well developed S-C fabric, which is best viewed by hand lens on a surface parallel to the lineation. The S-C fabric in this and other similar dikes shows a consistent top-to-the-east sense of flow.

Note that the lineated C-surfaces in the dike are parallel to the main foliation in the surrounding metasedimentary rocks and that the lineation in the dike parallels the sillimanite lineation in the enclosing rock. Yet, the border of the dike distinctly cuts across the foliation in the

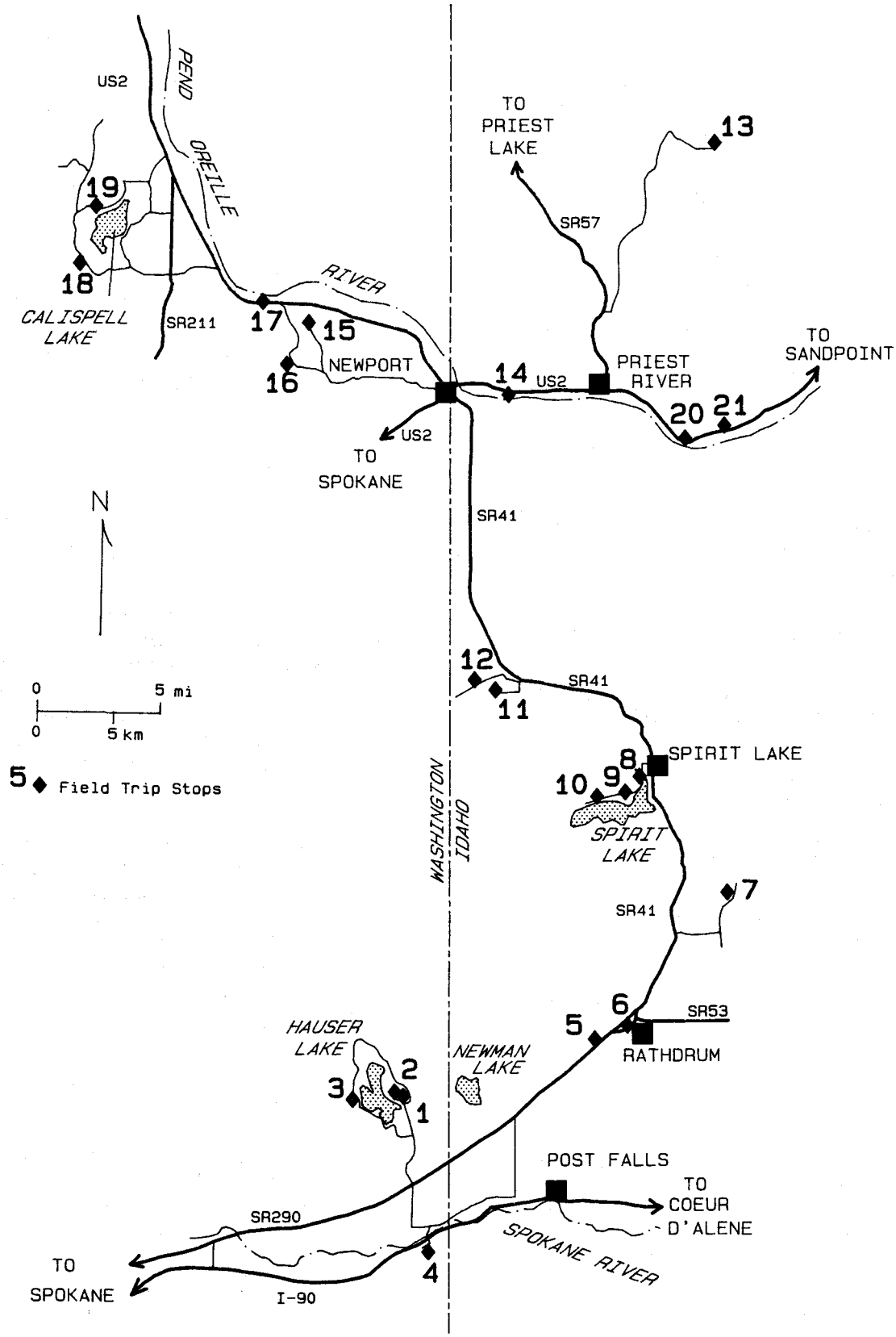

Figure 4. Fieldtrip route.

metasedimentary rocks. These relations are interpreted as evidence that the dike intruded during the mylonitization and that, as deformation continued following the solidification of the dike, the dike deformed with the surrounding rock with little if any ductility contrast.

To continue on to optional Stop 2, drive west on Newman Lake Drive for 0.7 mi. To skip Stop 2, turn around and drive back south on Starr Road.

STOP 2. Newman Lake Gneiss.

Park on the left side of the road near the roadcut. Be sure to leave driveways clear.

We have just crossed the contact between the Hauser Lake Gneiss and Newman Lake Gneiss. The contact itself is nowhere exposed. This exposure of the Newman Lake Gneiss is strongly lineated and lacks the sub-euhedral K-feldspar megacrysts typical of the Newman Lake elsewhere. This exposure may be part of a border zone, adjacent to an originally intrusive contact with the Hauser Lake, that was later smeared out into parallelism with the foliation during mylonitization. The gneiss here is also more strongly deformed than is typical of the Newman Lake; perhaps a large degree of deformation was concentrated along the contact with the Hauser Lake Gneiss.

Return to the vehicles, make a U-turn, and drive back toward Stop 1. Turn right onto Starr Road, where road log continues.

14.5 (1.5) Turn right on West Newman Lake Drive.

16.1 (1.6) Junction with Honeymoon Bay Drive. Bear left, staying on West Newman Lake Drive.

16.2 (0.1) Junction with Lakeview Drive. Continue straight on West Newman Lake Drive.

17.1 (0.9) Sutton Bay Resort. Bear left, staying on West Newman Lake Drive.

17.4 (0.3) Large roadcut of sillimanite-bearing Hauser Lake Gneiss.

17.7 (0.3) Crossing unexposed contact between Hauser Lake Gneiss and Newman Lake Gneiss.

18.4 (0.7) **STOP 3. Dike in Newman Lake Gneiss.**

Park in the wide gravel area across from the small roadcut around the sharp left bend in the road.

Here the Newman Lake Gneiss is cut by a dike of the Mount Rathdrum granite, which itself is deformed by top-to-the-east shearing. Thin pegmatitic bands parallel the mylonitic foliation in the Newman Lake Gneiss. One of these bands is cut by a 1- to 2-cm-thick ultramylonitic shear band that dips gently to the west and clearly offsets the pegmatitic band in a top-to-the-west sense. Late, top-to-the-west, west-dipping ultramylonitic shear zones are rare, but all cut across the mylonitic foliation. We believe the ultramylonitic shears are related to the Eocene extensional event, perhaps the same event that formed the Newport fault.

Return to the vehicles. Make a U-turn, and drive south.

20.7 (2.3) Junction with Honeymoon Bay Drive. Continue straight on West Newman Lake Drive.

22.3 (1.6) Stop sign. Turn right on Starr Road.

24.4 (2.1) Junction with SR 290. Continue straight through the intersection, staying on Starr Road.

26.0 (1.6) Stop sign just beyond railroad tracks; junction with Wellesley Road. Turn left.

27.2 (1.2) Turn right on State Line Road at the green sign pointing to the weigh station/port of entry.

27.4 (0.2) Bridge over the Spokane River.

27.7 (0.3) Stop sign. Turn left and pass under I-90.

28.0 (0.3) Turn right on Appleway Avenue.

28.2 (0.2) Large cut of high-grade metasedimentary rocks on the left.

28.6 (0.4) **STOP 4. Folded schist and gneiss.**

Park on the shoulder as close to the guard rail as possible and examine cuts on both sides of the road.

The exposed rock is sillimanite-bearing biotitic schist and gneiss, which correlates with the Hauser Lake Gneiss on the north side of the Spokane Valley. Metasedimentary rocks similar to these make up most of the hills immediately south of the valley.

The rock here has a complexly folded crystalloblastic foliation. Note the numerous, gently south dipping, lineated, nonpenetrative mylonitic foliation planes. These surfaces probably record the same mylonitic event that is much more penetrative on the north side of the valley. It is thought that the mylonitic deformation may be warped into a synform beneath the Spokane Valley, with this roadcut in part of the south limb. Furthermore, the mylonitic deformation fades out at structurally deeper levels. The rocks seen here may be near the base of the mylonitic zone, where the mylonitization has partially transposed an earlier crystalloblastic foliation. South of here (south end of Liberty Lake), the rock is dominated by a steeply dipping crystalloblastic foliation that is not cut by younger structures of the mylonitic event.

This is a good exposure at which to think about the processes involved during the transposition of the earlier foliation.

Return to the vehicles and continue to drive west on Appleway Avenue.

29.0 (0.4) Make a U-turn at this intersection and drive back east on Appleway Avenue.

30.2 (1.2) Stop sign. Turn left and pass beneath I-90.

30.7 (0.5) Bridge over the Spokane River.

30.9 (0.2) Junction with Wellesley Road. Continue straight on State Line Road.

31.2 (0.3) Stateline Village.

31.9 (0.7) Turn left on Becks Road and drive north.

32.7 (0.8) As you drive north on Becks Road across the wide Spokane River Valley, look toward 2 o'clock at the high, partially bald hill. This is the type locality of the Mount Rathdrum granite.

34.2 (1.5) Turn right on Idaho State Highway (SH) 53 toward Rathdrum.

36.8 (2.6) Outcrops north of the highway are southeast-dipping Hauser Lake Gneiss.

40.6 (3.8) Junction with Green Ferry Road. Continue straight on Idaho SH 53.

40.9 (0.3) **STOP 5 (optional). Hauser Lake Gneiss.**

Pull off onto the right shoulder opposite the roadcut on the left side of the highway. Watch out for traffic.

The rock in this cut consists of strongly mylonitic Hauser Lake Gneiss with a southeast-dipping foliation. Others (Rehrig and Reynolds, 1981) have proposed that this southeast-dipping foliation represents a second mylonitic event that occurred along the west side of the Purcell Trench and cut the earlier west-dipping foliation that characterizes most of Spokane dome. However, in fairly continuous exposures north of this cut, from west to east, the west-dipping foliation can be seen to progressively roll over to a south dip and finally to an east dip with no evidence of two mylonitic events. The exposure here is just east of the axis of the Spokane dome.

The west limb of the dome contains an approximately 4-km-thick section of mylonitic rocks, whereas the section on the east limb of the dome is perhaps only 3 km or less thick, suggesting that, at least locally, a fault exists beneath the Purcell Trench that cuts out the upper part of the mylonitic zone on the east limb of the dome.

Return to the vehicles and then drive east on SR 53.

41.2 (0.3) Entering the town of Rathdrum.

41.7 (0.5) Turn right at the second street that crosses the railroad tracks in the center of Rathdrum.

41.8 (0.1) Stop sign. Continue straight down a short hill.

41.9 (0.1) Stop sign at the bottom of a short hill. Turn left.

42.0 (0.1) **STOP 6. Chloritic alteration.**

Pull off on the left shoulder opposite the roadcut on the left.

This roadcut consists of metasedimentary rocks and pegmatite that contain some chloritic alteration. The rocks in this exposure have been

used as evidence that a low-angle fault and accompanying chloritic breccia zone exist along the Purcell Trench. However, this is the only known outcrop that contains any chloritic alteration along the entire trench. Furthermore, it is in an awkward location to connect with any fault hypothesized in the Purcell Trench; any such fault would have to loop into the Spokane Valley near Rathdrum. We believe that this alteration is localized and is not related to any major structure.

Return to the vehicles and continue to drive north.

42.4 (0.4) Rathdrum High School on the left. Continue straight.

42.7 (0.3) Turn left onto Idaho SH 41 and 53.

42.9 (0.2) Turn right on SH 41, toward Spirit Lake.

46.7 (3.8) Turn right on the unnamed gravel road opposite Twin Lakes Village.

48.6 (1.9) Turn left at the T-junction. Drive north toward Round Mountain.

50.2 (1.6) **STOP 7. East limb of Spokane dome.**

East side of Round Mountain. Park on the right shoulder opposite slabby outcrops that can be seen through the trees to the left. Climb the slabs for about 100 ft.

Views to the east are of the wide Rathdrum Prairie, which is part of the southern Purcell Trench. Hills in the distance are underlain by rocks of the lower Belt Supergroup, which are capped by flows of the Columbia River basalt along the edge of the Purcell Trench. The rocks below the basalt were affected by Precambrian burial metamorphism but are unaffected by any younger dynamothermal metamorphism.

The slabby outcrops on the east side of Round Mountain are dip slopes of medium- to coarse-grained mylonitic orthogneiss. This orthogneiss is found only locally and probably represents a small prekinematic granitic intrusion into the Hauser Lake Gneiss. It has a strongly developed S-C fabric. Peel back the moss to see the strong down-dip lineation, and look at surfaces parallel to the lineation and perpendicular to the foliation to see the S-C fabric.

Return to the vehicles, make a U-turn, and drive south.

51.8 (1.6) Turn right on the gravel road back toward SR 41.

52.8 (1.0) Road ascends a well developed outwash terrace.

53.8 (1.0) Turn right on SH 41 toward Spirit Lake.

60.1 (6.3) Junction with SH 47 (toward Athol). Continue straight (north) on SR 41.

60.6 (0.5) Entering town of Spirit Lake.

60.9 (0.3) Turn left on Main Street, pass through the old town center of Spirit Lake, and continue down the short, steep hill.

61.7 (0.8) Cross the short bridge over Spirit Lake narrows.

61.8 (0.1) **STOP 8. Base of mylonite zone.**

Park on the shoulder at the far end (around bend) of the large roadcut.

This cut consists of intensely folded, sillimanitic Hauser Lake Gneiss. Note that the folds are "enclosed" between gently dipping, lineated mylonitic surfaces, whereas the foliation around the folds is generally not well lineated. The orientations of the fold axes are not perfectly parallel to, but rather scatter around the average orientation of the lineation. This is probably due to the incomplete re-orientation of the axes into the stretching direction during mylonitization. This exposure is structurally just above the east edge of the Spirit Lake window, a region where erosion has penetrated through the mylonitic zone into underlying steeply dipping nonmylonitic rocks. Note the similarity between these rocks and those at Stop 4; it is thought that they lie in approximately the same structural position.

Return to the vehicles and continue to drive west on Spirit Lake Road.

63.2 (1.4) **STOP 9 (optional). Spirit Lake window.**

Turn left into small parking area and walk approximately 100 ft west along the road to the roadcuts on the right side of the road. These

rocks are below the Spokane dome mylonitic zone. Note the lack of a penetrative, slickenside-style lineation and the generally crystalloblastic nature of the foliation. Note also the rather open, concentric style of folding. Folds of this type do not affect the mylonitic rocks; thus it is inferred that these folds predate the mylonitization. Folds such as this probably became tighter and were reoriented during the mylonitic event. Higher in the zone, transposition is complete, and these folds are completely obliterated.

Return to the vehicles and continue to drive west.

63.7 (0.5) **STOP 10. Mount Rathdrum granite.**

Park well onto the left shoulder, beyond the long roadcut on the right side of the road.

The west part of the cut consists of fine-grained, massive or nearly massive Mount Rathdrum granite. The granite intrudes sillimanite-bearing Hauser Lake Gneiss in the east half of the cut. Note the steep dips of the crystalloblastic foliation in the metasedimentary rocks; such steep dips are typical of nonmylonitic rocks throughout the Priest River Complex. Note also the mats of sillimanite that are randomly oriented within the foliation and the general lack of consistent lineation.

Return to the vehicles. Make a U-turn and retrace the route back to the junction of Main Street and SH 41 in Spirit Lake.

66.5 (2.8) Junction with Main Street, center of Spirit Lake. Continue north on SH 41.

68.3 (1.8) Road descends a glacial outwash terrace and turns to the west, leaving the Purcell Trench.

68.6 (0.3) Barren Hill at 10 o'clock is underlain by east-dipping, mylonitic Hauser Lake Gneiss.

70.2 (1.6) Here, Idaho SH 41 cuts across the Spokane dome. At this latitude, erosion has not completely breached the mylonitic zone. The hills to the north are underlain by nearly horizontal Hauser Lake Gneiss that defines the broad apex of Spokane dome. The forested hills to the south are underlain by Hauser Lake Gneiss that locally contains sillimanite, kyanite, and andalusite together.

71.2 (1.0) Bear left on an unnamed dirt road before entering the town of Blanchard. The turnoff makes only a small angle with SH 41. If you reach the sign that says "Entering Blanchard", you've missed the turn.

71.3 (0.1) Bear left at the fork.

71.5 (0.2) Turn left on the gravel road that immediately crosses a small wooden bridge over a drainage ditch.

71.8 (0.3) Small outcrops in fields on either side of the road are amphibolite.

72.0 (0.2) Turn right (following the main road); the road straight ahead enters a tree farm.

72.6 (0.6) Golf course to the right.

73.0 (0.4) **STOP 11. Mylonitic quartzite.**

Park off the road (several spots available) before crossing a wooden bridge. Walk across the bridge and just on the far (west) side descend a steep trail (watch your step) and examine the outcrop underneath the bridge.

This excellent exposure consists of banded, mylonitic, biotitic quartzite. In thin section, the quartz is almost entirely annealed and extremely fine grained.

Study both the clean face that is perpendicular to the stream and the less clean face parallel to the stream. Note that the compositional layering appears planar when viewed parallel to the lineation, but clearly is tightly folded when viewed down the lineation, with the fold axes parallel to the lineation. The lineation is well displayed on the underside and is clearly defined by the intersection between the compositional layering and the axial planar foliation defined by biotite.

This locality is one of the few known where true quartzites occur in the Hauser Lake Gneiss. Most of the Hauser Lake contains much more feldspar and biotite, which makes the quartz-rich Prichard Formation an unlikely protolith.

Return to the vehicles. Make a U-turn and drive back toward Blanchard.

74.0 (1.0) Turn left toward Blanchard.

74.6 (0.6) Turn right after crossing a small wooden bridge onto an unnamed gravel road.

75.1 (0.5) T-junction with the Blanchard Road. Turn left.

75.8 0.7) **STOP 12 (optional). Hauser Lake Gneiss.**

Pull off to the right into a small quarry/borrow pit.

This exposure consists of sillimanitic Hauser Lake Gneiss, including numerous layers and pods of pegmatite. Kyanite occurs with sillimanite as small, anhedral, blue blades. Look carefully at the kyanite blades with a hand lens. You should be able to find some that are partially altered to anhedral, flesh-colored, or pink andalusite.

See the text of the preceding article and Rhodes (1986) for a discussion of the textural relations between the three Al_2SiO_5 polymorphs.

Return to the vehicles. Make a U-turn and drive back toward SH 41.

76.6 (0.8) Turn left on SH 41 toward Newport, Washington.

86.3 (9.7) Road descends a long hill just south of Newport. The partially forested hills straight ahead in the distance are underlain by essentially unmetamorphosed rocks of the Belt Supergroup that lie on the upper plate of the Newport fault.

88.1 (1.8) Entering town of Oldtown, Idaho.

88.3 (0.2) Junction with 4th Street. Continue straight on State Avenue.

88.7 (1.8) Junction with U.S. 2. Turn east (right) toward Priest River.

94.5 (5.8) Junction with Idaho SH 57 in the town of Priest River. Turn north (left) onto SH 57.

98.0 (3.5) Turn east onto Peninsula Road. Follow Peninsula Road as it bends north.

101.4 (3.4) At this point, Peninsula Road affords a good regional view to the north of the east flank of the Newport fault zone (NFZ). To the east, a series of west-trending ridges slopes westward down to the valley floor. The NFZ, which is generally north-south trending in this area, is present near the base, across the nose of each of these ridges. The westward dip of the fault (5-35 degrees) is slightly greater than the slope of the ridges. To the east, the fault projects above the ridges, which are underlain by footwall granitic bodies and associated pendants of metamorphic rock. The valley floor and hills to the west are underlain by the Prichard Formation and form the hanging wall of the NFZ. Resistant diabase sills within the Prichard crop out on several hills to the west. Northward along the axis of the valley, the Prichard Formation dips moderately to steeply (25-65 degrees) east toward the NFZ.

102.6 (1.2) Bridge over McAbee Falls. Here Peninsula Road changes from a paved surface to gravel.

104.2 (1.6) Roadcut in the Prichard Formation.

106.0 (1.8) North- and south-bound lanes of Peninsula Road divide.

106.2 (0.2) Turn east (right) onto an unnamed gravel road, which is the first turnoff immediately north of the reconvergence of the lanes of Peninsula Road.

106.5 (0.3) Follow the south (right) fork at the branch in the gravel road.

106.9 (0.4) Follow the main gravel road to the left along the north fork of the road.

107.4 (0.5) **STOP 13. Newport fault zone.**

There are discontinuous outcrops along the SSE bank of the road. Park as far off the road as possible to avoid local, recreational, and logging traffic.

Exposures along this road provide a nearly continuous section, west to east, across the NFZ from the hanging wall, through both the cataclastic and mylonitic subzones of the fault, and continuing up the hill well beyond the field trip stop, to structurally underlying undeformed rocks of the footwall. Along this part of the fault, quartzite of the Prichard Formation in the hanging wall, subjected only to burial metamorphism, is juxtaposed against mylonitized upper-amphibolite-grade rocks of the footwall.

Rusty weathering, fine-grained, impure quartzite of the Prichard Formation is folded into numerous outcrop-scale, tight, overturned folds

in the westernmost part of this outcrop. East of this, highly silicified and indistinctly bedded Prichard is in direct contact with the upper, cataclastic subzone of the NFZ. Locally, Prichard strata dip 64 degrees ESE to abut the NFZ surface, which in the immediate area dips 5 to 12 degrees WNW. This corresponds with the expected angular relation between bedding and fault attitudes following rotation along a listric fault that cut initially near-horizontal strata. This bedding-fault relation holds in general all along the eastern trace of the fault. The approximately 30 degree range in dip of the fault is accompanied by a corresponding range in dip in hanging wall strata. Hills to the east of this stop, which are underlain by footwall lithologies, rise topographically from the fault zone at a greater than 12 degree incline. This slope requires the projection of the NFZ to be curved in order to pass above the footwall and further constrains the original listric shape of the fault.

A thick section of cataclastic fault rock occurs structurally below the Prichard. Chloritic microbreccia at the top of this sequence grades downward into a zone of less penetrative fine-scale brecciation but which is characterized by wholesale disruption of fabric. The latter appears to have been derived from the immediately underlying mylonites.

Below the cataclastic fault rock a broader zone of well developed mylonite occurs. The mylonites are mica-rich and quartzo-feldspathic in composition. They are commonly sillimanite-bearing, but textural evidence for sillimanite stability during mylonitization is equivocal. The mylonite mineralogy may have been inherited from upper-amphibolite grade metapelites, siliceous marbles, and orthogneisses that occur as undeformed footwall lithologies gradationally below sheared rocks of the fault zone several kilometers east of this site. Mylonites at this stop are strongly foliated. In hand specimen, surfaces perpendicular to foliation clearly display both a flattening (S) fabric produced by elongation of quartz grains and mica alignment and a shear (C) fabric composed of crushed feldspar and mica that offsets the S-fabric. The mylonites also show the penetrative lineation, here composed of quartz rods and tails of crushed feldspar, which is ubiquitous in NFZ mylonites. In this outcrop, the mylonitic foliation has an anomalous shallow east dip which, a few meters farther east along the road, rolls over to dip west and parallel the attitude of the fault zone as defined by the chlorite microbreccia zone. Parallelism of fault zone and mylonitic foliation is characteristic of all other exposures along the eastern fault trace. The local anomalous east dip here is attributed to minor rotation within the fault zone. Regardless of dip direction, kinematic indicators within the mylonite fabric all along this outcrop show a top-to-the-west or regionally normal sense of shear.

120.3 (12.9) Return to the intersection of SH 57 and U.S. 2 in Priest River. Turn west (right) toward Newport on U.S. 2.

126.1 (5.8) Intersection of U.S. 2 with State Avenue on the Washington-Idaho state line in Newport. Turn south (left) onto State Avenue.

126.4 (0.3) At the first intersection immediately following the railroad crossing, turn east (left) onto East 4th Street South.

127.3 (0.9) Road surface changes from pavement to gravel.

128.3 (1.0) Road changes back to pavement.

128.4 (0.1) Turn north (left) off the paved road onto a small unnamed dirt road leading down to the railroad tracks.

128.5 (0.1) **STOP 14. Kinematics in the Newport fault microbreccia.**

The dirt road ends at the railroad tracks. From here east to the railroad bridge over the Pend Oreille River the tracks run through a large cut. (Note: osprey can commonly be observed on the large platform nests they have built on top of the railroad bridge over the river.)

This railroad cut and the Albeni Falls damsite are constructed within the chlorite microbreccia subdomain of the NFZ. Innumerable polished and slickensided planar fractures within the fault breccia are exposed in the railroad cut. Sense of displacement on the majority of surfaces where it is determinable is slightly oblique, normal dip-slip offset. These faults are not the primary surface of detachment of the hanging wall along the NFZ. They occur entirely within brecciated fault rocks. They are commonly steeply dipping and not parallel to the attitude of the fault zone as a whole. However, they do demonstrate dilatancy and extension within the fault zone and are interpreted as secondary synthetic and antithetic, brittle normal faults associated with displacement along the NFZ. Strain within the cataclastic subdomain of the NFZ is compatible with extension and normal offset determined for the

mylonitic subdomain of the fault; the two domains are kinematically linked.

130.9 (2.4) Return to the intersection of State Avenue and U.S. 2 in Newport.

Day 2: Newport fault (continued) and central Priest River Complex.

0.0 Begin road log for Day 2 at the intersection of State Avenue and U.S. 2 in Newport. *Reset odometers.* Drive west on U.S. 2.

0.4 (0.4) Turn west (right) off U.S. 2 onto First Street in Newport.

2.1 (1.7) At the fork in the road, bear north (right) onto Coyote Trail.

2.9 (0.8) Coyote Trail changes from pavement to a gravel surface.

6.4 (3.5) After skirting the south side of Saddle Mountain on Coyote Trail, turn north (right) onto an unnamed dirt road. This is a residential road; be alert for local traffic.

6.9 (0.5) Fork in the road. Bear west (left). Outcrops along this segment of the road are quartz-rich high-grade metasedimentary rocks that occur as large septa within the Eocene Silver Point Quartz Monzonite pluton in the footwall of the NFZ.

8.4 (1.5) This fork in the road begins a closed loop at the end of the road. Bear west (left).

8.5 (0.1) Just beyond the fork, a small dirt track leads off to the west. It is advisable to park near the fork. Walk along the dirt track approximately 70 m to where it ends in an open meadow. Cross the meadow to the northwest to another dirt track which leads to the top of a small hill (approximately 25 m above the meadow).

STOP 15. Cataclastic subdomain of the NFZ.

The structurally highest rock here, cropping out on the low north side of the exposure just at the line of trees, is a chloritic microbreccia. This is the most characteristic fault rock of the cataclastic subdomain. Its groundmass consists of an aphanitic chloritic matrix supporting small (1-5 mm) fragments of feldspar and quartz. Except for abundant chlorite overgrowths, the very fine grained components of the groundmass cannot be resolved petrographically. The chlorite microbreccia is extremely hard. The 30 degree north dip of this hill, of the adjacent hill to the west, and the crest of the next hill to the east are dip slopes of the NFZ developed on this very resistant fault rock. To the south, along the crest of the hill, the chlorite microbreccia grades structurally downward into a "mortar texture" fault rock in which the original fabric of the rock has been disrupted but not obliterated. One- to 2-cm fragments of less deformed protolith are surrounded by a "mortar" of chloritic fine-grained cataclasite. Enough of the character of the protolith is preserved in this mortar texture fault rock to recognize its derivation from the Silver Point Quartz Monzonite.

The Silver Point Quartz Monzonite intrudes basement metasedimentary rock in the footwall of the NFZ along the southern, east-trending trace of the fault. The NFZ cuts the Silver Point Quartz Monzonite and juxtaposes it against relatively unmetamorphosed Prichard Formation of the hanging wall. The Prichard Formation underlies the lower, broad rounded hill immediately below this site, extending north from the resistant line of the fault trace.

From the vantage point at this stop, standing on the southern fault trace looking essentially down the plunge of the structure, the architecture of the hanging wall of the NFZ is displayed in the panoramic view north (Fig. 3). The Pend Oreille River lies in a broad flat valley which from here westward bends gradually around to a north trend and continues off into the distant background. From this stop, the trace of the NFZ follows along the south side of the valley and continues north along the base of the mountains, rising on the west side of the valley. Silicified and recrystallized, extremely resistant NFZ rocks confine the Pend Oreille River on the west and cause it to mimic the spoon shape of the fault. The fault dips extremely shallowly (0-20 degrees) east under the Pend Oreille. Mountains to the west of the fault trace are underlain by footwall granite and metamorphosed Belt rocks.

Due north from this viewpoint, across the Pend Oreille River, a series of north-trending ridges have steep, planar west-dipping flanks. These are dip slopes developed on the 60 degree west dip of bedding within the Prichard Formation in the hanging wall. The Belt Supergroup youngs to the west from there. At the eastern limits of this view Prichard strata roll over and dip 30 to 60 degrees east, forming the broad,

open Snow Valley anticline (Schroeder, 1952). The lower hills adjacent to the westernmost Belt strata are underlain by flows of the Eocene Sanpoil Volcanics that overlap the tilted Belt strata with angular unconformity. The broad valley of the Pend Oreille River is underlain by Eocene Tiger Formation nonmarine clastic rocks. The Tiger dips gently to the west. The geometry of these hanging wall units is consistent with the development of (1) a roll-over anticline of Prichard strata in which both the 60 degree west-dipping west limb and 30 to 60 degree east-dipping east limb rotated down two inward-facing listric normal fault surfaces, and (2) a basin on the west limb of the hanging wall anticline in which syntectonic volcanic and sedimentary units unconformably overlap tilted Belt strata and are themselves rotated to lesser westward dips.

10.6 (2.1) Return to Coyote Trail, turn west (right).

11.6 (1.0) At the first intersection, turn north (right) onto McCloud Creek Road.

12.0 (0.4) **STOP 16. Silver Point Quartz Monzonite.**

This small roadcut on the west side of McCloud Creek Road provides an excellent example of fresh and undeformed Silver Point Quartz Monzonite. The primary igneous texture in these rocks can serve as a reference for comparison with both the cataclastically and mylonitically deformed Silver Point Quartz Monzonite of the preceding and following stops, respectively. The Silver Point Quartz Monzonite is hornblende-, biotite-, and sphene-bearing. It is medium to coarse grained (1-4 mm) and characterized by distinctive large, euhedral K-feldspar phenocrysts which range from one to several centimeters in length. In much of the northern part of the pluton, as at this site, the Silver Point Quartz Monzonite is weakly foliated and commonly is weakly lineated. The average orientation of the Silver Point Quartz Monzonite lineation coincides with the average for all NFZ mylonite lineations. This parallelism suggests that although the Silver Point Quartz Monzonite predates the NFZ, the regional attenuation which accompanied NFZ displacement occurred while the pluton was still sufficiently ductile to have undergone mineral alignment in response to that stress.

14.6 (2.6) Continue north on McCloud Creek Road to the intersection with SR 20. Turn west (left) on SR 20.

15.3 (0.7) **STOP 17. Mylonitized Silver Point Quartz Monzonite.**

Roadcuts are present on both sides of the highway here. From the south side of the road there is also easy access to the continuation of this outcrop along the railroad cut that parallels SR 20. (Note: you may be able to see osprey nesting on pilings in the river to the north of this site.)

Well developed, ductilely deformed NFZ mylonites exposed at this stop are derived from the Silver Point Quartz Monzonite. From here south, perpendicular to the fault trace and structurally downward into the footwall, mylonitic rocks grade through progressively decreasing amounts of strain into undeformed crystalloblastic Silver Point Quartz Monzonite like that at the previous stop. Here, mylonitization has rounded the distinctive feldspar phenocrysts which characterize the Silver Point into the porphyroclasts observed at this stop. Mylonitic recrystallization was accompanied by considerable mobilization of quartz, which in these rocks occurs in elongate ribbon grains defining a strong mylonitic foliation. Incomplete chloritization of mafic minerals of the Silver Point Quartz Monzonite protolith has also occurred.

Both cataclasis and mylonitization of the NFZ have penetratively deformed and cut the Silver Point Quartz Monzonite and both therefore must be Eocene, post-Silver Point Quartz Monzonite (post-48 Ma) in age. Both fault rock types are kinematically compatible subdomains of normal faulting. (See Stop 14.) The chloritic microbreccia does not significantly postdate mylonitization, and both result from one episode of displacement on the NFZ.

17.8 (2.5) Continue west on SR 20 into Dalkena where West Calispell Road intersects the highway. Turn west (left) onto West Calispell Road.

19.8 (2.0) Cross SR 211 and continue west on West Calispell Road.

23.2 (3.4) **STOP 18. Newport fault zone.**

From the intersection with SR 211 westward, the NFZ strikes roughly parallel to West Calispell Road, less than a kilometer south of the road. From this stop to the next, resistant, silicified chloritic microbreccia of the NFZ forms the hills that rise southwest and west of Calispell Lake. Here and along the route ahead, the road traverses the base of these hills and lies

within or immediately adjacent to the NFZ. This bend is part of the distinctive spoon-shaped trace of the fault; it curves north from its southern, west-trending segment to its western, north-trending flank. The brief stop here is intended simply to demonstrate the location of the NFZ.

Continue west, then north along West Calispell Road as it bends around the west side of the low marshland and fields surrounding Calispell Lake.

25.8 (2.6) Intersection of West Calispell Road and Pease Road. Continue on West Calispell Road. Here, the NFZ maintains its north trend, outcropping not more than a kilometer to the west. As it bends east, West Calispell Road diverges from the trace of the fault and continues onto the hanging wall.

26.7 (0.9) **STOP 19. Tiger Formation.**

The embankment on the north side of the road exposes poorly indurated, fluvial deposits of the Eocene Tiger Formation. To the east, across the valley of the Pend Oreille, the Tiger unconformably overlies Belt through Paleozoic strata. It is the highest stratigraphic level of the hanging wall. However, immediately south and west of this stop, the Tiger is in direct juxtaposition with metamorphosed Prichard Formation and possible pre-Belt basement gneiss (Harms, 1982) across the NFZ. The normal, dip-slip throw on this portion of the fault can be estimated by this stratigraphic separation (or stratigraphic thickness) between the Tiger and lowermost Prichard at approximately 9 km (Harms, 1982).

Clasts in conglomeratic horizons of the Tiger at this locality are derived predominately from Belt strata. Elsewhere the Tiger Formation includes granitic and mylonitic clasts which record uplift and erosion of the footwall and NFZ (Gager, 1984). Bedding in the Tiger at most localities dips 5 to 30 degrees westerly into the NFZ, which is less than but has the same sense of rotation as underlying Belt strata to the east. These data suggest the Tiger is a syntectonic deposit associated with hanging wall rotation and basin formation accompanying listric normal faulting along the west flank of the NFZ.

28.7 (2.0) Turn east (away from Chewelah) from West Calispell Road onto McKenzie Road.

30.9 (2.2) At the intersection of McKenzie Road and SR 20 in Usk, turn south (right) onto SR 20 to return to Newport.

46.6 (15.7) Junction of SR 20 and U.S. 2 in Newport. Turn east (left) onto U.S. 2.

46.7 (0.1) Junction of U.S. 2 and State Avenue. Continue east on U.S. 2 toward Priest River.

46.8 (0.1) Bridge across the Pend Oreille River.

51.8 (5.0) Entering the town of Priest River.

52.6 (0.8) Downtown Priest River. Continue east on U.S. 2.

53.3 (0.7) Bridge across the Priest River.

Stops 20 and 21 examine the mylonitic relations in the high-grade Precambrian (?) metasedimentary rocks and the megacryst-rich granitic augen gneiss which concordantly underlies the metasedimentary rocks. (See Rhodes and Hyndman, 1984, figs. 2 and 3.) These stops structurally underlie the Newport fault.

56.9 (3.6) **STOP 20. Metasedimentary rocks.**

Pull off the road to the right (south) onto a large paved turnout at the first towering roadcut. Examine the large roadcut on the south side of the road.

The rusty-weathering rocks in the large roadcut on the south side of the highway are sillimanite-bearing biotite-quartz schist and quartzite overlying amphibolite along a gently westward-dipping contact. A fairly well developed mylonitic foliation parallel to the compositional layering contains a fine, streaky mylonitic lineation trending east-west or slightly north of east. Deforming the mylonitic foliation and lineation are prominent east-verging, nearly isoclinal folds (Fig. 5). Fold axial surfaces strike east to south and dip 30 degrees south to west. Fold axes plunge 20 to 30 degrees southwest and parallel the foliation.

The schist and gneiss on the north side of U.S. 2 contain sillimanite and garnet, with the sillimanite defining the mylonitic lineation. High in the roadcut on the north side of the highway is a black amphibolite sill that is extended into lensoid boudins within the enclosing mylonitic quartzite. The metasedimentary foliation is deformed into folds as on the south side of the highway.

Return to the vehicles and continue east on U.S. 2. The highway passes large cuts in the same mylonitic metasedimentary rocks.

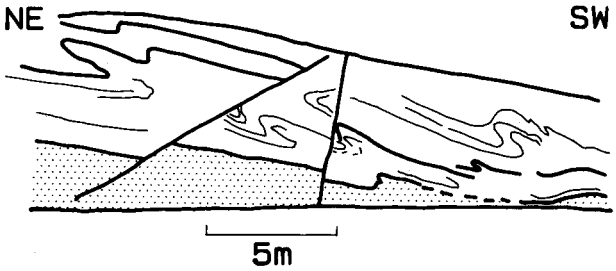

Figure 5. Sketch of folded metasedimentary rocks overlying amphibolite (shaded) at Stop 20.

58.4 (1.5) Contact (unexposed) between gently dipping mylonitic metasedimentary rocks and megacryst-rich granitic augen gneiss.

58.8 (0.4) **STOP 21. Augen gneiss.**

Pull off on the large gravel turn-off on the left (north) side of the road, park, and walk approximately 100 yd to the east to examine the large cut.

This large, vertical roadcut exposes coarse-grained biotite granite or augen gneiss rich in megacrysts of K-feldspar (5-35 % of rock). The original crystallization age of this granite is 1,576 Ma, as inferred from a U-Pb upper intercept from a moderately discordant assemblage of zircons (Evans and Fischer, 1986). The granite shows a moderately to strongly developed foliation dipping about 20 degrees east. A strong mylonitic lineation plunges about 15 degrees northeast. K-feldspar megacrysts or augen are rotated and drawn out into tails showing ambiguous vergence. In a roadcut approximately 0.3 mi to the east, megacrysts show an unambiguous top-to-the-east sense of shear. (See Rhodes and Hyndman, 1984, fig. 13.)

The north side of the roadcut at this stop contains a black amphibolite sill that is drawn out into spectacular, rectangular, rotated boudins (Fig. 6). The east side of each block is dropped down with respect to the adjacent boudin.

The mylonitic foliation in the granitic augen gneiss is in many places macro-crenulated on surfaces that dip gently to moderately west and has a top-to-the-west sense of shear. (See Rhodes and Hyndman, 1984, fig. 14.) Axes of the crenulations are oblique to the mylonitic lineation, which maintains its gently northeastward plunge. The spacing between crenulations is about 0.1 to 0.5 m.

An earlier (pre-crenulation) set of folds is well exposed on the south side of the highway in the east half of the roadcut. These older folds verge eastward and typically have strongly attenuated lower limbs.

Deformation appears to involve an earlier east-verging set of folds, perhaps associated with mylonitization. Later extension, with a top-to-the-west vergence, formed the boudins and macro-crenulations. This later movement may be related to formation of the Newport fault to the west and above.

End of road log.

To reach Newport, drive approximately 12 mi west on U.S. 2. To reach Sandpoint, drive approximately 17.5 mi east on U.S. 2.

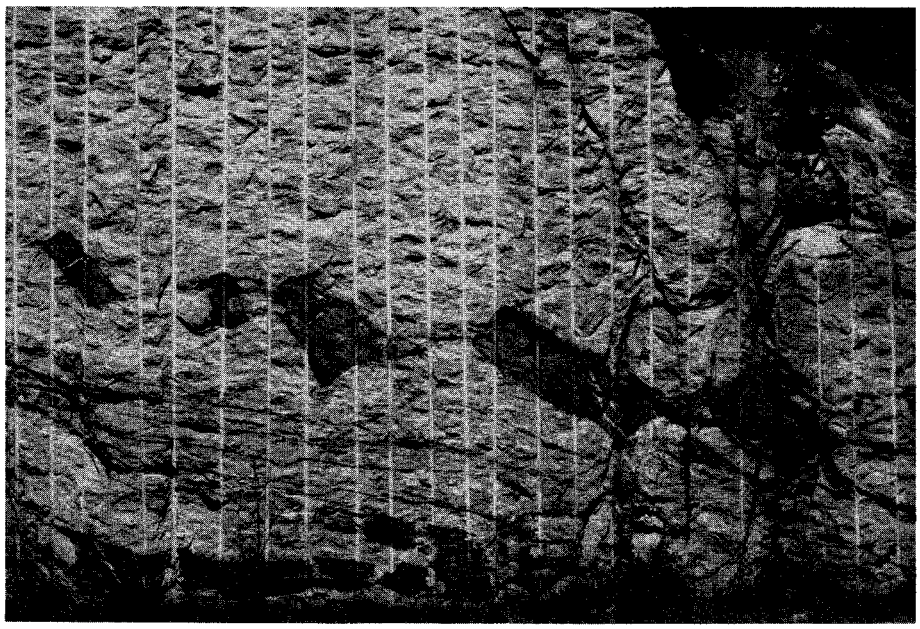

Figure 6. Amphibolite boudins in matrix of augen gneiss at Stop 21.

Volcanism, Plutonism, and Sedimentation, Central Okanogan Highlands

R. Wade Holder, David R. Gaylord, Grace A. M. Holder,
Kenneth F. Fox, Jr., and J. R. Wilson

Plutonism, Volcanism, and Sedimentation Associated with Core Complex and Graben Development in the Central Okanogan Highlands, Washington

R. Wade Holder
Department of Geology and Geography
Georgia Southern College
Statesboro, GA 30460

David R. Gaylord
Department of Geology
Washington State University
Pullman, WA 99164

and

Grace A. McCarley Holder
Department of Geology and Geography
Georgia Southern College
Statesboro, GA 30460

INTRODUCTION

The central Okanogan Highlands in north-central Washington, bounded by the Columbia River on the east and south and the Okanogan River on the west, is characterized by: (1) Paleocene-Eocene intrusions of the Colville batholith, (2) three en echelon, NNE-trending, volcanic- and volcaniclastic-filled grabens, and (3) dominantly amphibolite-grade metamorphic rocks of the Kettle and Okanogan core complexes (gneiss domes) (Fig. 1). These rocks comprise the southwesternmost part of the Omineca crystalline belt. The locations of 12 fieldtrip stops in and adjacent to the Republic graben are shown in Figure 1 and discussed below.

Plutonic rocks

The numerous plutonic igneous intrusions in the central Okanogan Highlands are referred to collectively as the Colville batholith. Originally named by Pardee (1918) for exposures on the Colville Indian Reservation, most of the batholith has been subdivided on the basis of field evidence, mineral composition, and major element chemical composition into three intrusive suites, which are, from oldest to youngest, the Keller Butte suite, the Devils Elbow suite, and the Herron Creek suite (Holder and Holder, 1988). Distinctive characteristics of these suites are summarized in Table 1. Locations of intrusions in the suites are shown in Figure 2.

Rocks of the Keller Butte suite are texturally varied (fine to very coarse grained), light colored, hornblende-free biotite granite and granodiorite (Fig. 3) with abundant aplo-pegmatite veins, dikes, and pods. Distinctive features of the Keller Butte suite include its lack of hornblende, low color index, and widespread penetrative mineral fabrics where these intrusions are within or adjacent to the gneiss domes or metamorphic core complexes in the region.

The Devils Elbow suite includes several medium-grained, equigranular biotite-hornblende diorite-quartz monzodiorite-granodiorite plutons (Fig. 3) that are much darker than those of the Keller Butte suite; mafic minerals typically comprise 20 to 25 percent of Devils Elbow suite rock. Unambiguous cross-cutting relations documented at several localities indicate that the Devils Elbow suite is younger than the Keller Butte suite (Atwater and Rinehart, 1984; Carlson, 1984; C. D. Rinehart, oral commun., 1984; Moye, 1984; G. M. Holder, 1985; Holder, 1986). In contrast to the Keller Butte suite, the rocks of the Devils Elbow suite have been affected only very locally and mildly by deformation associated with core-complex development.

Each member of the Herron Creek intrusive suite is composed of: (1) an older medium- to coarse-grained, inequigranular or alkali feldspar phyric, gray to pink,

From: Joseph, N. L., and others, editors, 1989, Geologic guidebook for Washington and adjacent areas: Washington Division of Geology and Earth Resources Information Circular 86.

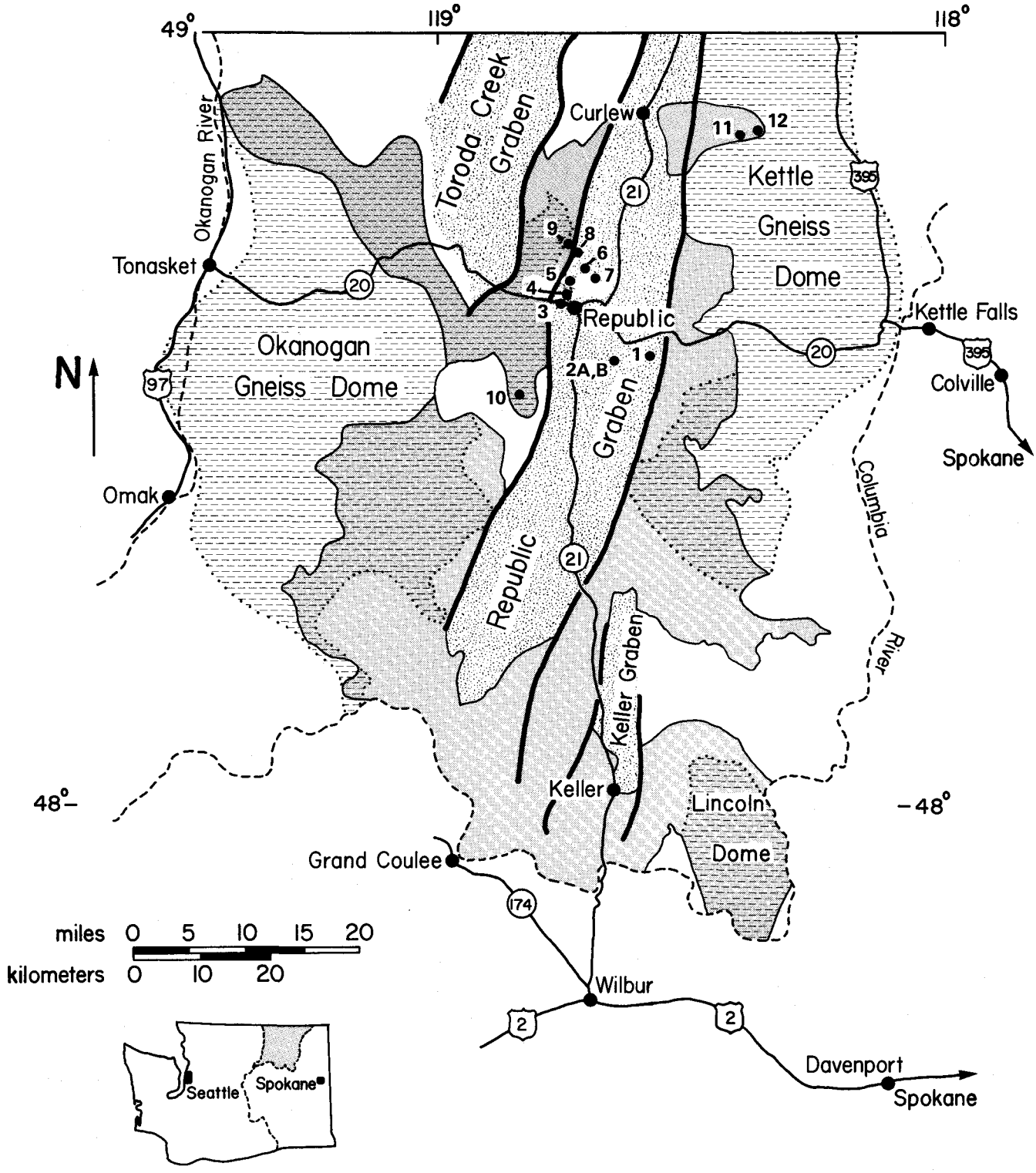

Figure 1. Generalized geologic map of the central Okanogan Highlands showing intrusive rocks of the Colville batholith (shaded), dominantly volcanic and volcaniclastic rocks in the grabens (stippled), and areas affected by penetrative mylonitic deformation associated with the gneiss domes (dashed). Graben-bounding faults, solid bold lines; limit of core complex deformation, dotted line; major highways, intermediate weight solid lines. Bold numerals are fieldtrip stops.

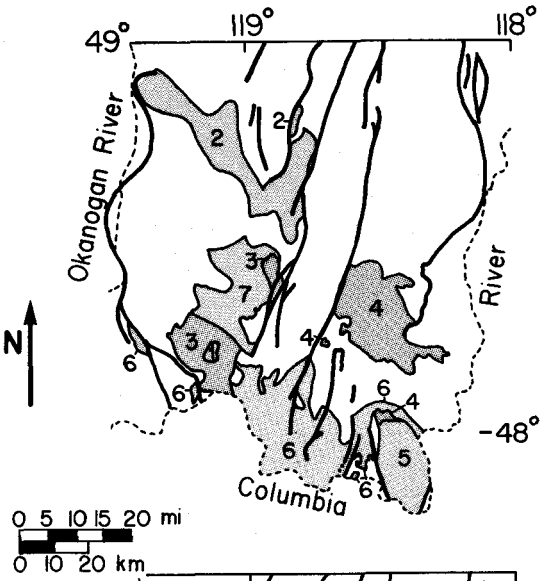

Keller Butte suite

1) granite west of Armstrong Mountain
2) Mount Bonaparte pluton*
3) Coyote Creek pluton
4) granite of Daisy Trail
5) plutonic complex of Johnny George
6) granite and granodiorite of Keller Butte**
7) Moses Mountain pluton

* includes homophanous granodiorite (Waters and Krauskopf 1941) and syntectonic granodiorite of Pearson (1967)

**includes, granite of Swawilla Basin, porphyritic granodiorite of Manila Creek, and porphyritic granite of Keller Butte (Atwater and Rinehart, 1984)

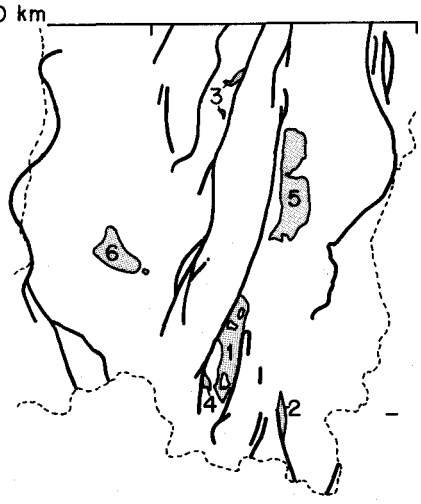

Devils Elbow suite

1) Devils Elbow pluton
2) Friedlander Meadows pluton
3) Henry Creek diorite
4) granodiorite of Joe Moses Creek
5) Kettle Crest pluton
6) Swimptkin Creek pluton

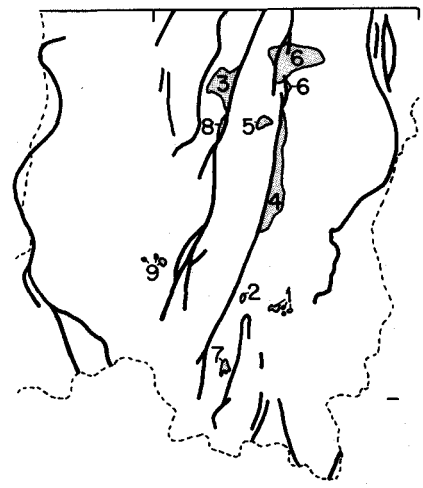

Herron Creek suite

1) Bridge Creek intrusions
2) granite of Deadhorse Creek
3) Empire Lakes pluton
4) Fire Mountain pluton
5) Herron Creek intrusion
6) Long Alec Creek pluton
7) seriate granite
8) monzonite east of Storm King Mountain
9) upper Stepstone Creek intrusions

Figure 2. Index map showing the names and locations of intrusions in the Keller Butte suite, Devils Elbow suite, and Herron Creek suite. (From Holder and Holder, 1988; with permission, Geological Society of America Bulletin, v. 100, p. 1971-1980.)

Table 1. Summary of the characteristics of the Keller Butte (KBS), Devils Elbow (DES), and Herron Creek (HCS) suites of the Colville batholith; see Figure 2 for a list of intrusions in each suite. AFM below refers to chemical trends on the Na2O + K2O (A) - FeO* (F) - MgO (M) ternary variation diagram. FeO* is total Fe expressed as FeO.

Intrusive Suite	Predominant Rock Type	Distinctive Mineralogy	Textural Features	Major Element Chemistry					Structural Features
				K2O	MgO	Alkali-Lime Index	Overall SiO2	AFM	
KELLER BUTTE SUITE	granite and granodiorite C.I. usually < 5 some granodiorite with C.I. = 10	- cpx -hbl +gnt +musc sphene rare	fine and even grained to coarse and even grained or seriate to mega-crystic, aplo-pegmatite common	--	< HCS < DES	calcic	acid > 64% SiO2 only	relatively immature Fe-rich trend	structurally concordant with gneiss domes
DEVILS ELBOW SUITE	diorite-monzodiorite-granodiorite C.I. = 25 avg. mafic margin	hbl cpx sphene -musc -gnt	equigranular medium grained	< HCS	> KBS	calc-alkalic	basic to intermediate, acid rocks rare	relatively mature, slightly more Fe-rich than HCS	typically discordant, locally deformed within gneiss dome, weak, locally mylonitic, fabric common
HERRON CREEK SUITE	quartz monzonite-monzogranite (C.I. = 8-26) microgranite (C.I. = 5 - 10) mafic margin	hbl cpx sphene -musc -gnt	quartz monzonite/ monzogranite: inequi-granular euhedral biotite (1mm-7mm) and mafic clots (1mm-1cm) distinctive. Locally porphyritic with K-feldspar phenocrysts. microgranite: typically fine and even grained, locally contains plagioclase and K-feldspar phenocrysts.	> DES	> KBS	ranges from calc-alkalic to alkali-calcic, overall alkali-calcic	basic to acid	relatively mature, slightly less Fe-rich than DES	discordant, generally lacks mylonitic fabric

hornblende-biotite quartz monzonite with abundant mafic clots, commonly containing cores of clinopyroxene, and (2) a younger, fine-grained, gray to brown, hornblende-biotite granite or "microgranite" (Fig. 3). In some Herron Creek suite intrusions, the microgranite is the dominant lithology, whereas in others inequigranular quartz monzonite is most abundant. In every place where relative age relations can be ascertained, the microgranite cuts or contains inclusions of the quartz monzonite. Herron Creek suite intrusions are normally associated with the Devils Elbow suite intrusions. Quartz monzonite of the Herron Creek suite contains foliated quartz monzodiorite inclusions of the Devils Elbow suite along the southern contact between the Kettle Crest pluton and Fire Mountain pluton (Fig. 2; G. M. Holder, 1985), and a dike of Herron Creek suite cuts the Henry Creek diorite (Fig. 2) (G. M. Holder, unpublished data). Contacts between Herron Creek suite quartz monzonite and the Devils Elbow suite range from gradational to razor sharp; relative age determinations are generally difficult to make. Herron Creek suite microgranite also cuts rocks of the Devils Elbow suite (see below).

Compilations of K-Ar ages for biotite in rocks in the central Okanogan Highlands (Fox and others, 1976, 1977; Pearson and Obradovich, 1977; Atwater and Rinehart, 1984) indicate a Paleocene to Eocene age (61-49 Ma) for the Keller Butte suite. However, thermal degradation of biotite in this suite in response to emplacement of the younger Devils Elbow and Herron Creek suites (Fox and others, 1976) requires that these ages be regarded as minimum. Biotite and hornblende ages from the Herron Creek and Devils Elbow suites indicate an Eocene age of between 45 and 53 Ma. The most believable and geologically significant ages are the concordant or nearly concordant biotite and hornblende ages from samples of the Swimptkin Creek pluton (49 Ma) and Kettle Crest pluton (45-47 Ma), both of the Devils Elbow suite.

Volcanic Rocks and Volcaniclastic Sedimentary Rocks

Eocene volcanic and volcaniclastic sedimentary rocks in the Republic graben have been subdivided into three formal stratigraphic units, in ascending order: O'Brien Creek Formation, Sanpoil Volcanics, and Klondike Mountain Formation (Muessig, 1967; Pearson and Obradovich, 1977) (Fig. 4). The O'Brien Creek Formation consists mainly of crystal-lithic tuffs and tuffaceous epiclastic (reworked volcanic) sediments; the maximum exposed thickness of O'Brien Creek strata exceeds 1,200 m (Muessig, 1967). Correlative strata in northeastern Washington yield a K-Ar biotite age of 54.5 Ma (Pearson and Obradovich, 1977, as corrected by Fox and Beck, 1985).

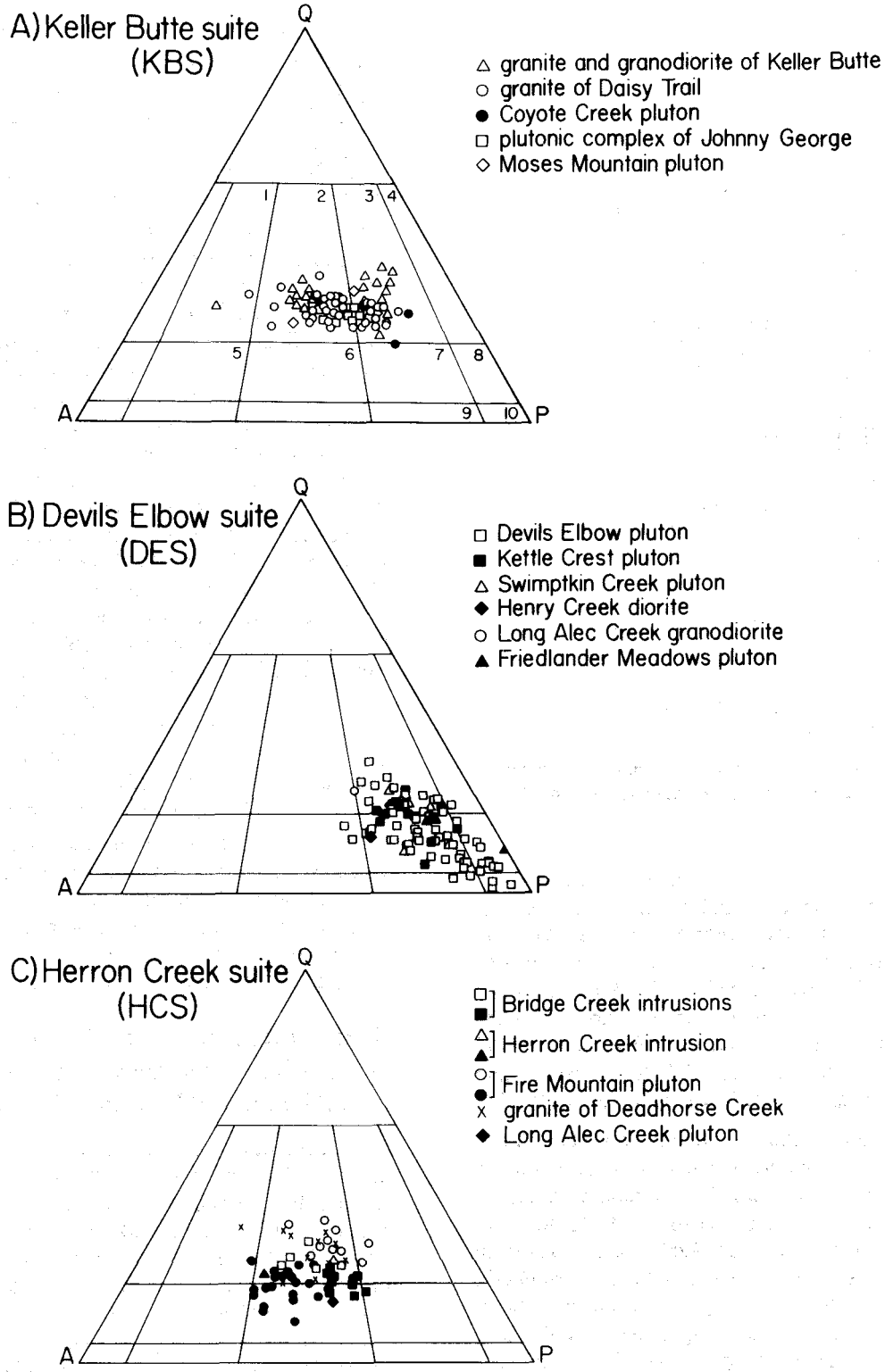

Figure 3. Modal analyses from the Herron Creek, Devils Elbow, and Keller Butte suites. Q, quartz; A, alkali feldspar; P, plagioclase feldspar. Field boundaries after Streckeisen (1976): (1) syenogranite; (2) monzogranite; (3) granodiorite; (4) tonalite; (5) syenite; (6) quartz monzonite; (7) quartz monzodiorite and quartz monzogabbro; (8) quartz diorite and quartz gabbro; (9) monzodiorite and monzogabbro; (10) diorite and gabbro. In (C) the open symbols and Xs represent modes of younger fine-grained rocks (microgranite), and the solid symbols represent modes of older medium-grained, inequigranular rocks. The Long Alec Creek granodiorite of the Devils Elbow suite occurs as large xenoliths in the Long Alec Creek pluton (Charles Knaack, Washington State Univ., oral commun., 1988). (From Holder and Holder, 1988; with permission, Geological Society of America Bulletin, v. 100, p. 1971-1980.)

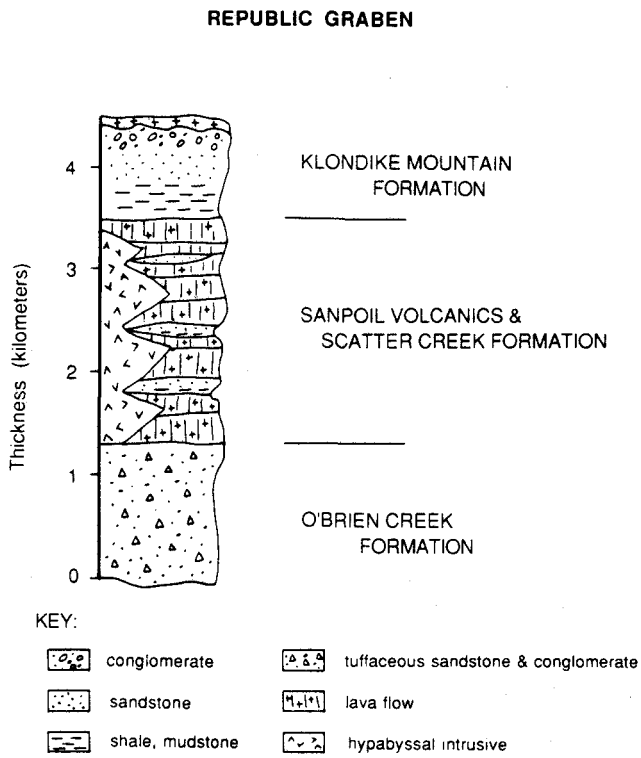

Figure 4. Generalized stratigraphic section of Paleogene volcanic, pyroclastic, and epiclastic strata in the Republic graben.

The Sanpoil Volcanics are composed primarily of lithoidal, porphyritic andesite and dacite lava flows, volcanic breccia and tuffs, and minor glassy lava flows and epiclastic sediments (Muessig, 1967; Pearson and Obradovich, 1977; Moye, 1984). The thickness of the Sanpoil Volcanics in the Republic graben exceeds 2,500 m (Muessig, 1967). K-Ar ages from the Sanpoil Volcanics range from 53.8 to 49.6 Ma (Pearson and Obradovich, 1977, as corrected by Fox and Beck, 1985).

The Klondike Mountain Formation consists of interstratified fine- to coarse-grained fossiliferous epiclastic sediments and minor andesite flows overlain by glassy lava flows (Muessig, 1967; Pearson and Obradovich, 1977; Gaylord and others, 1987, 1988). Recent research suggests that the total thickness of Klondike Mountain Formation strata in the Republic graben exceeds 1,000 m (D. R. Gaylord and S. M. Price, unpub. data). K-Ar dates from this stratigraphic sequence are inconclusive but suggest that deposition occurred during the Eocene between about 50.4 and 42.4 Ma (Pearson and Obradovich, 1977, as corrected by Fox and Beck, 1985).

Extensive dike swarms and small hypabyssal bodies of older high-K rhyolite and younger high-K hornblende dacite and andesite also occur within and adjacent to the Republic graben. The rhyolite dikes riddle plutonic rocks of the Keller Butte suite but predate the Devils Elbow suite (Atwater and Rinehart, 1984; Holder, 1986) and are thought to be the intrusive equivalent of the O'Brien Creek Formation (Pearson and Obradovich, 1977). The dacite and andesite dikes are correlative with the Scatter Creek Formation (nomenclature of Parker and Calkins, 1964), which is a hypabyssal intrusive equivalent of the Sanpoil Volcanics (Muessig, 1967).

Several lines of evidence lead to the conclusion, inferred by Moye (1984), that the Devils Elbow and Herron Creek suites are largely coeval and possibly comagmatic with the Sanpoil Volcanics and rhyolite domes that intrude the Sanpoil. The evidence includes: (1) the Devils Elbow and Herron Creek suites postdate the biotite rhyolite dikes but predate Klondike Mountain Formation volcanism (Muessig, 1967); (2) both the Devils Elbow suite and the medium-grained quartz monzonite intrusions of the Herron Creek suite grade into the hypabyssal Scatter Creek Formation (Muessig, 1967; Carlson, 1984; Moye, 1984; G. M. Holder, 1985; Holder, 1986); (3) the younger microgranite intrusions in the Herron Creek suite cut across the hornblende dacite bodies in several locations (Muessig, 1967; G. M. Holder, 1985; Holder, 1986), suggesting the microgranite may correlate with rhyolite domes that intrude the Sanpoil (Moye, 1984); and (4) the Devils Elbow suite and medium-grained quartz monzonite intrusions of the Herron Creek suite are chemically similar to the Sanpoil Volcanics (Moye, 1984; G. M. Holder, unpub. data).

Klondike Mountain Formation sedimentation and volcanism appear to postdate any recognized plutonic activity. Deposition of sedimentary strata in the lower part of the formation appears to have been restricted to local basins whose original margins are, in many places, obscured by postdepositional faulting.

Structural Relations of Plutonic, Volcanic, and Sedimentary Rocks with Associated Graben and Gneiss Dome Structures

Keller Butte suite intrusives were largely emplaced during Paleogene regional mylonitic deformation that formed the gneiss domes (Waters and Krauskopf, 1941; Pearson, 1967; Fox and others, 1976; Atwater, 1985; R. W. Holder, 1985), although some may predate dome formation. As a result, they commonly display the penetrative, generally west-trending mineral lineation characteristic of high-grade metamorphic rocks of the domes. In addition, at least one Keller Butte suite intrusion, the Coyote Creek pluton (Fig. 2), was emplaced during contemporaneous development of the Okanogan gneiss dome and the Republic graben (Atwater, 1985). Other suspected Keller Butte suite intrusives are so intensely deformed that they form layers of granitic orthogneiss within the high-grade metamorphic rocks of the domes.

Field evidence indicates that emplacement of the Devils Elbow suite was also contemporaneous with the formation of the Republic graben and Okanogan and Kettle gneiss domes. Intrusive contacts of this suite and associated Scatter Creek dike swarms commonly strike parallel to graben-bounding faults (Fig. 2) (Atwater and Rinehart, 1984; Moye, 1984; Holder, 1986), reflecting structural control by the graben on their emplacement. Some of the graben faults remained active long after solidification of the Devils Elbow suite, truncating both Devils Elbow suite and Herron Creek suite rocks (G. M. Holder, 1985; see below). These field relations require that the graben faults were active both before and after emplacement of the Devils Elbow suite, related Scatter Creek dikes, and any Sanpoil Volcanics coeval with the Devils Elbow suite and that the grabens must be, at least in part, Eocene in age.

Both the Swimptkin Creek and the Kettle Crest plutons of the Devils Elbow suite cut across deformed rocks in adjacent gneiss domes (Fox and others, 1976; Singer, 1984; G. M. Holder, 1985; Holder, 1986). However, both the western part of the Swimptkin Creek pluton adjacent to the Okanogan dome and the southern and southeastern parts of the Kettle Crest pluton adjacent to the Kettle dome are deformed along with the rocks they intrude. Locally, they are thoroughly mylonitized. The deformed rocks have mineral lineations parallel to the characteristic lineations of the gneiss domes (Singer, 1984;G. M. Holder, 1985; R. W. Holder, 1985, 1986). The observation that these two intrusions both cut and are deformed along with gneiss dome rocks suggests that the Devils Elbow suite was emplaced during the waning stages of mylonitic deformation associated with the domes. This indicates that dome formation extended well into Eocene time, and confirms Atwater's (1985) conclusion (noted above) that the Okanogan gneiss dome and Republic graben are contemporaneous.

The Herron Creek suite intrusions and those Scatter Creek dikes and upper Sanpoil Volcanics flows thought to be coeval with the Herron Creek suite predate the last movements along graben-bounding faults. However, these rocks have nowhere revealed any hint of deformation related to gneiss domes and may postdate dome formation.

It follows from the discussions above that the early biotite rhyolite intrusives and those Scatter Creek dikes and Sanpoil Volcanics flows correlative with the Devils Elbow suite were intruded or erupted during deformation of the gneiss domes. Though these dikes have not been observed to have been affected by dome-related regional mylonitic deformation, the extensive dike swarms flanking the east side of the Republic graben on the Colville Indian Reservation strike and dip perpendicular to stretching lineations in adjacent foliated granite in the Kettle gneiss dome (Holder, 1986). Tertiary regional extension in the central Okanogan Highlands was apparently accommodated by largely simultaneous regional ductile stretching (gneiss domes) and brittle development of extension fractures (grabens and dike swarms) with parallel ductile stretching and fracture dilation. In summary, intrusion of the Keller Butte and Devils Elbow suites, deposition of the O'Brien Creek Formation and the Sanpoil Volcanics, core complex emplacement, and Republic graben development are broadly contemporaneous and largely of early Tertiary (Paleogene) age. Extrusion of the upper Sanpoil Volcanics, intrusion of the Herron Creek suite, epiclastic sedimentation associated with Sanpoil volcanism, and Klondike Mountain Formation deposition apparently postdate regional mylonitization but predate the final stages of graben subsidence.

ACKNOWLEDGMENTS

The authors are grateful to P. R. Hooper, J. H. Bush, K. L. Stoffel, and R. E. Powell for constructive reviews of the manuscript. Financial support from the Washington Mining and Mineral Resource Institute, Washington State University Office of Grant and Research Development, Washington Department of Natural Resources, and Hecla Mining Company is gratefully acknowledged.

REFERENCES CITED

Atwater, B. F., 1985, The contemporaneity of the Republic graben and Okanogan gneiss dome [abstract]: Geological Society of America Abstracts with Programs, v.17, no. 6, p. 338.

Atwater, B. F.; Rinehart, C. D., 1984, Preliminary geologic map of the Colville Indian Reservation, Ferry and Okanogan Counties, Washington: U.S. Geological Survey Open-File Report 84-389, 4 sheets, scale 1:100,000 [sheets 1-3].

Bouma, A. H., 1962, Sedimentology of some flysch deposits–A graphic approach to facies interpretation: Amsterdam, Elsevier, 168 p.

Carlson, D. H., 1984, Geology and petrochemistry of the Keller Butte pluton and associated intrusive rocks in the south half of the Nespelem and the north half of the Grand Coulee Dam quadrangles, and the development of cataclasites and fault lenses along the Manila Pass fault, northeastern Washington: Washington State University, Doctor of Philosophy thesis, 181 p.

Fox, K. F., Jr.; Beck, M. E., Jr., 1985, Paleomagnetic results for Eocene volcanic rocks from northeastern Washington and the Tertiary tectonics of the Pacific Northwest: Tectonics, v. 4, no. 3, p. 323-341.

Fox, K. F., Jr.; Rinehart, C. D.; Engels, J. C., 1977, Plutonism and orogeny in north-central Washington–Timing and regional context: U.S. Geological Survey Professional Paper 989, 26 p.

Fox, K. F. Jr.; Rinehart, C. D.; Engels, J. C.; Stern, T. W., 1976, Age of emplacement of the Okanogan gneiss dome, north central Washington: Geological Society of America Bulletin, v. 87, no. 9, p. 1217-1224.

Gaylord, D. R.; Lindsey, K. A.; Thiessen, R. L., 1988, Eocene sedimentation and volcanism–Upper Sanpoil Volcanics to lower Klondike Mountain Formation transition, Republic graben, Washington [abstract]: Geological Society of America Abstracts with Programs, v. 20, no. 6, p. 415.

Gaylord, D. R.; Thiessen, R. L.; Mohl, G. B., 1987, Geology of Republic graben and implications for Eocene sedimentation in north-central portion of the Columbia Basin [abstract]: American Association of Petroleum Geologists Bulletin, v. 71, no. 8, p. 1006.

Holder, G. M., 1985, Geology and petrology of the intrusive rocks east of the Republic graben in the Republic quadrangle, Ferry County, Washington: Washington State University Master of Science thesis, 87 p.

Holder, R. W., 1985, The emplacement and geochemical character of the Colville batholith [abstract]: Geological Society of America Abstracts with Programs, v. 17, no. 6, p. 381.

Holder, R. W., 1986, Emplacement and geochemical evolution of Eocene rocks in the Colville batholith: Washington State University Doctor of Philosophy thesis, 189 p.

Holder, R. W.; Holder, G. M., 1988, The Colville batholith–Tertiary plutonism in northeast Washington associated with graben and core complex (gneiss dome) formation: Geological Society of America Bulletin, v. 100, no. 12, p. 1971-1980.

Moye, F. J., 1984, Geology and petrochemistry of Tertiary igneous rocks in the western half of the Seventeenmile Mountain quadrangle, Ferry County, Washington: University of Idaho Doctor of Philosophy thesis, 187 p.

Muessig, S. F., 1967, Geology of the Republic quadrangle and a part of the Aeneas quadrangle, Ferry County, Washington: U.S. Geological Survey Bulletin 1216, 135 p.

Parker, R. L.; Calkins, J. A., 1964, Geology of the Curlew quadrangle, Ferry County, Washington: U.S. Geological Survey Bulletin 1169, 95 p.

Pardee, J. T., 1918, Geology and mineral deposits of the Colville Indian Reservation, Washington: U.S. Geological Survey Bulletin 677, 186 p.

Pearson, R. C., 1967, Geologic map of the Bodie Mountain quadrangle, Ferry and Okanogan Counties, Washington, U.S. Geological Survey Geologic Quadrangle Map GQ-636, 4 p., 1 pl., scale 1:62,500.

Pearson, R. C.; Obradovich, J. D., 1977, Eocene rocks in northeast Washington–Radiometric ages and correlation: U.S. Geological Survey Bulletin 1433, 41 p.

Singer, S. H., 1984, Geology of the west half of the Disautel 15′ quadrangle, Okanogan County, Washington: University of Idaho Master of Science thesis, 101 p.

Streckeisen, A., 1976, To each plutonic rock its proper name: Earth Science Reviews, v. 12, no. 1, p. 1-33.

Waters, A. C.; Krauskopf, K. B., 1941, Protoclastic border of the Colville batholith: Geological Society of America Bulletin, v. 52, no. 9, p. 1355-1418.

Wolfe, J. A.; Wehr, Wesley, 1987, Middle Eocene dicotyledonous plants from Republic, northeastern Washington: U.S. Geological Survey Bulletin 1597, 25 p.

Road Log

Cumulative mileage is given on the left, interval mileage in parentheses.

0.0 (0.0) Start at the junction of Washington State Routes (SR) 20 and 21 N, 3 mi east of Republic. *Set odometer to 0.* Drive 6.8 mi east on SR 20 to the O'Brien Creek Road. Turn right (south) and proceed 1.0 mi on the O'Brien Creek Road.

7.8 (7.8) **STOP 1. O'Brien Creek Formation.**

Gray-white epiclastic and pyroclastic rocks of the O'Brien Creek Formation, which form the white flaggy bench midway up the slope 100 m north of the road, are the oldest of the Paleogene sedimentary and volcanic strata in the Republic graben. O'Brien Creek rocks are characterized by tuffaceous sandstone and conglomerate that unconformably overlie Paleozoic and Mesozoic metasedimentary units. Dark gray, angular, granule-sized slate and phyllite clasts are abundant in the O'Brien Creek sequence. Alteration of the ash obscures stratification and makes distinction between epiclastic and pyroclastic sequences in this unit difficult.

At this stop, the O'Brien Creek Formation exhibits evidence of rapid deposition and loading, including massive to crude stratification, normal grading, and flame structures. Elsewhere in the graben, O'Brien Creek Formation sediments are generally poorly sorted and crudely stratified. Primary sedimentary structures and lithofacies associations suggest that deposition occurred primarily in subaerial (probably alluvial) settings.

The O'Brien Creek Formation at this exposure, as in many other places near the graben margin, is intruded by a Scatter Creek dike. The Scatter Creek forms gray cliffy exposures upslope of the O'Brien Creek Formation. The contacts and chill zones between these two units are not well exposed; however, xenoliths of O'Brien Creek Formation have been incorporated in the Scatter Creek dike.

Continue south on the O'Brien Creek Road 3.0 mi. Turn right (west) onto the Snow Peak Road (unlabeled, T-junction). Drive 0.7 mi to the junction with the Hall Creek Road (U.S. Forest Service Road [FSR] 2050). Turn left (south). Bear right at Y-junction (2.0 mi) onto the Ninemile Road (FSR 2053). Drive 4.5 mi along the Ninemile Road to the junction with the Refrigerator Canyon Road. Turn right (north) and continue 0.1 mi.

18.1 (10.3) **STOP 2A. Sanpoil Volcanics.**

Sanpoil Volcanics form the bulk of exposures in the Republic graben. One of several displays of columnar jointing in andesitic to dacitic Sanpoil lavas is present across the small valley to the east. This exposure and localized horizontal colonnades visible in cliffs along the Sanpoil River and its side canyons may represent intracanyon flows that filled drainages eroded into older Sanpoil flows.

Continue north on the Refrigerator Canyon Road for an additional 1.0 mi.

19.1 (1.0) **STOP 2B. Sanpoil Volcanics.**

On the cliff to the east, the dip of the Sanpoil flows is highlighted by bands of columnar-jointed lavas. The structure of the Sanpoil Volcanics in the Republic graben is complex. However, in general, the central part of the Republic graben, from just north of Republic south to the Colville Indian Reservation, forms a poorly defined, asymmetric, north-trending syncline, the axis of which roughly corresponds to the Sanpoil River valley (Muessig, 1967).

Continue north on the Refrigerator Canyon Road 1.0 mi to the junction with the Hall Creek Road. Turn left (west) and drive 1.75 mi to SR 20. Turn left (west) onto SR 20 and drive 7.7 mi to the intersection of 6th and Clark Streets (at the flashing yellow light) in the center of the town of Republic. Turn left on SR 20 (toward Tonasket) and continue 0.55 mi to the outcrop on the right (north) side of the road.

30.1 (11.0) **STOP 3. O'Brien Creek Formation and upper Sanpoil Volcanics.**

The bleached, tuffaceous, epiclastic sediments of the O'Brien Creek Formation also seen at the first stop are well exposed along this part of the roadcut. Note the abundance of angular, granule-sized phyllite and slate clasts in the sandstones and conglomerates of these gently dipping strata. Gray-brown intrusive rocks of Scatter Creek, with near-vertical contacts, cut O'Brien Creek strata in this exposure.

Walk along the north side of the road east toward town. The NNW-trending valley you traverse corresponds with the trace of the Eureka fault, a major intragraben structure along which an estimated 500 m of displacement between the O'Brien Creek Formation strata (footwall) and Sanpoil Volcanics (hanging wall) has occurred. Highly altered strata of the upper part of the Sanpoil Volcanics, including a thick sequence of altered sandstones and cobble and boulder conglomerates, are exposed in the roadcut closest to town.

Return to the vehicles and drive 0.55 mi east on SR 20 back to the intersection of 6th and Clark Streets (flashing red light) in the center of Republic. Turn left at this intersection and drive 0.15 mi to the T. Turn left at the T and drive 0.15 mi along the Trout Creek Road. Park on the left (west) side of the road.

30.95 (0.85) **STOP 4. Contact of the Sanpoil Volcanics and Klondike Mountain Formation.**

The 10-m-high roadcut across the road from where you are parked exposes strata just above the contact between the Sanpoil Volcanics and the Klondike Mountain Formation (following the stratigraphic guidelines of Muessig, 1967). As noted by Muessig (1967), the contact is nowhere well exposed in the Republic Mining District. The conglomerates at the base of the exposure contain reworked pebble- to boulder-sized andesite and dacite clasts of the Sanpoil Volcanics. These conglomerates are overlain by laminated and thin-bedded mudstones and siltstones of the lowermost strata of the Klondike Mountain Formation. The conglomerate beds are alluvial in origin, whereas the mudstones and siltstones reflect dominantly lacustrine sedimentation.

Exposures of the Klondike Mountain Formation in the Republic graben are concentrated in two areas. The first encompasses approximately 50 km^2 in the Republic Mining District and the second covers about 100 km^2 (15 km to the north) near Curlew, Washington. Klondike Mountain Formation strata in the Republic Mining District are apparently conformable with the underlying Sanpoil Volcanics (Fig. 5). Detailed sedimentologic studies of the Klondike Mountain Formation have been undertaken only in the Republic Mining District. The limited extent of Klondike Mountain Formation strata in the graben largely reflects preferential preservation due to intragraben faulting. Gold mineralization

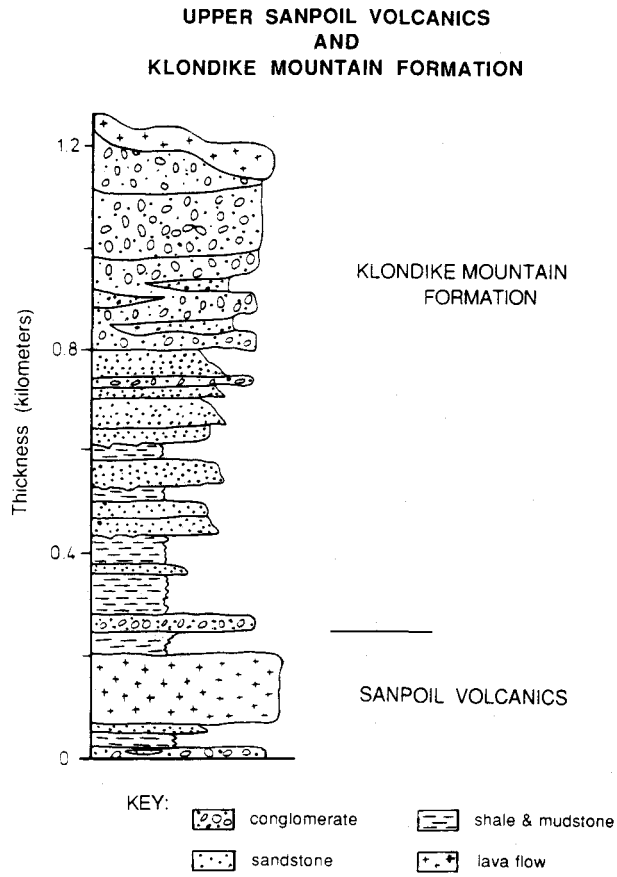

Figure 5. Composite stratigraphic section of upper Sanpoil Volcanics and Klondike Mountain Formation in the Republic Mining District.

(in older strata) commonly occurs beneath areas where Klondike Mountain Formation strata are preserved.

Sedimentary strata of the Klondike Mountain Formation coarsen upward from mudstones and siltstones in the lower one-third to sandstones in the middle one-third, to conglomerates and interstratified coarse sandstones and conglomerates in the upper one-third of the unit (Fig. 5). An episode of erosion and fluvial incision that followed deposition of the coarse-grained sediments in the upper part of the unit produced a local topographic relief of at least 150 m. Laterally extensive, black, glassy andesite flows cap the Klondike Mountain Formation sequence in this area and preserve the underlying paleorelief. The total composite thickness of the Klondike Mountain Formation in the Republic Mining District is approximately 1,000 m (D. R. Gaylord and S. M. Price, unpub. data).

Continue north 0.4 mi on the Trout Creek Road to the Couse Road (a private road). Turn right and drive 0.15 mi past the building. Park vehicles and walk approximately 150 m along the abandoned drill site access road.

31.50 (0.55) **STOP 5. Fossiliferous beds in the lower part of the Klondike Mountain Formation.**

The mudstones, siltstones, and some heterolithic sandstones from the lowest one-third of the Klondike Mountain Formation are renowned for their preservation of abundant plant, fish, and insect fossils. Wolfe and Wehr (1987) have identified 24 species of dicotyledonous plants in equivalent (Eocene) strata in the Republic and Toroda Creek grabens. They surmise that the flora grew in an upland microthermal mixed coniferous forest 700 to 900 m above sea level.

Drive back 0.15 mi to the Couse Road-Trout Creek Road intersection and turn right. Proceed 0.9 mi to the county road with a sign 'Not the Mine Entrance' on the right. Turn right and drive 0.3 mi along the county road (past the baseball field on the right) until you reach the T-intersection. At the T, turn left onto the gravel mine road and proceed 0.4 mi uphill to the tailings pond.

33.25 (1.75) **STOP 6. Lacustrine and turbidite deposits of the Klondike Mountain Formation.**

The lake basins in which much of the Klondike Mountain Formation accumulated were subject to periodic rapid infilling by sediment-laden streams. As a result, the fine-grained suspension deposits of the lakes are intercalated with both proximal and distal turbidites. Coarse-grained turbidites are most common in the middle third of the Klondike Mountain Formation sequence (Fig. 5). A number of 10- to 15-cm-thick (Bouma) ABE turbidite sequences (Bouma, 1962) are visible in this exposure. Notice that mafic dikes and sills have baked, intruded, and altered this epiclastic sequence.

Drive back along the mine road 0.4 mi to the T-junction. Continue east past the T along the county road. Turn left (north) 0.3 mi from the T in order to continue along the county road. Drive for 2.8 mi on the county road past the radio tower at the crest of the ridge.

36.75 (3.5) **STOP 7. Conglomerate beds and glassy volcanic flows of the Klondike Mountain Formation.**

The conglomerates and coarse-grained sandstones that characterize the upper one-third of the Klondike Mountain Formation typically are poorly exposed. This stop is no exception. However, as you walk toward the black, glassy, andesite flows prominently exposed on the ridge crest you will see a matrix-supported pebble, cobble, and boulder conglomerate exposed on the surface. The andesite and dacite clasts were derived from erosion of the Sanpoil Volcanics. Deposition probably occurred on alluvial fans. Fluvial incision during a subsequent hiatus created deep valleys into which the overlying andesites flowed. The flows are less than 100 m thick in the Republic Mining District but are two to three times thicker in the northern Republic graben and in the Toroda Creek graben (Parker and Calkins, 1964; Pearson, 1967).

Return to the Trout Creek Road intersection (3.4 mi), turn right and drive 2.1 mi north.

42.25 (5.5) **STOP 8. Bacon Creek fault zone.**

The scarp of the Bacon Creek fault is clearly exposed on the east side of the road. The graben margin fault juxtaposes plutonic rocks of the Herron Creek suite (to the west) against Sanpoil Volcanics (to the east). The fault zone is characterized by intense brecciation of wall rocks; slickensides are visible on the overhanging surface of the outcrop. The lithology and composition of the fragments within the fault zone are difficult to determine due to alteration.

Drive north 250 ft, turn left onto a logging road through the green metal gate, and continue 0.5 mi to outcrop on left (west). Climb 15 ft to natural outcrop exposure above the roadcut.

42.80 (0.50) **STOP 9. Quartz monzonite and microgranite of the Herron Creek suite.**

Both principal rock types of the Herron Creek suite are well exposed on the eastern slope of Stormking Mountain adjacent to and west of the Bacon Creek fault; Herron Creek suite microgranite intrudes Herron Creek suite quartz monzonite. The contact here is a textbook example of a chilled margin, but the contact is more commonly gradational over a few inches or is sharp, without chilling (see below).

Chlorite-filled fractures with slickenside striations at the base of the outcrop reflect proximity to the Bacon Creek fault.

Return 4.5 mi to the stoplight in Republic. Drive 2.5 mi west on SR 20; turn left (south) at junction with Swamp Creek Road. At 9.8 mi, turn right onto FSR 5314. Bear right at Y-junction at 5.0 mi, odometer reading 54.25, and follow directions to Swan Lake (FSR 5330). After 1.8 mi on FSR 5314, turn left (east) onto a small spur road (FSR 5314-450) and drive 0.1 mi onto the quarry floor.

61.25 (18.45) **STOP 10. Leucocratic biotite granite and granodiorite of the Keller Butte suite.**

The Keller Butte suite consists of large plutons of light colored biotite granite and granodiorite with locally abundant and commonly garnetiferous aplo-pegmatite (Figs. 2, 3). Penetrative mineral fabrics are characteristic of these intrusions adjacent to or within areas affected by mylonitic deformation associated with the Kettle and Okanogan domes and are largely absent away from these areas. In this quarry on the eastern edge of the Okanogan gneiss dome, main phase granodiorite with a well-developed mineral fabric is cut by several pegmatite veins and dikes. Both the granodiorite and pegmatite contain garnet. Garnet in the main phase of Keller Butte suite rocks is atypical. Xenoliths of garnet-biotite schist in various stages of digestion have been observed in this area and suggest the garnet in the main phase may be xenocrystic.

Return 0.1 mi to FSR 5314, and drive south (left) 4.5 mi to the Scatter Creek Road (FSR 53). Turn right and continue 7.3 mi to the junction with SR 21. Turn left (north) and drive 7.0 mi. Turn right at the junction with SR 20; drive 3.0 mi. Then bear left at breakoff of SR 21 north to Curlew. After 19.0 mi, turn right onto the West Deer Creek Road (unlabeled) across from the Blue Cougar Cafe. At 0.3 mi, keep right and follow arrow to U.S. Highway 395, bypassing the town of Curlew on the east. Park at the east end of the roadcut on the spur road on the north side of the road, 9.55 mi past the junction with the fork into the town of Curlew.

120.00 (50.75) **STOP 11. Herron Creek suite microgranite and quartz monzonite of the Long Alec Creek pluton.**

The largest known mass of microgranite in the Herron Creek suite makes up most of the Long Alec Creek pluton (Fig. 2). Xenoliths of quartz monzonite of the Herron Creek suite are included in the microgranite. Basaltic dikes of unknown age, representing a very late episode of magmatism in the Okanogan Highlands, cut both the quartz monzonite and the microgranite.

Continue east on the West Deer Creek Road 1.8 mi to Deer Creek Summit. Walk about 150 ft along the road to the large outcrop on the left.

113.80 (1.8) **STOP 12. Quartz monzodiorite of the Devils Elbow suite.**

At the Deer Creek Summit, microgranite dikes of the Herron Creek suite cut medium-grained, equigranular biotite-hornblende quartz monzodiorite of the Devils Elbow suite. Devils Elbow suite rocks have a remarkably uniform texture and composition throughout the region. The large outcrops of Devils Elbow suite at this stop are thought to be stope blocks in the Herron Creek suite Long Alec Creek body (Charles Knaack, Washington State Univ., oral commun., 1988).

End of road log. To return to the junction of SR 21N and SR 20, turn around and drive west 11.65 mi, back to the junction of the West Deer Creek Road with SR 21N. Turn left (south) and continue 19.0 mi to the junction at the start of this road log. From this point, Republic is 3.0 mi to the west (right) and Kettle Falls and Colville are approximately 40 and 50 miles to the east, respectively.

Kettle Gneiss Dome: A Metamorphic Core Complex in North-Central Washington

Kenneth F. Fox, Jr.
U.S. Geological Survey
Box 25046, MS 913, Federal Center
Denver, CO 80225
and
J. R. Wilson
Law Environmental
112 Townpark Drive
Kennesaw, GA 30144

INTRODUCTION

The Kettle gneiss dome is one of several bodies of lineated and foliated high-grade metamorphic and syntectonic plutonic rocks that are commonly referred to as metamorphic core complexes (Davis and Coney, 1979) and that occupy extensive areas of north-central and northeastern Washington. The complexes (Fig. 1) include, in addition to the Kettle gneiss dome, the Okanogan gneiss dome (Fox and Rinehart, 1988), the metamorphic rocks of Tenas Mary Creek (Parker and Calkins, 1964), the Lincoln gneiss dome (Atwater and Rinehart, 1984), the Selkirk crest complex (Miller, 1983), and the Spokane dome (Cheney, 1980, p. 470).

The gneiss domes are distinguished by the presence of rocks of medium to high metamorphic grade with flat to shallowly outward-dipping layering and foliation, which define a large-scale domal or antiformal structure, and by the presence of penetrative lineation and cataclastic fabrics[1]. The degree of cataclasis typically intensifies upwards and outwards toward low-angle extensional (detachment) faults that locally bound the gneiss domes. Metamorphic rock in the interiors of the domes consists chiefly of orthogneiss and(or) paragneiss, schist, marble, quartzite, and amphibolite, dominantly of amphibolite facies but grading locally to greenschist facies.

Country rocks outside these metamorphic complexes in the eastern part of the region consist chiefly of unmetamorphosed to strongly metamorphosed Precambrian sedimentary rocks (Deer Trail Group and Belt Supergroup) and Paleozoic strata, locally invaded by plutonic rocks of Jurassic to Eocene age. Country rocks in the western part of the region consist chiefly of weakly to strongly metamorphosed Ordovician (Covada Group, Snook and others, 1981), Permian (Anarchist Group and its correlatives, Rinehart and Fox, 1972; Fox and others, 1977), and Upper Triassic (Kobau Formation, Rinehart and Fox, 1972; Cave Mountain Formation, Rinehart and Fox, 1976) rocks, locally invaded by Upper Triassic to Eocene plutonic rocks. The western rocks are inferred to be part of Quesnellia, an allochthonous terrane or superterrane that was sutured to the craton during the Jurassic (Monger and others, 1982).

[1] Terminology for cataclastic rocks follows that of Higgins (1971). He divides cataclastic rocks that have fluxion structure (a cataclastically produced foliation) into two groups. Those in which cataclasis was dominant over recrystallization include protomylonite, mylonite, and ultramylonite. Those in which recrystallization was dominant include mylonite gneiss and blastomylonite. Ultramylonite consists of sparse porphyroclasts generally less than 0.2 mm in diameter dispersed through an aphanitic matrix of finely crushed minerals. Mylonite consists of 10 to 50 percent porphyroclasts generally larger than 0.2 mm embedded in an aphanitic to very fine grained matrix of crushed minerals. Protomylonite consists of lenticular masses of rock separated by megascopic gliding surfaces filled with finely crushed rock. Blastomylonite is similar in megascopic fabric to the rocks listed above, but porphyroclasts are embedded in a granular mosaic of unstrained, metamorphically recrystallized minerals.

From: Joseph, N. L., and others, editors, 1989, Geologic guidebook for Washington and adjacent areas: Washington Division of Geology and Earth Resources Information Circular 86.

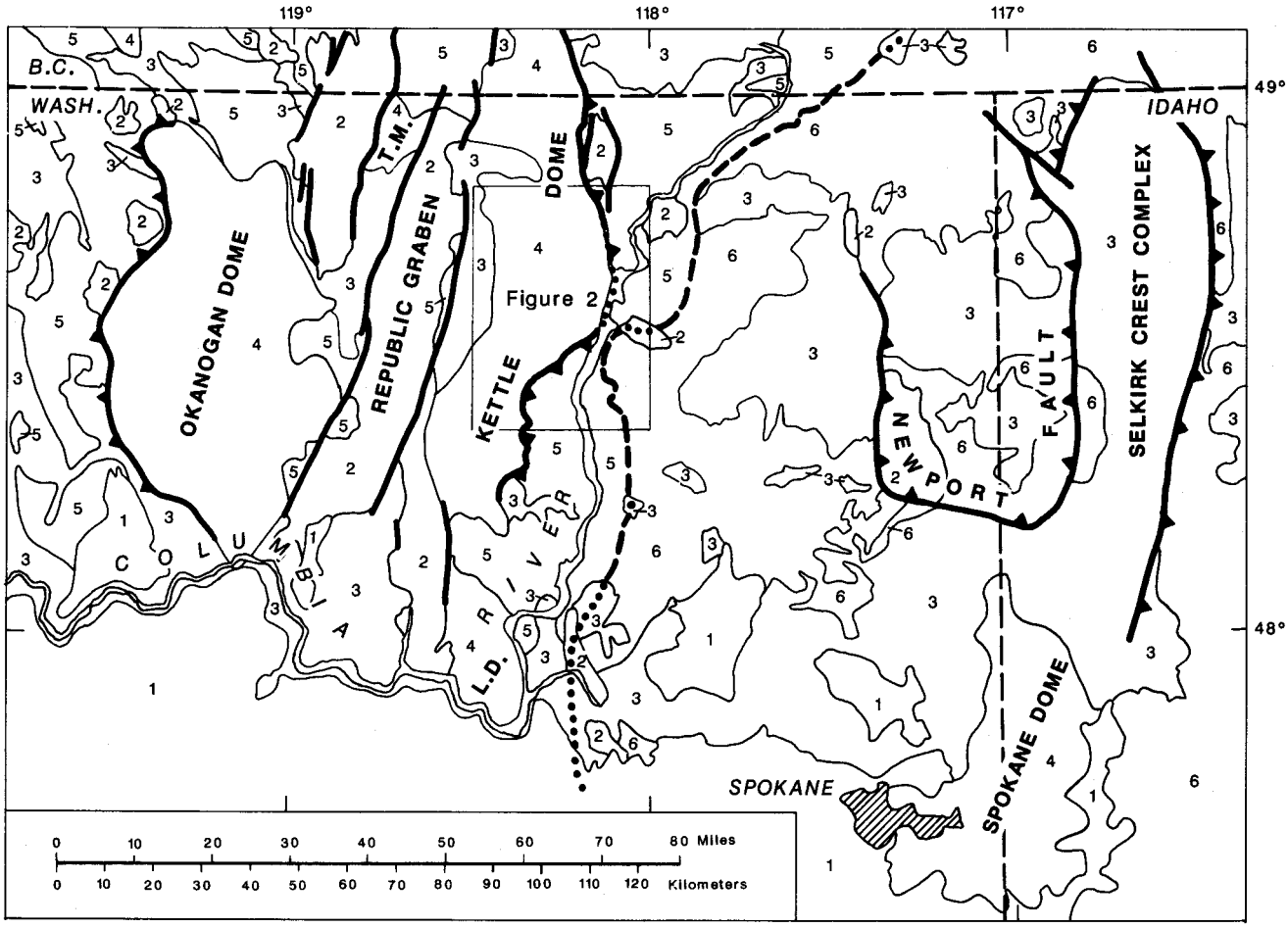

EXPLANATION

1	Columbia River Basalt Group (Miocene)
2	Volcanic and volcaniclastic rocks (Eocene)
3	Plutonic igneous rocks (Upper Triassic to Eocene)
4	Foliated and lineated paragneiss, orthogneiss, quartzite, marble, amphibolite, and schist (age of protolith: Precambrian to Cretaceous) and syntectonic plutonic rocks (Paleocene(?) to Eocene)
5	Oceanic rocks (Ordovician to Upper Triassic, possibly includes Lower Jurassic)
6	Miogeoclinal rocks (Precambrian to Mississippian)

Contact

Low-angle extensional faults (teeth on upper plate)

High-angle extensional faults

Inferred suture. Dotted where concealed

Figure 1. Distribution of gneiss domes and associated features in north-central and northeastern Washington (modified from plate 1, Cady and Fox, 1984). L.D., Lincoln gneiss dome; T.M., metamorphic rocks of Tenas Mary Creek.

Eocene volcanic and volcaniclastic rocks and intercalated breccias (Pearson and Obradovich, 1977) discontinuously overlie older sedimentary and plutonic rocks and fill grabens fringing the gneiss domes. Depositional contacts of the volcanic rocks on the Kettle and Okanogan gneiss domes have not been found. However, dikes and Eocene plutonic rocks, thought to be the hypabyssal equivalents of the volcanic rocks, intrude the gneiss domes. (See, for example, the map encompassing part of the Kettle gneiss dome by Pearson, 1977.)

The Kettle dome was recognized as an area of cataclastically deformed para- and orthogneiss by Little (1957), Preto (1965, 1970), and Fox and others (1976) and named and described by Cheney (1976, 1980). According to Cheney, the Kettle dome is antiformal, exposing a sequence of metamorphic rocks greater than 3,400 m thick, and consists of interlayered granitic gneiss, amphibolite, feldspathic quartzite, biotite schist, and marble. The gneiss dome encompasses a linear, north-trending gneissic terrain that is approximately 125 km long and 30 km wide. In its central part the dome is an asymmetrical antiform; it has a steeply west-dipping western limb, a broad, nearly flat medial arch, and a shallowly east-dipping eastern limb (Fig. 2). The western flank of the gneiss dome has been extensively invaded by syntectonic and post-tectonic granitic plutons. The eastern flank of the gneiss dome is faulted against lower grade country rocks along the Kettle River fault (Rhodes and Cheney, 1981), an east-dipping low-angle fault. Rocks of granitic composition within the dome consist chiefly of mylonitic gneiss in the central part, grading upward and outward to blastomylonite, mylonite, and ultramylonite.

DISCUSSION

Campbell (1938, 1946) suggested that the rocks now believed to be the eastern part of the Kettle gneiss dome (near the intersection of U.S. Highway 395 and State Route 20) were the crushed border facies of a large batholith, whose main mass lay to the west. He (1946) attributed the crushing to protoclasis attending emplacement of the batholith.

Cheney (1980) postulated that the low-angle fault zones bordering the gneiss domes in the region were zones of decoupling—possibly major thrusts or a series of thrusts, or purely local phenomena—between batholithic and pre-Beltian(?) rocks below and Precambrian to Tertiary layered rocks above. He suggested that the batholithic and pre-Beltian(?) rocks were exposed through post-Eocene folding and erosion. In his view, the Kettle dome forms the core of one of these arch-like folds, which regionally have amplitudes of a few kilometers and wave lengths of tens of kilometers. The Republic graben, adjoining on the west, forms one of the complementary synclines.

Wilson (1981b) suggested that the Kettle dome comprised a series of nappe-like diapirs, each cored by granitic gneiss enveloped within a mantle of metasedimentary rocks. In his interpretation, the diapirs flowed horizontally northward, then flattened, with the dominant extension direction during flattening perpendicular to the initial northward direction of horizontal flow.

Price (1980) attributed the gneiss domes to crustal-scale megaboudinage associated with lithospheric stretching. Fox and Beck (1985, p. 334) postulated that areas of relatively undeformed upper crustal rock between or alongside the gneiss domes are the megaboudins and that the gneiss domes are the ductile matrix. Expanding on this idea, Fox and Rinehart (1988) suggested that the Okanogan dome is a part of the ductile middle crust that flowed laterally and bulged upwards at a crustal pull-apart and finally froze into place in the upper crust in middle Eocene time. The Kettle dome may have formed through an analogous process.

In evaluating the applicability of these and other hypotheses to the Kettle dome, certain key features should be considered. These include (1) internal and external contact relations with datable units, which bears on the age of the protolith, the age of dynamic metamorphism, and the age of the bordering low-angle faults; (2) fabric of the cataclastically deformed rocks, which bears on the nature of internal strain; (3) metamorphic petrology of the rocks within the gneiss dome, which bears on the depth and temperature at which metamorphic minerals crystallized.

ACKNOWLEDGMENTS

The authors appreciate constructive reviews of the manuscript by F. Barker, G. A. McCarley Holder, W. D. Johnson, Jr., K. L. Stoffel, and R. E. Powell.

REFERENCES CITED

Atwater, B. F.; Rinehart, C. D., 1984, Preliminary geologic map of the Colville Indian Reservation, Ferry and Okanogan Counties, Washington: U.S. Geological Survey Open-File Report 84-389, 20 p., 4 pl., scale 1:100,000.

Cady, J. W.; Fox, K. F., Jr., 1984, Geophysical interpretation of the gneiss terrane of northern Washington and southern British Columbia,and its implications for uranium exploration: U.S. Geological Survey Professional Paper 1260, 29 p., 1 pl., scale 1:1,000,000.

Campbell, C. D., 1938, An unusually wide zone of crushing in the rocks near Kettle Falls, Washington: Northwest Science, v. 12, no.4, p. 92-94.

Campbell, C. D., 1946, Structure in the east border of the Colville batholith, Washington [abstract]: Geological Society of America Bulletin, v. 57, no. 12, pt. 2, p. 1184-1185.

Cheney, E. S., 1976, Kettle dome, Okanogan Highlands, Ferry County, Washington [abstract]: Geological Society of America Abstracts with Programs, v. 8, no. 3, p. 360.

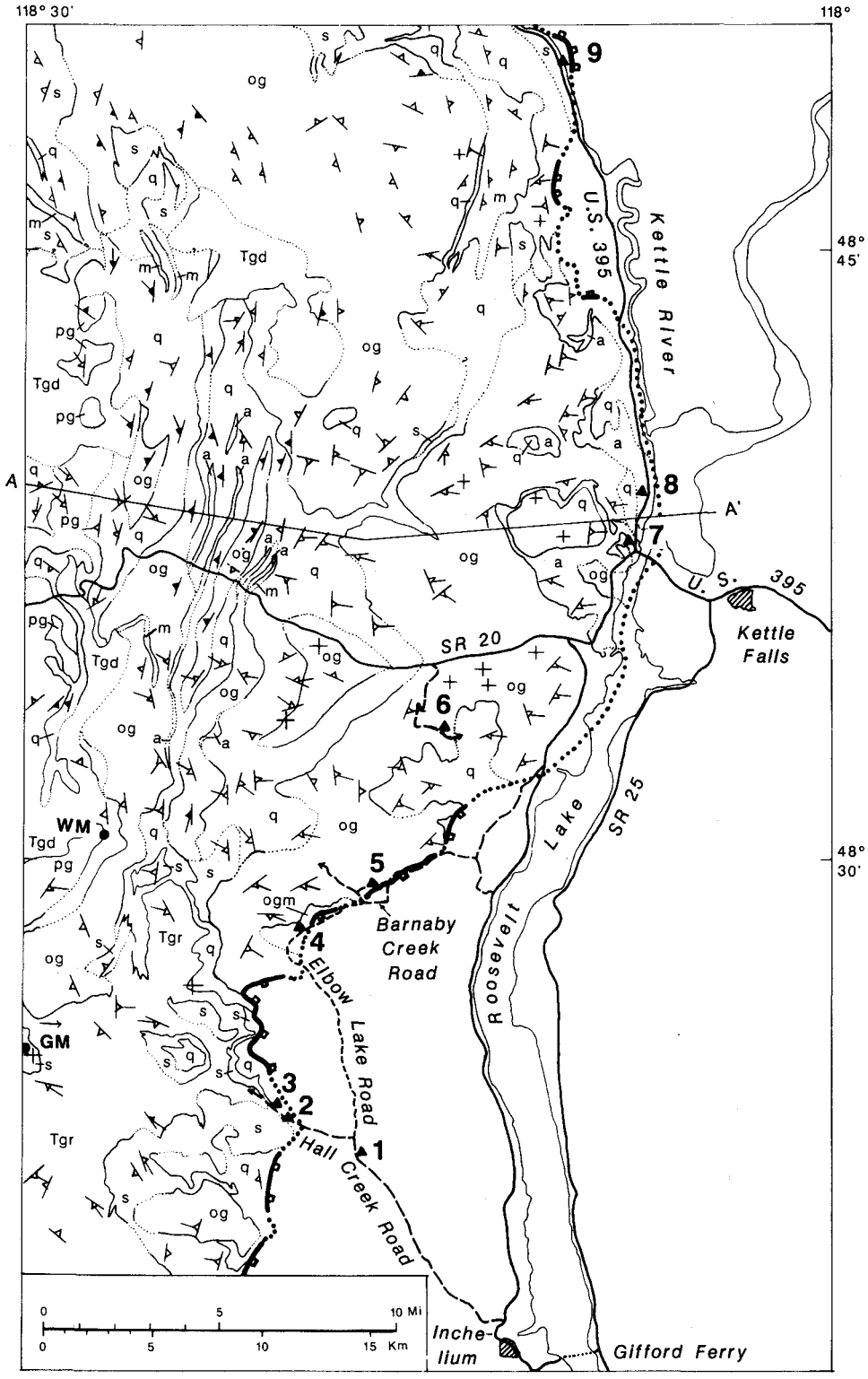

Figure 2. Geologic map of a portion of the Kettle gneiss dome, route of field trip, and localities described in road log. Location of map area is shown on Figure 1. GM, Grizzly Mountain; WM, White Mountain.

EXPLANATION

Tgd	Eocene	Chiefly hornblende-biotite granodiorite
Tgr		Biotite- and muscovite-biotite granite and pegmatite with intercalated schist
pg, a, q, m, s, og, ogm	Eocene to Paleocene(?) 1/	pg: Paragneiss; a: Amphibolite; q: Quartzite; locally includes interlayers of schist; m: Marble; s: Schist; includes interlayers of calc-silicate gneiss, quartzite; og: Orthogneiss, augen gneiss (light gray); ogm: Orthogneiss (medium gray)
MzPzs	Paleozoic to Mesozoic	Sedimentary rocks (in cross-section)

1/Refers to age of penetrative dynamic metamorphism. Age of protolith unknown

Contact, dotted where concealed

Fault, low-angle extensional (detachment), teeth on upper plate

(0–15°) (>15–45°) (>45°) (with lineation)

Foliation, showing dip, and strike of lineation within plane of foliation

Unimproved Graveled Paved

Roads

Source of data

A	B	
C	D	
	E	
F		

A Pearson, 1977
B Rhodes, 1980
C Wilson, J.R., unpublished mapping
D Wilson, 1980
E Wilson, 1981a
F Fox, K.F., Jr., unpublished mapping

▲9

Field trip stop

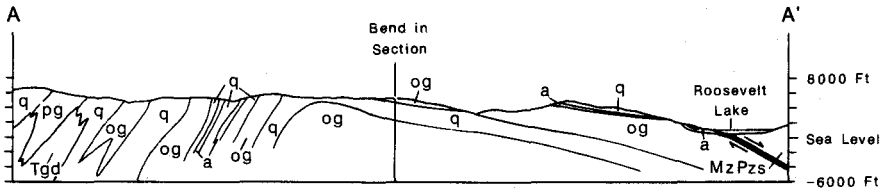

Cheney, E. S., 1980, Kettle dome and related structures of northeastern Washington. *In* Crittenden, M. D., Jr.; Coney, P. J.; Davis, G. H., editors, 1980, Cordilleran metamorphic core complexes: Geological Society of America Memoir 153, p. 463-483.

Davis, G. H.; Coney, P. J., 1979, Geologic development of the Cordilleran metamorphic core complexes: Geology, v. 7, no. 3, p. 120-124.

Donnelly, B. J., 1978, Structural geology of the Nancy Creek area, east flank of the Kettle dome, Ferry County, Washington: Washington State University Master of Science thesis, 251 p.

Fox, K. F., Jr.; Beck, M. E., Jr., 1985, Paleomagnetic results for Eocene volcanic rocks from northeastern Washington and the Tertiary tectonics of the Pacific Northwest: Tectonics, v. 4, no. 3, p. 323-341.

Fox, K. F., Jr.; Rinehart, C. D., 1988, Okanogan gneiss dome – A metamorphic core complex in north-central Washington: Washington Geologic Newsletter, v. 16, no. 1, p. 3-12.

Fox, K. F., Jr.; Rinehart, C. D.; Engels, J. C., 1977, Plutonism and orogeny in north-central Washington–Timing and regional context: U.S. Geological Survey Professional Paper 989, 27 p.

Fox, K. F., Jr.; Rinehart, C. D.; Engels, J. C.; Stern, T. W., 1976, Age of emplacement of the Okanogan gneiss dome, north-central Washington: Geological Society of America Bulletin, v. 87, no. 9, p. 1217-1224.

Higgins, M. W., 1971, Cataclastic rocks: U.S. Geological Survey Professional Paper 687, 97 p.

Little, H. W., 1957, Kettle River (east half), Similkameen, Kootenay and Osoyoos districts, British Columbia: Geological Survey of Canada Map 6-1957, 1 sheet, scale 1:253,440.

Lyons, D. J., 1967, Structural geology of the Boulder Creek metamorphic terrane, Ferry County, Washington: Washington State University Doctor of Philosophy thesis, 115 p.

Miller, F. K., 1983, Preliminary geologic map of the Priest Lake area, Idaho: U.S. Geological Survey Open-File Report 82-1063, 25 p., 1 pl.

Mills, J. W., 1985, Geologic maps of the Marcus and Kettle Falls quadrangles, Stevens and Ferry Counties, Washington: Washington Division of Geology and Earth Resources Geologic Map GM-32, 18 p., 2 pl., scale 1:24,000.

Monger, J. W. H.; Price, R. A.; Tempelman-Kluit, D. J., 1982, Tectonic accretion and the origin of the two major metamorphic and plutonic welts in the Canadian Cordillera: Geology, v. 10, no. 2, p. 70-75.

Parker, R. L.; Calkins, J. A., 1964, Geology of the Curlew quadrangle, Ferry County, Washington: U.S. Geological Survey Bulletin 1169, 95 p., 4 pl.

Pearson, R. C., 1977, Preliminary geologic map of the Togo Mountain quadrangle, Ferry County, Washington: U.S. Geological Survey Open-File Report 77-371, 1 sheet, scale 1:48,000.

Pearson, R. C.; Obradovich, J. D., 1977, Eocene rocks in northeast Washington–Radiometric ages and correlation: U.S. Geological Survey Bulletin 1433, 41 p., 1 pl.

Preto, V. A., 1965, Structural relations between the Shuswap terrain and the Cache Creek Group in southern British Columbia [abstract]: Canadian Mining Journal, v. 86, no. 1, p. 90.

Preto, V. A. 1970, Structure and petrology of the Grand Forks Group, British Columbia: Geological Survey of Canada Paper 69-22, 80 p.

Price, R. A., 1980, The southeastern Canadian Cordillera–Superimposed divergent, convergent, and strike-slip displacements at the western margin of the North American Plate [abstract]: Geological Association of Canada Programme and Abstracts, v. 5, p. 77.

Rhodes, B. P., 1980, Structure of the east flank of Kettle dome, Ferry and Stevens Counties, Washington: University of Washington Master of Science thesis, 97 p., 2 pl.

Rhodes, B. P.; Cheney, E. S., 1981, Low-angle faulting and the origin of Kettle dome, a metamorphic core complex in northeastern Washington: Geology, v. 9, no. 8, p. 366-369.

Rinehart, C. D.; Fox, K. F., Jr., 1972, Geology and mineral deposits of the Loomis quadrangle, Okanogan County, Washington: Washington Division of Mines and Geology Bulletin 64, 124 p., 3 pl.

Rinehart, C. D.; Fox, K. F., Jr., 1976, Bedrock geology of the Conconully quadrangle, Okanogan County, Washington: U.S. Geological Survey Bulletin 1402, 58 p.

Snook, J. R.; Lucas, H. E.; Abrams, M. J., 1981, A cross section of a Nevada-style thrust in northeast Washington: Washington Division of Geology and Earth Resources Report of Investigations 25, 9 p.

U.S. Geological Survey, 1974, Comparison of Anarchist and Covada Groups of north-central Washington: U.S. Geological Survey Professional Paper 900, p. 50.

Wilson, J. R., 1980, Preliminary geologic map of the Boyds quadrangle, Ferry and Stevens Counties, Washington: U.S. Geological Survey Open-File Report 80-983, 2 sheets, scale 1:24,000.

Wilson, J. R., 1981a, Geologic map of the Bangs Mountain quadrangle, Ferry and Stevens Counties, Washington: U.S. Geological Survey Open-File Report 81-581, 2 sheets, scale 1:24,000.

Wilson, J. R., 1981b, Structural development of the Kettle gneiss dome in the Boyds and Bangs Mountain quadrangles, northeastern Washington: Washington State University Doctor of Philosophy thesis, 156 p.

Road Log

Cumulative mileage is given on the left; mileage from previous locality is in parentheses.

0.0 (0.0) Start of trip. (*Set odometer to 0.0 miles.*) Gifford Ferry, western landing. Proceed westward on highway.

2.6 (2.6) Enter Inchelium. Gasoline and groceries available.

2.7 (0.05) Intersection with Twin Lakes Road. Continue straight ahead.

4.35 (1.65) Intersection. Turn left (west) on Hall Creek road.

8.45 (4.1) Intersection with Lynx Creek road on the left. Continue straight ahead toward Hall Creek. Note scattered outcrops of phyllite and graywacke of Covada Group.

11.2 (2.75) **STOP 1. Covada Group.**

Pass the outcrop and roadcuts on the right (east) and park off the road on the right (east). Walk back to the roadcuts.

The roadcuts expose rubbly, medium-gray slate and light brownish-gray to light greenish-gray calcareous phyllitic wacke. Foliation strikes N30°W and dips 65 degrees to the northeast. Rocks are multiply folded; horizontal fold axes striking N85°W; a second set plunges approximately 10 degrees S35°E.

Rocks of the Covada Group form much of the country rock southeast of the Kettle gneiss dome. The rocks at this locality were probably metamorphosed within the greenschist facies, typical of the Covada Group close to the gneiss dome. Correlative strata to the east and southeast appear distinctly less metamorphosed. In addition to lithologies observed here, the Covada Group includes black slate and argillite, greenstone, limestone, and dark bluish-gray quartzite. Wackes are composed in part of coarse-grained granitic detritus and locally include as much as 30 percent K-feldspar. The Covada Group probably formed as thick, bathyal marine turbidites (U.S. Geological Survey, 1974). Fossils from the eastern part of the Covada Group are of Ordovician age (Snook and others, 1981).

Continue northward on Hall Creek road.

12.85 (1.65) Intersection. Elbow Lake road continues straight ahead (north), Hall Creek road to the left (west). Turn left toward Hall Creek. Rocks in the rubbly outcrop to the east are calcareous greenish- to brownish-gray phyllite of the Covada Group.

14.65 (1.8) **STOP 2. Quartzite forming outer layer of gneiss dome.**

Park off the road and hike to the low cliff at the base of slope to the north.

Rocks are interlayered light-gray mylonitic quartzite and dark-gray mica schist containing tiny garnet porphyroblasts. Lineation is penetrative, plunging gently S80°-86°E. Layering and foliation are parallel, rolling from gentle south to northeast dips. One intrafolial (isoclinal recumbent) fold was observed, plunging gently S60°E, with lineation curving obliquely around the fold hinge.

This unit forms the outer layer of the gneiss dome in this area. It dips homoclinally a few degrees to the southeast. The contact with the Covada Group uphill to the north is concealed, but it appears to parallel the quartzite and to truncate strata of the Covada Group.

Continue northward on Hall Creek road.

15.45 (0.8) **STOP 3. Interlayered quartzite and schist with infolded pegmatite dikes.**

Park off the road on the right (north); elevation is approximately 2,275 ft. Hike to the base of the ledgy slope to the north; then climb to the top of the rounded, treeless cliff (elevation approximately 2,880 ft or 600 ft above road level). In climbing, work to the west and north around the upper cliff.

At the base of the ledgy slope (elevation 2,315 ft), protomylonitic light-gray pegmatite containing coarse-grained muscovite and tiny red garnets is infolded with interlayered quartzite and biotite schist. The quartzite has thin muscovite-rich laminae. Layering and foliation are concordant, dipping approximately 5 degrees eastward. Lineation is penetrative in all lithologies, lying in the plane of foliation and trending approximately S75°E.

Higher on the slope (elevation approximately 2,500 ft), slightly discordant (to foliation and layering) protomylonitic granitic dikes are exposed. At first glance, the dikes appear to be sills, but in places the sill-like bodies can be followed into and through fold hinges. At approximately 2,630 ft elevation, the granitic dikes weather into cavernous zones under steep cliffs developed in massive white quartzite above. (Work to the west and north on benches below the upper cliff.) The granitic dikes cut the quartzite and are folded into recumbent isoclinal folds; the fold axis of one well-exposed hinge is approximately horizontal and trends S75°E. The original attitude of the dikes is unknown. If steep, as seems possible, it is likely that the dikes were subsequently transposed to near horizontal attitudes though movement (simple shear) along the foliation planes.

Rocks above the cliff, underlying the false summit at 2,880 ft elevation, are dark gray, garnetiferous biotite schist in which lineation trends S67°E. To the north of this point, the tree-clad skyline and ledgy slopes below expose weakly metamorphosed rocks of the Covada Group, in which primary depositional textures and structures are preserved. The contact between the gneiss dome and the Covada Group is covered, but it must truncate section in the Covada Group and conform approximately to the homoclinal, east-dipping quartzite and schist unit below us. To the south, however, the dip of foliation and layering within the gneiss dome near its eastern contact locally reverses and turns west. There the contact dips moderately to the east and cuts across structure and stratigraphy of both the Covada Group and the gneiss dome.

The massive white quartzite exposed in the cliff below can be traced northwestward in discontinuous outcrop for 8 mi, cropping out at an elevation of 5,200 ft on the eastern flank of White Mountain (Fig. 2). Erosional outliers of white quartzite, probably correlative with this unit, form Paint Rock (northern summit area of Grizzly Mountain) approximately 7-1/2 mi to the west at an elevation of 6,397 ft. If the quartzite on or near these summits occupies the same structural position relative to the outer surface of the gneiss dome as the supposedly correlative unit does here and at Stop 2, then dissection of the dome through erosion of nearby canyons (such as Hall Creek Canyon) exposes a scant 1.3 km of structural relief in this area. For the gneiss dome as a whole, Cheney (1980) has estimated that less than 3 km of structural relief is exposed.

Descend to the vehicles. Turn the vehicles around and drive eastward, retracing route to the intersection with Elbow Lake road.

18.05 (2.6) Intersection with Elbow Lake road. Turn left (north) toward Elbow Lake. (This is a fair weather road only.)

22.45 (4.4) Cliffs and ledgy slopes to the west and north outline a re-entrant in the eastern exterior wall of the gneiss dome.

23.25 (0.8) **STOP 4. Cataclastic orthogneiss.**

Park vehicles and hike to outcrops forming a ledgy slope 75 to 100 m to the north.

The rock is a greenish-gray orthogneiss without coherent foliation or lineation, although locally a crude foliation parallel to the slope is present. In places, the rocks appear to have two intersecting foliations, of which the earlier (F1) is crudely parallel to slope. F1 is cut, dragged, and distorted by multiple intersecting shears spaced 1 to 10 cm apart, dipping steeply, and striking N10° to 30°E. Neither foliation is judged to be a fluxion structure since porphyroclasts do not appear to be rotated. The gneiss appears to be a crushed, brecciated, and rehealed granitic rock. It forms a lensoidal body, armoring the southern flank of the gneiss dome in this area.

Hills to the south and east (Ant Mountain) are underlain by phyllite of the Covada Group. The contact is concealed, but it is presumed to be a fault conformable with the south-facing slope at this locality.

Return to the vehicles and continue eastward on the Elbow Lake Road.

25.45 (2.2) Northern boundary of Colville Indian Reservation and junction with Barnaby Creek Road. Turn left (west) toward Barnaby Creek.

25.85 (0.4) Intersection. Turn right (east) on U.S. Forest Service Road 028.

26.15 (0.3) **STOP 5. Internal and external contacts of gneiss dome.**

Park in the borrow pit. The ledgy slope to the east exposes rubbly, rusty brown to greenish-gray weathering, brecciated to fractured granite. The granite is composed of quartz, microcline, zoned plagioclase, relict biotite, chlorite, with accessory sphene and apatite. The granite forms

a small pluton of about one square kilometer area, tapering northeastward to a sill-like body. The granite intrudes interlayered medium gray limestone and brownish gray silty limestone of the Covada Group.

Brecciation and fracturing within the granite increase gradually toward its contact (concealed) with the gneiss dome to the west.

Hike 100 m north to outcrops at the base of the northwest-facing slope. Outcrops expose 30 to 40 m of medium gray biotite- and tourmaline-bearing, laminated, impure quartzite interlayered with light gray micaceous quartzite. The sequence dips homoclinally to the south-southeast 20 to 40 degrees. Rocks are strongly lineated and penetratively foliated, locally boudinaged and isoclinally folded. Lineation and fold axes plunge 70° to 87°E in the plane of foliation. These rocks probably are part of the gneiss dome.

Hike 150 m northeast, crossing the east-northeast-trending meltwater channel (forested, with much brush and deadfall). Ledgy slopes expose protomylonitic augen gneiss with foliation dipping 20 to 25 degrees to the south-southeast, and penetrative lineation plunging to S82°E in the plane of foliation. The augen gneiss is homogeneous except for thin layers of sheared pegmatites that are nearly conformable with foliation. The protomylonitic augen gneiss forms much of the slope to the north; foliation dips 25 to 30 degrees to south-southeast, nearly parallel to the slope.

Contour around the slope approximately 400 m ENE to the contact of the quartzite unit described above with the protomylonitic augen gneiss. The quartzite is exposed low on the slope, where it forms flatirons overlying the gneiss and dips conformably with foliation noted above. Near the contact, the gneiss consists of interlayered (and intergradational) ultramylonite, mylonite, and protomylonite. Lineation is penetrative, defined by a micro-ripple in the foliation surface. From a distance, the lineation resembles fine grooving or streaking. Layering is folded into recumbent isoclinal folds, with fold axes parallel to lineation, both lying in the plane of foliation and trending S86°E. Second generation folds are present, but rare, with the axis of one fold plunging S30°W, parallel with the exterior contact of the gneiss dome.

The quartzite is only about 20 to 25 m in exposed thickness. It is conspicuously boudinaged in places, with mylonitic quartzite boudins elongated parallel to lineation. The quartzite contains micaceous zones composed of quartz, biotite, muscovite, and sillimanite.

The contact of the gneiss dome with the pluton is inferred to be a fault striking N60°E along the linear, 8-km-long erosional (glacial meltwater) furrow occupied by Lake Ellen and Elbow Lake. The dip cannot be demonstrated along this segment, but by analogy to relations demonstrated at Stops 2 and 3, the fault probably dips parallel to foliation and layering in the gneiss dome—that is, 20 to 30 degrees to the southeast. The fault truncates units within the hanging wall, such as the small pluton noted above. In the footwall, units within the gneiss dome wedge out or pinch out against the fault, and as previously noted, the fault locally crosscuts layering and foliation. Nevertheless, the fault tracks layering and foliation around bends such as that at Elbow Lake, and in general it is broadly conformable with layering and foliation within the gneiss dome.

The eastern contact of the gneiss dome is judged to be a fault throughout its entire extent. To the north, the fault is referred to as the Kettle River fault (Rhodes and Cheney, 1981).

Return to the vehicles. Retrace the route, turning left (south) on Barnaby Creek road.

26.85 (0.7) Intersection with Elbow Lake Road. Continue straight ahead (east) on Barnaby Creek Road.

28.75 (1.9) Lake Ellen on the left (north). Cliffs and ledgy slopes to the north expose protomylonitic gneiss. The rubbly slope with scattered outcrops to the south exposes carbonate rocks and phyllite of the Covada Group. At trip mileage 29.3 outcrops on the left and right sides of the road bracket the contact (fault) between the gneiss dome and the Covada Group.

31.5 (2.75) Intersection. Turn left (north). Abandoned school house on the left.

32.3 (0.8) Phyllite of Covada Group in roadcuts.

34.6 (2.3) Ledgy slope to the north is a dip slope on gneiss.

35.2 (0.6) Intersection with paved road. Turn left (north). Scattered outcrops and roadcuts in the next 4 mi expose shallowly east-dipping protomylonitic granitic gneiss.

39.7 (4.5) Intersection with State Route (SR) 20. Turn left (west).

43.3 (3.6) Junction. Turn left (south) on Canyon Creek Road (Bangs Mountain Scenic Drive). Continue past the campground ahead on the left.

45.7 (2.4) **STOP 6. Protomylonitic gneiss cut by late ultramylonite zone at Donaldson Draw.**

Park off the road on the right near the sign describing glaciation.

Roadcuts on the east expose medium-gray protomylonitic granodiorite gneiss and sheared pegmatite dikes. Foliation strikes N75°E and dips 17 degrees to the southeast. A penetrative lineation on foliation planes plunges gently S77°E. Early dikes form intersecting layers to 20 cm thick with feathery to irregular contacts and are semi-concordant with foliation in the gneiss. Later dikes are planar, strike approximately east-west, and dip 35 to 45 degrees to the south.

The protomylonite and early and late dikes are cut by one thin (to 2 cm thick) zone of ultramylonite. The ultramylonite is dark gray and has tiny white porphyroclasts scattered through an aphanitic matrix. Although subconcordant, the ultramylonite locally cuts obliquely through foliation in the gneiss at a small angle.

Retrace the route to SR 20; turn right (east).

51.7 (6.0) Intersection with Inchelium road. Continue straight ahead. Road cuts on the north expose shallowly east-dipping protomylonitic granitic gneiss.

55.8 (4.1) **STOP 7. Interlayered mylonitic granitic gneiss and amphibolitic gneiss.**

Junction of SR 20 and U.S. 395. Barney's Junction on left. Turn left (north) and park on the wide shoulder of the road to the left (west), adjacent to the motel and this side (south) of the deep highway cut ahead. Hike northward and examine rocks in the roadcut.

West of the road, amphibolitic gneiss overlies mylonitic augen gneiss, which in turn overlies thinly interlayered amphibolitic gneiss and mylonitic granitic gneiss and pegmatite. Layering and foliation are concordant, dipping 17 degrees east. All rocks are penetratively lineated, the lineation lying in the plane of foliation and trending approximately N75°E. In the granitic gneiss, mylonite grades to or is thinly interlayered with ultramylonite. The mylonite is typically light gray and medium to fine grained and has conspicuous foliation and lineation and abundant larger grains (porphyroclasts) of light-gray feldspar, which are milled to spindle shapes. The ultramylonite is darker and much finer grained than the mylonite and has scattered sand-sized light-gray feldspars and poorly developed lineation.

The railroad cut east of the road exposes the upper amphibolitic gneiss. This amphibolite is mottled by lenses of coarse-grained amphibole (and garnet), evidently recrystallized following cataclasis. Recumbent isoclinal (intrafolial) folds are abundant. Trends of fold axes in this area show considerable scatter (Lyons, 1967; Donnelly, 1978), but many trend approximately parallel to the lineation. At the north end of the cut, axes of sheath folds and refolded intrafolial folds trend obliquely to the lineation. Small boudins, some of amphibolite within mylonitic granitic gneiss, others of amphibolite, are exposed in cross-section. A small white boudin above the prominent fold in the central part of the cut trends approximately N76°E.

The mylonitic character of the rocks in this area was recognized by Campbell (1938). His carefully worded descriptions are well worth reading. Campbell considered these rocks to be part of the crushed border zone of the Colville batholith. He concluded (1938, p. 94) that the "...brecciated appearance of the rock, the slicing and displacement of the feldspars, the warping of quartz and feldspars as shown by strain shadows, and the lens-like grouping of fine particles about rounded and strained relic crystal..." were evidence of the pressure that had acted on the batholith.

Return to the vehicles and continue northward on U.S. 395.

58.25 (2.45) **STOP 8. Amphibolitic gneiss cut by pegmatite dikes.**

Pull off the road and park on the left (west) side at the northern of two turnouts. Examine exposures of amphibolitic gneiss on the west side of the road to the north.

The amphibolite is dark gray to black and has undulating subhorizontal thin lamination and foliation. Lineation is penetrative, trending N80°E to S35°E, thus exhibiting greater scatter than is typical of the gneiss dome. The amphibolite is cut by several generations of dikes, most of which strike from N25°E to S60°E

(average strike of 13 dikes is N81°E). All dikes show some degree of cataclasis. Late dikes have sharp contacts with the amphibolite, dip steeply, and crosscut earlier dikes. Early dikes have ragged to feathery contacts with the amphibolite, are variously mylonitized, dip shallowly or are nearly concordant with foliation in the amphibolite, and have been folded. The hinge of one folded dike, trending approximately S85°E, is exposed above the bench cut into the southern part of the outcrop.

As at Stop 2, the dikes provide an indication of the character and direction of slip during cataclasis. The amphibolite or its protolith was evidently fractured and the steep, east-trending fractures dilated as dikes were injected along them; the amphibolite and dikes were then deformed through slip (simple shear) on fluxion structures (the foliation planes). At this locality, this process was repeated at least three times. The inferred transposition of early dikes from initially steep attitudes to nearly horizontal attitudes implies substantial thinning of the amphibolite and extension in a north-south direction, perpendicular to early fold axes and to the strike of dikes and lineation. Two assumptions are implicit in this interpretation: (1) that the strike of the latest dikes is primary—that is, they have not been rotated through east-west extension to their present attitude; and (2) that earlier dikes also were not rotated to east-west strikes through east-west extension prior to intrusion of the latest dikes.

Return to the vehicles and continue northward on U.S. 395.

60.3 (2.05) Mylonitic quartzite is exposed at the water line on Kamloops Island to east and in roadcuts. Marble overlies the quartzite to the west. U.S. 395 follows the west bank of the Kettle River northward. Outcrops east of the river are massive, little-metamorphosed greenstone of probable Triassic age (Mills, 1985). The concealed eastern contact of the dome is bracketed between the mylonitic quartzite exposed along the road and at Kamloops Island and the greenstone to the east.

62.85 (2.55) Massive greenish-gray greenstone, weathering rusty brown in scattered roadcuts. This unit is probably correlative with the greenstone noted above. Here it extends west of the road, forming a roof flap overlying the east flank of the gneiss dome (Wilson, 1981a).

70.05 (7.2) **Stop 9. Folded and refolded rocks.**

Pull off the highway and park at the turnout on the right (east) side of the highway. Hike northward 100 m and examine the roadcut.

The roadcut exposes a recumbent cylindrical fold in interlayered diopside(?) marble, calc-silicate gneiss, and pegmatite. The fold axis plunges 10 to 15 degrees N65°E. *If samples are desired, please collect them from the roadcut, not from outcrops to the east.*

Follow the upper (south) limb of the fold east-northeast to the Kettle River. In places, boudins of fine-grained gneissic granite trending approximately N70°E are present in the upper limb of the fold. Near the river, the fold is intersected by later folds which are overturned to the east and have fold axes plunging as much as 5 degrees to S30°E. The surfaces of the later folds are armored by thin varnish-covered layers of quartzite and fine-grained leucocratic gneissic granite.

Late, post-mylonitization folds are ubiquitous in the Okanogan and Kettle gneiss domes. In the interiors of the domes, the folds are typically upright and open. Near the western margin of the Okanogan gneiss dome and the eastern margin of the Kettle gneiss dome, the folds are tight and commonly overturned toward the adjacent low-angle bounding faults. Fold axes are subhorizontal and generally have a northerly strike, although they show considerable scatter.

The folds may reflect a force couple produced by late-stage down-dip movement on the bounding faults—that is, by upward movement of the gneiss domes.

End of field trip.

Paleogene Strike-slip Basins of Central Washington

James E. Evans and Samuel Y. Johnson

Paleogene Strike-Slip Basins of Central Washington: Swauk Formation and Chumstick Formation

James E. Evans
Department of Geology
Bowling Green State University
Bowling Green, OH 43403
and
Samuel Y. Johnson
U.S. Geological Survey
Box 25046, MS 939, Federal Center,
Denver, CO 80225

INTRODUCTION

Geologic Overview

Paleogene right-lateral displacements occurred along several major fault zones in central Washington, including the Straight Creek, Leavenworth, Entiat, and Eagle Creek fault systems (Fig. 1; Frizzell, 1979; Vance and Miller, 1981; Tabor and others, 1984; Johnson, 1985; Evans, 1988; Taylor and others, 1988). Within this strike-slip framework, nonmarine sediments accumulated in a number of basins, forming some of the thickest (>6,000 m) alluvial sequences in North America. Participants in this field trip will examine the syntectonic fill of two of these basins, the Swauk basin (Swauk Formation) and the Chumstick basin (Chumstick Formation), and discuss their sedimentology, paleogeography, and structural history.

The fluvial and lacustrine rocks of the Swauk and Chumstick basins show clear evidence for syndepositional tectonics, including major changes in sediment source regions, drainage pattern, drainage type, and sediment-transport competence related to localized uplift in fault zones. Disruption of regional drainage patterns led to several intervals of internal drainage in both basins and axial-drainage systems that paralleled fault zones in the Chumstick basin. Evidence that movement on the bounding fault systems was oblique slip includes: the geometry of secondary faults and folds; the development of a Chumstick sub-basin in the transtensional step-over zone between two parallel, dextral faults; features interpreted as horsetail splays; features interpreted as positive flower structures; and evidence for conveyor-belt-style sedimentation in part of the Chumstick basin. The displacement on these major faults probably ranges from kilometers to tens of kilometers.

DISCUSSION

Stratigraphy and Age

Swauk Formation

Outcrops along Swauk Creek were named the Swauk Sandstone by Russell (1900) and the Swauk Formation by Smith (1904). Later workers mapped various exposures of the Swauk Formation over an extensive area in central Washington (for example, Waters, 1930; Chappell, 1936; Page, 1939; Willis, 1953; Alexander, 1956; Foster, 1957; Rector, 1962). Because of lithologic similarity and lack of dating control, strata presently assigned to the Chumstick Formation were originally mapped as part of the Swauk Formation.

The Swauk Formation has been divided into one formal and several informal members. A number of silicic tuff interbeds were originally called the Silver Pass Volcanic rocks by Foster (1957, 1960) and revised as the Silver Pass Volcanic Member of the Swauk Formation by Tabor and others (1984). Tabor and others (1982a) recognized and mapped five sedimentary facies: conglomerate, arkosic sandstone, shale of Tronsen Ridge, monolithologic fanglomerate, and ironstone deposits (paleolaterite). Recent sedimentologic studies have identified seven mappable lithostratigraphic units that repre-

From: Joseph, N. L., and others, editors, 1989, Geologic guidebook for Washington and adjacent areas: Washington Division of Geology and Earth Resources Information Circular 86.

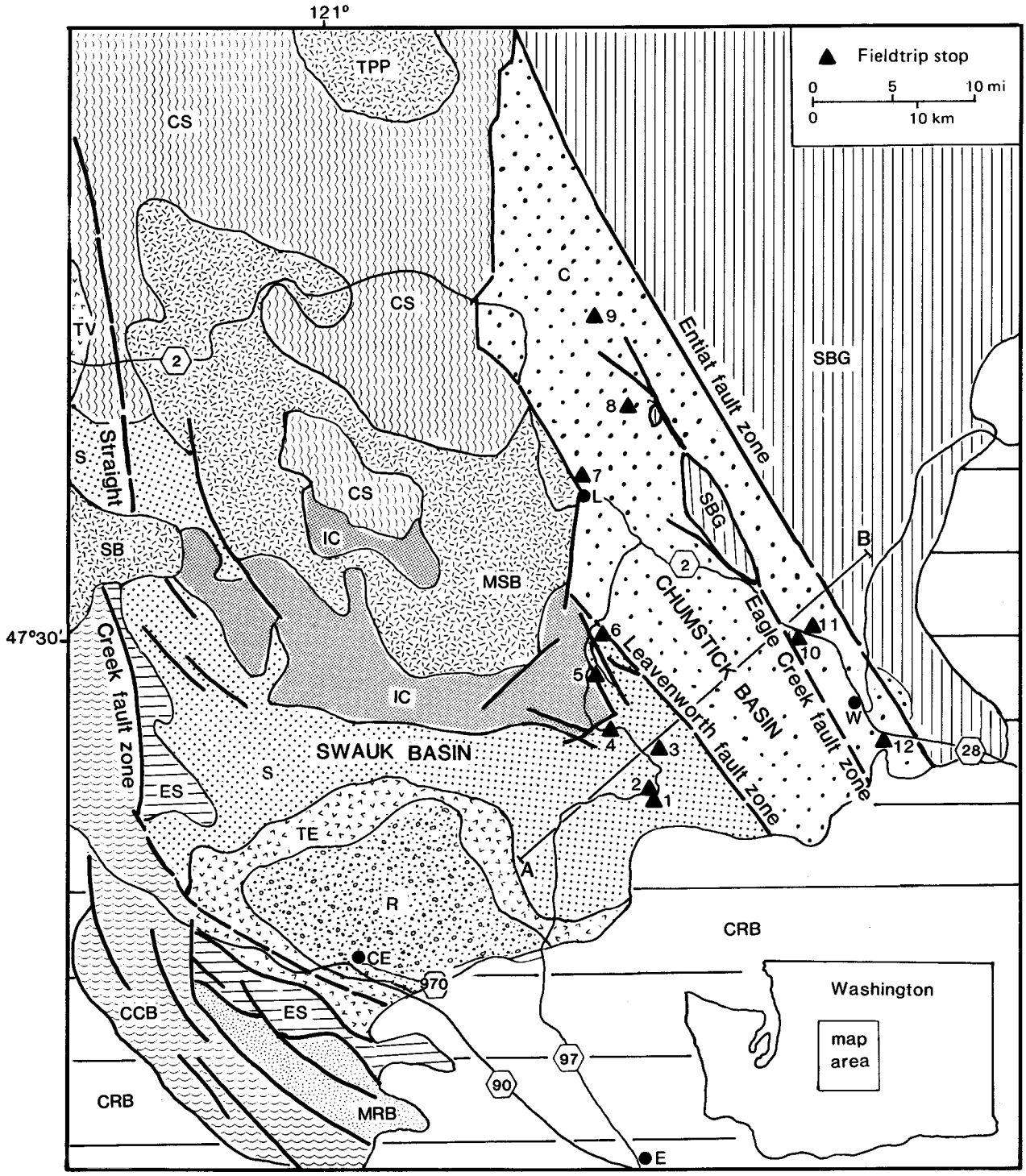

Figure 1. Generalized geologic map of the Swauk and Chumstick basin area of central Washington, showing fieldtrip stops (based on mapping by Tabor and others, 1982a, 1982b, 1987; Frizzell and others, 1984). Abbreviations for rock units: C, Chumstick Formation; CCB, Cabin Creek block of Tabor and others (1984); CRB, Columbia River Basalt Group (Miocene); CS, Chiwaukum Schist and associated metamorphic rocks; ES, Easton Metamorphic Suite; IC, Ingalls Tectonic Complex; MRB, Manastash River block of Tabor and others (1984); MSB, Mount Stuart batholith (Cretaceous); R, Roslyn Formation; S, Swauk Formation; SB, Snoqualmie batholith (Miocene); SBG, Swakane biotite gneiss; TE, Teanaway Formation; TPP, Ten Peak pluton (Cretaceous); TV, undifferentiated Tertiary volcanic rocks. Abbreviations for towns: CE, Cle Elum; E, Ellensburg; L, Leavenworth; W, Wenatchee. Line A-B is line of restored stratigraphic cross-section of Figure 2.

sent strata deposited in alluvial-fan, braided stream, meandering stream, lacustrine, and lacustrine-deltaic environments (Taylor, 1985; Roberts, 1985; Fraser, 1985; Taylor and others, 1988). These stratigraphic relations are shown in Figure 2.

Paleobotanical samples from the Swauk Formation have been considered early Tertiary (F. H. Knowlton *in* Smith, 1904) and Paleocene (Chappell, 1936; Alexander, 1956; Foster, 1960; Rector, 1962). Palynology studies (Newman, 1981) established that the Swauk Formation was early to middle Eocene in age. Tuff beds of the Silver Pass Volcanic Member have zircon fission-track ages ranging from 54.1 ± 2.1 to 48.4 ± 2.3 Ma (Tabor and others, 1984). The Swauk Formation is unconformably overlain by the basaltic flows of the Teanaway Formation, which have K-Ar ages ranging from 48.3 ± 1.8 to 44.9 ± 1.3 Ma (Tabor and others, 1984).

Chumstick Formation

The Chumstick Formation was defined by Gresens and others (1981). Both Russell (1900) and Alexander (1956) considered these strata to be distinct from the Swauk Formation (Russell's Camas Sandstone). Most workers, however, considered the sedimentary rocks in the Chumstick basin to be part of the Swauk Formation due to lithologic similarity. The basin was recognized as fault-bounded by Waters (1930) and was labeled the "Chiwaukum graben" by Willis (1950). Generally, attempts by earlier workers to define stratigraphic units and depositional history were hampered by poor stratigraphic control and by lack of radiometric dating (for example, Young, 1963; Rosenmeier, 1968; Pongsapich, 1970; Lupe, 1971).

Recent work has revised the stratigraphic position of these rocks. Newman (1981) found that pollen from the Chumstick Formation is middle to late Eocene in age. Additional pollen studies (reported in Evans, 1988) indicate the upper Chumstick units may extend to the Eocene-Oligocene boundary (E. Leopold, Univ. of Washington, 1987, oral commun.). Plant macrofossils (Evans, 1988) are similar to those in middle to upper Eocene floral assemblages from the Puget Group (Wolfe, 1968).

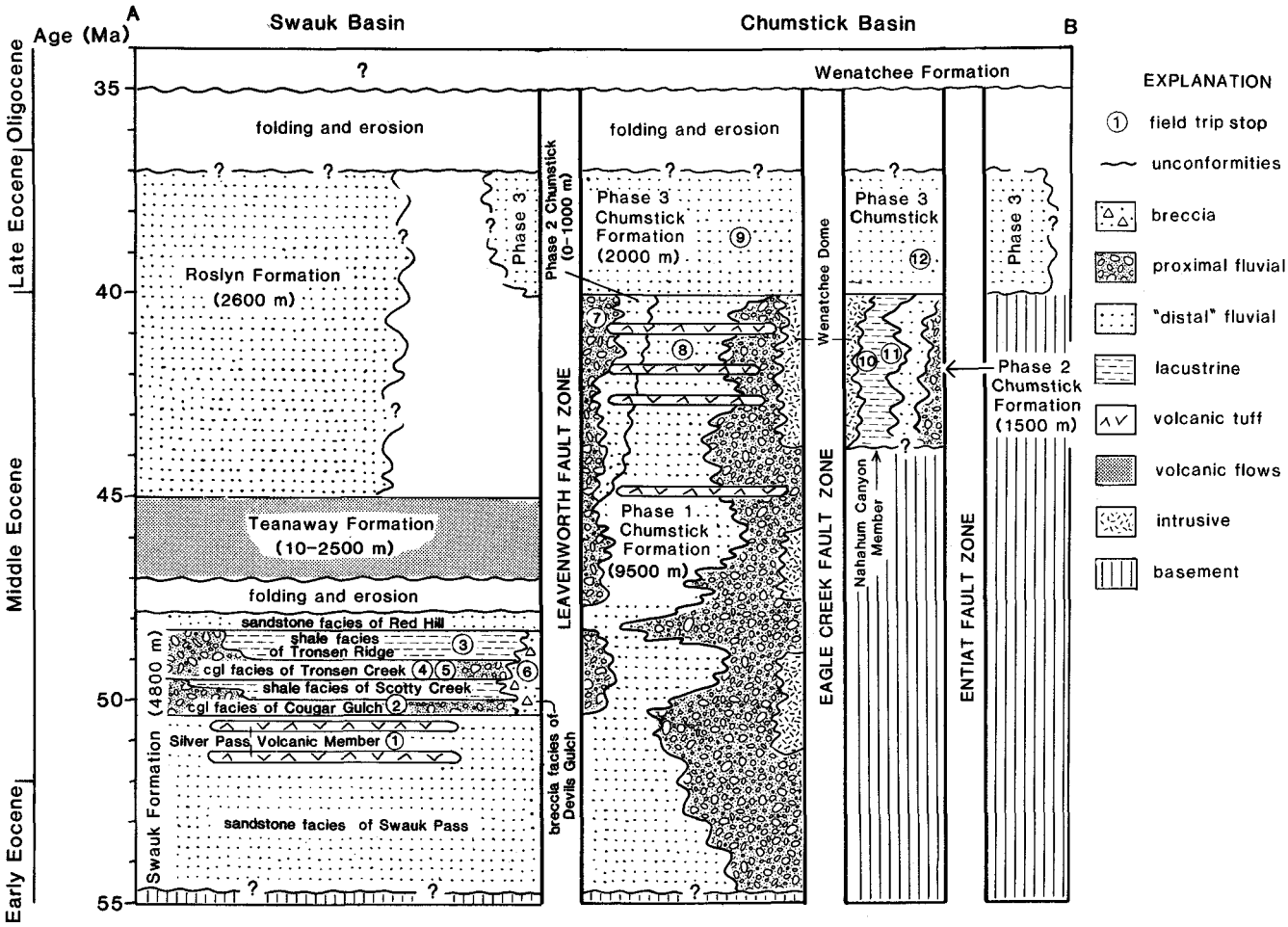

Figure 2. Schematic correlation diagram of restored stratigraphy along the trace of line A-B in Figure 1. Cgl, conglomerate. Other symbols given in explanation.

The Chumstick Formation contains 17 interbedded air-fall and ash-flow tuff beds of local to regional extent, each with a distinctive trace-element chemistry (McClincy, 1986). Zircon fission-track ages of these tuff beds range from 48.8 ± 7.2 to 41.9 ± 6.8 Ma (Gresens and others, 1981; Tabor and others, 1987). Intrusive rocks in the Chumstick Formation include a number of mafic and intermediate dikes and a felsic dike swarm associated with a rhyolite dome emplaced in the Eagle Creek fault zone near Wenatchee. An andesite porphyry dike in Chumstick rocks near the Eagle Creek fault zone yielded a K-Ar age of 50.3 ± 3.9 Ma (Ott and others, 1986), providing an important constraint on the age of the lowermost Chumstick rocks. A diabase dike in Number One Canyon near Wenatchee has a K-Ar age of 48.3 ± 2.8 Ma, while another diabase in Walker Canyon near Leavenworth has a K-Ar age of 41.5 ± 2.6 Ma (Gresens, 1983). There are five K-Ar dates from the felsic intrusive rocks near Wenatchee, ranging from 44.2 ± 1.9 to 40.2 ± 1.6 Ma (Tabor and others, 1982a; Gresens, 1983; Margolis, 1987). Additional stratigraphic age control is provided by provenance data, such as the occurrence of basalt clasts probably derived from the Teanaway Formation or the occurrence of flow-banded rhyolite clasts probably derived from the Wenatchee dome.

Gresens and others (1981) defined the Nahahum Canyon Member of the Chumstick Formation as a dominantly lacustrine, fine-grained unit that conformably overlies the undivided lower part of the formation and that interfingers with alluvial fan deposits near the basin margin. Evans (1988) geographically and stratigraphically restricted the Nahahum Canyon Member to lacustrine sequences located in the eastern sub-basin (between the Eagle Creek and Entiat fault zones during Phase 2 sedimentation; Fig. 2); we here confirm this revision. Fine-grained deposits in the northern part of the basin, mapped by Tabor and others (1987) as Nahahum Canyon Member, are actually younger fluvial deposits (Phase 3 deposits; Fig. 2); these strata are here reassigned as part of the undivided Chumstick Formation.

Gresens (1983) believed that there were as many as three stratigraphic units in the Chiwaukum graben: the "Swauk(?)", Chumstick, and Wenatchee Formations. Gresens distinguished the "Swauk(?)" Formation from the Chumstick on the basis of lithologic differences, such as calcite content or abundance of fresh biotite versus chloritized biotite. Recent studies, however, have shown that Gresens' "Swauk(?)" exposures are actually hydrothermally altered outcrops of the Chumstick Formation that surround the Wenatchee dome (Margolis, 1987). The Wenatchee Formation is a lower Oligocene fluvial and lacustrine unit that overlies the Chumstick and postdates regional strike-slip tectonism (Gresens and others, 1981). Because the entire syntectonic fill of the "Chiwaukum graben" is the Chumstick Formation, the simpler term "Chumstick basin" is recommended (Evans, 1988).

Basin Evolution

The evolution of these two basins, as recorded in the strata of the Swauk and Chumstick Formations, permits reconstruction of a regional strike-slip system that includes the Straight Creek, Leavenworth, Entiat, and Eagle Creek fault systems. At various times, uplift in

Figure 3. (on facing page) Evolution of the Swauk basin (between the Straight Creek and Leavenworth fault zones) and Chumstick basin (between the Leavenworth and Entiat-Eagle Creek fault zones). Layers shown in black are mudstones.

A. Interval from about 55 to 51 Ma, showing uplift on the Entiat-Eagle Creek fault system, coarse-grained fluvial systems in the Chumstick basin (earliest Phase 1 deposits) transitional to fine-grained fluvial systems in the Swauk basin (sandstone facies of Swauk Pass) and interbedded Silver Pass Volcanic Member of the Swauk Formation.

B. Interval from about 51 to 49 Ma, showing uplift in the Straight Creek fault zone and east-directed fluvial systems (conglomerate facies of Cougar Gulch). Several episodes of drainage disruption (lacustrine facies of Scotty Creek and Tronsen Ridge) and coarse-grained fluvial systems (conglomerate facies of Tronsen Creek, breccia facies of Devil's Gulch) in the eastern Swauk basin indicate uplift in the Leavenworth fault zone. Chumstick drainage was redirected southeast, parallel to the Leavenworth fault zone.

C. Interval from about 49 to 48 Ma, showing lack of relief in the Leavenworth fault zone, coarse-grained fluvial systems in the Chumstick basin (Phase 1 deposits) transitional to fine-grained fluvial systems in the Swauk basin (sandstone facies of Red Hill).

D. Interval from about 48 to 47 Ma, showing deformation of the Swauk basin (more intense near fault zones). Chumstick deposition continues (late stage of Phase 1 deposition).

E. Interval from about 47 to 45 Ma, showing deposition of basaltic flows of the Teanaway Formation across folded and eroded Swauk Formation.

F. Interval from about 45 to 41 Ma, showing Phase 2 deposition in the Chumstick basin. Sediment sources in the Leavenworth fault zone suggest transpressive uplift at restraining bends in a dextral system. The eastern sub-basin opens as a transtensional step-over basin between the parallel and partly overlapping dextral Eagle Creek and Entiat fault zones. Drainage disruption caused by relief in the Eagle Creek fault zone results in an extensive lacustrine-deltaic system in the eastern sub-basin (Nahahum Canyon Member of the Chumstick Formation).

G. Interval from about 41 to 37 Ma, showing low relief on all fault systems, overtopping of fault zones by fine-grained fluvial systems (Phase 3 Chumstick Formation, Roslyn Formation).

H. Interval from about 37 to 34 Ma, showing deformation of Chumstick basin in zone of dextral transpression.

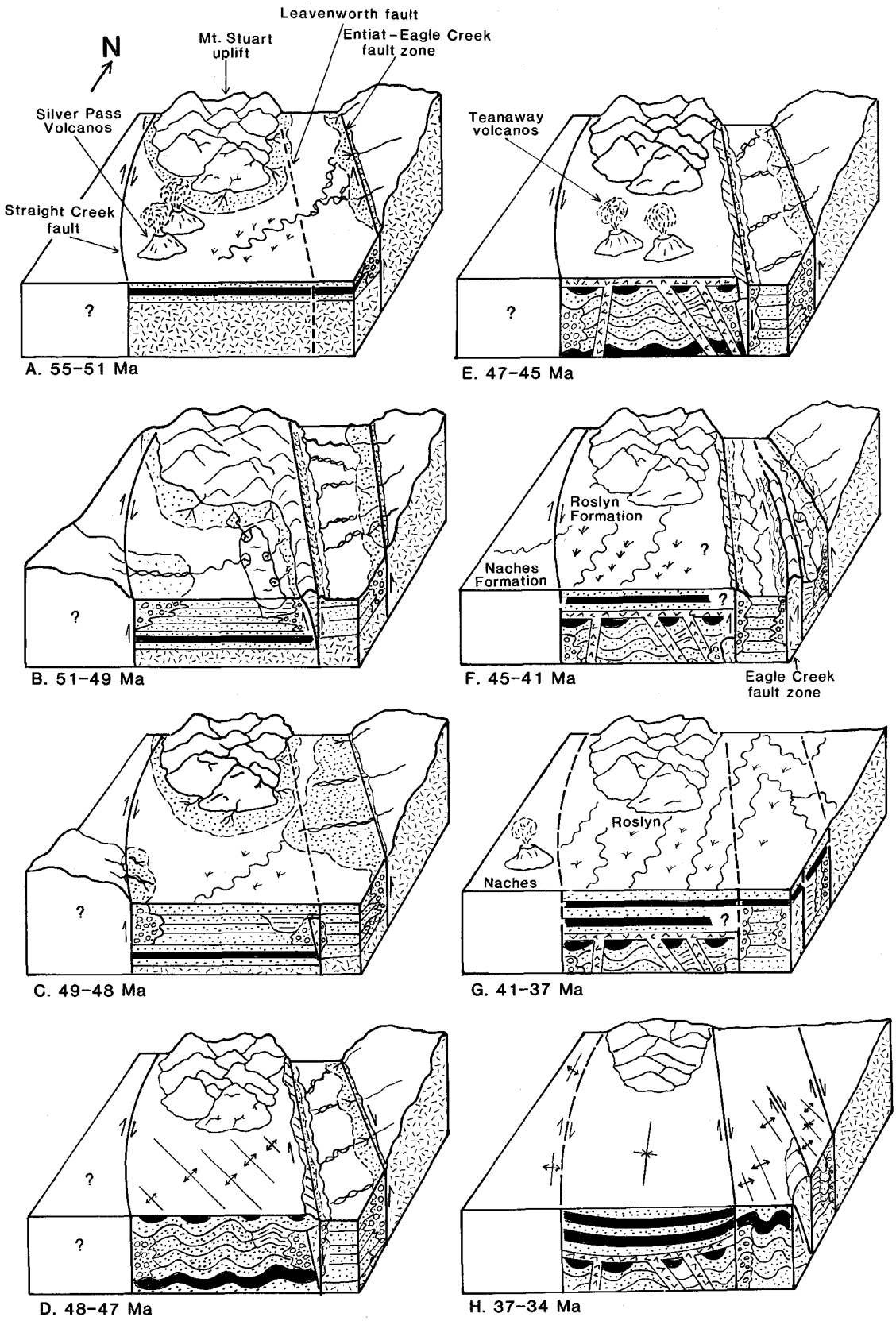
N
Leavenworth fault
Mt. Stuart uplift
Entiat-Eagle Creek fault zone
Silver Pass Volcanos
Straight Creek fault
?
A. 55-51 Ma
Teanaway volcanos
?
E. 47-45 Ma
?
B. 51-49 Ma
Roslyn Formation
Naches Formation
?
F. 45-41 Ma
Eagle Creek fault zone
?
C. 49-48 Ma
Roslyn
Naches
?
G. 41-37 Ma
?
?
D. 48-47 Ma
H. 37-34 Ma

these fault zones resulted in major changes in drainage type, drainage pattern, and sedimentary facies (Fig. 3).

Fairly fine grained sediments, deposited by southwest-flowing rivers, form the oldest exposed units of the Swauk Formation (sandstone facies of Swauk Pass, Fig. 2). This unit contains interbedded tuffs (Silver Pass Volcanic Member) whose ages range from about 54 to 48 Ma (Fig. 3A). The relatively fine-grained sandstone facies of Swauk Pass probably passed up-paleoslope to coarser grained fluvial deposits in the Chumstick basin (Phase 1 deposits of the Chumstick Formation). Accordingly, we hypothesize that Swauk-Chumstick rivers in this single depositional system drained uplifted fault blocks east of the Entiat-Eagle Creek fault system.

Between about 51 and 49 Ma, an episode of basin-margin faulting can be discerned in major drainage adjustments (Figs. 2, 3B). Coarse-grained Swauk fluvial deposits with east-directed paleocurrents (conglomerate facies of Cougar Gulch) suggest uplift on the Straight Creek fault system. In the eastern Swauk basin, drainage disruption resulted in two separate phases of lacustrine depositional systems (shale facies of Scotty Creek and shale facies of Tronsen Ridge). Coarse-grained fluvial deposits (conglomerate of Tronsen Creek) and talus-cone deposits (breccia facies of Devil's Gulch) indicate at least local uplift in the Leavenworth fault zone.

We recognize two possibilities for the Chumstick basin during this interval. Taylor and others (1988) have suggested that uplift east of the Leavenworth fault resulted in erosion and removal of some or all older Phase 1 Chumstick deposits, with renewed deposition beginning at about 48 to 49 Ma. This hypothesis requires either unconformities in the Chumstick section (which are not observed) or that the Chumstick Formation is entirely younger than about 49 Ma—in other words, the isotopic ages of the oldest Chumstick intrusive rocks, 50.3 ± 3.9 and 48.3 ± 2.8 Ma, must fall into the younger portion of the standard error. In the preferred hypothesis, given in Figures 2 and 3B, Chumstick Phase 1 depositional systems continued through this interval. The basin drainage system was apparently asymmetrical, with southwesterly flowing drainage crossing most of the basin (Buza, 1979; Evans, 1988) to connect with a southeast-directed axial drainage system at the basin margin, just east of the Leavenworth fault.

By about 49 to 48 Ma, relief in the Leavenworth fault zone was reduced, and southwest-directed, relatively fine-grained fluvial sediments (sandstone facies of Red Hill) were again deposited in the Swauk basin (Fig. 3C). On the basis of facies relations, paleocurrents, and provenance, these deposits are interpreted as distal Chumstick (Phase 1) deposits. Thus, the depositional systems inferred for 55 to 51 Ma (Fig. 3A) were re-established at this later time.

A probable episode of transpression in the Swauk basin, beginning about 48 Ma, resulted in the formation of broad, northwest-trending folds (Fig. 3D). Deformation was most intense in the vicinity of the Leavenworth fault. The Swauk Formation was uplifted and eroded prior to the deposition of the basalt flows of the Teanaway Formation at about 47 to 45 Ma (Fig. 3E).

In the Chumstick basin, major reorganizations of drainage systems were contemporaneous with Swauk deformation. Dextral movement on the Leavenworth, Eagle Creek, and Entiat faults segmented the two basins (Fig. 3F). Dextral movement on the left-stepping Leavenworth fault resulted in transpressive uplifts at two restraining bends (Fig. 1). Coarse-grained fluvial systems flowed east off these uplifts, initiating Phase 2 of Chumstick deposition. Farther east, dextral movement on the Eagle Creek-Entiat fault system resulted in the formation of a transtensional step-over basin. Formation of this sub-basin and uplift in the Eagle Creek fault zone caused drainage from the Entiat highlands to be redirected southeast, down the axis of the sub-basin. Ponding of drainage resulted in an extensive lacustrine-deltaic system (Nahahum Canyon Member) that filled the southeast part of this sub-basin.

Subsequent Chumstick fine-grained fluvial deposits (Phase 3) indicate an interval of tectonic quiescence between about 41 and 37 Ma (Fig. 3G). The Chumstick basin was folded in an interval of dextral transpression between about 37 and 34 Ma (Fig. 3H). The Oligocene Wenatchee Formation unconformably overlies the Chumstick Formation.

Paleoclimatology and Paleogeography

Paleoclimate can be interpreted on the basis of leaf fossils, pollen, and paleosols. Evans (1988) demonstrated that the Chumstick paleoflora contains mixtures of fully tropical and subtropical species, dominated by broad-leaved evergreen and broad-leaved deciduous taxa and minor conifer pollen. A physiognomic analysis (based upon morphological characteristics of leaves, independent of their taxonomic classification) shows that 41 percent of Chumstick taxa have entire (smooth) leaf margins, which in modern floras can be correlated (Wolfe, 1978) to mean annual temperatures of about 14° to 15°C (58°F).

Paleosols in the Chumstick Formation are recognized on the basis of fossil rootlets, mottling, destratification, trace fossils, rhizoconcretions, and calcretes that range from isolated nodules to laminated K horizons. Most of these alluvial soils have poor horizonal development (entisols), probably due to vertical accretion rates that averaged as much as 1 m/1,000 yr. Other soil types show incipient Cca or K horizons (Inceptisols) and or-

ganic-rich horizons (Histosols). Trace fossils are primarily unlined vertical burrows (*Skolithos*); surface traces (for example, *Sinusites*) are rare.

The paleogeography of the Chumstick basin can be established by reference to other paleobotanical studies in the region. The fluvial-deltaic Puget Group (middle and upper Eocene) contains a broadleaved evergreen paleoflora that was fully tropical and had mean annual temperatures of about 17°C or 63°F (Wolfe, 1968, 1978; Buckovic, 1979). To the northeast, the lower middle Eocene Klondike Mountain Formation (Republic graben) contains a mixed conifer-broadleaved deciduous paleoflora that represents upland subtropical forest where mean annual temperatures were less than 13°C or 55°F (Wolfe and Wehr, 1986).

Given the coastal setting of the Puget Group, assuming a smooth regional gradient, and using an elevation lapse rate of 0.55°C/100 m elevation (Wolfe and Wehr, 1986), the Chumstick basin would have been located about 150 km inland from the coast, with average elevations between 350 and 550 m. The assumption of a smooth regional gradient is supported by lack of evidence for rain-shadow effects on the composition of the paleoflora. The average regional paleoslope calculated in this manner is close to paleohydraulic calculations based upon independent evidence (the minimum paleoslope of channel reaches necessary to transport the observed bedload through observed paleochannel geometries; Evans, 1988).

Depositional Systems

Evans (1988) interpreted the Chumstick Formation as a humid-tropical, alluvial-fan system, on the basis of depositional facies and on tectonic and paleoclimatic setting. Comparable facies in the Swauk basin can be similarly interpreted. Both the Swauk and Chumstick Formations are characterized by proximal coarse-grained fluvial facies that consist of gravel braid-bars and by distal fine-grained fluvial facies consisting of multistory sandstone channel deposits and overbank deposits (Roberts, 1985; Fraser, 1985; Taylor, 1985; Evans, 1988).

Characteristics of the Chumstick Formation that are interpreted to indicate a humid-tropical, alluvial-fan system include the following:

(1) Fluvial architecture was strongly affected by active basin-margin faulting. Coarse-grained fluvial deposits (boulder-cobble conglomerate) with tabular geometry occur adjacent to basin margins. In cross-section, these deposits consist of laterally stacked (that is, overlapping ribbons), broadly lenticular fanhead channels. Distal fan deposits are comprised of cobble-pebble conglomerate and sandstone with a sheet-like geometry. Distal fan deposits grade into a basin fill consisting of vertically stacked, multistory channel deposits encased in extensive overbank deposits.

(2) Rapid subsidence has resulted in preservation of compositionally immature sediments (sublithic, feldspathic arenites) with thin, shallow soils. This is the expected trend for aggrading systems in a subsiding basin, but it runs contrary to generalizations made about tropical climates, such as the development of lateritic soils. Indeed, there is evidence that thick lateritic soils formed on bedrock in this region prior to Swauk-Chumstick basin development (Tabor and others, 1982a).

(3) Paleohydraulic reconstructions for the Chumstick Formation indicate that streams carried coarse-grained bedload through channel reaches with paleoslopes of <5 m/km, possibly indicative of short but intense rainfall events.

(4) Rapid vegetative growth resulted in the bank stabilization of sandy sediments, development of soils and leaf-litter layers on emergent bar-tops, and introduction of woody debris into the channels. Even sequences of coarse-grained, proximal fluvial deposits have a significant overbank component and show evidence of bank stability, cutbanks, and cohesive bank failures.

(5) Debris-flow deposits are relatively minor, with the exception of local talus-cone deposits adjacent to basin-margin faults. The rarity of debris flows throughout the basin is probably due to hillslope stability imparted by vegetation.

ACKNOWLEDGMENTS

We express our appreciation to many people who have aided our research in these basins. Chumstick basin studies represent a doctoral dissertation by J. E. Evans at the University of Washington, under the supervision of Joanne Bourgeois. Chumstick basin studies owe a debt of thanks to the earlier work by the late R. L. Gresens. The first author also wishes to thank S. Y. Johnson, S. W. Bogue, T. J. Walsh, M. McClincy, J. A. Vance, J. Margolis, and R. J. Burnham for their assistance with his project.

Data and interpretations reported from the Swauk basin are derived mainly from studies conducted at Washington State University by S. Y. Johnson and the four graduate students he supervised (G. T. Fraser, D. Peoples, J. W. Roberts, and S. B. Taylor) between 1982 and 1985. The contributions of these students as reported in this guide are greatly appreciated.

Both authors also benefited substantially from stimulating discussions of regional geology with R. W. Tabor and V. A. Frizzell, Jr. We thank E. A. Johnson, Marguerite McLellan, J. W. Whipple, and T. J. Walsh for their helpful reviews.

REFERENCES CITED

Alexander, Frank, 1956, Stratigraphic and structural geology of the Blewett-Swauk area, Washington: University of Washington Master of Science thesis, 62 p., 3 pl.

Buckovic, W. A., 1979, The Eocene deltaic system of west-central Washington. *In* Armentrout, J. M., Cole; M. R.; Ter-Best, Harry, Jr., editors, Cenozoic paleogeography of the western United States; Pacific Coast Paleogeography Symposium 3: Society of Economic Paleontologists and Mineralogists, Pacific Section, p. 147-163.

Buza, J. W., 1979, Dispersal patterns and paleogeographic implications of lower and middle Tertiary fluviatile sandstones in the Chiwaukum graben, east-central Cascades, Washington. *In* Armentrout, J. M.; Cole, M. R.; Ter-Best, Harry, Jr., editors, Cenozoic paleogeography of the western United States; Pacific Coast Paleogeography Symposium 3: Society of Economic Paleontologists and Mineralogists, Pacific Section, p. 63-73.

Chappell, W. M., 1936, Geology of the Wenatchee quadrangle, Washington: University of Washington Doctor of Philosophy thesis, 249 p., 1 pl.

Evans, J. E., 1988, Depositional environments, basin evolution, and tectonic significance of the Eocene Chumstick Formation, Cascade Range, Washington: University of Washington Doctor of Philosophy thesis, 325 p.

Foster, R. J., 1957, The Tertiary geology of a portion of the central Cascade Mountains: University of Washington Doctor of Philosophy thesis, 186 p., 2 pl.

Foster, R. J., 1960, Tertiary geology of a portion of the central Cascade Mountains, Washington: Geological Society of America Bulletin, v. 71, no. 2, p. 99-125.

Fraser, G. T., 1985, Stratigraphy, sedimentology, and structure of the Swauk Formation in the Swauk Pass area, central Cascades, Washington: Washington State University Master of Science thesis, 219 p., 4 pl.

Frizzell, V. A., 1979, Petrology of Paleogene non-marine sandstone units in Washington. *In* Armentrout, J. M.; Cole, M. R.; TerBest, Harry, Jr., editors, Cenozoic paleogeography of the western United States; Pacific Coast Paleogeography Symposium 3: Society of Economic Paleontologists and Mineralogists, Pacific Section, p. 113-118.

Frizzell, V. A., Jr.; Tabor, R. W., 1977, Stratigraphy of Tertiary arkoses and their included monolithological fanglomerates and breccias in the Leavenworth fault zone, central Cascades, Washington [abstract]: Geological Society of America Abstracts with Programs, v. 9, no. 4, p. 421.

Frizzell, V. A., Jr.; Tabor, R. W.; Booth, D. B.; Ort, K. M.; Waitt, R. B., Jr., 1984, Preliminary geologic map of the Snoqualmie Pass 1:100,000 quadrangle, Washington: U.S. Geological Survey Open-File Map 84-693, 43 p., 1 pl.

Gresens, R. L., 1983, Geology of the Wenatchee and Monitor quadrangles, Chelan and Douglas Counties, Washington: Washington Division of Geology and Earth Resources Bulletin 75, 75 p., 3 pl.

Gresens, R. L.; Naeser, C. W.; Whetten, J. T., 1981, Stratigraphy and age of the Chumstick and Wenatchee Formations–Tertiary fluvial and lacustrine rocks, Chiwaukum graben, Washington: Geological Society of America Bulletin, v. 92, no. 4, Part I, p. 233-236, Part II, p. 841-876.

Johnson, S. Y., 1985, Eocene strike-slip faulting and nonmarine basin formation in Washington. *In* Biddle, K. T.; Christie-Blick, Nicholas, editors, Strike-slip deformation, basin formation, and sedimentation: Society of Economic Paleontologists and Mineralogists Special Publication 37, p. 283-302.

Johnson, S. Y.; Miller, R. B., 1987, Ingalls Tectonic Complex and Swauk Formation, Ruby Creek area, Cascade Mountains, Washington. *In* Hill, M. L., editor, Cordilleran Section of the Geological Society of America: Geological Society of America Centennial Field Guide 1, p. 363-368.

Lupe, R. D., 1971, Stratigraphy and petrology of the Swauk Formation in the Wenatchee Lake area: University of Washington Master of Science thesis, 27 p., 1 pl.

Margolis, Jacob, 1987, Structure and hydrothermal alteration associated with epithermal Au-Ag mineralization, Wenatchee Heights, Washington: University of Washington Master of Science thesis, 90 p.

McClincy, M. J., 1986, Tephrostratigraphy of the middle Eocene Chumstick Formation, Cascade Range, Douglas County, Washington: Portland State University Master of Science thesis, 125 p., 2 pl.

Newman, K. R., 1981, Palynologic biostratigraphy of some early Tertiary nonmarine formations in central and western Washington. *In* Armentrout, J. M., editor, Pacific Northwest Cenozoic Biostratigraphy: Geological Society of America Special Paper 184, p. 49-65.

Ott, L. E.; Groody, Diane; Follis, E. L.; Siems, P. L., 1986, Stratigraphy, structural geology, ore mineralogy, and hydrothermal alteration at the Cannon Mine, Chelan County, Washington. *In* MacDonald, A. J., editor, Gold '86, An international symposium on the geology of gold deposits, Proceedings Volume: Gold '86 Symposium, Toronto, p. 425-435.

Page, B. M., 1939, Geology of a part of the Chiwaukum quadrangle, Washington: Stanford University Doctor of Philosophy thesis, 203 p., 2 pl.

Pongsapich, Wasant, 1970, A petrographic reconnaissance of the Swauk, Chuckanut, and Roslyn Formations, Washington: University of Washington Master of Science thesis, 63 p., 3 pl.

Rector, R. J., 1962, Geology of the east half of the Swauk Creek mining district: University of Washington Master of Science thesis, 73 p., 2 pl.

Roberts, J. W., 1985, Stratigraphy, sedimentology, and structure of the Swauk Formation along Tronsen Ridge, central Cascades, Washington: Washington State University Master of Science thesis, 188 p., 2 pl.

Rosenmeier, F. J., 1968, Stratigraphy and structure of the Table Mountain-Mission Peak area in the Wenatchee Mountains, central Washington: University of Washington Master of Science thesis, 44 p., 1 pl.

Russell, I. C., 1900, A preliminary paper on the geology of the Cascade Mountains in northern Washington: U.S. Geological Survey Annual Report, v. 20, part 2, p. 83-210.

Smith, G. O., 1904, Description of the Mount Stuart quadrangle, Washington: U.S. Geologic Atlas Folio 106, 10 p.

Steel, Ron; Gloppen, T. G., 1980, Late Caledonian (Devonian) basin formation, western Norway: signs of strike-slip tectonics during infilling. *In* Ballance, P. F.; Reading, H. G. (editors), Sedimentation in oblique-slip mobile zones: International Association of Sedimentologists Special Publication 4, p. 79-103.

Tabor, R. W.; Waitt, R. B., Jr.; Frizzell, V. A., Jr.; Swanson, D. A.; Byerly, G. R.; Bentley, R. D., 1982a, Geologic map of the Wenatchee 1:100,000 quadrangle, Washington: U.S. Geological Survey, Miscellaneous Investigations Series Map I-1311, 26 p., 1 pl., scale 1:100,000.

Tabor, R. W.; Frizzell, V. A., Jr.; Booth, D. B.; Whetten, J. T.; Waitt, R. B., Jr.; Zartman, R. E., 1982b, Preliminary geologic map of the Skykomish River 1:100,000 quadrangle, Washington: U.S. Geological Survey Open-File Report 82-747, 31 p., 1 pl.

Tabor, R. W.; Frizzell, V. A., Jr.; Vance, J. A.; Naeser, C. W., 1984, Ages and stratigraphy of lower and middle Tertiary sedimentary and volcanic rocks of the central Cascades, Washington–Application to the tectonic history of the Straight Creek fault: Geological Society of America Bulletin, v. 95, no. 1, p. 26-44.

Tabor, R. W.; Frizzell, V. A., Jr.; Whetten, J. T.; Waitt, R. B.: Swanson, D. A.; Byerly, G. R.; Booth, D. B.; Hetherington, M. J.; Zartman, R. E., 1987, Geologic map of the Chelan 30' x 60' quadrangle, Washington: U.S. Geological Survey, Miscellaneous Investigations Series Map I-1661, 29 p., 1 pl., scale 1:100,000.

Taylor, S. B., 1985, Stratigraphy, sedimentology, and paleogeography of the Swauk Formation in the Liberty area, central Cascades, Washington: Washington State University Master of Science thesis, 199 p., 2 pl.

Taylor, S. B.; Johnson, S. Y.; Fraser, G. T.; Roberts, J. W., 1988, Sedimentation and tectonics of the lower and middle Eocene Swauk Formation in eastern Swauk basin, central Cascades, central Washington: Canadian Journal of Earth Sciences, v. 25, no. 7, p. 1020-1036.

Vance, J. A.; Miller, R. B., 1981, The movement history of the Straight Creek fault in Washington state. *In* Monger, J. W. H., editor, The last 100 million years (mid-Cretaceous to Holocene) of geology and mineral deposits in the Canadian Cordillera: Geological Association of Canada, Cordilleran Section, Programme and Abstracts, p. 39-41.

Waters, A. C., 1930, Geology of the southern half of the Chelan quadrangle, Washington: Yale University Doctor of Philosophy thesis, 256 p., 2 pl.

Willis, C. L., 1950, Geology of the northeastern quarter of Chiwaukum quadrangle, Washington: University of Washington Doctor of Philosophy thesis, 158 p., 4 pl.

Willis, C. L., 1953, The Chiwaukum graben, a major structure of central Washington: American Journal of Science, v. 251, no. 11, p. 789-797.

Wolfe, J. A., 1968, Paleogene biostratigraphy of nonmarine rocks in King County, Washington: U.S. Geological Survey Professional Paper 571, 33 p.

Wolfe, J. A., 1978, A paleobotanical interpretation of Tertiary climates in the northern hemisphere: American Scientist, v. 66, no. 6, p. 694-703.

Wolfe, J. A.; Wehr, W., 1986, Middle Eocene dicotyledonous plants from Republic, northeastern Washington: U.S. Geological Survey Professional Paper 1597, 25 p., 16 pl.

Young, R.E., 1963, Geology of the Swauk Formation in the Leavenworth, Washington area: University of Washington Bachelor of Science thesis, 49 p.

Road Log

Day 1: Swauk Formation

From Spokane, travel west on Interstate Highway 90 (I-90) about 174 mi to Ellensburg. Take U.S. Highway (U.S.) 97 exit 4 mi west of Ellensburg. Proceed north on U.S. 97 to the junction with State Route (SR) 970, approximately 16 mi. Cumulative mileage is given on the left below; interval mileage is given in parentheses. *Set odometer.*

0.0 (0.0) From the junction of U.S. 97 and SR 970, travel north on U.S. 97 toward Wenatchee.

0.2 (0.2) Cross Swauk Creek.

0.7 (0.5) Gravels from placer gold mining in Swauk Creek.

1.0 (0.3) Begin discontinuous outcrops of Teanaway Formation.

3.0 (2.0) Turnoff for Liberty historic townsite.

3.4 (0.4) Begin discontinuous outcrops of Swauk Formation cut by Teanaway Formation dikes.

6.3 (2.9) Mineral Springs campground and store.

9.4 (3.1) Turnoff for Old Blewett Pass Highway on the left.

10.6 (1.2) Turnoff for Porky Basin road on the right.

11.4 (0.8) Quarry exposing Swauk Formation with interbedded Silver Pass Volcanic Member, both cut by basalt dikes of the Teanaway Formation.

13.4 (2.0) **STOP 1. Sandstone facies of Swauk Pass.** Use the pulloff to the right for parking.

This outcrop consists of more than 20 m of interbedded sandstone and mudstone (Fig. 4). The sandstone forms thick (>2 m), sheet-like (laterally continuous for 200- >300 m) bodies and thin (<2m) sheet-like to lenticular bodies. Thick intervals of sandstones are typically trough cross-bedded, have sharp erosional bases, and fine upward in their upper portions. Thin intervals of sandstone are typically ripple cross-laminated to planar-laminated, have sharp upper and lower contacts, and are commonly mottled and rooted. Mudstone beds are typically massive, planar-laminated, or ripple cross-laminated. Abundant organic debris and plant fossils are commonly preserved on laminae surfaces.

Fraser (1985) and Taylor (1985) interpreted these strata as meandering stream deposits. Thick-bedded sandstone, thin-bedded sandstone, and mudstone are interpreted as channel, crevasse splay, and overbank deposits, respectively. This outcrop is typical of the sandstone facies of Swauk Pass (Fig. 2 and 3A; Taylor and others, 1988), which is the thick (>2,200 m) basal unit of the Swauk Formation. The upper half of this unit includes at least four tuffaceous interbeds of the Silver Pass Volcanic Member of the Swauk Formation, dated at about 51 Ma (Tabor and others, 1982a, 1984). Paleocurrent data indicate sediment transport to the southwest (Taylor and others, 1988).

Figure 4. Fluvial deposits of the sandstone facies of Swauk Pass of the Swauk Formation (Fig. 2) at Stop 1, Swauk Pass. People at the base of the outcrop indicate scale.

13.9 (0.5) Summit of Swauk Pass (elev. 1,250 m). Turn left on a gravel road at the summit of the pass. Follow the main gravel road 1.1 mi.

15.0 (1.1) **STOP 2. Vista of Tronsen Ridge facies.** Park along the edge of the road, and walk up the saddle to the left.

Walk upslope on the south side of the road for a geologic and scenic vista. The Stuart Range, underlain by the Late Cretaceous Mount Stuart batholith (Fig. 1; Tabor and others, 1982a) forms the high peaks to the north-northwest. In the

foreground to the north are bold outcrops of the Swauk Formation on the northeast side of Scotty Creek. These exposures include the alluvial fan deposits of the conglomerate facies of Cougar Gulch, lacustrine deposits of the shale facies of Scotty Creek, and alluvial fan deposits of the conglomerate facies of Tronsen Creek (Fig. 2; Taylor and others, 1988). (The latter unit will be examined at stops 4 and 5.) These units record a major drainage reorganization in the Swauk basin initiated by uplift on the northern and western basin margins (Fig. 3B). These strata are folded on northwest-trending axes and intruded by NNE-trending dikes of the Teanaway Formation. In the background to the northeast are good exposures of the shale facies of Tronsen Ridge (Stop 3).

16.2 (1.2) Retrace route to Swauk Pass. Turn left (east) on U.S. 97 toward Wenatchee.

17.1 (0.9) Lunch stop at Tronsen Campground (U.S. Forest Service, Wenatchee National Forest).

20.9 (3.8) Continue northeast on U.S. 97. Turn right on Five Mile Road (Forest Service Road 7724). This unpaved road is maintained by logging companies. Its quality is dependent on recent logging activity. Most of the time it can be easily traveled by passenger car.

24.3 (3.4) **STOP 3. Shale facies of Tronsen Ridge.**

Park at the ridge crest. Follow the trail along the ridge crest about 2 km (about 30 min) southwest.

Through the trees to the east are views of the Leavenworth fault zone, which juxtaposes the Swauk Formation and the lighter colored Chumstick Formation.

Turn west off the trail and walk to the summit of the first major peak (elev. 1,515 m). Walk southwest down the southwest-facing slope of Tronsen Ridge through several hundred meters of the shale facies of Tronsen Ridge (Fig. 5), which is cut by basaltic dikes of the Teanaway Formation.

The shale facies of Tronsen Ridge is more than 1,100 m thick and is present only in the easternmost part of the Swauk basin; its stratigraphic correlatives to the west have been eroded. The shale facies consists, in significant proportion, of coarsening-upward cycles (Fig. 6) that ideally include (from base to top): (1) fissile black and(or) greenish-gray mudstone, (2) planar-laminated or ripple cross-laminated mudstone and very fine grained sandstone, and (3) planar-laminated to ripple cross-laminated fine- to medium-grained sandstone (Roberts, 1985). Cycle thickness varies considerably, but it is typically about 10 m, and cycles can generally be traced laterally for as much as 2 km. Cross-bedded, medium- to coarse-grained sandstone fills erosional channels in the tops of some cycles, and fluvial sandstone bodies comprise a few thick (tens of meters) intervals in this facies. Laterally to the SSE, this unit is significantly more fine grained.

Roberts (1985) interpreted the coarsening-upward cycles as lacustrine margin deposits, each cycle representing progradation of a lacustrine

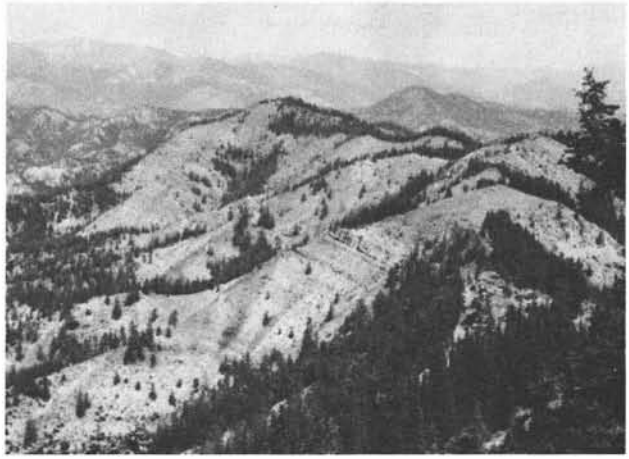

Figure 5. View from the south-southeast of the shale facies of Tronsen Ridge of the Swauk Formation (Fig. 2) at Stop 3 on Tronsen Ridge.

Figure 6. Coarsening-upward cycles of the shale facies of Tronsen Ridge of the Swauk Formation, Stop 3. Resistant sandstone ledges of inferred lacustrine-margin origin form the upper parts of the cycles. Person indicates scale.

delta lobe or shoreline. Channel sandstones represent fluvial facies of a delta plain. The significant proportion of fluvial deposits in this interval as well as lack of cyclicity in portions of the section probably reflect pulses of lake expansion and contraction driven by varied basin-margin tectonism and basin subsidence. Paleocurrent directions from the fluvial channel deposits suggest sediment transport to the east (Roberts, 1985).

The shale facies of Tronsen Ridge interfingers with and overlies the conglomerate facies of Tronsen Creek (Stops 4 and 5). The transition from fluvial deposition in southwest-flowing rivers in the sandstone facies of Swauk Pass (Stop 1) to alluvial fan-lacustrine deposition at higher stratigraphic levels (Fig. 2) in the eastern part of the basin records a major reorganization of drainage type and direction (Figs. 3A and 3B).

27.5 (3.2) Retrace route back to U.S. 97. Turn right (north) toward Wenatchee.

29.1 (1.6) **STOP 4. Conglomerate facies of Tronsen Creek.**

Park on the highway shoulder at the northern end of the outcrop.

Figure 7. Sandstone, conglomerate, and mudstone of the conglomerate facies of Tronsen Creek of the Swauk Formation (Fig. 2) at Stop 5, interpreted as distal alluvial fan deposits. Vertical feeder dike to the Teanaway Formation cuts the northern end (at left) of the outcrop. Two-lane road provides scale.

Roadcuts on both sides of the highway (Fig. 7) expose interbedded conglomerate, fine- to coarse-grained sandstone, and mudstone. Conglomerate beds are as much as a few meters thick, typically lenticular, massive to crudely stratified, and poorly sorted and have minimal erosional relief at their bases. Both clast-supported and matrix-supported conglomerates can be found; maximum clast dimensions reach 30 cm. Pocket structures showing downward movement of clasts resulting from liquefaction are present in a few beds. Sandstones form sheet-like to lenticular beds that are cross-bedded, planar-bedded, or massive. Mudstones are both massive and laminated and locally contain abundant organic debris. On the north side of the road, Swauk beds are cut by a prominent vertical dike of the Teanaway Formation (about 47 Ma; Tabor and others, 1984).

Fraser (1985) interpreted the conglomerate facies of Tronsen Creek as a distal alluvial-fan deposit. Abundant channeling and cross-bedding suggests that stream processes were dominant. Relatively poor sorting of many conglomeratic beds indicates rapid deposition. Correlative strata to the southeast grade laterally into the shale facies of Tronsen Ridge (Stop 3). Paleocurrent data indicate flow to the east. Clasts were mainly derived from the Ingalls Tectonic Complex and Mount Stuart batholith. (See discussion at the next stop.)

30.6 (1.5) Continue north on U.S. 97 toward Wenatchee. Start of road outcrops of Ingalls Tectonic Complex—complexly deformed peridotite, metasedimentary rocks, and metavolcanic rocks.

30.9 (0.3) Turnoff for Old Blewett Pass Highway to the left.

32.3 (1.4) Prominent outcrop of sheared peridotite.

34.5 (2.2) **STOP 5. Conglomerate facies of Tronsen Creek.**

Turn right on Ruby Creek Road and park immediately. Walk up the road.

The contact between the Ingalls Tectonic Complex and the Swauk Formation is a north-striking, high-angle fault (Fig. 1; Tabor and others, 1982a; Johnson and Miller, 1987). Directly west of the fault are strongly sheared and slickensided serpentinites. Farther west, serpentinites are separated from altered gabbros, diabases, and basalts by a steep, southeast-dipping fault. Some of these rocks have been tectonically brecciated, and cataclastic microstructures are common.

East of the main fault, the Swauk Formation forms an east-dipping, well-exposed section

more than 32 m thick. This section consists of greenish-gray conglomerate, conglomeratic sandstone, and medium- to coarse-grained sandstone (Figs. 8 and 9) and is cut by several small faults of minor displacement. Conglomeratic beds are as thick as 6 to 7 m and are mostly massive to crudely stratified. Clasts are poorly sorted, typically subrounded to rounded, as large as 45 cm in maximum dimension, and are either framework-supported or are interspersed in a matrix of coarse-grained sandstone. Two paleocurrent measurements on rare imbricated clasts indicate sediment transport to the east. Sandstone and conglomeratic sandstone beds are as thick as 4 to 5 m, lenticular, and massive or characterized by crude horizontal or low-angle cross-bedding. Bedding contacts are sharp or, less commonly, erosional.

From a count of 306 pebbles, conglomerate clasts have the following lithologies: 51.3 percent greenstone; 27.4 percent gabbro to granodiorite; 10.5 percent graywacke and argillite; 4.6 percent chert; 3.6 percent quartz and quartzite; 2.0 percent rhyolite to andesite; and 0.6 percent serpentinite. Sandstones are rich in lithic fragments.

The upper part of the Swauk section adjacent to the fault consists of highly faulted sandstone beds that were not measured and that are succeeded by a covered interval. For the next several hundred meters to the southeast on the Ruby Creek Road, trough cross-bedded to planar-bedded, fine- to coarse-grained sandstone, massive to crudely stratified pebble conglomerate, and massive mudstone are sporadically exposed. These strata differ from the Swauk adjacent to the fault in that they are much finer grained, and the sandstones are arkosic and contain a much smaller proportion of lithic fragments. Six paleocurrent measurements on pebble imbrication and axes of trough cross-beds have a vector mean of 170° ± 17°, indicating sediment transport to the south.

Figure 8. Massive to crudely stratified conglomerate and minor sandstone of the conglomerate facies of Tronsen Creek of the Swauk Formation (Fig. 2) at Stop 5, interpreted as proximal alluvial fan deposits. Person indicates scale.

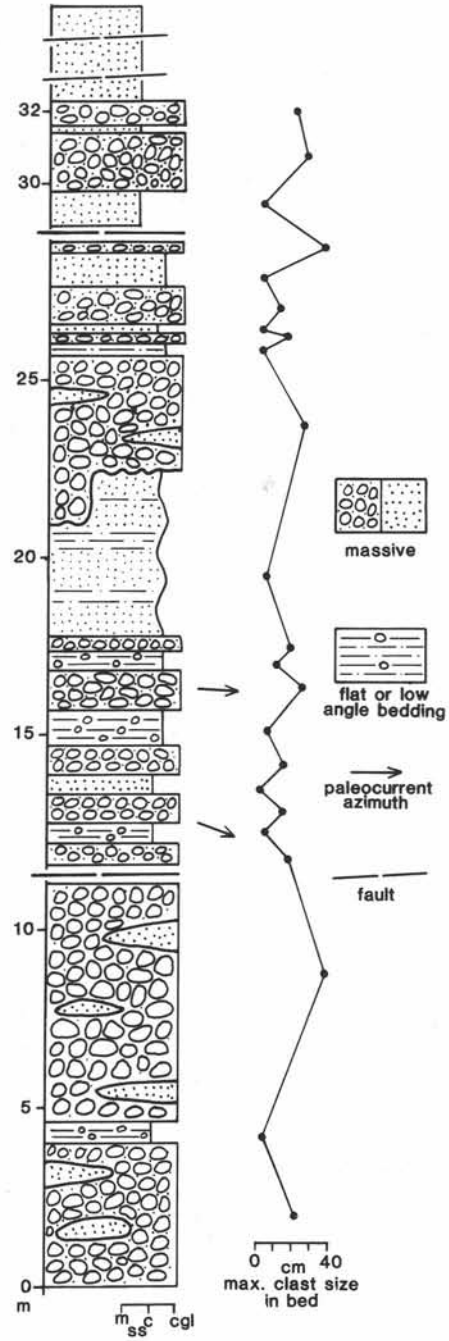

Figure 9. Stratigraphic section of the conglomerate facies of Tronsen Creek of the Swauk Formation at Stop 5 (Ruby Creek).

Swauk conglomerate and sandstone adjacent to the fault contact at Ruby Creek are interpreted as proximal alluvial-fan deposits on the basis of coarse grain size, poor sorting, and thick, lenticular bedding. The general lack of internal structure in conglomerates suggests that mass-flow depositional processes were important. Framework-supported conglomerates might represent partially winnowed debris flows. Rare erosional surfaces and horizontally aligned and imbricated clasts suggest that stream processes were also active. Most of the clast types occur as bedrock to the west in the Ingalls Tectonic Complex, the apparent sediment source. Granodiorite clasts were probably derived from a more distant source in the Mount Stuart batholith. We believe that the alluvial fan formed along a scarp related to offset on the fault at Ruby Creek. The abrupt grain-size change in the Swauk outcrops a few hundred meters to the southeast of the fault suggests that the inferred alluvial fan was quite small. Paleocurrents and lithologic contrasts suggest that this small fan interfingered to the east with a fluvial system carrying arkosic debris that was probably derived from a northern crystalline source.

36.4 (1.9) Continue north on U.S. 97. Outcrop of granodiorite fanglomerate behind Ingalls Creek Lodge (store).

STOP 6. Granodiorite Fanglomerate (Optional Stop).

Park at the northern end of the parking lot, north of the store and gas pumps. Walk east a few hundred meters to the cliff.

Exposed here is an outcrop of granodiorite breccia, included by Taylor and others (1988) in the breccia facies of Devil's Gulch, within the Swauk Formation. The rock consists of angular clasts of granodiorite as much as 3 m in maximum dimension in a matrix of angular, granodioritic sand (Gresens and others, 1981). Where well indurated, the rock is difficult to distinguish from granodiorite. The fanglomerate grades upward in these exposures to massive and cross-bedded sandstones that have paleocurrents to the west.

These rocks now lie east of the main trace of the Leavenworth fault zone (Tabor and others, 1982a). Following their deposition, they were down dropped into the Chumstick basin by a westward shift (as much as 1 km) of the main trace of the Leavenworth fault and a reversal of its sense of vertical offset (Taylor and others, 1988). Similar facies occur discontinuously in the Leavenworth fault zone on both sides of its main trace (Frizzell and Tabor, 1977; Tabor and others, 1982a). These relations indicate that the Leavenworth fault zone is best thought of as a broad, branching zone in which lithologically similar facies of the Swauk and Chumstick Formations have been complexly juxtaposed.

38.2 (1.8) Start of discontinuous outcrops of Chumstick Formation.

43.3 (5.1) Junction of U.S. 97 and U.S. 2. Turn left (northwest) on U.S. 2 toward Leavenworth.

45.5 (2.2) Prominent outcrop of Chumstick Formation on the left.

46.9 (1.4) Prominent outcrop of Chumstick Formation on the left.

48.5 (1.6) Enter Leavenworth.

End of Day 1 road log.

Day 2: Chumstick Formation

Start in the town of Leavenworth. Go to the junction of U.S. 2 and Ski Hill Drive (paved town road that goes north, located west of the city center). *Reset odometer.*

0.0 (0.0) Junction of U.S. 2 and Ski Hill Drive. Turn north on Ski Hill Drive.

0.7 (0.7) Junction with Ranger Drive. Turn left (west).

1.2 (0.5) Ranger Drive turns sharply right and becomes a dirt road. Continue on the dirt road (signs to Tumwater Mountain). This road has deep washouts and is barely passable with passenger car.

3.2 (2.0) **STOP 7A. Overview of Tumwater Mountain section.**

Stop and park at the junction of dirt roads.

Stops 7A and 7B examine coarse-grained fluvial deposits from rivers that flowed ENE into the Chumstick basin from uplifts west of the Leavenworth fault zone. The development of west-derived sediment sources indicates a major change in Chumstick drainage patterns and drainage directions, and this is referred to as Phase 2 in the Chumstick basin evolution (Evans, 1988). Deposition of these units fol-

lowed folding, uplift, and erosion of the Swauk Formation. Farther south, similar Chumstick deposits contain basalt clasts probably derived from the Teanaway Formation (about 47-45 Ma; Fig. 3E). To the northeast, these units are interstratified with Chumstick basin-fill deposits whose age is approximately 44 to 41 Ma. These age relations help constrain the interval of Phase 2 deposition to between about 45 and 41 Ma (Fig. 3F).

The field trip starts at this locality because it is the best access to coarse-grained fluvial deposits in the proximal regions of a humid-tropical, alluvial-fan system. From this viewpoint, one can observe virtual cross-sectional views of broadly lenticular (width to thickness ratio of 10:15), laterally stacked (that is, overlapping ribbons), fanhead channels filled with boulder-cobble conglomerate (Fig. 10). Paleoflow was directed to the northeast, which is into the face of the outcrop. Typical channel deposits are 3 to 5 m thick and 40 to 80 m wide. (Note that some erosional loss of the top of each channel sequence is likely.)

The lateral stacking of these channels is interpreted as evidence for channel switching (avulsions) in the fanhead regions. As individual channels became choked with sediment, subsequent floods formed new channels in the topographic lows between earlier deposits.

Continue on the road to examine some of these deposits more closely. Take the right fork, and continue on the dirt road.

3.5 (0.3) Outcrops of Chiwaukum Schist in the Leavenworth fault zone.

3.7 (0.2) **STOP 7B. Proximal fan deposits (Phase 2).** Stop and park at the sharp bend in the road.

The accessible outcrops along the road consist of channel fills (massive to crudely stratified cobble conglomerate) and interbedded sandstone units. The latter are predominantly massive to planar-bedded, coarse-grained sandstone, and less commonly trough cross-bedded and planar-laminated coarse- to fine-grained sandstone. These sandstone units have a sheet-like geometry. Paleocurrent directions from trough cross-beds are polymodal and suggest that some of these may have represented sheetflood deposits that flowed down-fan, while other units may represent proximal onlaps of basin-fill. Proximal onlaps have been observed in a number of strike-slip basins (Steel and Gloppen, 1980) and are attributed to depocenter migration sourceward in response to oblique slip on the bounding fault.

Conglomerate clasts were derived from source rocks exposed just west of the Leavenworth fault zone (53% biotite-quartz schist, 42% granodiorite, 4% quartz or quartzite, 1% rhyodacite porphyry clasts; 102 clasts counted). Clasts are subrounded to subangular and are set in a matrix that is lithologically similar to disaggregated granodiorite. Clast imbrication is rare. Many of the conglomeratic channel fills have basal coarsening-upward sequences over the basal 3 to 5 clast layers, then exhibit coarse-tail normal grading to the top of the bed.

Plant macrofossils recovered from some of the finer grained units at this locality indicate a mixture of broad-leaved evergreen and broad-leaved deciduous types and include several genera of climbing vines. This fossil assemblage appears to be a mixture of upland forest types and riparian vegetation (Evans, 1988).

Turn around and retrace the route back to Leavenworth.

6.6 (2.9) Junction of Ranger Drive with Ski Hill Drive. Turn right toward town.

7.3 (0.7) Junction with U.S. 2. Turn left into town.

8.0 (0.7) Junction of U.S. 2 with SR 209. Turn left on SR 209.

8.5 (0.5) Junction with Peshastin road. Stay left on SR 209.

13.9 (5.4) Junction with Clark Canyon road (dirt). Turn right onto Clark Canyon road.

15.0 (1.1) Resistant ridge to the left is tuff unit Tctc2 ("zeolite tuff" of Tabor and others, 1987).

15.1 (0.1) Begin almost continuous outcrops of Chumstick Formation.

16.2 (1.1) **STOP 8. Distal fan deposits (Phase 1).** The vans will unload here, turn around, and meet us about 2 hr later about 0.5 mi back down the canyon (at the prominent bend in the road).

There are approximately 1,400 m of continuous section exposed on the north side of

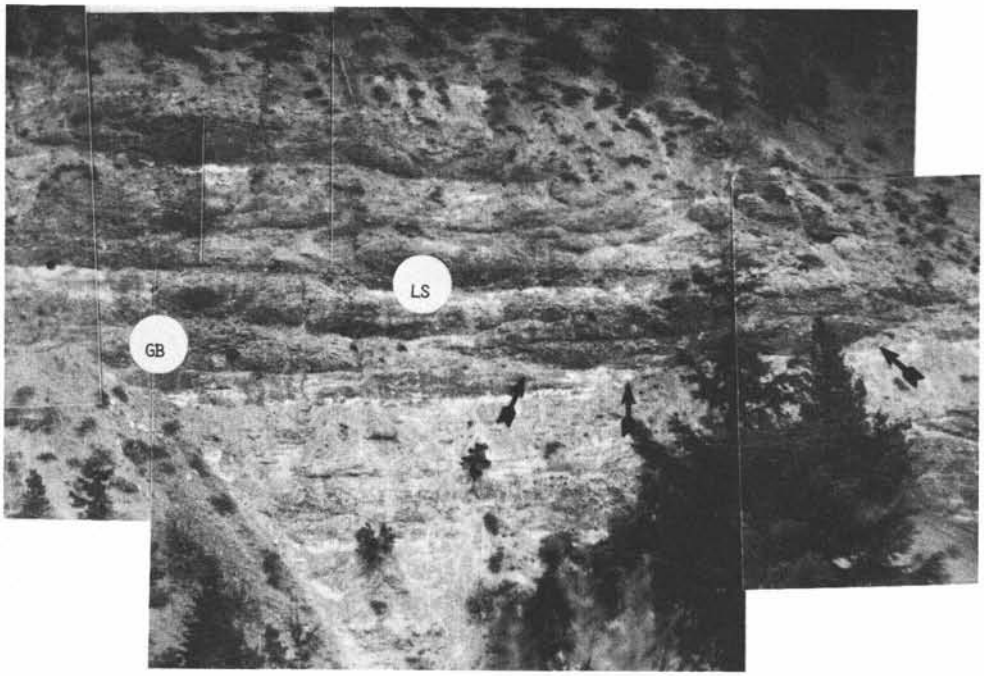

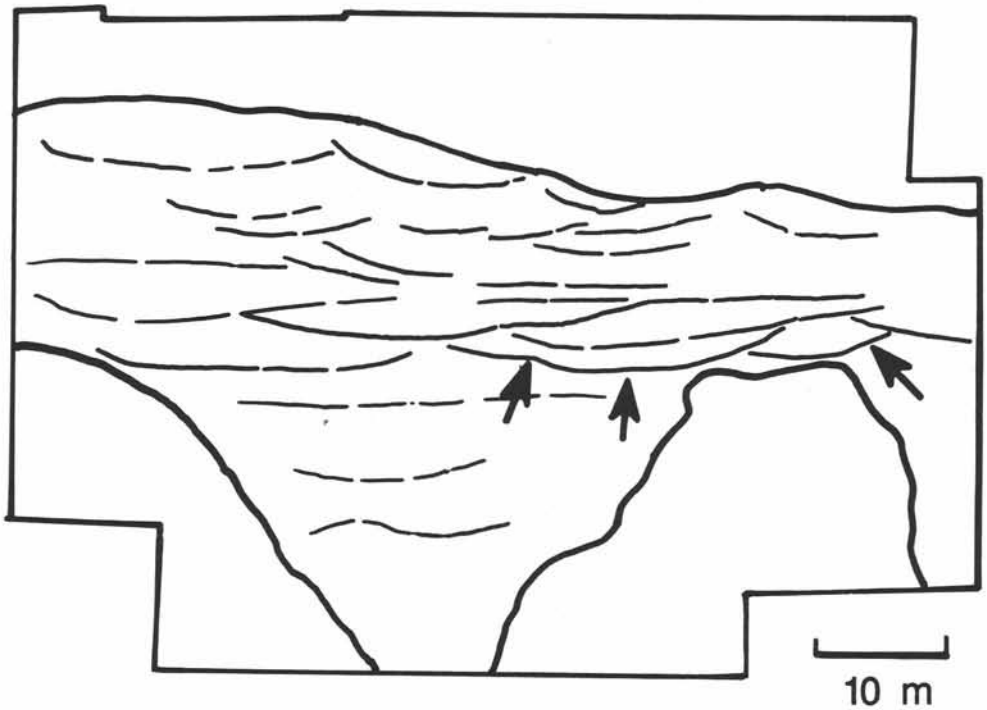

Figure 10. Photomosaic and interpretive sketch of cliff exposure at Stop 7 (Tumwater Mountain section), showing approximate cross-sections of broadly lenticular fanhead channels (paleoflow directed into outcrop). GB, gravel bedform; LS, layered sand sheet.

Clark Canyon, and isolated intervals on the south side can be correlated across the canyon. Nine air-fall and ash-flow tuffs are interbedded within this section (Fig. 11). Each tuff bed has a distinctive trace-element chemistry (McClincy, 1986) that permits its use as a marker bed. At this stop, we will examine the section between tuffs Tctc7 and Tctc5.

Depositional units that have been identified in this section include: gravel bars (massive to crudely stratified conglomerate); bar-platform deposits (planar-bedded and trough cross-bedded sandstone, and laminated to massive fine-grained sandstone and mudstone); channel deposits (trough cross-bedded sandstone); channel-margin slumps (mudstone intraclasts); and overbank deposits (ripple cross-laminated, planar-laminated, and massive sandstone and mudstone). Detailed correlation using tephrostratigraphy permits studies on the architecture of depositional units (Fig. 12). Gravel-bar and bar-platform deposits are sheet-like in geometry, average 2 to 3 m in thickness, and are laterally continuous for several hundred meters. Paleosols are present in many of the overlying bar-platform deposits. Broadly lenticular, multistory, trough cross-bedded sandstones are interpreted as deposits from inter-bar channels that transported sand bedload during lower flow conditions.

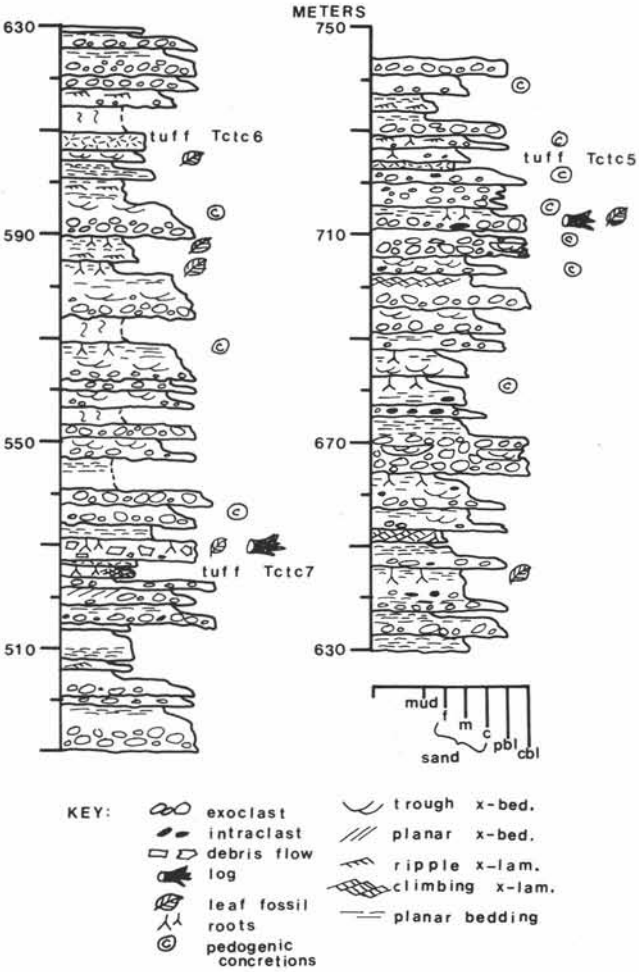

Figure 11. Stratigraphic section showing distal fan deposits of the Clark Canyon section. Location of interbedded tuffs shown. Field trip Stop 8 will examine the part between tuff units Tctc7 and Tctc5 (Tabor and others, 1987).

Gravel-bar deposits consist of subrounded to rounded, pebble-cobble conglomerate (Fig. 13). Clast composition (909 clasts) reflects two sources: crystalline rocks (22% granite and granodiorite, 11.3% biotite gneiss, 11.5% vein quartz, 0.7% hornblende schist); and felsic volcanic rocks (47% rhyodacite porphyry, 3% vitric tuff, 3% flow-banded rhyolite, 1% andesite porphyry). The crystalline rock clasts were derived from plutonic and metamorphic sources east of the basin. The felsic volcanic component was derived from sources either northeast of the basin (for example, Duncan Hill pluton) or from the intrabasinal dome complex near Wenatchee (about 44-40 Ma). The percentage of felsic volcanic clasts increases stratigraphically upward at the expense of plutonic and metamorphic clasts throughout Phase 1 deposition.

The Clark Canyon section contains both air-fall and ash-flow tuffs. The tuffs at the field trip locality are green-gray vitric tuffs that include pumice clasts and incorporated exoclasts. The lowermost tuff unit, Tctc7, comprises two vitric tuff layers, each capped by a diamictite. The lower diamictite is about 1 m thick and consists of angular clasts of tuff and pumice. The upper diamictite is 2 m thick and contains leaves, branches, and carbonized plant fragments. Both diamictites are interpreted as debris flows, which probably originated from hillslope instability in the basin headwaters following the destruction of vegetation by ash fall. Tuff unit Tctc6 is about 3 m thick and massive at its base, and becomes planar-bedded and detrital-rich near the top. Tuff unit Tctc5 is about 60 cm thick and grades upward into tuffaceous sandstone. Note that tuffaceous sandstone units are distinctive in these outcrops due to strong induration and greenish coloration (chalk white on weathering).

The Clark Canyon section was deposited during Phase 1 sedimentation, which was characterized by gravel- and sand-bedload

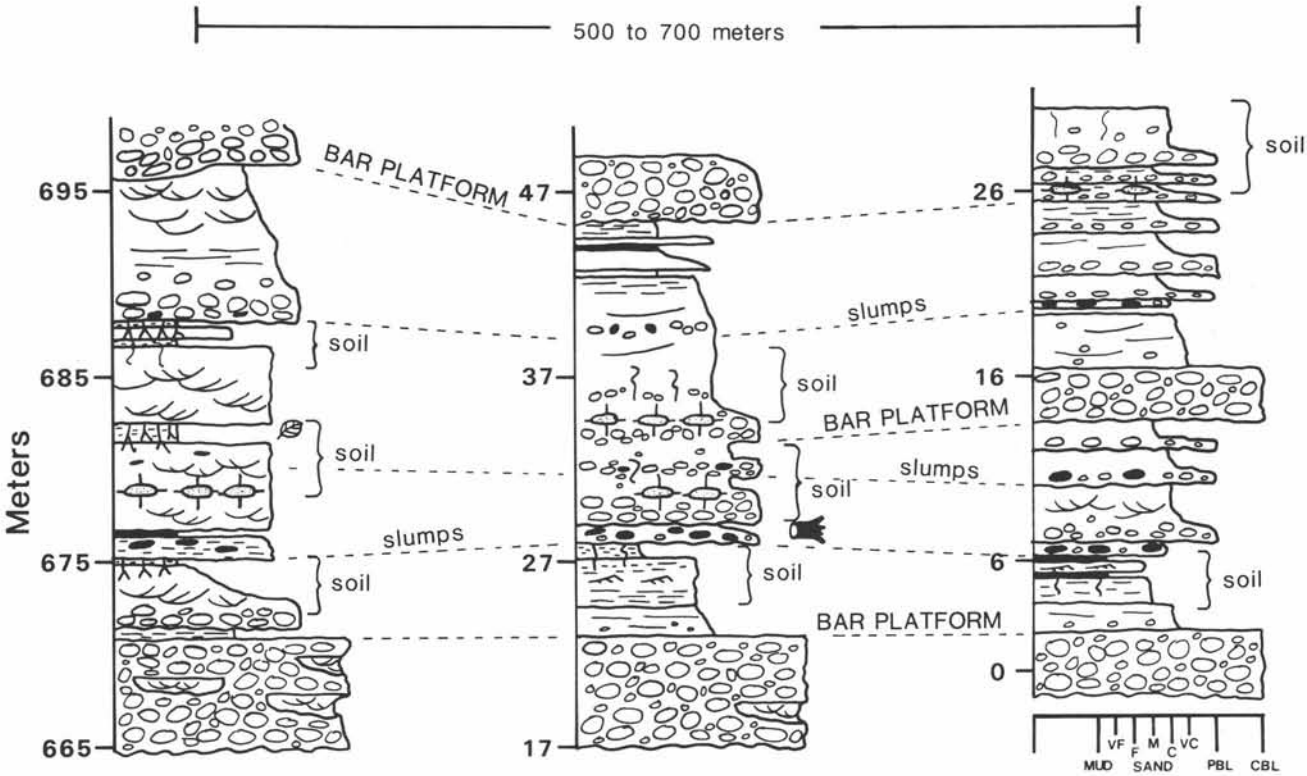

Figure 12. Three stratigraphic sections in Clark Canyon immediately above tuff unit Tctc5 (Tabor and others, 1987), showing laterally continuous, sheet-like gravel-bar and bar-platform deposits with soils. Left section includes vertically stacked, multistory sandstone channel deposits. These are interpreted as deposits from inter-bar channels that transported sand bedload during low-flow conditions. Symbols are the same as in Figure 11.

Figure 13. Typical gravel-bar and bar-platform deposit, Clark Canyon section. Gravel-bar deposits consist of massive to crudely stratified framework conglomerate. Bar-platform deposits are planar-bedded to laminated sandstone and mudstone. Hammer for scale (30 cm).

streams that flowed west to the vicinity of the Leavenworth fault zone. At times during Phase 1, there was no relief in the Leavenworth fault zone, and these depositional systems were continuous with Swauk depositional systems (Figs. 3A and 3C). At other times, deformation in the Leavenworth fault zone resulted in southeast- (and possibly northwest-) flowing axial drainage systems in the Chumstick basin, parallel to the Leavenworth fault zone (Figs. 3B and 3D).

Return to the vehicles and retrace route to SR 209.

18.5 (2.3) Junction of Clark Canyon road and SR 209. Turn right (north).

26.4 (7.9) Cross the Wenatchee River.

31.2 (4.8) Junction of SR 209 and SR 207. Turn left on SR 207.

31.4 (0.2) Junction of Lake Wenatchee road. Turn right.

31.7 (0.3) Enter Lake Wenatchee State Park.

32.3 (0.6) Lunch stop in picnic grounds of state park.

33.2 (0.9) Retrace route to SR 207. Turn left.

33.4 (0.2) Junction of SR 207 and SR 209. Turn right on SR 209.

36.4 (3.0) Prominent outcrop of Chumstick Formation with excellent preservation of leaf fossils.

38.7 (2.3) Junction of SR 209 and Wenatchee River road. Stay left on SR 209.

40.3 (1.6) **STOP 9. Mixed-load fluvial deposits (Phase 3).**

Park in pulloffs along the right side of the road. Set parking brakes. *Use extreme caution at this outcrop because of traffic.*

The last stage of Chumstick deposition (Phase 3, Figs. 2 and 3G) is recorded by mixed-load fluvial deposits, which have been preserved in the northern and southeastern parts of the basin. In comparison to older Chumstick strata, Phase 3 sediments have finer overall grain sizes and less steep paleoslopes. Unlike older Chumstick strata, the paleocurrent data from these outcrops display no consistent drainage pattern or any relation to the major fault zones. These data are interpreted as evidence for tectonic quiescence and low basin relief during Phase 3 deposition.

At this stop, depositional units are organized into vertically stacked, multistory-channel deposits encased in thick sequences of overbank deposits. Channel sequences overlie scoured basal surfaces and consist of massive to trough cross-bedded sandstone and pebbly sandstone. Rare lateral-accretion surfaces can be observed, including a poorly exposed example in the road cut (Fig. 14). Cutbanks, channel-margin slumps, and intraclasts attest to bank cohesion. An abrupt grain-size reduction at the top of this channel sequence is interpreted as evidence for channel abandonment due to channel switching and avulsion.

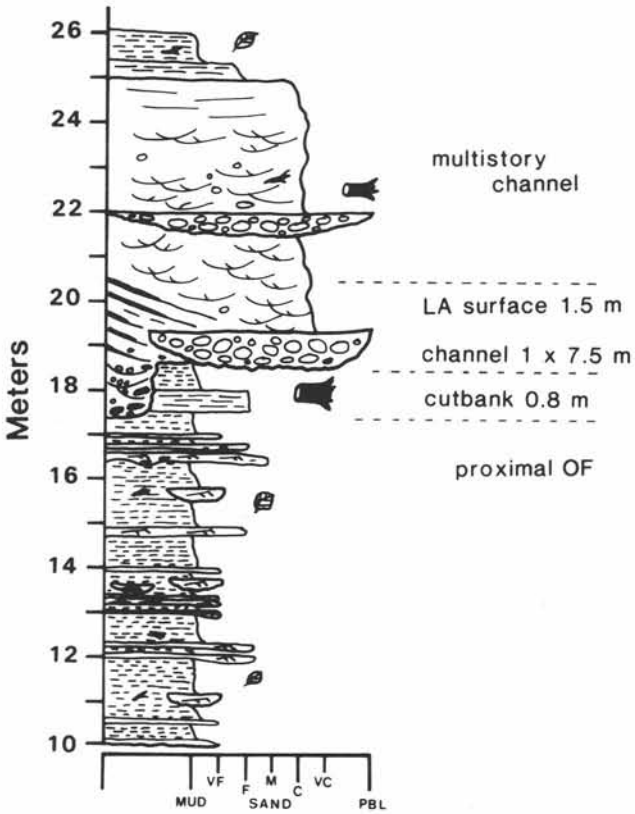

Figure 14. Stratigraphic section of a part of the South Plain section (Stop 9), showing multistory sandstone channel deposits, lateral-accretion surfaces (LA), and thick sequences of proximal overbank deposits (OF). Symbols are as in Figure 11.

Fine-grained units include thin, lenticular bodies of ripple-laminated and planar-laminated sandstone, laminated and massive mudstone, and carbonaceous mudstone. The maximum total organic carbon (TOC) content of these units is 4 percent (Evans, 1988). Although fossil rootlets and rootcasts are rare, most of the fine-grained units are destratified and probably supported soils. Preservation of leaf fossils is poor at this exposure.

51.9 (11.6) Retrace the route to Leavenworth. At the junction of SR 207 and U.S. 2, turn left on U.S. 2, toward Wenatchee.

61.9 (10.0) Prominent outcrop of Chumstick Formation.

62.6 (0.7) Junction of U.S. 2 and the Cashmere turnoff. On the left side of U.S. 2 are coarse-grained fluvial deposits of Phase 1 in the Eagle Creek fault zone. Continue on U.S. 2.

66.5 (3.9) Exit U.S. 2 onto Main Street into the town of Monitor. The road immediately crosses the Wenatchee River.

66.7 (0.2) The road crosses railroad tracks.

67.0 (0.3) Turn left on Richared Drive.

67.3 (0.3) Turn left at "T" junction onto West Richared Drive.

67.6 (0.3) The road jogs right and becomes Sleepy Hollow Road.

68.2 (0.6) **STOP 10. Mixed-load fluvial deposits (Phase 2).**

Park along the right shoulder of the road.

This stop is in the eastern sub-basin of the Chumstick Formation, east of the Eagle Creek fault zone and west of the Entiat fault zone. The eastern sub-basin opened as a transtensional step-over basin during an interval of dextral motion on the parallel, partly overlapping Eagle Creek and Entiat fault systems (Fig. 3F). Uplift in the Eagle Creek fault zone truncated the earlier, predominantly westward-flowing drainages. Gravel-bedload streams flowed west off the Entiat highlands into an axial drainage system that flowed southeast into a lacustrine-deltaic complex (Stop 11).

These deposits represent the fluvial channel and delta plain deposits that overlie the delta-front turbidites we will see at the next stop. Broadly lenticular, multistory-channel sequences consist of trough cross-bedded sandstone and planar-laminated and climbing ripple cross-laminated sandstone. Channel deposits are extensively bioturbated (*Skolithos*). Overbank deposits include laminated and ripple cross-laminated sandstone, laminated and massive mudstone, and carbonaceous mudstones with as much as 5 percent TOC. An example of the influence of floodplain topography on subsequent channel switching or avulsion is shown in Figure 15.

Continue east on Sleepy Hollow Road.

69.5 (1.3) The road jogs left.

69.7 (0.2) Cross the railroad tracks.

69.9 (0.2) Cross the Wenatchee River.

70.1 (0.2) Junction with Lower Sunnyslope Road. Turn left.

70.4 (0.3) Junction with U.S. 2. Continue straight across U.S. 2 on Lower Sunnyslope Road.

70.6 (0.2) **STOP 11. Lacustrine-deltaic deposits (Phase 2).**

Junction with Sunnyslope Road (also called Upper Sunnyslope Road, Lower Monitor Road, and(or) Easy Street). Park along the right side of the road.

This stop is one of the reference sections for the Nahahum Canyon Member of the Chumstick Formation (Gresens and others, 1981) and comprises fluvial and lacustrine deposits in a delta-front setting. Lenticular channels (Fig. 16) were cut and filled predominantly by massive sand units and less commonly by turbidite sequences (Bouma ABE, AE, or BCE divisions), channel-margin slumps, or dunes. Nonchannelized deposits typically consist of BCE and DE division turbidites. A maximum of 5 percent TOC is recorded in mudstones at this outcrop. Organic debris in channel deposits includes leaf fragments and logs. Biogenic structures are rare.

Paleocurrent indicators include trough cross-bedding, flute casts, grooves, current lineation, and asymmetric straight ripple crests. Paleoflow

Figure 15. Part of the Monitor section (Stop 10), showing floodplain topography (differential compaction of mudstones created topographic low, filled by subsequent channel deposit). Person indicates scale.

was directed down the trough of the eastern subbasin to the southeast. Paleoslope orientation can be obtained from slump fold orientations that indicate that paleoflow was approximately perpendicular to paleoslope.

Evidence for high sedimentation rates and high levels of lake turbidity include lack of macrofossils, abrasion of pollen grains, and rarity of biogenic structures. The fairly high TOC content of the shales suggests that rapid burial facilitated preservation of the original organic material. Lake depth is difficult to gauge from these deposits. Periodic subaerial exposure may be indicated by mudcracks and ripple marks with planed-off tops.

Continue east on Sunnyslope Road (Easy Street).

72.7 (2.1) Junction with U.S. 97. Turn right; follow signs into Wenatchee on Business U.S. 2 (Wenatchee Avenue).

77.4 (4.7) Continue on Wenatchee Avenue. (Do *not* take U.S. 2 and SR 28 turnoff.)

79.2 (1.8) **STOP 12. Mixed-load fluvial deposits (Phase 3).**

Park along the right side of the road. *Be extremely careful of traffic at this stop.*

Phase 3 deposits in the southeastern part of the basin do not show any relation to the main fault zones, and they unconformably overlie the hydrothermally altered and folded older Chumstick rocks near the Wenatchee dome (Fig. 3G). The deposits at this stop include placer gold and mineralized clasts from these older, hydrothermally altered Chumstick rocks (J. Margolis, Univ. of Washington, oral commun., 1987). Conglomerate clast composition reflects local volcanic sources (65% rhyodacite porphyry, 2% vitric tuff, 6% flow-banded rhyolite, 11% vein quartz, 10% granite, 2% biotite gneiss, and 4% sedimentary clasts; 190 clasts).

These deposits are organized into vertically stacked, multistory-channel deposits encased in overbank sequences (Fig. 17). Channel deposits have basal scoured surfaces and consist of massive to trough cross-bedded sandstone and pebbly sandstone, with lesser amounts of planar-laminated and climbing ripple cross-laminated sandstone. Cutbanks, channel-margin slumps, lateral-accretion surfaces, and intraclasts attest to bank cohesion. Overbank deposits include ripple cross-laminated and laminated sandstone, laminated and massive mudstone, and carbonaceous mudstone. Fossil rootlets, destratified layers, *Skolithos*, and leaf-litter layers indicate extensive biologic activity along channel margins and in floodplains. Pollen from this locality (analyzed by Shell Offshore,

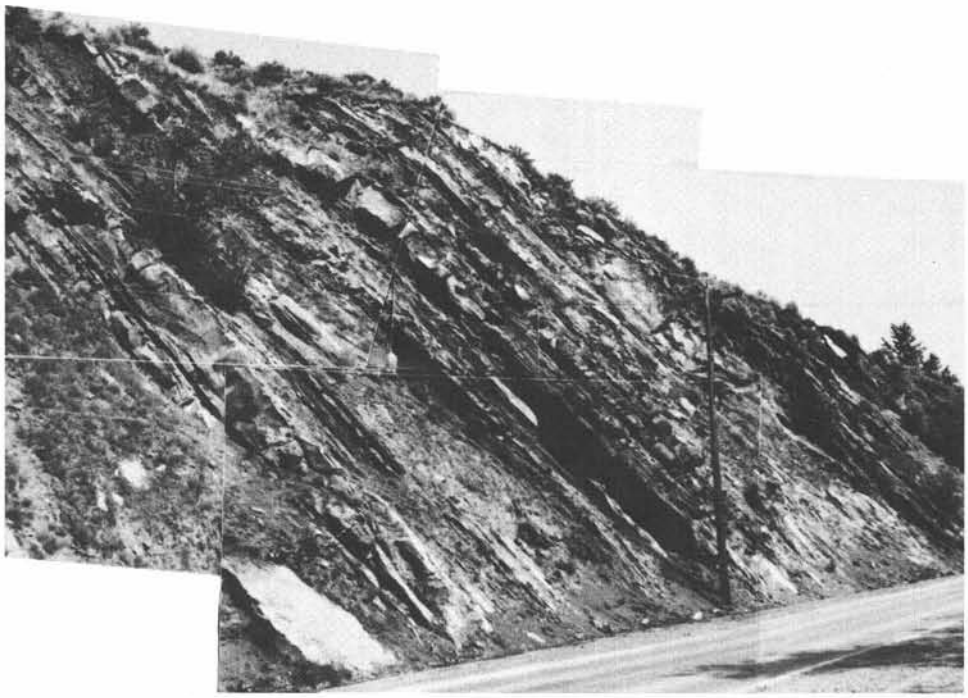

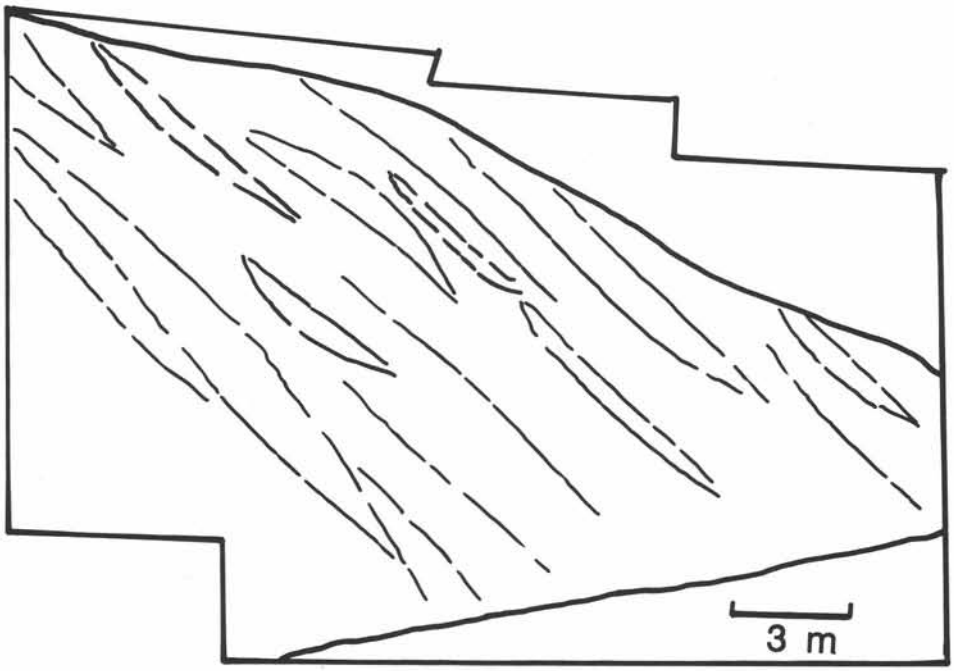

Figure 16. Photomosaic and interpretive sketch of lacustrine-deltaic deposits at the Sunnyslope Road section (Stop 11), showing lenticular channels infilled by massive sandstones, by turbidite sequences (dominated by Bouma ABE or BDE divisions), or by channel-margin slumps.

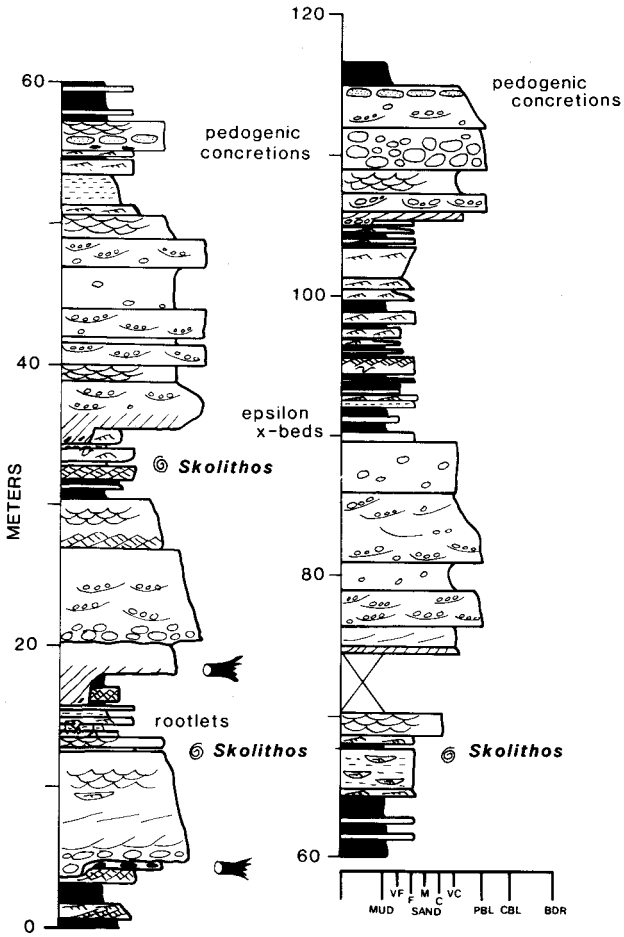

Figure 17. Stratigraphic section for the Malaga Road section (Stop 12), showing multistory sandstone channel deposits separated by intervals of proximal overbank deposits. Symbols are as in Figure 11.

Incorporated, for J. Evans) contains latest Eocene indicators (E. Leopold, Univ. of Washington, 1987, oral commun.).

End of Day 2 log and field trip. Turn around and retrace the route into Wenatchee.

81.2 (2.0) Junction of Wenatchee Avenue and U.S. 2. Turn left on Ferry Street (immediately after U.S. 2 overpass).

81.3 (0.1) Turn left on Mission Street.

81.4 (0.1) Turn left on Stevens Street (becomes U.S. 2 and SR 28 in 0.1 mi).

81.5 (0.1) Junction with U.S. 2 and SR 28. Cross the Columbia River.

81.7 (0.2) Turn off SR 28 toward Rock Island and Quincy.

Take SR 28 southeast from Wenatchee to Quincy (about 30 mi). Take SR 281 south from Quincy to George (about 10 mi). Junction with I-90. Take I-90 east to Spokane (about 133 mi).

Gold Deposits in Northern Ferry County

Richard J. Tschauder

Gold Deposits in Northern Ferry County, Washington

Richard J. Tschauder
Hecla Mining Company
Box 467
Republic, WA 99166

INTRODUCTION

The north half of Ferry County has the most consistent record of large gold production of any area of comparable size in the Pacific Northwest. High-grade gold deposits were generally known in the area prior to the opening of the Colville Indian Reservation to mineral entry in 1896, and were put into production shortly thereafter. Although gold deposits are scattered throughout the county, 99 percent of the production to date has come from the Republic Mining District. By January 1, 1989, that district had produced more than 2.5 million oz of gold and 14 million oz of silver from less than 4.5 million tons of ore.

Remarkably, major exploration companies paid little attention to the area until Hecla Mining Company discovered the Golden Promise ore body in late 1984. Since that discovery, several companies acquired and drilled properties in the area, but the only additional successes are by Echo Bay Mining Company at the Key and Kettle River properties. As of September 1988, published ore reserves on four mining properties in the county exceeded 1.4 million oz of gold.

Early geologic work in the area was by Umpleby (1910) and Lindgren and Bancroft (1914) in the Republic Mining District. In spite of its importance as a gold producing region, northern Ferry County received very little scientific attention. The Republic graben was not recognized until 1960 (Staatz, 1960), and regional geologic maps were first published only two decades ago (Muessig, 1967; Staatz, 1964; Parker and Calkins, 1964). Although Lindgren recognized the epithermal nature of the deposits, no major study of the district appeared until 1968 (Full and Grantham, 1968).

Recently, the pace of scientific investigation has increased, in part as a response to renewed mineral-industry interest in the area. Several studies have contributed to a better understanding of mineral deposits. E. R. Braun (Hecla Mining Co., unpub. study, 1986) attempted the first major wallrock geochemical study of the Republic Mining District. R. M. Fifarek and others (Southern Illinois University, Carbondale, unpub. data) are expanding on this work and are examining light stable isotope patterns. Gaylord and others (see Holder and others, this volume) are re-examining the Eocene volcanic and sedimentary stratigraphy. Atwater and others (1984), Holder (1986) and Holder (1985) have examined Tertiary plutons in the area.

GEOLOGIC SETTING

All known gold deposits in northern Ferry County lie in the Republic graben, a down-dropped block 6 to 10 mi wide that extends from near the Canadian border south to the Columbia River. Within the graben, basement consists of metamorphosed Permian and Triassic flows and sedimentary rocks (Parker and Calkins, 1964). Overlying these rocks are, from oldest to youngest, sedimentary and volcanic rocks of the O'Brien Creek Formation, the Sanpoil Volcanics, and the Klondike Mountain Formation (Muessig, 1967), all of early Tertiary age. The O'Brien Creek Formation is dominated by reworked tuffs, shales, and conglomerates; the Sanpoil Volcanics consists of rhyodacitic flows and pyroclastic rocks; and the Klondike Mountain Formation comprises epiclastic rocks derived principally from the Sanpoil Volcanics. The Eocene Herron Creek suite of intrusive rocks intrudes both the metamorphic basement rocks and the lower part of the Eocene extrusive assemblage. (See Holder and others, this volume).

Outside the graben, nearby rocks consist of high-grade metamorphic rocks of the Kettle and Okanogan gneiss domes and epizonal batholithic intrusions of calcic, calc-alkalic, and alkali-calcic affinity (Holder, 1986; Holder, 1985; R. W. Holder and G. M. Holder, unpublished mapping).

From: Joseph, N. L., and others, editors, 1989, Geologic guidebook for Washington and adjacent areas: Washington Division of Geology and Earth Resources Information Circular 86.

Permian and Triassic Rocks

Permian and Triassic rocks crop out north of Curlew and along the flanks of the Republic graben. Rock types include basic flows and tuffs, limestone, argillite, quartzite, chert, and graywacke, all of which have been metamorphosed to greenschist facies (Parker and Calkins, 1964; Muessig, 1967). Most common is a sequence of graywackes with lesser amounts of argillite and limestone. This package does not form prominent outcrops. Two other important groups are present: basic flows and limestones. These pre-Tertiary rocks have been intruded by stocks, dikes, and sills of Eocene rhyodacite, and outcrops are sparse, perhaps explaining why these rocks have not been studied in detail.

Several bodies of serpentine are associated with the Permian and Triassic rocks north of Curlew and elsewhere (Parker and Calkins, 1964) and in adjacent parts of British Columbia (Little, 1983). The age of the serpentine is not known, but it is cut by dikes of Scatter Creek Rhyodacite, and therefore must be pre-Eocene.

Tertiary Rocks

O'Brien Creek Formation

The O'Brien Creek Formation consists of reworked tuffaceous sandstones, shales and conglomerates. The formation is distinguished from other rocks in the area by the abundance of small, black argillite chips, detrital quartz, distinct bedding,and its distinctive white color. In contrast to overlying units, conglomerates in the O'Brien Creek Formation contain rounded clasts of hornblende-free granodiorite and high-grade metamorphic rocks, but no clasts of volcanic origin. Diamond drilling by Hecla Mining Company and underground mine development by Crown Resources Corporation have demonstrated that the contact between the O'Brien Creek Formation and the overlying Sanpoil Volcanics is gradational; flows and tuffs of the Sanpoil are interbedded with epiclastics of the underlying formation over an interval of at least 100 ft.

Sanpoil Volcanics

The Sanpoil Volcanics consists of porphyritic flows, pyroclastic breccias, and lithic tuffs (generally confined to the upper part of the unit), epiclastics ranging in grain size from mudstones to boulder conglomerates, and an upper "rubble zone".

Flows are the dominant rock type and form massive cliffs along the river valleys and the higher peaks within the graben. They are of various hues, and their composition is dominantly rhyodacitic but ranges from rhyolite to andesite (Tschauder, unpublished data). Flows similar in appearance and composition to the Sanpoil Volcanics have been detected in the Klondike Mountain Formation in the Republic Mining District, as well as in other locations in the graben.

Pyroclastic rocks occur in the upper Sanpoil Volcanics in a number of places in the graben. Rock types are dominantly massive lithic tuffs, with abundant tuff breccias. Some of these pyroclastic rocks were assigned to the Tom Thumb Tuff Member of the Klondike Mountain Formation by Muessig (1967) and Parker and Calkins (1964), while rocks stratigraphically and lithologically equivalent were elsewhere assigned to the Sanpoil Volcanics. For this discussion, all these rocks are assigned to the Sanpoil Volcanics, and the term Tom Thumb Tuff is dropped.

The contact between the Klondike Mountain Formation and the Sanpoil Volcanics is not well defined. Parker and Calkins (1964) and Muessig (1967) describe an unconformity at the base of the Klondike; however, Holder and others (this volume) show that it is not of regional extent. Data from more than 120 diamond drill hole penetrations of the contact area by Hecla Mining Company and other diamond drill holes near Mount Elizabeth and in the First Thought graben (Stevens County) indicate that the contact is gradational.

Conglomerates, sandstones, and mudstones interbedded with the pyroclastic rocks appear in at least four stratigraphic positions within the Sanpoil Volcanics in the Republic Mining District and elsewhere. Hand specimens of these rocks, where they are not hydrothermally altered, are very similar to samples of sediments higher in the stratigraphic section, in the middle part of the Klondike Mountain Formation.

Within the Republic Mining District, a conglomerate (the so-called rubble zone) marks both the paleosurface at the time of mineralization and the temporary cessation of regional volcanism. This conglomerate in places contains angular to subrounded clasts of various Sanpoil lithologies, including vein fragments and altered rock fragments (both silicic and argillic), and it is silicified and argillically altered. Geologists presently working in the district place the top of the Sanpoil Volcanics at the top of this conglomerate.

Klondike Mountain Formation

Because diamond drilling in the Republic district and elsewhere suggests much of what was mapped by Muessig (1967) as Klondike Mountain Formation belongs in the Sanpoil Volcanics, it is necessary to redefine the Klondike Mountain Formation here. The Klondike Mountain Formation comprises two units: a broadly coarsening-upward epiclastic sequence overlain by a lithoidal to glassy flow sequence. The epiclastic sequence consists of a lower unit of evenly laminated organic-rich shales and silts, a middle unit consisting of graded-bedded and massive sandstones, and an upper conglomeratic unit. The flow sequence consists of black glassy to lithoidal flows overlying a regional unconformity (Muessig, 1967; Parker and Calkins, 1964). The Klondike Mountain For-

mation is discussed in detail elsewhere in this volume (Holder and others).

Intrusive Rocks

Muessig (1967) gave the name Scatter Creek Rhyodacite to widespread porphyritic hypabyssal intrusive dikes, sills, and irregular masses that are younger than the O'Brien Creek Formation but older than the Klondike Mountain Formation. The typical rhyodacite is a light gray to dark greenish-gray porphyry containing equant plagioclase phenocrysts and hornblende prisms. Unless crosscutting relations can be established, the rock is virtually impossible to distinguish in the field from porphyry flows.

The alkalic rocks of Shasket Creek occur 2 mi SSW of Danville along a narrow WNW-zone (Parker and Calkins, 1964). Four units have been recognized: monzonite, shonkinite, trachytic syenite, and syenite porphyry, in that order of abundance (Herdrick and Bunning, 1984). The alkalic rocks crosscut and have thermally altered Permian and Triassic rocks and are in turn crosscut by the Scatter Creek Rhyodacite.

Epizonal intrusive rocks cropping out in and adjacent to the graben are discussed in detail by Holder and others (this volume).

Structure

The dominant structural feature in northern Ferry County is the NNE-trending Republic graben. The nature and age of the graben have been a source of debate ever since its recognition. The majority of workers (Muessig, 1967; Staatz, 1960; Parker and Calkins, 1964; Holder, 1986; Holder, 1985) suggest an extensional origin during the Eocene, related either to magma-chamber evacuation or gneiss dome formation. However, the appearance of granodioritic and high-grade metamorphic clasts in conglomerates in the O'Brien Creek Formation strongly suggests that graben formation in part predated the Sanpoil Volcanics and postdated gneiss dome formation.

Several independent lines of evidence suggest that the Republic graben marginal faults experienced dextral transcurrent movement through the deposition of the Sanpoil Volcanics, followed by normal movement at the beginning of and possibly through deposition of the Klondike Mountain Formation. The evidence includes: clockwise rotation of an average of 25 degrees in the direction of remnant magnetization at 102 sites in Eocene volcanic rocks, with wide variation in the data (Fox and Beck, 1985); a clockwise rotation of as much as 30 degrees of isolated structural blocks containing the Knob Hill No. 3 vein near the western graben margin; small-scale dextral transcurrent offsets of veins close to faults within the graben but parallel to the graben margin faults; strike-slip slickensides on several faults; and dextral transcurrent displacement of 1,500 ft on the Eureka fault and no apparent dip-slip displacement by the Hermes and Crosby faults, which parallel the graben marginal faults.

Several faults which appear to be dextral transcurrent in nature are truncated at or near the base of the Klondike Mountain Formation and must predate that formation. Normal faulting during and after deposition of the Klondike Mountain Formation unroofed co-magmatic epizonal plutons in the graben walls.

GOLD DEPOSITS

Gold deposits in northern Ferry County include epithermal veins and disseminated deposits (Republic District and Kettle River mine), gold-bearing replacement deposits related to calc-alkaline intrusion and volcanism (Overlook, Oversight, and Key deposits), gold hosted in alkalic dikes (the Gold Dike mine), and gold-copper veins associated with serpentine (the Morning Star mine). From the standpoint of past production, epithermal precious metal veins are the most significant.

Epithermal Precious Metal Deposits

Epithermal precious metal deposits in northern Ferry County are of the low-sulphur adularia-sericite type (Hayba and others, 1985) and are genetically related to hot-spring activity at the paleosurface marking the top of the Sanpoil Volcanics (as defined here). Geometric ore controls vary from a near-paleosurface disseminated environment consisting of sinter and silicified rock, which grades downward into stockworks, which grade downward into tightly confined veins. The veins are the most productive. The following discussion of epithermal vein systems is based on work in the Republic Mining District.

A cross-section through a typical epithermal hot-spring system is shown in Figure 1. The paleosurface is expressed as a porcelaneous silica sinter underlain by a circular to elliptical breccia zone that grades downward and outward into a stockworks of chalcedonic veinlets. The stockworks ultimately coalesce downward into a series of veins; finally, these veins join to form a large vein (the low-resistance conduit of Fig. 1). This large vein gradually decreases in width downdip. Adjacent to the main vein are several secondary veins that are also mineralized, but not to the extent of the main vein.

Tenor varies throughout the vein system. Near the paleosurface, ore grades normally range from 0.05 to 0.10 oz/ton gold, increasing gradually with depth through the stockworks. The zone in which the stockworks coalesce into large veins and into a main vein has the highest grade ore of the system (the throttle zone of Fig. 1); gold grades here commonly exceed 1.00 oz/ton gold and locally are in excess of 100.00 oz/ton.

Tenor in adjacent veins (secondary vein, Fig. 1) is normally one-half to one-third that of the main vein. Both

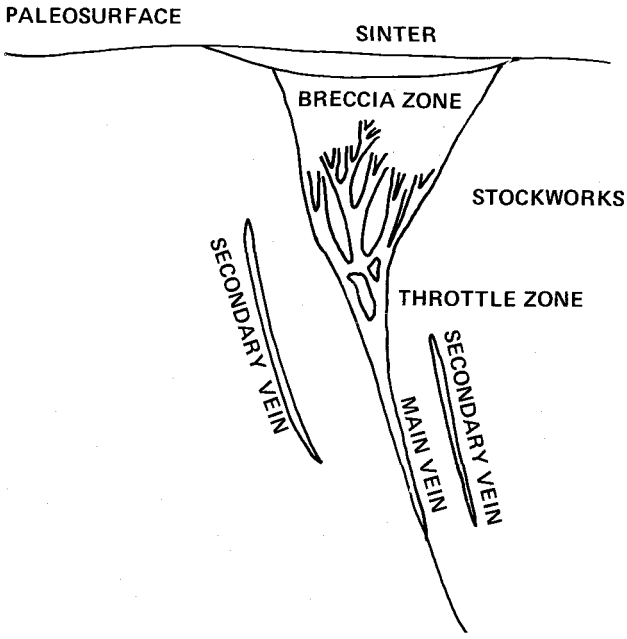

Figure 1. Components of an epithermal precious metal hot spring system, modeled after the deposits in the Republic Mining District. No scale is implied.

the Knob Hill and the Golden Promise vein systems are good examples of this difference. The Gold Dollar vein in the Knob Hill system averaged 0.862 oz/ton gold, while the secondary veins averaged 0.435 oz/ton gold. The Golden Promise vein system exhibits a similar variation.

Vein mineralogy of the Republic District consists of electrum, native gold, naummanite, chalcopyrite, and pyrite in a gangue of chalcedony, calcite, and clay. Metallic minerals rarely constitute more than 5 percent of the vein; exceptions are in the upper levels, where pyrite can constitute as much as 25 percent of the vein.

R. M. Fifarek, M. Sollman, and Tschauder (unpub. data) have studied the silica phases in the veins in the Republic Mining District. Three major types of chalcedony can be recognized; these are, from oldest to youngest, banded, brecciated, and vug and fracture fillings. Paragenetic position has been determined by cross-cutting relations and crustification sequences.

Banded chalcedony consists of banded white and black chalcedony and clay in approximately equal proportions. Band geometry ranges from planar to intricately convoluted, and ore tenor increases with the complexity of banding. Bands range in thickness from 1 mm to 5 cm. Banded chalcedony contains significant amounts of gold, silver, and selenium.

Brecciated chalcedony is generally dark gray to black and contains locally visible, but normally microscopic grains of pyrite and marcasite. The dark chalcedony occurs as matrix to most vein breccias and as filling in small fractures and as filling in medial cavities in banded veins. The breccias consist of fragments of wallrocks (some of which are altered or replaced by chalcedony) and of earlier banded chalcedony. The fragments range from less than a millimeter to several centimeters in their greatest dimension. Brecciated chalcedony generally decreases in abundance with depth. It contains more mercury, iron, arsenic, and antimony and less silver, gold, and selenium than the banded chalcedony. Although the brecciated chalcedony is depleted in gold and silver, it is enriched in silver relative to gold.

The vug and fracture fillings consist of bilaterally symmetrical medium-gray to white banded veinlets, massive brown chalcedony, and vug fillings. This phase is relatively depleted in all elements listed above.

The distribution of trace elements and the alteration patterns in the wallrocks around the veins in the Republic Mining District are typical of an epithermal system (Hayba and others, 1985; Silberman and Berger, 1985). In general, wallrocks adjacent to a vein are enriched in gold, silver, and antimony, while erratically distributed mercury and arsenic anomalies are located near the paleosurface.

The wallrocks have been silicified and argillically altered. The silicified zone, in the shape of a downward-tapering funnel centered on the vein, tends to grade outward into an argillic zone, which in turn grades outward and downward into a propylitic zone.

Epithermal precious metal deposits in northern Ferry County are spatially and genetically related to a paleosurface which marks the waning stages of calc-alkaline volcanism in the Eocene. The relation of the deposits to this paleosurface is evident by constraints placed on the age of ore-controlling faults, the lack of mineralized rock in overlying sediments, and by the presence of mineralized and altered clasts in the sediments which define the paleosurface. This same paleosurface also marked the beginning of the coarsening-upward sedimentary sequence in the Klondike Mountain Formation and the onset of normal faulting. While the relative timing of mineralization has been well established, an absolute date of mineralization has not been determined. Hence, a genetic tie between epithermal mineralization and replacement mineralization, discussed below, cannot be definitively established.

Replacement Deposits

Replacement deposits occur in Permian and Triassic metasedimentary rocks. The deposits consist of two zones: (1) a massive magnetite, pyrrhotite, and pyrite zone replacing limestone and superjacent siliceous argillite, and (2) stockworks of quartz and pyrite and disseminated sulfides in the siliceous argillite.

The replacement zone consists of two phases: a lower oxide phase consisting of magnetite, and an overly-

ing, thinner, massive sulfide zone consisting of pyrrhotite and pyrite. The zone of stockworks and disseminated sulfides occurs immediately above the replacement zone and is not everywhere present. Minerals in the stockworks consist of pyrite and pyrrhotite in quartz and minor chalcopyrite, arsenopyrite, and magnetite. Gold is enriched in, but not confined to the sulfide phases in both zones.

Known replacement deposits occur as small tabular and apparently isolated masses near Cooke Mountain, along the east margin of the Republic graben; they lie in a northeast belt approximately 1 mi long roughly parallel to and just west of the graben margin. Three ore zones have been discovered to date: the Key East, the Key West, and the Overlook. A fourth zone, the Oversight, is not economic. The ore zones at the Key East and the Key West are about 20 ft thick, while the ore zone at the Overlook, where stockwork ore is dominant, is at least 100 ft thick.

Garnet and other calc-silicate minerals typical of a skarn deposit are rare, and alteration seems to be confined to minor chlorite and sericite adjacent to the ore bodies. No widespread geochemical halos have been detected, although bismuth, arsenic, and copper are enriched proximal to the replacement bodies.

Intrusive rocks exposed on Cooke Mountain are dominantly sills and dikes of Scatter Creek Rhyodacite. Not all mineralized zones are in contact with the intrusive rocks, nor are they strictly stratabound. The zones are known to cut across bedding at angles as much as 25 degrees.

The age of replacement mineralization is not known definitively. It is inferred to be approximately the same as that of the associated intrusions (which have not been dated on Cooke Mountain), and it must be older than the last movement on the Sherman fault, which forms the eastern margin of the graben in this area. Nearby brecciated slices of mineralized rock assumed to be correlative with those on Cooke Mountain occur in the Sherman fault zone, and magnetite veins have been found along structures adjacent to and striking parallel to the Sherman fault.

Deposits Related to Alkalic Rocks

Fox (1973) recognized two subparallel belts of alkalic diatremes and stocks, which, including related rocks in British Columbia, have an aggregate length of 130 mi. The alkalic intrusive bodies range in size from 0.15 to 1.2 mi^2 and consist of brecciated rock and fenitized wallrock. Although radiometric ages of ~190 Ma have been obtained on some of these complexes, others clearly crosscut the O'Brien Creek Formation (Pearson, 1967) and must, therefore, be Tertiary in age.

Most of the alkalic bodies are mineralized to some extent; the metals generally present are molybdenum and copper. However, gold has been produced from the Shasket Creek group of alkalic stocks and dikes near Danville.

Economic minerals in the Shasket Creek intrusive group are hosted in alkalic dikes of two types: a trachytic syenite, and a syenite porphyry (Parker and Calkins, 1964). A trachytic syenite dike hosts copper and silver at the Comstock mine, while a syenite porphyry dike hosts copper and gold at the nearby Gold Dike mine. Cross-cutting relations between the trachytic syenite and the syenite porphyry have not been established, and the two rock types may represent spatially coincident, but temporally separate events. The Shasket Creek alkalic rocks intrude Permian and Triassic metamorphic rocks. Scatter Creek Rhyodacite dikes crosscut the alkalic rocks.

Gold at the Gold Dike mine occurs as micron-thick coatings on disseminated pyrite and chalcopyrite; minor amounts of auriferous pyrite occur as fracture fillings and in quartz-pyrite veinlets (D. Herdrick, Vulcan Mountain Mining Company, oral commun., 1986). Although no systematic study has been attempted, the gold content seems to be proportional to pyrite content and inversely proportional to pyrite grain size.

Alteration consists of minor late-stage fenitization, thermal metamorphism of the Permian and Triassic rocks adjacent to the intrusive bodies, and perhaps some carbonitization. The dikes contain concentrations of silver, tungsten, copper, tellurium, platinum, and palladium, and smaller concentrations of fluorine, antimony, arsenic, and mercury (Herdrick and Bunning, 1984). The geochemical signature is similar to that at other gold deposits associated with alkaline porphyries (Mutschler and others, 1985).

Deposits Associated with Serpentine

Until 1988, the final type of gold deposit discussed here was not studied, explored for, nor mined in Ferry County for more than 40 yr. The deposit consists of quartz and calcite veins striking more or less parallel to a serpentine body in Permian or Triassic greenstones. The veins contain varied amounts of native gold, auriferous pyrite, and chalcopyrite. Ore zones within the veins are normally small but relatively enriched in gold. Gold may be genetically tied to serpentinization, as this type of mineralization coincides with serpentine outcrops in at least three widely separated areas in and around northern Ferry County, including the California mine, near Republic, and the Morning Star mine, near Danville.

ACKNOWLEDGMENTS

The author wishes to acknowledge the assistance and discussions provided by the staffs of Hecla Mining Company, Echo Bay Mining Company, Crown Resources Corporation, and Vulcan Mountain Mining Company. Critical comments by reviewers Tom Salzer of Hecla

Mining Company, Walt Hunt and his associates of Echo Bay Mining Company, and Kevin Brackney of Crown Resources Corp. helped improve the manuscript. I also thank Hecla Mining Company for permission to publish. Special thanks go to David Gaylord of Washington State University and his students, and to Richard Fifarek of Southern Illinois University and his students for the creative effort they have put into the Republic Mining District on behalf of Hecla Mining Company. Nancy Joseph and Thor Kiilsgaard reviewed the manuscript.

REFERENCES CITED

Atwater, B. F.; Rinehart, C. D.; Fleck, R. J., 1984, Preliminary geologic map of the Colville Indian Reservation, Ferry and Okanogan Counties, Washington; with a table of potassium-argon ages: U.S. Geological Survey Open-File Report 84-389, 20 p., 4 pl.

Fox, K. F. Jr., 1973, The geology of alkalic complexes in north-central Washington: U.S. Geological Survey Open-File Report 73-73, 249 p., 5 pl.

Fox, K. F. Jr.; Beck, M. E. Jr., 1985, Paleomagnetic results for Eocene volcanic rocks from northeastern Washington and the Tertiary tectonics of the Pacific Northwest: Tectonics, v. 4, no. 3, p. 323-341.

Full, R. P.; Grantham, R. M., 1968, Ore deposits of the Republic mining district, Ferry County, Washington. *In* Ridge, J. D., ed., 1968, Ore deposits of the United States, 1933-1967; Graton-Sales Volume: American Institute of Mining Metallurgical and Petroleum Engineers, v. 2, p. 1481-1494.

Hayba, D. O.; Bethke, P. M.; Heald, Pamela; Foley, N. K., 1985, Geologic, mineralogic, and geochemical characteristics of volcanic-hosted epithermal precious-metal deposits. *In* Berger, B. R.; Bethke, P. M., editors, 1985, Geology and geochemistry of epithermal systems: Society of Economic Geologists Reviews in Economic Geology, v. 2, p. 129-135.

Herdrick, Melvin; Bunning, B. B., 1984, Geology of the Gold Dike mine, Ferry County, Washington: Washington Geologic Newsletter, v. 12, no. 1, p. 20-22.

Holder, G. A. M., 1985, Geology and petrology of the intrusive rocks east of the Republic graben in the Republic quadrangle, Ferry County, Washington: Washington State University Master of Science thesis, 87 p.

Holder, R. W., 1986, Emplacement and geochemical evolution of Eocene plutonic rocks in the Colville batholith: Washington State University Doctor of Philosophy thesis, 189 p.

Huntting, M. T., 1956, Inventory of Washington minerals, Part II, Metallic minerals: Washington Division of Mines and Geology Bulletin 37, 2 v.

Lindgren, Waldemar; Bancroft, Howland, 1914, The Republic mining district, Washington. *In* Bancroft, Howland, 1914, The ore deposits of northeastern Washington: U.S. Geological Survey Bulletin 550, p. 133-166.

Little, H. W., 1983, Geology of the Greenwood map area, British Columbia: Geological Survey of Canada, Paper 79-29, 37 p., 1 pl.

Muessig, S. J., 1967, Geology of the Republic quadrangle and a part of the Aeneas quadrangle, Ferry County, Washington: U.S. Geological Survey Bulletin 1216, 135 p., 1 pl.

Mutschler, F. E.; Griffin, M. E.; Stevens, D. S.; Shannon, S. S. Jr., 1985, Precious metal deposits related to alkaline rocks in the North American Cordillera–An interpretive review: Geological Society of South Africa Transactions, v. 88, no. 2, p. 355-377.

Parker, R. L.; Calkins, J. A., 1964, Geology of the Curlew quadrangle, Ferry County, Washington: U.S. Geological Survey Bulletin 1169, 95 p., 4 pl.

Pearson, R. C., 1967, Geologic map of the Bodie Mountain quadrangle, Ferry and Okanogan Counties, Washington: U.S. Geological Survey Geologic Quadrangle Map GQ-636, 1 sheet, scale 1:62,500, with 4 p. text.

Silberman, M. L.; Berger, B. R., 1985, Relationship of trace-element patterns to alteration and morphology in epithermal precious-metal deposits. *In* Berger, B. R.; Bethke, P. M., editors, 1985, Geology and geochemistry of epithermal systems: Society of Economic Geologists Reviews in Economic Geology, v. 2, p. 203-232.

Staatz, M. H., 1964, Geology of the Bald Knob quadrangle, Ferry and Okanogan Counties, Washington: U.S. Geological Survey Bulletin 1161-F, 79 p.

Staatz, M. H., 1960, The Republic graben, a major structure in northeastern Washington: U.S. Geological Survey Professional Paper 400B, p. B304-B306.

Umpleby, J. B., 1910, Geology and ore deposits of the Republic mining district: Washington Geological Survey Bulletin 1, 67 p.

Road Log

Day 1: The Republic District

The first day of the field trip will examine an Eocene epithermal hot spring system at various levels below the paleosurface in the central portion of the Republic Mining District. Characteristics of the deposits in the Republic Mining District and the Eocene rock package as well as the major structural features will be discussed.

The trip route and stops are shown on Figure 2. *All the stops listed for Day 1 are on private land. Permission must be obtained prior to entering.*

Cumulative mileage is given on the left; interval mileage is shown in parentheses.

0.0 (0.0) Intersection of Washington State Route (SR) 20 and Clark Street, in Republic. Go north on Clark Street.

0.15 (0.15) End of Clark Street; turn left on Knob Hill Road.

0.3 (0.15) The outcrop on the right is one of the few places where the contact between the Sanpoil Volcanics and the Klondike Mountain Formation is exposed. Note the clasts of chalcedonic quartz in the light-green conglomerate.

0.75 (0.45) **STOP 1. The Quilp and Surprise mines.** Pull off on the primitive road to the right.

Bedrock geology of this area is shown in Figure 3. Rock outcrops are tuff breccias and lithic tuffs of the upper Sanpoil Volcanics. Both of these mines are on the Eureka fault, a northwest-striking, northeast-dipping structure. Production from the mineralized portion of the Eureka fault, which extends from the Bailey ore body southeast 5,000 ft to the Quilp mine, totals 444,161 tons of ore, yielding 237,179 oz gold and 1,215,271 oz of silver. Historic production grades decrease from northwest to southeast; production from the Bailey ore body on the north averaged 0.686 oz/ton gold, while production from the Quilp ore shoot averaged only 0.410 oz/ton gold. The Eureka fault is not mineralized south of the Quilp mine.

Production from the upper part of the Quilp ore shoot, mined from the small glory hole on the hill, totaled 50,393 tons of ore at an average grade of 0.186 oz/ton gold and 1.14 oz/ton silver. The small pit is a good example of the style of mineralization near the bottom of the stockworks zone (approximately 200-300 ft below the paleosurface). Underground, the stockworks merge into a vein.

Two important structural elements can be seen in the glory hole. The most obvious is the northwest-striking Eureka fault at the north end of the pit. The second is the northeast-striking faults and veins near the south end of the pit. The northeast-striking structures parallel the Hermes fault, which lies buried in the gulch southeast of the Quilp mine. The Hermes fault, first recognized underground in 1985, does not crop out. It is part of a major northeast-striking structural zone that displaces the Eureka fault to the west 1,500 ft with little dip-slip displacement evident.

The Surprise mine lies on the Eureka fault north of the Quilp mine and is offset from the Quilp by a minor northeast-striking normal fault. Because of this structural offset, the Surprise ore shoot crops out at a level approximately 400 to 500 ft below the paleosurface. At this level, the stockworks have merged into two veins: the Clark and the Surprise.

0.85 (0.1) Continue on the primitive road back to Knob Hill Road, then turn right.

1.8 (0.95) The Knob Hill mill on the right was constructed in 1937 to concentrate ore from the Mud Lake pit, and it has been in near-continuous operation ever since. The mill currently is running at capacity (240 tons/day), processing ore from the Golden Promise mine. After crushing and grinding, ore is fed through a primary flotation circuit and a secondary cyanide vat leach circuit. Gold recovery exceeds 95 percent, and silver recovery exceeds 80 percent.

1.95 (0.15) The Ben Hur vein crops out on the west side of the road. This vein lies in the footwall of and parallel to the Eureka fault. Production from the vein totals 120,161 tons of ore that contained 69,940 oz of gold and 381,714 oz of silver.

2.2 (0.25) Turn right onto a gravel road.

2.4 (0.2) **STOP 2. Knob Hill mine.**

Turn left at the stop sign, veer right around the building, and park at the edge of the mine yard. *This is a congested area. Please watch for traffic. Please wear your hard hats at this stop.*

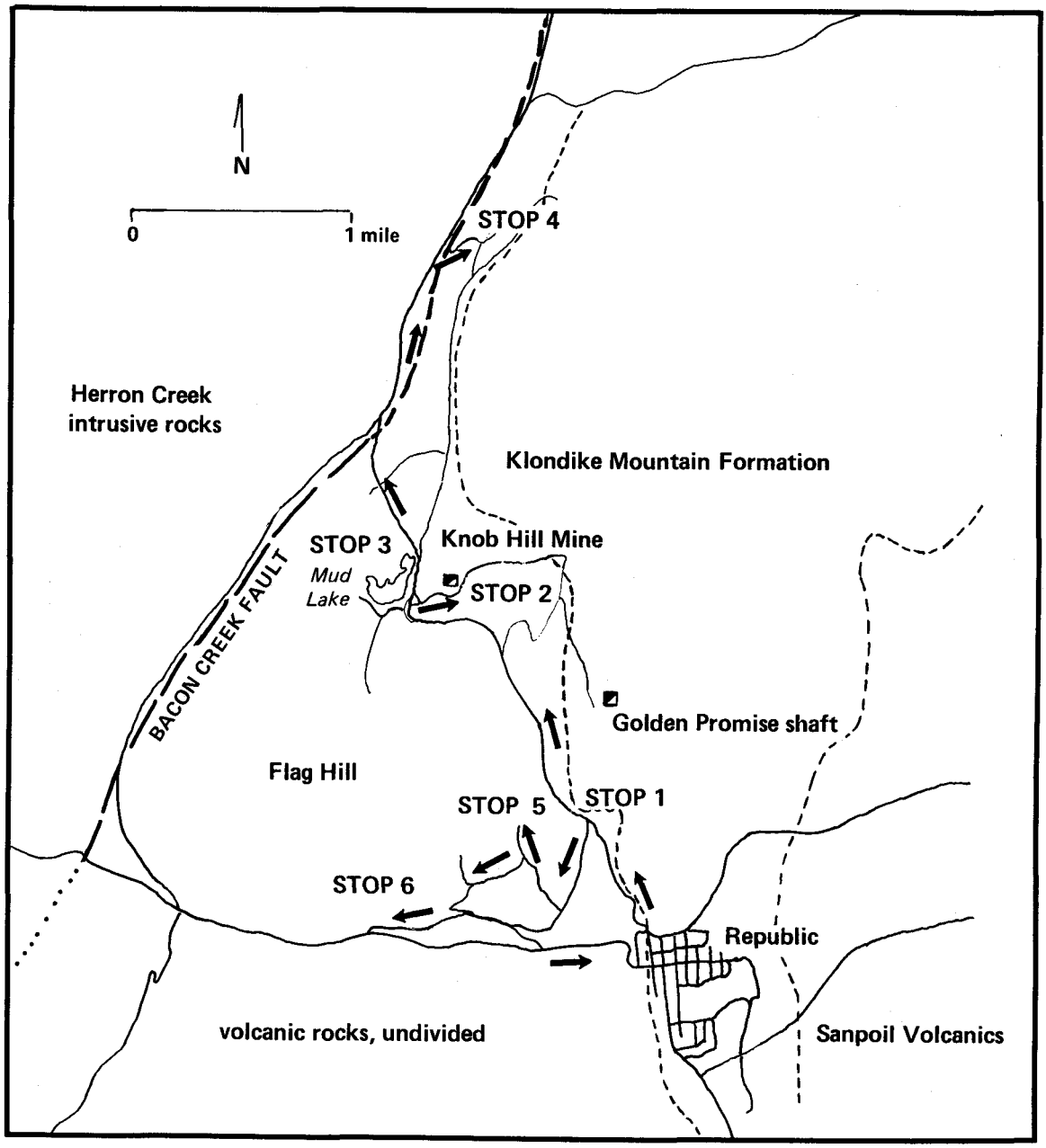

Figure 2. Stops for Day 1 of the excursion and locations of places and features named in the text. Dashed lines, geologic contacts.

The Knob Hill shaft has been in operation since 1941. Sometime in 1989, the 2 millionth ounce of gold will be hoisted from this facility. The shaft is inclined at approximately 65 degrees and is 1,700 ft deep.

The contact between the Sanpoil Volcanics and the Klondike Mountain Formation lies just to the east of the pits. To the north is the Mud Lake pit; the Stewart pit lies to the west. Both pits lie at and just below the paleosurface.

Production from the Stewart pit and underlying stope totals 44,197 tons of ore at an average grade of 0.280 oz/ton gold and 1.43 oz/ton silver. Mining has exploited an oval breccia body that tapers downward into a vein. Carbon fragments are encapsulated in silica within the breccia body, and a layer of organic carbon trash crops out along the north wall. Pyritic mineralization has occurred in places, and the wall rocks are argillically altered.

Ore production from the Mud Lake pit totals 499,067 tons at an average grade of 0.097 oz/ton gold and 0.85 oz/ton silver. As mined in the pit, the somewhat tabular breccia body (which is

capped by milky chalcedony) extends to a depth of about 40 ft and does not physically connect with a known ore body. The breccia body walls are well exposed in places in the west wall of the Mud Lake pit, and the white chalcedonic mantle is exposed on the highwall.

Both pits expose mineralized rocks at or near the Eocene paleosurface. The overall geometry of the ore body at the Stewart pit, the brecciated nature of the ore body, and the abundant carbon trash suggest that the Stewart ore body formed in a hydrothermal eruption crater. The presence of brecciated material representing at least two hydrothermal eruptive events (one above and one below the carbon trash) suggests the area was the site of episodic hydrothermal explosions during the mineralizing event. The geometry of the Mud Lake deposit, its physical isolation from an underlying vein, and the presence of a silica cap suggest a zone of lateral discharge from a hot spring.

The Mud Lake and Stewart deposits are paleosurface expressions of the underlying Knob Hill vein system, production from which (since 1941) has totaled 2.2 million tons of ore at an average grade of 0.55 oz/ton gold and 4.92 oz/ton silver.

2.6 (0.2) Go back to Knob Hill Road, and turn right.

3.2 (0.6) **STOP 3. Mountain Lion mine.**

Turn left and park.

The Mountain Lion mine lies just to the west of the parking area. Like the Quilp, the Mountain Lion exposes veins and upper-level stockworks. Production from the Mountain Lion mine area has totaled 75,000 tons of ore at an average grade of 0.11 oz/ton gold from the stockworks, and 77,600 tons at an average grade of 0.211 oz/ton gold from the vein.

Vein mineralization consisting of both early banded and late black chalcedony phases can be seen in the large open stopes. At this location, the stockworks are dominated by black chalcedony.

At the north end of the Mountain Lion stope, a large, funnel-shaped breccia mass can be observed. The breccia seems to originate in the vein, truncates veinlets in the stockworks, and is weakly mineralized. The breccia may represent crater fill following an explosive hydrothermal event.

Approximately 200 ft to the west is the South Penn pit. The mineral deposit in the pit is unusual in that it is hydrothermally and tectonically brecciated and recemented with silica, and it is relatively rich in pyrite. Production from this area from 1941 to 1947 totalled 45,000 tons of ore that averaged 0.122 oz/ton gold and 0.27 oz/ton silver (K. Brackney, Crown Resources Corporation, oral commun., 1988). Recent production statistics from the pit are not available; however, samples taken from the pit average 0.080 oz/ton gold. The mineral deposit in the pit strikes nearly perpendicular to the Mountain Lion vein system.

3.5 (0.3) Continuing north, pass a small outcrop of conglomerate on the right. The conglomerate contains abundant chalcedony clasts and lies at the top of the Sanpoil Volcanics.

3.9 (0.4) Cross the Bacon Creek fault. The Bacon Creek fault is the western marginal structure of the Republic graben. Rocks to the west are part of the Eocene Herron Creek suite of intrusives (G. M. Holder, Georgia Southern College, oral commun., 1987) and are slightly younger than the Sanpoil Volcanics, which they intrude elsewhere in the graben.

4.4 (0.5) Turn right onto a dirt road.

4.6 (0.2) **STOP 4. The Rebate mine.**

The Rebate mine is the southern end of a discontinuous mineralized zone 2,400 ft in length that is characterized by brecciated chalcedony veins that occur along the contacts of several plagioclase-biotite-hornblende rhyodacite flows. The chalcedony veins occur at six stratigraphic locations, but production from the largest ore shoot (on the Tom Thumb vein) has totaled only 25,000 tons of ore at an average grade of 0.334 oz/ton gold and 1.61 oz/ton silver. Drilling has demonstrated that these veins are discontinous. The same stratigraphic intervals that contain veins also contain carbonaceous bedded sediments or flow breccias along strike.

All the veins in this area contain brecciated and recemented banded chalcedony typical of the banded chalcedony elsewhere in the district. Isolated chalcedony clasts can be found in brecciated flows adjacent to the veins.

The Rebate mineralized zone is an area where hydrothermal fluid flow was controlled by stratigraphic contacts rather than by steeply dipping faults. Mineralization was apparently con-

temporaneous with tilting and bedding plane adjustments. Both the vein and the flows were sheared, vein clasts became mixed with flow clasts in the gouge, and the gouge was recemented by continuing silica deposition.

8.05 (3.45) Return to the Quilp mine, and turn right (southwest).

8.3 (0.25) The dikes in the road cut to the left and the Eureka fault in the gulch below have been displaced to the east approximately 1,500 ft along the Hermes fault and the Crosby shear zone. The dikes have been intersected in drill holes in the footwall of the Eureka fault north of the Quilp mine. Turn right onto a primitive road at this location.

8.45 (0.15) Continue through gate.

8.55 (0.1) Take the right fork.

8.75 (0.2) View of the Golden Promise mine site to the east. The Golden Promise currently contains the bulk of the ore reserves in the district. It is a blind deposit, located beneath an average of 600 ft of post-mineral Klondike Mountain Formation sediments. It was originally intersected by diamond drilling from an exploration drift in 1963. That drilling program resulted in three mineralized intercepts that contained in excess of 0.20 oz/ton gold; the best intercept was 3 ft at 6.62 oz/ton gold and 32.46 oz/ton silver.

This area was not explored for 20 years, partly because the geologists in 1963 believed the pyroclastic rocks of this area were poor hosts for gold mineralization. In 1984, faced with nearly depleted ore reserves at the Republic unit, Hecla Mining Company redrilled the area. Nine of ten holes drilled intersected intervals in excess of 5 ft of 0.25 oz /ton gold, including one intercept of 28 ft at 1.57 oz/ton gold and 11.95 oz/ton silver.

To date, seven veins have been discovered in the Golden Promise area. In 1988, Hecla Mining Company reported Golden Promise ore reserves of 650,000 tons at an average grade of 0.70 oz/ton gold and 2.94 oz/ton silver.

9.2 (0.45) **STOP 5. The Sanpoil vein.**

The vein on this hillside is the south extension of the Ben Hur vein mentioned above. It is exposed here at a level at least 600 ft below the paleosurface.

9.85 (0.65) Return to the fork in the road; turn right.

10.2 (0.4) **STOP 6. The Iron Mask area.**

Veins in this part of Flag Hill intersect the lower stratigraphic parts of the Sanpoil Volcanics and the top of the O'Brien Creek Formation. Six veins have produced ore. Production from the largest vein, the Seattle, totals 10,469 tons at an average grade of 0.813 oz/ton gold and 1.317 oz/ton silver (Crown Resources Corporation, unpublished reports). The ore bodies are small and were likely deposited at some depth.

10.6 (0.4) Turn left (downhill), then left again.

11.1 (0.5) Continue east, past the substation.

11.15 (0.05) Turn right (downhill).

11.3 (0.15) SR 20; turn left and return to Republic.

11.6 (0.3) Cross the Eureka fault (in the gulch). Footwall rocks are O'Brien Creek Formation sediments cut by Scatter Creek Rhyodacite dikes; hanging-wall rocks are upper Sanpoil Volcanics. Although the rocks appear to be argillically altered, alteration extends only a few tens of feet below the surface, and the area is not geochemically anomalous in any of the pathfinder elements, suggesting that alteration here is supergene acid leaching resulting from the breakdown of pyrite.

End of road log for Day 1.

Day 2: Gold Deposits outside the Republic District

The second day of the trip is devoted to four gold deposits outside the Republic District. Of the four, only one, the Kettle River mine, belongs in the epithermal class. Along the way, the regional geologic history, and the possible relations between these deposits and the deposits in the Republic Mining District will be discussed.

The stops are shown on Figure 3. *Reset odometers. All of the stops listed for Day 2 are on private land. Permission must be obtained before entering.*

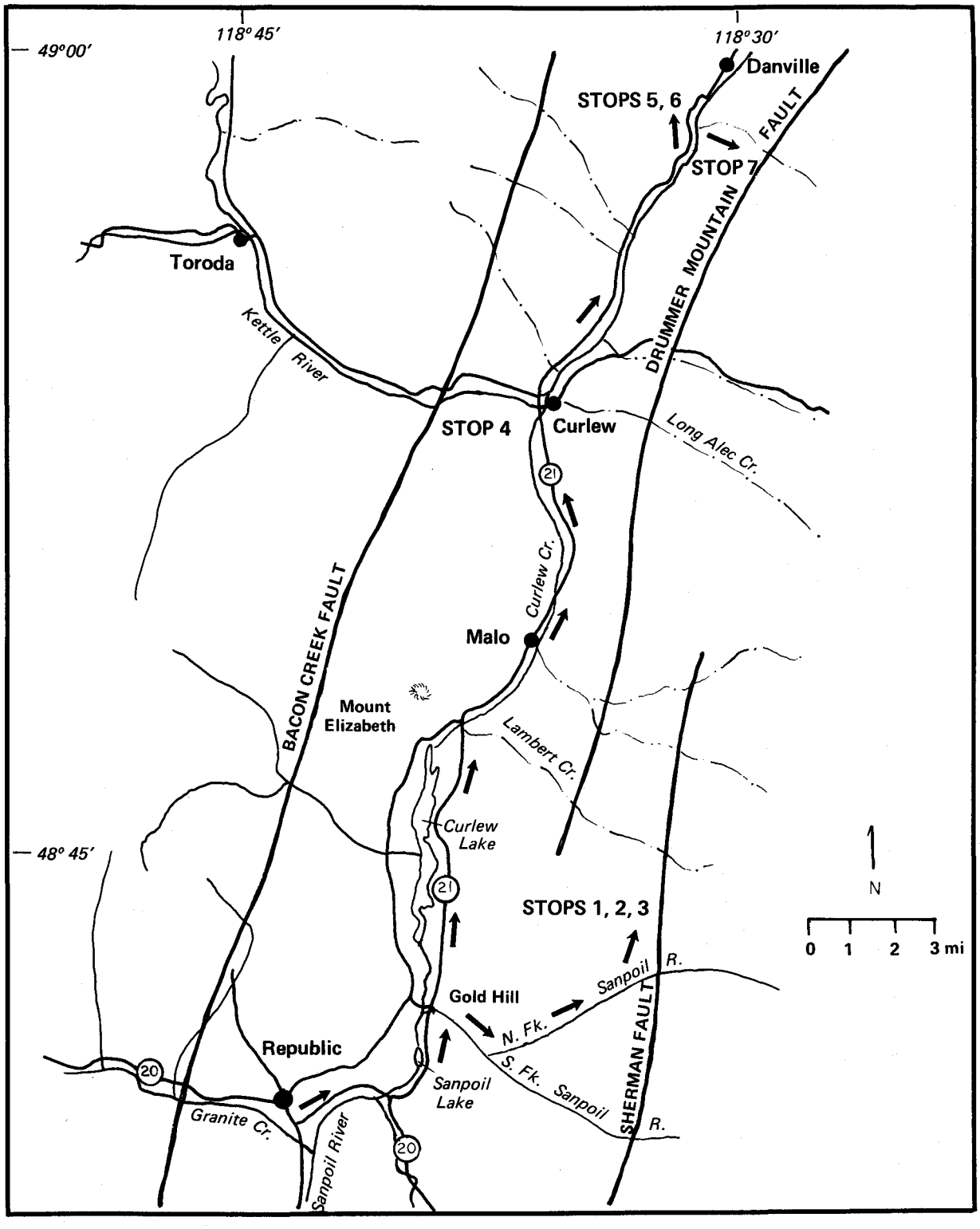

Figure 3. Route for Day 2 of the excursion and locations of places and features named in the text. Graben marginal faults are also shown.

0.0 (0.0) Intersection of SR 20 and Clark Street in Republic. Go east on SR 20.

3.1 (3.1) Turn north on SR 21.

4.0 (0.9) Turn east on Cooke Mountain Road.

6.3 (2.3) Turn north onto a dirt road.

7.15 (0.85) Take the fork to the right.

7.7 (0.55) Pass Echo Bay Mining Company's mill site (on the left).

8.4 (0.7) Turn left.

10.3 (1.9) Bear left.

10.5 (0.2) Turn left.

11.7 (1.2) **STOP 1. Overlook ore zone.**

The Overlook ore body lies as much as 800 ft below the surface at this location. The ore body consists of a basal magnetite/pyrrhotite blanket in limestone as much as 40 feet thick and similar to the deposits we will see later in the day. The basal blanket is overlain by a pyrite-quartz stockworks zone in siliceous argillites and quartzites. The stockworks zone is more than 100 feet thick in places. The blind ore body was detected by a ground magnetic survey.

Reported ore grades from drill hole intercepts are as high as 1.37 oz/ton gold over a 10-ft width (Crown Resources Corporation press releases, 1986-1988). The average grade of the deposit is estimated at 0.2 oz/ton gold. The ore body contains at least 315,000 oz of gold (W. Hunt, Echo Bay Exploration, Inc., oral commun., 1988).

12.9 (1.2) Return to the road intersection at mile 10.5; turn left.

13.5 (0.6) The Sherman fault, which bounds the Republic graben on the east, is in the valley below us. Rocks on the east side of the fault include the Herron Creek and Devils Elbow intrusive suites, and the metamorphic rocks of Kettle gneiss dome.

14.2 (0.7) Bear left.

14.9 (0.7) Bear left.

15.1 (0.2) **STOP 2. Oversight mine.**

The Oversight mine is a small replacement ore body in Permian and Triassic limestones; it resembles the Key East and Key West ore bodies. The nature of the mineralized deposit is evident in the upper adit, where a pyrrhotite blanket overlies magnetite. Both the oxide and sulfide phases contain gold and copper here, and the sulfide phase is enriched in these elements relative to the oxide phase.

15.3 (0.2) Turn left. The Key East ore zone is in the hill to the east. Published reserve estimates for the Key East and the Key West ore bodies are approximately 100,000 oz of gold in each deposit at an average grade of 0.16 oz/ton gold.

15.6 (0.3) **STOP 3. The Key West ore zone.**

The ore zone is exposed in a pit at this location. Again, pyrrhotite overlies magnetite, and both phases contain gold and copper.

26.0 (10.4) Return to SR 21 and turn right (north).

26.5 (0.5) Several small prospects on Gold Hill (to the right) expose quartz-pyrite veinlets that contain small amounts of gold. The rocks here are Permian and Triassic mafic tuffs, flows, and associated intrusive rocks metamorphosed to massive greenstone, phyllite, and some schist (Muessig, 1967).

32.1 (5.6) View of Mount Elizabeth, to the north. At least 1,200 ft of upper Klondike Mountain Formation is exposed on Mount Elizabeth. The upper part of the formation is dominantly black, aphanitic, glassy to stony andesite flows. The flows overlie several rock types in this area, including the metamorphic basement and Klondike Mountain Formation sediments. Relief at the base of the flows is in excess of 1,200 ft (Parker and Calkins, 1964). This relief suggests an unconformity probably related to graben formation.

43.3 (11.2) Turn left on West Kettle River Road.

51.8 (0.8) Turn left onto the Kettle River mine road.

55.5 (0.7) **STOP 4. The Kettle River mine.**

The Kettle River mine is an epithermal deposit similar to the deposits in the Republic Mining District. It consists of banded and brecciated chalcedony veins that contain electrum, pyrite, and pyrargyrite. While the veins are generally narrower and apparently somewhat lower in grade than those in the Republic Mining District, published drill results have been impressive. Vein intercepts from 35 selected diamond drill holes on the property average 13 ft (true width) at an average grade of 0.57 oz/ton gold (Crown Resources Corporation press release, 1985). Gold also occurs in stockworks near the base of a flow. Again, surface exposures are not impressive, and the ore body was a blind discovery. Vein and wallrock geochemistry is similar to that in the Republic Mining District, except selenium is not present at the Kettle River mine (Echo Bay Mining Company staff, unpublished data).

57.0 (1.5) Return to SR 21; turn left (north).

63.6 (6.6) Turn left onto Shasket Creek road.

64.2 (0.6) Turn left.

65.9 (1.7) Turn right.

66.0 (0.1) Mine gate.

66.4 (0.4) **STOP 5. Comstock mine.**

The Comstock mine exploits a WNW-striking, 5-ft-wide vertical trachytic syenite porphyry dike containing pyrite, chalcopyrite, and bornite, primarily as disseminated grains. The dike cuts Permian and Triassic limestone and greenstone similar to the rocks at the Key and Overlook areas. Total production from the Comstock is not known. A Tacoma Smelter settlement sheet in 1939 shows assay values of 7.21 percent copper, 0.02 oz/ton gold and 0.92 oz/ton silver, for a lot of 27 tons. Huntting (1956) reports anomalous platinum from the Comstock dike.

67.1 (0.7) Continue up the mine road and turn right.

67.5 (0.4) **STOP 6. Gold Dike mine.**

This small open pit mine came on stream in 1983 and it has produced approximately 150,000 tons of ore that had an average grade of 0.10 oz/ton gold, and 0.15 oz/ton silver. Ore is contained in a syenite porphyry dike as much as 60 ft wide which cuts a syenite stock (Parker and Calkins, 1964). The dike strikes WNW, parallel to the dike at the Comstock mine. Three types of mineralized rock have been reported: disseminated auriferous pyrite, quartz-pyrite veinlets, and pyrite coating fractures (Herdrick and Bunning, 1984). The mineralized rock is also anomalous in tellurium, platinum and palladium, copper, and tungsten.

71.4 (3.9) Return to SR 21 and turn left (north).

72.8 (1.4) Turn right onto Lone Ranch Creek road.

73.5 (0.7) Turn right.

73.9 (0.4) Turn right onto Day Creek road.

74.2 (0.3) Turn left onto the mine road.

74.4 (0.2) **STOP 7. The Bradley-Minniehaha adit.**

The recent trench work on the hill above exposed a vein similar to that mined underground approximately 1,000 ft to the south. Milky quartz veins, such as the one exposed here, contain free gold, chalcopyrite, and pyrite. The veins strike to the northwest and dip northeast, nearly parallel to the serpentine body exposed to the east. This type of occurrence in Ferry County has received no scientific scrutiny. The mines in this area have produced 7,387 tons of ore at a grade of 0.65 oz/ton gold, 2.00 oz/ton silver, and 1.61 percent copper (Parker and Calkins, 1964).

End of road log for Day 2.

Dikes and Vents Feeding the Columbia River Basalts

Peter R. Hooper and Stephen P. Reidel

Dikes and Vents Feeding the Columbia River Basalts

P. R. Hooper
Department of Geology
Washington State University
Pullman, WA 99164
and
S. P. Reidel [1]
Geosciences Group
Westinghouse Electric Co.
P.O. Box 1970
Richland, WA 99352

INTRODUCTION

The Columbia River basalts were erupted between approximately 17 and 6 m.y. ago (Miocene). They cover about 164,000 km^2 of southern Washington, northern Oregon, and west-central Idaho to form the Columbia Plateau lying between the Rocky Mountains and the Cascade Range in the Pacific Northwest. Recent estimates (Tolan and others, in press) suggest that there are as many as 300 individual lava flows, all of tholeiitic basalt, with a total volume of 171,000 km^3. Because they are younger than other examples of continental flood basalt volcanism, more accessible, better exposed, and less altered, the flows of the Columbia River Basalt Group (CRBG) have been studied in greater detail than those of other provinces. This province is, however, significantly smaller than other classic and older examples of continental flood basalts, such as the Deccan of India (67 Ma), the Parana of South America (130 Ma), and the Karroo of South Africa (190 Ma), each of which may have erupted well over 1 million km^3 of basalt.

All known feeder dikes and vents for the basalt flows lie in the southeast quadrant of the plateau. Some individual basalt flows are traceable for 600 km from their feeder dikes in Idaho to their terminations in the Pacific Ocean. Eruption occurred during the active east-west extension of the western Cordillera, and deformation of flows both during and after eruption has a consistent strain pattern similar to the pattern associated with structures ascribed to the 'Basin and Range' extensional regime (Hooper and Camp, 1981; Hooper and Conrey, in press).

This field guide focuses on those features exposed in the southeastern part of the Columbia Plateau that demonstrate: (1) the concentration of dikes and vents in the southeast corner of the plateau; (2) the control of dike locations by the nature of the underlying crust; and (3) the consistent orientation of virtually all feeder dikes formed over a 10-m.y. period and the importance of this to an understanding of the tectonic evolution of the Pacific Northwest. Consideration of these features leads to discussion of the nature of the magma plumbing system and the significance of that plumbing system to petrogenetic models.

THE LINEAR DIKE-VENT SYSTEMS

The realization that the CRBG was erupted from fissures (now dikes) dates back to the earliest studies on the Columbia Plateau (Russell, 1901; Lindgren, 1901; Washington, 1922). Since then, the CRBG has been seen as a type example of fissure eruption. Modern investigations began with the classic study by Waters in 1961, in which he defined a plateau-wide stratigraphy. He also recognized three areas of high dike density (dike swarms) in the southeast quadrant of the plateau: the Monument dike swarm in the John Day Basin of northeast Oregon (which we now know feeds only the flows of the Picture

[1] Also with Department of Geology, Washington State University, Pullman, WA 99164.

From: Joseph, N. L., and others, editors, 1989, Geologic guidebook for Washington and adjacent areas: Washington Division of Geology and Earth Resources Information Circular 86.

Gorge Basalt) and the Cornucopia and Grande Ronde dike swarms in the northeast and southeast corners of Oregon and Washington, respectively. This field trip visits the last two swarms.

Subsequent papers of particular significance include those by Taubeneck (1970) and Shaw and Swanson (1970). Taubeneck (1970) provides a comprehensive review of the feeder dikes—their number, thickness, distribution and orientations—while Shaw and Swanson (1970) give estimates of the astonishingly rapid rates of flow, both out of the dike/vent systems and across the gently sloping plateau surface, that are needed to account for the petrography, the sheet-like form, and the huge volumes of the individual cooling units. Their calculations suggest that in the two main eruptions of the Roza magma (each comprising approximately 700 km^3 of magma) the lava traversed the 30 to 40 km from a reservoir at the crust/mantle boundary to the surface in a matter of hours and then moved hundreds of kilometers across the plateau in a matter of days, rather than weeks or months. Swanson and others (1975) provide accounts of specific NNW-oriented linear-vent systems, emphasizing the complex of dikes feeding some flows and the many small shield-like vents built of scoria, spatter and numerous irregular dikelets that lie along each fissure system. Since 1975 many dikes and vents have been mapped in the southeast quadrant of the Columbia Plateau, and the use of precise analytical techniques has permitted correlation of many dikes and flows (Swanson and others, 1980; 1981; Camp, 1981; Hooper and Swanson, in press; S. P. Reidel, P. R. Hooper, G. D. Webster, and V. E., Camp, unpub. data on file with the Division of Geology and Earth Resources, Olympia).

THE PLUMBING SYSTEM AND PETROGENETIC MODELS

Most geoscientists working on the CRBG believe that the rapid extrusion of the large volumes of evolved, homogeneous basalt and the lack of evidence of crustal collapse is best explained by assuming the presence of large magma reservoirs at depth, most probably at the crust/mantle boundary (Hooper, 1984; Wright and others, in press). Recent geophysical evidence for the presence of thick accumulations of mafic and ultramafic rocks at the base of the crust beneath the central Columbia Plateau (Catchings and Mooney, 1988) appears to support this model and to emphasize the probability that crystal fractionation occurred in the reservoirs.

The restriction of the feeder dikes to the thinner and more mafic accreted terrains of the Blue Mountains province in northeastern Oregon suggests that these large magma reservoirs collected where the crust/mantle boundary would be at a slightly higher level than beneath the thicker cratonic crust to the east and north. The weaker accreted terrains would be more easily pulled away from the stable cratonic crust by the forces of the east-west (Basin and Range) extension that is evident in the consistent NNW orientation of all the feeder dikes (Hooper and Camp, 1981).

The processes responsible for producing the chemical variations among the flows of the CRBG remain more controversial. All authors appear to agree with Carlson (1984) that isotopic data require that these flows be derived from a variety of sources. Carlson cites four probable sources, of which three are in the mantle and the fourth is a crustal component. To this he adds significant crystal fractionation. Reidel (1983) and Hooper (1984, 1988) stress the geochemical evidence for crystal fractionation dominated by plagioclase (and occurring, therefore, in crustal reservoirs) but find less convincing evidence for crustal assimilation. Wright and others (in press) argue against significant crystal fractionation in the crust and suggest that the huge volumes of evolved homogeneous basalts are better explained by separate partial melts of a heterogeneous iron- and pyroxene-rich mantle.

ACKNOWLEDGMENTS

We thank our reviewers for their many useful comments: J. G. Evans, W. M. Phillips, D. R. Gaylord, and Bill Bonnichsen. H. C. Brooks and D. K. Schalck provided additional data and suggestions.

REFERENCES CITED

Anderson, J. L.; Beeson, M. H.; Bentley, R. D.; Fecht, K. R.; Hooper, P. R.; Neim, A. R.; Reidel, S. P.; Swanson, D. A.; Tolan, T. L.; Wright, T. L., 1987, Distribution maps of stratigraphic units of the Columbia River Basalt Group. *In* Schuster, J. E., editor, Selected papers on the geology of Washington: Washington Division of Geology and Earth Resources Bulletin 77, p. 183-195.

Armstrong, R. L.; Taubeneck, W. H.; Hales, P. O., 1977, Rb/Sr and K/Ar geochronometry of the Mesozoic granite rocks and their Sr isotope composition, Oregon, Washington, and Idaho: Geological Society of America Bulletin, v. 88, no. 3, p. 397-411.

Avé Lallemant, H. G.; Phelps, D. W.; Sutter, J. F., 1980, ^{40}Ar-^{39}Ar ages of some pre-Tertiary plutonic and metamorphic rocks of eastern Oregon and their geologic relationships: Geology, v. 8, no. 8, p. 371-374.

Barrash, W.; Bond, J. G.; Kauffman, J. D.; Venkatakrishnan, R., 1980, Geology of the La Grande area, Oregon: Oregon Department of Geology and Mineral Industries Special Paper 6, 47 p., 5 pl., scale 1:24,000.

Brooks, H. C., 1979, Plate tectonics and geologic history of the Blue Mountains: Oregon Geology, v. 41, no. 5, p. 71-80.

Byerly, G.; Swanson, D. A., 1978, Invasive Columbia River basalt flows along the northwestern margin of the Columbia Plateau, north-central Washington [abstract]: Geological Society of America Abstracts with Programs, v. 10, no. 3, p. 98.

Camp, V. E., 1981, Geologic studies of the Columbia Plateau – Part II. Upper Miocene basalt distribution, reflecting the source locations, tectonism, and drainage history in the Clearwater embayment, Idaho: Geological Society of America Bulletin, v. 92, no. 9, Part I, p. 669-678.

Carlson, R. W., 1984, Isotopic constraints on Columbia River flood basalt genesis and the nature of the subcontinental mantle: Geochimica et Cosmochimica Acta, v. 48, no. 11, p. 2357-2372.

Catchings, R. D.; Mooney, W. D., 1988, Crustal structure of the Columbia Plateau–Evidence for continental rifting: Journal of Geophysical Research, v. 93, p. 459-474.

Dickinson, W. R., 1979, Mesozoic forearc basin in central Oregon: Geology, v. 7, no. 4, p. 166-170.

Fleck, R. J.; Criss, R. E., 1985, Strontium and oxygen isotopic variations in Mesozoic and Tertiary plutons of central Idaho: Contributions to Mineralogy and Petrology, v. 90, no. 2, p. 291-308.

Gaylord, D. R.; Lundequist, J. H.; Webster, G. D., in press, Stratigraphy and sedimentology of the Sweetwater Creek interbed, Lewiston basin, Idaho and Washington. *In* Reidel, S. P.; Hooper, P. R., editors, Volcanism and Tectonism in the Columbia River Flood-basalt Province: Geological Society of America Special Paper.

Griggs, A. B., 1973, Geologic map of the Spokane quadrangle, Washington, Idaho, and Montana: U.S. Geological Survey Miscellaneous Investigations Series Map I-768, 1 sheet, scale 1:250,000. [Reprinted 1981].

Hooper, P. R., 1984, Physical and chemical constraints on the evolution of the Columbia River basalts: Geology, v. 12, no. 8, p. 495-499.

Hooper, P. R., 1988, Crystal fractionation and recharge (RFC) in the American Bar flows of the Imnaha Basalt, Columbia River Basalt Group: Journal of Petrology, v. 29, p. 1097-1118.

Hooper, P. R.; Camp, V. E., 1981, Deformation of the southeast part of the Columbia Plateau: Geology, v. 9, no. 7, p. 323-328.

Hooper, P. R.; Conrey, R. M., in press, A model for the tectonic setting of the Columbia River basalt eruptions. *In* Reidel, S. P.; Hooper, P. R., editors, Volcanism and Tectonism in the Columbia River Flood-basalt Province: Geological Society of America Special Paper.

Hooper, P. R.; Kleck, W. D.; Knowles, C. H.; Reidel, S. P.; Thiessen, R. L., 1984, Imnaha Basalt, Columbia River Basalt Group: Journal of Petrology, v. 25, part II, p. 473-500.

Hooper, P. R.; Knowles, C. H.; Watkins, N. D., 1979, Magnetostratigraphy of the Imnaha and Grande Ronde basalts in the southeast part of the Columbia Plateau: American Journal of Science, v. 279, no. 7, p. 737-754.

Hooper, P. R.; Swanson, D. A., in press, Columbia River Basalt Group and associated volcanic rocks in the Blue Mountains Province. *In* Walker, G. W., and others, editors, Geology of the Blue Mountains Region, Oregon, Idaho, and Washington–Cenozoic Geology of the Blue Mountains Region: U.S. Geological Survey Professional Paper 1437.

Hooper, P. R.; Webster, G. D., 1982, Geology of the Pullman, Moscow West, Colton, and Uniontown 7-1/2 minute Quadrangles, Washington and Idaho: Washington Division of Geology and Earth Resources Geologic Map GM-26, scale 1:62,500.

Hooper, P. R.; Webster, G. D.; Camp, V. E., 1985, Geologic map of the Clarkston 15-minute quadrangle, Washington and Idaho: Washington Division of Geology and Earth Resources Geologic Map GM-31, 11 p., 1 pl., scale 1:48,000.

Jacobson, R.; Milne, W.; Brooks, H. C.; Zollweg, J.; Brandsdottir, B., 1985, The 1984 landslide and earthquake activity on the Baker-Homestead highway near Halfway, Oregon: Oregon Geology, v. 47, no. 5, p. 51-57.

Lindgren, W., 1901, The gold belt of the Blue Mountains of Oregon: U.S. Geological Survey 22nd Annual Report, Part II, p. 551-776.

Mankinen, E. A.; Larson, E. E.; Grommé, C. S.; Prevot, M.; Coe, R. S., 1987, The Steens Mountain (Oregon) geomagnetic polarity transition; 3, Its regional significance: Journal of Geophysical Research (B), v. 92, no. 8, p. 8057-8076.

Martin, B. S., 1984, Paleomagnetism of basalts in northeastern Oregon and west-central Idaho: Washington State University Master of Science thesis, 150 p.

McDonald, E. V.; Busacca, A. J., 1988, Record of pre-late Wisconsin giant floods in the Channeled Scabland interpreted from loess deposits: Geology, v. 16, no. 8, p. 728-731.

Phelps, D. W.; Avé Lallemant, H. G., 1980, The Sparta ophiolite complex, northeast Oregon–A plutonic equivalent to low K_2O island arc volcanism. *In* Irving, A. J., editor, and others, The Jackson Volume: American Journal of Science, v. 280-A, Part 1, p. 345-358.

Price, S. M., 1978, An evaluation of dike-flow correlations indicated by geochemistry, Chief Joseph swarm, Columbia River basalt: Rockwell, Hanford Operations RHO-SA-59, 322 p.

Reidel, S. P., 1983, The stratigraphy and petrogenesis of the Grande Ronde Basalt from the deep canyon country of Washington, Oregon and Idaho: Geological Society of America Bulletin, v. 94, p. 519-542.

Reidel, S. P.; Hooper, P. R.; Price, S. M., 1987, Columbia River Basalt Group, Joseph and Grande Ronde canyons, Washington. *In* Hill, M. L., editor, Cordilleran Section of the Geological Society of America: Geological Society of America DNAG Centennial Field Guide, v. 1, p. 351-356.

Russell, I. C., 1901, Geology and water resources of Nez Perce County, Idaho: U.S. Geological Survey Water-Supply Paper 55, 68 p.

Shaw, H. R.; Swanson, D. A., 1970, Eruption and flow rates of flood basalts. *In* Gilmour, E. H.; Stradling, D., editors, Proceedings of the second Columbia River basalt symposium: Eastern Washington State College, p. 271-299.

Swanson, D. A.; Anderson, J. L.; Camp, V. E.; Hooper, P. R.; Taubeneck, W. H.; Wright, T. L., 1981, Reconnaissance geologic map of the Columbia River Basalt Group, northern Oregon and western Idaho: U.S. Geological Survey Open-File Report 81-797, 35 p., 6 pl., scale 1:250,000.

Swanson, D. A.; Wright, T. L.; Camp, V. E.; Gardner, J. N.; Helz, R. T.; Price, S. M.; Reidel, S. P.; Ross, M. E., 1980, Reconnaissance geologic map of the Columbia River Basalt Group, Pullman and Walla Walla quadrangles, southeast Washington and adjacent Idaho: U.S. Geological Survey Miscellaneous Geological Investigations Map I-1139, 2 sheets, scale 1:250,000.

Swanson, D. A.; Wright, T. L.; Helz, R. T., 1975, Linear vent systems and estimated rates of magma production and eruption for the Yakima Basalt on the Columbia Plateau: American Journal of Science, v. 275, no. 8, p. 877-905.

Taubeneck, W. H., 1970, Dikes of Columbia River basalt in northeastern Oregon, western Idaho, and southeastern Washington. *In* Gilmour, E. H.; Stradling, G., editors, Proceedings of the second Columbia River basalt symposium: Eastern Washington State College, p. 73-96.

Tolan, T. L.; Reidel, S. P.; Beeson, M. H.; Anderson, J. L.; Fecht, K. R.; Swanson, D. A., in press, Revisions to the estimates of the areal extent and volume of the Columbia River Basalt Group. *In* Reidel, S. P.; Hooper, P. R., editors, Volcanism and Tectonism in the Columbia River Flood-basalt Province: Geological Society of America Special Paper.

Vallier, T. L.; Batiza, R., 1978, Petrogenesis of spilite and keratophyre from a Permian and Triassic volcanic arc terrane, eastern Oregon and western Idaho, U.S.A.: Canadian Journal of Earth Sciences, v. 15, no. 8, p. 1356-1369.

Washington, H. S., 1922, Deccan traps and other plateau basalts: Geological Society of America Bulletin, v. 33, p. 765-804.

Waters, A. C., 1961, Stratigraphic and lithologic variations in the Columbia River basalt: American Journal of Science, v. 259, no. 8, p. 583-611.

Webster, G. D.; Kuhns, M. J. P.; Waggoner, G. L., 1984, Late Cenozoic gravels in Hells Canyon and the Lewiston Basin, Washington and Idaho. *In* Bonnichsen, B.; Breckenridge, R. M., editors, Cenozoic geology of Idaho: Idaho Bureau of Mines and Geology Bulletin 26, p. 669-683.

Wright, T. L.; Mangan, M.; Swanson, D. A., in press, Chemical data for flows and feeder dikes of the Yakima Basalt Subgroup, Columbia River Basalt Group–Constraints on a petrogenetic model: U.S. Geological Survey Bulletin 1821.

Road Log

The field trip follows U.S. Highway 195 south from Spokane to Lewiston, Idaho, and continues to Enterprise, Oregon, on Washington SR 129 and Oregon SR 3. On the second day the trip circumnavigates the Wallowa Mountains counterclockwise, returning to Enterprise. On the third and last day, the trip route returns from Enterprise to Lewiston by way of the lower Grande Ronde River. The route is shown on Figure 1. The formal road log begins at Baker and ends in Lewiston. The long drive from Spokane to Baker, via Lewiston and Enterprise, contains only one formal stop, and the geology passed is described in general terms. The basalt flow stratigraphy of the area is illustrated in Figure 2.

Day 1: Spokane to Enterprise

Spokane to Lewiston (106 mi)

Leaving Spokane, U.S. 195 passes through the valley of Hangman Creek, past Pleistocene deposits of glaciofluvial sediment, before climbing to the surface of the Columbia Plateau through a series of basalt flows of the Columbia River Basalt Group (CRBG). These include upper flows of the Grande Ronde Basalt (magnetostratigraphic unit N_2) which are overlain by flows of the Priest Rapids Member of the Wanapum Basalt (Fig. 2). A few miles farther south, just north of Spangle, the pine woods end abruptly. The lack of trees reflects the presence of loess, which covers the basalt plateau south to Lewiston. North of Spangle the loess was stripped away by the Spokane glacial floods. The low moisture retention by the loess prevents tree growth in the hot dry summers of the plateau.

This is the Palouse country: rolling loess hills, originally grasslands, which now form some of the richest wheatlands in the world. The loess probably formed as hills, or standing (silt) dunes as much as 100 m high, on a series of mesa-type (chocolate-tablet) surfaces which formed by stream erosion of the original horizontal basalt surface. Erosion has subsequently increased the asymmetry of the hills by steepening their northeastern slopes. Most of the loess was deposited during the last 1 m.y. It thickens to the southwest, and the grains of quartz and plagioclase are thought to have originated in slackwater deposits of earlier glacial floods to the southwest, whence they were transported by the Palouse westerly winds (McDonald and Busacca, 1988).

Most of the Palouse towns between Spokane and Lewiston are set in valleys between the loess hills in which the upper part of the basalt flow stratigraphy is exposed. Trees flourish in these valleys and are rooted in the water-retaining basalt.

Just north of Rosalia, the road passes down from the loess into Priest Rapids flows, below which lies a saprolite horizon. The saprolite separates the top of the Grande Ronde Basalt from Wanapum Basalt, and this horizon is recognized across most of the Columbia Plateau. It represents one major eruptive hiatus before eruption of the Saddle Mountains Basalt, in which most of the flows were separated by significant intervals of time.

The bypass to the east of Rosalia crosses quartzite. Similar rock forms Steptoe Butte, a prominent conical hill to the east of the road between Rosalia and Colfax. These outcrops represent mountain peaks and ridges of the pre-basalt topography that remained above the basalt flood. The quartzites have been variously correlated with the Precambrian Belt Supergroup (Griggs, 1973) and lower Paleozoic sequences (Hooper and Webster, 1982).

Entering Colfax, the road again passes down from the loess through the Priest Rapids Member (Lolo flow), then through the Roza Member of the Wanapum Basalt, and into the upper flows (N_2) of the Grande Ronde Basalt (Fig. 2).

Farther south the route by-passes both Pullman (site of Washington State University) and, 8 mi farther east, Moscow (site of the University of Idaho). Continue south for another 20 mi to the top of the Lewiston Grade.

(100) **STOP 1. Lewiston Grade overlook.**

If the weather is kind, this point will provide an excellent view south across the Lewiston Basin where the Clearwater River, flowing from the east, joins the Snake River, which flows from the south, to form the augmented Snake, which continues westward out of the basin. The towns of Lewiston, Idaho (east of the Snake) and Clarkston, Washington (west of the Snake) are at the confluence of the rivers.

Across the basin slightly east of south, the scarp of the Limekiln fault trends northeast-southwest; it is a normal fault with a downthrow to the northwest of more than 600 m. The fault appears to have formed over a fairly short time toward the end of the Grande Ronde R_2 eruptions.

South and southwest across the basin, the horizon is formed by the east-trending ridge of the Blue Mountains anticlinal uplift that terminates at the Limekiln fault. The ridge is capped by two obvious volcanic cones. Puffer Butte on the left is the source of the Umatilla Member, the oldest member of the Saddle Mountains Basalt (Fig. 2). The larger cone on the right is Big Butte, one of many cones associated with the eruption of flows of the Roza

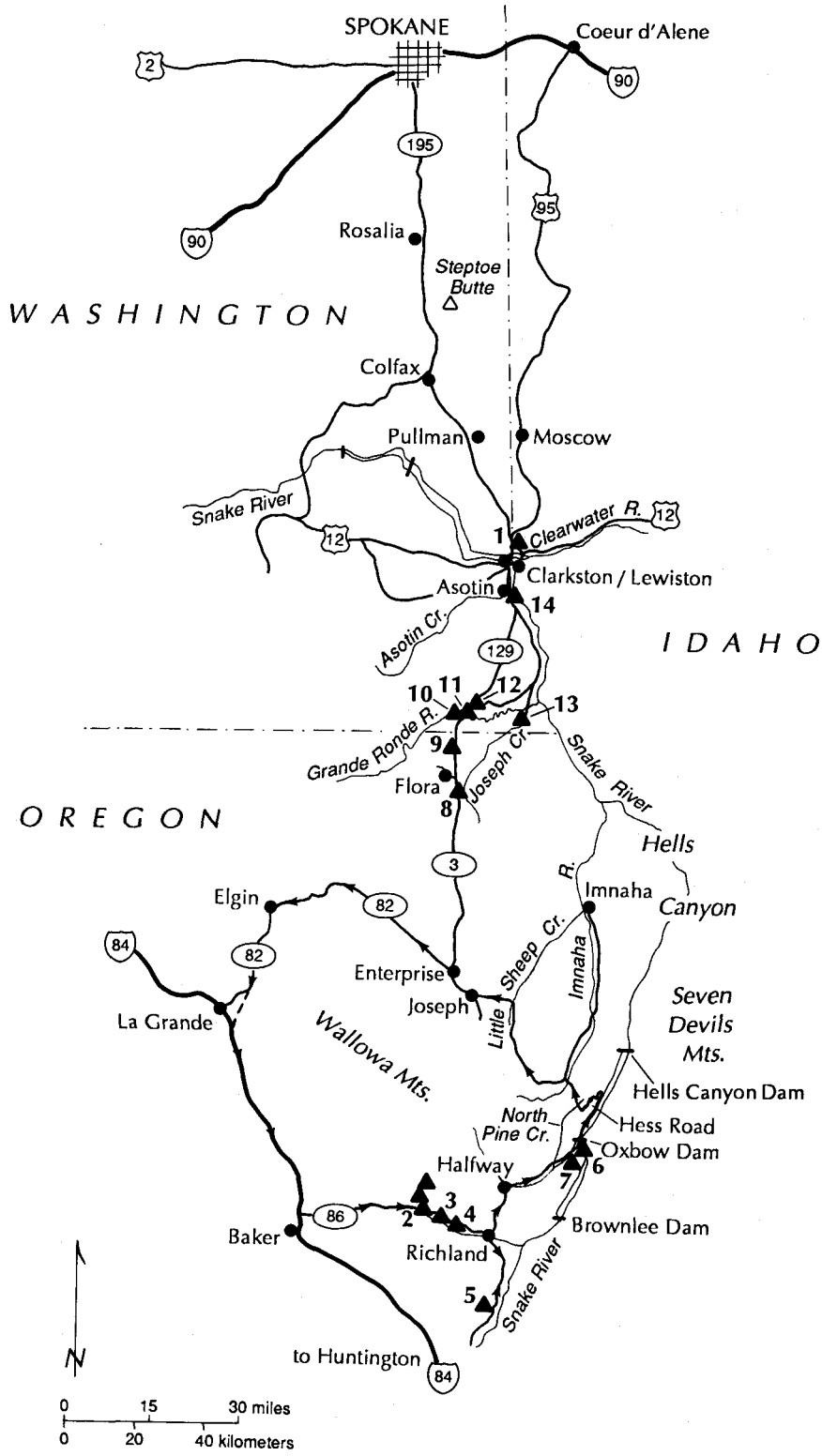

Figure 1. Route map showing stops (triangles) and principal topographic features. For geologic maps, see Swanson and others (1980, 1981;) Hooper and others (1985); and S. P. Reidel, P. R. Hooper, G. D. Webster, and V. E. Camp (unpub. data on file with the Division of Geology and Earth Resources, Olympia). For flow distribution maps, see Anderson and others (1987); Hooper and Swanson (in press); Tolan and others (in press).

	Formation	Member	Magnetic Polarity	K/Ar Dates
Columbia River Basalt Group	Saddle Mountains Basalt	Lower Monumental	N	6 my
		Ice Harbor	N,R	8.5 my
		Buford	R	
		Elephant Mountain	N,T	10.5 my
		Pomona	R	12 my
		Esquatzel	N	
		Weissenfels Ridge	N	
		Asotin	N	
		Wilbur Creek	N	
		Umatilla	N	13.5 my
	Wanapum Basalt	Priest Rapids	R	
		Roza	T,R	
		Frenchman Springs	N	
		Eckler Mountain	N	14.5 my
	Grande Ronde Basalt		N_2	
	Picture Gorge Basalt R_2		R_2	
	Picture Gorge Basalt N_1		N_1	
			R_1	16.5 my
	Imnaha Basalt		T	
			N_0	
			R_0	17.5 my

Figure 2. Stratigraphy of the Columbia River Basalt Group in the fieldtrip area. Magnetic polarity: N, normal magnetization; R, reverse magnetization; T, transitional magnetization.

Member (Swanson and others, 1975, 1980; S. P. Reidel. P. R. Hooper, G. D. Webster, and V. E. Camp, unpub. data on file with the Division of Geology and Earth Resources, Olympia).

The Lewiston Basin is a very gentle syncline that began to develop after the displacement on the Limekiln fault in early Wanapum time (approximately 14.5 Ma). The presence of a topographic basin is first indicated by the outcrop pattern of the Lolo flow and the pillow basalts at its base. Continued basining by synclinal warping through Saddle Mountains time (13.5-6 Ma) is demonstrated by the thickening of successive flows in the basin, the confinement of other flows to the basin, and the development of thick sedimentary interbeds between the flows in the basin (Swanson and others, 1980; Hooper and others, 1984; Gaylord and others, in press). Later, probably between the eruptions of the Elephant Mountain flow (~10 Ma) and the Lower Monumental flow (~6 Ma), the northern limb of the syncline broke to form a sharp upthrusted anticlinal wedge that we call the "Lewiston Structure".

The Lewiston Structure lies between the overlook, where we stand, and the rivers flowing west at the bottom of the grade. Behind us (north) are the horizontal basalt flows we have just driven across. These are the Wilbur Creek flows (Saddle Mountains Basalt), with well-developed entablature, and the Lolo flow (Wanapum Basalt), which overlies the saprolite horizon on top of the Grande Ronde flows (R_2, with typically oxidized tops). Immediately below the overlook lies the steep south-dipping, west-trending, reverse fault that forms the northern edge of the upthrust anticlinal wedge. A small replica of this fault can be seen displacing the red tops of the Grande Ronde flows in the roadcut due east of the overlook.

Descending to Lewiston, the road crosses the major reverse fault and then cuts a section through the uplifted anticlinal wedge. First, in the north, the flows dip north, then they dip to the south as the anticline is crossed. The crest of the anticline is fractured. Numerous vertical southeast- and southwest-trending slickensided fault planes contain sub-horizontal striae. The south-dipping limb of the anticline can also be seen as prominent flatirons to the west. This complex brittle structure wedges out immediately to the east of the grade, and, farther east, the flows form a fairly simple monocline. To the west, beyond the steeply dipping flatirons, the reverse fault swings southwest into a left-lateral strike-slip fault (Hooper and others, 1985).

The Lewiston Structure contains many of the structural elements characteristic of the whole Columbia Plateau: west-trending anticlinal folds associated with steep reverse faults, and northwest-striking (right-lateral) and northeast-striking (left-lateral) vertical strike-slip faults. The third major structural element characteristic of the plateau is the consistent trend of vertical fissures (dikes) that fed the lava to the surface. Together, these structural elements define a strain pattern that has remained unchanged from 17 Ma to the present: a pattern of relative shortening in a NNW direction and extension in a WSW direction.

Entering Lewiston at the base of the grade, the road cuts through black cliffs of the Lower Monumental flow (~6 Ma), the youngest dated flow of the CRBG.

Lewiston to Enterprise (89 mi)

From Lewiston, the route follows SR 129 south toward Enterprise, Oregon. Much of this route is retraced on the third day of the trip and is described later. On leaving Lewiston, notice the large gravel beds east of the Snake River; these include deposits from both the Bonneville and the Spokane floods (Webster and others, 1984). Note, also, the gentle north dip (2°) of the Grande Ronde flows as we approach Asotin; this is the southern limb of the Lewiston syncline. Climbing the "Asotin Grade", we pass older gravels with thick weathering rinds that underlie the Lower Monumental flow (Webster and others, 1984). Higher up the grade, observe the thick Sweetwater interbed (Hooper and others, 1985; Gaylord and others, in press) and the invasive nature of both the Umatilla flow and the Wilbur Creek flow into the sediment.

Day 2: Counterclockwise around the Wallowa Mountains.

Again, there is a full 2 hours' drive before the formal part of the field trip begins. During this day's trip, the route circumnavigates the Wallowa Mountains counterclockwise; we return to Enterprise for a second night (Fig. 1).

Enterprise to Baker

Take Oregon SR 82 northwest out of Enterprise, following the Wallowa River, which parallels the Wallowa fault.

The Wallowa Mountains are an uplifted fault block composed primarily of late Jurassic granites (160-143 Ma; Armstrong and others, 1977; Fleck and Criss,

1985) that intrude rocks of the Wallowa terrane. While probably already a topographic high when the first Columbia River basalts erupted (see below) approximately 17 Ma, continued uplift of the block is strikingly demonstrated by the presence of basalts high on the sides of the present mountains. These are the same flows of Imnaha Basalt that lie well below the surface in the Wallowa valley. The Wallowa fault appears to represent the southerly splay of the Olympic-Wallowa lineament (OWL) along which significant right-lateral transform displacement has recently been postulated (Hooper and Conrey, in press).

Proceeding northwest toward Elgin, SR 87 crosses a series of normal faults which lie en echelon (NNW) to the northwest trend of the main Wallowa fault. Whether any of these faults include significant strike-slip motion has not been determined. On the top of Cricket Flat the route crosses a series of normal faults that extend out from the Wallowa Mountains. Here, the Cricket Flat flow (Powder River basalt) is exposed between flows of Wanapum Basalt and the lowest member (Umatilla) of the Saddle Mountains Basalt. The Cricket Flat flow is an olivine-rich basalt similar to flows in the La Grande and Baker grabens that were first described by W. H. Taubeneck and which are now ascribed to the Powder River basalts (Swanson and others, 1981; Hooper and Swanson, in press). The exposure on Cricket Flat, where the flow is underlain by a conspicuous ash-flow tuff, is one of the few localities where the relative ages of the Powder River and Columbia River basalts can be determined.

At Elgin, SR 82 descends into a series of en echelon grabens from Elgin to south of Baker. These grabens represent significant east-west crustal extension on the southern side of the OWL and appear to be directly associated with the eruptions of Powder River basalt and younger sheets of andesite of calc-alkaline affinity. Their formation appears to postdate the eruption of the Grande Ronde Basalt. The stratigraphic sequence within the grabens is Grande Ronde Basalt (R_1 and N_1), overlain by Powder River basalt, overlain by thick andesite sheets, and finally overlain by thick sediment. The andesite sheets cap the hills on either side of the La Grande graben.

Near La Grande SR 87 joins Interstate Highway 84 (I-84), which is then followed to Baker. The stratigraphic succession in the grabens is well seen to the south of La Grande where I-84 climbs out of Ladd canyon. The lower flows on the roadside in Ladd canyon are Grande Ronde Basalt. Higher in the cliffs Powder River basalts crop out, and the hill to the east of the road is capped by andesite (Barrash and others, 1980).

At Baker, turn east onto Oregon SR 86, posted to Richland and Hells Canyon. *Set odometers to 0.0.* Cumulative miles are on the left below; interval mileage is in parentheses.

0.0 (0.0) I-84/SR 86 road junction. Drive east, crossing the old Oregon Trail, across outcrops of the Permian and Triassic rocks in the Wallowa terrane, and past roadcuts in Powder River basalt.

16.0 (16.0) Tertiary sedimentary rocks. These lacustrine strata formed in an east-west synclinal basin developed after eruption of early Grande Ronde basalts (R_1 and N_1).

21.0 (5.0) **STOP 2. Invasive flows of Grande Ronde Basalt** (at Sparta Road junction).

Immediately east of the Sparta road junction, R_1 Grande Ronde Basalt lies unconformably on weathered diorite of the Sparta ophiolite complex (Phelps and Avé Lallemant, 1980). Fresh exposures of the diorite are seen at Stop 3 (below). Stop 2 illustrates the invasive nature of a Grande Ronde basalt flow into sediments covering the diorite. The basalt is chilled against, yet locally underlies, the sediment. Sediment and lava are mixed together. This type of relation is common across the Columbia Plateau where hot basalt lava entered lakes and wet sediment. The basalt lava was denser and tended to dive into and below the sediment, forming pillows and intricate sediment/basalt glass mixtures. Such flows have been called invasive flows (Byerly and Swanson, 1978).

Optional stops: A post-basalt ignimbrite is well exposed about 2 mi up the Sparta road; it forms a small escarpment that is crossed by the road immediately beyond the first farmhouse. The degree of synclinal bending of the ignimbrite is less than that of the basalts but more than that of the sediments above, implying the continued development of the syncline before, during, and after the formation of the ignimbrite. Another 2 mi up Sparta road, a small outcrop above the road to the west is a coarse-grained plagiogranite (albite granite, trondjhemite) of the Sparta ophiolite complex. The plagiogranite includes large grains of bluish quartz.

Return to SR 86. *Reset odometer to 21.0.* Continue east along SR 86.

24.0 (3.0) **STOP 3. Diorite of the Sparta ophiolite complex.**

The diorite of the Sparta ophiolite complex has been dated at 223 Ma (Avé Lallemant and others, 1980). It is one of a series of ophiolitic complexes of Permian and Triassic age that are found in the northeast-trending Blue Mountains Province of northeastern Oregon (Dickinson, 1979; Brooks, 1979). The Sparta complex includes highly altered ultramafic rocks to the south, gabbros in the Powder River gorge (Stop 4), diorite, and the plagiogranite to the north. (See optional stops.) Like the other ophiolites in the Blue Mountains Province, those of Sparta have flat to depleted REE patterns. These and other geochemical signatures have led Avé Lallemant and others (1980) to suggest that these ophiolites are the roots of the island arc system that constitutes much of the Wallowa terrane (including the Clover Creek Greenstone and the basalts, andesites, and keratophyres of the Seven Devils Volcanics; Vallier and Batiza, 1978). The ophiolites were probably not formed at a distant mid-oceanic ridge. They are, however, entirely of oceanic origin, as is the whole Blue Mountains province. The terranes of this province were accreted to the old cratonic plate of North America north and east of the crustal suture (Fig. 3) in Jurassic to Cretaceous time. It is in this accreted crust that virtually all the feeder dikes of the CRBG are located.

Continue eastward through the Powder River gorge. A spectacular landslide blocked Powder River and the road in 1984 (Jacobson and others, 1985).

32.0 (8.0) **STOP 4. Gabbro of the Sparta ophiolitic complex.**

Note the gabbro is altered and partly amphibolitized.

Continue eastward on SR 86 to the town of Richland.

39.0 (7.0) Richland, Oregon.

Turn right (south) in the middle of Richland on the Huntington road. This road crosses the Powder River and runs east along the southern shore of the flooded lower reaches of that river (part of the Brownlee Reservoir). More exposures of the ignimbrite and very coarse volcaniclastic layers are exposed along this road. The road then turns south and climbs up to the rim of the Snake River canyon.

48.0 (9.0) Rim of the Snake River canyon.

To the east across the Snake River, Imnaha and Grande Ronde basalt flows rest unconformably on deeply eroded pre-Tertiary rocks. The same is true on the west side of the canyon, and as the road descends southward to the Snake River, it passes through Imnaha Basalt and then older flows, which are part of the Permian (Elkhorn Ridge) sequence of greenstones and cherts.

53.5 (5.5) Dike of Columbia River basalt intruding Burnt River Schist.

For the next 5 mi there are numerous dikes exposed along the river/road section. Most are of Imnaha Basalt, some are of Grande Ronde Basalt, and there are also some dikes that are much more altered and assumed to be feeders for the pre-Tertiary volcanic rocks.

58.5 (5.0) End of dike swarm. Turn around and retrace the route to a large composite dike of Imnaha Basalt.

61.7 (3.2) **STOP 5. Composite dike of Imnaha Basalt.**

This concentration of Imnaha and Grande Ronde dikes can be traced along strike to the poorly exposed hills west of Halfway and to near Cornucopia in the eastern Wallowa Mountains. It constitutes the Cornucopia dike swarm of Waters (1961). West of Stop 5 a large area of volcanic breccia of Imnaha Basalt composition is exposed at the head of Connor Creek (Hooper and Swanson, in press).

Five of the Imnaha dikes, together with three Imnaha flows near Oxbow Dam on the Snake River (near Stop 6, below), have been drilled for paleomagnetic data (Martin, 1984). The consistent results of this study demonstrate that this area has undergone approximately 17 degrees of clockwise rotation during the last 17 m.y. Such rotation contrasts with less than 5 degrees rotation in the Imnaha valley and areas farther north (Hooper and others, 1979). Although it is difficult to quantify, the average trend of dikes in this area is approximately N10°W, whereas farther north, in the Grande Ronde dike swarm, the average trend is N30°W (Fig. 3). This evidence suggests the local rotation of crustal blocks near the OWL, whereas the major blocks of the

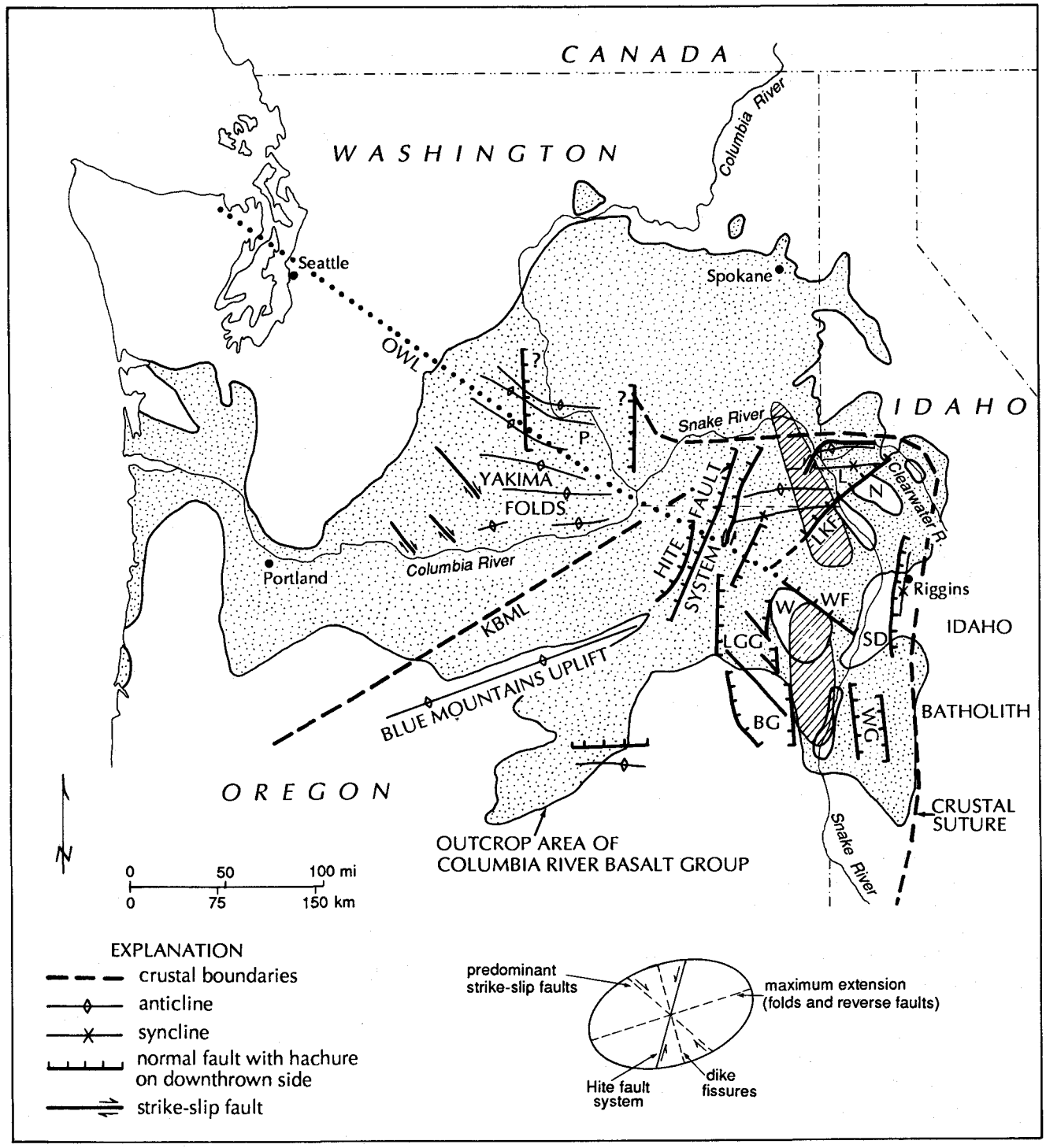

Figure 3. Major structural features of the Columbia Plateau and the strain ellipse defined by these structures (Hooper and Conrey, in press). L, Lewiston syncline; LKF, Limekiln fault; LGG, La Grande graben; W, Wallowa Mountains; WF, Wallowa fault; SD, Seven Devils Mountains; BG, Baker graben; WG, Weiser graben; OWL, Olympic-Wallowa lineament; KBLM, Klamath-Blue Mountains lineament; N, Nez Perce Plateau; P, Pasco Basin.

Columbia and Oregon plateaus to the north and south, respectively, remain unrotated (Hooper and others, 1979; Mankinen and others, 1987; Hooper and Conrey, in press).

Return to Richland.

78.0 (16.3) Richland, Oregon. Turn east on SR 86 toward Halfway and Oxbow Dam.

82.5 (4.5) View southwest over Richland valley. The west-trending syncline, with its axis near the bottom of the valley, is well seen from this point. Note the north-dipping flows of Imnaha and Grande Ronde Basalt in the south and the synclinal but gentler dips of the welded tuffs and sediments (Pliocene) exposed along the south bank of the Powder River.

Continuing northeast, the country between Richland and North Pine Creek is underlain by R_1 and some N_1 Grande Ronde Basalt flows dipping gently southwest or southeast. As we traverse these flows across their strike, note that the stratigraphy is repeated by many southwest-trending normal faults (Swanson and others, 1981).

93.5 (11.0) Hill on the right (south) side of the road. The highly oxidized nature of the lava forming this hill provides circumstantial evidence, in addition to the suggestive form of the hill, that it may be a Grande Ronde (R_1) vent.

99.4 (5.9) Descend into Imnaha Basalt. The road remains in Imnaha Basalt until it reaches the Snake River at Oxbow.

100.1 (0.7) Pine Creek road junction. Continue straight toward Oxbow Dam.

107.2 (7.1) Junction of roads to Hells Canyon Dam (north) and to Oxbow and Brownlee dams (south). Take the road to Oxbow and Brownlee dams, cross Pine Creek, and stop just across the bridge.

107.3 (0.1) **STOP 6. Typical flow of the American Bar (AB) type of Imnaha Basalt** (AB-4 chemical type, Hooper and others, 1984).

Note that the flow is mildly plagioclase phyric and has smaller phenocrysts of olivine and augite.

107.7 (0.4) **STOP 7. Imnaha Basalt section.**

Continue a short way along the Brownlee Dam road and park the cars opposite a small track leading uphill on the west side of the road. Walk up this track to the top of the ridge.

As you climb the ridge, observe various features of Imnaha Basalt flows. Most are of AB type, plagioclase phyric with a fairly fine-grained matrix. This is part of the Oxbow Dam section (Hooper and others, 1984). The crest of the ridge provides excellent views of the deep canyon country, of the differential erosion of Imnaha and Grande Ronde Basalts (the contact can be followed easily by eye), and of the unconformity between the Seven Devils Group and the CRBG. From this vantage point, we will discuss the feeder systems of the CRBG, the nature of the tectonic control of the eruption, the significance of the type of crust traversed by the magma on its way to the surface, the nature of the magma plumbing system, and various petrogenetic models that have been proposed for the CRBG.

Return to the cars and retrace the route across Pine Creek. Turn right (north) at the road junction. Then, almost immediately, take the left fork and continue north through Oxbow village along the west bank of the Snake River on an unpaved mining road. The road passes flows and breccias of the Seven Devils Volcanics (a Permian to Triassic primitive island arc). Participants may wish to make a brief stop to note the contrast of these rocks with the CRBG lying with marked unconformity above.

115.9 (8.2) Turn left (west) away from the river up Hess Road. This is an open switch-back gravel road that goes directly up the side of Hells Canyon. *Only vehicles with a fair clearance should attempt this route, and then only in dry weather.* Otherwise, drivers should head back along SR 86 towards Halfway for 7 mi where they should turn right (north) up North Pine Creek on the Imnaha River road. This road and Hess Road meet at the watershed between the Pine Creek and the Imnaha drainages.

In good weather Hess Road provides an excellent view of Hells Canyon. Observe the unconformity between the Seven Devils Volcanics and the CRBG, the varied dip of the deformed flows of the Seven Devils Volcanics, and the clearly folded Martin Bridge Limestone (Late

Triassic, Norian), which rests on the volcanics. Only the very uppermost flows of the Imnaha Basalt breached the Seven Devils/Wallowa Mountains divide. It is almost certain, therefore, that the peaks of both these ranges remained above the basalt flood; that is, both were mountain ranges before the eruption started. That they continued to rise during and after that eruption is demonstrated by the offlap of successive basalt units and the presence of Imnaha Basalts near the summits of both.

Join the Pine Creek-Imnaha road at the drainage divide and descend to the Imnaha River.

It is approximately 30 mi from the Oxbow road junction (Stop 6) to the Imnaha River by either road, but odometers will read differently depending on the route chosen. *Reset odometers to zero on the bridge crossing the Imnaha River.*

0.0 (0.0) At the T-junction, turn right on the west side of the Imnaha River, toward Imnaha.

0.2 (0.2) Take the left fork for Lick Creek, Joseph, and Enterprise. The road now winds through logging country around the head of the Imnaha drainage. Flows of Grande Ronde Basalt (mainly N_1 and R_2) dip off the Wallowas to the northeast.

9.5 (9.3) A highly oxidized zone of pyroclastic material is exposed at a switchback. This occurs close to the N_1/R_2 boundary and forms a conspicuous marker horizon for many square kilometers to the north. The route crosses the same horizon a number of times.

13.0 (3.5) The road to the right goes to Harl Butte. We do *not* follow this road, but it is noteworthy that Harl Butte is the southernmost cone in a series of small volcanic cones between here and the Limekiln fault. The cones sit on top of the Grande Ronde R_2 flows that form the surface of the lava plateau in this area. These cones have Grande Ronde chemistry, lie directly above the NNW-oriented Grande Ronde dike swarm (Fig. 3), and are normally magnetized. They are believed to represent Grande Ronde N_2 lava erupted on that part of the Plateau raised by the Limekiln fault toward the end of the R_2 period. The greatest volume of Grande Ronde N_2 lava erupted farther north from the same fissure system where it intersected the lower topographic surface on the northwest side of the Limekiln fault (Swanson and others, 1981; Hooper and Swanson, in press).

15.0 (2.0) Lick Creek campground.

30.7 (15.7) T-junction in Little Sheep Creek. Turn left (west) on the Enterprise-Imnaha road. As you drive uphill toward Enterprise on the side of Little Sheep Creek, note the same highly oxidized layer near the N_1/R_2 contact that was observed earlier; at this exposure you can see where basalt was pillowed by wet sediment.

38.7 (8.0) Enter Joseph. Note the large terminal moraine to the south. This was formed by an alpine glacier originating in the Wallowa Mountains. The moraine now dams Wallowa Lake. Turn right in the center of Joseph, onto SR 82 toward Enterprise.

45.7 (7.0) Enter Enterprise.

Day 3: Enterprise to Lewiston.

0.0 (0.0) *Reset odometer.* Leave on SR 3 north toward Lewiston.

For the first 3 mi the road traverses glacial gravel and alluvium derived from the Wallowa Mountains. Farther north the road again lies on Grande Ronde Basalt.

3.0 (3.0) Note the very oxidized flow top. This is the same horizon near the N_1/R_2 contact observed on Day 2. The road remains in Grande Ronde R_2 flows as it rises gently.

15.2 (12.2) Starvation Creek road junction on the right.

26.2 (11.0) Day Ridge road junction on the left.

30.7 (4.5) **STOP 8. Joseph Creek view point.**

The view point stands on the Umatilla flow (Fig. 2), a very fine grained flow with exceptionally high Ba content (>3,000 ppm). The flows exposed in Joseph canyon range from Grande Ronde R_1, which lie directly on Imnaha Basalt at the base of the canyon, to the upper parts of the R_2 Grande Ronde succession at the top where they are overlain directly by the

Umatilla flow. At the northern end of Joseph canyon numerous NNW-oriented dikes are exposed (Price, 1978). They form the center of the Grande Ronde dike swarm.

38.7 (8.0) Quarry on the east side of the road. This is the type locality for the Buford flow, a young and local flow of the Saddle Mountains Basalt. A well-exposed feeder dike for this flow is present in the Grande Ronde canyon below.

Descending the "Buford" Grade to the Grande Ronde River, the route passes through the Buford flow, then through a thick sedimentary interbed that shows much slumping, then the Umatilla flow, the Shumaker Creek flow and the Dodge flow (with saprolite horizons both above and below it), then the R_2, and lastly the N_1 flows of the Grande Ronde Basalt.

40.2 (1.5) **STOP 9. Upper CRBG units.**

Pull off on the bend opposite the Dodge flow.

Make a brief traverse of the upper flows of Grande Ronde Basalt below the bend (noting the oxidized flow tops), the saprolite, the Dodge flow, another saprolite, the Shumaker Creek flow, and the Umatilla flow in that order upward.

44.4 (4.2) Washington-Oregon border, where the road becomes Washington SR 129. From here to the Grande Ronde River various dikes can be seen both along the road and as lines across the hillsides. Some stand out as walls, others are trenches traversing the flat-lying flows.

48.8 (4.4) **STOP 10. Bridge across the Grande Ronde River.**

Rest stop at Oasis Cafe. Major Grande Ronde dikes cutting N_1 Grande Ronde Basalt flows stand out as walls close to the road at the north end of the bridge. Other dikes can be seen farther downriver. This is the western edge of the Grande Ronde dike swarm.

49.7 (0.9) On the left side of the road note reworked Mazama ash from the eruption that formed Crater Lake, 6,845 years ago.

50.2 (0.5) Breccia zone at the bend in the road. The breccia is formed along a 30-m-wide northwest-trending fault zone with a mainly horizontal offset. The brecciated flow top on the south side marks the top of the N_1 Grande Ronde Basalt. Vertical offset across the fault is only about 1 m. The same fault is crossed again higher up the "Rattlesnake Grade."

51.4 (1.2) **STOP 11. Roza dikes and strike-slip faults.**

Sharp bend in the road with space for parking. View of the Grande Ronde Basalt and the incised meanders of the Grande Ronde River. What is their origin?

Walk 0.3 mi up the road and observe several NNW-trending dikes of Roza composition (plagioclase phyric) cutting flows of Grande Ronde (R_2) Basalt. One dike (second from the south) has a splay, and the next one north has slickensides. Continue walking north around the next bend. Several small faults are seen and, in at least one locality, slickenside surfaces with horizontal striae are well displayed. This is the same fault zone observed near the bottom of the grade.

57.6 (6.2) The red oxidized zone with overlying saprolite represents the top of the Grande Ronde Basalt (Fig. 2).

57.8 (0.2) Umatilla flow.

58.5 (0.7) Turn right into Field Springs State Park. Keep left past the park camp (on right) until the end of the road.

STOP 12. The Puffer Butte volcano.

The park is located on the top of Puffer Butte, the flat-topped volcanic cone observed from the Lewiston Grade (Stop 1). The cone is the eruptive center for the Umatilla Member. This member (two flows) has a distinctive appearance and chemical composition. A feeder dike is present in the Grande Ronde canyon below. One lobe of the flow went north from Puffer Butte across the Lewiston Basin, but the main volume of basalt flowed up the Grande Ronde River, across the Blue Mountains uplift southeast of Walla Walla, and into the southern part of the Pasco Basin, where it ponded. We speculate that this path followed an earlier Snake River drainage, which had not yet breached the divide of the Blue Mountains uplift (along the Limekiln fault) to flow northward into the Lewiston Basin. The Umatilla flow may have blocked that earlier drainage, hastening the breakthrough to the north, which appears to have occurred soon afterward. The greatly increased volume of water entering the Lewiston Basin resulted in the

formation, for the first time, of deep canyons similar to those seen today. This major change in the drainage pattern would also have caused a reversal of the flow direction in the Grande Ronde River. Might this provide an explanation for the incised meanders ?

Exposures are poor on top of the butte, but a circuit around the volcano shows oxidized flow material. It is surprisingly unimpressive.

Return to SR 129, turn right, and continue eastward.

61.4 (2.9) Summit of rise. A Weissenfels Ridge flow (Saddle Mountains Basalt) is exposed to the right and is overlain by small remnants of the Buford flow. The group of four Weissenfels Ridge flows and their feeder dikes are confined to the Lewiston Basin.

62.7 (1.3) Turn sharp right onto Montgomery Ridge Road. More outcrops of the Weissenfels Ridge flow can be seen.

63.7 (1.0) Shumaker Creek road on the right.

Optional Route down the Shumaker Creek road (15 mi).

64.5 (0.8) Begin steep descent into the Grande Ronde canyon. A thick saprolite is developed between the Weissenfels Ridge flow and the underlying Shumaker Creek and Dodge flows.

64.7 (0.2) Dodge flow exposed, with another saprolite below.

64.8 (0.1) Meyer Ridge flow (top of the Grande Ronde) exposed at the bend in road.

65.9 (1.1) Approximate position of the R_2/N_1 contact in Grande Ronde Basalt. The dike just east of the road is a feeder to the Cloverland flow of the Weissenfels Ridge Member.

68.5 (2.6) Axial trace of a gentle west-trending syncline.

69.2 (0.7) Road junction. Turn right.

69.5 (0.3) Feeder dike to the Buford flow.

70.8 (1.3) Road mile marker 7.

71.1 (0.3) Feeder dike to the Cloverland flow of the Weissenfels Ridge Member at bend in river.

72.0 (0.9) **Optional Stop. Dike to the Sillusi flow of the Umatilla Member.**

The dike feeds the Puffer Butte volcano above and cuts flows of the R_1 Grande Ronde sequence.

Return to Montgomery Ridge Road and *reset odometer to 63.7 mi.*

83.4 (19.7) Junction with Weissenfels Ridge road. Keep right, toward the Snake River.

87.8 (4.4) Road junction. Again, keep right, toward the Snake River.

91.5 (3.7) Road junction. Keep left on the Snake River road and begin the descent down Montgomery Gulch. The flow sequence here is, from top to bottom, two flows of the Weissenfels Ridge Member, the Asotin flow, the Umatilla flow, then the R_2 Grande Ronde, N_1 Grande Ronde, and finally the R_1 Grande Ronde as we approach the Snake River. The Umatilla flow is hidden in the road section by massive slumping of the Asotin flow on a thick sedimentary interbed which underlies it in the Lewiston Basin.

91.8 (0.3) Weissenfels Ridge flow.

92.0 (0.2) Asotin flow.

92.5 (0.5) Landslide.

93.1 (0.6) R_2 Grande Ronde Basalt.

94.3 (1.2) R_2/N_1 Grande Ronde Basalt contact.

94.8 (0.5) Mazama ash in the creek for several miles.

98.6 (3.8) N_1/R_1 Grande Ronde Basalt contact.

99.4 (0.8) Junction with the Snake River road. Turn right (south), up the Snake River.

100.9 (1.5) End of paved road. Begin gravel road.

102.3 (1.4) Thick andesite flows of Seven Devils Volcanics, with significant dip. The andesite exposure continues for 1.5 mi. Note prehistoric Indian paintings.

103.0 (0.7) From here to Beamers Bar, the Limekiln fault runs southwest on the other side of the Snake River. Note pre-CRBG metasedimentary and metavolcanic rocks (Seven DevilsVolcanics) on the southeast side of the fault. Vertical displacement on the fault in this area is >600 m, decreasing along the fault in both directions, the fault finally giving way to simple monoclines. On our side of the river, the flows are all R_1 Grande Ronde Basalt.

110.0 (7.0) Beamers Bar. Rest stop when open in summer.

110.9 (0.9) Confluence of Snake and Grande Ronde rivers. The road continues up the Grande Ronde River.

111.2 (0.3) Imnaha Basalt (Rock Creek type) underlying R_1 Grande Ronde Basalt in a roadcut. Across the Grande Ronde River, flows of Imnaha Basalt dip toward us, away from the Limekiln fault. Displacement on this fault itself and the uplift of older flows by drag against the fault played significant roles in the emplacement of later flows.

113.4 (2.2) Bridge over the Grande Ronde River. Note, again, the spectacular meanders that give the river its name. Behind us, the north wall of the Grande Ronde River canyon is the type section for the Grande Ronde Basalt (R_1 through R_2). Heading south, the road now descends through Imnaha Basalt overlain by deposits of the Pleistocene Lake Bonneville floods.

114.8 (1.4) Lake Bonneville flood gravels. The road leaves the Grande Ronde valley and follows Joseph Creek.

116.6 (1.8) Bridge over Joseph Creek.

116.7 (0.1) **STOP 13. Dike feeding flow** (Reidel and others, 1987).

Park cars on the far side of the bridge and prepare for a difficult scramble up scree. Sturdy boots are essential.

The Grande Ronde dike is well exposed as a wall across the river to the south. Starting from the south side of the old bridge ramp, follow the dike up the northwest side of Joseph Creek by passing through a gate in a fence along the old road and following the north side of a small stream. The dike can be recognized by its horizontal joints and aphanitic texture, which contrasts with the coarse and porphyritic textures of the Imnaha flows at the base of the canyon. At the Imnaha/Grande Ronde contact, the dike appears to change trend from northwest to north. Above this, the dike becomes vesicular and forms a negative topographic feature before spreading out into an oxidized, glassy, banded, and scoriaceous flow half way up the canyon wall well above the Imnaha/Grande Ronde Basalt contact. Near the dike/flow contact, the dike contains blocks of cooled lava and scoria.

Return (carefully) to the cars.

Optional Stop. Imnaha and Grande Ronde Basalt (3.6 mi).

The climb up the canyon wall is not recommended for participants not in the best of health or without strong boots. Those not wishing to make the climb should proceed 1.8 mi farther up Joseph Creek and examine a well-exposed section of Imnaha Basalt overlain by Grande Ronde Basalt. The thick flows of Imnaha Basalt in the roadcut are of Rock Creek type (Hooper and others, 1984). They are very coarse and dark and have thick scoriaceous tops full of zeolites—chabazite, thomsonite, and analcite are the most abundant. Paleomagnetic work (Hooper and others, 1979) has shown (1) that there are many more flows in this section than there are farther from the dike swarm and (2) that many of these additional flows have transitional magnetic orientations between the N_0 of the Imnaha below and the R_1 of the lower Grande Ronde above. From this we conclude that there is no significant time gap between the eruption of the Imnaha and Grande Ronde basalts and that many small flows were erupted along the line of the Grande Ronde dike swarm which did not spread significant distances across the Columbia Plateau.

Return to Stop 13 and reset odometers to 116.7.

Retrace the route to the Snake River, past Beamers Bar, and back down the Snake River toward Lewiston.

132.6 (15.9) Leave the gravel road and begin the paved road.

138.6 (6.0) N_1 Grande Ronde Basalt at road level. A Weissenfels Ridge feeder dike can be seen in the

cliff directly ahead. On top of the ridge to the east of the dike is an exposure of the Elephant Mountain (Saddle Mountains) intracanyon flow.

141.4 (2.8) Bridge. Exposure of an intracanyon Pomona flow (Saddle Mountains) high on the ridge on the left above the road.

141.9 (0.5) For the next 3 to 4 mi patches of both Elephant Mountain and Pomona flows can be seen across the Snake River perched high on the edge of the present canyon. These are remnants of flows that filled an earlier Snake River canyon, cut less deep than the present one at this point.

145.0 (3.1) Enter southern limits of the town of Asotin.

145.5 (0.5) **STOP 14. Pomona flow.**

Turn right off the main road to the river front between houses.

Across the river is a photogenic view of the Pomona flow filling the older Snake River canyon. The Pomona flow is multi-tiered here and has a significant hyaloclastic horizon half way up. The columns of the well-developed colonnade at the base are everywhere perpendicular to the cooling surface. The continuation of the lava-filled canyon can be seen in Swallow Rock some miles north, downriver.

146.1 (0.6) Stop sign. Junction with SR 129. Continue straight, toward Lewiston.

148.7 (2.6) Swallow Rock. The Pomona flow and the Elephant Mountain flow crop out on the rock. Both flows filled sequentially developed canyons that trended northwest on the southwest side of Clarkston.

End of road log. Drive north to return to Spokane.

Structure of the Yakima Fold Belt, Central Washington

Stephen P. Reidel and Newell P. Campbell

Structure of theYakima Fold Belt, Central Washington

S. P. Reidel [1]
Geosciences Group
Westinghouse Electric Company
Richland, WA 99352
and
N. P. Campbell
Department of Geology
Yakima Valley College
Yakima, WA 98908

INTRODUCTION

The Yakima Fold Belt is a series of anticlinal ridges and synclinal valleys that covers about 14,000 km^2 of the western Columbia Plateau (Fig. 1). The fold belt formed as basalt flows of the Columbia River Basalt Group (CRBG), intercalated sediments of the Ellensburg Formation, and correlative units were folded and faulted under north-south-directed compression. Interest in the fold belt has increased over the past several decades because of hydrocarbon exploration and the siting of nuclear power plants. Despite the wealth of information from several decades of research, the Yakima Fold Belt is still incompletely understood. Although field studies have greatly increased our knowledge of the structure of the Columbia Plateau and the fold belt, timing of deformation, and growth rates of the folds, very little is known about the subsurface structure and the origin of the fold belt.

Many structural and tectonic models have been proposed to explain the origin and geologic evolution of the Columbia Plateau (for example, Laval, 1956; Davis, 1977, 1981; Bentley, 1977, 1980; Barrash and others, 1983; Reidel, 1984), but no one model has gained general acceptance because of differing interpretations of the nature of the geologic structures, extrapolation of structures to depth, character of basement involvement, and the timing and rates of deformation.

This field guide is designed to provide an introduction to the geology of the Yakima Fold Belt. It consists of two parts. The route for Day 1 of the trip is along the western margin of the Columbia River basalt west of Yakima. This part of the trip examines evidence for the influence of pre-Miocene structures on the Yakima folds and the nature of the folds along the margin of the Columbia Plateau. The route for the trip on Day 2 covers the central portion of the Yakima Fold Belt in the Pasco Basin area. This part of the trip examines the geology of the Yakima folds and the style of folding and faulting. Together, the two parts of the field guide provide not only an introduction to the geology of the Yakima Fold Belt, but also locations of easily accessible sites that demonstrate the structural characteristics of the fold belt.

REGIONAL SETTING

The Columbia Plateau is a broad plain situated between the Cascade Range to the west and the Rocky Mountains to the east and is constructed of the Miocene CRBG. In the central and western parts, the basalt is underlain predominantly by Tertiary continental sedimentary rocks and overlain by late Tertiary and Quaternary fluvial and glaciofluvial deposits.

The CRBG covers four general structural-tectonic regions or subprovinces of the Columbia Plateau, each of which has a distinctly different structural style: the Yakima Fold Belt, the Palouse, the Blue Mountains, and the Clearwater and Weiser embayments (Fig. 1). The Yakima Fold Belt consists of a series of generally west-trending (N50°W to S50°W) anticlinal ridges and synclinal valleys (Fig. 2). The Palouse paleoslope is the least deformed region and has only minor faults and low-amplitude, long-wavelength folds on an otherwise gentle

[1] Also with Department of Geology, Washington State University, Pullman, WA 99164

From: Joseph, N. L., and others, editors, 1989, Geologic guidebook for Washington and adjacent areas: Washington Division of Geology and Earth Resources Information Circular 86.

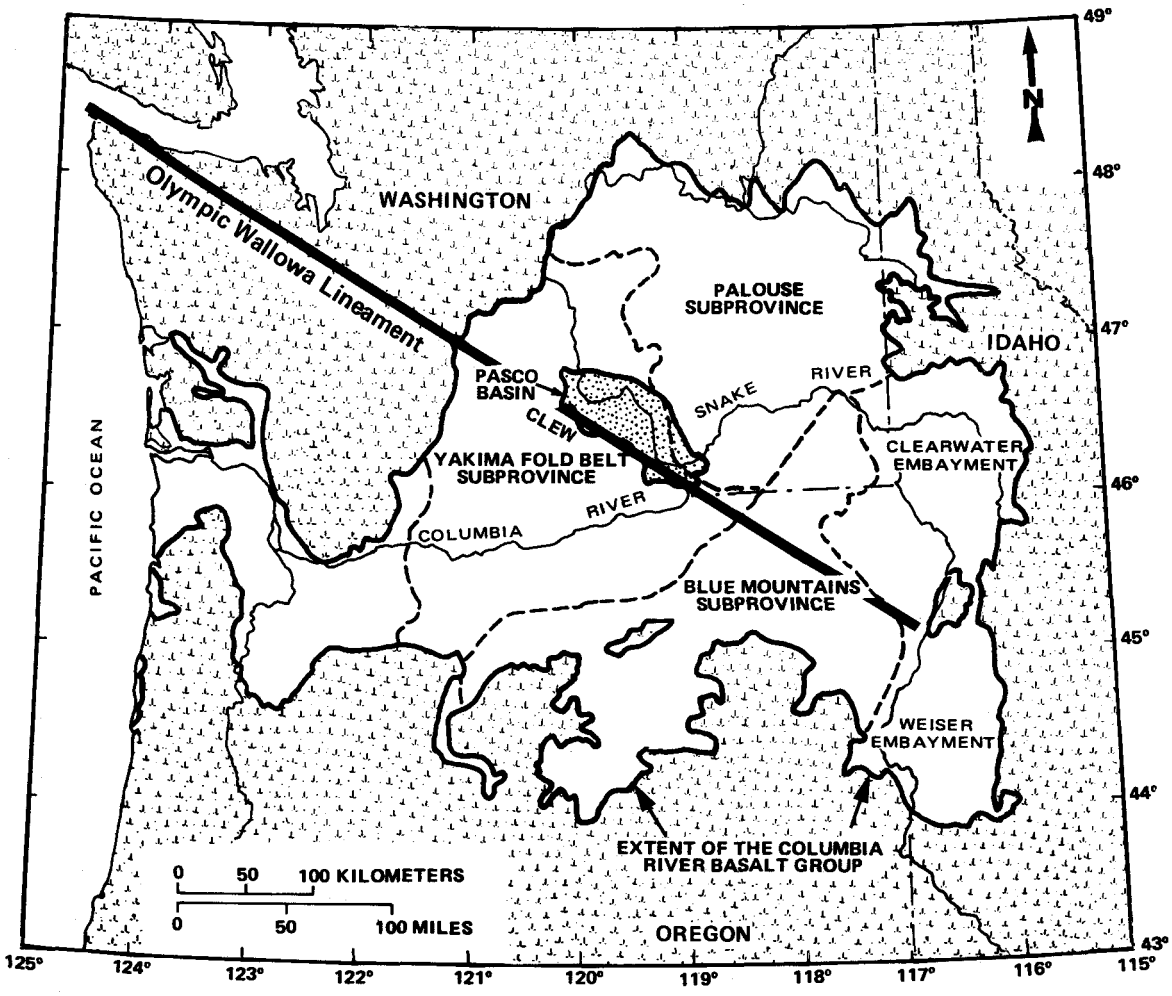

Figure 1. The Columbia Plateau. Shown are the areal extent of the Columbia River Basalt Group, the four major structural-tectonic subprovinces (the Yakima fold belt, Palouse, Blue Mountains, and Clearwater-Weiser embayments), the Pasco Basin, the Olympic-Wallowa lineament, and the CLEW, which is the central portion of the OWL that passes through the western part of the Columbia Plateau.

west-dipping paleoslope (Swanson and others, 1980). The Palouse paleoslope marks the eastern boundary of the Yakima Fold Belt and has been a relatively stable feature since at least the middle Miocene (Swanson and Wright, 1976). The Blue Mountains is a northeast-trending anticlinorium that extends 250 km from the Cascades to the eastern part of the plateau. The Blue Mountains form the southern boundary of the Yakima Fold Belt.

Two regional structures cross-cut the central and western part of the Columbia Plateau: the Olympic-Wallowa lineament (OWL) (Figs. 1 and 2), and the Hog Ranch-Naneum Ridge anticline (Fig. 2). The segment of the OWL that crosses the Yakima Fold Belt is referred to as the Cle Elum-Wallula deformed zone (CLEW; Keinle and others, 1977) and is marked by a rather diffuse zone of anticlines that has a N50°W orientation (Fig. 2). The Hog Ranch-Naneum Ridge anticline is a basement-controlled anticline that extends southward from the North Cascades (Tabor and others, 1984) and forms the western boundary of the Pasco Basin (Reidel, 1984), one of the larger basins in the fold belt (Figs. 1 and 2).

STRATIGRAPHY

The dominant rocks of the area of this field guide are the Columbia River basalts and intercalated sedimentary rocks of the Ellensburg Formation. These are overlain by younger sedimentary rocks of the Ringold Formation and the Pleistocene catastrophic flood deposits of the Hanford formation (informal). Sedimentary and volcanic units of the Naches, Ohanapecosh, and Fifes Peak formations underlie the basalt along the western margin. The stratigraphy in the area covered by the field guide is shown in Figure 3.

Pre-Columbia River Basalt Group Units

In the central Cascade Range west of Yakima, early Tertiary sedimentary and volcanic rocks underlie the middle Miocene CRBG (Fig. 3). The late Eocene Naches

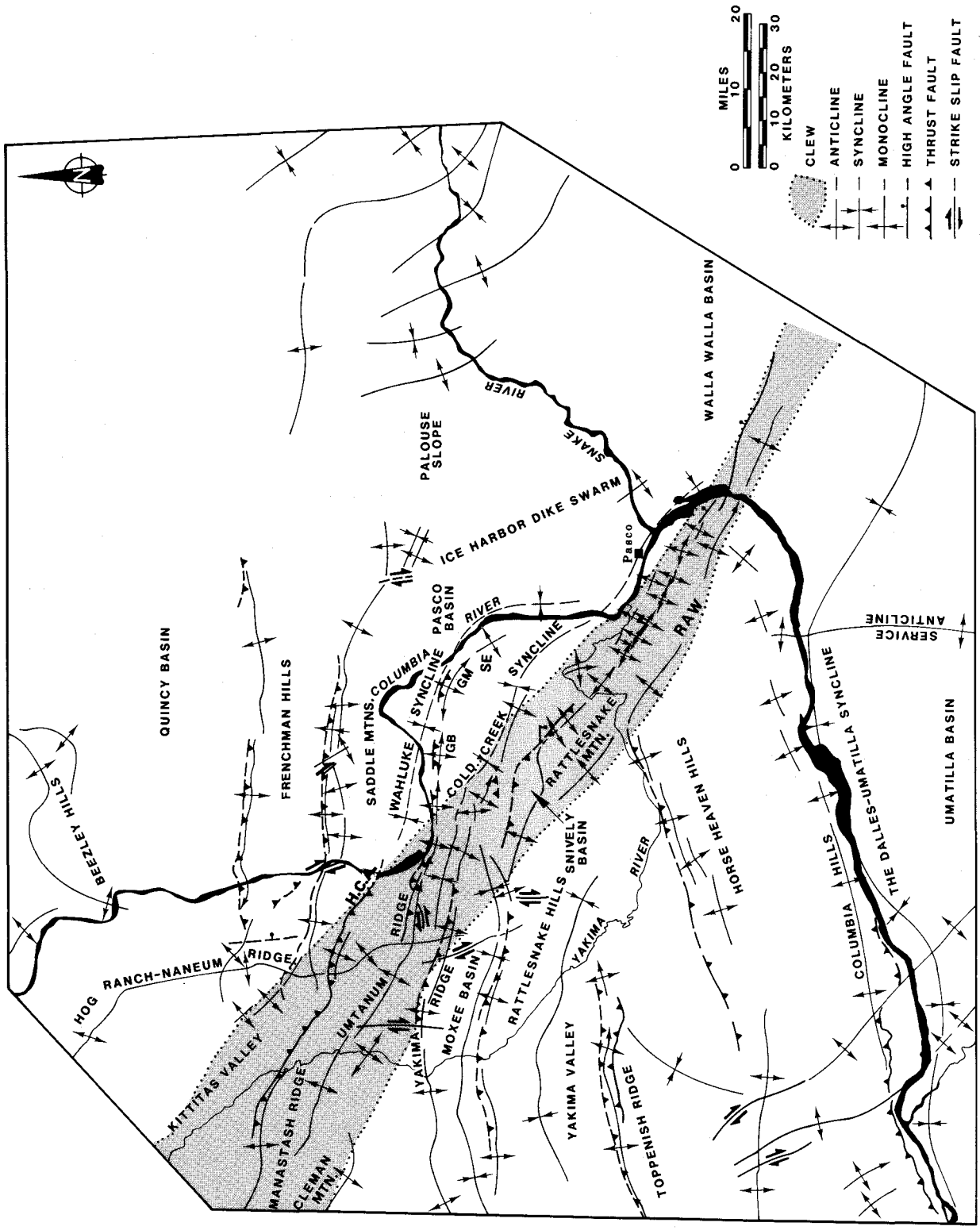

Figure 2. Major faults and folds in the central part of the Yakima Fold Belt and the western part of the Palouse (from Reidel and others, in press [b]). Shown are the Hog Ranch-Naneum Ridge anticline that forms the western boundary of the Pasco Basin, the Cle Elum-Wallula Deformed zone (CLEW, stippled), and the Rattlesnake-Wallula alignment (RAW) that forms that portion of the OWL and CLEW in the Pasco Basin. GB, Gable Butte; GM, Gable Mountain; SE, Southeast anticline along the Umtanum anticline; H.C.A., Hansen Creek anticline.

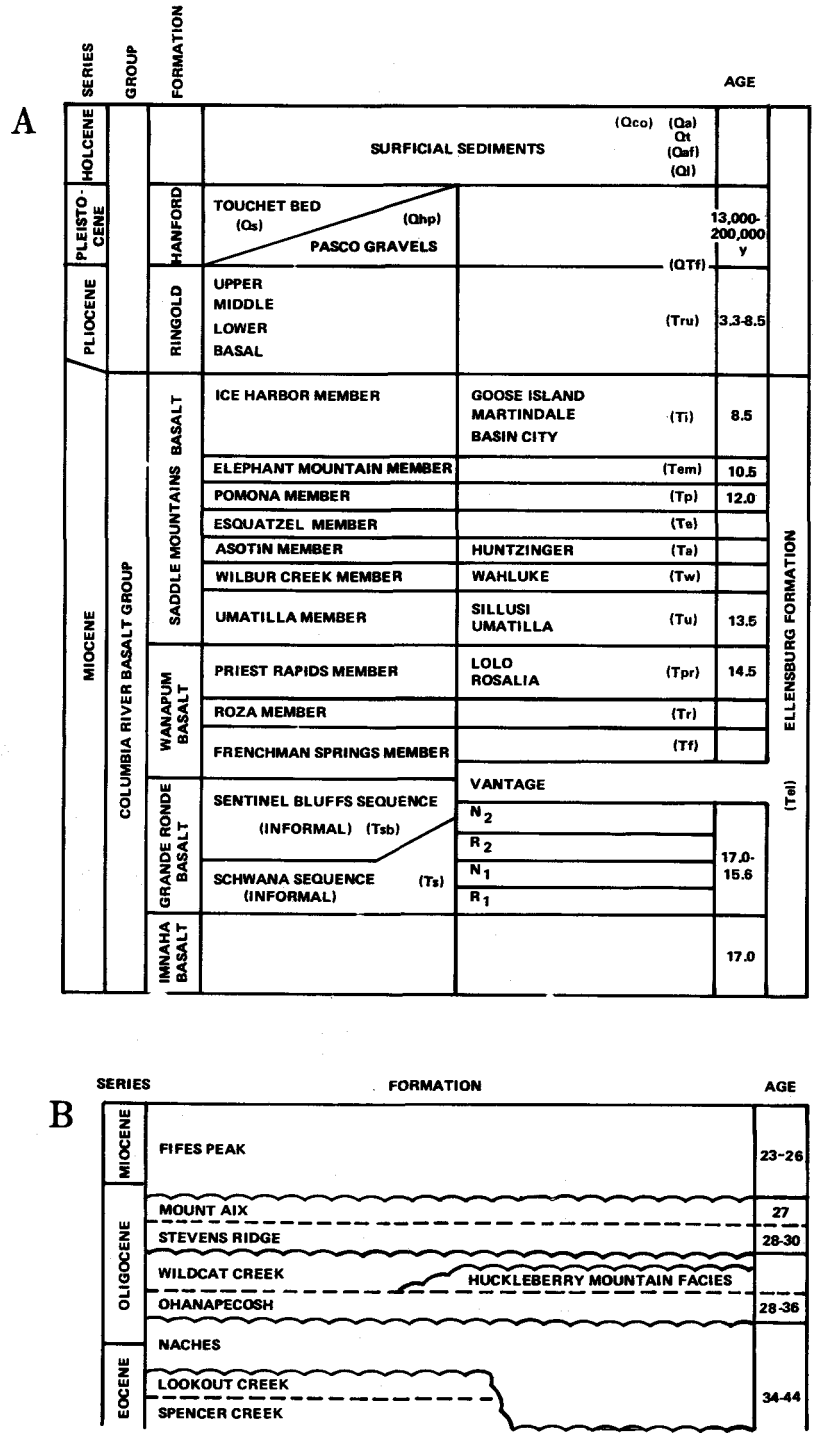

Figure 3. Major Tertiary stratigraphic units in the area covered by the field guide. Ages in million years. A. Units of the Columbia River Basalt Group, intercalated sediments, and overlying sediments. Symbols in parentheses are used on geologic maps of Figs. 12, 13, and 14. B. Units older than the Columbia River Basalt Group that are exposed along the margin of the Columbia River basalt. Holocene surficial sediments are generalized as: alluvium (Qa), talus (Qt), alluvial fans (Qaf), colluvium (Qco), and loess (Ql). Older alluvial fans of uncertain age are shown as (QTf). Goose Island, Martindale, Basin City, Huntzinger, Wahluke, Umatilla, Lolo, and Rosalia are individual basalt flows. Vantage is the sedimentary interbed between the Wanapum and Grande Ronde Basalts. The Grande Ronde is divided into four magnetostratigraphic units, N_2, R_2, N_1, R_1.

Formation is composed of fluvial, feldspathic sandstones and rhyolite flows and tuffs; basalt and andesite flows are present in the upper part. K-Ar dates near the base of the Naches Formation give ages of 40 to 44 Ma (Tabor and others, 1984). The Naches Formation is principally confined to the area bounded on the south by the White River-Naches River fault zone and on the north by splays of the Straight Creek fault (Fig. 4).

Younger volcanic rocks of the Ohanapecosh and Fifes Peak Formations are found along the Naches River drainage. The Ohanapecosh Formation consists of multicolored andesitic tuffs and volcaniclastic sediments interbedded with rhyolite and andesite flows. Fission-track ages on zircons range from 28 to 36 Ma (Vance and others, 1987). Ohanapecosh rocks are more voluminous south of the White River-Naches River fault (Fig. 4). The

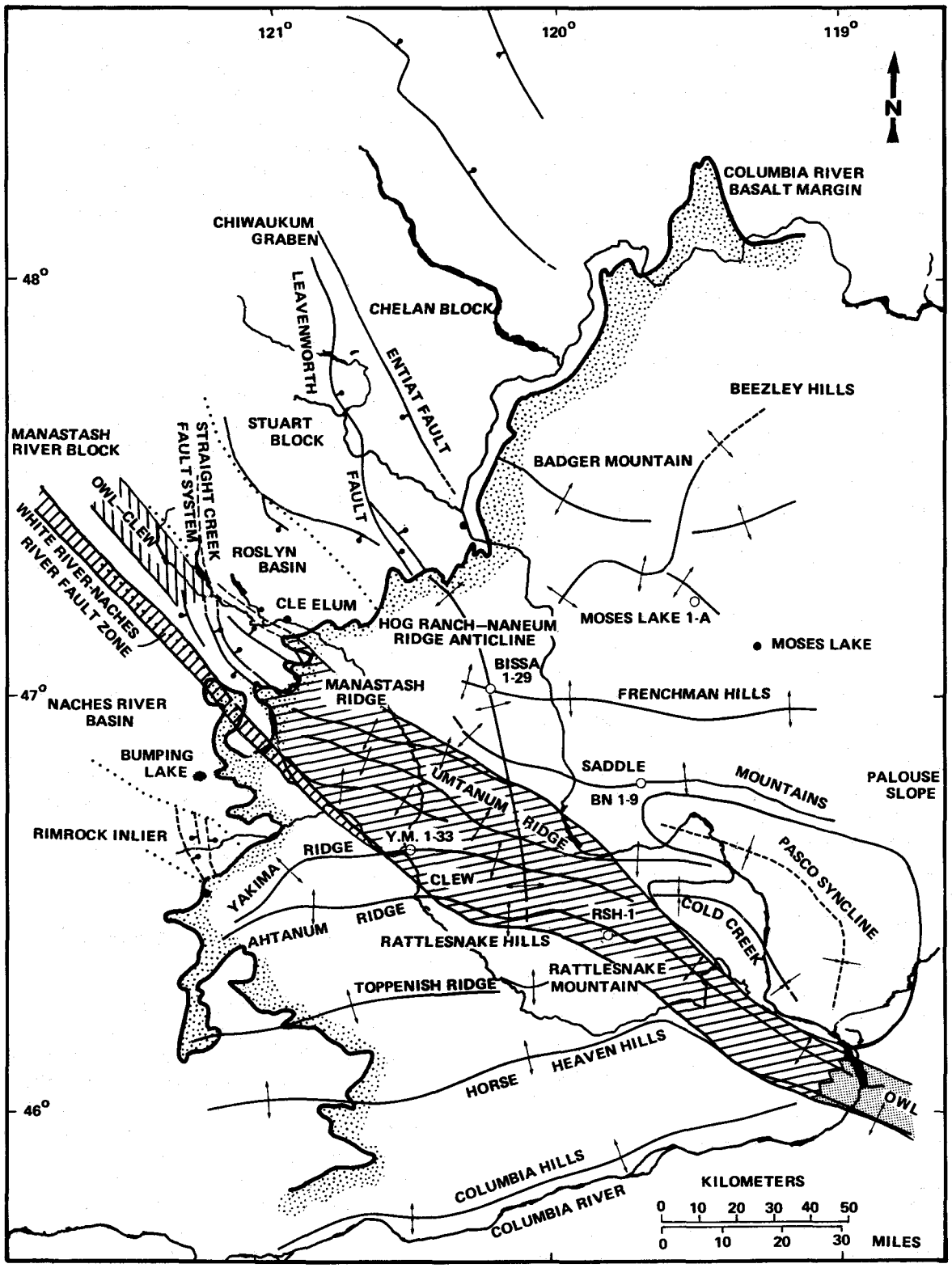

Figure 4. Generalized map of major faults and folds along the western margin of the Columbia Plateau and Yakima Fold Belt. Hydrocarbon exploration boreholes are shown as open circles.

Fifes Peak Formation consists of three or more eroded volcanic cones along the eastern flank of the Cascade Range. The Edgar Rock volcano is dissected by the Naches River and contains both an apron facies of ash-flow tuffs and a cone facies of andesitic brecciated lavas (Campbell, 1975, 1988; Carkin, 1988). These rocks range in age from about 23 to 26 Ma (Vance and others, 1987). The Edgar Rock volcano was built above the surrounding topography during the early Miocene. Lavas of the CRBG were forced to flow around the cone before they could spread up the Little Naches River.

Columbia River Basalt Group

The CRBG, the principal rock unit in the Yakima Fold Belt, is a sequence of tholeiitic flood-basalt flows that were erupted between 17 and 6 Ma. The CRBG now covers approximately 164,000 km^2 and consists of 174,000 km^3 of basalt (Tolan and others, 1987). The CRBG has been divided into five formations (Fig. 3; Picture Gorge Basalt is not shown but intercalates with the Grande Ronde Basalt) (Swanson and others, 1979a); only the Grande Ronde Basalt, the Wanapum Basalt, and the Saddle Mountains Basalt are exposed within the western Columbia Plateau.

The basalt flows of the CRBG can be distinguished by using a combination of lithology, chemistry, and paleomagnetic data (Swanson and others, 1979a). Chemical composition and paleomagnetic data have proven to be the most reliable criteria for flow recognition and correlation; lithology is reliable for many flows primarily within the Wanapum and Saddle Mountains Basalts, but chemical compositions are still used to confirm identifications. Chemical composition and paleomagnetic data are most important in identifying flows of the Grande Ronde Basalt because of the similarity of their lithology. In the field the Grande Ronde Basalt has been divided into four magnetostratigraphic units (msu) (Fig. 3) which, from oldest to youngest are: Reversed 1 (R_1), Normal 1 (N_1), Reversed 2 (R_2), and Normal 2 (N_2) (Swanson and others, 1979a). The composition has been broadly subdivided into two groups based on relative concentrations of MgO (Swanson and others, 1979a) (Fig. 3, high MgO is Sentinel Bluffs and low MgO is Schwana), but recent studies have provided more detailed compositional subdivisions (Reidel, 1983; Mangan and others, 1986; Reidel and others, in press [b]).

Ellensburg Formation

The Ellensburg Formation includes epiclastic and volcaniclastic sedimentary rocks that are intercalated with and overlie the CRBG (Waters, 1961; Swanson and others, 1979a). Most volcaniclastic material in the Ellensburg Formation was produced by volcanic events in the Cascade Range. In the Naches drainage, deposition was primarily by volcanic debris flows (lahars) and related stream and sheet floods. Some air-fall and pyroclastic-flow deposits are also present. The age of the formation in the Naches drainage is between 16.5 and 7.4 Ma (Smith and others, 1988). The bulk of the material in the Naches River drainage was derived from a single source near Bumping Lake (Fig. 4). Farther east in the central plateau, the Ellensburg Formation is mixed with sediments deposited by the ancestral Clearwater and Columbia Rivers (Fecht and others, 1982, 1987).

Suprabasalt Sediments

Sediments continued to be deposited in most synclinal valleys long after the eruptions of the Columbia River basalt. During the late Neogene, epiclastic and volcaniclastic rocks of the Ringold Formation were deposited in the central Columbia Plateau. The Ringold Formation of Pliocene age represents main- and side-stream facies of the ancestral Columbia River. The Ringold has been divided into four units (Fig. 3) primarily on the basis of texture. The basal unit represents a complete fining-upward fluvial cycle deposited by a braided-river system associated with the ancestral Columbia River system (Fecht and others, 1982, 1987). The lower and upper units are fine-grained sediments that were deposited in a low-energy lacustrine and(or) fluvial overbank depositional environment. The middle unit is composed of stream gravels, which were also deposited by the ancestral Columbia River system.

The most recent deposits are the sediments deposited by cataclysmic flood waters during the Pleistocene and post-flood alluvium and eolian deposits. The flood deposits are informally called the Hanford formation and are divided into the fine-grained, slackwater sediments, the Touchet beds, and the Pasco gravels.

Regional Thickness Variations of Units and Tectonic Implications

The greatest thickness of both Tertiary pre-CRBG rocks (Campbell, in press) and Columbia River basalt (Reidel and others, 1982, in press [a]) is in the central Columbia Plateau. Magnetotelluric data (Berkman and others, 1987) and seismic-reflection data (Catchings and Moody, 1988) suggest that both the CRBG and sub-basalt sediments thicken from the Palouse paleoslope into the area covered by Yakima Fold Belt. The CRBG ranges from 500 to 1,500 m thick on the Palouse paleoslope but abruptly thickens to more than 4,000 m in the Pasco Basin area (Reidel and others, 1982, in press [a]). Although the total thickness of the sub-basalt sediments is not known, these sediments appear to thicken dramatically beneath the Yakima Fold Belt (Campbell, in press; Reidel and others, in press [a]).

The regional thickness pattern of both the CRBG and underlying Tertiary sediments indicates that prior to the eruption of the basalts, the area encompassing the present-day Yakima Fold Belt had subsided relative to the Blue Mountains and Palouse paleoslope and filled with sediments. There is no evidence of encroachment by the sea into the central Columbia Plateau during the Tertiary. The continental nature of the sediments (Campbell, in press) suggests that aggradation kept pace with subsidence, and the subaerial nature of the CRBG (Reidel and others, 1982, in press [b]) indicates that subsidence continued through the eruption of the basalts and that basalt accumulation kept pace with subsidence. Furthermore, the suprabasalt sediments in the Pasco Basin indicate that subsidence continued beyond the Miocene and into the Pliocene. Evidence for the thinning and pinchouts of basalt flows onto the Blue Mountains (for example, Ross, 1978; Hooper and Camp, 1981; Fox and Reidel, 1987) indicates that the Blue Mountains were growing during the eruption of the CRBG and while the central part of the plateau was subsiding. The regional tectonic setting of the central Columbia Plateau throughout much of the Cenozoic, therefore, appears to be one of a subsiding intermontane basin that is bounded on the west by the rising Cascade Range, on the south by the slowly growing Blue Mountains, and on the east by a relatively stable westward-dipping paleoslope.

GEOLOGY OF THE NACHES RIVER AREA

The Naches River area along the northwest margin of the Columbia Plateau is an important place to develop an understanding of the effects of pre-basalt structures on the Yakima Fold Belt. The principal structural elements that border the basalt include the Straight Creek fault, faults thought to be associated with the Olympic-Wallowa lineament (OWL), and the White River-Naches River fault zone (Fig. 4).

Straight Creek Fault

The Straight Creek fault of the Cascade Range is a major fault zone extending from north of the Canadian border to at least as far south as Snoqualmie Pass in central Washington. There is little or no evidence to extend this fault south of the drainages of the White River-Naches River fault zone (Fig. 4). Instead, the Straight Creek fault turns southeastward and splays into a series of subparallel faults (Tabor and others, 1984; Frizzell and others, 1984). These fault splays pass under the CRBG and align with northwest-trending folds in the Yakima Fold Belt (Manastash Ridge). However, at the plateau margin, only small faults of low displacement and broad, flat folds are present in sub-basalt rocks. Farther to the southeast, within the Yakima Fold Belt, the deformation becomes more intense.

Olympic-Wallowa Lineament

The OWL has been recognized as a major throughgoing topographic feature in Washington (Raisz, 1945; Fig. 1). This feature aligns with pre-basalt structural trends northwest of the Columbia Plateau. Within the Yakima Fold Belt, deformation along Manastash Ridge and abrupt bending of the eastern ends of Umtanum Ridge, Yakima Ridge, and Rattlesnake Ridge (Fig. 2) are considered to be evidence for Miocene or younger deformation along the OWL. This portion of the OWL is called the Cle Elum-Wallula deformed zone (CLEW).

Just northwest of the Columbia River basalt margin, on Manastash Ridge, numerous northwest-trending faults and shear zones of the Straight Creek fault system are subparallel to the OWL (Tabor and others, 1984). It is not known whether the OWL affects Tertiary rocks here or if deformation is solely related to the Straight Creek fault system.

White River-Naches River Fault Zone

The Naches River and Little Naches River flow in a rather straight, southeasterly direction from near the crest of the Cascade Range toward Yakima (Fig. 5). The White River-Naches River fault zone is a major fault zone and is aligned with this 50-km-long Naches-Little Naches valley system that separates two terranes of dissimilar structure, stratigraphy, and topography (Campbell, 1988). Northeast of the White River-Naches River fault zone, faults and folds in pre-Tertiary through Pliocene rocks parallel (N60°W) splays of the Straight Creek fault zone. Southwest of the White River-Naches River fault zone, faults in pre-Tertiary rocks trend N5°E to N20°W. Middle and late Tertiary rocks in this area reflect Miocene folding and are commonly aligned east-west.

Within the basalts the White River-Naches River fault zone appears to influence fold development in the Yakima Fold Belt as far southeast as Yakima. The fault zone separates a domain of ENE-trending folds on the southwest from dominantly northwest-trending folds on the northeast, and it defines structural low points along the Yakima Ridge and Rattlesnake Hills anticlines. The fault zone can be shown to offset flows of the CRBG for several kilometers southeast of the margin (Campbell, 1988).

The White River-Naches River fault zone derives its name from an alignment northwest of this area between this fault zone in the Naches River and the White River fault (Hammond, 1963; Frizzell and others, 1984), a major fault that continues at least 50 km WNW of the area. The length of the entire fault zone, from Enumclaw to Naches, exceeds 90 km.

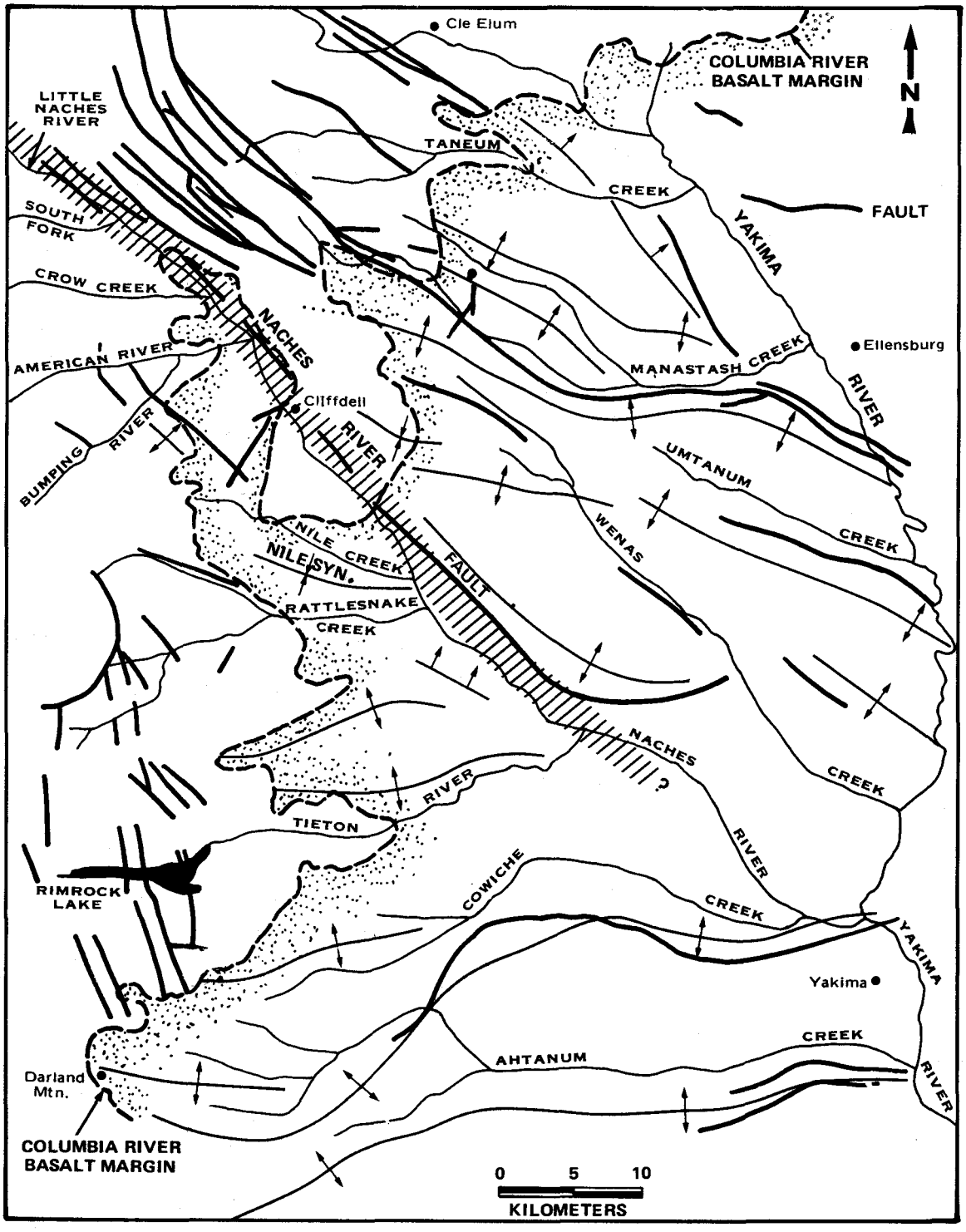

Figure 5. Comparison of drainage orientation and geologic structural patterns on both sides of the Naches-Little Naches rivers. The Naches River-White River fault zone is the striped pattern superimposed on the map. Thin lines are drainage systems, and heavy lines are major faults.

Deformation of the CRBG in the Naches River Drainage

Along the Naches River drainage at the margin of the CRBG, the Cleman Mountain anticline is the dominant structure in the Columbia River basalt (Fig 2). Cleman Mountain has the greatest amplitude and west structural closure of any anticline in the Yakima Fold Belt. A large folded thrust fault along the southwest limb of the fold places the R_2 msu of the Grande Ronde Basalt over the N_2 msu. Some of the complex faulting on this limb is attributed to movement on the White River-Naches River fault zone.

THE YAKIMA FOLDS

Introduction

The anticlines of the Yakima Fold Belt consist of non-cylindrical, asymmetrical anticlinal ridges and synclinal valleys. The anticlines are typically segmented and have a general north vergence, although some folds such as the Columbia Hills have a south vergence. Synclines typically have a gently dipping north limb and a steeply dipping south limb. Fold length is varied, ranging from several kilometers to more than 100 km; fold wavelengths range from several kilometers to as much as 20 km. Structural relief is typically about 600 m but varies along the length of the fold. The greatest structural relief along the Frenchman Hills, the Saddle Mountains, Umtanum Ridge, and Yakima Ridge occurs where they intersect the south-trending Hog Ranch-Naneum Ridge anticline (Fig. 2).

In general, the axial trends produce a "fanning" pattern across the fold belt (Figs. 2 and 4). Anticlines on the western side of the fold belt generally have a N50°E trend (Swanson and others, 1979b). Anticlines in the central part of the fold belt have west trends except along the CLEW where a N50°W trend predominates. The Rattlesnake Hills, Saddle Mountains, and Frenchman Hills have overall west trends across the fold belt, but Yakima Ridge and Umtanum Ridge change eastward from due west to N50°W in the zone of the CLEW. In the central part of the fold belt, the Horse Heaven Hills, the Rattlesnake Hills, and the Columbia Hills have eastward terminations against the CLEW. There is no evidence for continuation of any anticline to the northeast across the CLEW.

Fold and Fault Geometry

Within the east-central fold belt, the fold geometry typically consists of steeply dipping to overturned north flanks and gently dipping (5 degrees) south flanks. Exceptions, however, include the doubly plunging anticlines within the Rattlesnake-Wallula alignment (RAW) of the CLEW (Fig. 2) and the conjugate box-fold geometry of parts of the anticlines such as the Smyrna segment of the Saddle Mountains (Reidel, 1984). The main variable in fold profiles is the width of the gently dipping limb. The lengths of the gently dipping limbs range from as little 5 km to as much as 35 km.

Segmentation of the anticlines is common throughout the fold belt and is defined by abrupt changes in fold geometry or by places where regional folds die out and become a series of doubly plunging anticlines. Segment lengths range from 5 to 35 km in the central plateau; some of the larger segments contain subtler changes in geometry, such as different amplitudes that could also be considered segment boundaries. Segment boundaries are marked in many places by cross or tear faults that trend from N20°W to north and display a principal component of strike-slip movement (for example, Saddle Mountains; Reidel, 1984). In the central Columbia Plateau these cross faults are confined to the anticlinal folds and normally occur only on the steeper limb, dying out onto the gentler limb. In the southwest plateau, some cross faults can be traced as far as 100 km (Swanson and others, 1979b).

Some segment boundaries are also marked by relatively undeformed areas along the fold trend where two fold segments plunge toward each other. For example, the Yakima River follows a segment boundary where it crosses the RAW at the southeast termination of Rattlesnake Mountain (Fig. 2).

The steep limb of the asymmetrical anticlines in the east-central fold belt is almost everywhere faulted (Fig. 6). In the eastern portion of the Yakima Fold Belt, the steep limb is typically the northern flank, but elsewhere, as at the Columbia Hills (Swanson and others, 1979b), the south limb is faulted. Where exposed, these frontal fault zones have been found to be imbricated thrusts—for example, at Rattlesnake Mountain, Umtanum Ridge near Priest Rapids Dam (Bentley, 1977; Goff, 1981; Bentley, *in* Swanson and others, 1979b), the Horse Heaven Hills near Byron Road (Hagood, 1986), and the Saddle Mountains near Sentinel Gap (Reidel, 1984).

Yakima folds of the central Columbia Plateau have emergent thrust faults at the ground surface (Fig. 6). The tops of the youngest lava flows at the Earth's surface serve as a plane that becomes a low-angle thrust fault; the structural attitude of the surface flow controls the angle of the emergent fault plane. This type of apparent structural control led many investigators to conclude that faults associated with the Yakima folds are low-angle thrust faults with detachment surfaces within the CRBG, in the sediments below the basalts, or at the basalt-sediment contact. Where erosion provides deeper exposures into the cores of folds, the frontal faults are observed to be reverse faults (as at the Columbia water gap in the Frenchman Hills, 45 degrees to the south [Grolier and Bingham, 1971]; the Columbia Hills at Rock Creek, 50-70 degrees to the north [Swanson and others, 1979b]).

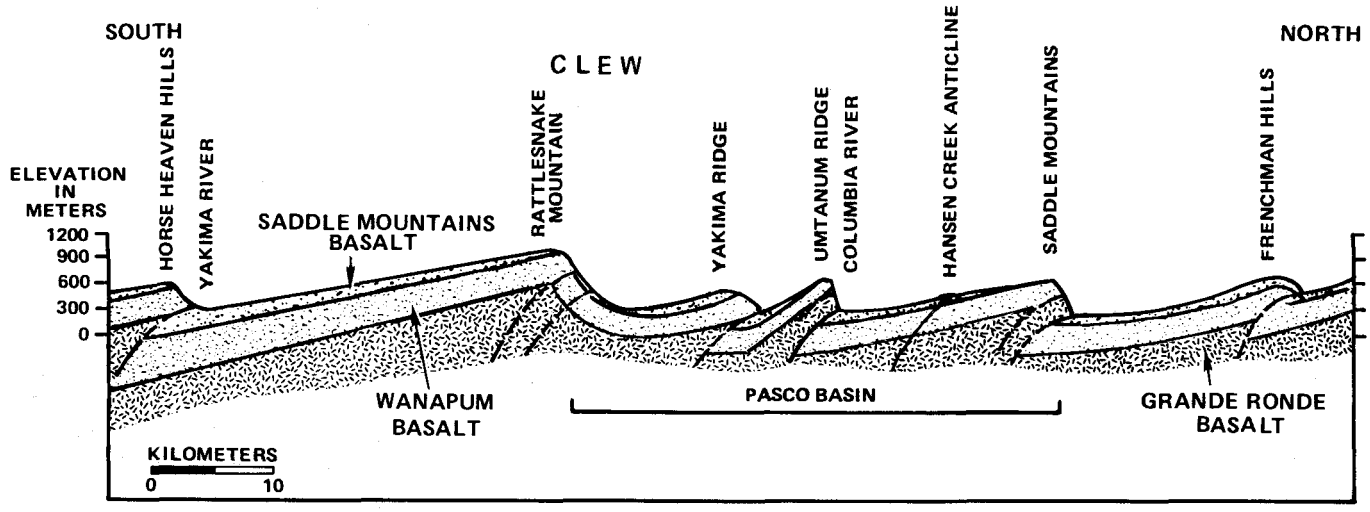

Figure 6. Schematic cross-section through the Yakima Fold Belt in the central Columbia Plateau at about long. N120°W.

Subsurface Structure

The dip of the frontal fault plane and the structure of the anticlines at depth remain controversial. A multitude of possible models (such as Suppe's [1983, 1985] fault-bend fold or fault-propagation fold, Jamison's [1987] detachment fold, and Mitchell and Woodward's [1988] kink-detachment fold) can all produce similar surface geometries and thus have provided abundant food for thought influencing many of the models that have been proposed for the fold belt. However, no clear answers have come forth because of the lack of direct observations.

ACKNOWLEDGMENTS

This manuscript benefited from valuable reviews by Robert D. Bentley, Virginia A. Pfaff, Gary A. Smith, Jim C. Evans, and Henry Schasse.

REFERENCES CITED

Barrash, W.; Bond, J. G.; Venkatakrishnan, R.;1983, Structural evolution of the Columbia Plateau in Washington and Oregon: American Journal of Science, v. 283, no. 9, p. 897-935.

Bentley, R. D., 1977, Stratigraphy of the Yakima Basalts and Structural Evolution of the Yakima Ridges in the western Columbia Plateau. *In* Brown, E. H.; Ellis, R. C., editors, Geology Excursions in the Pacific Northwest: Western Washington University Press, p. 339-389.

Bentley, R. D., 1980, Wrench tectonic model for the late Cenozoic evolution of Oregon and Washington [abstract]: Geological Society of America Abstracts with Programs, v. 12, no. 7, p. 385.

Bentley, R. D.; Campbell, N. P., 1983, Geologic Map of the Yakima Quadrangle, Washington: Washington Division of Geology and Earth Resources Geologic Map GM-29, 1 pl., scale 1:48,000.

Berkman, E. A.; Orange, A.; Bergstrom, K. A.; Mitchell, T. H., 1987, Interpretation of magnetotelluric data, Rattlesnake Mountain, Pasco Basin, Washington: Rockwell Hanford Operations Report SD-BWI-TI-354, 31 p.

Bingham, J. W.; Lundquist, D. J.; Baltz, E. H., 1970, Geologic investigation of faulting in the Hanford Region, Washington: U.S. Geological Survey Open-file Report, 103 p.

Campbell, N. P., 1975, A geologic road log over Chinook, White Pass, and Ellensburg to Yakima highways: Washington Division of Geology and Earth Resources Information Circular 54, 81 p.

Campbell, N. P., 1988, Structural geology along the northwestern Columbia River basalt margin, Washington: Washington Division of Geology and Earth Resources Open File Report 88-5, 108 p., 8 pl.

Campbell, N. P., in press, Structural and stratigraphic interpretation of the rocks under the Yakima Fold Belt based on recent surface mapping and well data. *In* Reidel, S. P.; Hooper, P. R. editors, Volcanism and Tectonism in the Columbia River Flood-basalt Province: Geological Society of America Special Paper 239.

Carkin, Brad, 1988, The geology and petrology of the Fifes Peak Formation in the Cliffdell area, central Cascades Washington: Western Washington University Master of Science thesis, 157 p., 2 pl. scale 1:24,000.

Carson, R. J.; Tolan, T. L.; Reidel, S. P., 1987, Geology of the Vantage area, south-central Washington–An introduction to the Miocene flood basalts, Yakima Fold Belt, and Channeled Scabland. *In* Hill, Mason, editor, Geological Society of America Centennial Field Guide, Cordilleran Section, p. 357-362.

Catchings, R. D.; Moody, W. D., 1988, Crustal structure of the Columbia Plateau–Evidence for continental rifting: Journal of Geophysical Research, v. 19, no. B1, p. 459-474.

Davis, G. A., 1977, Tectonic evaluation of the Pacific Northwest Pre-Cambrian to recent–Preliminary Safety Analysis Report. *In* Washington Public Power Supply System, 1977, Washington Public Power Supply System nuclear project number 2, Preliminary Safety Analysis Report: Washington Public Power Supply System, Appendix 23, Subappendix 2R C, p. 1-46.

Davis, G. A., 1981, Late Cenozoic tectonics of the Pacific Northwest with special reference to the Columbia Plateau. *In* Washington Public Power Supply System, Washington Public Power Supply System nuclear project number 2, Final Safety Analysis Report: Washington Public Power Supply System, Appendix 23, Subappendix 2.5 N, p. 1-44.

Fecht, K. R., 1978, Geology of the Gable Mountain-Gable Butte area: Rockwell Hanford Operations Report RHO-BWI-LD-5, 70 p.

Fecht, K. R.; Reidel, S. P.; Tallman, A. M., 1982, Evolution of the Columbia River system in the central Columbia Plateau of Washington from Miocene to present [abstract]: Geological Society of America Abstracts with Programs, v. 14, no. 4, p. 163.

Fecht, K. R.; Reidel, S. P.; Tallman, A. M., 1985, Paleodrainage of the Columbia River system on the Columbia Plateau of Washington State–A summary: Rockwell Hanford Operations Report RHO-BW-SA-318p, 55 p.

Fecht, K. R.; Reidel, S. P.; Tallman, A. M., 1987, Paleodrainage of the Columbia River system on the Columbia Plateau of Washington State–A summary. *In* Schuster, J. E., editor, Selected Papers on the Geology of Washington: Washington Division of Geology and Earth Resources Bulletin 77, p. 219-248.

Fox, T. P.; Reidel, S. P., 1987, Stratigraphy of the Standard Kirkpatrick No. 1, Gilliam County, Oregon–New insights into Tertiary tectonism of the Blue Mountains: Oregon Geology, v. 49, no. 2, p. 15-22.

Frizzell, V. A., Jr.; Tabor, R. W.; Booth, D. B.; Ort, K. M.; Waitt, R. B. Jr., 1984, Preliminary geologic map of the Snoqualmie Pass 1:100,000 quadrangle, Washington: U.S. Geological Survey Open-File Report 84-693, 43 p., 1 pl., scale 1:100,000.

Goff, F. E., 1981, Preliminary geology of eastern Umtanum Ridge, south-central Washington: Rockwell Hanford Operations Report RHO-BWI-C-21, 100 p.

Grolier, M. J.; Bingham, J. W., 1971, Geologic map and sections of parts of Grant, Adams and Franklin Counties, Washington: U.S. Geological Survey Miscellaneous Geologic Investigations Series Map I-589, 6 sheets, scale 1:62,500.

Hagood, M. A., 1986, Structure and evolution of the Horse Heaven Hills, south-central Washington: Rockwell Hanford Operations Report RHO-BW-SA-344, 176 p., 1 pl., scale 1:24,000.

Hammond, P. E., 1963, Structure and stratigraphy of the Keechelus volcanic group and associated Tertiary rocks of the west-central Cascade Range, Washington: University of Washington Doctor of Philosophy thesis, 294 p., 2 pl.

Hooper, P. R.; Camp, V. E., 1981, Deformation of the southeast part of the Columbia Plateau: Geology, v. 9, no. 7, p. 323-328.

Keinle, C. F.; Bentley, R. D.; Anderson, J. L., 1977, Geologic reconnaissance in the Cle Elum-Wallula Lineament and related structures. *In* Washington Public Power Supply System, 1977, Washington Public Power Supply System nuclear project number 2, Preliminary Safety Analysis Report: Washington Public Power Supply System, v. 2A, Amendment 23, Subappendix 2R D, p. 1-33.

Jamison, W. R., 1987, Geometric analysis of fold development in overthrust terranes: Journal of Structural Geology, v. 9, no. 2, p. 207-220.

Laval, W. N., 1956, Stratigraphy and structural geology of portions of south-central Washington: University of Washington Doctor of Philosophy thesis, 221 p.

Mackin, J. H., 1961, A stratigraphic section in the Yakima Basalt and Ellensburg Formations in south-central Washington: Washington Division of Mines and Geology Report of Investigations 19, 45 p.

Mangan, M. T.; Wright, T. L.; Swanson, D. A.; Byerly, G. R., 1986, Regional correlation of Grande Ronde Basalt flows, Columbia River Basalt Group, Washington, Oregon, and Idaho: Geological Society of America Bulletin, v. 97, no. 11, p. 1300-1318.

McMillian, Kent; Cross, R. W.; Long, P. E., 1987, Two-stage vesiculation in the Cohassett flow of the Grande Ronde Basalt, south central Washington: Geology, v. 15, no. 9, p. 809-812.

Mitchell, M. M.; Woodward, N. B., 1988, Kink detachment fold in the southwest Montana fold and thrust belt: Geology, v. 16, no. 2, p. 162-165.

Myers, C. W.; and others, 1979, Geologic Studies of the Columbia Plateau – A status report: Rockwell Hanford Operations Report RHO-BWI-ST-4, 326 p., 10 pl.

Price, E. H., 1982, Structural geology, strain distribution, and tectonic evolution of Umtanum Ridge at Priest Rapids Dam, and a comparison with other selected localities within the Yakima Fold Belt structures, south-central Washington: Rockwell Hanford Operations Report RHO-BWI-SA-138, 197 p., 3 pl.

Raisz, E., 1945, The Olympic-Wallowa Lineament: American Journal of Science, v. 243-a, no. 5, p. 479-485.

Reidel, S. P., 1983, Stratigraphy and petrogenesis of the Grande Ronde Basalt from the deep canyon country of Washington, Oregon and Idaho: Geological Society of America Bulletin, v. 94, no. 4, p. 519-542.

Reidel, S. P., 1984, The Saddle Mountains–the evolution of an anticline in the Yakima Fold Belt: American Journal of Science, v. 284, no. 8, p. 942-978.

Reidel, S. P., 1988[1989], Geologic Map of the Saddle Mountains, south central Washington: Washington Division of Geology and Earth Resources Geologic Map GM-38, 5 pl., scale 1:48,000.

Reidel, S. P.; Fecht, K. R., 1986, The Huntzinger flow–Evidence of surface mixing of the Columbia River Basalt Group and its petrogenetic implications: Geological Society of America Bulletin, v. 98, no. 6, p. 664-667.

Reidel, S. P.; Fecht, K. R.; Hagood, M. A.; Tolan, T. L., in press (a), Geologic evolution of the central Columbia Plateau. *In* Reidel, S. P.; Hooper, P. R., editors, Volcanism and Tectonism in the Columbia River Flood-basalt Province: Geological Society of America Special Paper 239.

Reidel, S. P.; Long, P. E.; Myers, C. W.; Mase, Jack, 1982, New evidence for greater than 3.2 kilometers of Columbia River basalt beneath the central Columbia Plateau: Eos (Transactions of American Geophysical Union), v. 63, no. 8, p. 173.

Reidel, S. P.; Scott, G. R.; Bazard, D. R.; Cross, R. W.; Dick, B., 1984, Post-12 million year clockwise rotation in the central Columbia Plateau, Washington: Tectonics, v. 3, no. 2, p. 251-273.

Reidel, S. P.; Tolan, T. L.; Hooper, P. R.; Beeson, M. H.; Fecht, K. R.; Anderson, J. L.; and Bentley, R. D., in press (b), The Grande Ronde Basalt, Columbia River Basalt Group–Stratigraphic descriptions and correlations in Washington, Oregon, and Idaho. *In* Reidel, S. P.; Hooper, P. R., editors, Volcanism and Tectonism in the Columbia River Flood-basalt Province: Geological Society of America Special Paper 239.

Ross, M. E., 1978, Stratigraphy, structure, and petrology of Columbia River basalt in a portion of the Grande Ronde-Blue Mountains area of Oregon and Washington: University of Idaho Doctor of Philosophy thesis, 407 p., 1 pl.

Schmincke, H.-U., 1964, Petrology, paleocurrents, and stratigraphy of the Ellensburg Formation and interbedded Yakima Basalt flows, south-central Washington: The Johns Hopkins University Doctor of Philosophy thesis, 384 p.

Schmincke, H.-U., 1967, Flow direction in Columbia River basalt flows and paleocurrents of interbedded sedimentary rocks, south-central Washington: Geologisches Rundschau, v. 56, no. 3, p. 992-1019.

Shannon & Wilson, Inc., 1973, Geologic studies of the Columbia River basalt structures and age of deformation: Report to Portland General Electric Company, Portland, Oregon, 45 p.

Smith, G. A., 1989, Neogene synvolcanic and syntectonic sedimentation in central Washington: Geological Society of America Bulletin, v.100, no. 9, p. 1479-1492.

Smith, G. A., 1988b, Sedimentology of proximal to distal volcaniclastics dispersed across an active fold belt–Ellensburg Formation (late Miocene), central Washington: Sedimentology, v. 35, no. 6, p. 953-977.

Smith, G. A.; Campbell, N. P.; Deacon, M. W.; Muhammad Shafiquallah, 1988, Eruptive style and location of volcanic centers in the Miocene Washington Cascade Range–Reconstruction from the sedimentary record: Geology, v. 16, no. 4, p. 337-340.

Smith, G. O., 1903, Anticlinal mountain ridges in central Washington: Journal of Geology, v. 11, no. 2, p. 166-177.

Suppe, J., 1983, Geometry and kinematics of fault-bend folding: American Journal of Science, v. 283, no. 7, p. 648-721.

Suppe, J., 1985, Principles of Structural Geology: Prentice-Hall, Inc., N. J., 537 p.

Swanson, D. A.; Wright, T. L., 1976, Field Guide to field trip between Pasco and Pullman, Washington, emphasizing stratigraphy, vent areas, and intracanyon flows of the Yakima Basalt. *In* Proceedings, Geological Society of America Cordilleran Section meeting, Pullman, Washington, Field Guide 1, 33 p.

Swanson, D. A.; Wright, T. L.; Hooper, P. R.; Bentley, R. D., 1979a, Revisions in stratigraphic nomenclature of the Columbia River Basalt Group: U.S. Geological Survey Bulletin 1457-G, 59 p.

Swanson, D. A.; Anderson, J. L.; Bentley, R. D.; Camp, V. E.; Gardner, J. N.; Wright, T. L., 1979b, Reconnaissance geologic map of the Columbia River Basalt Group in Washington and adjacent Idaho: U.S. Geological Survey Open-file Report 79-1363, 7 pl., scale 1:250,000.

Swanson, D. A.; Wright, T. L.; Camp, V. E.; Gardner, J. N.; Helz, R. T.; Price, S. M.; Reidel, S. P.; Ross, M. E., 1980, Reconnaissance geologic map of the Columbia River Basalt Group, Pullman and Walla Walla quadrangles, southeast Washington and adjacent Idaho: U.S. Geological Survey Miscellaneous Investigations Map I-1139, 2 sheets, scale 1:250,000.

Tabor, R. W.; Frizzell, V. A., Jr.; Vance, J. A.; Naeser, C. W., 1984, Ages and stratigraphy of Lower and Middle Tertiary sedimentary and volcanic rocks of the central Cascades, Washington–Application to the tectonic history of the Straight Creek fault: Geological Society of America Bulletin, v. 95, no. 1, p. 26-44.

Tolan, T. L.; Reidel, S. P.; Anderson, J. L.; Beeson, M. H.; Fecht, K. R.; Swanson, D. A., in press, Revisions to the areal extent and volume of the Columbia River Basalt Group. *In* Reidel, S. P.; Hooper, P. R., editors, Volcanism and Tectonism in the Columbia River Flood-basalt Province: Geological Society of America Special Paper 239.

Vance, J. A.; Clayton, G. A.; Mattinson, J. M.; Naeser, C. W., 1987, Early and Middle Cenozoic stratigraphy of the Mount Rainier-Tieton River area, southern Washington Cascades. *In* Schuster, J. E., editor, Selected Papers on the Geology of Washington: Washington Division of Geology and Earth Resources Bulletin 77, p. 269-290.

Walsh, T. J.; Korosec, M. A.; Phillips, W. M.; Logan, R. L.; Schasse, H. W., 1987, Geologic Map of Washington–Southwest quadrant: Washington Division of Geology and Earth Resources Geologic Map GM-34, 28 p., 2 pl., scale 1:250,000.

Waters, A. C., 1961, Stratigraphy and lithologic variations in the Columbia River basalt: American Journal of Science, v. 259, p. 583-611.

Road Log

The route covered by the road log is shown in Figure 7. Swanson and others (1979b) and Walsh and others (1987) provide geologic maps that include areas covered by this field guide. More detailed maps are available for parts of the areas described below: the western margin of the Columbia Plateau (Campbell, 1988); the Yakima area (Bentley and Campbell, 1983); the Saddle Mountains (Reidel, in press); out of date but useful color maps by Myers and others (1979) for the Pasco Basin and Grolier and Bingham (1971) for Franklin and Grant Counties. Bentley (1977), Campbell (1975), and Carson and others (1987) provide guides for portions of the Yakima Fold Belt.

Cumulative mileage is given on the left below; interval mileage is in parentheses.

Day 1: Columbia River Basalt Group Margin in the Naches River Drainage

Yakima to the Naches River area

0.0 Begin at Red Lion Inn parking lot. Turn right (north) on 1st Street. Stay in the right lane.

0.4 (0.4) Take U.S Highway 12 (west) turnoff toward Naches (sharp turn just beyond underpass). Proceed west on U.S. 12.

1.6 (1.2) 16th Avenue overpass.

1.7 to 2.5 (0.1) Cliffs on the right of the highway are in Columbia River Basalt Group (CRBG) and were exposed by breaching of the Yakima Ridge anticline by the Naches River. The bench above the river level marks the Vantage interbed. Grande Ronde Basalt (N_2 msu) flows below and Wanapum Basalt above the Vantage. The Pomona Member of the Saddle Mountains Basalt is exposed on the skyline (Fig. 3).

3.8 (1.3) The highway and Naches River cut diagonally through the Yakima Ridge anticline here. At 11 o'clock is the termination of the Tieton Andesite flow at Painted Rocks. (Direction notation in this guide uses a clock format.) The Tieton Andesite is a single flow that erupted from a volcano in the Goat Rocks area about 980,000 yr ago (Shannon & Wilson, Inc., 1973). Painted Rocks features numerous petroglyphs, restored for public viewing.

4.5 (0.7) Cross the Naches River at Twin Bridges. Cleman Mountain anticline is visible at 12 o'clock.

8.0 (3.5) Eschback Road intersection. Tieton Andesite forms cliffs at 9 o'clock. The flow traveled down the Tieton River canyon and filled the paleovalley of the Naches River just south of U.S. 12. The Naches River was forced to cut a new valley

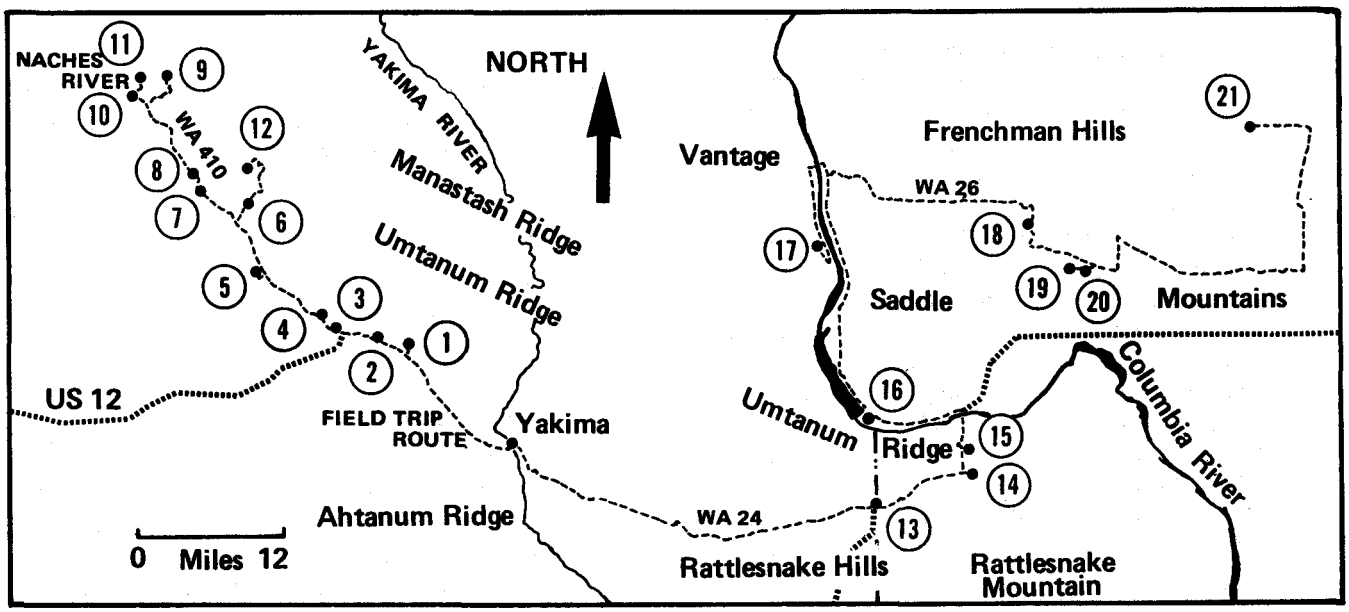

Figure 7. Fieldtrip route. Circled numbers locate trip stops. WA, Washington State Route (SR in text).

to the north. With a length exceeding 80 km, this flow may be the longest andesite flow in the world.

9.5 (1.5) Yakima Water Treatment Plant at 9 o'clock. The two interbeds exposed at 2 o'clock are the Selah and Vantage. Wanapum flows thin rapidly to the west in this area; at Cleman Mountain only one Wanapum flow remains.

10.8 (1.3) Cleman Mountain anticline at 12 o'clock. The type section of the Ellensburg Formation is exposed at 3 o'clock. Although Smith (1903) first described the Ellensburg Formation in the Kittitas Valley, the Naches section is the thickest known. About 366 m is exposed along these cliffs, and a nearby well penetrated 579 m of Ellensburg Formation before reaching basalt. There is nearly 1,930 m of structural relief between the Grande Ronde Basalt in the Naches syncline here and the Grande Ronde Basalt on top of the Cleman Mountain anticline.

12.3 (1.5) Turn right on Allan Road at Allan Brothers warehouse.

13.3 (1.0) Stop sign at Old Naches Highway. Continue straight ahead.

14.2 (0.9) **STOP 1. Upper Ellensburg Formation.**

Stop on the top of the Wenas Grade.

The Ellensburg Formation, described in detail by Schmincke (1964, 1967), Smith (1988a, b), and Smith and others (1988), shows a variety of volcanic-induced sedimentation units from the Cascade Range. Volcanic debris flows (lahars), hyperconcentrated flood flows, fluvial channel and overbank deposits, and paleosols are visible along the road (Fig. 8). Hornblende-dacite clasts plus air-fall and reworked ash and pumice dominate the section here. The material was deposited by volcanic events that choked streams (ancestral Naches River?) with fragmental debris. Ellensburg pyroclastics found in the Naches River watershed range in age from 13 to 7.4 Ma (Smith, 1988a). A single volcanic center may have deposited these rocks. Pyroclastic deposits can be traced nearly to a dacite intrusion dated at 8.8 Ma (Smith and others, 1988) thought to be part of an old volcano near Bumping Lake, 50 km to the west.

Return to U.S. 12 and continue west.

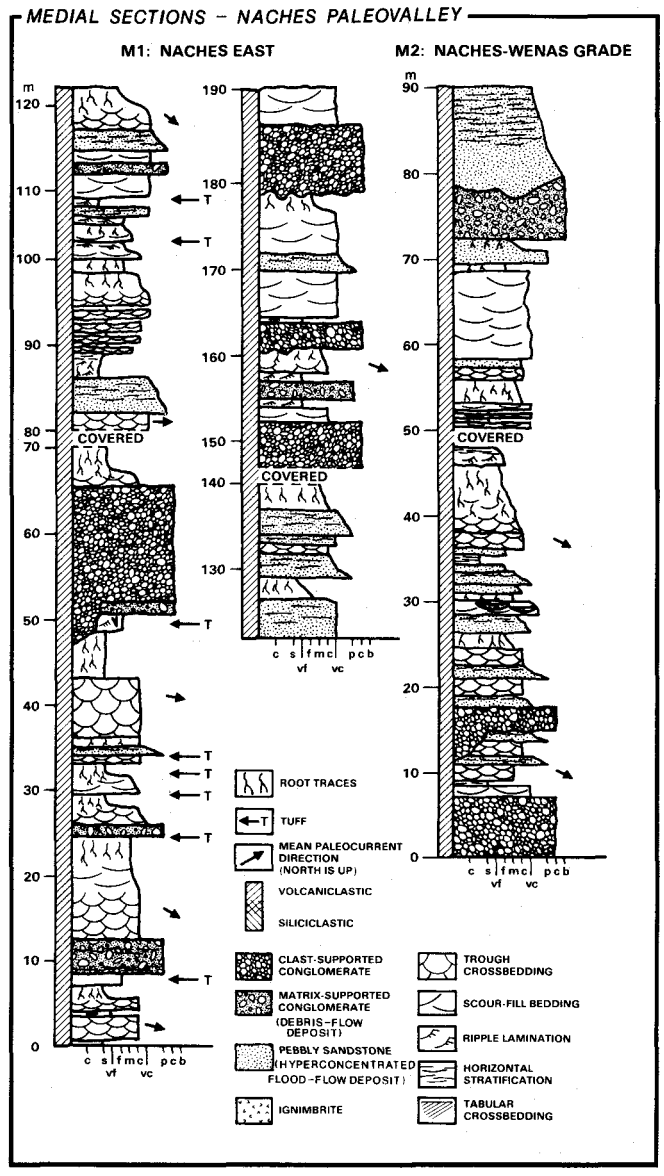

Figure 8. Ellensburg Formation stratigraphy from the type locality (from Smith and others, 1988).

17.2 (3.0) Entering Naches.

17.4 (0.2) Blinking yellow light. Continue west on U.S. 12.

18.0 (0.6) **STOP 2. Discussion of Cleman Mountain structure.**

Stop near Rose's Cafe, which is at 9 o'clock.

Cleman Mountain is not only the largest of the Yakima folds, it also has the greatest west structural closure measured on the top of the Grande Ronde Basalt, about 610 m. Cleman Mountain is unusual in other respects as well. A

folded thrust fault on its south limb places the Grande Ronde Basalt R_2 msu over the N_2 msu flows that form the steeply dipping rocks at 1 o'clock (Fig. 9). At 3 o'clock, the folded thrust may be overturned and displaced southward by a second thrust fault. Although a second thrust may exist just above road level, the folded thrust crosses U.S. 12 a few miles west of here. This large-scale fold and thrust of Cleman Mountain has deformed and perhaps covered part of the Naches syncline here (Fig. 9B).

Continue west on U.S. 12.

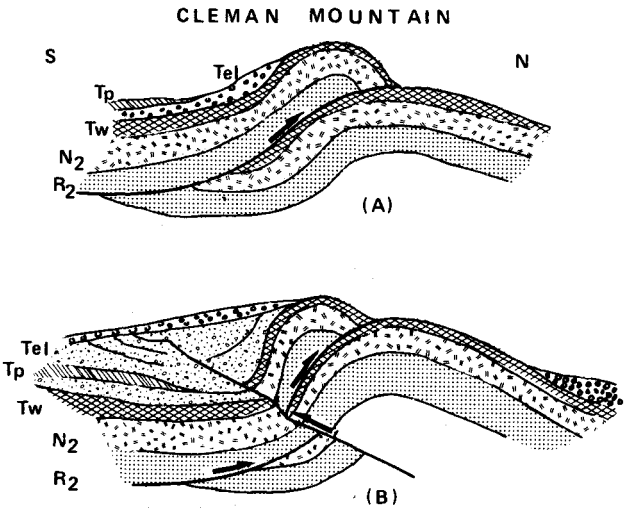

Figure 9. Generalized cross-sections of the Cleman Mountain structure (R. D. Bentley and N. P. Campbell, unpublished data). (A) is the interpreted structure at post-Wanapum time. (B) is the interpreted structure at post-Saddle Mountains time. Tel, Ellensburg Formation; Tp, Pomona Member; Tw, Wanapum Formation; N_2 and R_2, second normal and second reversed polarity intervals, respectively, of the Grande Ronde Basalt.

21.4 (3.4) Approaching the Chinook Pass-White Pass junction. Note steeply dipping, brecciated flows on the south limb of the Cleman Mountain fold at 3 o'clock.

21.8 (0.4) Junction of Highways U. S. 12 and Washington State Route (SR) 410. Proceed straight ahead on SR 410 toward Chinook Pass.

23.6 (1.8) **STOP 3. View of fault breccia and thrust fault.**

Turn right onto a small road and park.

Here the folded thrust seen at Stop 2 crosses SR 410. N_2 Grande Ronde basalt flows are exposed just west of this stop, whereas mostly sheared R_2 flows (?) crop out to the east. This is typical of many thrust faults in Columbia River basalt where the upper plate is highly brecciated and the overridden block is nearly undeformed. At 9 o'clock across the Naches River, N_2 Grande Ronde basalt flows, an interbed between the N_2 and R_2 basalt, R_2 basalt, and the trace of the thrust fault can be seen. This thrust fault presumably continues up the valley but has not been traced there to date.

Continue west on SR 410.

24.1 (0.5) Fault breccia associated with back thrust visible at 12 o'clock.

24.3 (0.2) **OPTIONAL STOP 4. Discussion of thrust fault and Sanford Pasture landslide.**

Turn off onto the wide shoulder and park.

The gray mass of breccia across the river at 9 o'clock is at the edge of an extremely large landslide known as the Sanford Pasture landslide. The breccia may be associated with the landslide, fault breccia transported by the landslide, or part of the Cleman Mountain folded thrust. Detailed mapping or trenching is needed to resolve this problem. The Sanford Pasture landslide continues upriver for more than 8 km.

Continue west on SR 410.

25.0 (0.7) Landslide debris at 3 o'clock in the roadcut. Grande Ronde Basalt in cliffs at 9 o'clock across the Naches River.

26.6 (1.6) Steeply dipping basalt in the Nile syncline (?) at 11 o'clock across the Naches River.

29.2 (2.6) Roadcut at 3 o'clock exposes pillows of Grande Ronde Basalt resting on a gravel interbed.

30.1 (0.9) Turn left (southeast) onto Rattlesnake Road.

30.3 (0.2) Cross the Naches River.

30.5 (0.2) N_2 flows at 9 o'clock.

30.9 (0.4) **STOP 5. View of Nile syncline and Cleman Mountain structure.**

Pull off along the road.

At 9 o'clock, the sediments in the Rattlesnake Creek section of the Ellensburg Formation near the axis of the Nile syncline (Fig. 5) are much coarser than those of the Naches section. Block- and ash-flow deposits, as well as rapid lateral clast-size changes, suggest that the source was only a few kilometers to the west.

Cleman Mountain anticline at 12 o'clock shows both steeply southwest-dipping N_2 Grande Ronde basalt flows and almost flat-lying R_2 basalt. The R_2 msu has probably moved southward as an in-place block, giving the false appearance of a tear fault.

The White River-Naches River fault zone parallels Cleman Mountain along this part of the river. This structure is thought to be a through-going cross-Cascade feature that follows the Naches River and has offset the basalt along the south flank of Cleman Mountain (Frizzell and others, 1984; Campbell, 1988). Figure 4 shows the relation of the White River-Naches River system to other structures along the margin of the Columbia River basalt. Both topographic and structural changes occur across this trend (Figs. 5 and 10).

Return to SR 410 and continue west.

32.1 (1.2) At 3 o'clock is a quarry in Columbia River basalt exposing a displaced segment of an interbed, probably at the R_2-N_2 Grande Ronde Basalt contact. This quarry is in the Sanford Pasture landslide.

33.0 (0.9) At 9 o'clock across the Naches River is a 244-m section of upper Ellensburg Formation volcanic debris-flow deposits, ash-flow tuffs, and fluvial gravels.

34.1 (1.1) Steeply dipping basalt flows at 12 o'clock mark the southwest limb of the Cleman Mountain anticline and the northeast limb of the Nile syncline.

35.7 (1.6) Nile Road turnoff at 9 o'clock.

35.8 (0.1) Slickensides and breccia in N_2 Grande Ronde Basalt at 3 o'clock mark the position of a thrust along the Cleman Mountain anticline. This fault does not appear to connect to the large

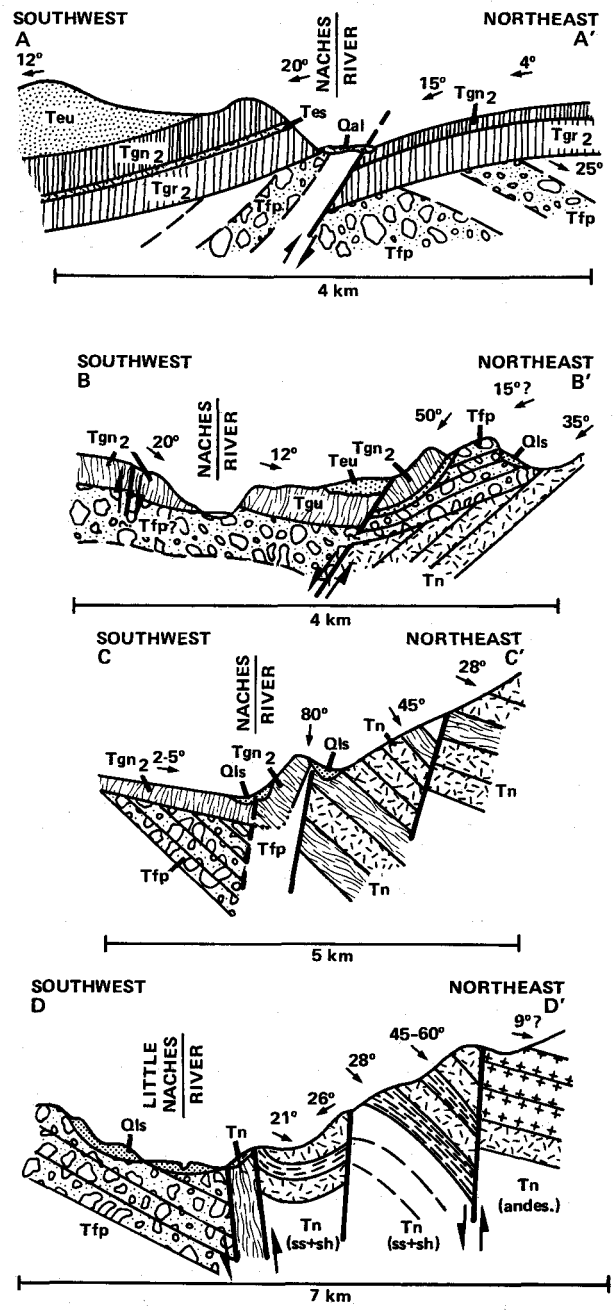

Figure 10. Diagrammatic sections across the Naches River-White River fault zone trend at selected locations along the Naches-Little Naches River canyon (not to scale; from Campbell, 1988). (A) at Rock Creek; (B) near Sawmill Flat; (C) at Longmire Meadow; and (D) west of profile (C) and beyond the margin of the Columbia River basalt. Tfp, Fifes Peak Formation; Tn, Naches Formation [ss, sandstone; sh, shale; andes., andesite]; Tel, Ellensburg Formation; N_2 and R_2, second normal and reversed polarity units, respectively, of the Grande Ronde Basalt; Qls, landslide. Arrows with numbers indicate dip angle.

folded thrust described at Stop 2 and may die out a few kilometers to the east.

36.6 (0.6) The stratigraphic section at 9 o'clock consists of both N_2 and R_2 Grande Ronde Basalt flows. These exposures are structurally high compared to the flows north of the road; offset occurs on a fault that parallels the road at this locality (Fig. 10, section a).

37.1 (0.5) Bald Mountain Road at 3 o'clock.

37.7 (0.6) **OPTIONAL STOP 6. Discussion of White River-Naches River fault zone.**

Fault breccia and slickensides in Columbia River basalt at 3 o'clock. This exposure is near the basalt margin. This fault is one of the few faults that can be found displacing basalt at the margin of the Columbia Plateau. The fault is thought to be part of the larger White River-Naches River fault zone and suggests that movement along this structure continued in post-basalt time. The fault here aligns with, and is related to the thrust described at trip mile 30.3. West of the basalt margin, the fault has been difficult to trace into the Fifes Peak Formation.

38.0 (0.3) Rock Creek turnoff at 3 o'clock. Up this road is a good view of the west-plunging Cleman structure; we will stop here late in the day when the light is best.

38.7 (0.7) Andesites, breccias, and tuffs of the Fifes Peak Formation are exposed here along cliffs at the sharp bend of the road.

39.2 (0.5) Across the river at 9 o'clock are steeply dipping volcanic rocks of the Edgar Rock volcano, a partly dissected cone of the Fifes Peak Formation (23-26 Ma). This is the southeast edge of the Edgar Rock volcano; the Naches River canyon cuts diagonally through the cone for the next 8 km. Fifes Peak rocks along this part of the Cascade Range are associated with these partly preserved volcanoes. Only rocks that are part of the Edgar Rock volcano will be seen on this field trip.

39.3 (0.1) Volcanic breccia and channel fill in Fifes Peak volcanics. The Edgar Rock volcano has both a cone facies (coarse breccias, andesite flows) and an apron facies (ash-flow tuffs and finer pyroclastics), but SR 410 exposes mainly cone facies.

39.6 (0.3) The Pond Restaurant at 3 o'clock.

40.4 (0.8) Passing through Forest Service work camp.

40.9 (0.5) Rocks at 3 o'clock for the next mile are altered volcanics of unknown age, possibly Fifes Peak Formation.

41.8 (0.9) Gold Creek Station and Cafe. This is the approximate center of the old Edgar Rock volcano, which probably exceeded 2,400 m in elevation.

42.0 (0.8) Edgar Rock at 12 o'clock is the northwestern flank of the old volcano.

42.7 (0.7) **STOP 7. Edgar Rock volcano and older(?) volcanic rocks.**

At 9 o'clock, Edgar Rock marks the highest remaining part of the Edgar Rock cone. At 3 o'clock the roadcut exposes sheared and altered older(?) rocks. Tuffs here gave a K-Ar age of 25.7 Ma (Neil Johnson, Shell Oil Company, oral commun., 1986) or in the age range of the Fifes Peak Formation, but the altered condition of the rock makes the date suspect. The shears and faults here are part of the White River-Naches River fault zone. Dips of more than 60 degrees in the rocks in the cone facies at Edgar Rock suggest tilting of the old cone due to faulting, but other evidence for faulting across this area has yet to be demonstrated.

Continue west on SR 410.

43.4 to 43.5 (0.7) **OPTIONAL STOP 8. Fifes Peak cone facies.**

Steeply dipping cone facies of the Fifes Peak Formation of the Edgar Rock volcano; we are now passing through the northwest edge of the old volcano.

44.0 (0.5) Entering Cliffdell.

45.0 (1.0) Old River Road at 9 o'clock.

45.1 (0.1) Columbia River basalt in cliffs along the road at 3 o'clock. Columbia River basalt flowed around the old Edgar Rock cone and continued up a paleodrainage that parallels the present Little Naches River.

47.7 (2.6) Milk Creek Road at 3 o'clock.

48.2 (0.5) Approaching the Little Naches Road. Prepare to exit SR 410.

52.4 (4.2) Right turn on U.S. Forest Service Road (FSR) 19, Little Naches River Road.

53.0 (0.6) We are now traveling westward on Columbia River basalt along Little Naches River syncline. There are four or five N_2 Grande Ronde basalt flows and one R_2 flow exposed. The White River-Naches River fault zone is north of the highway along the north limb of the syncline.

54.3 (1.3) FSR 1901 at 3 o'clock. Turn right and proceed to Optional Stop 9.

56.5 (2.2) Junction with FSR 1903; continue on FSR 1901.

57.2 (0.7) Beginning of exposures of Naches Formation in the roadcut at 3 o'clock.

57.4 (0.2) Kaner Flat Trail at 3 o'clock.

58.5 (1.1) Naches Formation at 3 o'clock.

58.6 (0.1) Rhyolite dome in the Naches Formation at 11 o'clock.

58.7 (0.1) FSR 1901-726 junction; stay left.

60.7 (2.0) Quartz Creek Trail, FSR 1916. Bear left downgrade.

60.8 to 61.5 (0.1) Section in the Naches Formation.

61.6 (0.1) **OPTIONAL STOP 9. Naches Formation and southern splay of Straight Creek fault.**

The Naches Formation has several different facies and probably should be subdivided into members. Several rhyolite dome-like masses are present in the Little Naches River drainage. The section exposed south of the fault contains both basalt flows and fluvial clastics. The fault observed here is the southernmost splay of the Straight Creek fault (Fig. 4), and it forms the south boundary of the Cabin Creek block of Tabor and others (1984).

Return to the main FSR 19 and continue west.

69.8 (8.2) FSR 1902 to Ravens Roost at 9 o'clock.

70.0 (0.2) Crossing Quartz Creek.

70.8 (0.8) Crossing the Little Naches River. Rapids are in N_2 Grande Ronde Basalt.

71.5 (0.7) FSR 750 at 3 o'clock. Turn right onto FSR 750 for Stops 10 and 11.

71.8 (0.3) At 9 o'clock N_2 Grande Ronde Basalt flows.

72.5 (0.7) **STOP 10. White River structure.**

Columbia River basalt flows are nearly vertical along the north edge of the Little Naches River syncline (Fig. 11). The main White River fault of Frizzell and others (1984) passes just to the north and may have as much as 1,000 m of north-side-up throw (Fig. 10, section D, and Fig. 11). No evidence for strike-slip movement is known from anywhere along the White River-Naches River structure. The main fault is not exposed, but small shears probably associated with it cut the basalt.

Continue on FSR 750 for Stop 11.

73.6 to 74.4 (1.1) Naches Formation in roadcuts.

74.5 (0.1) **STOP 11. Sandstone facies of the Naches Formation.**

The stratigraphy of the Naches Formation is not well known. It is possible that the thickness (1,500 to 3,000 m, Tabor and others, 1984) of the Naches is much less than published estimates due to stratigraphic duplication by faulting.

Return to FSR 19.

76.5 (2.0) Junction of FSR 750 and 19. Turn east onto FSR 19 (Little Naches Highway).

81.0 (4.5) Junction of FSR 19 and SR 410. Turn left onto SR 410.

91.4 (10.4) Turn north onto Rock Creek Road (FSR 1702/625) for Stop 12.

91.5 to 94.5 (0.1) We are traveling along Fifes Peak Formation at the margin of the Columbia River basalt.

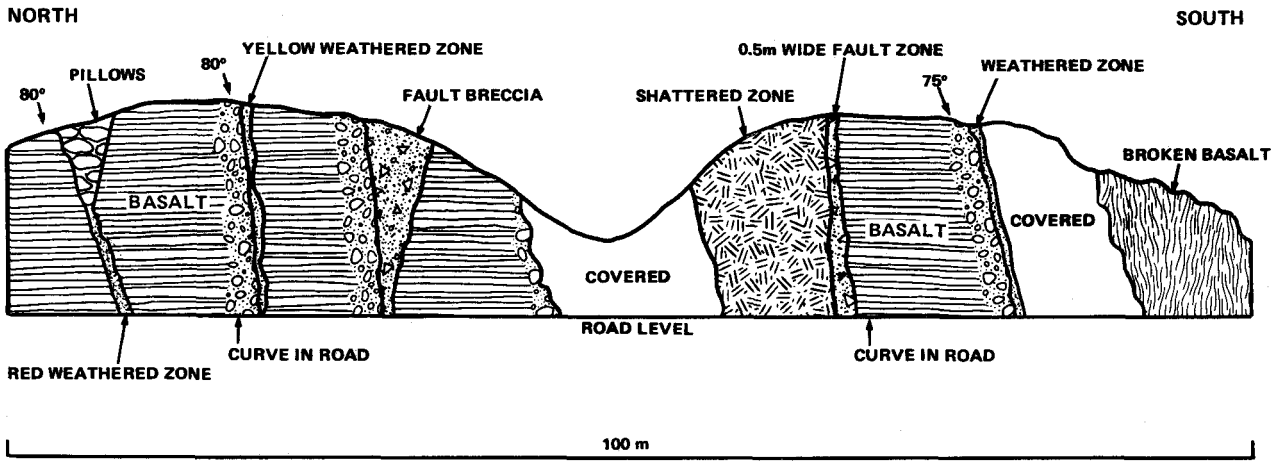

Figure 11. Sketch of near-vertical Columbia River basalt at Longmire Meadow, Little Naches River (from Campbell, 1988).

95.2 (0.7) Junction with FSR 1720; bear left on FSR 1702.

97.2 (2.0) Junction with FSR 1721; bear left to FSR 1721.

98.4 (1.2) Good exposures of Fifes Peak Formation for the next mile.

99.8 (1.4) Unmarked road junction; bear left on the lower road.

100.9 (1.1) Junction of FSR 1721 and 559; bear left on FSR 559.

102.1 (1.2) Bear right on the upper logging road.

102.3 (0.2) **STOP 12. Cleman Mountain anticline.** End of the road; park.

It is best to view this stop in the late afternoon. This stop provides an excellent view of the west-plunging Cleman Mountain anticline, the basalt margin, and the underlying Fifes Peak Formation. The Cleman anticline is typical of most Yakima folds in that the fold dies out before reaching the basalt margin. Clearly, pre-basalt structures here do not align with those in the Columbia River basalt (Campbell, 1988). Columbia River basalt is offset at the Little Naches River where the plateau margin is offset along the Naches River-White River fault zone.

Return to SR 410 and drive back to Yakima.

Day 2: Yakima Fold Belt, Columbia Plateau

Yakima to Spokane

0.0 Leave Red Lion Motel in Yakima. *Reset odometer.* Turn right on 1st Street and take Interstate Highway 82 southbound.

3.7 (3.7) Take exit 34 to Moxee. Turn left (east) on SR 24.

6.2 (2.5) Konnowock Pass in the Rattlesnake Hills anticline at 2 o'clock. This is an ancestral (late Miocene) water gap of the Yakima River through the Rattlesnake Hills (Smith, 1988).

23.4 (17.2) Mile marker 19. Road narrows.

26.0 (2.6) Approximate crest of the Hog Ranch-Naneum Ridge anticline (Fig. 2). The structural relief of the anticline exposed at the surface progressively decreases south from where it enters the Columbia Plateau near Wenatchee. The prominent ridge at 12 o'clock is the part of the Rattlesnake Hills anticline that extends northeast of the main trend.

35.2 (9.2) **STOP 13. Discussion of the western Pasco Basin.**

Pull into the parking lot of the Silver Dollar Cafe.

The Hog Ranch-Naneum Ridge anticline marks the western boundary of the Pasco Basin (Fig. 2). From the western boundary of the basin, the Yakima folds plunge gently eastward toward

the Palouse paleoslope. The structure of this area is complex because the CLEW trends across the area. To the north, Yakima Ridge trends northwest and is part of the CLEW, but the Rattlesnake Hills anticline to the south trends east-west and is separate from this zone. The Rattlesnake Hills display the typical geometry of a Yakima fold, whereas this part of Yakima Ridge is a series of en echelon folds superimposed on the main trend.

The first deep hydrocarbon exploration well, RSH-1 (Fig.4), was drilled in the 1950s on the Rattlesnake Hills east of here to a depth of 10,660 ft and was still in Columbia River basalt (Reidel and others, 1982).

35.5 (0.3) Benton County line. Pomona Member (Fig. 3) exposed on the left. The hill crest ahead is one of the en echelon anticlines that make up this segment of the Yakima Ridge anticline.

37.6 (2.1) Crest of another en echelon anticline on Yakima Ridge. Sediments of the Rattlesnake Ridge interbed at 3 o'clock. The Rattlesnake Ridge interbed is the packet of sediments of the Ellensburg Formation between the Pomona (12 Ma) and Elephant Mountain (10.5 Ma) Members (Fig. 3). The white layer is ash.

37.8 (0.2) The Saddle Mountains form the prominent ridge to the north; Gable Mountain is to the east. The highest point visible on the Saddle Mountains is Wahatis Peak, a channel fill of basalt of the Asotin Member (Reidel and Fecht, 1986).

40.3 (2.5) Cold Creek Road at 9 o'clock. Vineyards of Chateau Ste. Michelle on the left.

40.5 (0.2) Touchet beds along both sides of the road.

43.4 (2.9) **STOP 14. Central Pasco Basin.**

Junction of SR 24 and SR 240. The barricade at 12 o'clock is one of the entrances to the U.S. Department of Energy's Hanford Site. Proceed to the parking area before the guard station.

From here the eastward plunge of the Yakima folds is very apparent. In the distance only Gable Butte and Gable Mountain of the Umtanum Ridge anticline protrude above the sediment-filled basin (Fig. 2). A buried ridge east of Gable Mountain, called the Southeast anticline, marks the eastward termination of the Umtanum Ridge structural trend. Gable Mountain and Gable Butte are second-order en echelon anticlines developed on the Umtanum anticline (Fecht, 1978). The Yakima Ridge anticline also plunges southeast and is buried by sediments of the Ringold Formation and Hanford formation. To the south is the intersection of the east-trending Rattlesnake Hills and northwest-trending Rattlesnake Mountain. Both anticlines appear to terminate at this intersection. On the north side of Rattlesnake Mountain is the old Rattlesnake Hills gas field.

43.6 (0.2) Return to the main highway; turn right on SR 24. The road follows the Cold Creek bar, which contains multiple flood deposits from cataclysmic flood waters during the Pleistocene.

45.4 (1.8) **OPTIONAL STOP 15. Northern Pasco Basin.**

Pull over at the curve in the road near the top of the hill at Hanford Gate 122A.

The crest of this hill also marks the crest of Umtanum Ridge (Fig. 2), which is plunging to the east. The prominent basalt flow that we are on is the Pomona flow.

This stop provides a view of the northern part of the Pasco Basin. At 12 o'clock is the Sentinel Gap segment of the Saddle Mountains, at 2 o'clock is the Smyrna Bench segment. The geometry of the Saddle Mountains anticline changes here from an open fold in the Sentinel Gap segment to a box fold in the Smyrna Bench segment. Farther east in the Saddle Gap segment, the fold geometry is that of an open fold. At about 12 o'clock on the crest of the Saddle Mountains is the site where Shell and ARCO drilled the BN 1-9 wildcat well (Fig. 4). This well penetrated about 11,500 ft of basalt and bottomed (at more than 17,000 ft) in the Chumstick Formation of Eocene age (Campbell, in press). The well had subcommercial gas shows.

46.1 (0.7) Quarry in the Umatilla Member, Saddle Mountains Basalt, at 3 o'clock.

47.2 (1.1) Midway Road at 9 o'clock. From the bottom of the hill the road is on flood gravels of the Hanford formation. At 3 o'clock is Gable Butte, an en echelon anticline along the Umtanum Ridge structural trend that has been breached by Pleistocene catastrophic flood waters.

48.4 (1.2) Rest area.

48.6 (0.2) Return to the main road.

48.9 (0.3) Cross the Columbia River.

49.4 (0.5) Turn left on SR 243 toward Vantage.

50.6 (1.2) At 10 o'clock is a large landslide on Umtanum Ridge above the town of Midway; at about 12 o'clock is the large McCoy Canyon slide block.

53.2 (2.6) Road O-SW. Note the change from the north-dipping basalt flows along the north limb of Umtanum Ridge to overturned, south-dipping basalt flows farther west (at 12 o'clock).

54.2 (1.0) Type locality for the Umtanum flow, Grande Ronde Basalt at 3 o'clock. The Umtanum flow is the uppermost low-Mg flow, N_2 msu of the Grande Ronde Basalt in the area. It has a TiO_2 content (~2.3 wt %) that makes it fairly distinct and an important marker flow.

55.2 (1.0) Gravel pit in the Hanford formation.

58.2 (3.0) Turn left at Priest Rapids Dam Road.

59.6 (1.4) Where the main road bends to the right, continue straight on the asphalt/gravel road to the area below the dam. Stop at the river overlook.

59.9 (0.3) **STOP 16. Umtanum Ridge.**

Umtanum Ridge extends about 100 km from near the western margin of the Columbia Plateau to the Palouse paleoslope. The structural relief gradually decreases eastward to Gable Butte, where it becomes a series of en echelon anticlines. In the Priest Rapids Dam area the north limb is overturned and dips 40 degrees to the south. An upper fault, the Buck thrust, and a lower fault, the Umtanum fault, define the overturned flows of the fold (Price, 1982). The Buck thrust dies out to both the east and west, but the Umtanum fault has been inferred to extend from the western edge of the anticline to just east of Midway. Drilling has constrained the angle of the Umtanum fault in the near surface to between 30 and 60 degrees.

61.7 (1.8) Return to SR 243 and continue north (left). Glacial erratics left by catastrophic flood waters occur along the road side for the next mile.

63.0 (1.3) Desert Aire Resort. Pomona Member at 3 o'clock.

63.4 (0.4) At 9 o'clock north of Umtanum Ridge, an interbed of the Ellensburg Formation forms the white exposures (ash) across the Columbia River. The basalt flows in this area have been folded into a series of low-amplitude, east-trending anticlines and synclines.

64.3 (0.9) Sentinel Gap at 11 o'clock. Sentinel Gap is a water gap through the Saddle Mountains. Intracanyon flows and mainstream facies sediments indicate that the Columbia River flowed through this water gap from at least the middle to late Miocene (Reidel, 1984).

65.8 (1.5) Glacial erratics at 9 o'clock. Across the river is the Hanson Creek anticline (Fig. 2).

67.1 (1.3) Mattawa turnoff. At 10 o'clock on the west side of the river is the Huntzinger flow, a 13 Ma flow that filled an ancestral channel of the Columbia River (Reidel and Fecht, 1986).

67.7 (0.6) Glacial erratics form a boulder train from the Sentinel Gap area.

69.1 (1.4) At 2 o'clock in the quarry are exposures of the type locality of the Beverly interbed (Swanson and others, 1979a). The Elephant Mountain Member lies above, and the Priest Rapids Member below the interbed. Just east of the quarry, the Pomona is invasive into the Beverly interbed (Schmincke, 1967). This area is also the type locality for the Saddle Mountains Basalt (Swanson and others, 1979a).

70.9 (1.8) Entering Sentinel Gap.

71.1 (0.2) Cohassett flow, Grande Ronde Basalt, in roadcuts. The internal vesicle zone of the flow is exposed along the road (McMillian and others, 1987).

71.3 (0.2) Sentinel Gap, Saddle Mountains. This is Site 6 of Carson and others (1987).

72.1 (0.8) Flow top of the Umtanum flow, Grande Ronde Basalt, at 3 o'clock. The entablature is at 10 o'clock near the river level.

72.9 (0.8) Crab Creek. Saddle Mountains fault is inferred to pass through this area (Reidel, 1984, in press).

74.4 (1.5) Crab Creek Road at 3 o'clock.

75.2 (0.8) Beverly-Burke Road at 3 o'clock.

77.6 (2.4) Wanapum Dam turnout. The exposures of the Priest Rapids, Roza, and Frenchman Springs Members along the Columbia River near here (Mackin, 1961) form the type locality for the Wanapum Basalt (Swanson and others, 1979a). The Rosalia flow of the Priest Rapids Member is at 3 o'clock.

77.9 (0.3) Frenchman Springs Member at road level.

79.1 (1.2) Roza Member at 1 o'clock.

81.8 (2.7) Stop sign. Turn left on SR 26. Prepare to enter Interstate Highway 90 (I-90) westbound. At 12 o'clock from bottom to top on the cliff are the Ginkgo, Sand Hollow, and Sentinel Gap flows of the Frenchman Springs Member.

82.7 (0.9) Take the Seattle entrance on I-90.

84.7 (2.0) Take Exit 136 to Vantage.

85.0 (0.3) Turn right on Huntzinger Road. The white sediment is ash of the May 18, 1980, Mount St. Helens eruption. The basalt flows along the road for the next 2 mi are the Frenchman Springs Member.

87.9 (2.9) Wanapum State Park at 9 o'clock.

88.5 (0.6) Exposed from 15 to 30 m above the road at 3 o'clock is a south-dipping, northwest-striking thrust fault. In the creek and along the roadcuts is a series of thin (1-2-cm thick) breccia zones that parallel the fault (Fig. 2).

90.3 (1.8) Wanapum Dam abutment.

90.8 (0.5) The road climbs through the Frenchman Springs, Roza, and Priest Rapids members of Wanapum Basalt.

92.3 (1.5) Old railroad track crossing, now known as the John Wayne Trail.

92.4 (0.1) **STOP 17. The Saddle Mountains fault zone and core of the anticline.**

Turn right on the gravel road toward Doris and stop. Because it would take about 4 hours to walk through the entire exposure, we will examine it in two parts. For the first part (Fig. 12, area 1) we will observe one of the few places where the core of the Saddle Mountains anticline is well exposed. For the second part (Fig. 12, area 2) we will see the Saddle Mountains thrust fault.

Part 1. Deformation in the core of the Saddle Mountains anticline.

From the road walk due west toward the hummocky lower slope of the Saddle Mountains.

The Columbia River has exposed a zone of complex folding and faulting in the core of the Saddle Mountains anticline. Above the main fault, the Saddle Mountains fault, is an upper fault that does not penetrate the upper layers of basalt. The basalt flows between the two faults (the hummocky exposures) are vertical and strike west. The flows are shattered and brecciated, but their chemical compositions permit identification of the individual flows. The Cohassett and Umtanum flows are part of this group of flows. Above the upper fault, the flows are relatively intact but folded. The upper fault has about 100 m of offset measured on the Umtanum flow. Total shortening across this part of the Saddle Mountains anticline is about 3 km.

To reach Part 2, one can either walk north up through the stratigraphic section or return to the parking area and take the gravel road north.

93.0 (0.6) Follow the gravel road north to the quarry in Hanford formation gavels and then take the left fork.

93.4 (0.4) **Part 2.** The Saddle Mountains fault.

Drive up to the fence line and park by the gate.

The Saddle Mountains fault is covered along most of its length, but at this locality Wanapum Basalt is thrust northward over the Ringold Formation. The basalt flows are steeply north dipping to vertical south of the fault, and the Ringold sediments are nearly horizontal north of it. The youngest faulting here is older than the youngest catastrophic flooding (13,000 yr) because apparently undisturbed Hanford formation gravels overlie the fault.

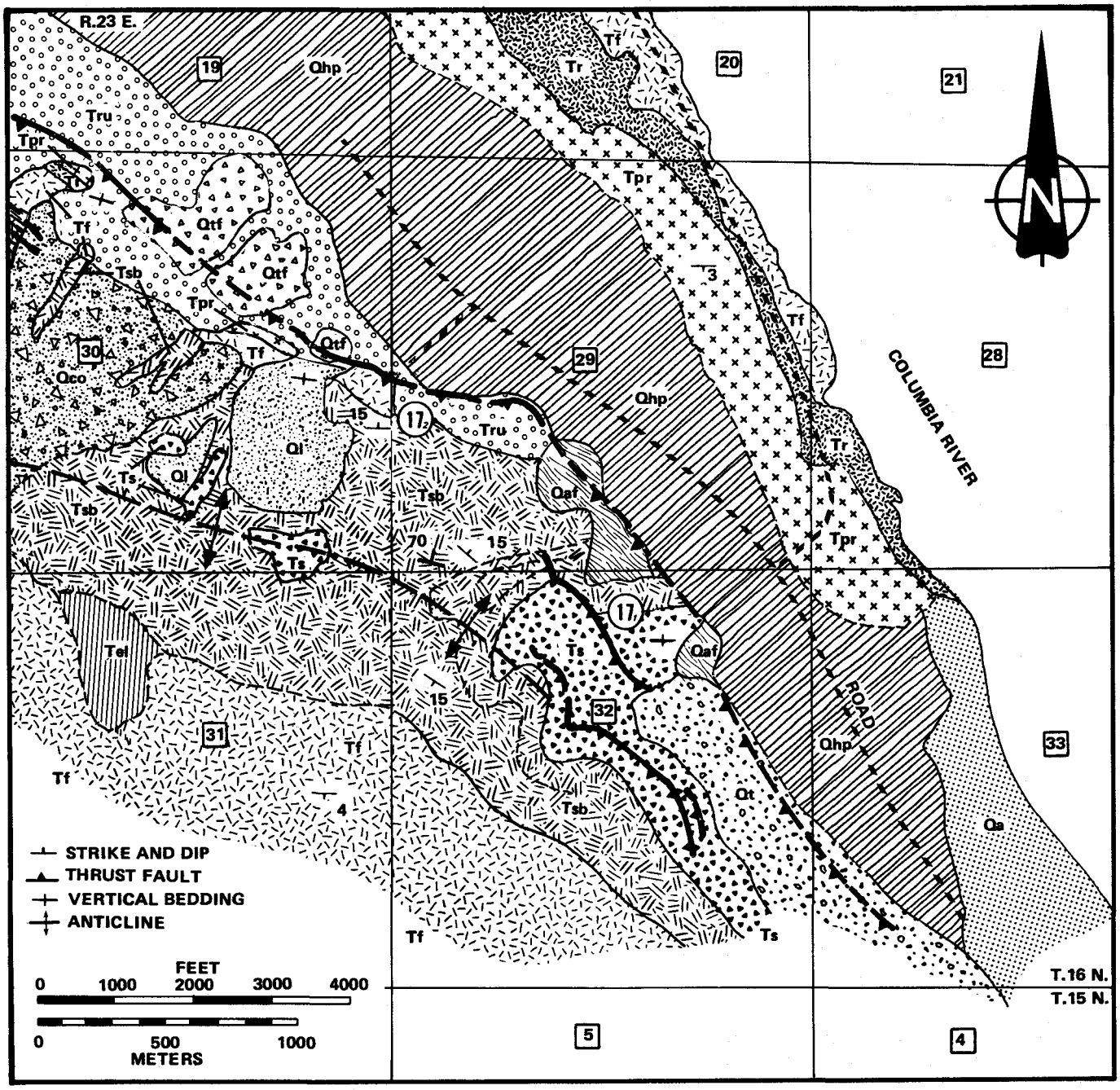

Figure 12. Geologic map of the west side of Sentinel Gap, Saddle Mountains (from Reidel, in press). The area covered by Part 1 of Stop 17 is indicated by 17_1 and Part 2 is indicated by 17_2. See Figure 3 for explanation of stratigraphic unit symbols. Numbers in squares refer to sections.

93.8 (0.4) Return to the quarry.

94.3 (0.5) Return to Huntzinger Road and retrace the route to I-90.

101.0 (6.7) Enter I-90 and proceed east toward Spokane.

103.2 (2.2) Exit I-90 onto SR 26 and proceed east toward Colfax and Pullman.

104.6 (1.4) Pillow complex of Ginkgo flow, Frenchman Springs Member. This is a classic locality to examine pillow complexes and has been described in several field guides (for example, Site 5 of Carson and others, 1987). This

pillow complex is composed of foreset beds of basalt that built out into a lake that had developed during Vantage time. Some of the best fossilized wood in Washington has come from this zone.

110.4 (5.8) Beverly-Burke Road. The route now heads east, parallel to the Saddle Mountains anticline. Note some of the smaller scale folds along the north face.

119.1 (8.7) Caliche horizon in the Ringold Formation.

121.2 (2.1) Royal City turnoff.

122.8 (1.6) Road E-SW, Brown's Corner. Turn right to Smyrna.

123.0 (0.2) Cross railroad tracks.

123.1 (0.1) **OPTIONAL STOP 18. View of Smyrna Bench.**

At 12 o'clock are dissected alluvial fans collectively known as Smyrna Bench. Smyrna Bench consists of several alluvial fans that developed as the Smyrna Bench segment of the Saddle Mountains anticline grew and was simultaneously eroded. Flood waters from the Pleistocene catastrophic floods removed much of the fan from Crab Creek coulee, which parallels the north side of the Saddle Mountains. Several trenches have been dug on Smyrna Bench in the past two decades to determine the youngest age of faulting (for example Bingham and others, 1970). Evidence to date suggests the youngest faulting is older then the most recent catastrophic flooding (13,000 yr).

123.4 (0.3) Descend into Crab Creek coulee. Basalt of the Elephant Mountain Member is exposed along roadcuts.

125.5 (1.1) Pomona Member outcrop at 8 o'clock. This is the easternmost exposure of the Pomona north of the Saddle Mountains.

126.9 (1.4) Turn left on Crab Creek Road. Cross the railroad tracks. Elephant Mountain Member and Ringold Formation at 3 o'clock.

130.3 (3.9) Roadcuts through the Elephant Mountain Member. Leaving Crab Creek coulee.

130.5 (0.2) CAUTION! Very rough cattle guard crossing.

130.8 (0.3) Top of the Elephant Mountain Member; Ringold Formation ahead and to the right. The Corfu landslide can be seen at 1 o'clock. The Corfu landslide resulted when catastrophic flood waters removed the north-dipping basalt along the Saddle Mountains, allowing the remaining basalt to slide on the interbed above the Priest Rapids Member.

132.1 (1.3) Turn right onto Smyrna Bench Road (gravel road).

132.3 (0.2) Cross the railroad tracks. On the right, the Asotin and Pomona Members form a small anticline with a thrust fault along the north side.

132.9 (0.6) View of the east side of Smyrna Bench. We will stop here on our return route.

133.6 (0.7) Road triple junction; bear left and then right (east) and stop at the top of the hill.

133.95 (0.35) **STOP 19. Smyrna Bench "graben".**

This low depression on Smyrna Bench in front of the Saddle Mountains (Fig. 13) has had many interpretations over the past several decades. (See Bingham and others, 1970.) The interpretations receiving the most attention are: (1) the depression is a graben that developed along with the Saddle Mountains anticline, and (2) the depression resulted from gravity sliding of Ringold sediments away from the Saddle Mountains after the catastrophic flood waters removed the northern part of Smyrna Bench. A structural origin is currently favored. Mapping by Reidel (in press) has shown that part of the "graben" is confined to the Saddle Mountains basalt flows and thick intercalated sediments of the Ellensburg Formation. Steep, north-dipping to overturned flows probably were extended during folding, allowing the "graben" to form as basalt flows slid along interbedded sediments. One of the most important questions is: How young is the movement? Evidence from recent trenching by Michael West and Associates suggests that there may be young scarps of unknown age but, unfortunately, the evidence is not conclusive.

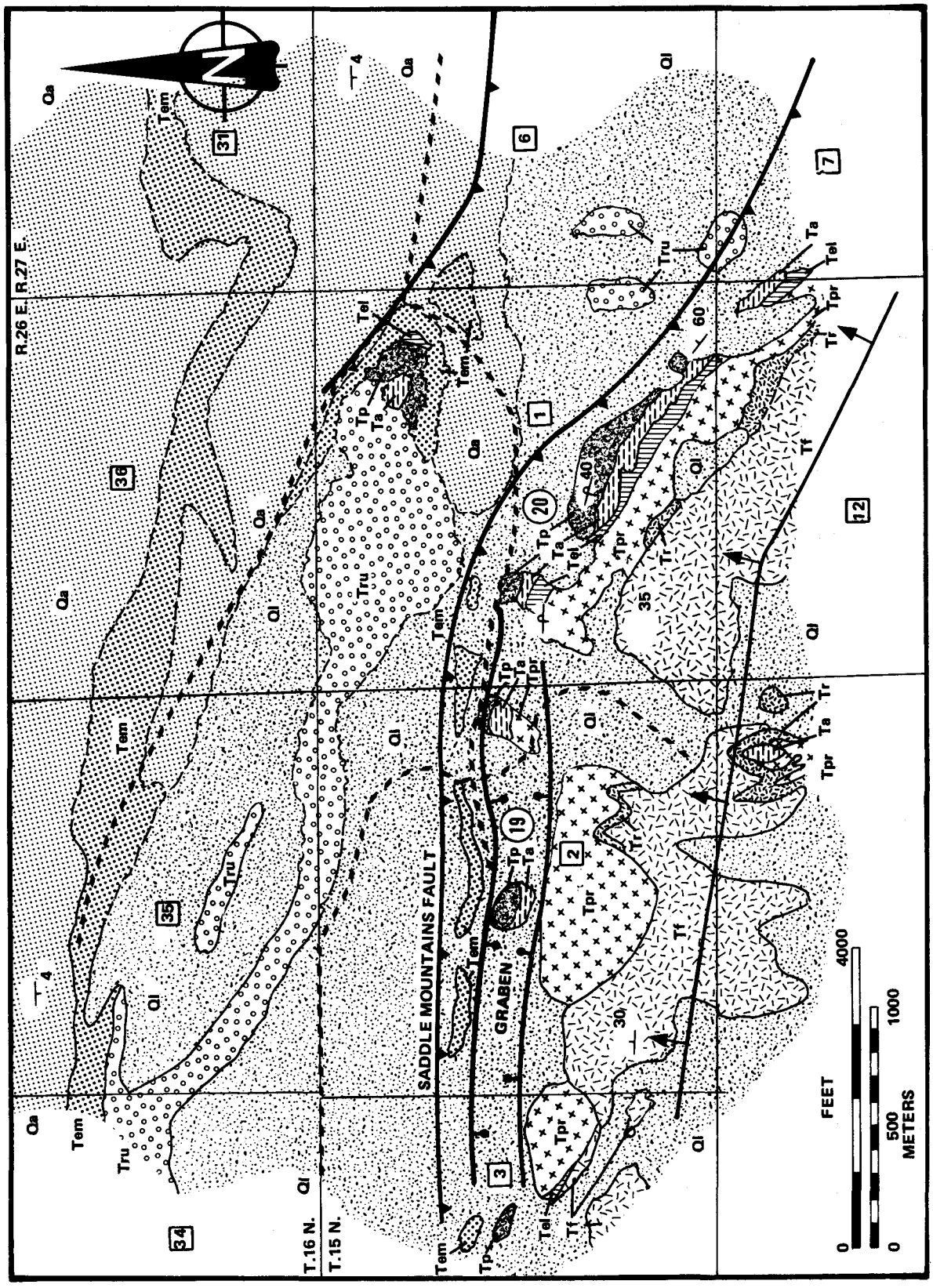

Figure 13. Geologic map of the west side of the Smyrna Bench area, Saddle Mountains. Shown are the location of the Smyrna Bench graben (Stop 19) and the junction between the Smyrna Bench and Saddle Gap segments (Stop 20) (from Reidel, in press). See Figure 3 for explanation of stratigraphic unit symbols and Figure 12 for explanation of structure and other symbols.

134.0 (0.05) Continue down the hill and turn around by the corral. Return by the same route to the road triple junction. We are at trip mile 134.5.

135.1 (1.1) **STOP 20. East side of Smyrna Bench.**

The east side of Smyrna Bench is geologically complex (Fig. 13). It marks the junction of two distinct segments, the Smyrna Bench segment on the west and the Saddle Gap segment on the east. The Saddle Mountains shows some of the most dramatic changes in geometry and style of folding across this segment boundary. The structure changes from a box fold with overturned beds that strike west in the Smyrna Bench segment to northeast-dipping and northwest-striking flows. Minor structures such as kink folds and small faults are well exposed in this area. We will examine both the large- and small-scale structures by walking about 2 km through the area where the two segments intersect.

135.9 (0.8) Return to Crab Creek Road. Turn right.

137.8 (1.9) Road B-SE, the Corfu Road. Turn left and proceed to SR 26. At 1 o'clock note the dipping basalt just above the road level. At this locality the Pomona Member has 25 degrees of clockwise rotation recorded by its magnetic declination (Reidel and others, 1984).

140.3 (2.5) Flood bar.

140.8 (0.5) SR 26. Turn right toward Othello. Corfu landslide at 2 o'clock.

145.6 (4.8) Adams County line.

155.3 (9.7) Junction with SR 240.

157.3 (2.0) Turn left on SR 17.

158.3 (1.0) Othello turnoff. Cunningham Road.

163.3 (5.0) Railroad underpass.

169.0 (5.7) Warden Road.

170.0 (1.0) Turn left on Potholes State Park Road and toward O'Sullivan Dam.

174.2 (4.2) Road M-SE. A Roza flow in the roadcuts.

174.6 (0.4) Turn right onto the dirt road that leads toward Lind Coulee.

174.7 (0.1) **OPTIONAL STOP 21. Lind Coulee fault.**

Grolier and Bingham (1971) mapped a reverse fault along the north side of the Frenchman Hills in Lind Coulee (Fig. 14). Their mapping shows that the fault cuts sediments that overlie the Roza Member in several places. Recent studies by Michael West and Associates for the Bureau of Reclamation show that Pleistocene loess is faulted and that still younger loess and flood deposits overlying the basalt are unfaulted. Although their study was not available at the time of the writing of this guidebook, it appears that movement occurred on the fault during the Pleistocene but that the latest movement is older than the most recent catastrophic floods. Loess that overlies the fault and is younger than the last fault movement is similar to loess dated at about 500,000 yr by Rockwell Hanford Operations (unpub. data) using paleomagnetic techniques. Although the trenches that Michael West and Associates dug are now filled in, there are several excellent exposures (A and B, Fig. 14) where the relations between faults and the overlying sediments can be seen.

Retrace the route to SR 17.

179.4 (4.7) SR 17. Turn left on SR 17 and proceed to Moses Lake. I-90 passes through Moses Lake and provides the most direct route to Spokane.

End of Road Log.

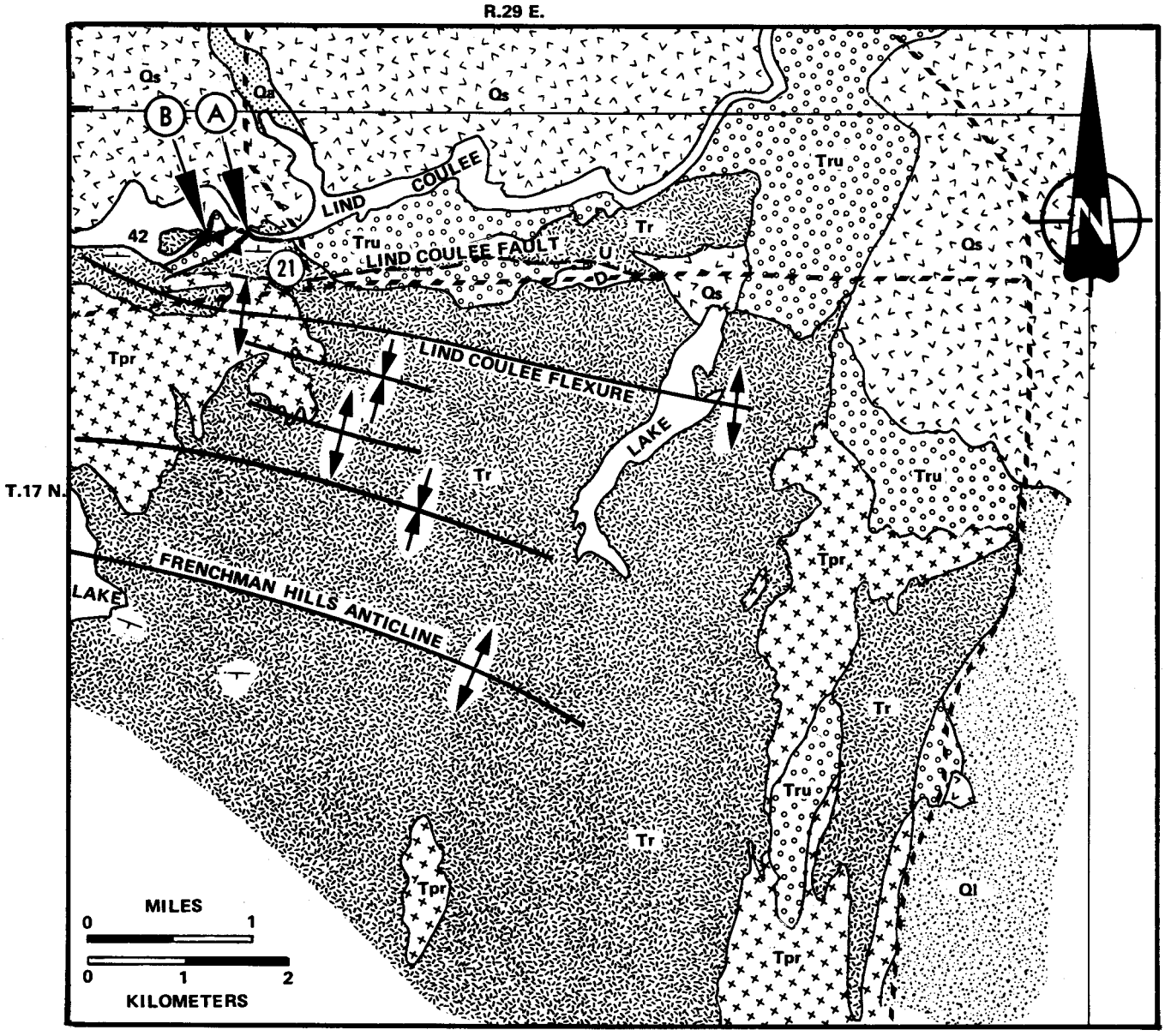

Figure 14. Geologic map of the area near Stop 21, the Frenchman Hills anticline and the Lind Coulee fault (from Grolier and Bingham, 1971). See Figure 3 for explanation of stratigraphic unit symbols and Figure 12 for explanation of structural and other symbols. Locations of good exposures of faults are shown by arrows; A is a northeast-facing exposure on the south side of Lind Coulee, and B is a northwest-facing exposure along the lake.

The Channeled Scabland: Lake Missoula Floods and Sediments and Loess Stratigraphy

Eugene P. Kiver, Dale F. Stradling, Roy M. Breckenridge, Eric McDonald, and Alan J. Busacca

Lake Missoula Floods and the Channeled Scabland

Eugene P. Kiver
Department of Geology
Eastern Washington University
Cheney, WA 99004

This sequence of three field trips provides an overview of the largest known catastrophic flooding events in the world. The introductory texts detail some of the research currently being pursued on features produced by the flood(s), processes operating during their formation, and chronology of flood events. The remarkable insights of J Harlen Bretz were presented in a series of papers beginning in 1923 that, decades later, led to the worldwide acceptance of his controversial hypothesis: that enormous amounts of water swept across eastern Washington and produced the landscape now known as the Channeled Scabland. Although most of the landforms and sedimentologic features on the Columbia Plateau do not prove the catastrophic flood hypothesis by themseves, when taken in total they overwhelmingly support the concept that thousands of cubic kilometers of water from an ice-dammed lake repeatedly ripped across eastern Washington in a matter of a few days, eroding a complex of channels through the thick loess blanket and into the underlying layers of flood basalt. Erosion by hydraulic vortexes (Baker and Nummedal, 1978) (also known as "underwater tornadoes") and other hydraulic processes on the well-jointed basalt produced a distinct topography of buttes, basins, dry falls, hanging valleys, bars, and giant current dunes.

Trip A provides a brief introduction to the glacial and flood histories of the area. The accompanying text (Breckenridge, this volume) offers a short review of pertinent literature. Recognition of Lake Missoula as the source of the floodwater and the ice dam failure mechanics are discussed in both the introduction and road log narrative. The fieldtrip route begins in Spokane, covers the area north to Pend Oreille Lake along the east side of the Purcell Trench, and then returns to Spokane along the west side of the trench.

Trip B (Kiver, Stradling, and Moody, this volume) follows the floodwater path out of the Spokane River valley and westward across the Channeled Scabland and loess uplands to Davenport, Washington. The route returns to the Spokane River valley at its confluence with the Columbia River, where the glacial history of the Columbia River continental ice lobe and its interaction with catastrophic flood(s) and glacial lakes are explored. At least three episodes of glaciation are recorded in the landforms, sediments, and soils; evidence for multiple catastrophic flooding is found in the landforms and glacial lacustrine sediments of the area.

Trip C (see McDonald and Busacca, this volume) also leaves from Spokane and proceeds southwestward into the heart of the Channeled Scabland where soil, ash, and geomorphic evidence indicate that extensive flooding occurred in pre-Wisconsin as well as Wisconsin time. Truncated paleosols and multiple tephra layers shed light not only on the catastrophic flood history but also on the development of the vast sheets of loess that blanket eastern Washington.

The three trips together provide a wide perspective of the events that created the unique geological phenomenon known as the Channeled Scabland. Many of the important papers on the Channeled Scabland are included in the references cited for the three trips. Some broad review works are listed below for those wishing more background information.

From: Joseph, N. L., and others, editors, 1989, Geologic guidebook for Washington and adjacent areas: Washington Division of Geology and Earth Resources Information Circular 86.

SELECTED REFERENCES

Allen, J. A.; Burns, M.; Sargent, S. C., 1986, Cataclysms on the Columbia: Timber Press, 211 p.

Baker, V. R., 1973, Paleohydrology and sedimentology of Lake Missoula flooding in eastern Washington: Geological Society of America Special Paper 144, 79 p.

Baker, V. R.; Bunker, R. C., 1985, Cataclysmic late Pleistocene flooding from glacial Lake Missoula: Quaternary Science Reviews, v. 4, p. 1-41.

Baker, V. R.; Nummedal, Dag, 1978, The Channeled Scabland: U.S. National Aeronautics and Space Administration, 186 p.

Bretz, J H., 1923, The Channeled Scabland of the Columbia Plateau: Geological Society of America Bulletin, v. 34, p. 573-608.

Bretz, J H., 1969, The Lake Missoula Floods and the Channeled Scabland: Journal of Geology, v. 77, no. 5, p. 505-543.

Moody, U. L., 1987, Late Quaternary stratigraphy of the Channeled Scabland and adjacent areas: University of Idaho Doctor of Philosophy thesis, 419 p.

Richmond, G. M.; Fryxell, Roald; Neff, G. E.; Weis, P. L., 1965, The cordilleran ice sheet of the northern Rocky Mountains and related Quaternary history of the Columbia Plateau. *In* Wright, H. E., Jr.; Frey, D. G., editors, 1965, The Quaternary of the United States: Princeton University Press, p. 231-242.

Richmond, G. M., 1986, Tentative correlation of deposits of the Cordilleran Ice Sheet in the northern Rocky Mountains. *In* Sibrava, V.; Bowen, D. Q.; Richmond, G. M., editors, 1986, Quaternary glaciations in the northern hemisphere – A report of the International Geological Correlation Programme, Project 24, International Union of Geological Sciences and UNESCO: Quaternary Science Reviews, v. 5, p. 129-144.

Stradling, D. F.; Kiver, E. P., 1984, Geomorphology of the Columbia Plateau. *In* Folsom, M. M., editor, 1984, Northern Columbia Plateau landscapes, narrative, and field guide: Eastern Washington University Press, p. 24-30.

Stradling, D. F.; Kiver, E. P., 1987, The great Lake Missoula Floods, when and how many: Social Science Perspectives Journal, v. 1, no. 3, p. 1-12.

U.S. Geological Survey, 1982, The Channeled Scablands of eastern Washington: U.S. Geological Survey [pamphlet], 25 p.

Waitt, R. B.; Thorson, R. M., 1983, The Cordilleran ice sheet in Washington, Idaho and Montana. *In* Wright, H. E. Jr.; Porter, S. C., editors, 1983, Late-Quaternary environments of the United States; The late Pleistocene: Vol. 1: University of Minnesota Press, p. 53-70.

Evidence for Ice Dams and Floods in the Purcell Trench: Trip A

Roy M. Breckenridge
Idaho Geological Survey
University of Idaho
Moscow, ID 83843

INTRODUCTION

In 1923, Professor J Harlen Bretz of the University of Chicago began a series of research papers explaining the origin of the Channeled Scabland in northeastern Washington. He attributed this system of dry channels, coulees, and falls to an episode of flooding on a scale larger than geologists had ever recognized. His "outrageous" hypothesis was disputed by prominent geologists, and the resulting controversy is one of the most famous in geologic literature. Bretz's ideas for such large-scale flooding were viewed as a challenge to the uniformitarian principles then ruling the science of geology. After additional evidence showed a source for the flood (Pardee, 1942), Bretz's persistence resulted in his ideas becoming accepted. The source of the immense flooding was finally attributed to glacial Lake Missoula. A great lobe of the Cordilleran ice sheet advanced down the Purcell Trench and dammed the Clark Fork valley. The resulting glacial lake held more than 2,000 km^3 of water. The failure of the ice dam released flood flows as great as 62.5 km^3/hr (Baker, 1973) through the Clark Fork valley.

This guide covers the first part of the three-part field trip to the Lake Missoula flood deposits and the Channeled Scabland. It describes the late Pleistocene geology of the ice dam area near Clark Fork, Idaho and the area initially inundated by outburst flooding from glacial Lake Missoula. The trip guide begins at Spokane, Washington, and proceeds to Coeur d'Alene, Idaho, via Interstate Highway 90 (I-90), then north on U.S. Highway 95 (U.S. 95) to Sandpoint, then east on State Route (SR) 200 to the town of Clark Fork, and from there by county road to Heron, Montana. An optional return route diverges at Athol, Idaho, and returns to Spokane by Spirit Lake and Rathdrum, Idaho. The trip route is shown in Figure 1.

DISCUSSION

Cordilleran Ice Sheet

During Pleistocene time the Cordilleran ice sheet advanced southward from Canada into Montana, Idaho, and Washington. A number of large glacially dammed lakes, including glacial Lake Missoula, formed along its margin. The regional extent of the Cordilleran ice sheet has been summarized by Waitt and Thorson (1983) and more recently by Richmond (1986). However, the area of the ice dam itself has received little attention. Unpublished mapping by Breckenridge, Kiver, and Stradling has refined the ice margin positions in northern Idaho and northeastern Washington. (See discussion in Richmond, 1986.) The mapped extent of the ice in the Idaho area and the location of the ice dam and outburst routes are shown in Figure 2.

Evidence of pre-late Wisconsin glaciation in the Idaho panhandle is sparse, probably due to obliteration by later glaciation and flooding. However, some older tills are exposed in cuts beneath the youngest till in the Purcell Trench near Cocolalla Lake and at Moravia, north of Sandpoint. These older tills and the glacial record in other parts of the Rocky Mountains indicate that early advance(s) of the Cordilleran ice sheet covered nearly all of the Selkirk Mountains and Cabinet Mountains (Alden, 1953; Richmond, 1986; R. M. Breckenridge, unpublished map). Richmond (1986) placed the latest advance of the Pend Oreille lobe of the Cordilleran ice sheet between 25 and 13 ka; an interstadial is represented by the 17-ka ice-free date of Clague (1978, 1981). Waitt (1985) interprets the same evidence to show that glacial Lake Missoula could have existed only between about 17 and 11 ka.

From: Joseph, N. L., and others, editors, 1989, Geologic guidebook for Washington and adjacent areas: Washington Division of Geology and Earth Resources Information Circular 86.

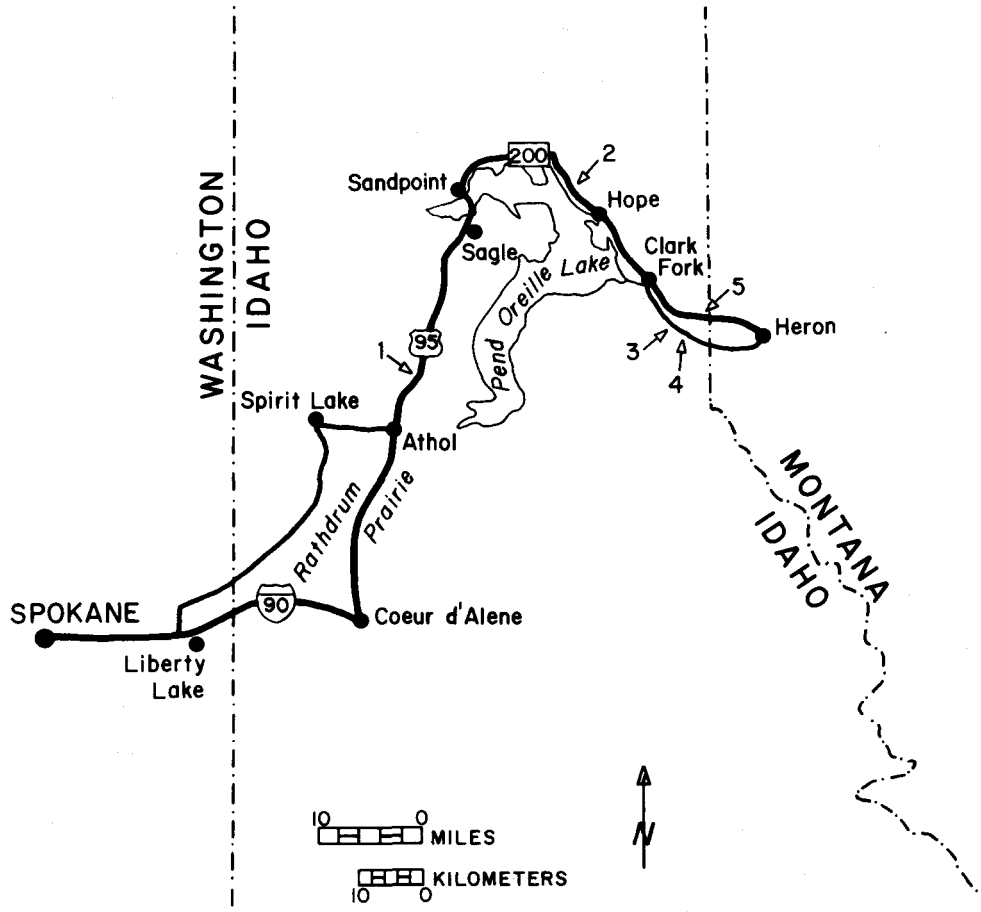

Figure 1. Route of Missoula Flood field trip A and locations of stops.

Source of the Flood

J. T. Pardee first reported on studies of glacial Lake Missoula in 1910, but not until 1942 did he present new evidence for rapid drainage of the large lake dammed by a lobe of the ice sheet (Pardee, 1910, 1942). His discussion of the unusual currents necessary to produce flood features in the lake basin provided the long-awaited source for the flooding that Bretz (1923) had suggested as the force that formed the Channeled Scabland. Alden (1953), in his summary of the glacial geology of western Montana and adjacent areas of Idaho, discussed aspects of the ice dam and the multiple glacial advances; he speculated on the lake and drainage routes of glacial Lake Missoula. Chambers (1971) described the sedimentation cycles of rhythmically bedded bottom sediments and interpreted them as multiple episodes of emptying and filling.

Pardee (1942) calculated that glacial Lake Missoula had a volume of 2,167 km^3 when it stood at an elevation of 1,265 m against the ice dam and estimated that the lake drained at a rate of 15.3 km^3/hr. Baker (1973) estimated the maximum rate of discharge to be 62.5 km^3/hr, and new calculations by Craig and Hanson (1985) have set the lake volume at that elevation at 2,514 km^3. These huge discharge magnitudes and rates are responsible for the megaripples and other large-scale sedimentary and geomorphic features formed by the floods.

Character of the Ice Dam and Location of Outburst Routes

Chambers (1971) noted the unstable characteristics of glacial dams and discussed four proposed mechanisms for the failure of ice dams: (1) subglacial failure by flotation (Thorarinsson, 1939); (2) deformation of ice by water pressure (Glenn, 1954); (3) enlargement of subglacial tunnels by water (Liestøl, 1955); and (4) enlargement of tunnels by icebergs (Aitkenhead, 1960). Waitt (1985) has proposed jökulhlaup releases when the depth of ice-impounded water at the dam reaches 90 percent of the thickness of the ice. He suggests that the increasing hydrostatic pressure progressively wedges into the ice-rock seal until the ice becomes buoyant. Subglacial tunnels then form and are enlarged by the flowing water until the tunnel roof collapses and the ice dam fails, causing the lake to empty. Waitt used the self-emptying model to explain the numerous rhythmite sequences preserved in areas flooded but adjacent to main courses of flood. He interprets each cycle in these rhythmite sequences as a separate flood. Recently Craig (1987) has modeled the in-

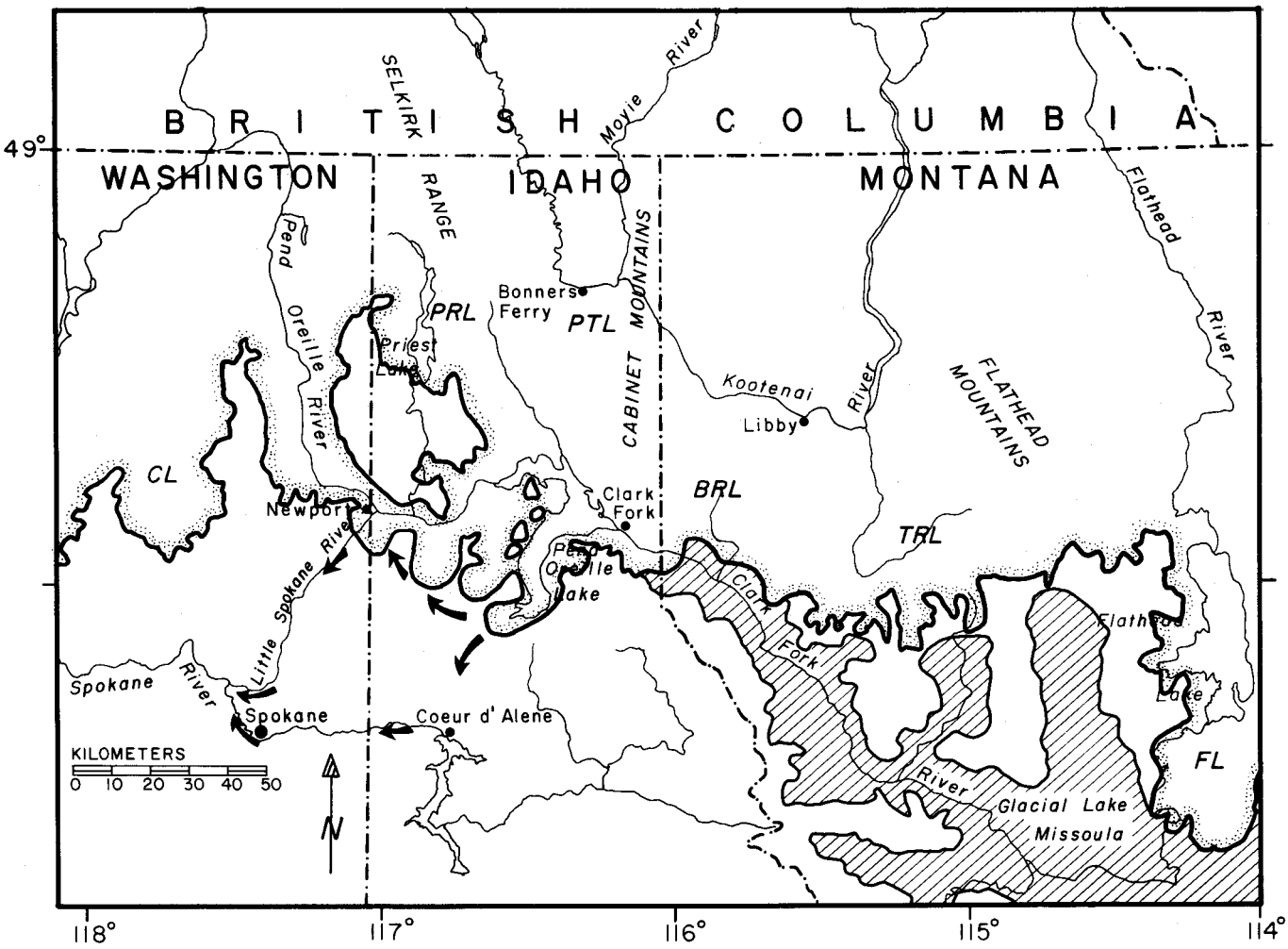

Figure 2. The Cordilleran ice margin (modified from Richmond, 1986), glacial Lake Missoula, and major flood outburst routes. BRL, Bull River lobe; CL, Colville lobe; FL, Flathead lobe; PTL, Purcell Trench lobe; PRL, Priest River lobe; TRL, Thompson River lobe. Glacial Lake Missoula; cross-hatched area. Arrows show major flood outburst routes.

teraction of water and ice dams and simulated cycles of ice damming, lake filling, and erosion of the ice dam using global climatic variations. Costa (1988) has compared the jökulhlaup models with modern ice-dammed lakes and regards the data as too diverse and the extrapolations as too great to be reliable.

The main path of Lake Missoula floods (Fig. 2) was from the end of Pend Oreille Lake through the Rathdrum Prairie and Spokane Valley. Another major flood route followed the Pend Oreille River, crossed divides, and followed the Little Spokane River valley. Other ice-dammed lakes existed in the valleys proximal to the Cordilleran ice sheet, and flooding from those sources must have also coursed down the Columbia River system. Another huge Pleistocene flood, from pluvial Lake Bonneville in Utah, traveled down the Snake River and the lower Columbia River sometime between 14,000 and 15,000 years ago (Scott and others, 1982). Both the Bonneville and Missoula flood deposits occur in the Lewiston Basin and have been described by Webster and others (1982).

ACKNOWLEDGMENTS

This guide benefited from the helpful comments and suggestions of Eugene P. Kiver, Robert L. Logan, Fred K. Miller, and Loudon R. Stanford. Field studies were supported in part by the U.S. Geological Survey surficial mapping project. I am grateful to Gerald M. Richmond and Robert R. Curry for comments in the field. Seismic information obtained from Pend Oreille Lake was supplied by the U.S. Navy David Taylor Research Facility, at Bayview. I thank Ken and Edie Kinucan of the University of Idaho Clark Fork Field Station for their hospitality and interest in my research. Many residents of the Clark Fork area granted access to their land and provided useful information.

REFERENCES CITED

Aitkenhead, N., 1960, Observation on the drainage of a glacier-dammed lake in Norway: Journal of Glaciology, v. 3, no. 27, p. 607-609.

Alden, W. C., 1953, Physiography and glacial geology of western Montana and adjacent areas: U.S. Geological Survey Professional Paper 231, 200 p.

Anderson, A. L., 1927, Some Miocene and Pleistocene drainage changes in northern Idaho: Idaho Bureau of Mines and Geology Pamphlet 18, 29 p.

Baker, V. R., 1973, Paleohydrology and sedimentology of Lake Missoula flooding in eastern Washington: Geological Society of America Special Paper 144, 79 p.

Bretz, J H., 1923, The channeled scablands of the Columbia Plateau: Journal of Geology, v. 31, no. 8, p. 617-649.

Bush, J. H., Jr.; Breckenridge, R. M., editors, in press, Guidebook to the geologic history of northern Idaho and southeastern Washington–Field trips originating from Moscow-Pullman: Idaho Geological Survey Bulletin 29.

Chambers, R. L., 1971, Sedimentation in glacial Lake Missoula: University of Montana Master of Science thesis, 100 p.

Clague, J. J., 1978, Mid-Wisconsin climates of the Pacific Northwest. *In* Current Research, Part B: Geological Survey of Canada Paper 78-1B, p. 95-100.

Clague, J. J., 1981, Late Quaternary geology and geochronology of British Columbia, Part 2: Summary and discussion of radiocarbon-dated Quaternary history: Geological Survey of Canada Paper 80-35, 41 p.

Conley, Cort, 1981, Idaho for the curious–A guide: Backeddy Books, Cambridge, Idaho, 704 p.

Conners, J. A., 1976, Quaternary history of northern Idaho and adjacent areas: University of Idaho Doctor of Philosophy thesis, 504 p.

Costa, J. E., 1988, Floods from dam failures. *In* Baker, V. R.; Kochel, R. C.; Patton, P. C., editors, Flood Geomorphology: John Wiley and Sons, p. 439-463.

Craig, R. G., 1987, Dynamics of a Missoula flood. *In* Mayer, L.; Nash, D., editors, Catastrophic flooding: Allen and Unwin, p. 305-332.

Craig, R. G.; Hanson, J. P., 1985, Erosion potential from Missoula floods in the Pasco Basin, Washington: Battelle Pacific Northwest Laboratory Document PNL-5684, 266 p., 5 appendices.

DeSmet, J. S., 1983, Geohydrology of the southside aquifer, Sagle, Idaho: University of Idaho Master of Engineering technical paper, 25 p.

Dort, Wakefield, Jr., 1960, Glacial lake Coeur d'Alene and bergrafted boulders: Idaho Academy of Science Journal, v. 1, no. 2, p. 81-92.

Finckh, Peter; Kelts, Kerry; Lambert, Andre, 1984, Seismic stratigraphy and bedrock forms in perialpine lakes: Geological Society of America Bulletin, v. 95, no. 9, p. 1118-1128.

Flint, R. F., 1936, Stratified drift and deglaciation of eastern Washington: Geological Society of America Bulletin, v. 47, no. 12, p. 1849-1884.

Glen, J. W., 1954, The stability of ice-dammed lakes and other water filled holes in glaciers: Journal of Glaciology, v. 2, no. 15, p. 316-318.

Liestøl, Olav, 1955, Glacier dammed lakes in Norway: Norsk Geografisk Tidsskrift, v. 15, no. 3-4, p. 122-149.

McLeod, J. R., 1987, Mysterious Pend Oreille Lake and its "monster"–Fact and folklore: Woodcraft Publishing, Coeur d'Alene, Idaho, 97 p.

McKiness, J. P., 1988, The Quaternary System of the eastern Spokane Valley and the lower, northern slopes of the Mica Peak Uplands, eastern Washington and northern Idaho: University of Idaho Master of Science thesis, 98 p., 1 pl.

Newcomb, R. C., [and others], 1953, Seismic cross sections across the Spokane River Valley and the Hillyard trough, Idaho and Washington: U.S. Geological Survey Open File Report 53-199, 16 p., 18 plates.

Pardee, J. T., 1910, The glacial Lake Missoula: Journal of Geology, v. 18, p. 376-386.

Pardee, J. T., 1942, Unusual currents in glacial Lake Missoula, Montana: Geological Society of America Bulletin, v. 53, no. 11, p. 1569-1600.

Richmond, G. M., 1986, Tentative correlation of deposits of the Cordilleran ice-sheet in the northern Rocky Mountains. *In* Šibrava, Vladimir; Bowen, D. Q.; Richmond, G. M., editors, Quaternary glaciations in the northern hemisphere: Quaternary Science Reviews, v. 5, p. 129-144.

Richmond, G. M.; Fryxell, R.; Montagne, J.; Trimble, D. E, 1965, International Association for Quaternary Research, 7th Congress, Guidebook for field conference E, Northern and middle Rocky Mountains. *In* Schultz, C. B.; Smith, H. T. V., editors, INQUA Guidebooks: Nebraska Academy of Sciences, 129 p.

Savage, C. N., 1965, Geologic history of Pend Oreille Lake region in north Idaho: Idaho Bureau of Mines and Geology Pamphlet 134, 18 p.

Scott, W. E.; Pierce, K. L.; Bradbury, J. P.; Forester, R. M., 1982, Revised Quaternary stratigraphy and chronology in the American Falls area, southeastern Idaho. *In* Bonnichsen, Bill; Breckenridge, R. M., editors, Cenozoic geology of Idaho: Idaho Bureau of Mines and Geology Bulletin 26, p. 581-595.

Thorarinsson, Sigurdur, 1939, The ice-dammed lakes of Iceland with particular reference to their values as indicators of glacier oscillations: Geografiska Annaler, v. 21, Ht. 3-4, p. 216-242.

Waitt, R. B., 1985, Case for periodic colossal jokulhlaups from Pleistocene glacial Lake Missoula: Geological Society of America Bulletin, v. 96, no. 10, p. 1271-1286.

Waitt, R. B.; Thorson, R. M., 1983, The Cordilleran ice sheet in Washington, Idaho, and Montana. *In* Wright, H. E., Jr.; Porter, S. C., editors, Late-Quaternary environments of the United States, Volume 1, The late Pleistocene: University of Minnesota Press, p. 53-70.

Webster, G. D.; Kuhns, M. J. P.; Waggoner, G. L., 1982, Late Cenozoic gravels in Hells Canyon and the Lewiston basin, Washington and Idaho. *In* Bonnichsen, Bill; Breckenridge, R. M., editors, Cenozoic geology of Idaho: Idaho Bureau of Mines and Geology Bulletin 26, p. 669-683.

Weis, P. L.; Richmond, G. M., 1965, Maximum extent of late Pleistocene Cordilleran glaciation in northeastern Washington and northern Idaho: U.S. Geological Survey Professional Paper 545C, p. C128-C132.

Road Log

In this road log, mileage is keyed to mileposts along the highways travelled. The numbers on the left are milepost numbers. No interval mileage is given.

Spokane to Coeur d'Alene

From Spokane, proceed east on Interstate Highway 90 (I-90).

The flood gravels of the Spokane Valley and Rathdrum Prairie are the sole-source aquifer for the greater Spokane area. Numerous wells tap the popularly termed "underground river" in the flood gravels.

289 Pines Road. North of I-90 a large Missoula flood pendant bar trails to the west (lee side) from the scoured bedrock knobs.

296 Liberty Lake, Otis Orchards, exit 296. To the south of I-90, note the scoured bedrock and the terraced gravel bars that dam the Liberty Lake basin. These deposits were interpreted by some to be moraines (Weis and Richmond, 1965). McKiness (1988) mapped the south side of the Spokane Valley and the Rathdrum Prairie and found no conclusive evidence of glaciation.

298 Missoula flood bar on the south side of the freeway.

1 Idaho/Washington border, Spokane River, and Port of Entry. Newcomb (1953) interpreted a seismic cross-section of the valley and estimated the base of the gravel aquifer to be at an elevation of 488 m near the state line, as compared to a base elevation of 567 m on the basalt at the Spokane Falls. The apparent deepening of the valley toward the east may be due to scour by floods and ice or preglacial streams. (See discussion at Stop 2.)

2 Pleasant View Road. Jacklin Seed Farm on the south. The ground water of Rathdrum Prairie and Spokane Valley is used to irrigate one of the world's largest producing areas of bluegrass lawn seed.

6 Treaty Historical Rock. At Post Falls, bedrock knobs are visible. Post Falls is the site of a low dam that controls the level of Coeur d'Alene Lake and the flow of the Spokane River.

8 Huetter Rest Area.

12 Junction of I-90 and U.S. 95 in Coeur d'Alene. Follow exit signs to U.S. 95, north toward Sandpoint. Coeur d'Alene has a history rooted in mining, logging, and recreation, but the city actually began as a military fort established by Gen. William Tecumseh Sherman in 1879. Coeur d'Alene Lake (second largest in Idaho) is dammed by Lake Missoula flood gravels and is the source of the Spokane River, a tributary of the Columbia River. Flood waters of glacial Lake Missoula inundated the area currently occupied by the lake basin and at times overtopped a pass to the south at Setters (Dort, 1960).

Some early workers put the ice limit as far south as Coeur d'Alene (Flint, 1936; Dort, 1960; Alden, 1953). Glacial grooves have been reported on bedrock near Post Falls and at Tubbs Hill in Coeur d'Alene. Weathered deposits just to the north of Coeur d'Alene near Hayden Lake have been interpreted as old till (Richmond and others, 1965) or Tertiary sediments (Conners, 1976). Late-glacial ice and flood features in northern Idaho are shown in Figure 3.

Coeur d'Alene to Sandpoint

Proceed north on U.S. 95.

447 Columbia River basalt cliffs on the east. Missoula floods scoured basalt blocks from the margins of the Rathdrum Prairie and Spokane Valley. Large basalt blocks and boulders are not uncommon in the Spokane aquifer (C. M. Breckenridge, Dickerson Pump and Irrigation Co., oral commun., 1988).

450 Athol. The large gravel plain that splays from the south end of Pend Oreille Lake is composed of till near the end of the lake, but within several kilometers it grades into flood gravels with large-scale ripples. Rathdrum Prairie has no surface drainage, but large volumes of ground water flow through the gravels.

452 Hoodoo Creek Rest Area. The Hoodoo valley is an abandoned channel that discharged flood and meltwater from the terminus of the Pend Oreille Lake sublobe. Current indicators show that at

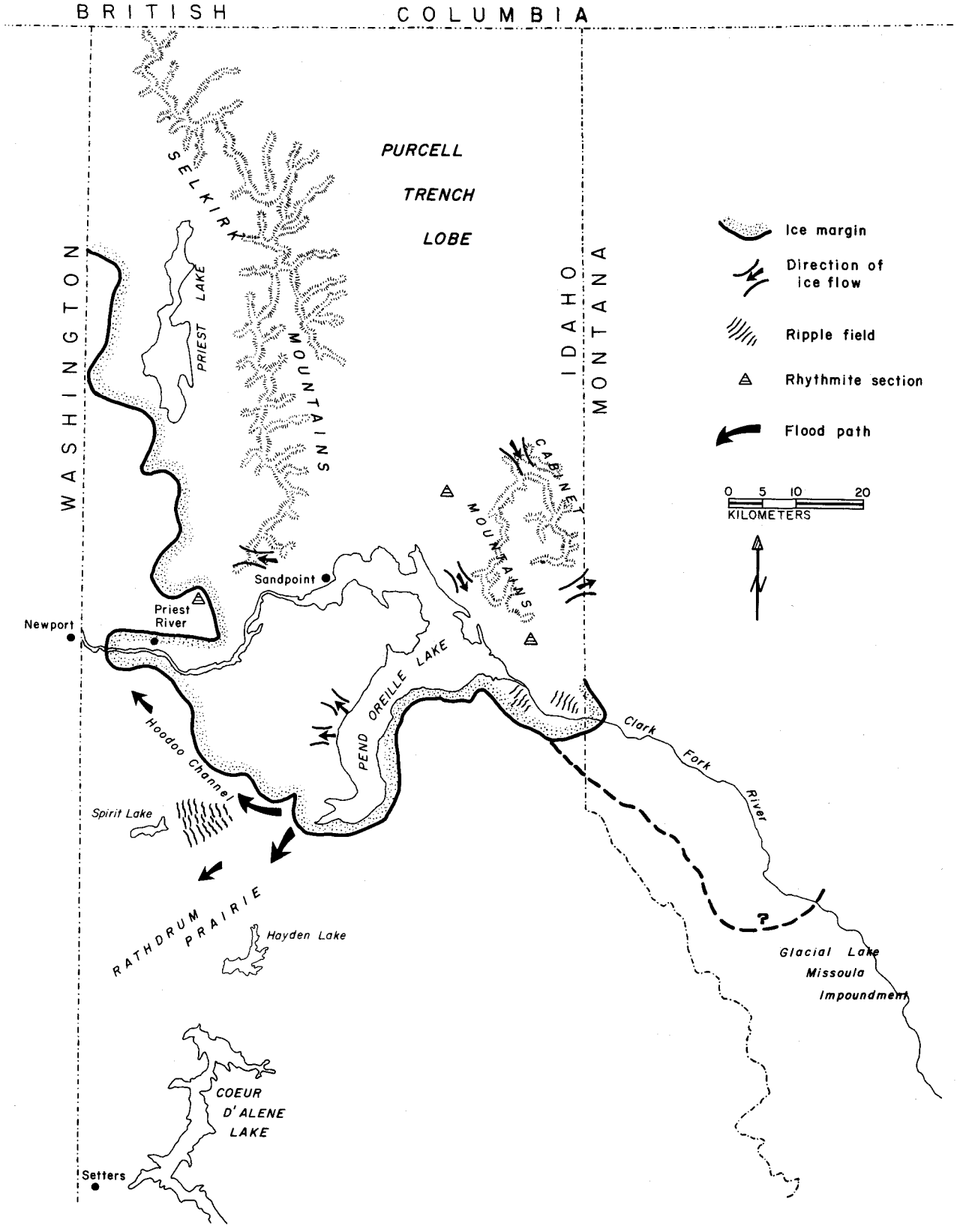

Figure 3. Major late-glacial features of the lower Clark Fork valley and adjacent areas.

least the latest phases of flooding traveled northwest through the channel toward Newport, Washington.

453 **STOP 1. Flood gravel.**

Turn left on Granite Lake road just past the rest area. Proceed to the railroad crossing and stop at the gravel pit.

Here, crudely bedded flood gravels dip northward along the Hoodoo channel. Note the scoured bedrock on the railroad right-of-way just across the road from the gravel pit.

Return to U.S. 95 and proceed north.

456 Careywood. A well-developed moraine marks the southernmost recognized extent of the latest Wisconsin ice advance in this valley.

463 Cocolalla Lake, a moraine-dammed lake. A prelate Wisconsin till is exposed in roadcuts on the right road bank. The ice limit on Huckleberry Mountain just to the west is at least elev. 1,160 m.

464 Westmond. The ice limit on Little Blacktail Mountain, the highest mountain to the east, was as high as elev. 1,220 m. Ice of the Pend Oreille Lake sublobe flowed west through several passes on Little Blacktail Mountain.

467 Algoma Lake, Heath Lake. Core from Algoma Lake to the west of the highway contained Mazama ash (6.7 ka) at a depth of 1.2 m and an unidentified ash at nearly 2.7 m. Note the scoured bedrock at the valley margin and elongated hills of till in the valley.

469 The Sagle area is composed mostly of till rather than flood deposits. Wells here penetrate blue clay and till. Ground water is relatively scarce, and septic drainage is poor due to impervious clay in these glacial deposits (DeSmet, 1983). This part of the valley apparently was not subjected to flood scour in latest glacial time. Either part of the ice lobe remained intact here while most of the Missoula flood water passed down the Pend Oreille Lake basin or the latest glacial flooding was not extreme.

470 Gravel pits west of the highway. Interbedded Missoula flood sands and gravels dip steeply to the south. Here the Pend Oreille River valley was a flood channel. Flood deposits are common to the west (Fig. 3).

472 U.S. 95 crosses the north arm of Pend Oreille Lake.

Sandpoint to Clark Fork

Follow U.S. 95 signs through Sandpoint. Just north of Sandpoint at the junction, proceed straight ahead on State Highway 200 toward Clark Fork.

Our route now crosses the Purcell Trench, along which a main lobe of the Cordilleran ice sheet moved south from Canada (Fig. 3). The ice sheet was joined by alpine glaciers from the Selkirk Mountains on the west as well as by ice from the Cabinet Mountains on the east. The Schweitzer Basin ski area is visible above Sandpoint on the west. The route along the north side of Pend Oreille Lake passes through some excellent examples of crag and tail topography, glacially scoured knobs, and molded till.

38 Cross the Pack River, a major drainage of the southern Purcell Trench and the Selkirk Mountains.

44 **STOP 2. Lake Missoula Highway geologic sign**

View of Pend Oreille Lake, one of largest lakes in North America, which is more than 350 m deep. The lake basin is impounded by moraines at the south end. Bathymetry of the lake shows immense deltas from the Clark Fork and the Pack Rivers. Like most of the world's large deep lakes, Pend Oreille is the subject of numerous legends, including bottomless depth and monsters like the "Pend Oreille Paddler" (McLeod, 1987).

The origin of the lake basin has been debated. Its anomalous depth (compared to that of adjacent formerly ice-covered areas in the trench) may be due to a preglacial river valley, more erodible sediments, or flood scour (Anderson, 1927; Savage, 1965; Conners, 1976). An interpretation of the lake basin and sediment based on new seismic reflection data is shown in Figure 4. These data are similar to seismic information from deep glacial lakes in Europe studied by Finckh and others (1984). The bottom of the lake basin is U-shaped, suggesting ice scour. Some evidence of fault control is shown by the fault bounding the east side of the basin. Although the basin was scoured earlier, it was not scoured or flushed of sediments by the latest episodes of flooding , but rather it contains more than 75 m of glaciolacustrine sediments.

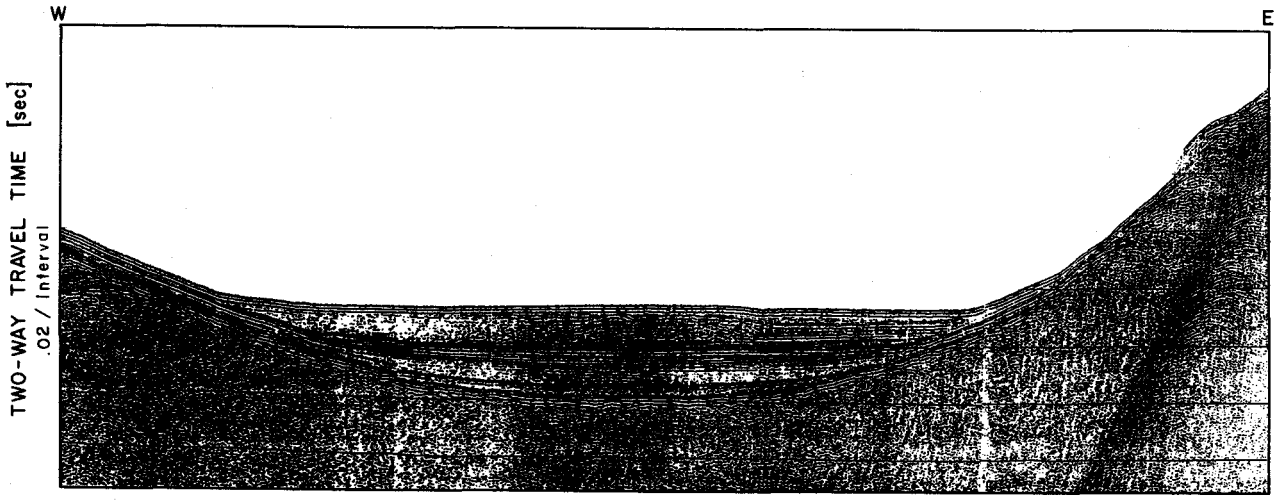

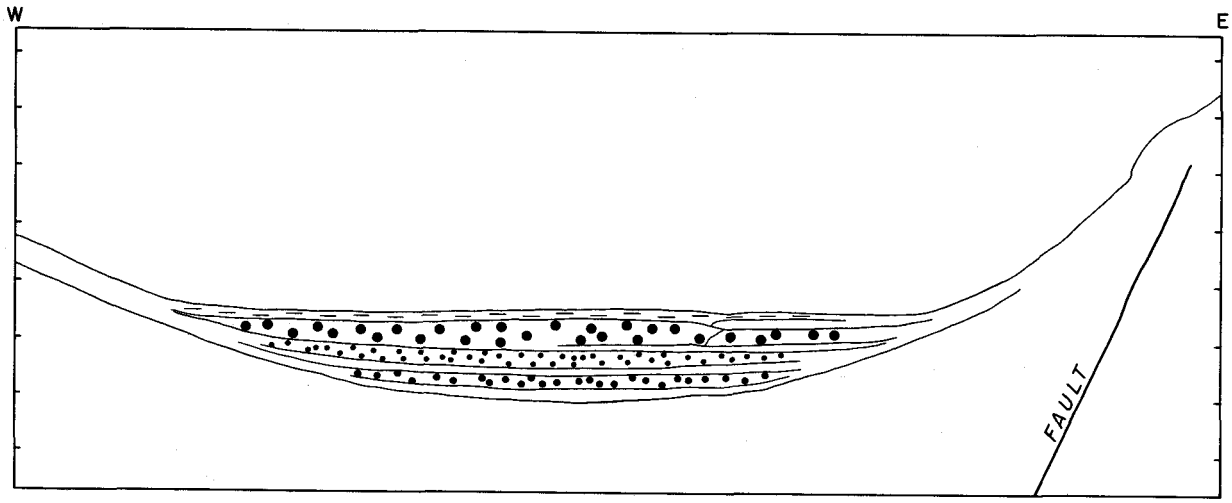

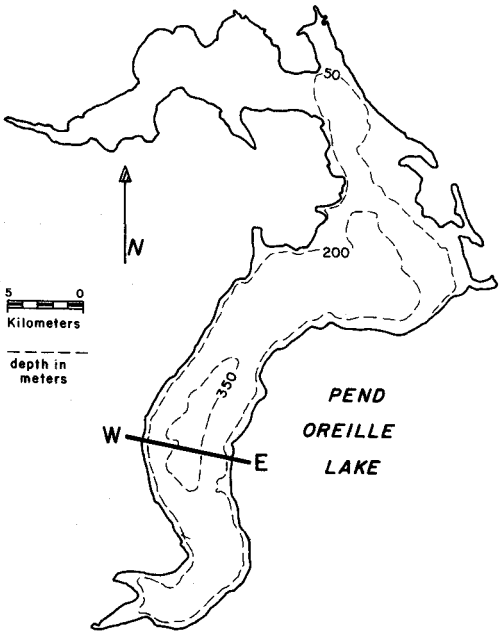

Figure 4. Generalized bathymetric map, seismic reflection profile, and interpretive reflection profile across the southern part of Pend Oreille Lake (from data provided by U.S. Navy).

Samples collected by the U.S. Navy indicate the uppermost lake-bed layer is Holocene ooze. At least two and probably four major depositional units exist below the uppermost layer. Although at present subsurface sampling cannot substantiate the content of the lower units, these units are probably coarse flood or till deposits, based on comparison with other lakes (Finckh and others, 1984)

45 Bridge over the boat basin.

49 Samowen Road. Kullyspel House Historical Highway Sign on the right. The Samowen peninsula exhibits ice-scoured bedrock and gravel deposits.

50 Denton Slough.

51 Delta of Clark Fork.

55 Lightning Creek Bridge. Lightning Creek is clogged with coarse Pleistocene flood and glacial boulders moved from upvalley terraces and redeposited here by periodic flash floods. Enter town of Clark Fork.

Clark Fork - Heron Loop

The route through the Clark Fork valley was an important one in the early exploration and settlement of the region. The first white explorer known to have visited the area was David Thompson, an Englishman who traveled through this area in 1809. He established fur trading posts at Selish House near Thompson Falls and at Kullyspell House near Hope. Both trading posts were short-lived because the Flathead, Kalispel, Spokan, and Coeur d'Alene tribes of the area were not traditionally trappers and because the marauding Blackfeet were hostile toward traders (Conley, 1981). David Thompson is best known, however, as the pioneer geographer and explorer during that era in northwest America. The Indians called him "koo koo sint," the man who looked at stars.

In 1876, the Northern Pacific Railway chose the Clark Fork route, and soon towns like Thompson Falls and Hope sprang up as sidings. These towns were the local jumping-off spots to the lumber and mining camps. Many prospectors were bound for the Coeur d'Alene district, just 40 km to the south, that is now the largest silver-producing district in the world.

In Clark Fork, turn south on the marked road to Lakeview. Use caution crossing the railroad tracks at the south end of town. Cross the Clark Fork River and turn east (left).

All water draining from glacial Lake Missoula passed through the mouth of the Clark Fork valley. At peak flow as much as 210 million m^3/sec of water from Lake Missoula passed through the valley. Note the water gap on the south skyline at an elevation of 1,000 m. The road crosses a large ripple field (Fig. 5) formed by flood waters below the Castle Rock cataract. A thin blanket of lacustrine silt overlies the flood gravels, indicating that the later stages of Lake Missoula drained quietly.

The ripple field is the site of the Ruen seed potato farm, the first and only in northern Idaho.

Note: *Mileage is given to Stops 3 and 4 because this road does not have mileposts.*

6 **STOP 3. Flood bar stratigraphy.**

At approximately 6.5 mi the road ascends terrace gravels. Stop at the freshest exposure in the roadcut. The road is excavated in a flood bar.

The quality of the exposures varies because of slumping. The bedding sets are several meters thick, and foresets dip in a downstream direction as much as 20 degrees. The clasts are of Precambrian Belt Supergroup rocks and are subrounded to rounded. Individual beds are general-

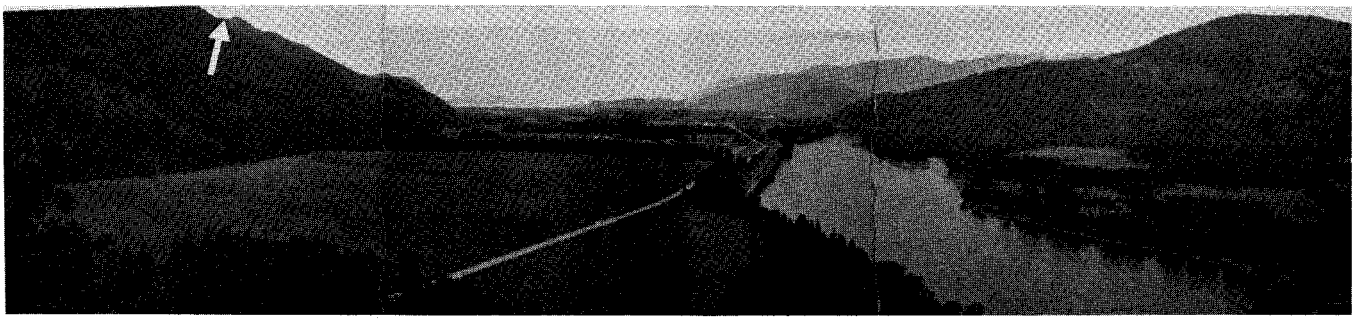

Figure 5. View from Castle Rock to the west of the mouth of the Clark Fork valley along the flood path. All flood water from glacial Lake Missoula passed through the field of view. Note the water gap on the south (arrow, left) skyline at 1,000 m. In the center of the view, long wavelength ripples are marked by the tree lines through the fields.

ly only poorly sorted. A perpendicular face in a private gravel pit (Fig. 6) just to the north under the power lines exposes well developed scour and fill troughs. The gravels are overlain by about a meter of silt. The section appears to have no major breaks in deposition. Note the texture, lithology, and bedding of these gravels for comparison with those at the next stop.

Travel east about 1/2 mi to the first turn to the right, marked Dry Creek. Turn south on Dry Creek road (U.S. Forest Service Road 280). The road reaches the mouth of Dry Creek in 3/4 mi. The gravel pit at the curve on the right side of the road is a private pit; however, much can be observed from the road right-of-way.

5 **STOP 4. Dry Creek gravel pit.**

The gravel deposit is at the mouth of Dry Creek (Fig. 7). The landform trails southeast from the valley side, in a direction opposite that of the flow of water that emptied glacial Lake Missoula. This pit is at an elevation of 817 m, more than 125 m above the floor of the valley. The foreset beds (Fig. 7) are several meters high and dip eastward. Clasts are poorly rounded, and some cobbles are striated. Although most clasts are Precambrian Belt metasediments derived locally, some clasts of granite and diorite exposed in and adjacent to the Purcell Trench are present, in addition to a few clay balls. The sediments are well cemented, and the pit walls must be ripped before gravel can be excavated.

These gravels probably represent glacial material that was deposited in glacial Lake Missoula. All the major drainages on the south side of the Clark Fork valley between here and Trout Creek, more than 30 km to the southeast, have similar deposits. Known occurrences of these deposits are restricted to the south side of the Clark Fork valley, opposite the source areas of ice on the north just where ice marginal channels would be expected. If these features represent ice-marginal outwash deposited in Lake Missoula, then the ice extended much farther up the Clark Fork valley than previously recognized—nearly to Thompson Falls—and the late phases of glacial Lake Missoula drained quiescently enough to leave them preserved.

Return to road junction. Turn east and follow signs for Heron. The route crosses flood gravels. Low-amplitude megaripples that are capped by lake silts are visible in many of the hay fields along the road. Bedrock hills in the valley have pendant bars trailing downriver.

Cross the Idaho/Montana border. At the junction just before Heron, turn left, then right, and cross the railroad tracks. Proceed across the bridge over Cabinet Gorge Reservoir (Clark Fork River) to SH 200 and turn left (west).

mile 1 Blue Creek. Deposits of Lake Missoula silts are exposed in the bay to the north.

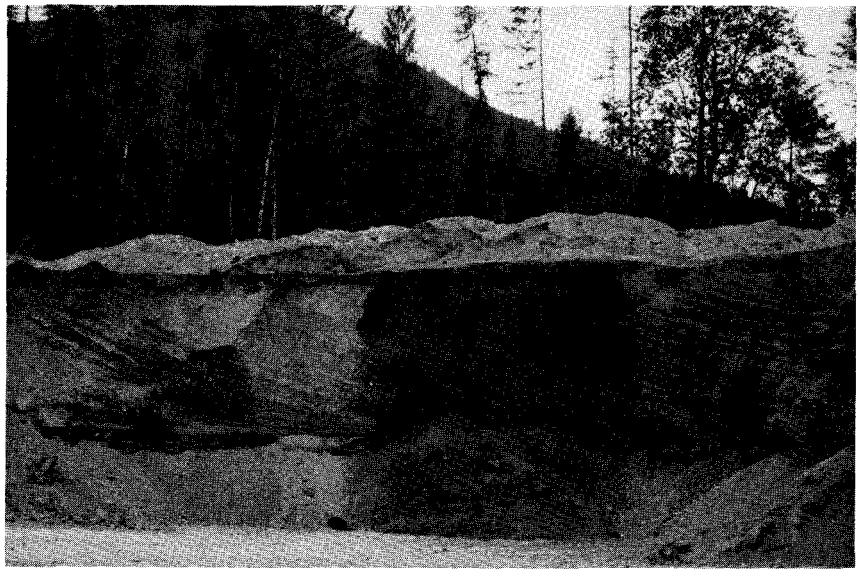

Figure 6. Coarse flood deposits exposed in a gravel pit near a power line. Bedding dips westward, down the Clark Fork valley. The section of gravel freshly exposed by the slump is 8 m high.

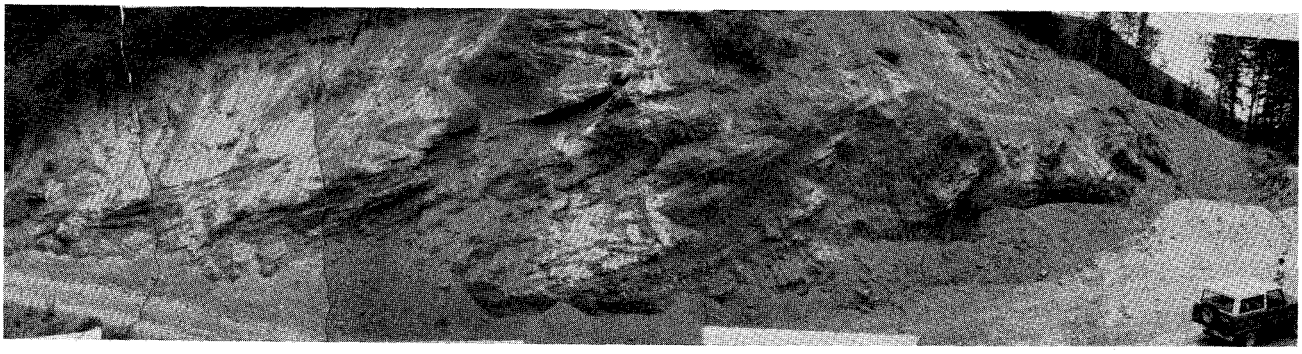

Figure 7. Panorama of Dry Creek gravel pit. Beds of poorly rounded, unsorted gravel dip steeply to the east. These deposits probably were formed by outwash into glacial Lake Missoula.

Note: *The following part of the road log is again keyed to mileposts.*

0 Montana/Idaho border. Turn south at the Cabinet Gorge Dam sign to the visitors parking area. For a better view, walk up the back (north) side of the prominent knob overlooking the dam site. Take care approaching the edge of the cliff.

STOP 5. Cabinet Gorge Dam viewpoint.

This dam was completed in 1952 by Washington Water Power (WWP). The 183-m-long and 63-m-high true arch dam is constructed on the Libby Formation of the Precambrian Belt Supergroup. This dam, in coordination with the Albeni Falls dam downstream, controls the water level of Pend Oreille Lake. A large new hatchery just downriver of the dam provides 2 million Kokanee salmon smolts to the lake annually.

The gravels capping the prominent terrace south of the river are mostly flood deposits but logs from monitor wells drilled by WWP in the terrace show cycles of clay till and interbedded lake deposits indicating multiple episodes of ice damming (H. T. Stearns, consulting geologist, unpublished data, oral commun., 1986). Glacial erosion and till deposits indicative of an ice margin are common in this area, so many publications show the ice lobe terminus near here. (See, for example, Alden, 1953; Weis and Richmond, 1965; Waitt, 1985.)

Note the truncated spurs and remnant strandlines on the south side of the Clark Fork valley. The nearly straight front along the north side of the valley here is controlled by the Hope fault, which may have been active in the Quaternary. If so, it is possible that tectonic or isostatic activity may have had a role in the failure of the ice dam.

The bedrock bench on the north side of the valley has abundant till cover interpreted to be ice-marginal deposits; possibly flood drainage was pushed to the south side of the valley by the ice from the north, at least in the waning stages of smaller late floods. Perhaps the bench represents the edge of the ice dam failure or the margin of subglacial flow. Just to the north, ice flowed through cols as high as elev. 1,830 m across the Cabinet Mountains between the Bull River and the Purcell Trench.

Return to SH 200 and proceed west toward Clark Fork.

60 River delta. Ground ice was reported by highway construction crews (oral commun., Idaho District 1 office, 1988). Ground ice has also been reported at several highway construction sites between Clark Fork, Idaho, and Thompson Falls, Montana, and at Lakeview on Pend Oreille Lake (McLeod, 1987). Although colloquially called glacial ice, these occurrences probably represent recent seasonal buildup rather than Pleistocene ice remnants.

59 Large ripples in the hayfield south of the highway.

58 Just past milepost 58, a state-owned gravel pit is on the right. Imbricated Missoula flood gravels dip generally west and are overlain by silt.

56 Just before we enter the town of Clark Fork, large glacial grooves and striations can be seen in roadcuts in the Wallace and Striped Peak Formations along the curves in the road (Bush and Breckenridge, in press).

Town of Clark Fork.

Return to Sandpoint and travel south toward Coeur d'Alene on U.S. 95 by the same route taken coming north. For an alternate return route to Spokane, turn right at Athol and proceed west toward Spirit Lake.

From Athol to Spirit Lake, the highway crosses the large fan of flood gravels discharged from the end of Pend Oreille Lake. The road also crosses a large-scale ripple field. This is one of the largest of the flood ripple fields and is most striking when viewed from the air. Flood water discharged from what is now the end of the Pend Oreille Lake basin directed flood outbursts toward this area and formed the gravel dam holding Spirit Lake. Bedding in flood gravels dips toward the west up the Spirit Lake basin.

At the Spirit Lake junction, turn south toward Rathdrum and Trentwood. This route passes several large gravel bars damming Spirit, Twin, and Newman Lakes. At Pines Road turn south and return to I-90, or proceed on Trent Avenue back to Spokane.

End of road log.

Glacial and Multiple Flood History of the Northern Borderlands: Trip B

Eugene P. Kiver
Department of Geology
Eastern Washington University
Cheney, WA 99004

Dale F. Stradling
Department of Geography and Anthropology
Eastern Washington University
Cheney, WA 99004

and
Ula Moody
Department of Natural Science and Math
Western Oregon State College
Monmouth, OR 97361

INTRODUCTION

The catastrophic release of as much as 2,000 km^3 of ice-dammed water from glacial Lake Missoula has had major impact on the topography and surficial geology of eastern Washington. Some of these flood features, as well as other geologic features, can be seen on this field trip, the second in a series of three. This trip proceeds from Spokane to Fort Spokane via the town of Davenport (Fig. 1). At Fort Spokane, some of the evidence that has aided in reconstructing the position of Pleistocene glaciers and the glacial and flood history in the upper Columbia River drainage system can be explored.

Soils are an important line of evidence used in tentative correlation of tills and flood deposits. Entisols and Inceptisols, with little or no horizonation, are found in relatively recent sediments. Alfisols in mid-Wisconsin tills show less development of structure and clay skins in the B horizons than those in early or pre-Wisconsin tills. Mollisols are now developing in this area under the present climatic regime (cool, wet winters and dry, hot summers). In contrast, the Alfisols of the Wisconsin developed under a climatic regime that was cool and wet throughout the year.

The field trip route can be followed on the U.S. Geological Survey 1:100,000-scale Coulee Dam, Nespelem, and Spokane quadrangle maps. For the Fort Spokane area, more topographic detail is available on the U.S. Geological Survey 1:24,000-scale Fort Spokane, Hunters, Inkster Lake, McCoy Lake, and Miller Mountain topographic maps.

The road log begins at the junction of Interstate Highway 90 (I-90) and U.S. Highway 2 (U.S. 2) just west of Spokane. West from Spokane on I-90, the route climbs out of the Spokane Valley, crosses the exposed edge of the Columbia River basalt, and passes onto the Columbia Plateau. Cumulative mileage for the trip is given on the left; interval mileage is in parentheses.

ACKNOWLEDGMENTS

Much of the field research was supported by the U.S. Bureau of Reclamation. A faculty research grant in 1988 from Eastern Washington University assisted greatly in the compilation of the road log. Careful reviews by F. K. Miller, J. R. Rigby, and H. W. Schasse are greatly appreciated. Trip logistics and publication policies were efficiently and cheerfully handled by Nancy Joseph. Candy Oswald typed an early draft, Dave Andersson drafted Figures 1 and 2, and Judy McMillan did the final drafting on Figures 4 and 5.

REFERENCES CITED

Becraft, G. E.; Weis, P. L., 1963, Geology and mineral deposits of the Turtle Lake Quadrangle, Washington: U.S. Geological Survey Bulletin 1131, 73 p.

Busacca, A. J., in press, Loess deposits of the Palouse and vicinity. *In* Morrison, R. B., editor, in press, Quaternary non-glacial geology of the conterminous United States: Geological Society of America Decade of North American Geology series, v. K-2.

From: Joseph, N. L., and others, editors, 1989, Geologic guidebook for Washington and adjacent areas: Washington Division of Geology and Earth Resources Information Circular 86.

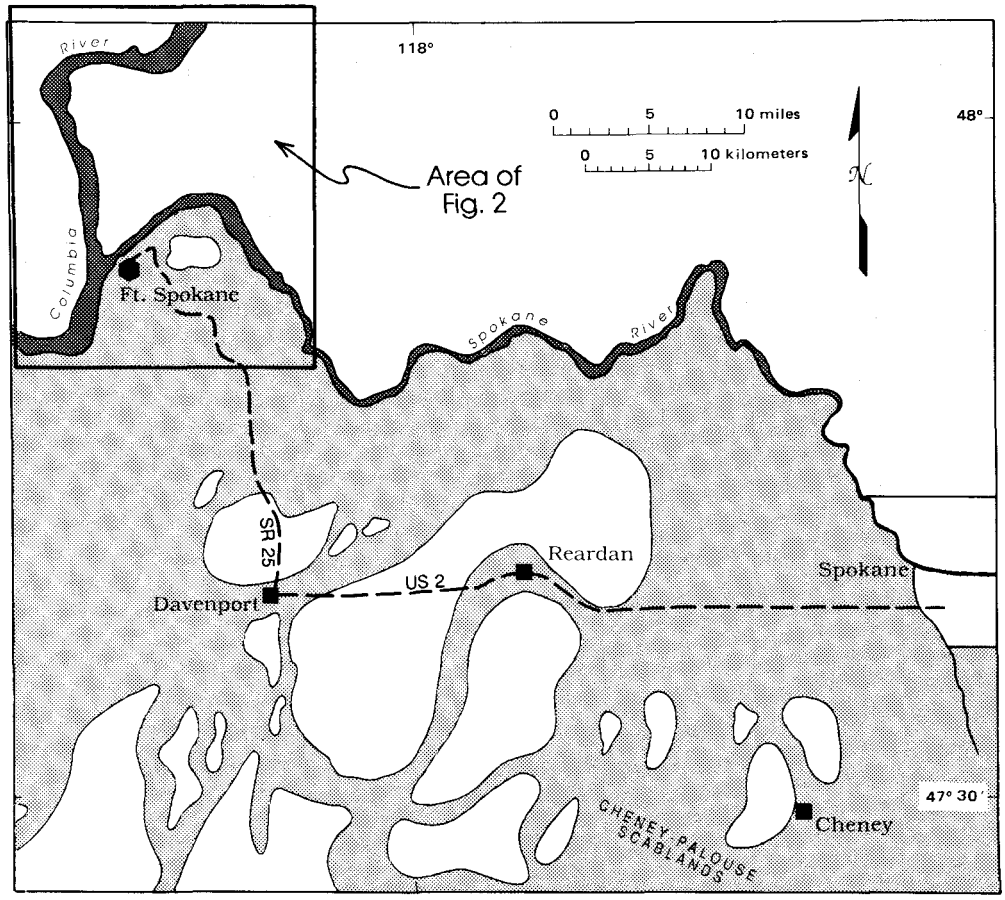

Figure 1. Fieldtrip route to the Fort Spokane area, shown by heavy dashed line. Scablands shown in gray pattern.

Chleborad, A. F.; Schuster, R. L., 1984, Stability of slopes below the Sherwood Uranium Mine, Spokane Indian Reservation, northeastern Washington: U.S. Geological Survey Open-File Report 84-627, 55 p.. 1 pl., scale 1:2,000.

Conners, J. A., 1976, Quaternary history of northern Idaho and adjacent areas: University of Idaho Doctor of Philosophy thesis, 504 p.

Garrey, G. H., 1902, Glaciation between the Rockies and the Cascades in northwestern Montana, northern Idaho, and eastern Washington: University of Chicago Master of Science thesis, 93 p.

Jones, F. O.; Embody, D. R.; Peterson, W. L, 1961, Landslides along the Columbia River valley, northeastern Washington: U.S. Geological Survey Professional Paper 367, 97 p.

Kiver, E. P.; Moody, U. L.; Stradling, D. F.; Rigby, J. G., in press, Late Quaternary stratigraphy of the Columbia Basin and adjacent areas. *In* Morrison, R. B., editor, Quaternary non-glacial geology of the conterminous United States: Geological Society of America Decade of North American Geology series, v. K-2.

Kiver, E. P.; Stradling, D. F., 1982, Upper Columbia River terrace system of eastern Washington–Preliminary interpretations [abstract]: American Quaternary Association Program and Abstracts, p.117.

Kiver, E. P.; Stradling, D. F., 1986, Lake Roosevelt shoreline study–Glacial geology, terraces, landslides, and lineaments: Unpublished U.S. Bureau of Reclamation report, [~90 p., available at Grand Coulee Project Office, Grand Coulee, Washington].

Pearson, R. C.; Obradovich, J. D., 1977, Eocene rocks in northeast Washington–Radiometric ages and correlation: U.S. Geological Survey Bulletin 1433, 41 p., 1 pl.

Richmond, G. M.; Fryxell, R.; Neff, G. E.; Weis, P. L., 1965, The cordilleran ice sheet of the northern Rocky Mountains, and related Quaternary history of the Columbia Plateau. *In* Wright, H. E., Jr.; Frey, D. G., editors, The Quaternary of the United States: Princeton University Press, p. 231-242.

Stradling, D. F.; Kiver, E. P., 1986, The significance of volcanic ash as a stratigraphic marker for the late Pleistocene in northeastern Washington. *In* Keller, S. A. C., editor, Mount St. Helens–Five years later: Eastern Washington University Press, p. 120-126.

Waitt, R. B., 1985, Case for periodic, colossal jökulhlaups from Pleistocene glacial Lake Missoula: Geological Society of America, v. 96, no. 10, p. 1271-1286.

Waitt, R. B.; Thorson, R. M., 1983, The Cordilleran ice sheet in Washington, Idaho, and Montana. *In* Wright, H. E., Jr.; Porter, S. C., editors, Late Quaternary environments of the United States, Volume 1, The Late Pleistocene: University of Minnesota Press, p. 53-70.

Washburn, A. L., 1988, Mima mounds–An evaluation of proposed origins with special reference to the Puget Lowland: Washington Division of Geology and Earth Resources Report of Investigations 29, 53 p.

Road Log

0.0 Begin trip at I-90 and U.S. 2 offramp. *Set odometer.*

0.7 (0.7) Priest Rapids Member of the Columbia River Basalt Group shows excellent, six-sided columnar jointing. Scabland topography along this route was produced by catastrophic Pleistocene floods generated when the ice dam in northern Idaho that held back Lake Missoula failed.

2.2 (1.5) Route continues westward on the west Spokane plains, which have a thin, discontinuous loess cover lying on sand and gravel deposited by the flood waters. Locally, outcrops of basalt protrude through the flood deposits. The west Spokane plains are part of the Cheney-Palouse Scablands (Fig. 1).

3.6 (1.2) Steptoes (kipukas) on the skyline to the left (south) were important in channeling the floods spilling southward.

5.4 (1.8) Proceed through Airway Heights, a strip development of stores and residences primarily serving Fairchild Air Force Base.

7.4 (2.0) Air Force survival school facilities on the left (south).

7.9 (0.5) The route passes through a field of giant current dunes (ripple field). These gravel-cored features can only be generated by floods of catastrophic proportions. Water depths here exceeded 40 m during the fairly short, but violent passage of Lake Missoula floodwaters. A giant ripple field to the southwest contains a Mount St. Helens S ash in the troughs; the ash is overlain by flood sediments. Thus, one or more floods occurred after 13,000 yr ago (Stradling and Kiver, 1986).

8.4 (0.5) Monument on the right (north) commemorates the 1858 Spokane Plains battle in which Col. George Wright's troops defeated the allied Coeur d'Alene, Palouse, and Spokan Indians.

10.6 (2.2) Descend into the valley of Deep Creek, a tributary of the Spokane River. Eolian dunes covering the surface contain Mazama ash from a Crater Lake eruption that occurred about 6,800 yr ago. The dune sand is derived from the underlying, sandy flood sediments. Interbedded varved clay and silt beds about 3.3 km northwest of here at an elevation of about 670 m indicate that one (or more) shoreline of glacial Lake Columbia (the lake produced by an ice dam near or below Grand Coulee) or perhaps glacial Lake Spokane (dammed by ice near Fort Spokane) was nearby.

12.1 (1.5) Twin steptoes to the left (south) near Medical Lake and steptoes to the southwest near Reardan.

13.5 (1.4) The road ascends onto the loess upland that was partially inundated by floods but was above the elevation of effective erosion. Erratic cobbles and boulders in the area were probably rafted into position by icebergs that grounded here during the Missoula Floods.

15.8 (2.3) Hanning and Magnison buttes (steptoes) to the left (south). The pre-Tertiary bedrock on Magnison Butte contains gold.

19.3 (3.5) Enter the town of Reardan. Note the small scabland channel to the right (north). This ephemeral stream is a headwater of Crab Creek, the only local stream to cross the plateau. Also note Mima-like mounds composed of silt along the road. The origin of the mounds is controversial but may be associated with runoff erosion combined with vegetation anchoring, swelling clays, eolian or periglacial processes (Washburn, 1988). Proceed through Reardan on U.S. 2.

22.6 (3.3) The road climbs onto a broad loess upland on which are pre-Wisconsin paleosols with petrocalcic horizons. The upland separates the Cheney-Palouse Scabland tract from the Davenport-Creston tract farther west. Loess is thinner here than in the southern Palouse because this area is north of the major source areas and the prevailing winds are from the southwest. Low annual rainfall necessitates dry-land farming techniques.

31.2 (8.6) Grain elevators in Davenport are visible to the southwest.

32.3 (1.1) Turn right (north) onto State Route (SR) 25 toward Fort Spokane. A large gravel pit in flood gravels is to the east. The thin, discontinuous loess cover on basalt gives way to thicker loess in upland areas.

35.3 (3.0) Reddish-brown paleosols are visible in roadcuts. Similar buried soils are present in numerous cuts between here and Fort Spokane. Loess-covered steptoes on the left and right sides of the road.

37.4 (2.1) Roadcut through loess-covered, pre- or early Tertiary granitic rock along the flank of a steptoe.

38.4 (1.0) Descend into the Davenport-Creston Scabland tract. Well-developed Mima-like mounds and youthful-appearing scabland topography occur locally.

39.3 (0.9) Highly weathered pre-Wisconsin flood gravel deposits with a strongly developed B horizon crop out immediately north of a fresh-appearing scabland channel. At least two buried paleosols are present in gravels in this outcrop. The oldest paleosol has a well developed, angular, blocky structure and clay skins. The upper soils are gravelly-clay loams. Granitic and basaltic clasts are so deeply weathered that no weathering rinds are discernible. Loess hills in the Davenport-Creston tract are elongated northeast to southwest, reflecting the direction of flood currents.

39.6 (0.3) Basalt lacking loess cover suggests inundation by late Wisconsin floods. Note the well-developed Mima-like mounds.

40.8 (1.2) This deep roadcut exposes five pre-Wisconsin paleosols in loess. The second from the top has a B horizon that has a high secondary calcium carbonate content.

43.8 (3.0) Turn left onto the gravel road, toward Stop 1.

44.2 (0.4) **STOP 1. Inkster Lake flood gravel pit.**

Flood water ascending Green Canyon from the Spokane River valley topped the divide at Inkster Lake (elev. 745 m) about 800 m north of here, creating a scour depression in the narrowest section of the canyon. The pass is the lowest point on the northeastern border of the 38-km-wide Davenport-Creston Scabland tract. Angular joint blocks and rounded core stones were ripped loose from the deeply weathered granitic outcrops to the north and deposited here by the Missoula floods.

Blockage of the Columbia and Spokane river valleys to the north and east during pre-late Wisconsin time helped divert considerable floodwater into this scabland tract. Late Wisconsin floods also topped many divides and spilled southwest through the Davenport-Creston tract into the Crab Creek channel. The largest boulders here are 2 m long, but flood erratics more than 4 m long have been found nearby. Transport distance of the largest boulders is probably less than 1 km. Nearby streamlined loess hills suggest flood crests were at least at elev. 793 m. Thus, flood depth through the Inkster Lake spillway exceeded 47 m.

Gently dipping foreset beds in the poorly sorted and poorly bedded sediments in the gravel pit walls indicate south- to southwest-directed currents. Numerous clasts of quartzite and other lithologies foreign to the area indicate an original source in the nearby Northern Rocky Mountains, but the gravels are likely redeposited from localized occurrences of glacial materials.

An Inceptisol (weakly developed B horizon) developed within the upper gravels indicates that late Wisconsin floods flowed through the Inkster Lake spillway. Weathering rinds on basalt clasts in the B horizon have thicknesses of less than 0.05 mm. Deep weathering of many granite and andesite clasts indicates reworking of older outcrops and deposits and short transport distance. Striated clasts here are very rare.

Return to SR 25.

44.6 (0.4) Turn left, back onto SR 25. Note the large granite erratics at the edge of the field.

44.8 (0.2) Deeply weathered granitic outcrops here could be the source of core stones found in local flood sediments.

45.2 (0.4) Turn right, toward Porcupine Bay. Leave SR 25.

45.5 (0.3) Deposit on the left is interpreted as Bull Lake till by Conners (1976). A thin veneer of rounded, commonly striated rocks overlies pre-Wisconsin loess and grus. A recent colluvial deposit containing striated cobbles is exposed in

the roadcut, but no unequivocal till was found. The road follows Green Canyon toward the Spokane River valley.

46.2 (0.7) Mafic dikes in granitic bedrock.

46.4 (0.2) Felsic dike in granitic bedrock.

47.4 (1.0) View (straight ahead) of presently inactive Sherwood uranium mine on the Spokane Indian Reservation. Large spoil piles on top of flood sand and lacustrine clays along the edge of valley wall create a potential pollution and landslide hazard (Chleborad and Schuster, 1984).

47.8 (0.4) Flood sands and gravels deposited in a glacial lake.

48.1 (0.3) Turn right onto a gravel road.

48.4 (0.3) Turn left onto a dead-end road. Note the extensive Sand Flat terrace system.

49.0 (0.6) Note the edge of a terrace at elev. 488 m to the east and the sequence of terraces on the opposite side of the Spokane River. Interpreting the terraces and their sediments is critical to properly understand Quaternary events in the Columbia River drainage system. The road descends from a 463-m terrace and continues past a farmhouse.

50.0 (1.0) Turn right at the Y. Good view of the Spokane River and terraces across the river. Descend from the 451-m terrace, which is capped by coarse flood gravels.

50.3 (0.3) Go through a farm gate.

50.4 (0.1) **STOP 2. Sand Flat boulder field.**

Park vehicles along the road and walk toward large boulders at the edge of a terrace at 402 m. Caution—steep cliffs!

This concentration of large, rounded boulders is one of six similar areas along Franklin D. Roosevelt Lake (the reservoir upstream of Grand Coulee Dam along the Columbia and Spokane Rivers) that are not of landslide origin. The largest boulder here is a 9-m-long granitic boulder, but andesite, quartzite, and other lithologies are present. The boulders are weathered, heavily spalled, and frost split, suggesting an age greater than late Wisconsin. Smaller rocks commonly have glacially snubbed forms, but no striations have been seen.

The boulders are at the edge of a terrace at elev. 402 m, although the 439-m terrace near here also locally displays a boulder concentration on its edge. The pool width of the reservoir increases dramatically both upstream and downstream of the boulder concentration where the resistance of the terrace to erosion abruptly decreases.

The boulder concentration here is believed to represent the southern terminus of a pre-late Wisconsin glacier that emerged from the Enterprise Valley about 12 km downstream (Fig. 2). Catastrophic floods later redistributed and reorganized the glacial debris. Sediments from glacial Lake Columbia buried the older deposits, and late Wisconsin and Holocene streams cut down and re-exposed them.

The boulders rest on, and are embedded in a coarse flood gravel displaying steep foreset beds as much as 8 m high (Fig. 3). An interbedded lag gravel layer and a thin, discontinuous bed of lacustrine sand indicate that two or more flood events occurred. The foreset beds are locally discernible in the terrace edge across the reservoir but are best seen on the south side in the bluff from a boat or by walking the base of the cliff when the reservoir is low enough to form a passable beach. Local pods of clast-supported, silt-matrix diamicton may be a water-laid till (deposited in a glacial lake) or perhaps a debris flow.

Retrace field trip route toward the Porcupine Bay turnoff on SR 25.

52.0 (1.6) Note the flood-scrubbed surfaces on the flank of Pitney Butte straight ahead (west). Immature soils at the butte summit indicate that late Wisconsin floods topped the butte whose summit is at an elevation of 808 m. Similar flood erosion limits upstream in Spokane suggest that there was very little slope in the floodwater surface between these two areas.

55.6 (3.6) Junction with SR 25. Turn right toward Fort Spokane. Columbia River basalt outcrops are on both sides of the road.

57.4 (1.8) View of Lilienthal Mountain (elev. 1,088 m) near Fort Spokane directly ahead. Lilienthal

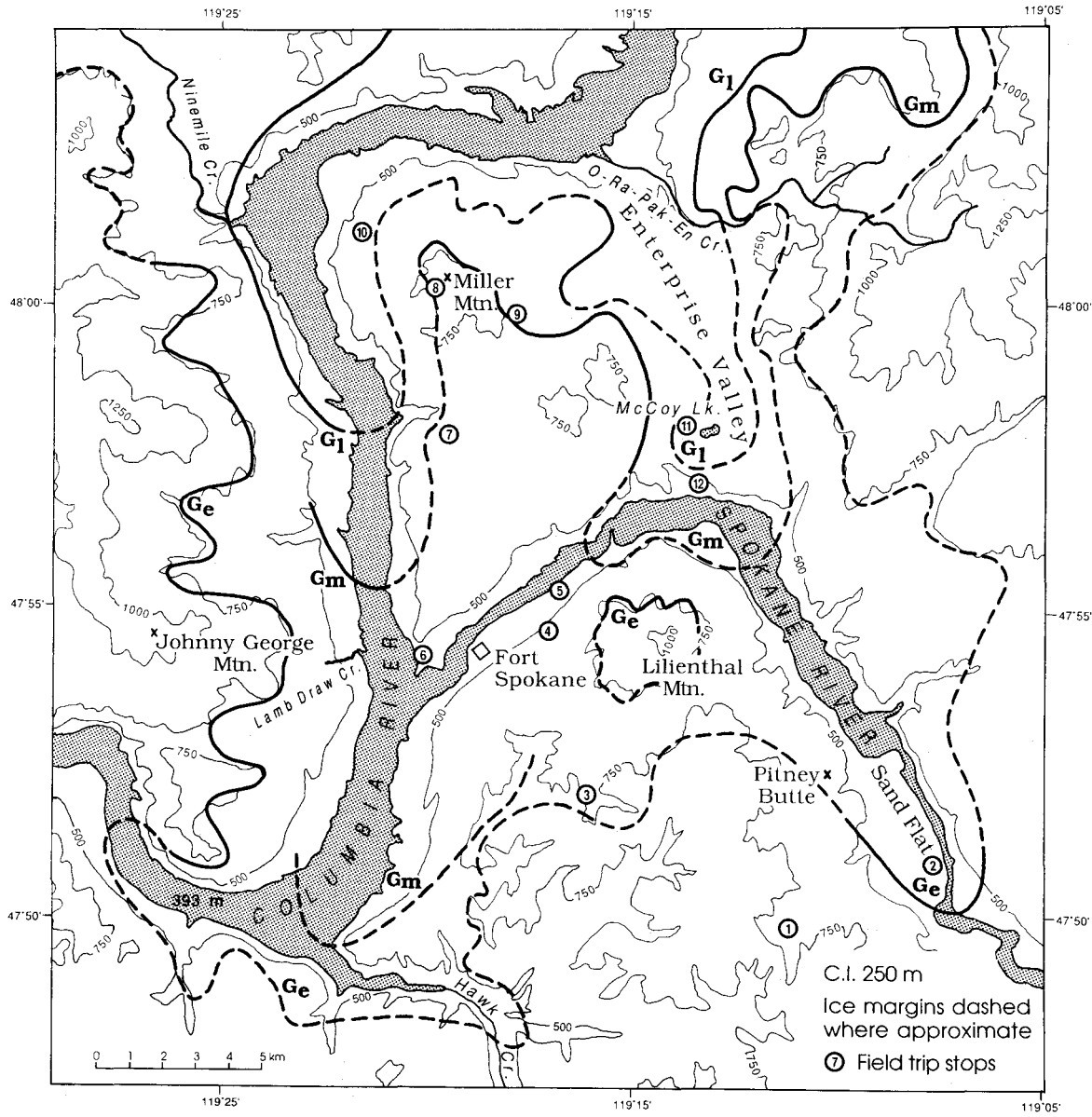

Figure 2. Ice-margin map of the Fort Spokane area. Ge, early glaciation(s); Gm, middle (intermediate?) glaciation(s); and Gl, late glaciation(s). Place names on this map are referred to in the road log. Stop 1, Inkster Lake; Stop 2, Sand Flat; Stop 3, Bockemuehl Canyon; Stop 4, Fort Spokane; Stop 5, Jackson Springs; Stop 6, confluence of rivers; Stop 7, Peters Road; Stop 8, Miller Mountains; Stop 9, West Enterprise Valley; Stop 10, Tavis Canyon; Stop 11, McCoy Lake; Stop 12, McCoy's Marina.

Mountain was a nunatak during older glaciations and stood well above the catastrophic flood levels. Johnny George Mountain is to the northwest.

59.7 (2.3) Christ Lutheran Church, constructed in the early 1890s, on the left; pillow basalts on the right.

60.5 (0.8) Begin the descent into Bockemuehl Canyon through exposures of the Columbia River Basalt Group.

61.4 (0.9) **STOP 3. Upper Bockemuehl Canyon till.**

Turn left onto the dead-end road and park. The till exposure is 0.15 mi from here, but a narrow shoulder there makes parking difficult.

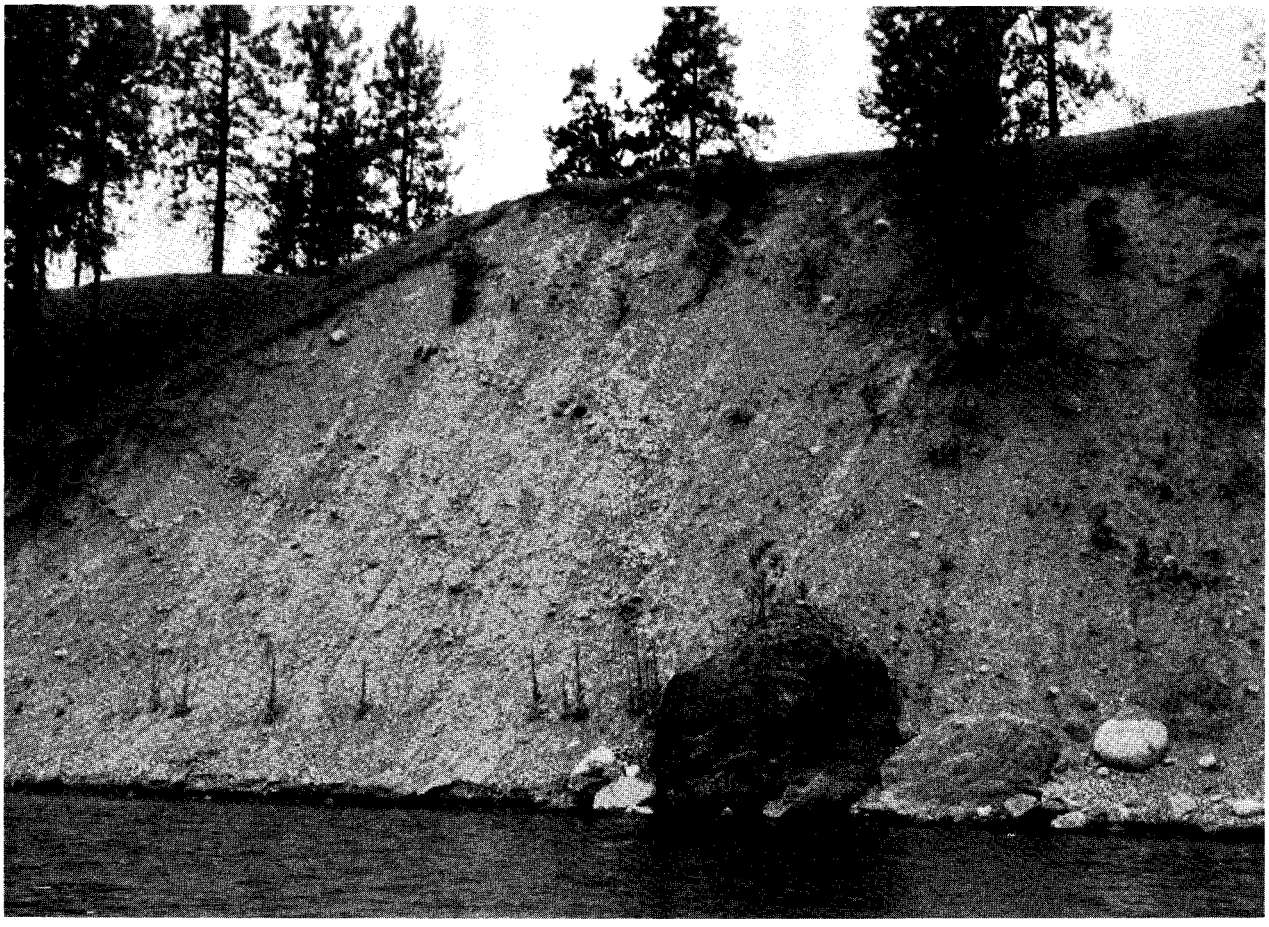

Figure 3. Sand Flat flood gravels. Note 2-m-long boulder at the base of the bluff and foreset beds.

Walk down the highway, past milepost 18 to just beyond a spring.

The till contains numerous striated rocks and rests on basalt in the upper part of the canyon. The B horizon in the paleosol is a yellow-brown to red-brown sandy loam and is moderately indurated by iron oxide. Clay skins on the ped surfaces thicken with depth. The soil is an Alfisol and is early Wisconsin or, more likely, pre-Wisconsin in age. Pre-Wisconsin ice must have extended across the Spokane River valley and pushed at least to the edge of the Columbia Plateau.

Return to the vehicle and continue the descent through the canyon.

62.2 (0.8) Emerge from the canyon. Old landslide material involving Latah Formation, Columbia River Basalt Group, and till occur in next few outcrops. The deep red color is old residual soil developed on basalt. Local blocks of till display a mid-Wisconsin(?) soil. The age is based on the thickness and development of the B horizon.

62.9 (0.7) Roadcut through the edge of the landslide; undisturbed Latah Formation lies underneath. Note the large basalt slide block on the landslide toe.

63.2 (0.3) The dune-covered surface at an elevation of 585 m is underlain by flood sand interbedded with lacustrine clay. Note the flood-scoured surfaces along the flank of Lilienthal Mountain to the right (east). Floodwaters spilled northwestward from the Spokane River valley over a pass on the flank of Lilienthal Mountain and across this surface.

65.3 (2.1) **STOP 4. Fort Spokane overlook.**

Park on the highway turnout to the right (north).

The panoramic view here looks across the confluence of the Spokane and Columbia Rivers to Johnny George Mountain (the mountain with the lookout tower) on the Colville Indian Reservation and north across the Spokane River to the Spokane Indian Reservation (Fig. 4). Lilienthal Mountain on the south side of the Spokane River is visible upstream, and the broad opening of the Enterprise Valley is just out of view to the northeast.

Other prominent features include flows of the Columbia River Basalt Group on the upper slopes of the hill across the Spokane River, the Mesozoic-Tertiary granitic rocks unconformably beneath the basalt, the large Jackson Springs landslide, and the parade grounds and buildings of Fort Spokane on the terrace between the overlook and the river confluence.

Mountains here contain mostly Proterozoic and lower Paleozoic rocks intruded by Cretaceous plutons. Structural elements generated or reactivated during and after the Laramide control the position of many stream segments.

Major drainage changes were caused by the eruption of the Sanpoil Volcanics beginning about 51 m.y. ago (Pearson and Obradovich, 1977) and by the Columbia River basalts during the Miocene. The Sanpoil Volcanics blocked the Enterprise Valley and diverted the ancestral Columbia River westward to near its present channel. The Columbia River basalts pushed drainages northward against the Rocky Mountains and partially filled the channel segment north of Fort Spokane, thus diverting the river back into the Enterprise Valley. Pleistocene glaciers blocked the Enterprise Valley and diverted the river back to its present channel. The floor of the Enterprise Valley is perched about 155 m above the Spokane River valley on the south and the Columbia River valley on its north end.

Numerous terraces lining the margins of the Columbia River drainage system record the changing base level produced by downstream ice dams and the lowering of the bedrock lip (now at 465 m) at Grand Coulee (Kiver and Stradling, 1982). Terrace elevations tend to cluster around 573, 518, 480, 426, 412, and 402 m (Fig. 5). The 573-m terrace was formed during ice blockage in the Fort Spokane area by a pre-late Wisconsin glaciation. Terrace remnants are confined to the Fort Spokane area and upstream in the Spokane River valley where they survived late Wisconsin floods. The 518-m terrace (Lake Columbia II of Waitt and Thorson, 1983) is the former lake bed of glacial Lake Columbia and formed after the Okanogan Lobe retreated from the Grand Coulee and before the lip of the coulee was eroded to a lower level. Erosion of the lip accounts for terrace levels down to the 465-m elevation (Lake Columbia III of Waitt and Thorson, 1983), although isostatic rebound could account for both slightly lower and higher

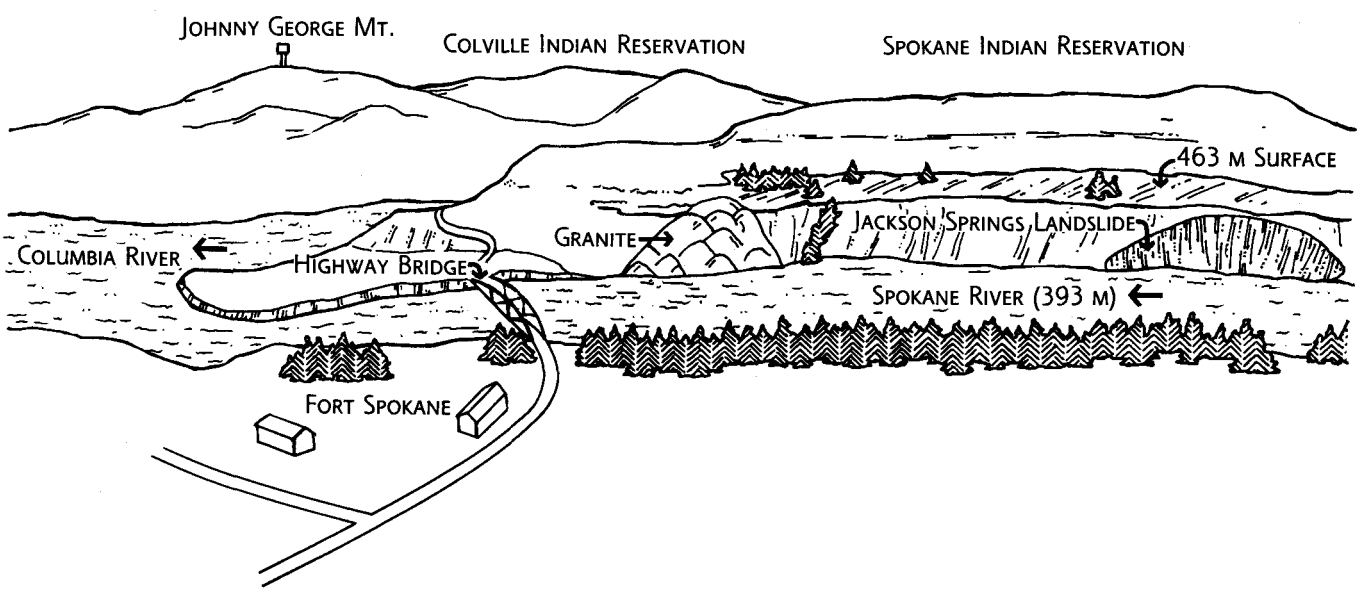

Figure 4. Panoramic view from the Fort Spokane overlook on Washington State Route 25.

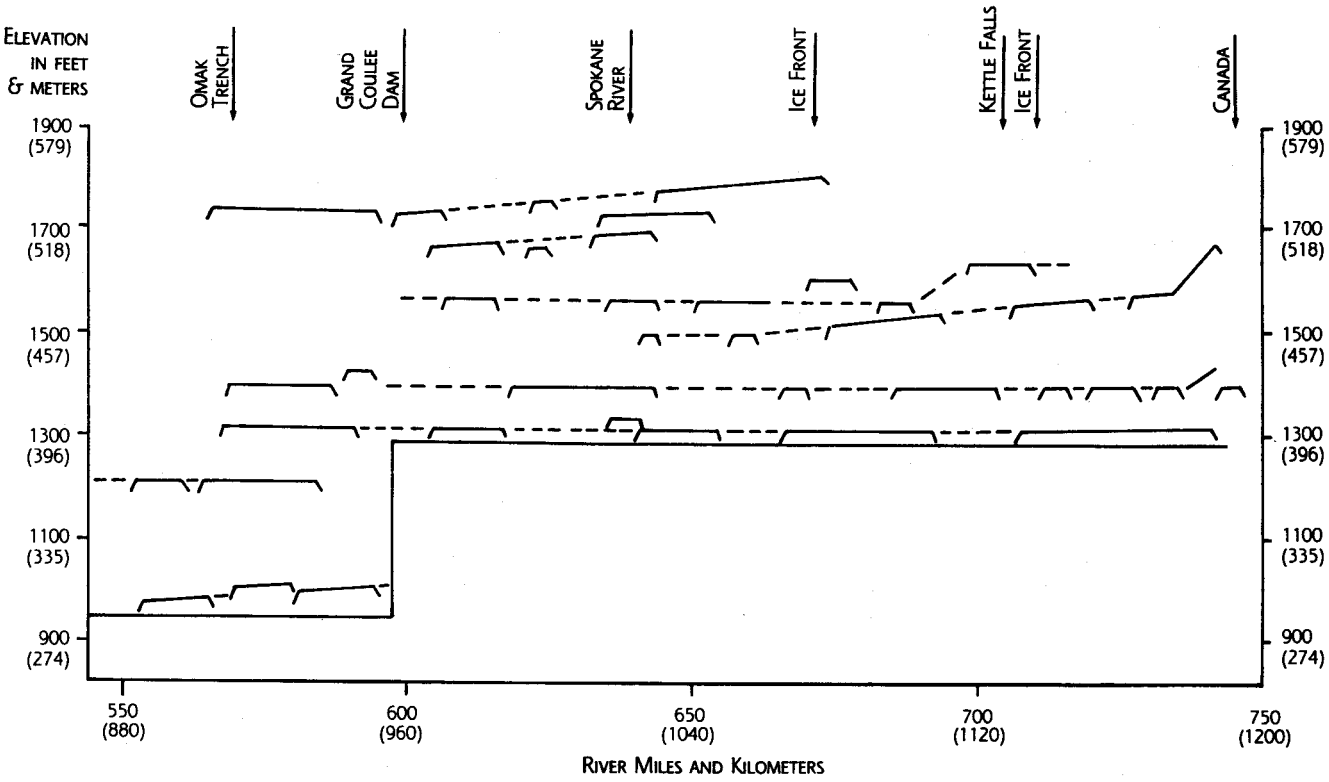

Figure 5. Generalized terrace profiles along parts of the upper Columbia River valley.

terraces. Terraces below elev. 460 m were controlled by the thickness and position of the Okanogan ice lobe or by downstream debris dams. The 426-m Lake Columbia IV (Waitt and Thorson, 1983) and lower terraces are capped by flood-reworked sand and gravel alluvium, although many higher terraces in the Spokane River valley, where flood energy was greater, display gravel caps in the form of pendant bars.

Three major groups of glacial deposits, distinguished by their ages, are recognized in the upper Columbia River valley area (Fig. 2): old (pre-Wisconsin), intermediate (middle Wisconsin or older), and young (late Wisconsin). The oldest glaciation (which may include more than one glacial event) was the most extensive of the three and is identified by highly indurated and weathered patches of till, many of which have reddish-brown, clay-rich soils. The deposits of intermediate age have less pedogenic development, less oxidation, and generally display a subdued morainal topography. Many of the young deposits show strong geomorphic form and thinner, less developed soils.

Construction of Grand Coulee Dam began in 1933, and filling of the reservoir was completed in 1941. In the first few years of filling the reservoir behind the dam, partial submergence of Pleistocene sediments along the valley wall produced hundreds of landslides. Approximately 80 percent of the 960-km shoreline is lined by Pleistocene sediment, and most of these areas have moderate to high slope stability problems (Jones and others, 1961; Kiver and Stradling, 1986). The Jackson Springs landslide across the Spokane River is the largest historic slide (11.5 m^3 x 10^6 of debris) along the reservoir. It failed on March 26, 1969, when the reservoir was at an unusually low level. Debris crossed the river to the left bank, pushing the channel southward. Undercutting, in turn, caused failure along the left bank beginning 2 days later.

Continue down the highway toward Fort Spokane.

66.2 (0.9) Turn right onto a paved road at the bottom of the hill. Proceed east through the historic town of Miles and onto a 439-m terrace. Small alluvial fans descend from the hills to the right.

67.5 (1.3) Continue straight at the Y in the road.

67.6 (0.1) Continue straight at another Y, onto a dirt road.

67.9 (0.3) **STOP 5. Jackson Springs landslide and terrace stratigraphy.**

Park at the refuse area.

The road behind the barrier leads to a sand pit where flood sediments interbedded with lacustrine clay beds can be observed. The flood sediments were deposited in a lake; planar bedding, rip-up clasts of fine lacustrine sediment, armored mud balls, and ice-rafted cobbles and boulders can be seen here. The graded and reverse-graded sediments and the numerous rip-up clast zones between fine lacustrine layers suggest that catastrophic flood energy changed appreciably during a single flood and that one-graded-bed-per-flood, as suggested by Waitt (1985), may not be the rule during all catastrophic floods.

The gravel cap on the terrace is clast supported and poorly sorted and locally displays crude bedding. Imbrication of clasts and other current-direction indicators are rare.

Similar gravel caps are present on all 439-m and lower terraces. Locally, particularly in the Spokane River valley, gravel caps also occur on higher terraces. The cap formed initially as alluvium as streams cut through the late Wisconsin valley fill and was later mixed and redistributed by late floods or was left as a lag deposit after finer sediment was winnowed from the gravel.

Walk downstream (southwest) across the Mima-like mound-covered terrace surface and carefully approach the steep, in some places overhanging edge of a landslide scar. *Use extreme caution here!*

Note the vegetated remnant of an older scar and landslide debris immediately upstream from the Jackson Springs landslide across the river. In addition to a low reservoir level (27 m below normal pool elevation) and thus greater relief from the top of the terrace to the reservoir, several other factors contributed to the Jackson Springs landslide. These included: (1) steep slopes, (2) ground-water loading in the spring after a record snowfall winter, (3) the presence of impermeable clay layers (suggested by the two bands of greener vegetation where small springs seep to the surface during wet times of the year), and (4) thick gravel layers indurated by calcium carbonate cementation near the clayey lake layers. The deposits here, as in most areas of the downstream part of the reservoir, contain clayey, varved sediments deposited in glacial Lake Columbia; these are separated by thick sand units deposited by Missoula Floods spilling into the lake. Varve counts indicate that floods occurred, on the average, every few decades. The source of the gravel in the cap is alluvium and locally, especially downstream of the Enterprise Valley, glacial moraine material reworked and redeposited by floods.

Missoula Floods were especially erosive where the larger floods flowed through valley segments lacking deep glacial lakes. Erosive energy was also high on the outside of river bends, where previously deposited sediment and rock debris tended to be cleaned off by flood waters. The segment of the large bend in the Spokane River valley from downstream of the Enterprise Valley to this site is a good example. An interesting granite scabland containing numerous water-filled depressions begins about 1 km east of Jackson Springs (northeast of the view point) and extends up to an elevation of 732 m. A pendant bar caps the Jackson Springs landslide surface, and the low ridges on the slope behind the landslide are likely giant current dunes deepened on the open valley side by small, ephemeral streams.

Return to SR 25.

69.5 (1.6) Intersection with SR 25. Turn right onto the paved road toward Fort Spokane. Descend through the gravel cap of a 427-m terrace onto the 402-m terrace.

70.3 (0.8) Cross the Spokane River on the highway bridge over a narrow, superimposed bedrock channel. Reservoir depth here is 82 m.

70.8 (0.5) Road follows the edge of a 1985 landslide that involved a lacustrine clay and flood sand section.

71.2 (0.4) **STOP 6. Confluence view point.**

Turn left into the view point by the bend in the road.

This stop offers an excellent panoramic view of the confluence but not a good place to be during a Missoula flood! The pre-Wisconsin glaciers and those of intermediate age smoothed and elongated the granitic slopes into whaleback

forms below 732 m; these can be seen on the east flank of Johnny George Mountain directly across the Columbia River valley from here. Local till remnants and an area of subdued moraine topography along George Creek just south of Johnny George Mountain (Fig. 2) record ice extent. Pre-Wisconsin ice is estimated to have reached a point downvalley of Hawk Creek (Fig. 2); a middle Wisconsin or pre-Wisconsin advance probably terminated just this side of Hawk Creek. A middle Wisconsin(?) ice front is marked by a bouldery diamicton due west of this site near Lamb Draw Creek. The late Wisconsin ice terminated near Castle Rock Creek, some 7 km north.

From near the mouth of the Spokane River to about 3.3 km upstream on the Columbia River (right bank) just north of Threemile Creek is a concentration of large boulders. The boulders locally overlie a cobbly flood gravel that has north-dipping foreset beds. The relation here is similar to that at Sand Flat except that the large boulders appear to rest on the flood deposit rather than being part of it. The deposit is interpreted as the result of an intermediate-age (middle Wisconsin?), north-flowing, subaerial flood followed by a glacial advance into a valley lacking a glacial lake. An alternative explanation for the boulder field is that it is part of an expansion bar formed by a late subaerial flood emerging from the mouth of the Spokane River valley.

All of the major terrace levels discussed at Stop 4 are visible, including remnants of the ~518-m terrace that steepens and rises as it approaches the Castle Rock ice position.

The prominent landslide scar to the southeast across the reservoir reveals interbedded lacustrine and flood sand units and three coarse lenses of basalt gravels that slid from the cliffs behind into glacial Lake Columbia. Directly to the right (north), below the confluence viewpoint, is a landslide alcove. Erosion has removed much of the landslide debris that formerly protected the slope, and wave action is now steepening the slope, all of which will eventually initiate another episode of slope adjustment.

The lowest basalt outcrops upstream along the Columbia are at 488 m, and downstream near Hawk Creek (southwest) in the far distance, they are at and below reservoir level (393 m). Thus, an important drainage system existed to the south near Hawk Creek prior to the Miocene flood basalt eruptions. Return to SR 25 and proceed north.

72.2 (1.0) Landslide debris in roadcuts includes Latah Formation, Columbia River basalt, and older tills for the next 2 km.

73.9 (1.7) Large basalt landslide blocks along the road.

74.7 (0.8) For the next 1.8 mi, an unusually old loess is overlain by till.

75.5 (0.8) **STOP 7. Peters Road pre-Wisconsin sediments.**

Turn right onto a farm road and park. Caution—Slight hill obscures view of oncoming traffic.

Approximately 20 cm of loess overlies a thin, discontinuous till. Tillstones have well-developed, snubbed forms, but striations are poorly preserved. The till in turn rests on a thick (at least 8 m locally) loess with a red-brown, strongly argillic subsoil.

Soil developed within the till is an Alfisol. The B horizon is a clay with strong columnar structure and thick, continuous clay skins. The soil development suggests an early Wisconsin or older age.

The rolling surface here is at about 744 m elevation and forms the drainage divide between the Columbia and Spokane Rivers. This area may have been inundated by Missoula Floods, but erosion was minimal because of shallow water depth and protection by rock hills to the east.

Return to the vehicles and continue north on SR 25.

76.6 (1.1) Road passes through older outwash and till outcrops.

76.9 (0.3) Miller Mountain and an outwash channel draining toward Castle Rock Creek on the left.

77.3 (0.3) Here the road crosses the terminus position of the middle Wisconsin(?) west Enterprise Valley glacier. Low end moraines and ground moraine continue for the next 3.5 km.

77.5 (0.3) Turn left onto a gravel road toward Miller Mountain. The road follows the former terminus of a middle Wisconsin glacier. Note large erratics (to 11 m long). Low moraine ridges and

shallow depressions are abundant. The gravel pit on the right is in outwash.

78.0 (0.5) Continue straight at the intersection toward Miller Mountain.

78.4 (0.4) Large glacial erratics of pre-Wisconsin age along the road.

78.8 (0.4) Proceed straight ahead at the intersection, over the cattle guard. This road is not recommended for cars with low clearance. Entering an area of glacial outwash from the west Enterprise Valley lateral moraine.

79.1 (0.3) Leave the outwash and enter an area of pre-Wisconsin soils developed in loess with a thin veneer of till stones.

79.5 (0.4) Highest occurrence of glacial rock veneer (814 m). No rounded rocks, tillstones, or other evidence of glaciation above this elevation.

80.2 (0.7) Road leaves the drainage divide between Enterprise Valley to the right (east) and the Columbia River valley to the left (west).

80.5 (0.3) **STOP 8. Miller Mountain summit (elev. 950 m).**

Tree growth since the abandonment of the lookout tower has obscured the vista and requires one to change locations to see clearly in different directions. The Columbia River valley separates the southern extension of the Kettle mountains on the west from Huckleberry Mountain to the east. At Whitestone Ridge (highest point 1,452 m at lookout tower visible to the west), pre-Wisconsin ice flowed up Ninemile Creek around the north end at about 762 m elevation into Friedlander Meadows and southward toward the Columbia River. Gold Mountain (elev. 1,429 m) to the northwest (with the lookout tower) was a nunatak in pre-Wisconsin time.

Just below the summit of Miller Mountain is a relict soil whose development indicates an early Pleistocene or older age. The profile is more than 1.5 m thick; displays well developed, blocky ped structure; has thick continuous clay skins; has loess and colluvium mixed in the upper part of the profile; and has a yellowish-brown (10 YR 5/4) color grading downward to a reddish brown (5 YR 4/4). The B horizon grades from a silt loam downward to a clay loam.

The Columbia River ice lobe flowed south along a major lineament and spilled into its southward continuation, the Enterprise Valley. Greater ice height and a more extensive front in the Enterprise Valley, compared to the Columbia River valley, indicates that ice flowed more effectively into the Enterprise Valley.

Miller Mountain was a nunatak in pre-Wisconsin time; ice reached about 814 m on the south side and 823 m on the north. Two younger moraines wrap around the north end of Miller Mountain; the higher one (801 m) is of intermediate age, and the lower (670 m) is late Wisconsin and connects with moraines and sediments of the late-Wisconsin Castle Rock and McCoy Lake (Enterprise Valley) ice positions. Kame terrace sediments along the edge of the "Tavis Canyon" surface immediately to the west of Miller Mountain and the sequence of descending surfaces on the north end of the Tavis Canyon surface were formed as the Wisconsin glacier decreased in thickness. While the glacier at Castle Rock Creek was calving and building a kame delta into glacial Lake Columbia, lateral moraines were forming subaerially a short distance upstream at Ninemile and Wilmont Creeks. Thus, assuming no, or very little isostatic rebound, the surface of glacial Lake Columbia II was between 549 m (the depositional surface in front of the calving glacier) and 585 m (the elevation of the lateral moraine) during the Castle Rock (late Wisconsin) ice advance.

The Columbia River ice lobe experienced a number of significant stillstands and at least one re-advance during its retreat to Canada. Just south of Hunters, before the major channel bend visible to the north, is the Hunters ice position, where a kame delta and till record a stationary position of the glacier. Stagnation and downwasting allowed local lake sediments to accumulate in kame terraces that are as high as 549 m in the massive bluffs just visible along the river about 15 km to the northeast. Melting of the stagnant ice permitted the waters of glacial Lake Columbia III (476 m) to follow the retreating ice northward.

Numerous landslide scars are visible in the river bluffs, and some large slope failures occurred along the edge of the high kame terrace surfaces near Ninemile and Wilmont Creeks to the west across the river. Jones and others (1961) attribute much of the instability there to groundwater flow in buried tributary channels.

Return to the intersection of gravel roads near the west Enterprise Valley terminal moraine.

82.9 (2.4) Turn left (north) at the intersection. The road follows outwash gravels and climbs onto a lateral moraine of middle Wisconsin(?) age.

83.4 (0.5) **STOP 9. West Enterprise Valley lateral moraine.**

The erratic-studded moraine here has good topographic expression and an Alfisol with a moderately well developed B horizon about 35 cm thick. The ped surfaces have discontinuous, thin clay skins, with moderate blocky structure and a sandy clay loam texture. The degree of soil development suggests a middle Wisconsin age.

The moraine (elev. 707 m) was topographically protected from effective erosion by Missoula Floods and was first recognized in 1901 by Garrey (1902). Basalt erratics, some of which are larger than 10 m in diameter, were torn from a basalt hill to the northeast. A number of low, nested moraines downslope to about 616 m represent recessional ice positions.

The existence of a middle Wisconsin glaciation in the Pacific Northwest is controversial; Busacca (in press) and Kiver and others (in press) summarize evidence for such an event.

Continue north on the gravel road.

83.9 (0.5) The roadcut to the right has a middle Wisconsin(?) till overlying a pre-Wisconsin till. The road descends across a number of recessional moraines of middle Wisconsin(?) age. Miller Mountain is to the left (west).

84.8 (0.9) Core stone in granite on the left.

84.9 (0.1) Turn left (west) on a paved road toward Miller Mountain. The road traverses moraines of middle Wisconsin(?) age. Note the glacial erratics.

86.8 (1.9) The road proceeds through a pass where middle Wisconsin(?) ice spilled from Enterprise Valley into the Columbia River valley. An ice fall and meltwater stream flowed westward toward the Tavis Canyon surface in the Columbia River valley.

87.7 (0.9) **STOP 10. Tavis Canyon surface.**

Park on the left side of the road across from the gravel pit.

The gravel pit here exposes outwash beds (kame deposits?) dipping westward overlain by a rocky till deposited in water. The sweeping beds of poorly sorted sand and gravel were deposited by meltwater derived from the middle Wisconsin(?) glacier in the pass to the east. The late Wisconsin Castle Rock glacier covered the Tavis Canyon surface, depositing the rocky till and helping to create some of the drumlinoid landforms on its surface.

The weakly developed soil on the till suggests a late Wisconsin age. Depending on soil-forming factors, late Wisconsin surfaces can have Inceptisols, Entisols, or thin Alfisols.

Retrace the route eastward back up through the pass and over middle Wisconsin(?) moraines. A bold, late Wisconsin terminal moraine is visible in the open field about 500 m to the left (south), east of the pass.

90.6 (2.9) Intersection. Continue straight ahead. Note rolling moraine topography and closed depressions.

91.9 (1.3) Roadcut through a ridge in pre-Wisconsin till. Middle Wisconsin ice overrode and streamlined the older till deposit.

92.1 (0.2) Intersection with SR 25. Turn left.

92.4 (0.3) The road crosses a low, late Wisconsin end moraine.

93.6 (1.2) Turn right at the intersection, toward Fruitland Bible Camp. The road drops into an extensive area of closed depressions that continues southward for more than 6 mi to the McCoy Lake area.

94.7 (1.1) Intersection. Turn right (south), toward McCoy Lake.

95.4 (0.7) Enter the Spokane Indian Reservation. McCoy Lake depression continues to the right (west). A large stagnant mass of late Wisconsin ice occupied the Enterprise Valley and helped protect it from major invasions by Missoula Floods.

97.4 (2.0) Lilienthal Mountain straight ahead.

97.9 (0.5) Our Lady of Lourdes Church, built in 1938.

98.1 (0.2) Turn left on reservation road 57, which leads down to the deepest part of the McCoy Lake depression.

98.4 (0.5) **STOP 11. McCoy Lake.**

McCoy Lake (elev. 502 m) lies in a closed depression more than 34 m deep located near the south end of the Enterprise Valley. Sanpoil volcanic rocks crop out on the north and east sides, and a mass of sediment with a flood-worked surface separates the lake from the Spokane River valley 1.8 km to the south. Eolian sand covers most of the flood-worked surface, but exposures of bedrock, lacustrine sand, and flood gravels can be found.

The lake depression could have been shaped by either glacial erosion or flood scour. The presence of the depression supports the hypothesis that the Enterprise Valley contained a large mass of protective ice when some of the later floods occurred. Without such an ice mass, the McCoy Lake depression would have filled with flood sediment. McCoy Lake is believed to be near the maximum late Wisconsin ice position. Floods swept across the stagnant ice and through the Enterprise Valley, as indicated by foresets in flood sands and coarse, poorly sorted gravels on the north end of Enterprise Valley along and near O-Ra-Pak-En Creek.

Retrace the route back to the main road. Note the thick accumulation of Mazama ash along the dirt access road.

98.8 (0.4) Turn left onto the main road. An intrusive phase of Sanpoil Volcanics crops out along the road (Becraft and Weis, 1963).

99.6 (0.8) McCoy Lake depression continues to the left (east).

99.8 (0.2) Entering unincorporated tribal village.

100.0 (0.2) Turn right onto a paved road.

100.1 (0.1) Turn left onto a gravel road toward McCoy's Marina. The road follows McCoy Creek. Eolian sand overlies flood gravel outcrops along road. Gravel beds dip northwestward into the Enterprise Valley.

100.4 (0.3) The Spokane River can be seen ahead. Floods descending the Spokane River valley were aimed directly at the south end of the Enterprise Valley and partially reworked sediments there into an elongate bar.

101.3 (0.9) **STOP 12. McCoy's Marina view.**

Pull off the road on the left by the last major switchback.

The upstream segment of the Spokane River valley here is a continuation of the 48-km-long Enterprise Valley lineament (Kiver and Stradling, 1986). Sand Flat (Stop 2) is about 9.6 km directly upstream to the southeast, and Pitney Butte (808 m) is the second peak to the right as one looks upstream.

Pitney Butte has a thin loess cap and was probably overrun by late Wisconsin floods. The lower flood-scoured peak near Tamarack Flat in front of Pitney Butte is at 768 m elevation, and Lilienthal Mountain directly across the river from here has thick colluvium and local patches of loess with deep argillic soils above 793 m that were not eroded by floods or glaciers.

Pre-Wisconsin glacial advances reached at least to the Sand Flat area and a maximum elevation of 793 m. The maximum extent of the intermediate glaciation here is unknown, but its surface was high enough to create a glacial lake that helped produce Tamarack Flat and the Bockemuehl Canyon surface (585 m). Small pendant bars on the outer edges of these surfaces were produced by later floods.

A stillstand or perhaps a re-advance of the middle Wisconsin(?) glaciers from Enterprise Valley stopped an unknown distance upstream in the Spokane River valley. The downstream ice position was probably where the narrow, boulder-armored meander neck is visible. Later floods reworked and distributed the glacial sediments onto downstream surfaces, just as the events described for the Sand Flat and Lamb Draw areas did.

An episode of meandering stream erosion occurred in late Wisconsin or (more likely) early Holocene time. Abandoned meanders upstream in the Spokane area have Mazama ash deposited in the channels, indicating that the meanders are older than 6,800 yr.

Descend to McCoy's Marina, turn around, and return to the main road.

104.0 (2.7) Turn left onto Peters Road toward the Fort Spokane area. The road climbs across flood-scoured Cretaceous and Tertiary intrusive rocks to a pass at elev. 734 m. A few areas of flood gravels are exposed near the pass.

105.2 (1.2) Buttes to the right (north) are nunataks capped by pre-Wisconsin soils.

106.1 (0.9) Cross through the pass. Closed depressions in the granitic scabland to the left (south) contain ponds. The road descends across granite and basalt and onto the old till-covered loess surface continuous with that visited at Stop 7.

108.4 (2.3) Intersection with SR 25. The road log ends here. Turn left toward Fort Spokane and follow the road south to Davenport, and then drive east to Spokane on U.S. 2.

Record of Pre-Late Wisconsin Floods and of Late Wisconsin Flood Features in the Cheney-Palouse Scabland: Trip C

Eric V. McDonald *and* Alan J. Busacca
Department of Agronomy and Soils
Washington State University
Pullman, WA 99164

INTRODUCTION

Many of the geomorphic features preserved in the Channeled Scabland are related to the episode of giant floods during the late Wisconsin, generally known as the Spokane Flood. The objective of this field trip is to present new evidence indicating that the processes that generated cataclysmic floods during the period from 16 to 12 ka also must have operated several, possibly many, times earlier in the Pleistocene. The trip also will take advantage of our route through the heart of the Cheney-Palouse scabland tract to view examples of scabland features.

Record of Scabland Flooding

Most of the voluminous literature on the history of the Channeled Scabland (reviewed in Baker and Bunker, 1985) concerns the latest floods from glacial Lake Missoula. Evidence elsewhere in the scabland suggests that the late Wisconsin Spokane Flood may have actually been an episode of multiple outbursts of the glacial lake that spanned a period of about 2,000 to 3,000 years between 16 and 12 ka (Waitt, 1985; Atwater, 1986). As defined here, a flood "episode" probably consisted of a few to many outburst floods that together may have spanned several thousand years during a glacial maximum. The stratigraphic resolution within the loess deposits is such that in most cases it is possible to detect only the signatures of flood episodes, not of individual floods.

Deposits from giant floods older than late Wisconsin crop out only sparsely on the Columbia Plateau. As reported by Patton and Baker (1978) and Foley (1982), loess deposits adjacent to flood coulees on the Columbia Plateau record episodes of pre-late Wisconsin cataclysmic floods. Additional evidence for older episodes of giant floods has been amassed from recent work in the loess (McDonald and Busacca, 1988a, b). This evidence consists of large unconformities that truncate buried soils and loess strata and of sediments associated with the unconformities. Sediments that overlie unconformities generally are fluvial and consist of basaltic gravel, lenses of basaltic sand, gravel to cobble-size fragments of indurated paleosols, and slackwater sand and silt; other deposits are eolian and fine upward. These unconformities and associated sediments are interpreted as having resulted from glacial outburst floods rather than from normal fluvial processes in the region because (1) they are similar in character to unquestioned late Wisconsin outburst flood sediments, (2) the fluvial sediments are interstratified in loess adjacent to coulees that are streamless today, and (3) some outcrops of fluvial sediment are in loess that is as much as 100 m above modern coulee floors.

The Palouse Loess

It is from deposits of loess, windblown silty sediment, adjacent to scabland channels that much of the evidence for older floods in the Channeled Scabland comes. Although this trip does not focus on the stratigraphy of the loess per se, some background information is in order: The loess that blankets a major part of the Columbia Plateau is one of the outstanding geologic and geomorphic features produced during the Quaternary Period in the Pacific Northwest. The core of this area, which is centered in eastern Washington and northern Idaho, is called "The Palouse". The Palouse is larger than 8,000 km^2 in area and the loess is more than 75 m thick in its central part (Treasher, 1925; Ringe, 1970). Loess that is generally much thinner than 75 m covers an area several times as large, extending approximately from Waterville in the northwest, to Spokane in the northeast, beyond Walla Walla and Pasco in the south and into the area between Pendleton and The Dalles in Oregon. The

From: Joseph, N. L., and others, editors, 1989, Geologic guidebook for Washington and adjacent areas: Washington Division of Geology and Earth Resources Information Circular 86.

Channeled Scabland lies at the center of this area (Fig. 1) and the history of the loess and the history of the Channeled Scabland are linked.

Dozens of buried paleosols (ancient soils) are interstratified with sheets of loess in the Palouse. The buried soils record episodes of landscape stability and the intervening silty layers record episodes of rapid accumulation of loess. Paleomagnetic measurements now prove that the geologic record in the loess spans at least the last 1 million yr (Packer, 1979; Kukla and Opdyke, 1980; Foley, 1982). Thin layers of ash in the loess, signatures of ancient volcanic eruptions, are being used to correlate and date loess strata (Foley, 1982; McDonald, 1987; Nelstead, 1988). Its potential was recognized early: "The inner core of the...hills remain as much a mystery as ever, but it is obviously a complex and relatively ancient deposit whose story, if known, would illuminate the history of Pleistocene time on the Columbia Plateau" (Bryan, 1927, p. 44). Unlike several other large loess fields around the world, however, the stratigraphy of the Palouse has not been the subject of sustained and coordinated research until the last quarter century (Busacca, in press).

The record of geologic events to be seen on this trip indicates that there were at least six episodes of floods during the Pleistocene. The oldest of those recognized at this time occurred prior to 790,000 yr B.P. on the basis of paleomagnetic measurements (McDonald and Busacca, 1988a). Tephra correlations and an accelerator radiocarbon age strongly suggest that the most recent episode of floods before the late Wisconsin occurred about 40 ka (McDonald and Busacca, 1988b).

Trip Description

The trip route proceeds from Spokane southwest to Ritzville along the northern part of the Cheney-Palouse Scabland. From Ritzville, the route continues south to Washtucna. From Washtucna, the route proceeds northeast across the heart of the Cheney-Palouse scabland tract, through Benge, then east to Endicott. The final leg from Endicott to Spokane leads north through the rolling loessial hills of the Palouse Formation. The locations of Stops 1 through 4 and the general route of travel are shown in Figure 1.

ACKNOWLEDGMENTS

We thank M. Purser, R. Breckenridge, N. L. Joseph, F. K. Miller, and R. L. Logan, for their review of the manuscript. We gratefully acknowledge the grant support of the National Science Foundation (EAR-8318909 and EAR-8707527).

REFERENCES CITED

Atwater, B. F., 1986, Pleistocene glacial-lake deposits of the Sanpoil River valley, northeastern Washington: U.S. Geological Survey Bulletin 1661, 39 p.

Bacon, C. R., 1983, Eruptive history of the Mount Mazama and Crater Lake caldera, Cascade Range, U.S.A.: Journal of Volcanology and Geothermal Research, v. 18, no. 1-4, p. 57-115.

Baker, V. R.; Bunker, R. C., 1985, Cataclysmic late Pleistocene glacial Lake Missoula–A review: Quaternary Science Reviews, v. 4, no. 1, p. 1-41.

Bjornstad, B. N.; Fecht, K. R.; Tallman, A. M., in press, Quaternary stratigraphy of the Pasco Basin area, south-central Washington. *In* Baker, V. R., and others, The Columbia Plateau, Chapter 3 *of* Morrison, R. B., editor, Quaternary non-glacial geology of the conterminous United States: Geological Society of America, The Geology of North America, v. K-2.

Bryan, Kirk, 1927, The Palouse soil problem, with an account of elephant remains in windborne soil on the Columbia Plateau of Washington: U.S. Geological Survey Bulletin 790, p. 21-45.

Busacca, A. J., in press, Loess deposits and soils of the Palouse and vicinity. *In* Baker, V. R., and others, The Columbia Plateau, Chapter 3 *of* Morrison, R. B., editor, Quaternary non-glacial geology of the conterminous United States: Geological Society of America, The Geology of North America, v. K-2.

Clague, J. J., 1978, Mid-Wisconsin climates of the Pacific Northwest. *In* Current Research, Part B: Geological Survey of Canada Paper 78-1B, p. 95-100.

Crandell, D. R.; Mullineaux, D. R.; Rubin, Meyer; Spiker, Elliott; Kelley, M. L., 1981, Radiocarbon dates from volcanic deposits at Mount St. Helens, Washington: U.S. Geological Survey Open-File Report 81-844, 16 p.

Fenton, M. M., 1984, Quaternary events Canadian Prairies–An example of correlation of Quaternary chronologies. *In* Mahaney, W. C., editor, Correlation of Quaternary chronologies: Norwich, England, Geo Books, p. 359-370.

Foley, L. L., 1982, Quaternary chronology of the Palouse loess near Washtucna, eastern Washington: Western Washington University Master of Science thesis, 137 p.

Johnson, R. G., 1982, Brunhes-Matuyama magnetic reversal dated at 790,000 yr B.P. by marine-astronomical correlations: Quaternary Research, v. 17, no. 1, p. 135-147.

Kiver, E. P.; Moody, U. L.; Rigby, J. G.; Stradling, D. F., in press, Late Quaternary stratigraphy of the Channeled Scabland and adjacent areas. *In* Baker, V. R., and others, The Columbia Plateau, Chapter 3 *of* Morrison, R. B., editor, Quaternary non-glacial geology of the conterminous United States: Geological Society of America, The Geology of North America, v. K-2.

Kukla, G. J.; Opdyke, N. D., 1980, Matuyama loess at Columbia Plateau, Washington [abstract]: American Quaternary Association Abstracts with Programs, p. 122.

McDonald, E. V., 1987, Correlation and interpretation of the stratigraphy of the Palouse loess of eastern Washington: Washington State University Master of Science thesis, 218 p.

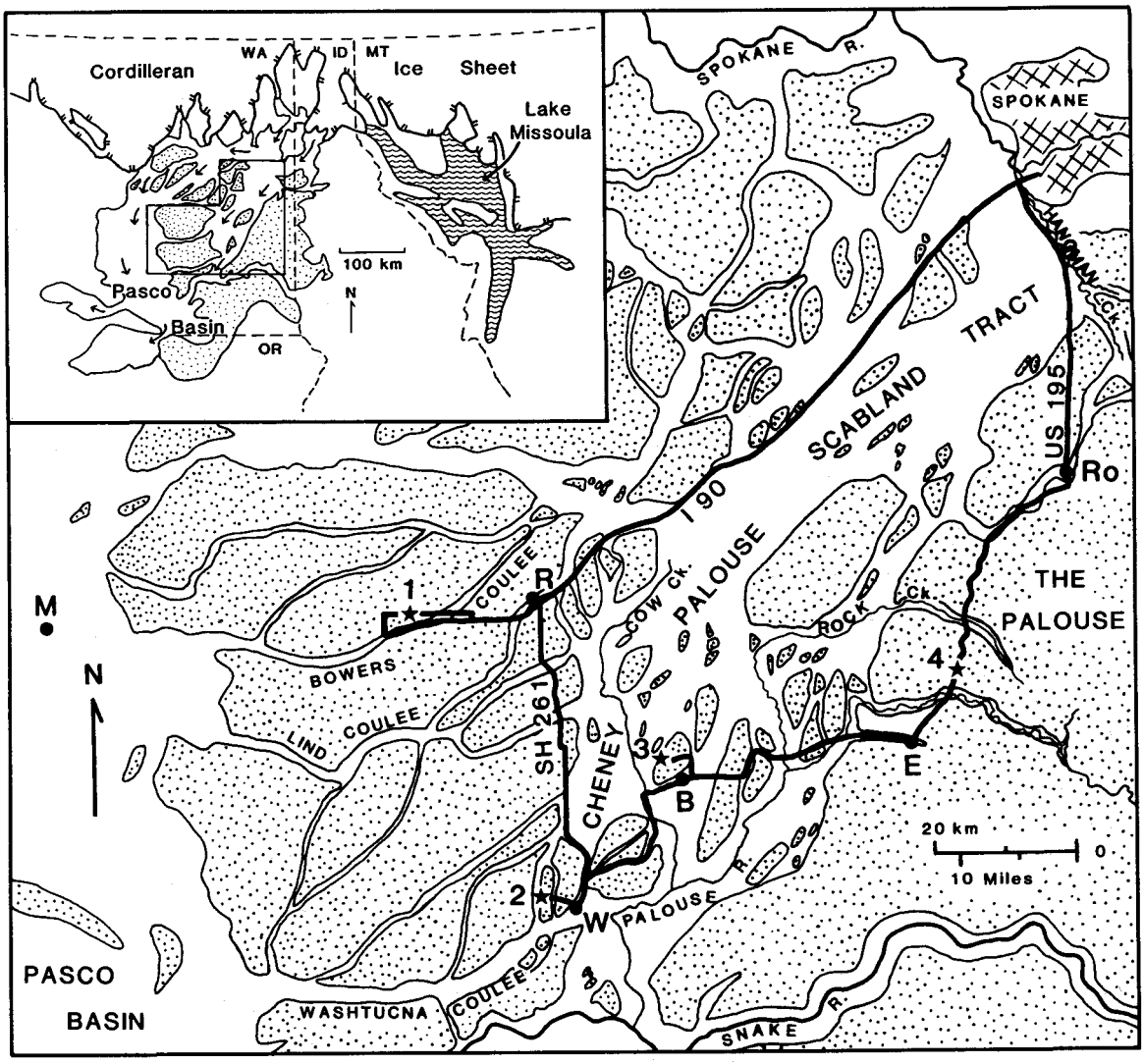

Figure 1. Generalized map (modified from Patton and Baker, 1978) of Cheney-Palouse scabland tract showing field trip route. Stippled pattern shows areas of deep loess cover. Fieldtrip stops are numbered stars. Towns are indicated by letters: B, Benge; E, Endicott; M, Moses Lake; R, Ritzville; Ro, Rosalia; W, Washtucna. Insert map shows generalized Lake Missoula-Channeled Scabland system. Arrows show major pathways of floods through scabland. Cordilleran ice sheet shown at its late Wisconsin maximum.

McDonald, E. V.; Busacca, A. J., 1988a, Record of pre-late Wisconsin giant floods in the Channeled Scabland interpreted from loess deposits: Geology, v. 16, no. 8, p. 728-731.

McDonald, E. V.; Busacca, A. J., 1988b, New evidence for middle Wisconsin glacial outburst flooding in the Channeled Scabland of eastern Washington [abstract]: Geological Society of America Abstracts with Programs, v. 20, no. 7, p. A373.

Mullineaux, D. R., 1986, Summary of pre-1980 tephra-fall deposits erupted from Mount St. Helens, Washington State, U.S.A.: Bulletin of Volcanology, v. 48, no. 1, p. 17-26.

Nelstead, K. T., 1988, Correlation of tephra layers in the Palouse loess: Washington State University Master of Science thesis, 78 p.

Packer, D. R., 1979, Paleomagnetism and age dating of the Ringold Formation and loess deposits in the State of Washington: Oregon Geology, v. 41, no. 8, p. 119-132.

Patton, P. C.; Baker, V. R., 1978, New evidence for pre-Wisconsin flooding in the Channeled Scabland of eastern Washington: Geology, v. 6, no. 9, p. 567-571.

Porter, S. C.; Pierce, K. L.; Hamilton, T. D., 1983, Late-Wisconsin mountain glaciation in the western United States. *In* Wright, H. E., Jr.; Porter, S. C., editors, Late-Quaternary environments of the United States, Vol. 1, The late Pleistocene: University of Minnesota Press, p. 71-111.

Ringe, L. D., 1970, Sub-loess basalt topography in the Palouse Hills, southeastern Washington: Geological Society of America Bulletin, v. 81, no. 10, p. 3049-3060.

Treasher, R. E., 1925, Origin of the loess of the Palouse region, Washington: Science, (n.s.), v. 61, p. 469.

Waitt, R. B., 1985, Case for periodic, colossal jokulhaups from Pleistocene glacial Lake Missoula: Geological Society of America Bulletin, v. 96, no. 10, p. 1271-1286.

Road Log

Cumulative mileage is shown in the left-hand column, and mileage between points is shown in parentheses.

0.0 (0.0) Spokane. Begin trip at Maple Street on-ramp to Interstate 90 (I-90) west toward Ritzville. *Set odometers.*

2.9 (2.9) I-90 ascends onto a broad expanse of scoured Columbia River basalt. This surface is characterized by numerous shallow coulees and has a thin and discontinuous covering of loess.

10.7 (7.8) One of many lakes and ponds formed from water accumulating in depressions that were scoured into the basalt by flood water.

31.5 (20.8) I-90 follows the Cheney-Palouse scabland tract (Fig. 1). Numerous loess islands, erosional remnants of a once-continuous loess cover, can be seen on either side of the highway. Mound-intermound microtopography has formed by deposition of Holocene loess on the flood-stripped basalt.

38.0 (6.5) Sprague Lake, just south (left) of I-90, is one of several lakes formed in large pothole basins that were carved into the basalt by flood water.

65.5 (27.5) I-90 enters the upper end of Bowers Coulee, a large flood channel that ends near the town of Moses Lake, approximately 44 mi (70 km) to the west (Fig. 1).

71.6 (6.1) Exit I-90 at State Route (SR) 21 exit. Turn right (north) onto SR 21.

74.2 (2.6) Turn right (east) toward Ritzville on Rossenhoff Road.

76.5 (2.3) **STOP 1. Ritzville -1 locality.**

Park on the gravel road just east of (above) the roadcut on the right side of road.

This roadcut, informally designated Ritzville-1 (RZ-1), exposes several loess layers and paleosols, a marker tephra, and Columbia River basalt. It also exposes an angular unconformity and two disconformities, all three of which are mantled by flood-derived sediments (Fig. 2). The older of the two disconformities (C, Fig. 2) is an erosional surface on the basalt, and it is overlain by a bed of subrounded basalt cobbles and gravel in a loess matrix. This bed is strongly cemented by calcium carbonate and silica to form the duripan of a paleosol. The abundance of basaltic cobbles and the proximity to Bowers Coulee suggest that this disconformity and the basaltic gravel were derived from an older episode of flooding, but at this site the age of flooding is unknown.

The angular unconformity, which is in the middle of the section (B, Fig. 2), forms a trough that is cut deeply into two older paleosols and down to the surface of the duripan formed in basaltic cobbles. The wedge of sediment that fills the trough contains lenses of basaltic sand and fragments of paleosols. The bedding pattern seems to define at least two crude rhythmite sequences that grade upward from coarse basaltic sand to thinly laminated quartz-rich silt. Within this wedge of sediment is a tephra that we correlate with the Mount St. Helens (MSH) tephra set C on the basis of electron microprobe analysis of glass shards and phenocrysts of magnetite and ilmenite and on its coarse texture (E. V. McDonald, unpublished data).

The MSH set C tephra provides a minimum age of about 36 ka (Mullineaux, 1986) for the episode of flooding that created the angular unconformity and deposited the slackwater sediments that fill the trough. This age estimate is based on radiocarbon isotopic dating of the Ape Canyon (set C) eruptive period of Mount St. Helens (>35,000 [W-2421(laboratory no.)], 36,000 ± 2,100 [W-2653], 36,000 ± 2,500 [W-2976], and 37,600 ± 1,300 [W-2661] yr B.P.; Crandell and others, 1981).

An additional radiocarbon age estimate for this episode of flooding comes from flood gravel in Lind Coulee, about 20 km south of Moses Lake. A duripan has formed in the gravel, indicating that the gravel is pre-late Wisconsin because soils formed in late Wisconsin flood gravels typically have only cambic or weak calcic horizons. In other words, the gravel layer at Lind Coulee was deposited prior to late Wisconsin flooding because the presence of a duripan indicates that the gravel has been exposed to soil-forming processes for substantially more than 12,000 yr. An age estimate for the gravel comes from charcoal from the base of the gravel

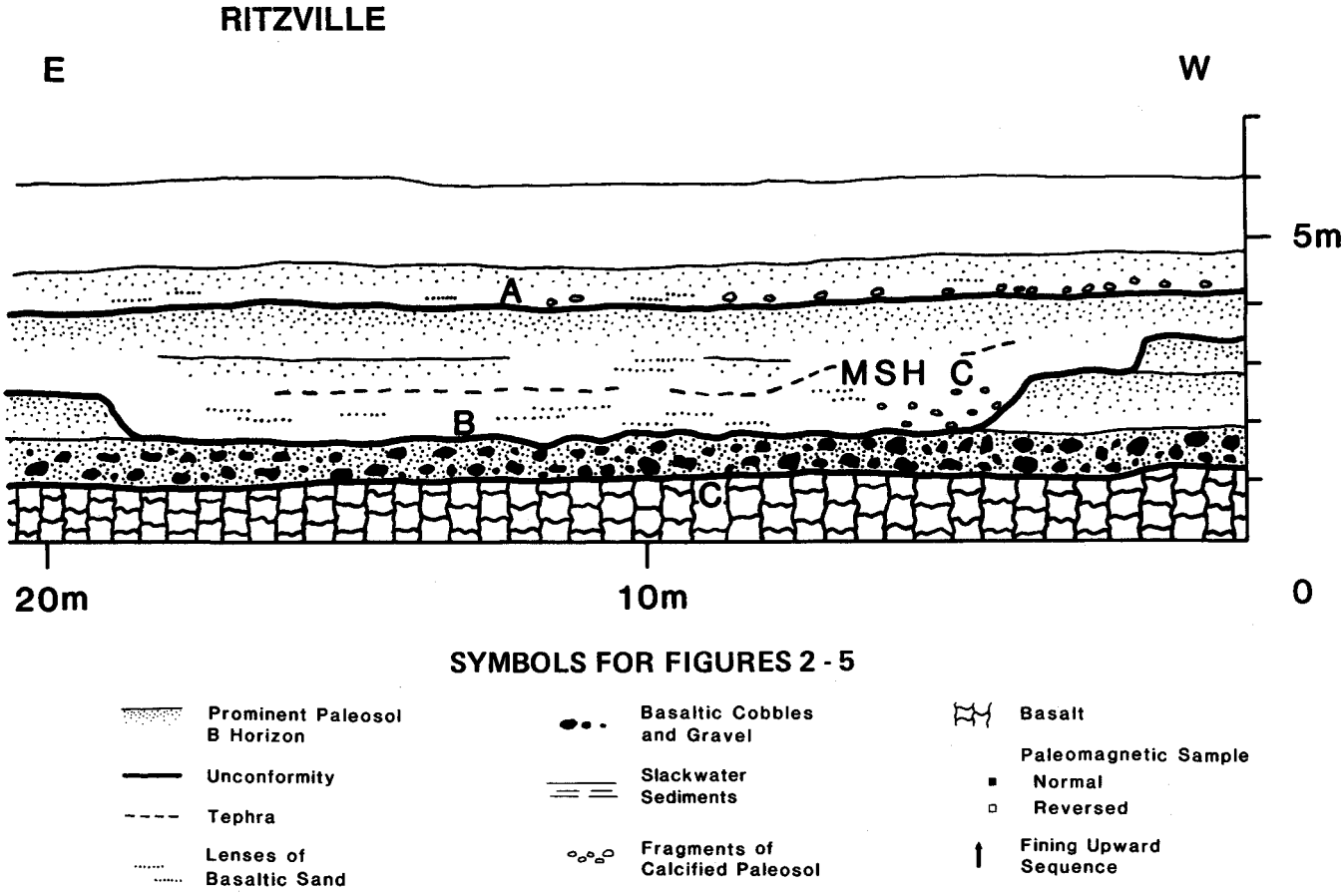

Figure 2. Stratigraphy of Ritzville-1 exposure (sec. 13-24 boundary, T. 19 N., R. 33 E., Willamette Base and Meridian (W.B.M.)). Line-and-stipple pattern marks approximate position of prominent paleosol B horizons. Dashed lines are tephras; those that are correlated are: MSH C, Mount St. Helens set C. Heavy lines are flood-cut unconformities and are labeled alphabetically in each exposure.

layer, which yielded an accelerator radiocarbon age of 40,650 ± 1,000 yr B.P. [Beta-24101, ETH-3668].

A correlative of the angular unconformity at RZ-1 was recognized as a disconformity at the WA-9 exposure (Stop 2, below) in the same stratigraphic position relative to the set C tephra. Flood sediment that contains the set C tephra and that overlies angular unconformities has been recognized in several exposures across the Columbia Plateau (McDonald, 1987; McDonald and Busacca, 1988a, b). These sites confirm the simultaneous development over a substantial part of the Columbia Plateau of an unconformity mantled by fluvial sediments and support the interpretation of its flood origin. Kiver and others (in press) also have presented evidence of a pre-late Wisconsin episode of flooding that may be no older than middle Wisconsin. Scabland flooding at about the time of the eruption of the set C tephra is inconsistent with the current glacial stratigraphy in southwestern Canada, where nonglacial conditions are thought to have existed from 65 to 25 ka (oxygen isotope stage 3; Clague, 1978; Fenton, 1984). Weathering rind and obsidian-hydration dating, however, has produced age estimates of 40 to 30 ka for end moraines of alpine glaciers in the Yellowstone area of the Rocky Mountains (Porter and others, 1983). This does not imply that alpine ice rather than a continental ice sheet was responsible for middle Wisconsin floods, instead it points out that this conflicting evidence increases the need for detailed stratigraphic and isotopic dating studies of glacial-climatic events in the late Pleistocene.

The upper disconformity at the RZ-1 site (A, Fig. 2) is the flood scoured and partially eroded surface of the duripan of a buried soil formed in loess. The disconformity is interpreted to be a

result of scabland flooding because it is covered by waterlaid fragments of cemented paleosols and scattered basaltic gravel. This in turn is mantled by about 1 m of Holocene loess. At many sites on the Columbia Plateau, flood sediments correlative to those overlying this disconformity contain the MSH set S tephra (ca. 13 ka, Mullineaux, 1986). The style of erosion and deposition exhibited by the upper disconformity and the angular unconformity at RZ-1 are typical of that found at sites in somewhat protected positions marginal to scabland channels; that is, floodwaters tended to scour into the loess down to the level of strongly cemented paleosols, in many places creating erosional troughs in the process. The veneer of flood sediment left behind is a few decimeters to about 1 m thick.

The buried soil that separates the two sets of flood sediments has been named the Washtucna geosol (McDonald, 1987) because it is a distinctive soil stratigraphic unit that can be found at many localities across the plateau. It represents a period of soil development between 36 and 13 ka.

Continue east on Rossenhoff Road to Ritzville.

82.6 (6.1) Turn right (south) onto Paha-Packard Road. Continue 1.5 mi south and proceed east on I-90 toward Ritzville.

89.6 (7.0) Exit I-90; turn right (south) onto SR 261.

99.1 (9.5) Town of Ralston. Ralston is in the upper reaches of Lind Coulee, a large flood channel that stretches approximately 80 km to the west (Fig. 1). South of Lind Coulee, the highway crosses Rattlesnake Flat, a broad expanse of flood-exposed basalt that has a thin cover of loess and flood sediments.

104.4 (5.3) Shallow roadcut exposes late Wisconsin flood deposits. Deposits consist of crudely bedded silts and sands with scattered granitic cobbles and a tephra that probably correlates with the MSH set S tephra.

108.4 (4.0) SR 261 enters the upper part of Staircase Rapids, a short flood channel that drops nearly 200 m in about 10 km. Staircase Rapids formed a constriction behind which flood water ponded onto Rattlesnake Flat. Note the several nickpoints in basalt and the loess islands.

112.7 (4.3) The broad, flat surface straight ahead is the top of a large gravel bar that has formed in the lower part of Staircase Rapids. SR 261 passes along the lower east side of the bar where several exposures of bedded flood gravels can be seen to the right.

116.3 (3.6) End of Staircase Rapids and bottom of Washtucna Coulee, one of the major flood channels in the southern part of the Cheney-Palouse scabland tract (Fig. 1). Turn right (west) onto SR 26. The highway rises out of Washtucna Coulee and onto thick loess deposits. Note the many buried soils and loess layers exposed in roadcuts.

120.2 (3.9) **STOP 2. Washtucna-9 locality**

This roadcut is informally designated Washtucna-9 (WA-9). It exposes about 20 m of loess in a loess hill adjacent to Collier Coulee. The complex arrangement of unconformities, loess layers, and paleosols indicates that this hill has been severely eroded several times in its history (Fig. 3). The site was first studied by Foley (1982) and more recently has been re-interpreted by McDonald and Busacca (1988).

Recent remapping by the authors has shown a total of five angular unconformities and one disconformity in the exposed part of the section. The oldest of these forms a trough that is deeply eroded into older, flat-bedded paleosols and loess layers at the base of the exposed section (F, Fig. 3). Three other angular unconformities truncate loess layers and paleosols in the middle of the exposure (C, D, and E, Fig. 3). The disconformable surface (B, Fig. 3) is recognized in the upper part of the exposure by scour along the surface of the duripan of the Washtucna geosol. A tephra bed in sediment that overlies the B disconformity is correlated with the MSH set C tephra (McDonald and Busacca, 1988a) and to the tephra in flood sediment at RZ-1 (Fig. 2). The B disconformity at WA-9 is correlated to the B disconformity at RZ-1, and both are attributed to the middle Wisconsin flood episode. The uppermost unconformity (A, Fig. 3) is associated with the late Wisconsin episode of flooding because the fresh scarp face is blanketed by loess that contains Mount Mazama tephra (Foley, 1982; about 7 ka, Bacon, 1983).

Because the ages of the five tephras exposed in the lower part of the section are not known, the probable ages of the older flood-cut unconformities (C-F, Fig. 3) can be estimated only from the stratigraphic sequence and from

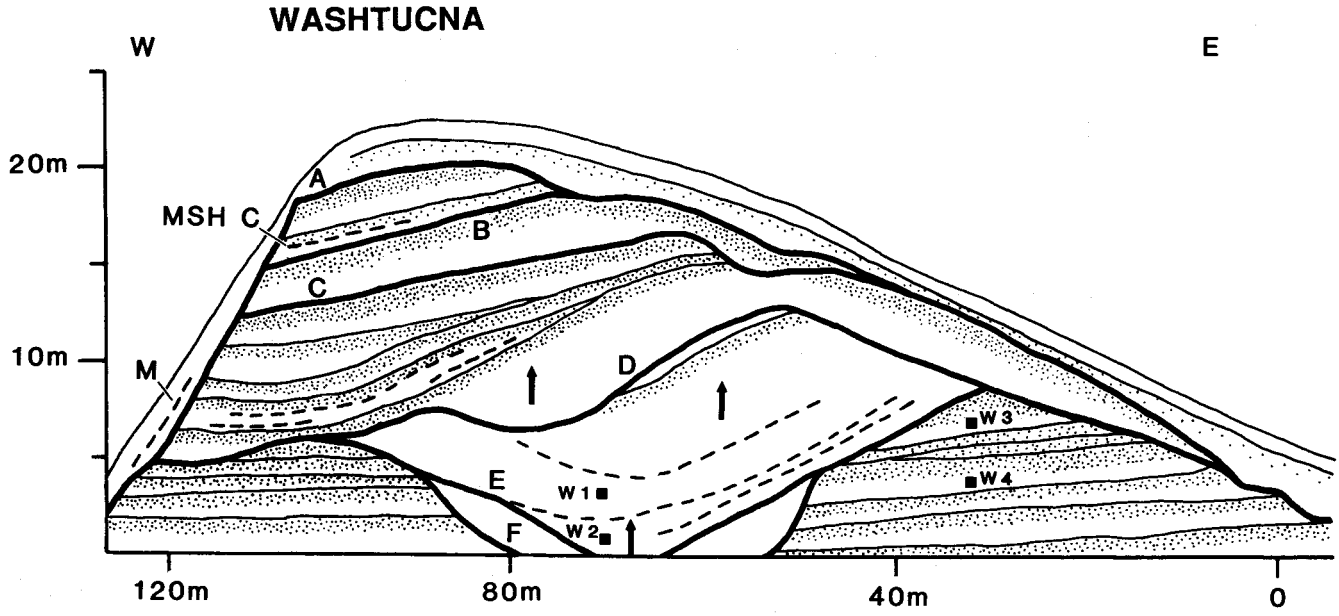

Figure 3. Stratigraphy of Washtucna-9 exposure (SW 1/4 sec. 14, T. 15 N., R. 35 E., W.B.M.). Line-and-stipple pattern marks approximate position of prominent paleosol B horizons. Dashed lines are tephras; those that are correlated are: M, Mazama; MSH C, Mount St. Helens set C. Heavy lines are flood-cut unconformities and are labeled alphabetically in each exposure.

paleomagnetic data. At least the lower one-half of the exposure is normally magnetized, based on reconnaissance sampling (Fig. 3). The current interpretation is that at least the part of the sequence above the lowest unconformity (F, Fig. 3) is Brunhes age because of its normal polarity signature. If so, the exposed section at WA-9 records six episodes of giant floods in the last 790,000 yr (Brunhes-Matuyama boundary; Johnson, 1982).

Continue west on SR 26 for 0.4 mi and make a careful U-turn at the gravel pad along the roadside. Go east on SR 26 to Washtucna.

123.0 (2.8) View of Washtucna Coulee, the bottom of which is incised more than 150 m into the basalt.

124.8 (1.8) Turn right (south) onto SR 260/261; enter the town of Washtucna.

125.5 (0.7) Turn right onto Spring Street, drive one block west to the town park for a lunch stop. After lunch, retrace route to the junction of SR 261/260 and 26.

126.2 (0.7) Cross SR 26 and drive north toward Ritzville.

128.4 (2.2) Turn right (east) toward Benge on the Benge-Washtucna Road. The road follows Stanley Coulee.

132.6 (4.2) The road enters a small, narrow branch coulee of Stanley Coulee. Note steep scarps in loess hills cut by flood water.

135.8 (3.2) The road descends to Cow Creek, which lies in the bottom of a large flood coulee. The general morphology is one of a narrow deep inner channel flanked by a higher, broadly scoured basalt surface consisting of a mixture of buttes, small potholes, and longitudinal grooves. The elevation of the upper surface of flood waters is defined by the tops of steep flood-cut scarps in the adjoining loessial hills. Scabland creeks and rivers are found in the deep inner channels.

136.9 (1.1) The road follows old Mullan Road, a military wagon road built in the early 1860s that connected Fort Walla Walla in south-central Washington with Fort Benton in Montana, a distance of about 1,000 km.

143.3 (6.4) Town of Benge. Turn left (north) onto the Ralston-Benge Road toward Ritzville. The road follows the edge of a large flood channel.

145.4 (2.1) The road turns west and onto a large loess island.

147.1 (1.7) **STOP 3. Benge-1 locality.**

Carefully pull onto the gravel apron on the left side of the roadcut.

Four distinct angular unconformities and seven buried paleosols are exposed at this site. Each of the three lowermost unconformities is overlain by a succession of fluvial sediment-eolian sediment-paleosol that is repeated upsection. For example, the lowest unconformity exposed at this site (D, Fig. 4) is cut into a strongly developed paleosol. A bed of laminated, waterlaid silt overlies the paleosol. Cobble-size (10-40 cm) fragments of carbonate-cemented paleosols lie on the unconformity, and the silt bed contains lenses of gravel-size pieces of paleosols. The waterlaid sediment grades upward into eolian silt that is capped by a paleosol.

The repeated sequence of angular unconformity-fluvial sediment-eolian sediment-paleosol(s) suggests that the exposed section of this hill has been subject to at least four episodes of giant floods that were widely separated in time. The waterlaid sediments and paleosols that overlie the lowest exposed unconformity (D, Fig. 4) are reversely magnetized, indicating that at least one episode of flooding had occurred before 790,000 yr B.P. Bjornstad and others (in press) also have found a floodlaid gravel bed enclosed by reversely magnetized sediment at the sites first reported by Patton and Baker (1978) and at sites elsewhere on the Columbia Plateau. A paleomagnetic sample from the waterlaid sediment above unconformity C is normally magnetized. If this indicates Brunhes-age sediment, then the episodes of flooding that created the flood-scoured surfaces at B and C (Fig. 4) occurred during the middle or late Pleistocene. Because the uppermost unconformity (A, Fig. 4) is overlain by a thin veneer of loess in which the modern surface soil has formed, it is probable that it resulted from late Wisconsin flooding.

It is possible that the stratigraphic record at the first three stops was created by more than six episodes of cataclysmic floods, because correlation has not been established among the sites and because the fluvial system in the scabland would have the potential to create large gaps in the stratigraphic record at any site. Regardless of the exact number of episodes of outburst flooding represented in the loess, the scabland appears to be the product of multiple episodes of glacial-outburst flooding. Because periods of glaciation are required to generate large-scale scabland floods, the record of multiple flood episodes in the loess may potentially be one of the better terrestrial proxy records of Quaternary climatic cycles in North America.

The repeating stratigraphic relations between unconformities, eolian sediments, and paleosols in the loess suggest an important link between scabland flooding and periods of loess deposition and soil formation. Sedimentologic features in the Washtucna and Benge exposures suggest that fine-grained sediment deposited by scabland floods has controlled the timing of at least some episodes of loess deposition and soil development. Sediments that cover flood-cut un-

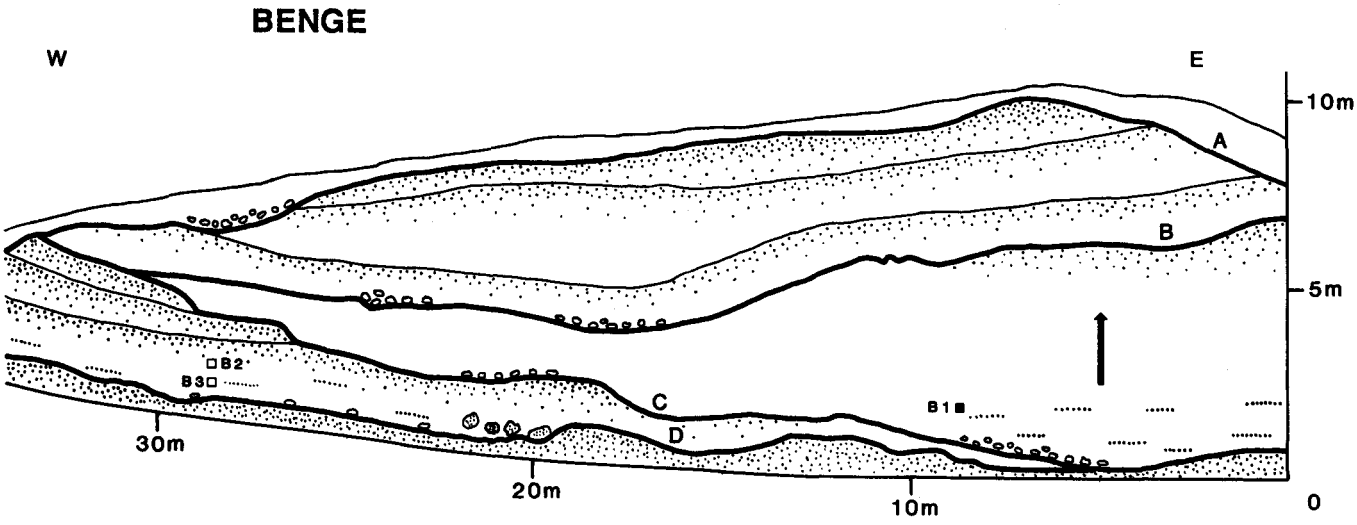

Figure 4. Stratigraphy of Benge-1 exposure (SE 1/4 sec. 27, T. 17 N., R. 37 E., W.B.M.). Line-and-stipple pattern marks approximate position of prominent paleosol B horizons. Dashed lines are tephras. Heavy lines are flood-cut unconformities and are labeled alphabetically in each exposure.

conformities generally fine upward (arrows, Figs. 3 and 4). The basal parts consist of dune sand, sandy loess, or fluvial sediments. The upper parts consist of fining-upward sequences of massive, uniform loessial silt. In most cases, these sequences are capped by paleosols, which began to form as deposition of loess decreased to a rate low enough for landscapes to stabilize. This does not imply that all of the dozens of loess-paleosol complexes in areas of thick loess cover were formed after episodes of flooding, but other possible causes of cyclic loess deposition such as climatic or vegetation changes remain to be documented.

Continue west for 0.1 mi and turn around on the gravel road on the right. Exposed in the roadcut across from the gravel road are late Wisconsin flood sediments consisting of finely bedded sands and silts, which are in turn overlain by a meter of Holocene loess. Proceed back to Benge (east) on the Ralston-Benge Road.

151.3 (4.2) Turn left (east) at Benge toward Winona and Endicott.

154.3 (3.0) The road enters a small flood channel cut through a large loess island separating two large flood channels.

159.4 (5.1) The large terrace-like feature to the left is a gravel bar deposited around two small loess islands.

161.1 (1.7) The road descends into an inner flood channel in which lies Rock Creek. Note the steep basalt walls that form the inner channel.

162.6 (1.5) Several loess islands can be seen to the south and north along the road for next 5 mi.

167.7 (5.1) Palouse River and the town of Winona. The flood channel carved along the Palouse River generally marks the eastern boundary of the Cheney-Palouse scabland tract. Continue east toward Endicott.

168.4 (0.7) Flood slackwater sediments are exposed in the creek bank on the right. Water backflooded into Rebel Flat Creek well past Endicott (5 mi ahead).

169.2 (0.8) Reworked Mazama tephra (about 7 ka, Bacon, 1983) is exposed in the creek channel on the left. The tephra lies in Holocene alluvium about 1 m below the surface.

173.2 (4.0) Enter the town of Endicott.

173.4 (0.2) Turn left (north) just past the school, proceed about 100 ft, and turn left at the stop sign onto St. John-Endicott Road.

177.4 (4.0) The roadcut on the left is at an elevation of 620 m and exposes late Wisconsin flood sediments. Endicott is at an elevation of 520 m, indicating that deep flood water backflooded the adjoining valleys.

180.0 (2.6) Palouse River (elev. 510 m). Water surged up the Palouse River for many kilometers during large flood events.

183.8 (3.8) **STOP 4. St. John-1 locality.**

Pull onto the gravel access road just past the right side of the roadcut.

Exposed in the roadcut are pre-late Wisconsin flood sediments (Fig. 5). About 3 m of poorly stratified slackwater sediments (horizontal lines, Fig. 5) overlie the scoured surface of two or three well-developed paleosols (A, Fig. 5). These sediments contain several rhythmites of poorly sorted basaltic sands that fine upward into thinly laminated silts. A very weak soil (not shown in Fig. 5) is formed in the lower meter of the bedded silts. On the opposing roadcut face, the corresponding sequence of sediments overlies an angular unconformity. A 20-cm-diameter cobble of basalt that was probably ice-rafted lies in the flood sediments.

Four tephra layers are stratified within the slackwater sediments. Preliminary analysis of major elements in the two lowermost tephras suggests that they may be correlative to two of the lowermost tephras in WA-9 (Fig. 3). The slackwater sediment that contains the tephras grades upward into about 2 m of loess that has strong prismatic structure. A well-developed paleosol in the loess appears to have been subsequently truncated by hillslope erosion (Fig. 5).

The elevation of this site is at about 674 m, or about 165 m above the Palouse River 6.4 km to the south. Deep flood water originating from the Cheney-Palouse scabland tract must have backflooded a large portion of the Palouse River and its tributaries for water to have reached this site. Several other sites have been found in the Palouse far to the east of the Cheney-Palouse scabland that contain flood sediments. Several episodes of floods penetrated into the area of the Palouse loess and may have had a significant

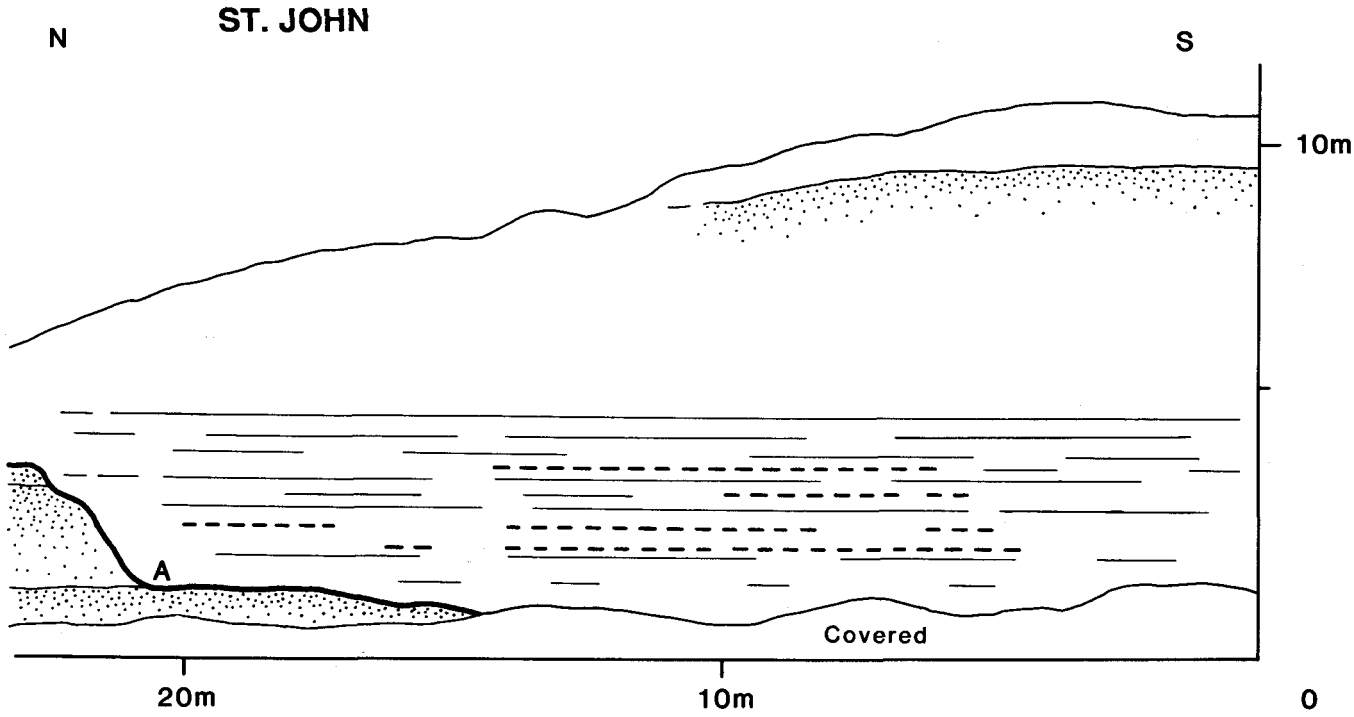

Figure 5. Stratigraphy of St. John-1 exposure (SE 1/4 sec. 24, T. 18 N., R. 41 E., W.B.M.). Line-and-stipple pattern marks approximate position of prominent paleosol B horizons. Dashed lines are tephras. Heavy lines are flood-cut unconformities and are labeled alphabetically in each exposure.

erosional impact on the topography. Floods might also have left large volumes of fine-grained slackwater sediments, which could have been transported and redeposited nearby as loess.

184.3 (0.5) Late Wisconsin flood sediments exposed in the top of the roadcut.

188.2 (3.9) The town of St. John. Turn left (west) onto SR 23.

189.0 (0.8) Turn right (north) on Pine City Road.

189.3 (0.3) The railroad cut on the right has a sequence of flood deposits similar to the ones at Stop 4. The flood channel just ahead is one of many that were backflooded.

196.9 (7.6) Large flood channel along Thorn Creek. Late Wisconsin flood sediments can be found more than 24 km up-valley (east) from here.

197.9 (1.0) Pine City is located in a flood channel that was eroded deeply into basalt. Some of the flood water that created this channel originated from spillover at the southern (headwater) end of Hangman Creek, approximately 32 km to the northeast (Fig. 1).

202.2 (4.3) Several borrow pits and roadcuts for the next 2 mi expose gravelly flood sediments. Note the large boulders in the deposit.

206.8 (4.6) Ridgetop view of the eastern boundary of the Palouse and of the Bitterroot Mountains approximately 25 km to the east.

207.3 (0.5) Turn left (north) toward Rosalia.

208.0 (0.7) Note Main Street clock on the left. Rosalia lies in the same flood channel as does Pine City.

209.4 (1.4) Turn right and drive 0.1 mi. Then turn left (north) onto SR 195.

223.0 (13.6) The highway enters a broad, flat expanse of flood-stripped basalt.

231.3 (8.3) SR 195 descends to Hangman Creek.

235.5 (4.2) The hillside ahead is composed of a thick sequence of flood gravel and sand.

Continue driving north on SR 195 to I-90 (about 2 mi). End of road log.

The Northern Columbia Plateau from the Air

Dale F. Stradling and Eugene P. Kiver

The Northern Columbia Plateau from the Air

D. F. Stradling *and* E. P. Kiver
Department of Geography
Eastern Washington University
Cheney, WA 99004

INTRODUCTION

The route (Fig. 1) of the flight for this field trip was selected to illustrate a variety of geomorphic and cultural landscapes representative of the northern Columbia Plateau. Many of the features are seen far better from the air because they are large and best examined in the context of other features around them. The most notable is the Grand Coulee, the largest and most spectacular of the Lake Missoula flood channels. Other features making up the landscape include scabland channels separated by loess-covered uplands and buttes, known as steptoes, which are composed of older plutonic and metamorphic rocks protruding through the Columbia River basalt (Fig. 2). Both glaciated and unglaciated landscapes bordering the Grand Coulee on the west will also be observed. On the return trip, circular sag flowout structures in the basalt and well-developed Channeled Scabland drainages, including Crab Creek, will be viewed.

Upon leaving Spokane International Airport, the airplane will take us WNW across the northern edge of the Columbia Plateau to Grand Coulee Dam, a distance of about 115 km. The low, rugged mountains of the Okanogan Highlands section of the Northern Rocky Mountains are to the north. The aircraft will circle the dam area and then fly about 16 km southwest to view Steamboat Rock, a small basalt mesa in the Grand Coulee. From there, the route continues southwesterly for about 20 km across Banks Lake in the upper Grand Coulee and then on to Sims Corner. After circling Sims Corner to observe glacial features, we will proceed south about 24 km to Dry Falls, which separates the upper and lower parts of the Grand Coulee. The return flight to Spokane of about 155 km passes an area along Crab Creek about 15 km east of Odessa. The total distance is about 340 km (or 210 mi) and will take about 2 hr of flight time.

The aircraft will circle at five locations that were selected to allow participants to observe particular features and take photographs. We hope you enjoy the flight and that the discussion and the accompanying map will contribute to your understanding and appreciation of the northern Columbia Plateau.

REGIONAL GEOLOGY

Two major "flood" events, fire and water, dominate the processes that formed the Columbia Plateau landscapes. First were the massive multiple Miocene extrusions of flood basalts of the Columbia River Basalt Group between 17 and 6 Ma (Hooper, 1982). Over most of the plateau, the flows are nearly horizontal; their upper surfaces generally reach no higher than elevation 760 m. The eruptions that created the three upper flows of the Wanapum Basalt in the area of the flight originated from fissures to the southeast. The Rosa Member of the Wanapum Basalt, for example, erupted from a narrow, linear vent system more than 150 km long in southeastern Washington and northeastern Oregon (Swanson and others, 1979; Hooper and Reidel, this volume; Reidel and Campbell, this volume).

The second major "flood" event in the area's geologic history is the cataclysmic glacial Lake Missoula floods, which formed the Channeled Scabland and provided a major source for the voluminous deposits of loess in eastern Washington and adjacent areas in Idaho and Oregon. The revolutionary concept proposed by J Harlen Bretz (Bretz, 1923, 1969; Bretz and others, 1956), however, did not receive general acceptance until the 1950s and 1960s. Initially, Bretz advocated only a single flood, but by 1956 he recognized at least seven. Since that time strong evidence has been developed for a significantly larger number of floods (Waitt, 1988, 1985; Kiver and Stradling, 1982a; Atwater, 1986, 1987; Kiver and others, this volume; McDonald and Busacca, this volume).

ACKNOWLEDGMENTS

Ernest H. Gilmour, Fred K. Miller, Henry W. Schasse, and Nancy L. Joseph reviewed this paper. We thank them for their constructive comments.

From: Joseph, N. L., and others, editors, 1989, Geologic guidebook for Washington and adjacent areas: Washington Division of Geology and Earth Resources Information Circular 86.

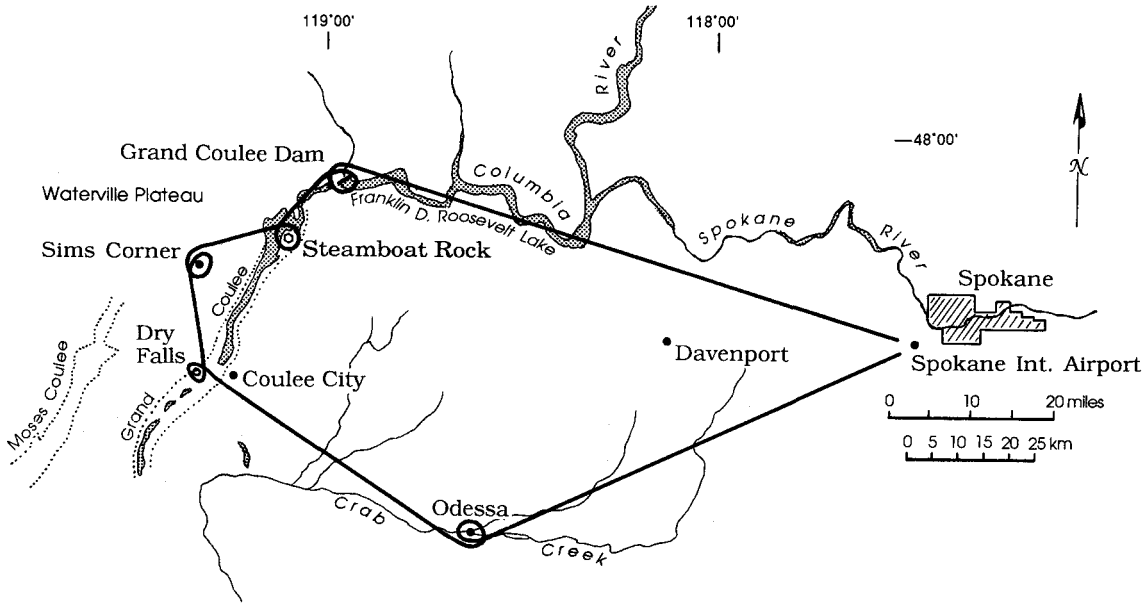

Figure 1. Flight route for the aerial field trip across the northern Columbia Plateau.

REFERENCES CITED

Atwater, B. F., 1986, Pleistocene glacial-lake deposits of the Sanpoil River valley, northeastern Washington: U.S. Geological Survey Bulletin 1661, 39 p., 3 pl.

Atwater, B. F., 1987, Status of glacial Lake Columbia during the last floods from glacial Lake Missoula: Quaternary Research, v. 27, no. 2, p. 182-201.

Baker, V. R., 1987, Dry Falls of the Channeled Scabland, Washington. *In* Hill, M. L., editor, Cordilleran Section of the Geological Society of America: Geological Society of America DNAG Centennial Field Guide, v. 1, p. 369-372.

Bretz, J H., 1923, The Channeled Scablands of the Columbia Plateau: Journal of Geology, v. 31, p. 617-649.

Bretz, J H., 1932, The Grand Coulee: American Geographical Society Special Publication 15, 89 p.

Bretz, J H., 1969, The Lake Missoula floods and the Channeled Scabland: Journal of Geology, v. 77, no. 5, p. 505-543.

Bretz, J H.; Smith, H. T. U.; Neff, G. E., 1956, Channeled Scabland of Washington–New data and interpretations: Geological Society of America Bulletin, v. 67, no. 8, p. 957-1049.

Flint, R. F., 1937, Pleistocene drift border in eastern Washington: Geological Society of America Bulletin, v. 48, no. 2, p. 203-232.

Hodges, C. A., 1978, Basaltic ring structures of the Columbia Plateau: Geological Society of America Bulletin, v. 89, no. 9, p. 1281-1289.

Hooper, P. R., 1982, The Columbia River basalts: Science, v. 215, no. 4539, p. 1463-1468.

Jones, F. O.; Embody; D. R.; Peterson, W. L., 1961[1962], Landslides along the Columbia River valley northeastern Washington: U.S. Geological Survey Professional Paper 367, 98 p.

Kiver, E. P.; Stradling, D. F., 1982a, Quaternary geology of the Spokane area. *In* Roberts, Shiela; Fountain, David, Tobacco Root Geological Society 1980 Field Conference Guidebook: Tobacco Root Geological Society [Spokane], p. 26-44.

Kiver, E. P.; Stradling, D. F., 1982b, Upper Columbia River terrace system of eastern Washington–Preliminary interpretations [abstract]: American Quaternary Association 7th Biennial Conference Program and Abstracts, p. 117. [Also presented as Poster Session 56].

McKee, B.; Stradling, D. F., 1970, The sag flowout–A newly described volcanic structure: Geological Society of America Bulletin, v. 81, no. 7, p. 2035-2044.

Richmond, G. M.; Fryxell, Roald; Neff, G. E.; Weis, P. L., 1965, The cordilleran ice sheet of the Northern Rocky Mountains and related Quaternary history of the Columbia Plateau. *In* Wright, H. E., Jr.; Frey, D. G., editors, 1965, The Quaternary of the United States: Princeton University Press, p. 231-242.

Stradling, D. F.; Kiver, E. P., 1986, The significance of volcanic ash as a stratigraphic marker for the Late Pleistocene in northeastern Washington. *In* Keller, S. A. C., editor, 1986, Mount St. Helens–Five years later: Eastern Washington University Press, p. 120-126.

Swanson, D. A.; Wright, T. L.; Hooper, P. R.; Bentley, R. D., 1979, Revisions in stratigraphic nomenclature of the Columbia River Basalt Group: U.S. Geological Survey Bulletin 1457-G, 59 p.

Symons, T. W., 1882, The upper Columbia River and the Great Plain of the Columbia: U.S. Congress, 47th, First Session, Senate Executive Document 186, 133 p.

Waitt, R. B., 1985, Case for periodic, colossal jökulhlaups from Pleistocene glacial Lake Missoula: Geological Society of America Bulletin, v. 96, no. 10, p. 1271-1286.

Willis, Bailey, 1887, Changes in river courses in Washington Territory due to glaciation: U.S. Geological Survey Bulletin 40, 10 p.

Flight Log

Spokane International Airport to Grand Coulee Dam

The flight starts from Spokane International Airport, which is located on the west Spokane plain. The plain lies across the Rathdrum Prairie-Spokane Valley flood path at an elevation near 790 m. The Spokane plain is mantled by flood sands and gravels and was exposed to all of the major floods. Because this was a spreading area for flood water, it was not significantly dissected except near the outlet channels leading southward between the buttes. Unequal scouring of the basalt and underlying metamorphic rock produced a number of depressions between the buttes; these now contain lakes that provide excellent sport fishing.

Early workers (Symons, 1882; Bretz, 1923; Flint, 1937), on the basis of studies of topography and sediments, believed that the west Spokane plain had been glaciated. However, Richmond and others (1965) and more recent workers, including the authors of this paper, support a Lake Missoula flood origin rather than a glacial origin for the sediments. Cobbles and pebbles in a coarse sand matrix are typical of the flood deposits here. Foreset beds and scattered imbricated gravels indicate a south or southwest flow direction. Giant current dunes superimposed on other flood deposits (and including older dune fields) were developed extensively in the region by successive floods. Several dune fields are present on the west Spokane plain, including a small one just north of Fairchild Air Force Base. A larger dune field is located about 10 km to the west of the base's runway. At least one major flood postdates the deposition of the 13,000-yr-old Mount St. Helens set S ash in this area (Stradling and Kiver, 1986). Immature soils associated with a thin, discontinuous loess cap support a late Wisconsin age for the last floods.

Steptoes (Fig. 2) are located south of the west Spokane plain as well as along the flight path and have protected the downstream areas of loess from severe erosion by flood water. They also channeled water between them, thus causing local dissection. The west Spokane plain has a loess cover less than 1 m thick, in contrast to the protected uplands, such as those north of Reardan and Davenport, which have as much as 10 m of loess. However, the loess in these areas is thinner than that in the Palouse region because they are not situated downwind of the source area; southwest winds apparently prevailed during deposition.

As the aircraft approaches Franklin D. Roosevelt Lake (or Roosevelt Lake), the confluence of the Spokane and Columbia Rivers can be seen about 10 km to the north. Lake Missoula floods interacted here with the south-flowing Columbia River glacial lobe of the Cordilleran ice sheet. At least once during the pre-late Wisconsin, Lake Missoula floods preceded the blockage of the Columbia River by the Okanogan lobe. Later, the floods flowed into glacial Lake Columbia, which formed upstream of the Okanogan lobe ice dam. It is still controversial whether Lake Missoula floods or other floods occurred following the retreat of the Okanogan lobe and the resulting drawdown of Lake Columbia. Atwater

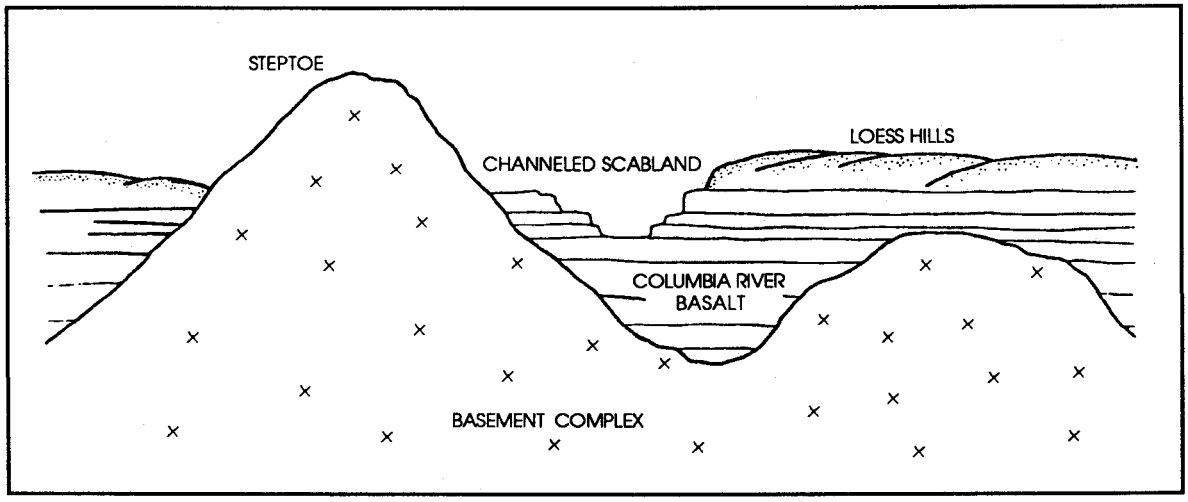

Figure 2. Sketch of general relations of stratigraphic units on the northern Columbia Plateau.

(1986, 1987), Waitt (1985), and Kiver and others (this volume) discuss the problems of chronology and relative interaction of the floods, Lake Columbia, and the Okanogan lobe.

Both the Spokane and Columbia Rivers follow the approximate contact between the Miocene Columbia River basalt and the pre-Miocene rocks of the Okanogan Highlands to the north and the North Cascades to the west. Willis (1887) first recognized this relation and attributed the displacement of drainages to northward and westward to advancing lava flows. Both rivers cut locally down through the basalt surfaces into the basement rock, creating some youthful channels. Many of these sites provide solid foundations for dams in the area.

Sixteen terraces have been identified along Roosevelt Lake and downstream to the Rocky Reach Dam (Kiver and Stradling, 1982b). Their internal composition, morphology, and extent vary considerably. Many of the upper terraces are capped by eolian sands and silts, whereas the lower ones are capped by gravels. Mount St. Helens set S ash is present in deltaic sediments on a terrace at an elevation of 520 m 5 km downstream from Grand Coulee Dam (Kiver and Stradling, 1982b; Stradling and Kiver, 1986). This occurrence indicates that the Okanogan lobe had retreated from the Grand Coulee entrance by 13,000 yr B.P., permitting meltwater and Lake Missoula floods to spill southward. Also, the 520-m terrace elevation indicates that the northern lip of the Grand Coulee was not eroded down to its present 468-m level until after 13,000 years ago. Presumably, later floods and the diverted Columbia River lowered the bedrock lip.

Numerous landslides can be observed in association with the terraces along Roosevelt Lake. The frequency of landslides greatly increased after the construction of Grand Coulee Dam, which backed up the Columbia River about 230 km upstream to the Canadian border and raised the water level 107 m. Jones and others (1961) studied 300 landslides along the lake shore and just downstream from Grand Coulee Dam. Fluctuating water levels, steep slopes, the presence of both permeable and impermeable sediments, and local irrigation have contributed to landslide activity. Note houses and at least one large development on the terraces adjacent to the reservoir. Not related to the filling of Roosevelt Lake is a large, relatively recent basalt landslide in the town of Grand Coulee located about 3 km south of Grand Coulee Dam.

Grand Coulee Dam to Steamboat Rock

The flight path proceeds down the Grand Coulee to Steamboat Rock. Light-colored sediments exposed just to the northeast of Steamboat Rock are part of the Nespelem Silt deposited in an extension of glacial Lake Columbia. Atwater (1987) suggests that deposition was by late lacustrine and small flood activity. Notice the difference in erosion of the massive granitic rock and that of the basalt with its dominant vertical jointing. Just south of Steamboat Rock is a pendant bar deposited by one or more large floods prior to deposition of the Nespelem Silt.

Steamboat Rock to Sims Corner

After circling Steamboat Rock, the flight heads WSW to Sims Corner to view ice sheet features. To the north and along the flight path are at least two partially covered Lake Missoula flood channels extending westward from Grand Coulee. Their presence indicates that the Grand Coulee could not accommodate all of the flood water. Following the flood erosion, the Okanogan glacial lobe deposited drift that partly covered the channels. Stagnant ice features, including kames and eskers, can be observed near Sims Corner. Thin soils, small tillable areas, and rocks at the surface create problems for wheat farmers in the glaciated areas of the Waterville Plateau.

Sims Corner to Dry Falls

From Sims Corner, the flight path turns south to Dry Falls. As the aircraft approaches Dry Falls, the loess-covered unglaciated part of the Waterville Plateau can be seen to the southwest. Dry Falls is the largest cataract in the Channeled Scabland. Its width is 5.5 km, and its height is nearly 120 m. Lakes occupy plunge pools nested in several alcoves. The complex of alcoves was formed as flood water preferentially eroded the most fractured parts of a zone of basalt along the Coulee monocline (Bretz, 1932, 1969). These grooves, as much as 3 m deep, are spaced 30 to 60 m apart (Baker, 1987). The Coulee monocline can be seen at several locations along the west wall of the Grand Coulee and on the east side of Banks Lake about 6 km north of Coulee City.

Dry Falls to Crab Creek

Upon leaving Dry Falls, the flight path heads southeast to an area along Crab Creek about 15 km east of Odessa. Several well-developed scabland channels, which are tributary to the Crab Creek channel, can be seen on the way. As we approach the area northwest of Odessa, numerous circular features or sag flowout structures in the basalt can be seen where they were exposed by flood water.

A Roza flow, as much as 100 m thick, is exposed in the cliffs bordering Crab Creek and tributary coulees. The circular sag flowout structures are developed in this flow (Fig. 3). McKee and Stradling (1970) suggested that subsidence of the flow crust caused cracking that provided circular openings for dikes to penetrate from the molten

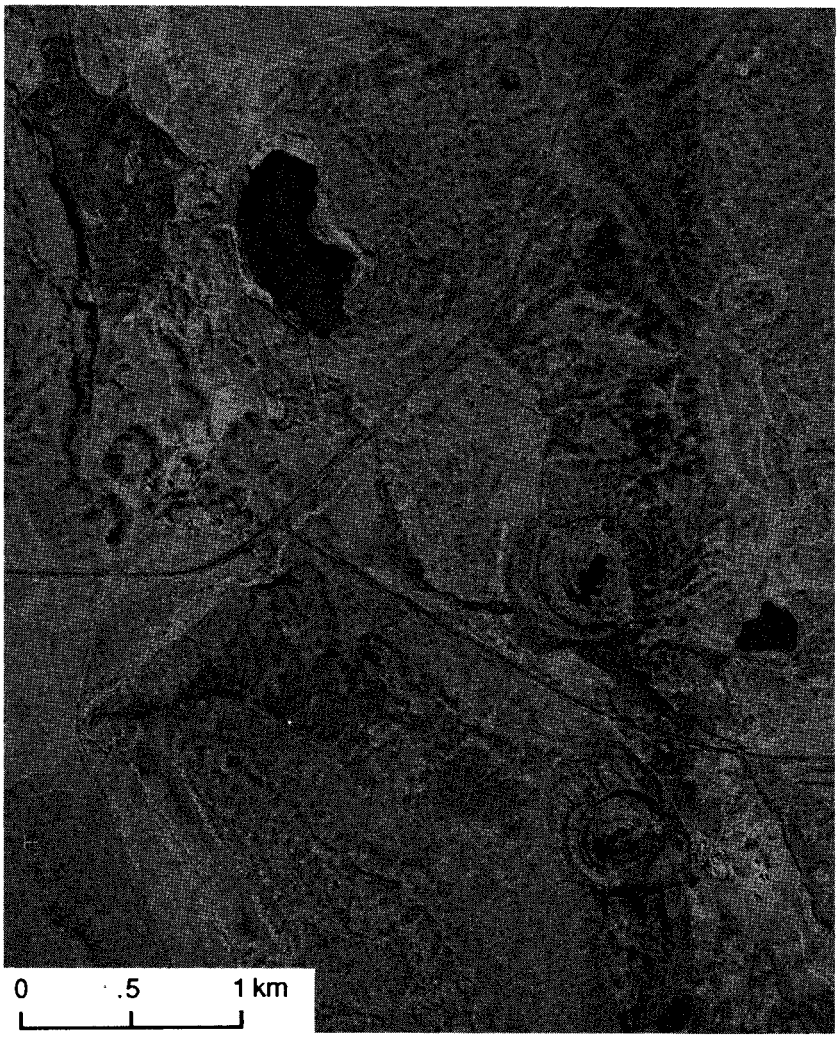

Figure 3. Circular sag flowout structures 8 km (5 mi) north of Odessa (Pacific Lake 7 1/2 minute quadrangle). U.S. Department of Agriculture Commodity Stabilization Service, Lincoln County, WA, flight of Aug. 16, 1957, image AAO25T8.

interior of the flow and serve as a source for lava sheets above. Flood waters subsequently removed the adjacent finely jointed basalt, leaving the circular dikes as residual features.

However, it is still not clear what effectively initiated the entire process. Hodges (1978) disagreed with McKee and Stradling's proposed origin for the features and suggested that the molten interior of the thick, ponded Roza flow was intersected by a rising ground-water table and that rapidly accumulating volatiles caused explosive venting. Subsidence caused by the venting would then permit intrusion of melt into predominantly concentric fractures. Her model, however, is incompatible with another relation seen in the area: several dikes can be traced in the cliffs along Crab Creek from the entablature base just above the colonnade upwards to the surface where the dikes form arcuate and circular ridges with no indication of explosive activity.

Whatever the features' origin, Lake Missoula flood water eroded these structures, leaving numerous overhanging cliffs that were later utilized by Indians as rock shelters. In addition, flood water deposited sands and gravels, forming pendant bars along Crab Creek and the tributary coulees.

Crab Creek to Spokane International Airport

After viewing the sag flowout structures along Crab Creek, we will fly northeast toward Spokane. Along the return leg of the trip, an increase in bunchgrass and sagebrush and eventually the appearance of Ponderosa pine, as well as evidence of greater agricultural productivity, are indicative of the increased precipitation between Odessa and Spokane. Also, the loess cover becomes thicker where it was not eroded by Lake Missoula floods.

Steptoe and Kamiak Buttes located in the heart of the Palouse are visible to the southeast. The buttes south of the west Spokane plain and their influence on flood erosion that was observed on the first leg of the trip can now be seen from a different direction.

Grand Coulee Dam

Greg W. Behrens and Phillip J. Hansen

Geology and Related Construction Problems of the Grand Coulee Dam Project

Greg W. Behrens *and* Phillip J. Hansen
U.S. Bureau of Reclamation
P. O. Box 620
Grand Coulee, WA 99133

INTRODUCTION

Grand Coulee Dam is the uppermost dam on the main stem of the Columbia River in Washington (Fig. 1). It is the key structure of the U.S. Bureau of Reclamation (USBR) Columbia Basin Project, a multipurpose development that provides irrigation water for agriculture in the central part of Washington, flood control, power generation, and recreational opportunities on project reservoirs and land (USBR, 1981).

The need to provide water for irrigation to the arid but fertile lands which now comprise the Columbia Basin Project prompted investigation by the newly established U.S. Reclamation Service as early as 1904. In 1918 local interests initiated a proposal for irrigation of the project area: that a high dam be constructed on the Columbia River at the head of the upper Grand Coulee. Such a dam would make use of the upper coulee to convey water to the irrigable lands as far as 50 mi to the south. Alternative proposals included (1) construction of a canal to convey water from the Pend Oreille River in northern Idaho generally westward across the plateau surface and into the middle portion of the project area, and (2) construction of a dam of sufficient height to create a lake which would allow gravity flow through Grand Coulee. In 1932 the Bureau of Reclamation recommended and the U.S. Army Corps of Engineers completed a conclusive engineering and economic study recommending construction of the high dam and pumping the water up into Grand Coulee and an irrigation plan for the Columbia Basin Project. This report was published as House Document No. 103, 73d Congress, 1st Session. As originally conceived, power generation other than that required for pumping of the irrigation waters was not a significant consideration.

The site of Grand Coulee Dam is characterized by topography dramatically altered and carved by events of the Pleistocene glaciation. The foundation of the dam consists of granitic bedrock which was overlain by considerable thicknesses of unconsolidated glacial and glaciofluvial sediments. Immediately downstream of the dam the Columbia River valley has been glacially sculptured into a U-shaped, granite-floored valley in which hundreds of feet of glacial, lacustrine, and glaciofluvial material were deposited. The sequence, thickness, and attitude of these deposits coupled with the ground-water conditions has introduced many engineering problems which had to be overcome.

The impoundment behind the dam, Franklin D. Roosevelt Lake (or FDR Lake), inundated more than 125 mi^2 of mostly unconsolidated sediments which are now being eroded along the reservoir rim. The Grand Coulee, an abandoned erosional channel carved into multiple layers of basalt flows, is a product of temporary occupation by the Columbia River and periodic floods of enormous size that issued from glacial Lake Missoula to the east. These floods encountered a pool of water, referred to as glacial Lake Columbia, that was formed by glacial damming of the Columbia near the site of the present Grand Coulee Dam. As the on-rushing waters from Lake Missoula floods encountered the Lake Columbia pool, the reservoir rim was over-topped, and flood waters rushed over the Columbia Plateau to the south, rapidly carving the features of the Channeled Scabland.

The enormous dam and its associated features cross a variety of geologic conditions, which played very significant roles in their design and construction. Use of the upper Grand Coulee as a stabilization reservoir made it feasible to pump water from the Columbia River up into Banks Lake. Hydrogeologic conditions of the Columbia River valley upstream of the dam were determined to be suitable for water impoundment, and seepage under the dam could be controlled by grouting. Excavation for the main dam cut through hundreds of feet of unstable glacial

From: Joseph, N. L., and others, editors, 1989, Geologic guidebook for Washington and adjacent areas: Washington Division of Geology and Earth Resources Information Circular 86.

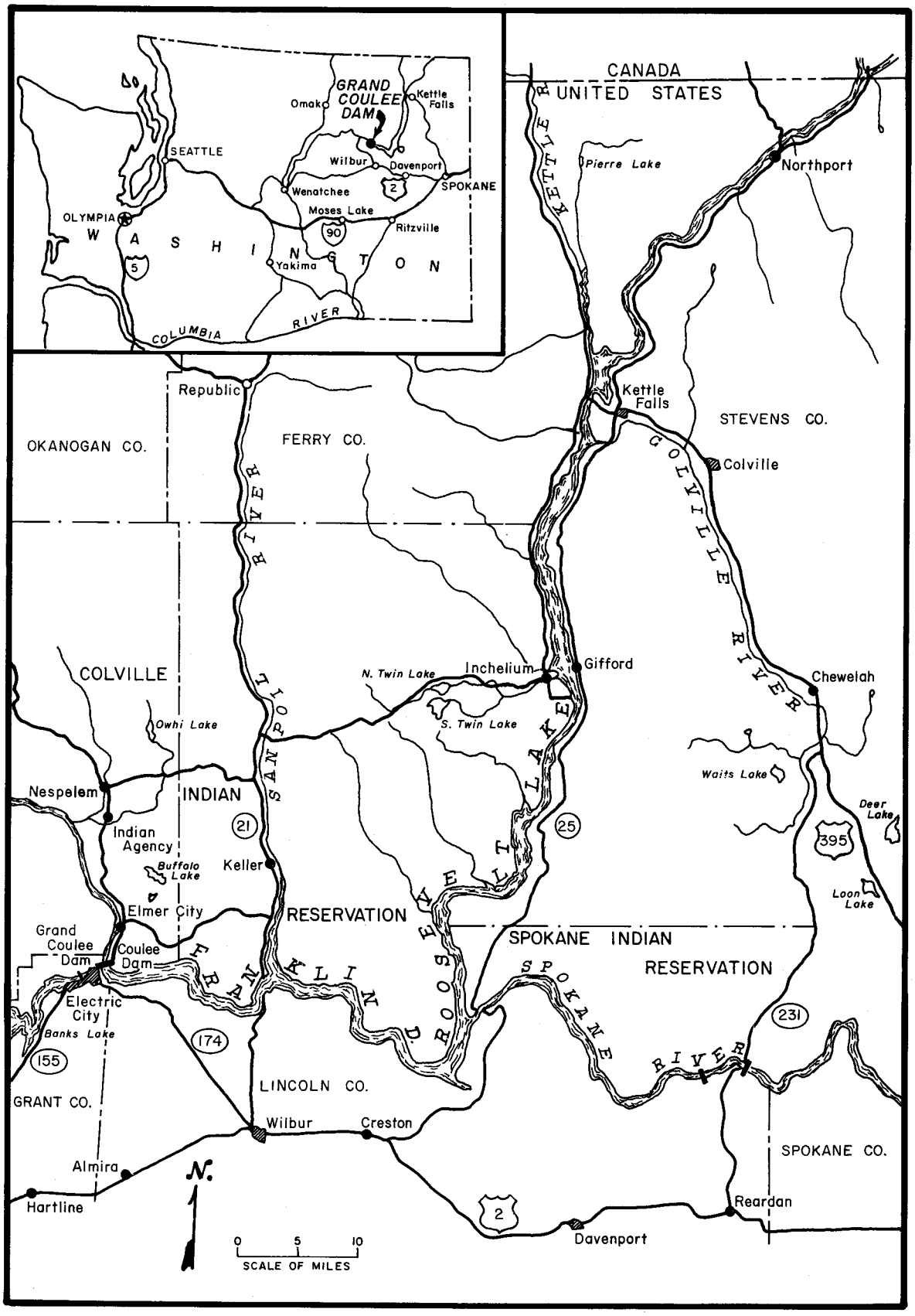

Figure 1. Grand Coulee Dam and vicinity, northeastern Washington.

and glaciofluvial deposits. Small- and large-scale land movements constantly plagued construction activities through this material. Stabilization measures as simple as complete removal of the slide material and as complex as construction of an ice barrier by freezing were employed. Construction of the Feeder Canal into Banks Lake was possible only through careful excavation and immediate burial of twin 25-ft-diameter concrete conduits through an active slide area. Daily tailbay fluctuations of as much as 20 ft impose extremely favorable conditions for landslide activity on the unconsolidated near-shore sediments for a 6-mi reach downstream of the dam on the right bank and a 1-mi reach on the left bank. Where economically feasible, engineering solutions for slope instability consist of laying the slopes back to a more gentle angle, riprapping, buttressing, dewatering of the slide material, and, least desirable, temporary operational restrictions imposed upon the powerplant.

GENERAL GEOLOGY

Pre-Miocene Geology

Grand Coulee Dam is located approximately on the physiographic boundary between the Okanogan Highlands to the north and east and the Columbia Plateau to the south and west. The Okanogan Highlands consist of south-trending mountains and valleys carved into the complex plutonic assemblage of the Colville batholith. These rocks range in composition from granite and granodiorite to quartz monzonite, quartz diorite, and diorite. Textural variations include medium- and coarse-grained nonporphyritic and fine- and medium-grained seriate. Pegmatite, aplite, and migmatite zones are locally abundant (Colville Confederated Tribes, 1984). These rocks have been divided into two basic types: an older coarse-grained granite, and a younger fine-grained granitic rock type that intrudes the older in a series of north-trending dikes. The older granite is characteristically moderately to lightly jointed (joint spacing typically 2-4 ft) and forms more massive outcrops. The younger rock is typically moderately to intensely jointed and forms outcrops that have a more blocky surface. At the dam, these granitic rocks have been identified as quartz monzonite, granodiorite, granite, and syenite porphyry.

Miocene Geology

During the Miocene periodic eruptions from elongate fissures, now exposed as dikes, released flows of highly fluid tholeiitic basaltic lava which ultimately inundated more than 100,000 mi^2 in parts of Washington, Oregon, and Idaho. More than 99 percent of these basalt flows, referred to as the Columbia River Basalt Group (CRBG), were erupted during a 2.5- to 3.0-m.y. interval centered about 15 Ma (Swanson and Wright, 1978). These flood basalts poured out onto an erosional surface of considerable relief, 3,000 ft or more in many places, forming a rather featureless surface whose gentle regional slope is towards the central part of the plateau. These flows ultimately pushed the Columbia River to its present channel which trends north at the site of the dam. The basalts cap the valley rim at the site of the dam and form portions of the reservoir rim, but they were not encountered in the dam foundation.

Sedimentary interlayers and unconformities that occur throughout the basalt sequence consist of weakly indurated shale, siltstone, sandstone, and claystone. These sedimentary units contribute to the slope stability problems characteristic of the area.

Pleistocene Geology

Pleistocene glaciation played the final part in forming geomorphic features that cause geologic engineering problems encountered within the area. The Cordilleran ice sheet pushed into the Columbia River valley from the north. The Okanogan lobe progressed south, covering a large area across the Waterville Plateau northwest of Grand Coulee Dam, and advanced down the Okanogan River valley to its confluence with the Columbia River, then up the Columbia River valley to the present location of Grand Coulee Dam. The glacier carved the originally V-shaped bedrock channel into a broad U-shaped glacial valley. Most of the soil cover and weathered or altered rock in the path of the glacier was stripped, leaving a lightly weathered or fresh bedrock surface. Deposits of till and outwash locally cover the bedrock surface. Damming of the Columbia River by the Okanogan lobe formed glacial Lake Columbia, the surface of which attained an elevation of 2,480 ft. Vast quantities of sediments were deposited into this lake in a sequence of varved clays and silts with sand interbeds. These sediments, locally referred to as Nespelem Formation, filled the preglacial drainages to elevations as high as 1,600 ft, more than 740 ft above the present granite floor of the valley. Periodic pulses and retreats of the glacier overrode the lake bed, forming override zones within the lacustrine deposits, overconsolidating them, and locally depositing till and outwash material. (See papers by Kiver, Breckenridge, and Stradling, this volume, for more detailed discussion of glacial events in the area.)

Periodic floods from glacial Lake Missoula in Montana resulted in cyclic deposition of coarser sands and (or) gravel within the varved sequence. Estimated flow rates, through the narrow parts of the Clark Fork Canyon, of the Lake Missoula flood waters are 9-1/2 mi^3/hr – a rate of about 386 million ft^3/sec or about 10 times the combined flow of all the rivers of the world (U.S. Geological Survey, 1976). Recent work by Atwater (1986) on the Sanpoil River valley suggests that floods from glacial Lake Missoula into glacial Lake Columbia

occurred periodically, perhaps as many as 100 times during the Pleistocene.

The Grand Coulee, immediately to the southwest of Grand Coulee Dam, is the result of catastrophic flooding that originated from glacial Lake Missoula in Montana and the southerly diversion of the Columbia River by the Okanogan lobe of the Cordilleran ice sheet. The Okanogan lobe ponded the Columbia River approximately at the present site of Grand Coulee Dam, creating glacial Lake Columbia; the river flowed southerly across the Columbia Plateau. As the Columbia River and periodic floods from glacial Lake Missoula flowed across the basalts of the plateau, a preferred drainage was established along the structurally weakened Coulee monocline, a Tertiary structure in the CRBG. Aided by the vertical jointing of the basalts and their susceptibility to be easily plucked and eroded, cataract recession eroded the lower Grand Coulee up to the present site of Dry Falls, 30 mi south of the dam, and along the upper Grand Coulee to the Columbia River valley near the dam site.

Today the Grand Coulee is filled with manmade Banks Lake, which is flanked by 800-1,200-ft-high basalt cliffs. Exposed on the flat valley floor, throughout the upper area of the coulee, are outcroppings of granite bedrock which exhibit glacial sculpturing (striations and grooving). This gives evidence for glacial occupation of the upper Grand Coulee after its breaching of the Columbia River valley.

Final retreat of the glaciers allowed the Columbia River to return to its preglacial course. The river has rapidly cut down through the varved lacustrine deposits to its present level. In many places the entire sequence of lake sediments has been cut through, exposing bedrock within the channel. Numerous erosional and depositional terraces have been left along the valley walls, evidence of the rapid downcutting of the river as it sought its preglacial level. The attitude and weakness of the varved clays and silt and the rapid downcutting have resulted in an extremely active landslide history that is characteristic of most of the upper reaches of the Columbia River.

GEOLOGIC AND GEOMORPHIC ASPECTS OF SITING AND DESIGN

The area's geological and geomorphic characteristics determined the present configuration of the project. The sound granite bedrock provided the foundation for the dam, and the upper reaches of the Columbia River within Washington provided adequate storage capacity for flood control, irrigation, and power generation. By using the upper Grand Coulee as a stabilizing reservoir, pumping lifts of 290 ft were needed to bring water from behind the dam up into manmade Banks Lake. The upper Grand Coulee provided a natural conveyance and reservoir for the irrigation water.

Construction Problems

Grand Coulee Dam

The generally fresh granite bedrock provided a suitable foundation for the dam. Geologic investigations undertaken by the State of Washington and the U.S. Army Corps of Engineers in the early 1930s consisted of drilling 15 exploration holes. The investigations indicated a bedrock surface beneath the river channel that varied in elevation from 780 ft to approximately 880 ft and was overlain by from 50 to more than 300 ft of alluvial sand and gravel and varved glacial lake deposits. Subsequent design investigations included numerous additional drill holes and test trench excavations to verify foundation conditions. These explorations verified the lightly weathered or fresh condition of the bedrock surface and revealed several deep, narrow crevices within the bedrock. Further construction investigations included open trench excavation and excavation of drifts to delineate the depth and extent of crevices and shear zones within the foundation rock.

Preparation of the foundations of both the original dam and the Third Powerplant involved excavation of enormous quantities of alluvial deposits and varved clays and silts. Shear zones encountered within the granite required extensive treatment, including scaling, over-excavation, and bolting.

The most challenging problems, then and now, result from the instability of the glacial lacustrine varved sediments. Initial excavation into the toe of the riverbank slopes resulted in landsliding. Between 1934 and 1937, 57 landslides occurred in the excavation area. Sliding into the left tailrace area began in March 1934, when a slide with nearly 100 ft of vertical displacement occurred. Treatment of this slide included extensive over-excavation, installation of drainage shafts, drifts, and radiating drain holes and construction of a rock-fill plug at the toe of the slope. Ultimately a riprap blanket was placed to protect the toe of the slope. Between 1934 and 1941, $2,726,000 in additional costs were incurred for treatment of this slide alone; placement of riprap between 1948 and 1953 brought the cost for treatment of this slide to more than $6 million (Jones and others, 1961).

As noted, solutions to landslide problems encountered in excavations in the unconsolidated materials ranged from laying back the slopes, to dewatering via drainage drifts and wells. Freezing the slide materials to form an arch dam to block flow of the slide materials into the excavation was also undertaken. This freezing approach was successfully used in the spring of 1936 to allow cleanup of a particularly deep bedrock crevice

filled with saturated unconsolidated sediments located directly below the forebay cut, on the east riverbank. This crevice became known as "Ice Dam Gulch".

Preliminary exploration of Ice Dam Gulch proved it to be a long, narrow gulch about 120 ft deeper than the average bedrock surface. Excavation into this gulch brought about construction problems which called for unusual methods of slope stabilization. More conventional methods, such as laying back the slope, were attempted but proved inadequate to the task. The volume of slide material involved and time constraints prohibited removal of the material, limited working space would not allow buttressing, and the slide mass would not withstand vibrations generated if sheet piling or caissons were to be installed. Arching of the toe of the slide mass with frozen ground was determined to be feasible and expedient, and this method was implemented.

Few data existed in 1936 on the mechanics and strength of frozen ground. Design calculations suggested an embankment thickness of 10 ft, but to provide an ample safety factor, the arch dam was made 20 ft thick. Freezing was accomplished by pumping brine through pipes driven into the ground. The freezing points were spaced 30 in. apart. Each point consisted of 3-in-diameter pipe driven 40 ft into the ground. A 1-1/2 in.-diameter pipe was then installed inside the larger pipe to allow circulation of the brine in through the smaller pipe and out through the annulus between the smaller and larger pipe. The points were connected in series by means of a rubber hose on the upper end. Freezing of the dam required installation of 377 freezing points. Two ammonia-brine refrigerating machines with a combined capacity of 80 tons of ice per day were installed. Construction of the ice dam was accomplished in about 6 weeks. The ice arch dam performed satisfactorily, and cleaning of the crevice continued without further problem. The arch was a means of saving, possibly, several hundred thousand cubic yards of excavation at a cost of $1 per yard and several months' time in preparing foundations and concreting in the area (USBR, 1936).

Construction problems of this type, though on a smaller scale, were the rule rather than the exception during construction of the main and, later, the forebay dam. Landslides occurred frequently when slopes were oversteepened during construction of the Third Powerplant. The only slide that caused damage occurred during placement of the cellular cofferdam. This slide moved recurrently from November 1968 to May 1969 as the contractor continued to undercut its toe. Its last movement damaged the partly erected cofferdam. The ultimate solution was laying back the slope.

Excavation for the Third Powerplant (1967-1974) generated more than 10 million yd^3 of waste material. This material was used in the construction of a staging area upstream of the dam for Third Powerplant construction and downstream, principally on the right (east) riverbank, to form the downstream stabilization embankment. Failures occurred frequently in the embankments where the waste material was underlain by varved clays and silts.

Feeder Canal

The Feeder Canal and other features of the irrigation project were constructed during the 1950s. Initial construction was by USBR forces. Excavation for the first portion of the canal prism was in granite bedrock. The excavation next penetrated bedded Miocene sediments dipping 4 degrees north and underlying remnants of a basalt flow. The alignment then crossed an ancient landslide in Miocene sediments and basalt slide blocks. Excavation through the sediments immediately became a problem. Undercutting by excavation led to sliding which threatened to fill the excavation. This problem was solved by changing this portion of the alignment to a "cut-and-cover" design. This cut-and-cover consisted of twin 25-ft-diameter concrete conduits placed along the canal alignment and immediately buried. This eliminated an open canal through this portion of alignment and minimized the chance for slope failure.

Modification of the Feeder Canal to allow reverse flow for pump/generation required widening the canal and eliminating the cut-and-cover section. The cut-and-cover section was to be replaced with a flume wall section. Construction began in the winter of 1979. Excavation for construction of the flume section would have to pass through the landslide deposits. This geotechnical problem was solved in two ways: the old cut-and-cover conduits were used as part of an anchored retaining system; and an automated instrumentation system was installed to monitor and warn of impending instability. The system consisted of a series of inclinometer wells emplaced upslope of the canal prism. In-place uniaxial inclinometers were installed within the wells and monitored by a centrally located microprocessor. The microprocessor was set to record hourly data from more than 100 individual instruments and to sound an alarm if movement of greater than 0.25 in. occurred. This system served as a model for the Riverbank Stabilization Monitoring System, which will be described in the last part of this text.

Anchoring the twin cut-and-cover conduits was accomplished by drilling and installing tensioned soil anchor tendons into the hillside from within the conduits. The anchor tendons did not penetrate bedrock. Pairs of tendons were installed on 25-ft centers in each of the conduits to depths adequate to pass through known failure surfaces. These depths ranged to as much as 150 ft. Drilling the holes for the tendons ultimately required use of horizontal drills capable of advancing casing through the

sandy material. Upon installation, the tendons were tensioned. This system proved effective, and the construction was completed with no major stability problems.

Landslides along FDR Lake

Construction of the dam was essentially complete by 1941, and filling of the reservoir began. Full reservoir pool was attained in 1942, creating a lake 151 mi long with approximately 635 mi of shoreline. About 70 percent of the shoreline is composed of unconsolidated Pleistocene clay, silt, sand, and gravel deposits. Landslides occurred frequently during reservoir filling—245 before the lake was full. Though the frequency of sliding decreased upon attaining initial full pool, annual reservoir fluctuations of 30 to 80 ft, coupled with wind and wave erosion, make landslides a continuing factor in engineering development and land use. Between 1943 and 1953, an additional 255 slides took place.

The relation between increasing frequency and magnitude of landsliding and increasing severity of reservoir drawdown was established by an intensive geologic investigation which was conducted between 1948 and 1955. The goal of the investigation was to develop criteria that could be used for predicting the probable amount of land impacted by sliding. These investigations are summarized in a comprehensive report by Jones and others (1961). This report provided a basis for procurement of additional lands, and it serves as a guideline for performance of current investigations along the lakeshore.

The Grand Coulee Project Office currently conducts an annual survey of landslides impacting the Lake Roosevelt shoreline. Currently, more than 130 active landslide areas are monitored under this program. To date, detailed mapping has been completed on U.S. Geological Survey 7-1/2- and 15-minute quadrangle sheets encompassing the entire shoreline. Additionally, detailed engineering geologic mapping has been accomplished for most of the shoreline, and zones of current and potential instability have been identified. The USBR is in the process of acquiring additional freeboard land in some areas and is providing shoreline protection (riprap and gabion bags) in others.

Riverbank Stabilization Program

Landslides downstream of the dam prompted the most recent construction. These landslides are mostly reactivations of ancient landslides that can be distinguished on maps and photographs predating the construction of the dam. Unusually high precipitation and seasonal runoff between 1948 and 1952 resulted in re-activation of several of these ancient slides. Peaking operations of the Third Powerplant were recognized as having the potential for further destabilizing the area. Power peaking operations, required during periods of high energy demand, will generate daily fluctuations in the tailrace elevations in excess of 20 ft. The added erosive force of this volume and velocity of water, coupled with fluctuation of pore pressures in the clays underlying the riverbanks, result in an unacceptably high potential for large rotational and planar-surface failures downstream of the dam. At the time of construction of the Third Powerplant, USBR designers determined that placement of an embankment along a 6-mi reach immediately downstream of the dam on the right (east) riverbank and a 1-mi reach of the left riverbank would be required to stabilize the area for peaking operations.

Failures which occurred both during and after placement of the stabilization embankment indicated that the embankment was inadequate to stabilize the hillsides. In 1975 the USBR commenced investigations targeted at identifying and correcting additional factors lending to the overall instability of the downstream riverbanks. In June 1978, landslides occurred along the entire 6-mi river reach downstream from the dam along the east bank. The most significant of these failures occurred just downstream of the east end of the State Route 155 bridge adjacent to the town of Coulee Dam. The slide, which had a maximum vertical displacement of approximately 4 ft and horizontal displacement of 0.5 ft, was triggered by a 13-ft drop in the mean elevation of water in the tailbay, which was caused by a failure of one of the units in the Third Powerplant. This drop in the mean tailbay elevation was slightly more than fluctuations anticipated for Third Powerplant peaking operations. As a result of this renewed landslide activity, investigations ultimately leading to the Riverbank Stabilization Program were intensified.

Numerous possible solutions to the riverbank stabilization problem were identified and evaluated. These included relocation of the downstream communities and resloping of the hillsides below the dam to reduce the driving force on the failure surfaces. Ultimately it was determined that an engineered solution was feasible, and the decision was made to approach the problem with minimal disruption to the downstream residents. The Riverbank Stabilization Program addressed the stability of the downstream slopes in three ways:

(1) Reshaping and rearmoring the previously placed stabilization embankment.
(2) Constructing drainage features to reduce pore pressure fluctuations within the clay/silt materials underlying the hillsides.
(3) Installing automated instrumentation to monitor the equipment operation, effectiveness of the completed drainage features (based upon relative reduction of pore pressures), and to warn of movement within the river banks.

The automated system has real-time alarming capability and is operational at this writing.

This stabilization work involved placement of additional fill and armor rock within the river channel, principally on the right riverbank. The grade of the face of the embankment was reduced from an original 1.5H:1V slope to slopes ranging to as little as 5H:1V. The embankment is protected with graded armor stone quarried from granite exposures on the right riverbank and the staging area immediately upstream of the Third Powerhouse on the FDR Lake shoreline. Approximately 3 million yd^3 of fill and 3 million yd^3 of riprap were used.

Ground-water recharge in the first 3 mi of riverbank downstream of the dam is essentially controlled by the river. From 3 to 6 mi downstream, the ground-water system is complicated by upslope artesian conditions. Features designed to control pore pressure fluctuations within the clay on the slopes consist of traditional pumped wells and, on the right riverbank below the community of Coulee Dam, three 12.5-ft-diameter shafts, as much as 239 ft deep, with near-horizontal drains (as much as 600 ft long) installed radially out into the clay and bedrock. The shaft concept was advanced as a method to more effectively collect and control water within disturbed landslide masses of complexly interbedded deposits of clay, silt, and sand. Wells were the method selected for dewatering in the undisturbed sediments, artesian areas, and on the left riverbank immediately adjacent to the Left Powerhouse. Well and shaft sites were determined by geohydrologic investigations which indicated sources of clay recharge, such as bedrock anomalies (areas of higher hydraulic conductivity), perched water tables, extensive sand interbeds, and the presence of basal gravels. This approach has proven highly successful to date.

The Riverbank Stabilization Monitoring System consists of: uniaxial inclinometers installed in wells penetrating identified failure surfaces; electronic pore pressure transducers in selected ground-water observation wells; river gaging stations at three locations downstream of the dam; flowmeters installed on discharge piping and horizontal drains; earth-pressure cells and structurally mounted strain gages to monitor shaft deformation; and equipment operation sensors to monitor their performance. The data from the instrumentation are collected at data scanner locations which are linked by a network to a central computer. The system is capable of operation in a continuous scan mode, but it normally queries the instruments on a 3-min cycle and records data hourly. Data are automatically compared to predetermined alarm criteria residing in the central computer. Once the monitoring system is fully operational, data will be collected from more than 600 remote locations.

ACKNOWLEDGMENTS

The authors are grateful to Nancy Joseph, Washington Division of Geology and Earth Resources, and Brent Carter, USBR, for their kind and competent assistance and comments on drafts of this report. Linda Phlug prepared the illustrations.

REFERENCES

Atwater, B. F., 1986, Pleistocene glacial-lake deposits of the Sanpoil River valley, northeastern Washington: U.S. Geological Survey Bulletin 1661, 39 p., 3 pl.

Colville Confederated Tribes, 1984, Revised geology and mineral potential of the Colville Indian Reservation, Washington: Colville Confederated Tribes, 81 p., 26 pl.

Jones, F. O.; Embody, D. R.; Peterson, W. L., 1961, Landslides along the Columbia River Valley, northeastern Washington: U.S. Geological Survey Professional Paper 367, 98 p.

Swanson, D. A.; Wright, T. L., 1978, Bedrock geology of the northern Columbia Plateau and adjacent areas. *In* Baker, V. R.; Nummedal, Dag, editors, The Channeled Scabland: U.S. National Aeronautics and Space Administration, p. 37-57.

U.S. Bureau of Reclamation, 1936, Grand Coulee Dam Project History: U.S. Bureau of Reclamation, Vol. IV, 360 p.

U.S. Bureau of Reclamation, 1981, Project Data Book:–Columbia Basin Project, Washington: Adams, Douglas, Franklin, Grant, Lincoln, and Walla Walla Counties: U.S. Bureau of Reclamation, 20 p.

U.S. Geological Survey, 1976, The Channeled Scablands of eastern Washington–The geologic story of the Spokane Flood: U.S. Geological Survey, 23 p.

Road Log

This trip will begin at the Grand Coulee Dam Visitor Arrival Center (VAC) and visit several of the project's major features (Fig. 2). Along the route we will discuss some of the local geology and some of the geotechnical problems overcome during construction of the project.

Cumulative mileage is given on the left below; interval mileage is shown in parentheses.

0.0 (0.0) **Visitor Arrival Center.**

Begin field trip. Take in the center's activities and collect some of the project-related handouts available. These will add some interesting highlights to the field trip. By convention, directions left and right are given facing downstream. Thus the left bank is on your left as you face downstream.

Grand Coulee Dam rises 550 ft above the lowest bedrock surface, is 500 ft wide at its base, and raises the water surface 380 ft above the old riverbed. The average tailbay elevation is 960 ft, and maximum full pool elevation of Franklin D. Roosevelt Lake behind the dam is 1,290 ft. The dam is 5,673 ft long, and contains 12 million yd^3 of concrete. The right and left powerhouses contain a total of eighteen 125,000-kilowatt units, for a total capacity of 2.25 million kilowatts. The Third Powerplant/forebay structure has six power generating units with a total capacity of 3.9 million kilowatts.

The dam is designed as a gravity-type dam. The foundation rock is a complex plutonic assemblage of granodioritic rocks of the Colville batholith. The foundation was excavated down to bedrock along the entire axis of the dam, and all undesirable rock was removed through blasting. Prior to placing of concrete the near-surface bedrock was grouted, using low pressures (generally less than 200 lb/in.^{2}) along the entire upstream portion of the dam and under the site of the pumping plant. Average grout take for these shallow holes (20-50 ft deep) was 1.9 ft^3/linear foot of hole. This "dental" grout provided a general solid upper layer of rock so that deeper penetration and more effective sealing could be obtained with the higher pressures used in the deeper grouting. As construction continued and successive lifts of concrete were placed, it was necessary (possibly because of the additional overlying weight) to increase the depth and grout pressures beneath the foundation to assure a proper cutoff wall. Intermediate pressure (maximum 400 lb/in.^{2}) grout holes were drilled as the poured concrete reached a minimum height of 25 ft. These holes were 50 to 80 feet in depth; average grout takes were 10.8 ft^3/linear foot. The deepest grout holes averaged 150 to 200 ft; some special holes were more than 500 ft deep. These holes had grout takes averaging 3.9 ft^3/ linear foot.

As construction neared completion, high pressure (greater than 300 lb/in.^{2}) grout holes were drilled from within the grouting and drainage gallery in the dam. These holes were generally 150 to 200 ft deep and accepted an average of 4.8 ft^3 of grout per linear foot. In all, more than 500 grout holes were drilled, and the total volume of grout was nearly 700,000 ft^3.

To provide drainage and reduce uplift pressure beneath the dam and Pump/Generator Plant, approximately 780 foundation drains 50 ft deep were installed. A similar grouting program was carried out during construction of the Pump/Generator Plant. There, a total of 734 holes were drilled, with average grout takes of 1.3 ft^3/linear foot.

Immediately in front of the Left Powerhouse is the elevation 970 riprap terrace. This terrace was placed for erosion control during times of high flow, and it also provides a buttress for the slide mass upslope, which also includes the area near the VAC. To further increase the stability to the immediate area, several drainage wells scattered throughout the park area immediately below the VAC can be observed. These are the rectangular steel vault lids covered with grass carpet flush with the ground. The area is also dotted with many observation wells (6-in. steel casing, about 4 ft high), which are used to monitor the drainage efficiency. To further add to the safety of the area are several inclinometer wells which can monitor very small movements within the ground at various depths.

Travel up the hill on State Route (SR) 155 towards the City of Grand Coulee.

0.5 (0.5) Pump/Generator Plant on left.

This pumping plant lifts water approximately 290 ft up to the Feeder Canal, which empties into Banks Lake. The plant is designed to accommodate 12 pumping units, six of which are

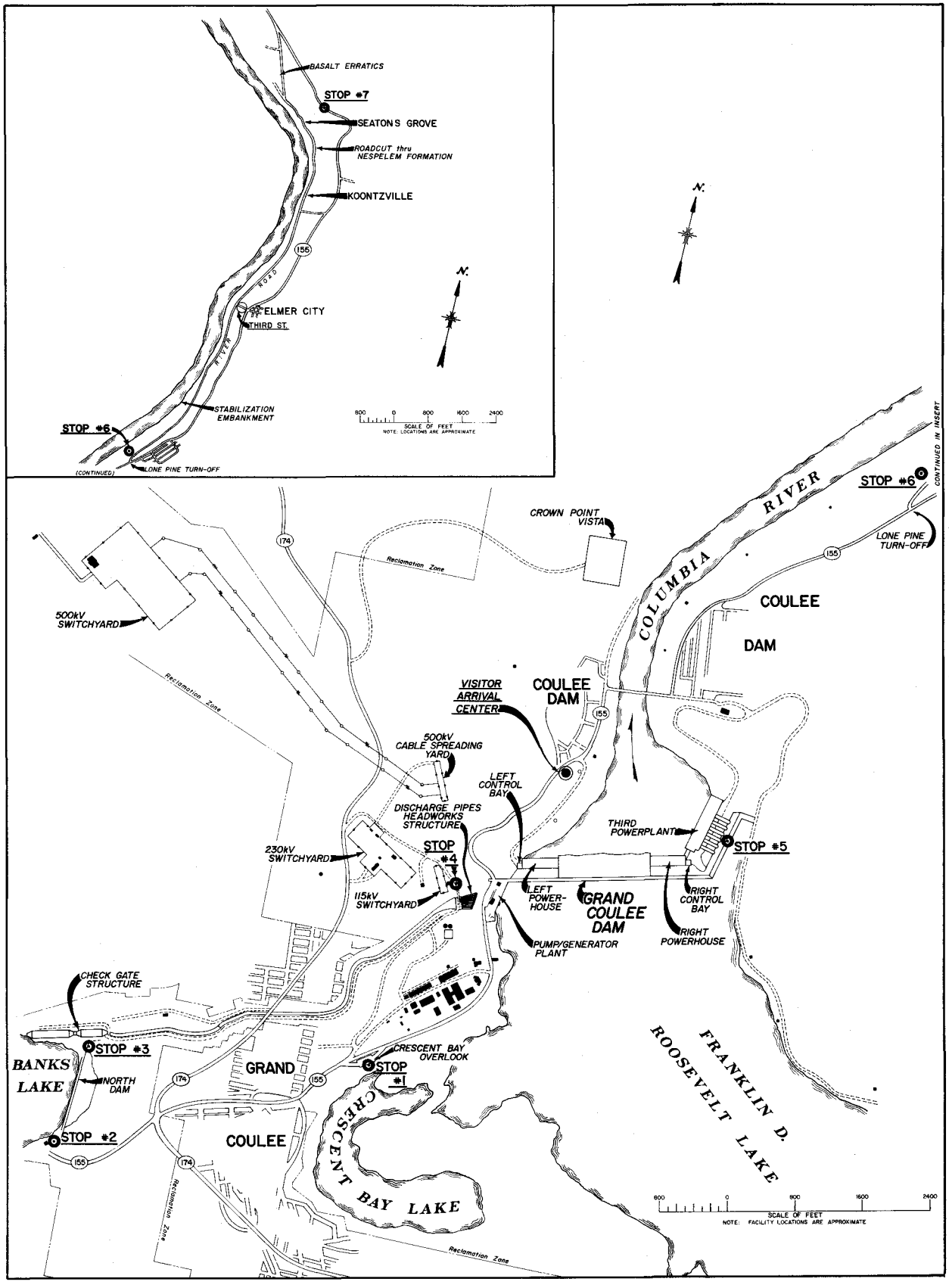

Figure 2. Fieldtrip stop locations, Grand Coulee Dam and project features.

capable of reverse flow and can be used to generate power during peak power demand periods.

0.6 (0.1) Granite in the roadcut on the right.

Exposed here are rocks of the Late Cretaceous Colville batholith. These are subdivided into an older, coarse-grained granitic rock and a younger, fine-grained granite that intrudes the older rock in a series of north-trending dikes. The older, gray biotite granite has an equigranular fabric and is characteristically moderately to lightly jointed; typical joint spacing is 2 to 4 ft. The younger rock consists of light-gray porphyritic granite with feldspar, quartz, and chloritized biotite phenocrysts in a fine-grained groundmass of the same composition and minor syenite and monzonite. The younger granite is typically moderately to intensely jointed; average joint spacing is about 1 ft.

The rock is exposed in what originally was a railroad cut, and has had a history of instability. Recent stabilization efforts included scaling of loose rock, rock bolting using 14- to 20-ft-long bolts, and installation of chain link mesh in zones of rock too intensely fractured to bolt.

1.4 (0.8) **STOP 1. Crescent Bay Lake Overlook.**

Turn left into the park.

This vantage point overlooks Crescent Bay Lake in the foreground and FDR Lake on the left. Columbia River Basalt Group (CRBG) rocks are exposed along the south and west shore of Crescent Bay Lake.

Granitic rock of the Colville batholith is exposed on the north side of Crescent Bay Lake. Glacial/fluvial sand and gravel are exposed in a landslide scarp above the south shore of a cove on FDR Lake on the left. Directly to the south, on the south shore of Crescent Bay Lake, a landslide is exposed. Crescent Bay Lake was formed by construction of a dike on the east end of a small crescent-shaped coulee. The lake is fed by springs and by discharge from the underdrain system of the Feeder Canal.

1.8 (0.4) Miocene sedimentary rocks are exposed in a roadcut on the right side of the road.

The poorly indurated claystone, siltstone, shale, and sand were deposited as interlayers between the CRBG flows. The sediment contains a variety of fossil leaf and stem fragments. The floral assemblage is typical of a wetter, subtropical environment. These Miocene rocks, particularly where bedding planes dip toward excavations, are unstable. Ground water, traveling along and through the sandstone beds, tends to saturate the finer grained interbeds and lubricates failure surfaces in the formation. Where exposed to erosion by streams and small drainages, the sedimentary rock is quickly undercut, leading to destabilization of the overlying rock mass. Many block failures have occurred as a result of this mechanism.

2.0 (0.2) City of Grand Coulee.

Grand Coulee is considered to be a classic "boom town". With the advent of the construction activities, businesses and homes sprang up wherever there was suitable—and not so suitable—ground. It is interesting to contrast the seemingly haphazard layout of Grand Coulee to that of "Engineer's Town" (Coulee Dam) below the dam. Grand Coulee was built upon private ground with no real civic entity to structure the development, while Coulee Dam was strictly government built with one controlling designer, the Federal Government.

2.8 (0.8) **STOP 2. North Dam Park.**

(Restrooms available here.)

Banks Lake, the equalizing reservoir (elevation 1,570), was created by building two rock-faced, earthfill dams at the north and south ends of the upper Grand Coulee. In the spring of 1952, the first water was delivered to the irrigation system to the south. This 27-mi-long reservoir has an active storage capacity of 715,000 acre-feet and can supply water in sufficient quantity to irrigate more than 1 million acres. Currently about 550,000 acres receive water from the Columbia Basin Project.

North Dam is a zoned earthfill dam with a structural height of 145 ft and a crest length of 1,450 ft. The crest width is 30 ft, and the maximum base width is 1,000 ft. The foundation material for the dam consists of a massive basalt slide block on the north end, interbedded basalt and shale overlain by Pleistocene sand, gravel, boulders, clay, and silt within the central two-thirds of the dam, and granite on the south end.

3.2 (0.4) **STOP 3. North end of North Dam/Feeder Canal outlet.**

The Feeder Canal was constructed during the 1950s. Initial construction was by federal forces. Excavation of this portion of the canal was in an

ancient landslide of Miocene sediments and basalt blocks. Undercutting these materials immediately led to landslides, which threatened to fill the excavation. During a cessation of construction necessitated by transfer of work from the USBR to contractors, this problem was solved by redesign of this part of the alignment to a cut-and-cover section. Twin 25-ft-diameter concrete conduits were placed in segments and buried to minimize length of open canal.

Construction began in 1979 to modify the canal to allow reverse flow for pumping/generating. This modification required widening the canal and replacing the cut-and-cover conduits with the flume wall section viewed from this stop. Excavation was required for the flume wall section through the materials that had failed during the initial construction. To stabilize the slope tensioned soil anchor tendons were installed in the hillside from within the conduits. Pairs of tendons were installed on 25-ft centers in each conduit to depths adequate to pass through failure surfaces identified during preconstruction exploratory drilling. Drilling the holes for the anchor tendons required horizontal drill rigs capable of advancing casing through the sandy materials.

Foundation treatment for the flume section included installation of driven and cast-in-place piles. An additional precautionary measure taken prior to construction was the installation of an automated inclinometer instrumentation system with the capacity to provide warning if movement of the slide mass begins to occur.

Turn around and travel back to the SR 155/174 intersection at the west end of the community of Grand Coulee.

4.1 (0.9) Intersection of SR 174 and 155. Turn left (north) on SR 174.

4.6 (0.5) Cross the Feeder Canal. You can see granite outcrops to your right (east) through which portions of the canal pass.

5.4 (0.8) Turn right at the paved road to the 230-kilovolt switchyard. This is one of the project's main switchyards which feeds the Bonneville Power Administration power grid. The 500-kilovolt switchyard is located on top of the coulee wall directly to the west (out of view).

5.9 (0.5) **STOP 4. View of Grand Coulee Dam.**

Stop at overlook.

This vantage point provides an excellent overview of the dam and other project features as well as the river valley downstream of the dam. On the opposite side of the river, above the community east of Coulee Dam, is Brett pit, which was the primary source of aggregate for construction of the dam. Below Brett pit is an immense sandpile that consists of undersized material screened from the aggregate source.

To the north, downstream, is the U-shaped glacial valley of the Columbia River which was sculpted by the Okanogan lobe of the Cordilleran continental ice sheet. This lobe moved down the Okanogan River to its confluence with the Columbia, then eastward up the Columbia River approximately to the present location of Grand Coulee Dam. Blockage of the Columbia drainage resulted in the formation of glacial Lake Columbia. This lake achieved a surface elevation of 2,500 ft. In comparison, the full pool elevation of FDR Lake is 1,290 ft. Materials deposited into Lake Columbia consisted of a sequence of varved clays and silts which choked the preglacial drainages of the Columbia and its tributaries. These sediments are the culprit in the numerous landslides that have occurred both up- and downstream of the dam.

Floodwaters released from glacial Lake Missoula in Montana entered the Lake Columbia pool, and the combined water overtopped the valley rim, spilling out over the Columbia Plateau to the south. This catastrophic flooding resulted in the formation of the Channeled Scabland, of which the upper and lower Grand Coulee are a part.

Along the east side of the 6 mi of river reach downstream of the dam, as well as on the west side of the river below the town of Coulee Dam, embankments have been placed and protected by armor riprap. The work, visible from this vantage point, was done as part of the project's Riverbank Stabilization Program. Landslides, clearly visible from this point, have occurred throughout the post-glacial history of the Columbia River valley. The years of 1948, 1950, and 1952, after construction of the dam was complete, were extremely wet years, and floods occurred. Flows as high as 614,000 ft^3/sec occurred as the flood waters peaked. The current average flow is less than 100,000 ft^3/sec.

Erosion along the toe of the riverbank, coupled with excessive recharge to the aquifer, led to reactivation of the landslides. The potential for aggravation of this condition by flows generated by peaking operation of the Grand Coulee Third Powerhouse was recognized during design of the powerhouse and forebay dam. The embankment placed during construction of the Third Powerhouse proved inadequate to stabilize the riverbank. Stabilization features since constructed consist of drainage wells and shafts, a reshaped and rearmored embankment, and instrumentation to detect changes in the geologic environment, such as excess pore pressures and slope movement. Construction of these stabilization features was completed during the spring of 1988.

6.6 (0.7) Continue travel down the road, past the canal headworks, to SR 155. Turn left onto the highway.

7.6 (1.0) Turn right across the dam.

8.4 (0.8) **STOP 5. Third Powerplant inclined elevator.**

Along the east end of the dam, the granite foundation rock and mafic dikes are exposed in a rock cut section. Also visible are shear zones, which extend into the dam foundation and required treatment during construction. Rock falls periodically occur from this cut slope.

Continue down the highway into the community of Coulee Dam towards the bridge.

9.6 (1.2) SR 155. Turn right.

10.0 (0.4) Football field on right.

10.2 (0.2) Lone Pine turnoff. Turn left.

10.5 (0.3) **STOP 6. Drainage Shaft.**

At the bottom of the hill, pull out onto the left side of the road.

As you look toward the river, immediately in front, about 100 yd through the trees, is one of the three drainage shafts. It is the fenced compound with a small substation box and concrete structure. As part of the Riverbank Stabilization Program, three drainage shafts were constructed in areas where a well point system proved inadequate for drainage desired. All three shafts are 12-1/2 ft in diameter and concrete lined; they are 175, 225, and 239 ft deep. From within each shaft were drilled 50 near-horizontal drains extending out to a maximum of 600 ft. These 2-in. gravity flow drains penetrate and dewater the slide-prone lacustrine clays and silts. The water is then pumped from the shaft invert into the river.

The individual shafts have inflows of 20, 100, and 260 gal/min. It is interesting to note that the 175-ft deep shaft, producing 20 gal/min, is equally as effective in lowering the pore water pressure within the clays as the higher flow shafts. The reason for this is the varied consolidation of the clays and silts and number and extent of sand interbeds present, which have the tendency to transmit more water than the fine sediment.

11.4 (0.9) The stabilization embankment along the river parallels the road from here.

Note the observation wells, drainage well vaults, and inclinometer wells scattered throughout this area.

12.2 (0.8) Community of Elmer City (Third Street).

13.4 (1.2) Community of Koontzville.

Notice the hummocky topography and lush vegetation. This is an area of historic instability. In addition to recharge to the aquifer from the river, the area is fed ground water from drainage upslope through coarser alluvial deposits which abut thick sequences of lacustrine clays and silts near the river. The ground water is then dispersed throughout the clays, via sand interbeds, lubricating them with high artesian heads and causing subsequent movement. Several springs which are contributing factors and indicators for the instability in this area are, interestingly, the attraction for human settlement and subsequent increase in slide-hazard potential.

13.8 (0.4) Roadcut through the Pleistocene Nespelem Formation.

14.0 (0.2) Community of Seatons Grove.

This is nearly the downstream extent of the stabilization work except for the embankment which extends another 1.5 mi downstream. This is also an area of high artesian pressure in addition to the recharge from the river. The area has

had a long history of instability. The granite bluffs along the east edge of the community mark the extent of sliding.

14.6 (0.6) Basalt erratics on left.

These are locally referred to as "haystack rocks" and were ripped up from the nearby basalt cliffs by the advancing glaciers, carried to their present location, and deposited upon stagnation of the ice mass.

15.2 (0.6) SR 155. Turn right.

16.2 (1.0) **STOP 7. View upstream to Grand Coulee Dam.**

A pullout at the south end of the rock cut offers a view upstream to the dam. Again note the historic landslide areas. Seatons Grove is immediately below the cut. Seatons pond at the base of the granite cliff is fed by water channeled from springs and artesian wells.

Just upstream of Seatons Grove is the community of Koontzville, which is identified by the hummocky topography and lush vegetation. Springs and free-flowing artesian wells are the main water source and, consequently, the contributing factor for the instability of this area.

Farther upstream, the town of Elmer City can be observed. This community is built on a large alluvial fan, and the area is considered stable due to the coarse-grained underlying deposits.

Along the east side of the valley can be seen the well-developed 1,700-ft terrace which marks one of the longer periods of occupation of this valley by glacial Lake Columbia. Along the opposite (west) bank is a long and continuous terrace known as Washington Flats. This terrace is composed predominantly of alluvial sands and gravels and contains only minor lacustrine deposits. It does not have the stability problems that plague the right bank.

Return to Visitor Arrival Center.